

# First and Second Symposia on DETONATION

First Symposium:
The Chemistry and Physics
of Detonation
11-12 January 1951
Main Navy Building
Washington, DC

Second Symposium
9-10 February 1955
National Academy of Sciences
Washington, DC
and
11 February 1955
U.S. Naval Ordnance Laboratory
White Oak, Maryland

and the second second

This document has been approved for public release and sale; its distribution is unlimited.

#### CONFERENCE ON THE CHEMISTRY AND PHYSICS OF DETONATION

Main Navy Building Washington, D.C. 11-12 January 1951

# SECOND ONR SYMPOSIUM ON DETONATION

National Academy of Sciences Washington, D.C. February 9 and 10, 1955

U.S. Naval Ordnance Laboratory White Oak, Maryland February 11, 1955

19950111 140

DTIC COPY INSPECTED

Both Sponsored by the Office of Naval Research Department of Navy

Reprinted by the Naval Surface Weapons Center

DTIC QUALLET INSPECTED S

NSWC MP 87-194

Accos	ion For
	CRA&I
Unann Justifi	cation
By Distrib	ution /
А	vailability Codes
Dist	Avail and/or Special
A-1	
NAN	NOUMOED

During my eight years organizing The Detonation Symposium, I have received inquiries about copies of the first three symposia (which were never published in hardback form). In response to your inquiries, the first three are now hardbound. The first two symposia are combined in a single hardbound volume. The third symposium is in a separate hardbound volume. All of the papers in these symposia are now unclassified.

Copies of these volumes, or Proceedings of any Detonation Symposium (the First through the Seventh) are available at a cost of \$35.00 each. Only prepaid orders can be accepted. Make your check payable to "The Detonation Symposium" Mail your payment to:

Dr. James M. Short, R12 Co-Chairman, The Detonation Symposium Naval Surface Weapons Center White Oak, Silver Spring, MD 20903-5000

> James M. Short June 1, 1987 White Oak

#### CONFERENCE ON THE CHEMISTRY AND PHYSICS OF DETONATION

#### CONTENTS

WELCOMING ADDRESS Rear Admiral T. A. Solberg, USN Chief of Naval Research	
SESSION I REVIEW OF RECENT STUDIES	
RECENT STUDIES IN BUORD Stephen Brunauer Bureau of Ordnance	7
RECENT WORK ON DETONATION AT ABERDEEN Jane Dewey Aberdeen Proving Ground	9
STUDIES ON DETONATION PHENOMENA  F. C. Gibson and C. M. Mason Bureau of Mines, Pittsburgh	12
RECENT WORK AT NOL Donna Price Naval Ordnance Laboratory	22
RECENT STUDIES AT THE NAVAL ORDNANCE TEST STATION John S. Rinehart NOTS, Inyokern	31
SOME RECENT STUDIES IN CANADA G. R. Walker Canadian Armament Research and Development Establishment	39
SESSION II CHEMICAL ASPECTS OF DETONATION	
CHEMICAL ASPECTS OF DETONATION Bernard Lewis Bureau of Mines	43
NONSTATIONARY DETONATION WAVES IN GASES George B. Kistiakowsky Harvard University	45
DURATION OF THE REACTION IN A DETONATING EXPLOSIVE S. J. Jacobs Naval Ordnance Laboratory	52
EXPERIMENTS ON THE TRANSITION FROM DEFLAGRATION TO DETONATION J. Roth Hercules Powder Company	57

## SESSION III PHYSICAL ASPECTS OF DETONATION

PHYSICAL ASPECTS OF DETONATION John G. Kirkwood California Institute of Technology	71
THE EQUATION OF STATE FOR DETONATION GASES Stuart R. Brinkley, Jr. Bureau of Mines, Pittsburgh	72
CONVERGENT SHOCK WAVES Arthur Kantrowitz Cornell University	79
SHOCK WAVES IN SOLIDS J. E. Ablard Naval Ordnance Laboratory	88
INTERACTIONS OF DETONATION WAVES WITH MATERIAL BOUNDARIES R. B. Parlin and H. Eyring University of Utah	93
SESSION IV PROBLEMS AND FUTURE DEVELOPMENTS	
PROBLEMS AND FUTURE DEVELOPMENTS George B. Kistiakowsky Harvard University	105
THEORETICAL DEVELOPMENTS IN DETONATION John G. Kirkwood California Institute of Technology	107

# SECOND ONR SYMPOSIUM ON DETONATION CONTENTS

CHARGE PREPARATION FOR PRECISE DETONATION VELOCITY STUDIES 119 Edward James, Jr. Los Alamos Scientific Laboratory
TECHNIQUE FOR THE MEASUREMENT OF DETONATION VELOCITY 136 A. W. Campbell, M. E. Malin, T. J. Boyd, Jr., and J. A. Hull Los Alamos Scientific Laboratory
A MICROWAVE TECHNIQUE FOR MEASURING DETONATION VELOCITY 151 T. J. Boyd, Jr., and P. Fagan Los Alamos Scientific Laboratory
MEASUREMENT OF DETONATION TEMPERATURES
A NEW CINE MICROSCOPE AND ITS APPLICATION TO DETONATION PHENOMENA J. S. Courtney-Pratt University of Cambridge
THE MEASUREMENT OF DENSITY CHANGES IN GASEOUS DETONATIONS 187 G. B. Kistiakowsky and P. H. Kydd Harvard University
THE ATTAINMENT OF THERMODYNAMIC EQUILIBRIUM IN DETONATION WAVES
ON THE STRUCTURE OF A DETONATION FRONT
HIGH TEMPERATURE THERMODYNAMICS AND GASEOUS DETONATIONS IN MIXTURES OF CYANOGEN, OXYGEN, AND NITROGEN
DETONATION IN GASES AT LOW PRESSURE
MEASUREMENTS ON GASEOUS DETONATION WAVES

B. Greifer, F. C. Gibson, and C. M. Mason U.S. Bureau of Mines
CONDENSATION SHOCKS AND WEAK DETONATIONS
THE STRUCTURE OF A STEADY-STATE PLANE DETONATION WAVE WITH FINITE REACTION RATE
THE MEASUREMENT OF CHAPMAN-JOUGUET PRESSURE FOR EXPLOSIVES
MEASUREMENT OF THE CHAPMAN-JOUGUET PRESSURE AND HEACTION ZONE LENGTH IN A DETONATING HIGH EXPLOSIVE
THE DETONATION ZONE IN CONDENSED EXPLOSIVES
CALCULATION OF THE DETONATION PROPERTIES OF SOLID EXPLOSIVES WITH THE KISTIAKOWSKY-WILSON EQUATION OF STATE . 383 W. Fickett and R. D. Cowan Los Alamos Scientific Laboratory
A SOLID-STATE MODEL FOR DETONATIONS
DIAMETER EFFECT IN CONDENSED EXPLOSIVES. THE RELATION BETWEEN VELOCITY AND RADIUS OF CURVATURE OF THE DETONATION WAVE William W. Wood, Ios Alamos Scientific Laboratory John G. Kirkwood, Yale University
THE DETONATION BEHAVIOR OF LIQUID TNT
DETONATION IN HOMOGENEOUS EXPLOSIVES

PARTICLE SIZE EFFECTS IN ONE- AND TWO-COMPONENT EXPLOSIVES	478
DETONATION WAVE FRONTS IN IDEAL AND NON-IDEAL DETONATION	500
DETERMINATION OF REACTION RATE OF SODIUM NITRATE AND THE EQUATION OF STATE OF 50/50 TNT-NaNO3	519
THE DECOMPOSITION OF AIPHA-IEAD AZIDE	529
THE DETONATION OF AZIDES BY LIGHT	547
DETONATION IN AZIDES WHEN THE DIMENSIONS ARE COMPARABLE WITH THE IENGTH OF THE REACTION ZONE	561
ORIGIN OF LUMINOSITY IN DETONATION FLAMES	571
THE ROLE OF GAS POCKETS IN THE PROPAGATION OF LOW VELOCITY DETONATION	582
SENSITIVENESS TO DETONATION	601
INITIATION OF MILITARY EXPLOSIVES BY PROJECTILE IMPACT J. M. Dewey Aberdeen Proving Ground	612
FACTORS AFFECTING THE TRANSMISSION OF DETONATION BETWEEN SMAIL EXPLOSIVE CHARGES	620
THE CORRELATION OF THE SENSITIVENESS OF EXPLOSIVES WITH  COMBUSTION DATA	643

PROBLEMS OF INITIATION IN TESTS OF SENSITIVENESS E. G. Whitbread Ministry of Supply, Great Britain	695
IEAD AZIDE PRECIPITATED WITH POLYVINYL ALCOHOL  T. Gaynor Blake, Olin Mathieson Chemical Corporation Donald E. Seeger, Picatinny Arsenal Richard H. Stresau, U.S. Naval Ordnance Laboratory	711
THERMO-HYDRODYNAMICS AND REACTION KINETICS IN SOME METALIZED EXPLOSIVES	733
CONDITIONS BEHIND THE REACTION ZONE OF CONFINED COLUMNS OF EXPLOSIVE - NOTIONS DERIVED FROM PLATE DENT EXPERIMENTS W. M. Slie and R. H. Stresau U.S. Naval Ordnance Laboratory	749
TNDEX TO AUTHORS	776

**PROCEEDINGS** 

conference on

# THE CHEMISTRY & PHYSICS OF DETONATION

MAIN NAVY BLDG. Washington, D.C. 11-12 January 1951

under the sponsorship of THE CHEMISTRY BRANCH

OFFICE OF NAVAL RESEARCH \* DEPARTMENT OF THE NAVY

#### **FOREWORD**

This report of the conference on "Physics and Chemistry of Detonation" is a record of the papers presented and the discussions held at the meeting called by the Office of Naval Research on 11 and 12 January 1951. The purpose of this meeting was to bring together scientists from government, contractor, and university laboratories to discuss the current status and problems in this field of chemical physics.

It is hoped that this report will be of value to those working in the field of detonation and stimulate the interest of scientists working in related fields of chemistry, physics, and mathematics in the problems related to detonation.

To all those who actively participated in the conference, the Office of Naval Research expresses its sincere appreciation.

C.M. Bolster, RADM, USN Chief of Naval Research

C.M. Tolotus

#### WELCOMING ADDRESS

#### Rear Admiral T. A. Solberg, USN Chief of Naval Research

Mr. Chairman, Ladies, and Gentlemen: It's always a pleasure to come to these meetings and in some respects embarrassing when you realize you have so little to contribute to the subject matter of the conference itself. Nevertheless I'm here, and it's nice to get away from a busy desk to do something like this.

I think this is the first conference in the field of physics and chemistry of detonation which has been sponsored by our office. I think it's also the first such conference that has been held since the end of World War II. One of the nice things about it is to get all the people together in this field. We haven't all been together before and perhaps it doesn't apply so much to me, but I'm sure with many of you, you see many of the faces that you probably haven't seen for a long time, or probably since the end of World War II. I think it's fortunate, too, that there are so many of the scientists here who contributed so much to Division 8 of NDRC in World War II.

As you know, the Office of Naval Research was set up under Public Law 588, and one of its duties is to coordinate research in the Navy. That is a tremendous job in itself. It is one of those things you can't force down people's throats, so you have to adopt other mechanisms. One of those mechanisms is such a conference as this one today. We've found that it has been very beneficial in various areas of urgent Naval interests—and I'm sure all of us will try to keep our efforts in urgent Naval interests—to have such symposia as this. It certainly gets the people together. It is one of the best means of disseminating information and getting exchanges of ideas. I am very much impressed with the logs of such conferences as this that I've read because of the amount of information that I see coming out of them. I learn a great deal more from reading the logs of these conferences than I could possibly get from reading a stack of reports on the same subject.

We've been trying to develop this scheme as much as possible, and about a year and a half ago we had a very successful one in another field and I felt that the method we adopted then was very important. In other words, previous to that time most of such gatherings as this had been only with the inclusion of Service personnel. At that particular one I thought it was well to bring in not only the people interested in the subject, such as our research contractors and Service people, but also to bring in the interested contractors from industry. In other words, we selected people from industry or firms whom we felt had the facilities and also the personnel to go into the development of whatever was going to come out of research in that particular subject.

One of our problems that we are striving hard to improve is the cutting down of the horrible time gaps that usually exist between the time you get some research information and you get it into use or into an end item. We felt that bringing in industry at the proper stage of the research would be a big help. As a matter of fact, in years past, I have complained because of the fact that industry doesn't allow Service people to get in on their research at some stage when we can be helpful to them in specifying the final engineering of whatever is going to come out of their research. Generally, we have to wait until we see a newspaper ad that here's something we need. Most of the time we have to go back to that particular industry and ask them to re-engineer it to suit our specifications.

I think I would like to say just a few words with regard to our present situation and our policies under present conditions. As you know, there is a great effort being made now to produce more hardware and more materials which are available and which are the best we can get. However, I think it is very important that we also produce items which are improvements over what we have if we are going to contend with the numbers which may be against us. Consequently, it is more than ever important that we get our research information into use. I feel that in a conference of this type you should give much attention to that. Most of you know the programs; you are familiar with them; you have an opportunity to discuss them and I feel that you should start roping in those programs and the information that has been made available to you. Think in terms of what implications are coming out of this particular field of research. How can it be applied even if it's only in bits and pieces? That is something that we try to do in the Office of Naval Research. We feel very strongly that you must not wait until a particular research project is finished before you take a hard look at it; as it progresses, try to find out where implications are coming out and at least warn the people who are going to be concerned with those particular implications.

I think, also, in this conference you have an opportunity of learning more about Naval requirements, where our urgent areas of interest are, and I hope you'll prospect that also and, if possible, give off-the-cuff solutions. If you don't have off-the-cuff solutions, when you go back carry those problems with you and bring us any information that might contribute to those particular solutions.

I particularly like the way this conference is named-"Physics and Chemistry of Detonation." I can't remember many other times when I've seen two fields of science married together this way, and I feel very strongly that marriage of the sciences in almost any activity is a matter of the greatest importance. In other words, no one particular scientific subject should have a wall built around itself or be compartmented. I might even be so bold as to suggest that, knowing our own projects in this field and also having the knowledge of how a great many of our projects in the mathematical sciences are contributing and speeding up the work that is being done in this particular subject, it might also be appropriate to name this "Physics, Chemistry, and Mathematics of Detonation." I had the pleasure of getting to know John von Neuman over in London, and it was kind of hard trying to find out what he was doing. He had another mathematician with him-John Calkin-who was continually working out mathematical formulae and problems for Dr. von Neuman. He was running around seeing what damage detonation had done and developing the mathematical formulae that were involved. We all know now that he was thinking in terms of something bigger than what we had over there. He was certainly trying to develop the art as mathematically as possible as to the results of detonations, and that made me realize how important mathematics was in this whole field, whether it's in actual manufacture or in observations of the results.

I would like to add just a little bit as to how we are handling our research at the present time under the present conditions and what our policy is. In our Office we feel it is well for everyone to continue the basic research program at its present level and on its present basis. However, in connection with that, we have continually, and more fervently since Korea, been looking at what we thought were the most urgent areas and also areas which seem to be nearing completion or fruition and putting a great deal more emphasis on those, trying to speed them up. Also, with the help of our university personnel and our own Office, we have been looking very hard for implications that are coming out of the program, and in those areas where it is desirable, getting those into the applied research stage. We are also increasing our coordination and dissemination of information particularly to industry where they'll be able to pick up the ball when it is ready for them. Consequently, the extra money that we are getting we're using principally for those two activities, to put more emphasis where it is necessary and getting some things started in applied research with the idea of having the Bureaus take it over as soon as they can. Many of those projects of that type are being done on a joint basis with the various Bureaus and the other Services.

I think that is all I have to say except that I'm glad to be here and glad to welcome you all to this conference.

#### SESSION I

#### 11 January 1951

#### REVIEW OF RECENT STUDIES

Stephen Brunauer Bureau of Ordnance Chairman

#### RECENT STUDIES IN BUORD

#### Stephen Brunauer Bureau of Ordnance

I feel very good about this meeting. I feel almost as though I were present at a class reunion to see some of the faces of the old friends with whom we worked together in World War II. At the same time I'm sorry for two things. First of all, the occasion that brought us together is not a joyful one. The peace that followed the war in which we worked together apparently was too short-lived, and we are again in a national emergency, and the chances seem to be awfully slim that we can get out of another world war which would be the third in the lifetime of most of us.

The second reason I feel sorry is that some of our friends are not here, some of our old collaborators like John von Neumann, E. Bright Wilson, MacDougall, Eyring, Gamow, and others. I know, however, that these men did not lose their interest completely in explosives. In fact, some of them are working full time in the field, and I do hope that when the next gathering comes, they will all be here, and in between they have helped us also in our work.

There is another reason why I feel good about this meeting, besides seeing the old faces. I see many new faces here. It is to the credit of the Services—and especially of the Office of Naval Research, the Ordnance Corps of the Department of the Army, and the Bureau of Ordnance of the Navy Department—that they kept up the interest in this field through the past years and frequently under rather adverse circumstances.

Now as far as the purpose of this meeting is concerned, I can not add much to Admiral Solberg's presentation. He gave it in more detail, but perhaps I'll repeat one or two points about the purpose of this gathering. The ultimate purpose as I see it - and I use the word "ultimate" as contrasted to the immediate purpose - is to improve the weapons of the Services of the United States and to improve them by the particular method that we are all interested in, namely, by explosive means. That improvement may be one of two types: It may be by putting new and better explosives in our weapons, and the other is by controlling the explosion process in such manner that we can get greater effectiveness out of our weapons. The immediate purpose of this gathering is to increase our fundamental understanding of the detonation process. I do not need to show to any of you that there is a very close connection between the ultimate and the immediate purpose, namely, that the increase in our understanding of the detonation process would in the long run, or perhaps not-so-long run, bring about improvements in our weapons by explosive means.

Now there are two ways in which this conference can help increase our fundamental understanding, as was pointed out by Admiral Solberg. One is by giving us an opportunity here to exchange ideas with each other; and the second, which perhaps is even more important, is that it gives you an opportunity to get acquainted with each other and to get acquainted with each other's problems. This conference will last only two days, so you can exchange ideas here for only two days, and perhaps we may not have another one for another year. But in the intervening period, if you know each other and each other's problems, you can keep on exchanging ideas among yourselves and thereby help each other in increasing our knowledge of the detonation process.

Those of us who worked together in World War II know it full well, and those of you who are newcomers in the field probably realize it too, although perhaps to a lesser extent, what

a tremendous contribution was made to explosive research by the increase in our understanding of the explosion process that was brought about by the work of men like Kistiakowsky, Kirkwood, Wilson, von Neumann, MacDougall, Brinkley, Richardson, Eyring, Gamow, Cook, and many others. The ideas that they developed, the understanding that they brought about, was a tremendous help to the experimentalists, and together the theorist and the experimentalist brought about very important improvements in the weapons of all three Services—or rather at that time there were only two Services of the United States—by explosive means.

At the end of World War II our theoretical understanding was almost adequate to explain the process, the actions of explosives that were used in that war. To be sure, it was realized that the theory was not entirely perfect. Certain limitations were known. It was believed, for example, that perhaps a better equation of state might be found, or that the evaluation of the parameters in the equation of state, especially the covolume factors, may be improved. However, now on the basis of the work that has been done since that time, we realize that the theory might have even greater limitations. We've been working since that time with explosives of the type we did not use in World War II. For example, when the Naval Ordnance Laboratory investigated the detonation velocity of the compound hydrazine mononitrate, a compound that contains no carbon, they discovered that the theoretical value of detonation of velocity was around 6000 meters per second, but the velocity actually measured was around 8000 meters per second. Other differences came in when we dealt with explosives that had much higher percentage of solid products than the explosives we used in World War II, which perhaps would require some modification or at least a more detailed understanding of the detonation process. Then difficulties came up also in the study of underwater-explosion phenomena. The Kirkwood theory gave very well the parameters of the shock wave, especially under water, but in air too, for action beyond several charge-diameter distances, but it isn't quite as good if we deal with the parameters of the shock wave closer to the explosion. What is more, only recently did we realize the great importance that the bubble produced in an underwater explosion plays in damage to underwater targets, and in order to evaluate the bubble parameters we probably need again a more detailed knowledge of the detonation process than we needed for the evaluation of the shock-wave parameters at greater distances.

Now, to say just a few words about the efforts since World War II. The situation was this: in the first two or three years following the war we were building up research. We were building up personnel to do the research and facilities and instrumentation for further research. So these two or three years were very meager in terms of results that you could use in your discussion today. Then in the last two years we were having economic and financial difficulties. You know about that—all of you—and these difficulties hit rather hard at explosive research and especially the phases of explosive research that will be discussed here, the fundamental phases of research. However, in spite of all of that, certain new things did come out and you'll hear those at this meeting.

In conclusion I would like to thank you together with Admiral Solberg for appearing at this meeting and giving your time to it, and I wish you a very pleasant and fruitful conference.

#### RECENT WORK ON DETONATION AT ABERDEEN

# Jane Dewey Terminal Ballistic Laboratory Aberdeen Proving Ground

#### MEASUREMENT OF DETONATION VELOCITY

One completed project(1) includes a study of errors in determining detonation velocities. In investigating detonation velocity in Primacord, it was found impossible to obtain the expected reproducibility. Fourteen measurements were made on the same strips using a rotating-mirror camera and 1.6-megacycle counter chronographs simultaneously. Although the precision of a measurement as estimated by comparison of the two methods is about 2%, the standard deviation of camera measurement estimated from the 26 rounds fired is 6%. The range of the measurements by the camera and electronic methods is 15 and 9%, respectively, in the 14 rounds studied by both methods. The difference between the standard deviations of the camera and electronic methods is insignificant. Both make it clear that the Dautriche method may introduce a 10-20% measurement error.

#### AIR SHOCK CLOSE TO CHARGES

Ultra-high-speed photographic measurements (2) (exposure time about  $3 \times 10^{-8}$  sec) on air shock close to spherical Pentolite charges have progressed to the point where a tentative report can be given. As in previous Bruceton(3) data, a linear decay is found close to the charge. All peak-pressure data obtained in this laboratory on these charges are represented to about 10% by the three-parameter formula

$$PZ = [2.18 + 71.4/(1 + 0.23 lb^{2/3} ft^{-2} Z^{2})] atm.ft/lb^{1/3},$$

where P is the peak pressure and Z the scaled distance. The range of Z's is from the charge surface  $(0.133 \text{ ft/lb}^{1/3})$  to  $100 \text{ ft/lb}^{1/3}$ . Gage as well as velocity measurements cover the range of pressures from 25 to 0.015 atmospheres. Further data at the high and very low pressure ranges are required. The lower portion of the curve gives a good representation of the data of other workers; especial attention was given to the measurements of Stoner and Bleakney(4).

#### INITIATION BY AN EXPLODING WIRE

For blast work close to small spherical charges, spherically symmetric initiation is almost essential. This has been obtained by using an exploding wire surrounded by handpacked PETN. Desensitized PETN from Primacord detonates as readily as the pure material, but a larger quantity is required to initiate Pentolite. In most of the work one gram of PETN from Primacord was tamped by hand into one-half-inch-diameter hemispherical cavities in matching pieces of Pentolite. Using the pulse from a 0.4-microfarad condenser and #40 Nichrome wire, initiation is obtained with 4 KV. Experimental studies with a circuit of 0.15 microfarad capacity and 0.06 microhenry inductance have shown that the resistance of this type of wire must be above 0.7 ohm to initiate at any voltage. Below 5.7 KV initiation is not obtained. As the resistance of the wire is increased above the minimum value, the voltage required to initiate increases rather slowly when the resistance is near the minimum or the critical damping resistance and very rapidly at other resistances. This work is continuing with the aim of investigating its value for study of the mechanism of initiation in solid explosives.

#### REFERENCES

- 1. Breidenbach, H. I., and Gehring, J. W., "Environmental Effects on Primacord Detonation Velocity," BRL Report No. 740 (1950)
- 2. Sultanoff, M., Rev. Sci. Instruments, 21, 653 (1950)
- 3. Boggs, E. M., and Hurwitz, M. D., "Optical Studies of Strong Shock Waves," OSRD 5613 (1945)
- Stoner, R. G., and Bleakney, W., "The Attenuation of Spherical Shock Waves in Air,"
   J. App. Phys., 19, 670 (1948)

#### DISCUSSION

DR. KISTIAKOWSKY: I would like to make a couple of short remarks. In about '44 rather extensive work was done on the Primacord velocities which for various reasons cannot be put in the form of a report. It was indeed found that the commercial Primacord as supplied by the Bickford Company did show a substantial variation. However, it was also found that by asking the Company to be a little more careful—and apparently not very much more careful since the price wasn't very much higher—it was possible to get Primacord which had very much better reproducibility than the commercial. After six years I don't remember what the actual figures were, but it was an improvement by a rather substantial factor in the magnitude of the random errors. Also, it was shown that the cord coming from a given spool within itself was very high in reproducibility. The variations from spool to spool were somewhat large. Then as to the PETN detonation by an explosive wire, it is a very good method to create spherical waves, but I have a suspicion that if you are interested in determining the minimum energy required to set off detonation, you'll have to produce extremely rigid chemical controls in the crystal habitats of the PETN.

DR. DEWEY: As to the Primacord, I'm sorry to say this is Primacord Bickford claims is the best that can be made and these jumps occurred within a roll. We do not expect to experiment directly on the sensitivity of the PETN but on the sensitivity of other explosives to an entire initiator set up by this method in which you can get the maximum control of the form of the detonation wave and know the pressure in the shock emerging from the initiator.

Those measurements have been published. Camera and electronic measurements on the same piece of Primacord check in every case very closely, but both of them change suddenly after nine or ten pieces of measurements. I think you'll see why we do not think it is an optical illusion.

DR. LEWIS: We have had better luck measuring Primacord. I believe we obtain reproducibilities to within half of one percent by the methods we use, and I might also suggest that you contact the Austin Powder Company because they have been recently making Primacord which is of a rather good quality.

I want to mention very briefly what we are starting to do in initiation from point sources and measurements of minimum energy for ignition. There are two methods: one, to insert a bubble of controlled size with the explosive and initiate by ultrasonic waves of known impulse. The other method is to insert a steel ball or other metal ball into a solid explosive or liquid explosive and to initiate by very short induction heating. That work has not progressed far enough yet to give any results but I believe it has some value.

DR. HARTMAN: I suppose I should add my voice to those who say they found no difficulty with Primacord, but I had a slightly different question. I understood you to say something about the pressure varying linearly in an air shock.

#### DEWEY

DR. DEWEY: Close to the charge.

DR. HARTMAN: And this is calculated from the velocities?

DR. DEWEY: Yes.

#### STUDIES ON DETONATION PHENOMENA

F. C. Gibson and C. M. Mason Bureau of Mines Pittsburgh, Pennsylvania

#### INTRODUCTION

The classical theory of the detonation wave applies to steady nondimensional propagation in which the chemical reaction in the detonation wave is sufficiently rapid so as not to affect the detonation velocity. This treatment provides a means of evaluating the parameter of an equation of state for the gaseous products of detonation, using experimentally determined detonation velocities. Information on the thermodynamic state of the gases is necessary to detailed study of detonation processes, as the detonation state is inaccessible by other experimental means. A systematic study of detonation velocities provides a comparatively simple means of estimating the properties of the detonation gases. To obtain high precision, it was necessary to study and develop methods of preparing suitable explosive charges of uniform quality and high purity. A versatile oscillographic method has been developed for precise determination of detonation velocities.

Although detonation velocity data are sufficient for the determination of the parameters of an equation of state of assumed form, it has been shown that the information is insufficient to determine whether or not the form assumed is adequate for the description of the thermodynamic state of the detonation gases. Since the direct experimental determination of the temperature of the detonation wave would provide criteria for selecting a proper form of the equation of state, a method has been developed for determining this quantity by optical means. Although the method appears to be promising, additional refinements of the experimental arrangement will be required to permit accurate determination of the temperature of the detonation wave.

#### MEASUREMENT OF DETONATION VELOCITY

The oscillographic method for determining velocity of detonation in explosives consists of an electronic system which produces a steplike calibrated trace on the cathode-ray tube of an oscillograph that is recorded by a simple photographic process. Figure 1 shows a block diagram of the apparatus. The impulse pickup through the explosive stick or cartridge depends on the change in resistance at the pickup station due to the highly ionic flame front passing the wires that comprise each make station.

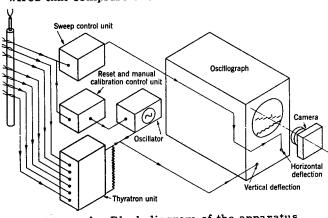


Figure 1 - Block diagram of the apparatus

A potential of approximately 100 volts exists between the two wires that comprise each station; the wires have been twisted and introduced through the explosive charge and are insulated from each other only by the enamel covering. When the front reaches a station, a sharp potential rise results, causing the thyratron associated with the station to trigger or conduct. This is a rapid phenomenon, requiring approximately 0.05 microsecond for conduction. Each thyratron station is influenced by the identical stimuli from the explosive

<sup>&</sup>lt;sup>1</sup>The detonation luminosity and temperature measurements described in this report were carried out by R. L. Boyer.

#### GIBSON AND MASON

charge so that, regardless of the position of the ionic cloud with respect to the detonation front, a true measure of detonation velocity is obtained. Thyratrons were chosen because a thyratron responds only to an initial pulse and is completely stable until the end of the test, at which time it is reset manually. The unit now in use at the Bureau of Mines Explosive Testing Station consists of five channels for determining average velocities of detonation across five adjacent short segments of an explosive charge. The unit employs seven thyratron tubes, a crystal-controlled oscillator, a standard laboratory high-speed oscillograph with a suitable recording camera, and the necessary associated power supplies. One thyratron is used for synchronization purposes and the remaining six for velocity determinations.

Since a driven sweep is employed, it is necessary to synchronize the sweep with the explosion so that the phenomena to be measured fall on the trace and can be photographed. Consequently, the sweep is started a few microseconds before the timing interval begins by a synchronization "make" station a few centimeters ahead of the first measuring station. The six thyratrons have a common resistor in their plate circuits. An increase in voltage drop appears across this resistor, which is between the vertical deflection plates of the cathoderay tube, as each thyratron conducts. Consequently, as the beam spot progresses across the face of the cathode-ray tube, it is deflected vertically as each station is reached by the flame front and the corresponding thyratron conducts. A steplike trace appears on the tube and is recorded by means of a still camera whose shutter has been opened for a time exposure just before the charge is fired. As soon as the explosion phenomenon has been recorded, a calibration time base is superimposed on the record by means of a 1-megacycle, crystal-controlled oscillator. This time base is highly reliable, since the quartz-crystal frequency is very stable and its resonant frequency can be compared with the standard frequency transmissions of Station WWV. This comparison is seldom necessary, since low-drift, temperaturecompensated quartz crystals are available. The record is analyzed by means of a standard 10-power laboratory microscope, utilizing a cross-hair eyepiece.

An actual velocity record is shown in Figure 2. The charge was prepared of 20-micron sized PETN. Each step interval represents the time required for the detonation to traverse 3 cm. The charge was prepared at three densities -1.51, 1.21, and 0.90 gm/cm<sup>3</sup>—with two segments of each and initiated from the high-density end. One step is shown for the highest-density segment and two for each of the lower-density segments. The velocities obtained for the composite are within 1.5 percent of those predicted by the linear relation between the velocity

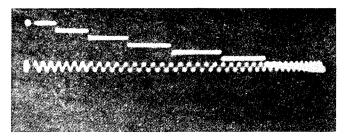


Figure 2 - Typical cathode-ray oscillograph trace for determining velocity of detonation across five adjacent segments of a three-density PETN charge

of detonation and the loading density, established by data obtained previously by several methods. The increase in the step length is easily discernible on the record by unaided visual inspection. The time between adjacent peaks of the calibration wave is 1 microsecond.

The apparatus has been thoroughly tested by measurement of average velocities of detonation over 10-cm lengths on solid explosive charges between two stations. Standard explosives were used, the early work being performed on Primacord. Typical values for charges prepared from adjacent segments of Primacord are shown in Table 1. The maximum deviation from the average for four charges is 0.5 percent. Typical data for cast charges of (50/50) Pentolite are also given, in which the maximum deviation from the average is less than 1 percent for six charges that were homogeneous and uniform in quality.

TABLE 1
Velocity of Detonation for Primacord\*

Charge No.	Station Distance, cm	Time, Microseconds	Velocity of Detonation, m/sec
1 2 3 4	10.0 10.0 10.0 10.0 Maximu	15.5 15.5 15.5 15.6 m deviation from average	6450 6450 6450 <u>6410</u> Average 6440 , 0.5 percent

### Velocity of Detonation for Pentolite (50 Percent TNT - 50 Percent PETN)

Charge No.	Density	Station Distance, cm	Time, Microseconds	Velocity of Detonation m/sec
1	1.69	10.0	13.30	7520
2	1.70	10.0	13.40	7465
3	1.70	10.0	13.40	7465
4	1.69	10.0	13.45	7435
5	1.69	10.0	13.35	7490
6	1.67	10.0	13.50	7405
J				verage 7465
		Maximum devi	lation from average, 0.8	percent

\*The deviations of these data would be further reduced if calculated to a common density by means of an appropriate D vs.  $\rho_0$  law.

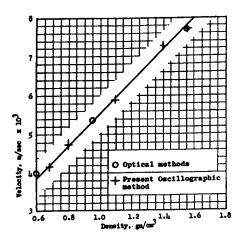


Figure 3 - Velocity of detonation for PETN of approximately 30-micron particle size

The reliability of the method is further illustrated in Figure 3, where velocities of detonation at five loading densities are compared with data accumulated by many tests, employing optical methods. The oscillographic rates were determined over 10-cm distances, and the average of two tests at each density is plotted. The variation is of the order of 1 percent.

A program has recently been initiated to study the decay of nonsteady detonation waves as affected by changes in particle size and loading density of TNT charges. Previously obtained data are not accurate enough for this purpose, much of them having been obtained as averages over segments of considerable length. Charges were prepared of two particle sizes, 500 and 1000 microns, at three loading densities. The charges were 3/4 inch in diameter and confined with a single wrap of cellulose acetate sheet. Each charge was amply initiated by a tetryl booster followed by a

#### GIBSON AND MASON

high-density pressed TNT pellet. In Figure 4, the average velocity over 2-cm segments of charge is plotted against distance from the high-density TNT booster. In the case of 500-micron sized material, velocities for the three loading densities, 1.28, 1.15 and 0.95 gm/cm<sup>3</sup>, tend to a stationary value in a distance of 7 cm or less. In the case of 1000micron sized material, a stationary value is obtained for a loading density of 1.27 gm/cm<sup>3</sup>; however, for densities of 1.13 and 0.95 gm/cm<sup>3</sup> the velocities do not attain stationary values over the distances investigated, and in the case of the lower density the detonation wave has nearly died out in a distance of 5 cm.

This instrument will permit study of the variation of detonation velocity between adjacent charge segments of unequal density, unequal charge diameter, and unlike materials. Since the velocity can be accurately determined over relatively short segments of charge, a comparatively small amount of material is required for each measurement. This constitutes a particularly attractive feature of the instrument, since preparation of charge material of high purity and controlled particle size is usually difficult and tedious.

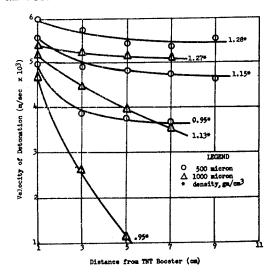


Figure 4 - Velocity of detonation decay for 500- and 100-micron particle sized TNT at three loading densities

#### MEASUREMENT OF DETONATION LUMINOSITY

The parameters of various forms of the equation of state for the gaseous products resulting from the detonation of solid explosives have been evaluated in recent years by Brinkley and Wilson,<sup>2</sup> Caldirola,<sup>3</sup> and Cook.<sup>4</sup> These calculations have been based on the classical hydrodynamic theory of detonation, together with thermochemical data and experimental values for the detonation velocity of high explosives at various loading densities. These equations of state permit the calculation of the pressure and temperature of the detonation wave. Pressures as high as 200,000 atmospheres for the detonation wave at high loading densities of explosives are indicated by the different equations of state. However, calculations of the detonation temperature vary between 3500° and 6500° K, depending upon the particular form of equation selected. The considerable variation of the detonation temperature as calculated by the several equations of state indicates that an experimental measurement of the detonation temperature at several loading densities would be useful to determine the proper form of the equation of state and provide approximate values for its parameters.

A radiation method appears to be most appropriate for measuring the high temperatures of the detonation wave. A method of this type has been developed in this laboratory, and preliminary tests of its application to the determination of detonation temperature have been carried out. The method is based on the change in spectral distribution and the density of the radiation energy as the temperature of a black body increases. Values of the radiation energy density at wavelengths between 0.30 and 1.50 microns for black body temperatures of 3000°, 4000°, 5000°, and 6000° K are shown in Figure 5. These values may be calculated directly from Planck's formula<sup>5</sup> for black body radiation and have also appeared in tabular form<sup>6</sup> for several temperature ranges.

<sup>&</sup>lt;sup>2</sup>Brinkley, S. R., Jr., and Wilson, E. B., Jr., OSRD Report No. 905 (1942)

Caldirola, P., J. Chem. Phys., 14, 738 (1946)

4 Cook, M. A., J. Chem. Phys., 15, 518 (1947); 16, 1081-1086 (1948)

5 Planck, M., Ann. Physik 4, 553 (1901)

6 Smithsonian Physical Tables, 8th ed., The Smithsonian Institution, Washington, D. C. (1934), Tables 309-311, pp. 314-316

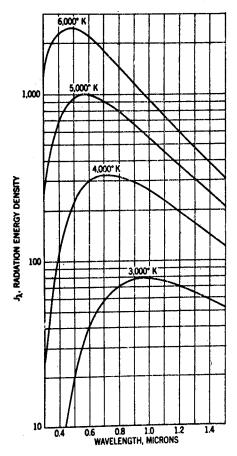


Figure 5 - Black body spectrum intensities

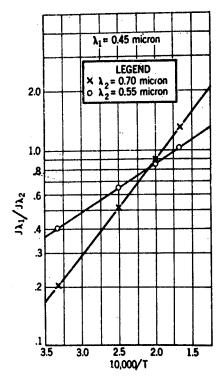


Figure 6 - Relative radiation intensities  $\lambda_1 = 0.45$  micron

The relative intensities of the radiant energy at two wavelengths,  $\lambda_1$  and  $\lambda_2$ , for each of the temperatures are determined from the values of radiation energy density. For example, at 3000°K, the ratio of radiant energy for  $\lambda_1$  = 0.45 micron to that for  $\lambda_2$  = 0.70 micron is 0.206. As the temperature increases, this ratio increases, and at 6000°K the relative intensity of the two wavelengths is 1.32. This change in relative intensity with black body temperature is shown in Figure 6 for two wavelength ratios, and a linear calibration is obtained when the logarithm of the intensity ratio is plotted as a function of reciprocal temperature. The line with the steeper slope shows the relative intensity of radiation for wavelengths of  $\lambda_1$  = 0.45 micron and  $\lambda_2$  = 0.70 micron, while the second line represents this ratio for the same value of  $\lambda_1$  but  $\lambda_2$  = 0.55 micron. This type of calibration line can be used in the experimental measurement of temperature, except that it is preferable to base the calibration on measurements of the radiation emitted at selected wavelengths by radiation sources at various temperatures.

Spectral zones of narrow range of wavelength are obtained with interference-type optical filters, and the transmitted radiation is detected by multiplier-type phototubes and amplifier networks. Incandescent lamps were used as radiation sources between 3000° and 3450°K; their temperatures were determined by operation of the projection-type filaments at voltages

#### GIBSON AND MASON

between 85 and 115 and the direct observation of the filament temperature with a potentiometer-type optical pyrometer. A xenon-filled, highintensity flash tube with an estimated color temperature of 6800° K was also used as a calibration point. Experimental calibration data for these radiation sources are shown in Figure 7 for optical filters with maximum transmissions at 4510 Å, 5420 Å, 6420 Å, and 6870 A; two additional calibration lines are obtained by using the relative intensity ratio for wavelengths 4510 Å and 6420 Å and for wavelengths 5420 A and 6870 Å. The use of four filters with transmission in various parts of the visible spectrum permits four observations of the radiation temperature for each measurement.

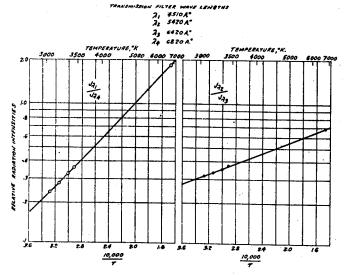


Figure 7 - Experimental calibration data for radiationtemperature measurements

The schematic diagram of the proposed apparatus for measuring deto-

nation temperatures is shown in Figure 8. The source of the radiant energy X corresponds to the lamps for the calibration data and to the explosive for determining the detonation temperatures. This source is placed in an enclosed bombproof approximately 1 meter from the optical filters and phototube detectors. Two "multiple" glass windows, each of 1-inch thickness, are used as transparent apertures through the bombproof wall. A steel tube with slit aperture near the radiation source protects one of these glass windows and also limits the effective radiation zone of the explosive that is incident upon the filters and phototubes. An insert is used with this steel tube to obtain narrow slit apertures; black masking tape over these inserts permits slit aperture widths down to 0.8 mm in the direction of the detonation wave along the length of the explosive charge. The explosive charges are set approximately 8 cm from this slit aperture, and plastic windows of 1-cm thickness are cemented over the aperture to prevent fracturing of the glass window by the exploding charge.

The luminosity from the explosive passing through the slit aperture is incident upon a set of four multiplier phototubes behind the glass window in the bombproof wall. Radiation intensities for the different regions of the visible spectrum are obtained by placing the narrow-band optical filters directly in front of the sensitive surfaces of the phototubes. Each of the phototubes is connected through a vacuum-tube amplifier to the vertical plates of a cathode-ray tube

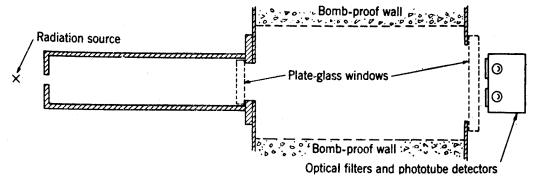


Figure 8 - Schematic diagram of optical system

so that luminosity-time records at four different wavelengths of radiation are obtained on the driven sweep of a four-channel oscilloscope. These four luminosity-time curves for the detonating explosive charge are photographed on a single frame of 35-mm film with a miniature-type camera and f:2.0 lens. Peak deflections on the luminosity-time curves are measured directly from the film negative with a traveling microscope, and the peak intensities are evaluated as equivalent currents in the phototube circuits by comparison with the experimental calibration of the current sensitivity of each phototube-amplifier network. Detonation temperatures can thus be determined for each explosive charge from the ratios of the equivalent phototube currents at the different wavelengths employing the experimental calibration curves.

Time synchronization between the detonation wave advancing along the explosive charge and the triggering of the sweep trace of the oscilloscope is obtained by an electrical circuit similar to that used in the velocity of detonation apparatus. The synchronizing signal from this circuit provided a timing accuracy of better than 1 microsecond, as determined by the distance of the trigger wire above the slit aperture section of the explosive and the occurrence of the luminosity peak on the oscilloscope sweep trace.

Several methods of photocurrent amplification have been used during the preliminary investigations. Initial tests were made with the phototube output connected through a megohm resistor coupled directly to the vertical plates of the cathode-ray tube. In later tests a single-stage dc amplifier with a type 6BA6 tube was used to obtain additional amplification for the input signal to the cathode-ray tube. Tests with unsheathed explosive charges have shown the necessity for higher amplification due to the lower luminosity of these charges and for a greater signal in the output stage to compensate for decreased deflection sensitivity of the cathode-ray tube.

In a verbal communication from James Taylor, I.C.I., Great Britain, to Dr. Bernard Lewis, it was noted that pronounced luminosity has been observed to emanate from inert pellets placed between pellets of explosives. A series of measurements showing the luminosity effects of layers of nonexplosive substances between explosive pellets has been carried out by us. Luminosity records have been obtained for the radiation emitted during passage of the detonation wave through pellets of sodium chloride and also through pellets of flake graphite and flake aluminum placed between explosive pellets. These layers of nonexplosive substances were more than 1 cm in length, permitting adequate definition of the radiation emitted by the material and excluding radiation from the explosive. PETN, tetryl, and TNT were used as the explosive substance, permitting investigation of the luminosity phenomena for a range of detonation pressure and temperature. Luminosity data were also obtained for plastic explosive compositions C-3 and C-4.

TABLE 2

Relative Luminosity for Detonation of Unsheathed Explosive Charges

Radiation Source	Pellet Density, gm/cm <sup>3</sup>	Relative Luminosity
PETN, micron diameter	1.50	1.0
Composition C-3	Plastic	3.0
Composition C-4	Plastic	3.0
Granular NaCl between		
PETN pellets	1.90	6.0
Flake graphite between PETN pellets	1.90	0.65
Flake aluminum between PETN pellets	2.00	1.5

#### GIBSON AND MASON

Some results of the luminosity tests are shown in Table 2. The values of the relative luminosity were derived by interpolation of the signal amplification required for constant deflection on the detonation peak on the cathode-ray tube.

Most of our tests have been made with the explosive charge surrounded by air. Most of the luminosity observed in such tests probably originates in the early portions of the blast wave generated by the charge. The experiments with nonexplosive pellets provide support for this conjecture. The estimation of detonation temperatures will require the elimination of such effects by changes of the geometry of the experimental procedure and of the nature of the atmosphere surrounding the charge.

Since the slit aperture has a finite width, the resultant wave form is the result of integrated radiation, and the recorded peaks are not actual peak values. Reduction of the slit aperture with the necessary additional amplification and broader frequency response of the phototube-amplifier network will reduce the error of experimental determination of the detonation temperatures.

#### DISCUSSION

DR. KIRKWOOD: What about the preliminary results on the temperatures?

DR. MASON: Our difficulty is that they are all plus and minus 500 or more degrees. I can give you some examples. With a radiation slit width of one millimeter, for PETN density of 1.64—five charges—5750 plus or minus 550 degrees. PETN 1.18—four charges—6000 plus or minus 650. Tetryl 1.6 density—three charges—4900 plus or minus 900. TNT (density of 1.56) 5500 plus or minus 350. Most of these traces have appeared in our quarterly reports and these temperatures have been in there. There is one exception to this which at the moment we can't explain. With the use of inert pellets, we get reproducible temperatures in the inert material, plus or minus 100 degrees, but we haven't explored that far enough yet to say any more.

QUESTION: What approximately are the shock temperatures in the pellets?

DR. MASON: About the same as those for the explosives.

DR. BRUNAUER: Is this the maximum range from the average?

DR. MASON: You get four temperatures from each stick, and this plus-minus represents the deviation between the four temperatures you get by comparing the intensity ratio from the four phototubes.

DR. KARTROWITZ: Have you taken any spectrograms of the light?

DR. MASON: Not yet.

DR. KARTROWITZ: I was wondering if perhaps some of the trouble in reproducibility had to do with the fact that the radiation is not black body.

DR. LEWIS: We feel it is necessary to study the quality of the radiation.

DR. BRUNAUER: Do I understand right that the detonation temperature of TNT was around 5000 degrees or something like that?

DR. MASON: For the TNT we have two values. For density of 1.56, 5500 plus or minus 350; density 1.29, 4850 plus or minus 400. I might say, I think Dr. Lewis will agree, due to the question as to whether we have true black body radiation—we don't like to commit

ourselves to saying these are the temperatures. We are skeptical of the translation of these luminosities into temperatures at the moment.

DR. BRINKLEY: I think perhaps it should be emphasized a little further that we are not certain that we are actually seeing the detonation waves. Until the effects have been thoroughly investigated in a systematic way, that question can't be answered. This explains our reluctance to call these detonation temperatures. We suspect that they are actually blast wave temperatures. For this reason, we have to be a little bit careful of interpreting the results. Before committing ourselves, we'll have to complete a greater number of tests.

MR. STRESAU: You mentioned that you did something with powdered aluminum. Did you ever use ordinary cast or raw aluminum and see what happened with that?

DR. MASON: I believe that is contemplated on the program. We just haven't got to it yet.

DR. LAWRENCE: I wonder if I might refer to the work carried out by the Hercules Laboratory in 1944 when J. G. Fox devised a spectrographic method of measuring detonation temperature. He carried out quite extensive tests in order to separate the detonation luminosity from the shock-wave luminosity and found, for example, that where he had an air surround he got very much more intense luminosity than when he had a propane or water surround. You'll run into trouble if you have air bubbles in the charge because you have the shock wave traveling through the air bubbles in the explosive column as well as outside. It was also our impression that probably most of the luminosity came from the light scattered by explosive particles in front of the detonation, and this can be very strikingly illustrated. For example, Fox found that the temperature he was getting for tetryl was very much out of line with those he was getting from other explosives. Then he found that if he measured the light-transmission curve for tetryl and then corrected for the color of the tetryl, it brought the temperatures in line with the other temperatures. Just as a check on this, Fox ran another experiment with Cyclonite which he dyed blue so that there was a change in the color of light which would be scattered, and this had the effect of raising the apparent temperature about 1000 degrees K.

To come back to the effect of shock waves, we didn't actually measure any temperatures on these, but, qualitatively, their temperatures were very much higher than the detonation temperatures. As I say, we did carry out a good deal of work to try to eliminate the shockwave luminosity in the surround and we would, for example, evacuate a charge and replace the air by propane as far as we could and then if desirable carry out the detonation under water using great care to get rid of all air bubbles which might carry shock waves.

We also carried on work with nitroglycerin where we felt that luminosity could be nothing but detonation luminosity. You could, if you wished, dye it black to cut down the scattered light. As I recall, the temperatures that Fox got were not unreasonably different from the calculated temperatures of Kirkwood and Brinkley and some others. But the main point I want to make now is that it is of very great importance to eliminate the shock-wave luminosity.

Fox carried out a number of experiments which indicated that the radiation was black body, but we all felt that more conclusive evidence was needed on that point.

DR. WALKER: The questions I was going to ask have been very well covered by the last speaker. I was going to ask what arrangement was made to eliminate luminosity of shock wave. What was the nature of the surround in these explosive charges? And the other thing—I was merely going to remark that in our studies we have been using salt pellets, length of three quarters of an inch and diameter about the same as in the explosive charge, and viewing them in a propane atmosphere which substantially eliminates all the shock waves. The luminosity seems to occur simultaneously over the salt pellets and commences as soon as the detonation wave reaches the initial surface of the salt pellets.

#### GIBSON AND MASON

DR. RINEHART: We have been studying the burning associated with the solid particles. In that connection you get aluminum oxide which is given off by the particle which burns rapidly. We have recently taken spectrograms and find that most of the spectrum is continuous but we have observed Al or AlO lines. While there is a background there is a lot of spectra associated with the luminosity and I think, when you take spectrograms, you may well find it to be the case.

DR. COOK: I wanted to make one remark in connection with what Dr. Brinkley said, and simply say that I wonder if we can ever measure a detonation temperature directly from luminosity. When we realize that the detonation temperature corresponds to the back of the reaction zone and that, because of opacity, this will be different from this observed luminosity and also from that observed from the side, due to an edge effect, it certainly will make one wonder if he is ever going to measure detonation conditions directly from any such means. Of course, the best we can do is to measure what we see. Perhaps a technique for evacuation would help a great deal instead of trying to work in media that don't have much shock light intensity.

DR. LAWRENCE: You have to have a different medium. Evacuation doesn't do it.

DR. MASON: We tried evacuating the shots but it complicated the picture by putting more peaks in it.

DR. JACOBS: I would like to make further comments on that of Dr. Cook - whether you can expect to measure the detonation temperature since the only one that is important is that corresponding to the Chapman-Jouget condition. Unless you can measure at the Chapman-Jouget point you'll have nothing to compare with the hydrodynamic theory. If you consider the charge with a shock wave coming off the side, generally the luminosity of the shock wave does not build up immediately so you do see a peak. I am quite certain that this is mainly the luminosity seen through the explosive charge ahead of the shock wave. Some of this luminosity comes by transmission through the unexploded charge. Some of it may be due to the air shock, but that is part of the detonation when we are speaking of a detonation wave, and therefore the air shock is just contributing to the head of the detonation wave and not a shock ahead of it and separate from it. It is one consecutive thing. The other point is this: In the bounding medium the pressure is very low because it is pressure of a shock in the outside atmosphere. Therefore, if you cannot see in very far, you're only seeing light due to reaction at relatively low pressure, and measuring temperatures of reaction at 500 atmospheres or thereabouts. The only way to get the pressure of a Chapman-Jouguet condition is to increase the pressure at the boundary. One way of doing that is to fool the detonation by having the wave impact on a solid in such a way that no rear effect and no shock wave is transmitted back into the explosive charge. If you can devise a transparent boundary which will allow you to see a detonation in this way, it is quite likely that you can get something which resembles the Chapman condition. Under these circumstances you'll have a pretty good chance of measuring the detonation temperatures.

#### RECENT WORK AT NOL

#### Donna Price Naval Ordnance Laboratory

#### INTRODUCTION

This paper summarizes various research projects carried out at NOL during the last three years. For each project, an effort has been made to describe the reasons the work was undertaken, the results of the program to date, and the current interpretation or proposed use of the data. Of necessity, the description of each program has been condensed and simplified. Similarly much of the specialized equipment and facilities (bombproofs, cameras, probetimers) developed for the experimental work cannot be included in this report. However, a bibliography of the original work is included and covers the complete programs.

#### SENSITIVITY TESTS

The practical necessity of meaningful sensitivity tests is obvious. In an attempt to develop such a test, which can also be simply made, that will give test values on a continuous scale, and that utilizes a test charge of large enough dimensions to eliminate propagation difficulties, the wax-gap test (1) has been evolved.

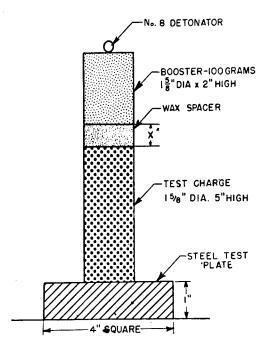


Figure 1 - Setup I for sensitivity test

#### Wax-Gap Test

Figure 1 shows the standardized Setup I finally selected to satisfy these criteria. In each test, a 100-gram tetryl booster is used, and the acceptor charge is 1-5/8 inch in diameter x 5 inches long. The wax gap is varied by 0.05-inch increments during preliminary trials to locate the 50% point—the height of wax for which detonation occurs for half the trials made. Detonation is judged by the denting of the steel plate; failure, by lack of effect on the plate.

Table 1 shows typical results obtained with this standardized setup. You will note that the range of test values obtained was about a 2-inch height of wax. (Numbers in parentheses indicate the number of trials.) Statistical computations indicate a standard deviation of about 0.1 inch as a significant difference in test values.

The data in Table 1 have been arranged to show the usual sensitivity variation noted between cast and pressed charges. It should be pointed out, however, that in no case is the density of the cast and pressed material the same. Data obtained for various pressed densities of TNT indicate that extrapolation to the same density might eliminate

PRICE

TABLE 1

Wax-Gap Sensitivity Test

Errologica	Density		50% Gap	(Inches)	
Explosive	(g/cc)	Pre	ssed	Ca	st
Hydrazine Mononitrate	1.60	2.51	(14)	-	-
Pentolite	1.61	2.36	(13)	_	-
Pentolite	1.65	-	`-	2.08	(12)
Fivonite	1.52	1.81	(13)	-	_
Fivonite	1.58	-	-	1.12	(12)
TNT	1.55	1.68	(12)	<del>-</del>	_
TNT	1.60	-	`- '	0.82	(23)
Composition B	1.69	-	-	1.40	(59)
Baratol 73/27	2.55	-	-	0.32	(12)

TABLE 2

50% Point vs. Spacer Material for Tetryl

Spacer Material	50% Gap (Inches)	
Acrowax B	1.89	(12)
Aluminum	1.90	(17)
Polystyrene	1.85	(15)
Copper	1.69	(13)
Oak	1.39	(17)
Air	5.04	(10)

this difference. Initiation difficulties on small quantities of highly compressed, highly confined materials in another study also point to rapid fall in sensitivity with approach to the crystal-density value.

Exploratory work on variations of the standardized setup has been sufficient to show that the test values obtained are definitely functions of the chosen conditions. Thus, while the results are fairly insensitive to the diameter of the acceptor charge, they are sensitive to booster height and, in this case, do not follow a linear scaling law. All results reported are, therefore, dependent on the standardized setup shown in Figure 1.

On the other hand, minor variations in the wax will probably have little effect. Table 2 shows typical results for wax and other materials used in the gap while testing tetryl. These data are interesting in several ways: the practically identical effect of wax and Al— and as Dr. Ablard's paper shows, we have considerable information about shocks in Al— and the very great difference between any solid-filled gap and an air gap. In the case of the solids, the initiation must result entirely from shock; no detonation products from the donor can make contact with the test charge. For an air gap, however, both shock and hot detonation products as well as the very different properties of the medium may play a role in the initiation.

The standardized wax test showed the expected decrease in sensitivity with addition of wax to the usual explosives (except for TNT). In general, it showed no effect of a temperature drop of about  $100^{\circ}$ C on sensitivity. Grit (sand and carborundum) had no effect on the test values. Although the test was satisfactory for most materials, a few were beyond the scale it covered. Thus, melted TNT and frozen nitromethane (NM) could not be detonated at 1-5/8-inch diameter even with a zero gap, although Fivonite (1) gave 0.47 inch and Fivonite (c) gave 1.12 inches. Since both TNT (1) and NM (c) gave detonations and partial detonations when tested at 2-1/4 inches diameter, it is probable that the standardized conditions chosen do not always avoid a diameter effect.

#### Air-Gap Sensitivity

The second sensitivity test that will be briefly described resulted from an investigation of critical variables in fuze explosive train components (2). Those results obtained for an air gap which are analogous to the wax-gap test work are the only portion of this program we will consider.

In this case, both the donor (booster) and acceptor are highly confined. The test arrangement, sensitivity Setup II, is shown in Figure 2. At the left is a brass cylinder bored to contain the initiator and the donor; at the right is a copper cylinder (with lip for ease in mounting) bored to contain the acceptor. The two parts are mounted and aligned on a lathe; the initiator (dextrinated lead azide) is fired by a condenser discharge.

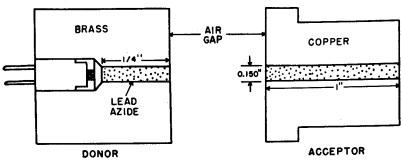


Figure 2 - Setup II for sensitivity test

The criterion for detonation is, in this case, spalling or change of diameter of acceptor container (end farther from donor).

Various factors affecting the test values have been studied. It was found, for instance, that the critical air gap increased with increasing donor diameter, increasing donor length, increasing donor density, and decreasing accep-

tor density. Of these factors, the donor diameter and the acceptor density were found to have the greatest effects. Figure 3 shows three of these effects for shots on tetryl. Each curve shows critical air gap vs. tetryl density for the lead azide donor density indicated by the number written at the end of the curve. The acceptor diameter was kept constant at 0.200 inch. For the curves on the left, the donor diameter was 0.200 inch; on the right, 0.100. Doubling the donor diameter has increased the critical gap 4-5 times (top curves). In general, the gap length and donor diameter showed a linear dependence.

Figure 3 also shows the trend of increasing gap length with increasing donor density. A significant difference amounts to about 15% of the measured gap length. Hence, the crossing of curves shown at the left cannot be established without further work. The trend of increasing gap length with decreasing acceptor density is the conventional and expected one for tetryl; a similar trend was found in the wax-gap test for TNT. In the set of curves at the right, under these conditions, the sensitivity evidently decreases very rapidly as crystal density is approached.

#### PRICE

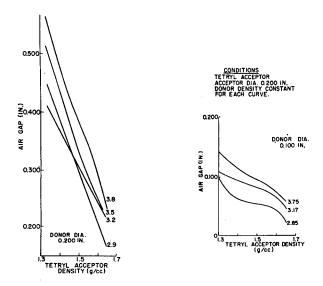


Figure 3 - Critical gap as function of acceptor density

After consideration of the factors affecting the test values, the standardized testing conditions finally chosen were:

Donor: Dextrinated Lead Azide

0.150-inch diameter x 0.500-inch length

Acceptor: 0.150-inch diameter x 1.00-inch length

Loading pressure: 10,000 psi

Number of shots for each determination: 15 - 20

Four materials have been tested in this manner as well as by the wax-gap test. The results and the corresponding densities are given in Table 3. In the three cases where both densities are known, they are nearly the same. This justifies some comparison of the airgap and wax-gap lengths for these materials. This is shown in Figure 4 which does suggest a definite correlation between the two tests. The nature of the correlation will have to be determined by examination of more materials by both methods. The curvature of the line in Figure 4 indicates that initiation, in part by factors other than shock, plays a role in the airgap test, particularly for explosives of lower sensitivity. Thus, if the trend RDX to tetryl were extended, no initiation of TNT would be obtained at zero air gap. Instead, initiation did occur and at an appreciable gap length. This agrees with the large difference for wax- and airgap lengths found with tetryl in Setup I.

#### **DETONATION VELOCITY MEASUREMENTS**

In contrast to the sensitivity measurements, the detonation velocity of explosives can be determined quite accurately. Moreover, detonation velocity-loading density measurements provide data from which velocity of the medium surrounding the explosive (shell case, water, or air) can eventually be computed. Both their accuracy and their potential use to predict explosive effects make these measurements an important part of the present program.

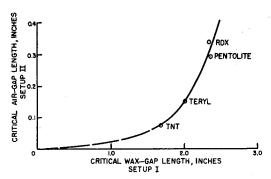


Figure 4 - Comparison of results of two sensitivity tests

TABLE 3

Critical Air Gap and Loading Densities of Pressed Charges

Explosive	Critical Air Gap (Inches)	Density Estimated for 10,000 psi	Density Obtained in Setup I
RDX	0.338	1.52	1.54
Pentolite	0.293	-	1.61
Tetryl	0.153	1.56	1.58
TNT	0.076	1.50	1.55

An immediate application of these data is a determination of the behavior of the detonation products. In Jones' recent formulation of the detonation theory (3), he expressed the detonation pressure as:

$$\mathbf{p} = \frac{\mathbf{D}^2 \, \boldsymbol{\rho}_0}{\kappa + 1}$$

where  $\kappa$  is the adiabatic exponent, and

$$\kappa + 1 = (2 + \alpha) \quad \left(1 + \frac{\rho_0}{D} \frac{dD}{d\rho_0}\right),$$

where  $\alpha$  is a dimensionless quantity related to the variation with volume of the internal energy of the detonation products at constant pressure. The rate-density curve is linear at practical loading densities  $(\rho_0 \ge 0.8)$ . In this region, therefore, $(dD)/(d\rho_0) = B$ , a constant, and we can define

$$\epsilon = \frac{\kappa \pm 1}{2 + \alpha} = \left(1 + \frac{B\rho_0}{D}\right).$$

The quantity  $\epsilon$  is a measure of the departure of the detonation products from ideal gas behavior, and it can be determined entirely from the experimental D vs.  $\rho_0$  data. For an ideal gas,  $\epsilon$  = 1; for explosives at a loading density of 1.6 and above,  $\epsilon$  varies from 1.5 to 2.0.

We have found that there is an empirical relationship (4) between  $\epsilon$ , D, and Q, the detonation energy per gram of explosive. This may be expressed as

$$\frac{\left[0.04613 \frac{Q}{n} + 5.413 \times 10^{-5} \frac{D_{C}^{2}}{\epsilon_{C}^{2}} - 630\right]}{Q \rho_{C}} = 1.00 \pm 0.03,$$

where Q in cal/g and n, the number of moles of gas product per gram, have both been determined for an arbitrary decomposition with detonation products formed in the order:  $H_2O$ , CO, and  $CO_2$ . The subscript "c" indicates that this equation is applied only at crystal density, but under this restriction twenty of the twenty-one sets of available D vs.  $\rho_0$  data fit it to within the indicated 3 percent.

The significance and extent of utility of this relationship have not yet been determined. It is being used at the present time as a test of consistency of the experimental data. For instance, an error in crystal density for one explosive resulted in a deviation of about 10 percent rather than 3 percent or less. Similarly, for another material, the D vs.  $\rho_0$  data used in the first trial did not lie on the curve for an infinite-diameter stick and the variation was again large. In both cases, accurate data reduced the variation to 3 percent or less.

The numerous D vs.  $\rho_0$  data now available for conventional explosives were used in evaluating  $\epsilon$  and in developing the empirical relationship just described. For the experimental program, however, attention has been directed to less familiar materials: hydrazine mononitrate (HN), nitromethane, and high-oxygen-content explosives.

#### Hydrazine Mononitrate

Hydrazine mononitrate is a solid (m.p. 70°) and differentiated from the usual high explosives by (a) containing no carbon and (b) containing excess oxygen. Its detonation products would, therefore, be expected to contain a relatively high amount of water, and its study to yield information about the covolume of this gas as well as gas mixtures encountered in explosion products in general.

Rate-density studies were, therefore, carried out on HN with a conventional rotating-mirror camera setup (5). Although the material is quite sensitive to shock initiation, the charges were initiated by a two-inch length of tetryl booster. The results of this study, summarized in Figure 5, are both interesting and unexpected. D vs. $\rho_0$  curves were

obtained at four diameters. A conventional diameter effect appears at low  $\rho_0$  for diameters 0.5 inch to 1.0 inch. At high densities, however, there is also a diameter effect for diameters of 0.5 to 1.62 inches which results in maxima in these curves and actual failure of 2 charges of 0.5-inch diameter at a loading density of 1.63. The curves have been terminated at the highest density charge detonated except for the top curve which ends at crystal density. The only known similar diameter effect at high density is that reported for 60-40 Amatol for which the D vs.  $\rho_0$  curves are flattened at high density but show no maxima (6).

Coupled with the very large diameter effect, we would expect HN to show a curved detonation front. Preliminary examinations of the front profile confirm the presence of a marked curvature (as compared to the nearly planar front for Comp. B) and, for a 1-inch diameter, a greater curvature at

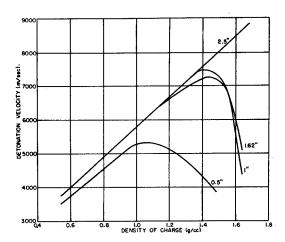


Figure 5 - Detonation velocity of hydrazine mononitrate

 $ho_0$  = 1.6 than at  $ho_0$  = 1.3. In addition, HN shows a high D and a steep D vs.  $ho_0$  slope for ho diameter. The high D is typical of oxygen-rich explosives, as the next project shows.

High-Oxygen-Content Explosives — Measurement of D vs.  $\rho_0$  on Small Quantities of Explosives

Most of the newer explosives of high oxygen content are available only in limited amounts. To obtain D vs.  $\rho_0$  data, therefore, it was necessary to devise a new method requiring but a few grams of the material for each test. It was found possible to obtain D measurements to about 5 percent by high confinement of small charges. Figure 6 shows the setup developed (7).

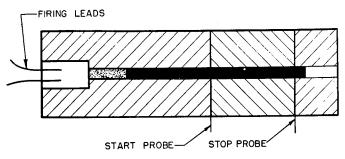


Figure 6 - Setup for measuring detonation rate on small charges

TABLE 4

D vs.  $\rho_0$  Data for Oxygen Rich Explosives

Explosive	Slope (D vs. $\rho_0$ )	Crystal Density	D <sub>c</sub> (m/sec)				
RDX Medina BTNEU BTNEN TNEB Nitromannite	3533	1.82	8700 (9024)				
	4487	1.74	8772				
	5038	1.86	9091				
	3340	1.96	8719				
	3459	1.78	8337				
	3637	1.82	8441				

It consists of three metal blocks with holes of 0.1-0.2-inch diameter bored through the center. The first block at the left contains the initiator followed by a half-inch length of lead azide, a half-inch length of PETN or RDX, and a half-inch of the test material. The middle block contains a one-inch length of the test material; and the end block, 0.2-0.3-inch of the test material. As indicated in the figure, the rate measurement is made by a probe timer on the one inch of material in the middle block.

This method is new, and there are many points yet to be investigated for specific materials. Complications can be introduced by such factors as different diameter, particle size, and sensitivity effects at different loading densities. The present tentative results are shown in Table 4. RDX is included as an example of more familiar materials. Medina and BTNEU show large values for the slope D vs. $\rho_0$  as did HN, another oxygen-rich material. Although the slopes of the other three materials are more conventional, all five of these oxygen-rich explosives exhibit high detonation velocities at

crystal density,  $D_c$ . In fact, the actual rate values are probably higher than those shown under  $D_c$ , for the second value in parentheses for RDX is that obtained by extrapolating the optical data. It is about 300 m/sec higher than the value obtained by this probe method.

The extrapolated values of D at the crystal density are listed because they are only slightly higher than the highest rates measured. For example, RDX pressed to a  $\rho_0$  of 1.81 had D = 8650 m/sec as compared to D<sub>C</sub> of 8700; and TNEB pressed to  $\rho_0$  = 1.77 showed D = 8300 (D<sub>C</sub> = 8337). On the basis of D values of high-density pressed charges, RDX, Medina, and BTNEN seem about comparable; BTNEU, slightly superior; and TNEB and nitromannite, slightly inferior.

Some work has been conducted on the detonation of nitromethane. It will not be described here. For those who are interested in this material, however, the factors investigated were diameter effect, sensitizers, and desensitizers.

## COMPUTATIONS

The present detonation theory permits calculation for a given material of D, P,  $\rho$ , U, and T (detonation velocity, pressure, density, particle velocity, and temperature). The theory depends on the use of the usual detonation equations, the Chapman-Jouget condition, and an assumed equation of state for the gaseous detonation products. Such calculations, which are extremely tedious, have been carried out in great detail by Dr. Brinkley and others (8) for many of the more conventional explosives.

Dr. Snay and his associates have done a great deal of recent work on such computations (9). It is difficult to indicate in a short time how very helpful the resulting systematization and simplification has been. However, anyone who has made such calculations will appreciate the advantage of requiring only two computation sheets and the reading of three permanent diagrams to compute all parameters for a single explosive. These numbers are for an arbitrary decomposition and a known heat of formation for the explosive. One additional sheet is required for estimating the heat of formation (if unknown), one additional sheet for a mixed explosive, and several additional sheets for the calculation of equilibrium composition. The sheets are available in ozalid form and contain all necessary constants and operation directions.

TABLE 5 - TYPICAL COMPUTATION SHEET

DETONATION TEMPERATURE Iteration Process. Begin with an assumed $T_D$ , later enter result of previous step. Repeat until result does not change further.										
	First Step	Second Step	Third Step	Fourth Step						
(a) $T_D = (T_D/T_B) \cdot T_B$	preb	step	preb	preh						
(b) $n_g \tilde{C}_V = A + B \cdot T_D$										
(c) $T_B = Q/n_g \bar{C}_v + 300^{\circ} K$										
(d) $T_{\mathbf{B}}^{\frac{1}{\mu}}$				:						
(e) $x_B = h \rho_{eg} / T_B^{\frac{1}{4}}$										
(f) $1/\bar{C}_V = n_g/n_g\bar{C}_V \cdot 10^3$										
(g) $T_D/T_B$ Read from diagram.										
Final Result: $T_D = ; T_D^{\frac{1}{4}} =$										
DETONATION '	VELOC	ITY								
(h) Read $I_D(x_B, 1/\overline{C}_V)$ from diagram	1.									
(i) $D^2 = \frac{n_g T_B I_D(x_B, 1/\overline{C}_v)}{10^5}.10^5$										
$M_0 (1 - \eta v_s \rho_0)^2$	D =	D = m/s								
DETONATION PRESSURE										
(j) Read $I_2(x_D)$ from diagram using $x_B$ and $1/\overline{C}_{V}$ .										
(k) $p_D = \frac{n}{k}g \left[T_D^{5/4}I_2(x_D)\right]$	·	pD =		kbars						
Further Detonation Parameters:	Expl	Explosive								
$U = p_D/\rho_0 D$ $D = \frac{\rho_0}{1 - U/D}$ $c_D = D - U$										

Table 5 illustrates one computation sheet. In the iterative process, to find TD, represented in the upper portion of the table, an initial value is assumed in (a). All other values are available from previous sheets, are computed by the operations indicated, or are read from one of the three diagrams. This sheet calls for three such readings, one from each diagram. The diagrams are:

$$\begin{array}{lll} \text{(a)} & \mathbf{T_D/T_B} \text{ vs. } \mathbf{x_B} & \text{various } \overline{\mathbf{C}_v} \\ \text{(b)} & \mathbf{I_D} \text{ vs. } \mathbf{x_B} & \text{various } \overline{\mathbf{C}_v} \\ \text{(c)} & \mathbf{I_2} \text{ vs. } \mathbf{x_B} & \text{various } \overline{\mathbf{C}_v} \end{array}$$

These are plotted on coordinate paper and a satisfactory device for rapid interpolation between curves has been developed.

For these calculations, the equation of state used was the Kistiakowsky-Wilson equation:

PVM = NRT 
$$(1 + Ke^{\beta X})$$
,  
 $x = \frac{K}{T^{\alpha}VM}$ , where K is a covolume.

where

The values  $x_B$  and  $\overline{C}_V$  are determined on the sheet shown in Table 5 and correspond to a constant-volume process (explosive  $\rightarrow$  products). From them the necessary functions for computing T, D, and P are obtained from single readings of each diagram. The calculation is then completed by the simple operations indicated on the sheet.

In addition to this project, the same group is now in the process of finding the correct covolume factors from all available experimental data. Present results indicate that the correct values (especially for  ${\rm H_2O}$ ) are different for those in current use.

# REFERENCES

- 1. Eyster, Smith, and Walton, NOLM 10336, 1949
- 2. Stresau and Starr, NOLM 10577, 1950
- 3. Jones, H., Third Symposium on Combustion Flame and Explosion Phenomena, p. 590, Williams and Wilkins Co., Baltimore, Md., 1949
- 4. Price, D., NavOrd 1733, 1950
- 5. Drosd, R., NavOrd to be published, 1951
- 6. Martin and Messerly, OSRD 3411, 1944
- 7. Stresau, R.H.F., NavOrd to be published, 1951
- 8. Brinkley and Wilson, OSRD 1707, 1943
- 9. Snay, H., NavOrd to be published, 1951

# RECENT STUDIES AT THE NAVAL ORDNANCE TEST STATION

John S. Rinehart U. S. Naval Ordnance Test Station, Inyokern, China Lake, California

#### INTRODUCTION

The purpose of this talk is to describe work at the Naval Ordnance Test Station relating to the physics and chemistry of detonation. Generally, the level of effort in this field is not particularly high. The major efforts of the physicists and chemists at the Station are directed toward propellant rather than explosives investigations. The Station, in many cases, relies heavily on the work of other military establishments for the data which it needs in this work.

In the past, much excellent work was done by the Station's former Physics Division under the direction of Dr. W. M. Cady. Most of this work was stopped, however, when the group disbanded in September 1950. J. S. Stanton and his co-workers have published the results of several of their investigations as NavOrd reports and as technical memoranda of the Shaped Charge Working Panel. Cady, B. Cassen, Stanton, D. Marlow and others have published some of their results in the open literature.

Their more recent investigations include (1) an investigation of shock-wave reinforcement from simultaneously detonated charges (Stanton is continuing this work as an employee of Old and Barnes), (2) a study of the collapse of shaped-charge liners using luminous tracers, (3) the development of a number of micro-time techniques, particularly the development of a satisfactory Kerr cell camera, (4) a study of transient stresses in photoelastic substances, (5) an investigation of the decay of shock waves, and (6) the development of a method for the instantaneous measurements of velocity and temperature in high-speed air flow by the use of ultrasonic methods.

At the present time, three groups at the Station are actively engaged in studies relating to detonation. Dr. R. W. VanDolah's group in the Chemistry Division of the Research Department has been determining some of the physical properties of trinitrotoluene, and another group under Dr. A. L. Olsen in Chemistry has conducted a study leading to the design of a powder train delay. A group under my direction in the Physics Division of the Research Department has been interested in the reaction of metals to the impulsive type of loading generated by an explosive charge. In addition, we have been exploring various explosive systems with a view to obtaining very-high-velocity particles of predetermined size and shape. Mr. Guy Throner's group in the Rocket and Explosives Department is making valuable contributions in the way of novel, effective, and practical explosive systems and is conducting a number of shaped-charge studies on which he will report at this meeting.

In addition to these main efforts, miscellaneous studies are carried out at the Station from time to time by other groups or individuals. Recently, for example, Mr. K. S. Skaar, of the Rocket and Explosives Department, has undertaken the design of a waveguide that would give peripheral detonation of the explosive surrounding a shaped-charge cone. The design will be used to determine the efficacy of a waveguide in increasing the penetration of an antitank shaped-charge head for rockets. As part of the design study, the velocity of the pressure wave induced in maple by a detonating explosive charge has been determined experimentally. A value of approximately 12,800 ft/sec was obtained across the grain through 2 inches of maple. However, it appears that the velocity is an exponential function of distance through the wood since thinner sections give higher apparent velocities.

Mr. Shook of the Physics Division is investigating the role that radiation plays in the ignition of propellants. It may turn out that some of the results will also be applicable to problems in the detonation of explosives.

# CHEMISTRY PROGRAM

# Physical Properties of Trinitrotoluene

Studies in the Chemistry Division at the Station under Dr. VanDolah brought on a discussion of the conflicting statements found in the literature as to the crystal system in which TNT crystallized. X-ray studies were made in an effort to resolve this conflict. It was found that TNT was polymorphic in character, showing both orthorhombic and monoclinic forms.

The observation of the polymorphic character of TNT tended to emphasize the meagerness of existing data on TNT and its reaction to varying environments. A program for a general study of the physical properties of TNT was then developed. This program was initiated with studies considered most likely to yield immediately useful information. The present work has been concerned with the phenomena of crystallographic transition and grain growth.

Experiments to determine the orthorhombic-monoclinic transition temperature led to the conclusion that this temperature is below 25°C. At lower temperatures, the rate of transition is so slow as to make the usual methods of detecting such changes inapplicable and work along these lines has been temporarily suspended. It has been found that various materials, including some which are normal impurities in TNT, are capable of affecting the rate of transition; some increase the rate of transition while others reduce the rate markedly, even at temperatures as high as 70°C.

TNT shows a marked tendency toward grain growth even at relatively low temperatures. Noticeable grain growth was observed in samples of TNT stored at room temperature for a period of two years. In general, it has been found that materials which, when added to TNT, increase the rate of transition from the orthorhombic to the monoclinic form also increase the rate of grain growth. On the other hand, those materials which reduce the transition rate reduce the rate of grain growth proportional to their effect on the rate of transition.

# Time Delay Element

The Chemistry Division has also developed, under Dr. Olsen's direction, a powder train delay element for use in the fuze of the 2.75 rocket. Several mixtures of explosive materials were tried. In the final design, the flash primer mixture within the delay cartridge is 53 percent potassium chlorate, 17 percent antimony sulfide, 25 percent lead thiocyanate and 5 percent TNT. The main body of the delay is 3,5-dinitrobenzoic acid, loaded incrementally under approximately 4000 lb/in.<sup>2</sup> pressure. The results of 36 test shots gave a mean delay of 491 microseconds, with a standard deviation of 164 microseconds. The delay cartridge is stainless steel, approximately one-half inch long with an internal diameter of 0.116 in. and a 0.042-in. wall. Its mechanical strength is such that it will not be ruptured by the explosion of the Mk 120 primer used to initiate the delay element. The results are purely empirical. No explanation of the mechanism responsible for the delay has been advanced.

### PHYSICS DIVISION PROGRAM

As mentioned above, my group in the Physics Division has been interested in the reaction of metals to the impulsive type of loading produced by an explosive charge. Our interests have been from both a phenomenological and a structural point of view. Much of

#### RINEHART

our work so far has been exploratory and qualitative. Generally, the action of an explosive is to produce fracturing and plastic flow. Our investigations are directed largely toward obtaining a better understanding of (1) the conditions that will lead to fracturing, (2) the type of fractures produced, (3) the conditions under which plastic flow will take place, (4) the structural character of the plastic flow that does occur, and (5) the mechanical properties of the materials that are significant under this type of loading.

One of the most instructive experiments has been that in which a small cylinder of charge is placed on the surface of a metal plate and then detonated. I will exercise a speaker's prerogative and discuss my own work in greater detail, devoting most of my time to a discussion of the results of these tests.

The experimental arrangement is shown in Figure 1. Composition C3, packed by hand into cardboard containers, has been used in all of the tests. Engineer's Special Caps were used to detonate the charges.

In such an explosive-metal system, three classes of fracture have been observed. These can be characterized in the following way: (1) scabbing, or spalling, the fracturing of the metal near one of its free surfaces which is relatively far removed from the area of application of the pressure (or stress) impulse, (2) fracturing of a type that probably can be attributed to sudden release of the applied pressure, and (3) fracturing that results from the lateral dilation that accompanies a vertical compression. Of these three types of fracture we have investigated scabbing most extensively and have obtained considerable quantitative data.

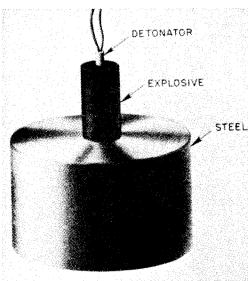


Figure 1 - Experiment arrangement

### Scabbing

Geometrical considerations indicate that, if a plate scabs as the result of reflection of a high-intensity compressional stress wave at a free surface, the thickness of the scab ought to be governed principally by two factors: (1) the shape of the stress wave and (2) a critical normal fracture stress  $\sigma_{\mathbf{C}}$  characteristic of the material acted upon. These same considerations indicate that the thickness of the scab ought to be equal to one half the distance within the wave that corresponds to a decrease in stress equal to  $\sigma_{\mathbf{C}}$ . Scabbing should never occur when the maximum value of the stress within the wave is less than  $\sigma_{\mathbf{C}}$ .

The method that has been employed to obtain stress information is somewhat similar to that used first by Hopkinson and later by others. Essentially, it consists of the experimental determinations of successive increments of momentums, i.e., areas under the stress-time curve, and, from these, construction of the complete curve.

Our experimental procedure includes determining the stress wave, measuring the scab thickness, and then deducing  $\sigma_{C}$  from these data. This has been done for plates of four thicknesses, 1-1/2 in., 2 in., 2-1/2 in., and 3 in. for each of five metals, annealed 4130 steel, annealed 1020 steel, 24 S-T4 aluminum alloy, annealed brass, and annealed copper.

A small cylinder (2 in. long, 1 in. in diameter) of explosive is placed on one face of a heavy metal plate and a small pellet (1/2 in. in diameter) of the same material on the opposite face, in line with the charge. A cutaway section of the arrangement is shown in Figure 2.

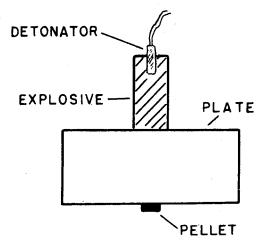


Figure 2 - Cutaway section

The plates were about 5 inches in diameter. Usually, five different thicknesses of pellets were used. Nominal thicknesses were 1/16 in., 1/8 in., 3/8 in., and 3/4 in.

The velocity-versus-distance curve obtained experimentally is then transformed to a stress-time curve through the relation,

$$\sigma = \rho c v$$
,

where  $\sigma$  is the pressure (or stress) at a particular point, v is the particle velocity at that point,  $\rho$  is the density of the material, and c is the velocity of the wave.

A set of typical curves obtained in this way for annealed 1020 steel have been drawn in Figure 3. The curves have been plotted as histograms

since this type of plot represents most accurately the experimental data. The dotted smooth curve, sketched on each histogram, is the author's guess as to the probable shape of the true pressure curve. Similar curves have been obtained for annealed 4130 steel, annealed brass, 24S-T4 aluminum alloy, and annealed copper.

The deduced critical normal fracture stress for each of the five metals is listed in Table 1. No values for  $\sigma_c$  could, of course, be determined for those plates that did not scab.

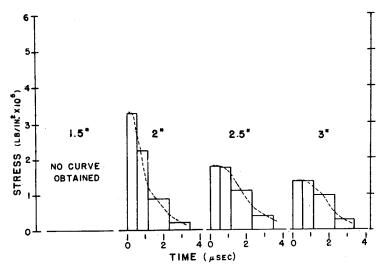


Figure 3 - Typical curves for 1020 steel

Two significantly different values of  $\sigma_C$  were found for 1020 steel. It is possible that the state of stress that exists in the region of the fracture at the time the fracture occurs may affect the value of  $\sigma_C$ . The higher value of  $\sigma_C$  was obtained for the higher ambient pressure. Such an increase in normal stress to fracture is in qualitative agreement with Bridgman's observations that resistance to cleavage fracture is increased by application of hydrostatic pressure.

## RINEHART

TABLE 1

# Comparison of Data with Clark and Wood's Critical Impact Velocities

Metal Critical normal fracture stress $\sigma_{\mathbf{c}}$ (lb/in.2)		Associated critical impact velocity (ft/sec)	Clark and Wood's critical impact velocity (ft/sec)				
24S-T4	140,000	202	290*				
Copper	430,000 400,000	277 258	235*				
Brass	310,000	216	**				
1020 Steel	230,000 130,000	120 68	100				
4130 Steel	440,000	235	**				

<sup>\*</sup>Calculated from static stress-strain curve.

# The relationship

# $\sigma = \rho cv$

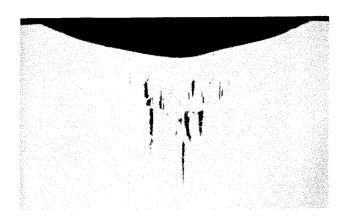
can be used to associate a critical particle velocity with each critical normal fracture stress. Values of critical particle velocities obtained in this way are listed in the same table. These critical velocities and the critical impact velocities found by Clark and Wood agree rather closely. It seems not unlikely that, through further study, they can be shown to be physically equivalent.

# Second Type of Fracture

Among the more unexpected fractures are those that can probably be attributed to the sudden release of the applied pressure. Numerous examples of this type of fracture have been observed. One of the most interesting is in the upper half of Figure 4, which is a photograph of a section cut from the middle of a plate that had been acted upon by a small cylindrical charge. A curved fracture resembling the arc of a circle was found about one-half inch below the surface of the crater. The shape of this fracture can be seen somewhat better in the lower half of Figure 4 which is a photograph of a section so cut that the material could be separated at the fracture.

It seems reasonable to assume that, in the present case, a very large portion of the energy of the compressional wave is stored in the form of a recoverable volumetric change. Upon release of the applied pressure, the body finds itself in an extremely unstable condition, with the energy very inhomogeneously distributed within it. The body will attempt to attain a stable condition as rapidly as possible. Fracturing, which is an energy-absorbing process, is undoubtedly one way in which the energy is dissipated.

<sup>\*\*</sup>Not determined.



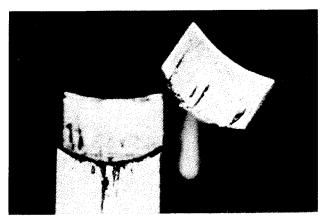


Figure 4 - Typical fracture due to sudden release of applied pressure

# Third Type of Fracturing

The over-all effect on steel of explosive cylinders of several diameters is illustrated in Figure 5. Many fractures, parallel to the direction of the applied stress, are seen to have been generated within the plate. The size, number, and extent of these are seen to increase with increasing charge diameter. They are brittle-type fractures. The tensile stresses that produced them probably originate in the dilation that accompanies application of a compressive stress. The tensile stresses will be expected to act normal to the direction of the applied compressive stress. Under slow loading rates, the material will flow plastically in a lateral direction. At very high loading rates, steel is known to behave more nearly as a brittle than a ductile material; hence, fracturing and not plastic flow can be expected to occur.

#### Plastic Deformation

The plastic deformation that takes place within the plate is also being studied extensively, but time does not permit a detailed account of these studies here. Of particular interest, however, is a clearly defined region (Figure 5) that surrounds the crater and which, when etched heavily, contrasts markedly with the remainder of the section. The metal within this region has undoubtedly undergone severe coldworking. The hardness of the material within this region was found to be very much greater than the hardness of the material

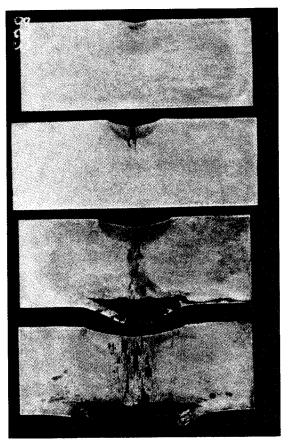


Figure 5 - Third type of fracture

just outside of the region. The microstructures of the sections have also been studied. Typical structures are shown in Figure 6. The parent material is in the upper-left corner. The microstructure of the material below the highly worked region (bottom photograph in Figure 6) is characterized by the presence of a large number of Neumann bands or shock twins. Material within the highly worked region is shown in the upper-right corner. We do not yet understand the nature of the structural changes that have been wrought here. It appears probable that extreme shock-twinning occurs, but that, superimposed on it is extensive slip and some actual breakup of the grains into crystallites.

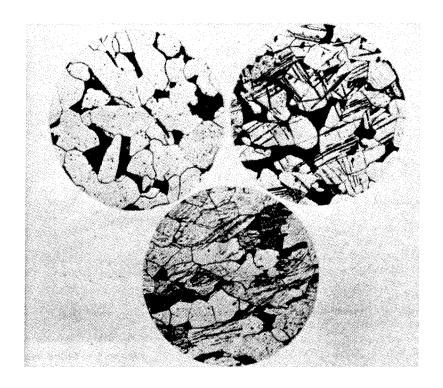


Figure 6 - Typical microstructures

# SOME RECENT STUDIES IN CANADA

# G. R. Walker Canadian Armament Research and Development Establishment

This work was started back in 1943 when Dr. Hertzberg was at the University of Saskatchewan. He was asked by the National Research Council or one of its associated committees—that's the Canadian National Research Council—whether he would undertake some investigation into the field of explosives. He was advised by many people not to attempt it, because it was rather a difficult field and we had no facilities for setting off big charges, or anything of that sort, but he went ahead anyway.

I was with him as a student-assistant from the spring of 1944, and we carried on for about 18 months in that way. Dr. Hertzberg left the University in September 1945, and for the next few months we had some correspondence, but after that we were largely left to our own resources, and I carried on there until September of 1949. Since that time, I've been at the Canadian Armament Research and Development Establishment, or CARDE, as the initials would be pronounced; but up to the present time I haven't had any detonations there.

I have done some work, though, in attempting to study further the photographs which had already been taken at the University of Saskatchewan.

Now, very briefly, our facilities there were rather crude. We didn't have any concrete at all; we had very little steel in our bomb cell. It was mostly a wooden structure with earth banked around it and a few sand bags here and there. Our camera was one which Dr. Hertzberg had designed. We thought it would be rather suitable for this sort of investigation. It's of the rotating-mirror type streak camera. Its "F" number is relatively poor. It's about F-20. But its image speed is relatively large—5000 meters, which is comparable to detonations.

This camera, then, gives very good resolving power in the time direction—slits about a tenth of a millimeter wide, image speed, 5000 meters—that's 5 millimeters per microsecond. Also, it enabled us to study very small portions of the charge. We were setting off very small charges. And so the nature of initiation came to be one of the topics that we dealt with. I'll say something more about that in a moment.

We have done some work measuring detonation velocity. We were limited, of course, in the diameters of charges we could use, but ordinarily our accuracies were something like 0.2 or 0.3 percent. Rather considerably better accuracies were obtained for one liquid where we were using the differential method—measuring the velocity in this liquid at various diameters by measuring the difference between its velocity in various tubes and that in a standard tube filled with the same liquid.

The results there would probably be of some interest to a theoretician. We haven't done anything except to report them. Our work throughout has been almost entirely experimental reporting these things as we found them.

The question of detonation time— I am glad to notice that it has been given considerable attention here. We have photographed the zone of detonation following Dr. Lawrence's suggestion of using the stationary image, that is, using the image velocity as given by the mirror to compensate for the velocity of the detonation so that the image on the film is a

stationary one. You make the slit wide or narrow, and the image remains unchanged—it merely becomes brighter.

And by measurement of such images, while I have no figures with me, and while such measurements are only now being made with a good microdensitometer, I can say roughly that the peak luminosity lasts something of the order of 0.02 microsecond and the total luminosity of detonation something like ten times that amount—perhaps not more than 0.2 microsecond.

Another thing which occupied some of our attention was observing Mach waves in detonations. And we observed all the usual things—that is, the incident wave, the reflected wave, and the Mach wave. These detonation waves are actually curved, as someone pointed out this morning. It is also true for shock waves. And the reflected detonation waves are extremely weak. But they do show up in the photographs.

Initiation—I can't very well say much about that, but we did study various high-density explosives, and a certain amount, also, of low-density explosives, initiated by detonator. We also have initiated them by the impact from what's now called a shaped charge, an aluminum-alloy jet.

But perhaps the more interesting results were the ones which I presented at the tripartite conference last fall at CARDE. I indicated at that time the means by which we could measure the velocity of the low-order detonations obtained when you have a jet, initiating high-density powders. The initial stages of the detonation are a low-order detonation.

Now, I indicated at that time how we had succeeded in measuring the velocity of this low-order detonation, which, incidentally, proceeds only down along the axis of the charge. It's not in itself visible, but by slightly indirect means we measured that velocity. I have no figures with me. The velocities were something of the order of 2000 meters, although they were not constant for one of the explosions. It would seem to depend on how far the lower wave travels.

We also have attempted to produce these low-order detonations artifically, in a manner somewhat analogous to what has been presented here at this meeting, by using a plain detonation wave, passing it through an inert material, and then passing the shock wave thus transmitted through the specimen concerned. We have used high-density solids and also liquid explosives. That shock wave passing through the solid or liquid seems to cause initiation not everywhere over its surface but just at one point on its surface, and from that point on the ordinary detonation spreads. There is a little more definite information in our reports dealing with these low-order detonation waves, including one or two attempts which we have made to cause two low-order detonation waves to intersect. However, that is something which hasn't been followed up very much as yet.

Now, I think I've said a few words about all the various things that we have poked around at, and I'm sure the impression you got is that we haven't really done much of anything in any one field but that we have just dug around a little bit and then tried to find out a little here and there as best we could.

Reports 1, 2, and 3 of our work, are, I believe, available from the National Research Council of Canada at Ottawa. And the other two reports, which I have numbered 4 and 5, are available as a single report from the Defense Research Board, also of Ottawa. Several other reports are in the process of preparation, and they'll be issued from CARDE as time allows us to get them finished.

# SESSION II

11 January 1951

# CHEMICAL ASPECTS OF DETONATION

Bernard Lewis Bureau of Mines Chairman

## CHEMICAL ASPECTS OF DETONATION

# Bernard Lewis Bureau of Mines

The chemical aspects of detonation present a difficult subject for discussion. What we appear to be concerned with are those detonation phenomena that are neither predicted nor understood by the classical hydrodynamic theory. It would seem that our interest should gravitate toward solid explosives rather than toward gases. But we know generally more about gases than solids, so that it is perhaps more profitable to talk about gases.

It is quite natural to be interested in gas-phase detonation, since we have become acquainted with the striking phenomena of discontinuous progress and spin of the detonation wave in tubes filled with detonable gas mixtures; and it is intriguing to speculate how these phenomena might be harmonized with the classical concepts of the detonation wave. Von Neumann has provided us with the concept of the structure of such a wave, according to which there is a family of Hugoniot curves, each referring to a plane behind the shock front and representing stages of chemical reaction. Somewhere behind the shock front is the Chapman-Jouguet plane, in front of which the released chemical enthalpy is available for reinforcement of the shock front. There is nothing in the theory to indicate in detail the chemical and physical processes that occur behind the shock front in the various planes of Von Neumann. It is here that there is some leeway for further speculation.

We may introduce two different concepts of chemical transformation, each type being well-illustrated from other experience. One is exemplified by a gas element passing through the shock front and being thrown into a state of chemical reaction. In this process, diffusion and heat conduction between the various wave layers play a negligible role. One feature about the reaction may be assumed a priori, namely, the reaction rate is self-accelerating because heat is released and the temperature rises. It is, therefore, admissible to some degree to apply the concept of induction period whereby the element, after some time and corresponding distance of travel, will suddenly release the bulk of its chemical enthalpy.

In contrast to this type of process is the transformation in a combustion wave. Let us suppose that the reaction rate behind the shock front is at first very slow, permitting the element to travel some distance virtually unchanged, and that subsequently the reaction goes to completion within a distance of travel of only a few mean free paths. In that case, a zone is formed within which the rates of transport of molecules and heat by diffusion and conduction become of high order. The zone remains stable if the molecules of reactants that enter the zone can undergo complete reaction within a few (10 to 100) collisions.

This is no extravagant assumption because here the entering molecules are exposed to a combination of high temperatures and high chain-carrier concentrations. The concentration of chain carriers (atoms and free radicals) is large, even in the completely burned gas behind the zone, so that collisions with chain carriers constitute a substantial fraction of the molecular collisions. It is thus possible to visualize that the shock-generating thermal expansion takes place in a zone in which heat conduction and diffusion are controlling processes; in other words, a combustion wave is established behind the shock front. In contrast to the shock front which tends to be plane and perpendicular to the tube axis, the combustion wave is not stable toward fluctuations of particle velocity over the tube cross section. It must tilt and wander; and, since it is coupled with the shock wave, being the seat of the shock-generating force and thereby

producing the medium within which it propagates, numerous phase relations appear possible which lead to more or less regular periodic phenomena.

Interesting possibilities arise when we consider that both types of combustion mechanisms operate simultaneously. There is no recognizable stability condition that limits the growth of area of the combustion wave. The chief limiting process that is operative in ordinary combustion-wave propagation along a tube is viscous drag at the wall, which is negligible here. Consequently, as time passes the wave area increases; and, since the tube walls provide confinement, the combustion wave assumes a tilted position of increasing angle of tilt. Simultaneously, since the total mass rate of burning is proportional to the area of the wave, the pressure signal to the shock front grows continuously, so that the detonation velocity increases. However, as the combustion wave becomes more tilted, certain gas elements "explode" before they have reached the combustion-wave front. This means a sudden additional release of chemical enthalpy which gives rise to a retonation wave. At the same time, however, the release of enthalpy in the pocket that is bounded by the combustion wave and the tube wall brings about a decrease of the area of the combustion wave and therefore a decrease of mass burning rate and weakening of the pressure signal to the shock front. The detonation velocity thus decreases and picks up again as the combustion wave oscillates between tilted and plane positions. Such periodic increase and decrease of the detonation velocity, interspersed with retonation waves, may be seen in the photographs of Bone and Fraser.

This concept leads further to an explanation of the "spin," which experimentally is known to be an intensely luminous spot that moves in a spiral path at high frequency along the tube and is capable of making a spiral trace in a silver film or in dust on the tube wall and to break a glass tube into spiral fragments, all of which is evidence of a local blast of hot gas. Such blast must occur at the upstream tip of the tilted combustion wave. Since conditions here are subsonic and since the gas expands in the combustion wave, there must be a refraction of the stream tubes entering the wave because of the continuity principle. This means that, at the tip, stream tubes expand on the unburned side of the wave and contract on the burned side and thus, because of refraction, direct a concentrated blast of hot gas against the tube wall. There is no stability for such a spot on the tube circumference, and it is quite readily imagined that the spot travels around the circumference. Since the whole disturbance moves forward, a spiral track is traced.

Whatever the merits of these suggestions, they certainly point to an interplay of chemical and physical aspects of detonation. The fact that spinning detonations seem to be generally observed as one approaches either limit of detonability lends further support to this interplay of chemical and physical factors.

In this particular theory the combustion wave would coincide with the Chapman-Jouguet plane. It is quite imaginable that, in other cases, the reaction mechanism is such that the reaction is more or less quenched before the total enthalpy is released, so that reaction is not complete in the Chapman-Jouguet plane. Thus only part of the chemical enthalpy is available for the detonation process. This at any rate might explain the occurrence of several detonation rates that have been observed with nitroglycerin and other high explosives. Incomplete reaction in front of the Chapman-Jouguet plane must also be a determining factor in the limits of detonability. It presages considerable difficulty in the search for a satisfactory theory of the limits of detonability, but perhaps it is less formidable than a theory of the limits of inflammability. In this connection I venture the opinion that, as difficult as the problems of detonation processes may be in their finer details, they probably are always considerably simpler than the formidable problems associated with combustion-wave propagation.

# NONSTATIONARY DETONATION WAVES IN GASES

# George B. Kistiakowsky Harvard University

Since 1946, my interests, as far as personal research goes, have been limited to gases which in comparison with actual explosives are rather feeble phenomena. But I agree with Dr. Lewis that in some way the study of gases is very useful, even as far as the understanding of solid explosives is concerned.

I'm afraid, however, that the particular phenomena which I wanted to discuss this afternoon happen to be very closely related to the detonation spin which Dr. Lewis has just discussed and don't have a parallel in solid explosives, largely because the phenomena in gases are very strongly influenced by the walls—the confining walls of the tube in which the experiments are made.

Dr. Lewis has mentioned that it's well known that these fluctuating detonation waves, so to speak, and spinning detonations, occur near to detonation limits. In our effort to understand the effect, so to speak, of chemical variables—reaction rates and such—upon detonation phenomena, we came upon the very old work of Dixon, who claimed that in very dry carbon monoxide mixtures, detonations were very seriously slowed down. Later work seemed to discount it.

Now, from the study of flames in carbon monoxide-oxygen mixtures, it's been definitely established that water or hydrogen are needed as intermediates in the chain mechanism - presumably the hydroxyl radicals and the dry carbon monoxide-oxygen mixtures burn at much slower flame velocities and have high ignition temperatures. We have studied the detonations in such mixtures, and I might perhaps say a few words about how these measurements are taken.

Most of the velocity determinations were carried out in stainless steel pipes of 10 cm diameter. The flanged pipes were made in two sections, bolted together, with a thin cellophane diaphragm clamped between the flanges. The ends of the pipes were closed by flat plates bolted to the flanges. To insure airtight connections, grooves were machined in the flanges, into which fitted rubber "O" rings. All other connections were welded airtight. The first "initiator" section was 50 cm long and was normally filled with readily detonable acetylene-oxygen mixtures, which were ignited by a powerful spark in a spark plug screwed centrally into the end plate. The other, "experimental," section, 120 cm long, was filled with the gas mixture to be examined. The initial spark ignition of the acetylene-oxygen mixtures was found to change into a detonation within a distance of a few centimeters. The experimental mixtures were detonated, therefore, by a nearly plane detonation wave striking them through the rupturing cellophane diaphragm. This technique eliminated the long run-up distances required to produce detonation waves from flames in less readily detonable mixtures.

The sensitivity of the method is about two-tenths of a microsecond, and the gages are spaced 10 cm apart so that we can get successive velocity intervals to certainly one percent. Now, when we plot the velocity of the initial shock which triggers the gages against the distance along the pipe, we find that a moist, essentially stoichiometric carbon monoxide-oxygen mixture has a perfectly normal detonation wave to—within the accuracy of the measurement—a few tenths of a percent.

However, careful drying changes the phenomena completely. It becomes very difficult to initiate the wave. The wave has to be very definitely overdriven by a rather strong initiating mixture to get anything self-propagating in the dry mixture. And secondly, the velocity undergoes essentially periodic pulsations, of which we have observed, altogether, three, on a distance of two meters. If you wish to call it wavelengths, it's about 50 centimeters.

Incidentally, that ratio of wavelengths of these pulsations to the tube diameter is not very far from what has been observed in early work, particularly by the English school, using optical methods for observation and using narrow tubes. They worked usually with half an inch or, at most, one-inch glass tubes, in which case their moving film traces, instead of being straight, appear as wriggly records.

And again with these records are associated the so-called detonation spins. The variations in detonation velocity are by no means small. The normal excess, if you can call it normal at all, is maybe thirty percent in excess of Chapman-Jouguet. After these observations were made I started remembering the earlier work done by other students of mine in which detonating mixtures—hydrogen-oxygen, and so on—were under initiated. In that case, one usually observes a decaying shock, well under the Chapman-Jouguet value, then a violent rise in velocity. Of course, the gages being several centimeters apart, we cannot assert that it is an instantaneous thing, but it always occurs in the interval between two gages. The velocity becomes higher than Chapman-Jouguet—maybe sometimes as much as twice—and then drops to the Chapman-Jouguet value.

Furthermore, the thing that puzzled us then—two years ago—was that this surge was delayed about 50 centimeters which we now observed in the periodic situation. So I now think that the two types of phenomena have very close connections, and they have to do with initiation of detonations. And I want to speak now about a possible mechanism which I am very glad to see actually is very closely connected with what Dr. Lewis has spoken to us about just now. As he pointed out already, there is inevitable existence of an induction period between the initial shock and the onset of chemical reactions.

I was going to call this the Von Neumann zone, but actually I must warn you that it shouldn't be called the Von Neumann zone. Not so long ago I was reading a Russian article by Zeldovich published in a journal in 1940, which contains all the elements of the Von Neumann theory in detail. So if there is to be a name attached, I'm afraid it has to be Zeldovich rather than Von Neumann.

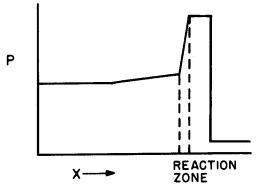


Figure 1

So, as shown in Figure 1, we have to draw the pressure-distance curve because we have to remember that, if there is a zone where there is no chemical reaction and we are to have a stationary phenomenon, there can't be any pressure gradient. Now, what happens with these periodic detonations? I feel that it has to do with the fact that the reaction mixture is not sufficiently reactive to undergo chemical reaction within a very short interval after the compression by the shock front.

Now, what is "short"? "Short," I think, is a relative word in this case and relates completely to the tube diameter; these periodic fluctuations observed by others are only a few centimeters in

wavelength—again, only just a few tube diameters. So the whole phenomenon is tied into the tube diameter—that is, to the effects of the walls—and I imagine, although I'm not sure, that it has probably something to do with the turbulent boundary layer which must spread into the interior of the pipe. I don't know these details; they're certainly unclear to me.

#### KISTIAKOWSKY

But now, let's see what will happen in either a poorly detonating mixture—that is, a mixture near the detonating limits—or in a mixture which has been deliberately made nonreactive—although an intrinsically good detonating mixture—by drying—like carbon-monoxide-oxygen. Let's start with the driven wave, which has been made to have higher intensity than the stationary Chapman-Jouguet intensity. At this point, we can assume that the initial shock is adequately strong, and in this case the temperature of the initial shock may be as high as 2000 or 2500 degrees Kelvin—enough to cause instant reaction. In other words, the profile is such that the chemical zone follows the shock almost immediately. But, the wave being overdriven, the energy dissipation by the wave is greater than the energy provided by the chemical reactions. And the wave must gradually decay to the Chapman-Jouguet stationary state.

When that happens, let's say at this point, the shock becomes not strong enough to insure the ignition of the gases in a region which is still nonturbulent and is free of wall effects. Consequently, the shock intensity begins to decrease, since it isn't being provided any more with a flame which follows it at the same velocity as the shock. The induction period must increase in duration, and the burning zone falls further and further behind the shock.

Well, if the flame front falls behind the shock and the pressure gradient becomes positive toward the shock, then the shock can be looked upon as a decaying shock, because there's a rarefaction wave behind it. And so, we have, then, the falling velocity of the shock; as the shock decreases in intensity, the induction period for ignition lengthens, and the flame falls further and further behind. The question now is, what causes sudden explosion? I feel the same way as Dr. Lewis does, although in detail a little differently, that it must be a fresh, spontaneous ignition. Because I cannot conceive of any mechanisms, even allowing for turbulence— after having had several discussions on the subject with several people—I can't think of any mechanism by which the same flame, after falling back into the turbulent region, could all of a sudden pick up such velocity that it could catch up with the shock.

And so I am inclined to think at present that a new ignition sets in. If the old flame is somewhere in the intermediate region, a new ignition sets in, so that there is a positive pressure gradient forward. Then presumably a new shock—maybe a pressure wave—then a flame front, which, of course, always means pressure drop inward; then a second flame which is moving backwards from this new spontaneous ignition region. I'll describe it as shock—to differentiate from flames—although there's no proof that they are real shocks since the whole thing is speculation.

And finally, somewhere farther back, is the initial flame. When the rear disturbance meets the original flame, that is the end of it. But when the forward disturbance reaches the original shock, you will have a very much higher mass velocity than is predicted by the Chapman-Jouguet theory, since you have a mass velocity due to the first shock and mass velocity due to the second disturbance—and, of course, once you're given the mass velocity you can see that the rest follows—that you have a sudden rise of velocity as detected by the gages.

If that is the correct interpretation of pulsating detonations, then the delayed initiations must be understood as follows. The first shock is moving forward, and is a decaying one. And by mechanisms which I freely admit I do not understand, our delayed ignition sets in, in a space between the initial shock and the air piston pushing the explosive gases forward, and this ignition spreads out. And when it catches the initial shock, we have, again, this extreme overshoot.

But now, since the explosive mixture is a good explosive, the phenomenon is a non periodic one, because the originally overdriven wave, insofar as its energy is dissipated, settles to a stationary regime of Chapman-Jouguet.

## DISCUSSION

DR. COOK: I'd like to call your attention to the fact that Parisot and Lafitte have observed the "spinning detonation" in amatol, and they found the same sort of thing that Dr. Kistiakowsky described here for gases.

DR. KISTIAKOWSKY: In a solid explosive?

DR. COOK: Yes, maybe Dr. Lawrence recalls.

DR. LAWRENCE: I'm a little bit hazy on that.

DR. COOK: Then I'd like to make one more comment. Becker, in his original treatment of this "spinning detonation," talks about dying out and reforming of the detonation wave—getting the effect that we get here, merely from the fact that we have a positive particle velocity in detonation, and a negative particle velocity in the deflagration process, so that you get a sort of a "retonation wave" effect. In other words, when the particle vector turns around, you have to conserve momentum by creating a "retonation wave" which now moves into the unreacted explosive and may be the reason detonation starts up again. I just wanted to add that as a possibility—and I believe it is a good possibility—that you have a periodic reinitiation of detonation in the "spinning detonation." But I think there's also a possibility that one obtains such a reinitiation by means of a "retonation wave" created as the particle vector turns around. In other words, perhaps this "retonation wave" is an explanation for the reinitiation suggested by Dr. Kistiakowsky.

DR. KISTIAKOWSKY: But how would that fit with the subinitiated good explosives?

DR. COOK: Well, this would always occur with materials that are right on the threshold of detonation. The threshold of detonation might be associated either with controlled boostering or controlled sensitivity. I think that may be the correlation, at least—that you require the detonation really dying out—but if you get right on that threshold of detonation by controlled initiation as well as by controlled sensitivity then you have a possibility of reforming an impulse of the detonation wave by means of a "retonation" wave.

In other words, we always talk of particle velocities being positive in detonation and negative in deflagration. The transfer from positive to negative would thus require a sort of "retonation wave." I'm just mentioning this as the Becker statement of it.

DR. KISTIAKOWSKY: May I say something? Just ten minutes before I started talking, Dr. Roberts gave me a report by Mooradian and Gordon which tickled me no end—because this is a measurement of the pressure phenomena—time-pressure curves in gaseous explosions. On inadequate initiations, when he plots the pressure-time curve, he finds a shock, and then another pressure pulse. The pressure pulse catches up with the initial shock—which to me is extremely encouraging, as suggesting that basically this idea of ignition far behind the front catching up with the front is not unreasonable.

DR. LEWIS: Why does it have to catch up with the front?

DR. KISTIAKOWSKY: Because, you see, this ignition is taking place in a medium with respect to which the shock velocity is subsonic. And therefore such a wave, which moves with at least sonic velocity, must catch up with it.

DR. VON ELBE: With respect to those criss-cross patterns in Bone and Fraser's photographs of spinning detonations, it seems to me that we must consider a mechanism of accelerating and decelerating wave propagation much as you have proposed, except that the frequency is higher than in the example described by you and that the zone of periodic change of reaction rate is at a much smaller distance from the shock front, perhaps a few centimeters

#### KISTIAKOWSKY

only. The spinning detonation seems to be a transition stage between ordinary steady-state detonation and the extreme case of discontinuous ignition that you have discussed. If I remember correctly, Bone and Fraser found spinning detonation in stoichiometric mixtures of carbon monoxide and oxygen to which a very small percentage of water vapor was added as a catalyst. When the water-vapor content was increased above some limit, the spin was eliminated.

Spinning detonation seems always to be observed when a mixture is weakened. It has been stated by Lafitte and his co-workers that spinning detonation or discontinuous progress is observed in any mixture when one approaches the limits of detonability.

DR. KISTIAKOWSKY: I might say that we have found, if not full periodicity, at least an irregular propagation of detonations in all such mixtures.

DR. HORNIG: Von Neumann points out that, with exponential reaction rates, it doesn't much matter whether you call it an initiation or let the reaction start immediately. But the rate of reaction after a finite period increases because of the exponential reaction rate with temperature behind the front as the reaction proceeds and heats up the gases, first slowly, and then very rapidly. And I think that's basically a correct point.

I'd like to comment, if I may, that I think that the Russians also have some data that bears on this question of the wall effect. I think it was also Zeldovich and the people associated with him who observed that, in cases of underinitiated gas mixtures where they got auto ignition after a period of travel, the auto ignition was very much speeded up by having rough-walled tubes as opposed to smooth-walled tubes. I think that ties in very well with what Professor Kistiakowsky has said.

DR. LEWIS: I have been looking over some old photographs that I took in 1930 in which an induction period is shown very clearly. These were Schlieren photographs. I wish to emphasize that one should not study detonation only with piezoelectric or other gages, because important phenomena may be missed. These photographs of gaseous detonation show clearly a separation in time between the shock front and a wave in which heat is involved, i.e., the combustion wave, of about  $10^{-5}$  second. This time represents a distance separation of the order of a centimeter.

DR. KAUFMAN: I just want to ask this question: We've heard a lot about the combustion wave. Now, I'm not sure - are there really two mechanisms possible for the propagation of this wave? In the Zeldovich-Von Neumann picture you have first a shock wave, which heats the gas to a temperature at which the induction period for reaction is very short—perhaps long enough to give the effect known as spin—but at any rate very short. The energy released by the reacting gases then supports the shock wave. Now, is it possible to reach the same sort of picture with a combustion wave in the ordinary sense? I think you can prove quite simply that gradients which lead to diffusion and heat flow are totally insufficient to make the phenomenon stationary at the extremely high velocities that are actually observed. Therefore, diffusion and heat flow which present a sound mechanism for slow burning are not enough to explain detonation. I'm just wondering whether anyone has any suggestions. I can only see how a gas is heated rapidly to a temperature at which it's beginning to react, perhaps, with a short delay, but a combustion zone in the sense of the lower end of the Hugoniot curve I cannot picture at all because I don't see its mechanism.

DR. VON ELBE: I don't think that these gradients are necessarily small. It is conceivable that reaction goes to completion in a zone of only a few mean free paths width. In such a zone diffusion and heat conduction would not be negligible. The concept is that the gas passes through the shock front without undergoing rapid reaction until it reaches a zone within which reaction goes to completion in a few molecular collisions. In a sense, such a zone constitutes a combustion wave behind the shock front.

DR. KAUFMAN: Isn't the width, first of all, actually wider than the normal width of a flame—and also, isn't the shock temperature quite high?

DR. VON ELBE: No, the width of the zone that I have in mind is only of the order of a few mean free paths. The total width of the detonation wave is much larger and usually considerably in excess of the normal width of a flame. What is meant—and this is at present only an idea, not a proven fact-is this: A gas element crossing the shock front indeed attains a very high temperature and pressure, but this by itself is insufficient to initiate the rapid chemical reaction demanded by the detonation process. When neutral molecules such as  $\hbox{CO}$  and  $\hbox{O}_2$ collide, nothing much happens even at those temperatures. The additional requirement is a high concentration of atoms and free radicals which act as chain carriers. When this concentration attains the order of the other molecular concentrations, the molecules of reactants, CO and O2, have a chance to react in a few molecular collisions. Let us now suppose that the reaction itself produces such high chain-carrier concentrations after an induction period which starts from the moment at which a gas element crosses the shock front. In that case the element travels for some distance in a state of high temperature and pressure with little chemical change; then suddenly the reaction goes to completion over a distance of only a few mean free paths. The resulting gradients of temperature and chain-carrier concentrations are such that heat conduction and chain-carrier diffusion are no longer negligible, and thus a zone of chemical reaction is formed whose propagation is controlled by heat conduction and diffusion in the manner of a combustion wave. This zone is unstable with respect to fluctuations of mass flow over the tube cross section; it must continuously tilt and wander. As it is coupled to the shock front by the fact that it furnishes the piston energy for maintaining the shock wave and is in turn dependent on the preheating and precompression occurring in the shock front, all manners of phase relations and periodic changes are imaginable. I think there is some evidence for such combustion waves in the photographs of Bone and Fraser.

DR. KISTIAKOWSKY: I agree with Dr. Von Elbe and also with Dr. Kaufman—that what is known as a spin is probably just a shock wave created behind the lagging combustion zone, the details of which I don't understand.

Now, more in detail to your remarks, Dr. Lewis. As little as I understand of hydrodynamics, I think the pressure gradient across the chemical reaction zone is defined completely by hydrodynamic considerations—the increase in volume, the heat released by the reaction, and the speed with which the reaction zone moves through the medium.

Now, as I see it, for instance, this pressure gradient across the chemical reaction zone, being caused by the considerations of propagation velocity and the nature of the reaction, is determined by the same laws in the reaction zone which exist behind the shock and what might be called the true deflagration of the flame.

There is one fundamental difference in my own thinking between the two phenomena. A normal deflagration is propagated by transport mechanisms—be it transport of chain carriers or transport of heat—but so long as you have these phenomena controlling propagation there is a certain finite velocity beyond which it can't accelerate—the limiting flame velocity. In distinction to that is a detonation, where the propagation of the reaction zone does not depend any more on the transport phenomena because a fresh reaction—if I may use such a crude expression—is generated in unreacted gas by an adiabatic compression of the shock so that the propagation mechanisms are different.

But I think the hydrodynamic laws of the zone itself are the same, whichever way it is propagated. But of course, actually, for instance, say in the Chapman-Jouguet detonation wave, the pressure drop across the reaction zone is very, very much higher than it is in a normal flame going through, say, hydrogen-oxygen. In a normal flame it moves with the velocity of maybe a hundred or two hundred centimeters, as against a thousand meters or so in this enforced propagation of a detonation. And that permits, incidentally, a perfectly logical definition of the instant initiation of detonation by deflagrations. And that is the one

#### KISTIAKOWSKY

where the mechanism of propagation of a deflagration changes from a transport mechanism to an adiabatic heating by the shock wave.

- DR. LEWIS: In the deflagration wave or combustion wave that trails the shock wave the same mechanism obtains as in ordinary combustion waves except that the entire reaction occurs in a very much shorter time, because the gas leaving the shock wave is prepared.
- DR. KISTIAKOWSKY: I don't know that it isn't essential. In our initiation experiments, when a shock enters an explosive mixture from air, the detonation picks up right at the boundary and just goes on, and there's no preparation by the chain carrier.
- DR. KIRKWOOD: In connection with the relationship between the Hugoniot curve and burning, I'd like to ask if any one believes any more that burning has anything to do with this lower part of the Hugoniot curve. That is, you don't have shock.

The facts are pretty clear that you must have reignition in order to have this pulsating phenomena, and I wanted to ask both Dr. Kistiakowsky and Dr. Lewis whether you had any detailed ideas of how this reignition works.

- DR. LEWIS: This is explained in my introductory remarks, and it concerns an induction period for ignition of the gases passing through the shock front coupled with the phenomenon of flame tilt.
- DR. KISTIAKOWSKY: A chemically controlled induction period? Then it won't work, because it would depend on tube diameter.
- DR. LEWIS: Yes, it does depend on the tube diameter. The frequency in the spin phenomenon is a function of tube diameter.
- MR. STRESSAU: The question I had was, when you get this effect—whether it's rotating or pulsating or what-not—in the large tubes, is it obtained under the same conditions of pressure and mixture, and so forth, as it's obtained in the small tube? Or is the critical point that divides the detonable mixture different in the small tube from what it is in the large tube?
  - DR. LEWIS: I don't think we know, do we?

# DURATION OF THE REACTION IN A DETONATING EXPLOSIVE

# S. J. Jacobs Naval Ordnance Laboratory

## INTRODUCTION

The Hydrodynamic Theory of Detonation, with its concept that the detonation is a shock followed by a deflagration, has attained to a rather satisfactory stage of development and acceptance. In this theory the idea of a finite reaction time is present, but hydrodynamics and thermodynamics alone shed no light on the kinetics of the reaction even to the limited extent of establishing its duration. To gain knowledge about the reactions duration, one must consider explosives finite in one or more dimensions. Only in this way does one obtain observable parameters concerning the duration. This is true both in experiment and in the accompanying theory. As a consequence we have the observation that detonation velocity is a function of charge diameter, and we have H. Jones' and H. Eyring's theories to explain this dependence in terms of a finite reaction zone. Similarly we have the experimental observations and theories of failure diameter and of over-and-under-boostering. More recently we have acquired further knowledge of the reaction zone in the experiments suggested by R. Goranson on the impact of detonations on metal plates. This is to be described by Dr. Ablard.

All of these experiments and theories relate an observable effect in bounded explosives to the presence of a finite reaction zone. In spite of the fact that a fairly large number of papers dealing with this subject have been written, there seems to be a feeling of dissatisfaction among the workers in the field concerning the significance and validity of the conclusions drawn in these papers. I think the trouble lies in our having insufficient understanding of the basic facts concerning the deviation from plane wave theory encountered when one begins to think of detonations which are finite in time and space. As a consequence the conclusions drawn by one author frequently contradict those of others and are even self-contradictory. As a result this phase of detonation theory is due for a thorough review. It is encouraging to find that some of the ideas of supersonic flow, shock waves, and rarefaction waves are catching on so that this mathematical field of hydrodynamics is being used, as it should, as a tool in the solution of problems of finite explosions.

# STEADY DETONATION IN TWO-DIMENSIONAL FLOW

I should like, now, to make a few remarks concerning the steady detonation conditions met in homogeneous explosives in two-dimensional flow, one dimension being the direction of propagation the other being thickness or radius. These can be termed slab and cylindrical symmetry respectively. I should like to consider the case when the explosive is bounded by an infinite low-density medium, for example air. These are the conditions under which most detonation velocity measurements are made. A profile of the detonation wave as I see it is shown in Figure 1. In this conception, which contains the combined and sifted ideas of many workers, the shock front is considered to be curved. The shock in the bounding medium is closely followed by the discontinuity between shocked medium and explosion products. The condition of reaction controlling the shock propagation in the explosive is drawn as the line designated as the general C-J surface. (The general C-J surface is here defined as that locus of points in the reaction back of the shock at which the outflow velocity is equal to the local sound speed.) The locus of complete reaction is drawn as the curve n = 1. As long as the shock front is curved, stream lines back of the shock can have radial component directly behind the shock. Several generalities can be stated concerning detonations in this configuration:

**JACOBS** 

Point 1. The front is generally non-planar. At the boundary of the explosive, the pressure in the explosive shock is determined by the pressure in the surrounding medium. For air this pressure will be of the order of magnitude of 500 atmospheres, corresponding to an air shock velocity of about 7000 meters per second. Because of the low pressure, the explosive shock will be very weak and only slightly supersonic. The front will therefore be inclined at an angle whose sin is  $C_0/D$ . The quantity  $C_0$  is the sound speed in the intact explosive. In this way curvature is accounted for at the edge. In general, curvature to the center will exist so long as the detonation is at a velocity

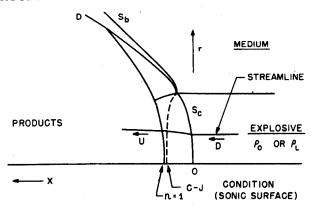


Figure 1 - Detonation in a bounded explosive

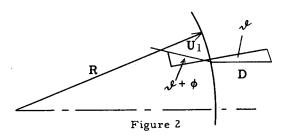
below that for infinite media. The reason for this is that rarefaction eating into the reaction must exist if the detonation is slowed. The only alternate to sidewise rarefaction is axial rarefaction to the rear. This is unlikely to exist alone in the presence of a low-density medium at the sides. If the stream lines diverge at the front corresponding to sidewise rarefaction, the front must be nonplanar. Near the charge axis the curvature will depend on the relative magnitude of the distance to the sonic surface compared to the distance at which rarefaction from the edge reaches the axis. I think it is possible to demonstrate that the ratio of these distances will always be less than one: On the other hand the condition of complete reaction is restricted only to being at or behind the sonic surface.

Point 2. The reaction zone length is not constant throughout. The very low pressure existing at the charge boundary with its accompanying weak shock in the explosive should mean that initiation temperature near the boundary is much lower than at the center. This, coupled with the lower pressure, should be reason enough to establish the existence of a lower reaction rate relative to the center and probably so low in many explosives that part of the explosive near the boundary may not react at all. In addition, the reaction temperature and products near the boundary will be quite different from those at the center. For this reason we might parenthetically remark it would appear undesirable to attempt to measure detonation temperatures in charges bounded by low-density media.

Point 3. <u>Curvature at the axis plus the extent of the completion of the reaction at the sonic surface determine the detonation velocity</u>. The outflow divergence of the stream lines will be determined by the curvature at the front plus the shock conditions met at the front. The latter are a function of the propagation velocity. Curvature alone cannot determine the propagation velocity since for weak shocks corresponding to low-rate detonations the curvature should be less than for some detonations propagating at higher velocity. This is due to the fact that the velocity can never be less than sound speed in the explosive. Low-rate detonations have less velocity difference between center and edge than do high-rate detonations. For very large radius of charge, most of the curvature will exist at the edge. As radius is reduced, curvature will move in to the axis and pass a maximum at the axis. If propagation continues, then reduction of radius will tend to reduced curvature as a result of the sonic limit.

# THE RELATION OF DETONATION VELOCITY TO CURVATURE AND REACTION

In conclusion I should like to present a simple analysis of the conditions near the axis of a charge. If we consider the front as having constant curvature near the axis, we can obtain simply the initial stream lines in this region. Referring to Figure 2., at the shock



front we must conserve the tangential component of the flow through the jump so that

$$U, \sin (\mathcal{J} + \phi) \quad D \sin \mathcal{J}, \tag{1}$$

where  $\mathcal{L}$  and  $\mathcal{L} + \phi$  are the angles of the stream lines relative to the normal.

Therefore

$$\phi = \arcsin \left[ \frac{D}{U_1} \sin \mathcal{A} \right] - \mathcal{A}, \qquad (2)$$

and for small

$$\phi = \mathcal{L}\left(\frac{D}{U_1} - 1\right). \tag{3}$$

But  $\mathcal{I}$  is given by  $\frac{\mathbf{r}}{R}$  so that

$$\phi = \frac{\mathbf{r}}{\mathbf{R}} \left( \frac{\mathbf{D}}{\mathbf{U}_1} - 1 \right). \tag{4}$$

The radial component of flow velocity acquired in the shock is then given by

$$\mathbf{U}_{\mathbf{r}} = \mathbf{U}_{1} \sin \frac{\mathbf{r}}{\mathbf{R}} \left( \frac{\mathbf{D}}{\mathbf{U}_{1}} - 1 \right). \tag{5}$$

If we consider this radial component to be conserved in passing through the reaction zone, then

$$\Delta \mathbf{r}(t) = U_1 \left[ \sin \frac{\mathbf{r}}{\mathbf{R}} \left( \frac{\mathbf{D}}{\mathbf{U}_1} - 1 \right) \right] \mathbf{t},$$
 (6)

which for small angle eis

$$\Delta \mathbf{r}(t) = \frac{\mathbf{r}}{\mathbf{R}} \left( \mathbf{D} - \mathbf{U}_1 \right) \mathbf{t}$$
 (7)

If we define

$$\alpha = \frac{A(t)}{A_1}$$
 ,  $A = area$  (8)

we obtain for

$$\alpha = \left(\frac{\mathbf{r} + \Delta \mathbf{r}}{\mathbf{r}}\right)^{2}$$

$$\alpha = \left[1 + \frac{\mathbf{D} - \mathbf{U}_{1}}{\mathbf{R}} t\right]^{2}$$
(9)

This therefore gives a pretty good approximation to the axial stream tube expansion in terms of the stream velocity immediately behind the shock and the radius of curvature of the shock front. We can now consider a perturbation on the plane detonation conditions in which mass and axial component of momentum are conserved in the stream expansion.

The initial equations become

$$D\rho_0 = \alpha U_{\mathbf{X}} \rho_2 \tag{10}$$

$$\alpha p_2 - p_0 = D^2 \rho_0 - U_X^2 \alpha \rho_2$$
 (11)

$$\mathbf{E}_{2} - \mathbf{E}_{1} = \frac{\mathbf{p}_{2}}{\boldsymbol{\rho}_{2}} - \frac{\mathbf{p}_{0}}{\boldsymbol{\rho}_{0}} + \frac{1}{2} \left( \mathbf{D}^{2} - \mathbf{U}^{2} \right)$$
 (12)

These can be reduced to yield the following set of equations when  $U_X$  is assumed to equal U:

$$p_2 - \frac{p_0}{\alpha} = \frac{D (D - U)}{\alpha V_0}$$
 (13)

$$\mathbf{p}^2 = (\alpha \mathbf{V}_0)^2 \frac{\mathbf{p}_2 - \frac{\mathbf{p}_0}{\alpha}}{\alpha \mathbf{V}_0 - \mathbf{V}_2}$$
 (14)

$$\mathbf{E}_{2} - \mathbf{E}_{1} = \frac{1}{2} \left( \mathbf{p}_{2} + \frac{\mathbf{p}_{0}}{\alpha} \right) \left( \alpha \mathbf{V}_{0} - \mathbf{V}_{2} \right)$$
 (15)

where  $V = \frac{1}{\rho}$ .

These equations are identical to the equations for plane detonations, with the exception that the initial conditions are transformed to a new volume and pressure:

$$V_0^* = V_0 \alpha \text{ and } P_0^* = \frac{P_0}{\alpha}$$
.

Since  $P_0$  is negligible for detonation of solid explosive, the value of  $\alpha$  can be determined from the detonation velocity <u>provided we assume the C-J condition applies at the point of complete reaction</u>. Under these circumstances the velocity of propagation of the finite charge is given by the velocity of an infinite charge of lower loading density. The equivalent loading density  $V_0$ \* immediately defines  $\alpha$ . The equations can be equally well applied to slab symmetry by redefining  $\alpha$  in terms of r. This changes the exponent of equation 9 to 1 instead of 2. The combination of detonation-velocity data with wave-front curvature therefore offers a method of determining the reaction time at the charge axis. If the sonic surface does not coincide with the end of reaction, more data will be needed to obtain the time to the sonic surface. For such cases, however, the propagation will be determined by the condition of tangency of the detonation velocity line (Equation 14) as defined above to a partial reaction Hugoniot which we can define in terms similar to that of Equation 15 as:

$$\left(\mathbf{E}_{2}\right)_{\mathbf{n}} - \mathbf{E}_{1} = \frac{1}{2} \left(\mathbf{p}_{2} + \frac{\mathbf{p}_{0}}{\alpha_{\mathbf{n}}}\right) \left(\alpha_{\mathbf{n}} \ \mathbf{V}_{0} - \mathbf{V}_{2}\right) \tag{16}$$

Of course  $\alpha_n$  is understood to apply to Equation 14 as well. In the limit of very low propagation velocity, such as in the low rate of detonation of nitroglycerine,  $\alpha_n$  will approach unity in agreement with statements which I made before. This viewpoint therefore includes an explanation, in principle, of the low rate of detonation frequently encountered for explosives.

It might be pointed out here that the Eyring point of view on the stream expansion considers the particles as moving radially toward the curved front. It is easy to demonstrate that this viewpoint imposes a slightly different assumption than mine on the stream lines. His point of view gives  $\mathbf{U_r}$  decreasing with time as  $\mathbf{U_r}$  is defined as proportional to (D-U) throughout the reaction zone.

When one inserts reasonable values for U(t), the effect on (t) for the completed reaction turns out to be about 50 percent of that obtained if  $U_r$  is considered constant. The correct solution probably lies somewhere between the limits set by these alternate assumptions. It should be pointed out that both assumptions show the off-axis stream lines as curving toward lines parallel to the axis.

#### DISCUSSION

- DR. ROTH: Do you know what (t) is, roughly I mean, from whatever data you have?
- DR. JACOBS: We made one comparison on hydrazine mononitrate. We had already calculated the reaction time for particular charges of hydrazine mononitrate on the basis of the Eyring theory and on the basis of the Jones theory and have come up with answers of the order of magnitude of two microseconds. This results in similar answers. Namely, the theory is not different in magnitude but I think only makes it a little bit clearer as to what you're looking at.
- DR. VON ELBE: This is somewhat off the point, but speaking about the curved detonation wave when it comes to the end of the charge a jet is emitted, which I think shows up in numerous photographs, at the end of the explosive cartridge. And the front of the jet is extremely luminous. I just wondered—do you think that since the expansion occurs against a very low pressure so that there is little loss of internal energy, would it pay, perhaps, to make temperature measurements of this first gas, which shows up very well in photographs, and seek a relation between this temperature and the temperature in the detonation wave?
- DR. JACOBS: Actually, this is aside from the subject, but I'd like to make a comment anyway. When you consider detonation reaching an end boundary, the detonation ceases as an entity and is replaced by a rarefaction wave running away from the boundary, a shock wave is sent out into the surrounding media, if there is a surrounding media, and a rarefaction wave eats into the explosion. Now if it takes a certain amount of time for the reaction to be completed, then a rarefaction wave begins to eat into it before the reaction has even started, and there is a great likelihood that one will have disturbed the reaction so much that it no longer will conform to the plane conditions that one associates with the detonation wave; and therefore any temperatures you measure will be associated with another phenomena and should not be interpreted as detonation phenomena.
  - DR. KIRKWOOD: To what order of 1/R are these approximations on Hugoniot?
- DR. JACOBS: The only approximations on Hugoniot, as far as I can see, is that, when you conserve momentum and you have a  $U_{\mathbf{X}}$  and a vector U, I have substituted the vector U for the vector  $U_{\mathbf{X}}$ . Therefore, if the angle is small, I think the order of difference is going to be quite small.
- DR. STERNE: A question for my own information. I think you can adduce reasons—I don't know whether it's been done before or not—for part of the stability of a detonation. I'm thinking back to the previous talk of the oscillations. If for any reason the detonation process occurs at too high a rate, I think one can argue with considerable mathematical support that a rarefaction is going to eat away the detonation wave, reduce pressures, and get down to the Chapman-Hugoniot velocity. On the other hand, suppose the reaction velocity is less than Chapman-Hugoniot. What is the tendency that tends to bring the velocity up to the Chapman-Hugoniot? Can anyone answer that?
  - DR. KIRKWOOD: Dr. Brinkley and I have published a theory.
  - DR. STERNE: I think I remember the theory, but I don't know all the details of it.
- DR. KIRKWOOD: It shows that if you've overdriven it, the pressure decreases towards the Chapman-Jouguet point. If you are underneath, you rise to it.

# EXPERIMENTS ON THE TRANSITION FROM DEFLAGRATION TO DETONATION

# J. Roth

Hercules Experiment Station, Hercules Powder Company,
Wilmington, Delaware

## INTRODUCTION

It is well known that, given the right conditions, many burning explosives will detonate. This transition from burning to detonation offers features of considerable practical and theoretical interest. In the handling and disposal of explosive materials, one often encounters fires. From safety considerations it is important to know when such fires can turn into explosions. On the other hand, one must know the conditions under which a properly initiated explosive will detonate, particularly in the case of primary explosives. Turning now to theoretical implications, it can be said that any complete description of detonation phenomena must account for these transitions. Conversely, the experimental study of the transition of burning to detonation provides a test for existing theories of the initiation of detonation. Our paper deals largely with this latter aspect.

Since we shall have occasion to refer to it, we would like to present here a brief outline of the theory of initiation championed by Prof. Kistiakowsky (1):

- 1. The flame from a burning explosive penetrates into the interior of the explosive mass, setting up pressure gradients due to the resistance to gas flow in the interstices between particles.
- 2. The rising pressure increases the deflagration rate. This further increases the rate of gas-volume production, which further increases the pressure, etc.
- 3. Gas flow from the center of deflagration, during the rising violence of burning, is accompanied by constantly rising backing pressure and temperature, which causes formation of shock waves.
- 4. Shock waves with their discontinuous rise in temperature and pressure greatly enhance the deflagration. The latter in turn reinforces the shocks. Eventually, all the grains of the explosive are consumed in one passage of the shock wave, and, therefore, the entire energy of the explosive can be utilized for the propagation of this wave. This is detonation.

When our work was begun, Dr. Cairns and Dr. Lawrence of Hercules Powder Company had already shown(2) that diazodinitrophenol, when initiated by a hot wire, shows a period of deflagration prior to detonation. Also, Prof. Bowden (3,4), of Cambridge, had published photographs showing that nitroglycerin and mercuric fulminate, initiated by impact, show similar predetonation deflagrations. We have extended these studies by obtaining rotating-drum photographs of primary and secondary explosives and smokeless powder under varying conditions of initiation, confinement, and packing density.

## RESULTS AND DISCUSSION

## **Primary Explosives**

Mercuric Fulminate. - Of the primary explosives considered, mercuric fulminate best lends itself to our type of study. The transition from burning to detonation can be relatively slow, and the processes involved are sufficiently luminous to be recorded without difficulty. We found that confinement is the most important single factor in determining if the deflagration will change over into detonation. These trials were all made with the powder loosely packed in cellulose acetate tubes and initiated by a bridge wire imbedded in the explosive. Confinement was varied by altering the number of wraps of cellulose acetate used in making up the tubes.



Figure 1 - Mercuric fulminate—10-ply, 0.68-cm i.d. cellulose acetate foil tube; density 1.49 g/cc, aperture F:2.8

Figure 1 shows the transition for mercuric fulminate in a 10-ply cellulose acetate foil tube. The little luminous dot at "A" is probably due to the explosion of a few grains of powder adhering to the bridge wire, since the bridge wire fused by the discharge of a ten-cap machine will not register on film. Between "A" and "B" is a nonluminous zone lasting for about 300 microseconds. Deflagration starts at "B" and proceeds uniformly at a rather low rate up to point "C." Here an accelerating deflagration becomes visible. For the most part this deflagration moves at around 300 to 400 m/sec, but just prior to detonation at "D" it accelerates to 1100 m/sec. Detonation proceeds both upwards and downwards, indicating that it started in the interior of the powder column. There is appreciable afterburning. The total predetonation period lasts 8.5 milliseconds.

Figure 2 shows much the same sort of traces as Figure 1, except that all primary processes are much shorter, and the deflagration just prior to detonation proceeds at 1500 m/sec. The predetonation period lasts for 0.2 millisec. If the confinement is increased even further, say with a glass tube, the preliminary processes can no longer be resolved.

Figure 3 is typical of the record obtained if there is just barely insufficient confinement to obtain detonation. Up to "C" the traces are similar to those in Figures 1 and 2. At "C" accelerating deflagrations of short duration are discernible. Considerable luminosity is observed at "D." Possibly this is caused by shock waves, formed by the deflagration, striking the stopper at the top of the tube. Again there is vigorous afterburning.

To summarize, we have observed nonsteady accelerating deflagrations and start of detonation in the interior. It is also possible that we have seen the manifestation of shock waves and their reflection in instances where no detonation regime existed.

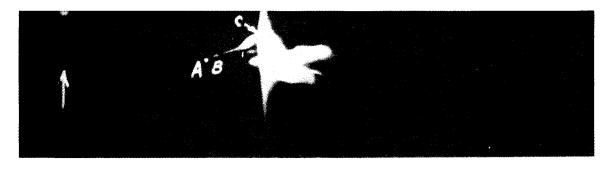


Figure 2 - Mercuric fulminate-12 ply, 068-cm i.d. cellulose acetate foil tube; density 1.54 g/cc, aperture F: 2.5



Figure 3 - Mercuric fulminate--5 ply, 0.68-cm i.d. cellulose acetate foil tube; density 1.52 g/cc, aperture F:3.5

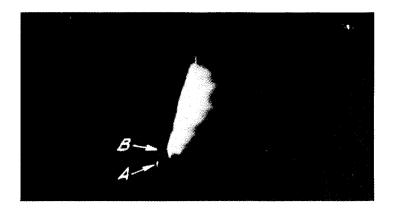


Figure 4 - Diazodinitrophenol—2 ply, 0.46-cm i.d. cellulose acetate tube; density 0.61 g/cc, aperture F:2.5

<u>Diazodinitrophenol</u>. - We were unable to obtain very significant photographs for the transition of burning to detonation for diazodinitrophenol because of the rapidity with which this takes place. However, Figure 4 shows an accelerating deflagration which rapidly turns into detonation.

Lead Styphnate. - Lead styphnate, the next explosive studied, is peculiar in that we were unable to obtain any detonation traces when initiation was by hot bridge wire. In every case, however, the container was completely destroyed. The luminosity was too weak to show up in an illustration. However, the luminous track occurs above the powder column. From the horizontal separation of the bridge wire and the start of the luminous track, we would judge that the process, whatever it is, occurs at an average rate of only several hundred meters per second. This would account for its lack of luminosity as well as for the well-known lack of brisance of lead styphnate. In agreement with this, Bowden(5) states that styphnate initiated by impact does not propagate at a rate greater than 700 m/sec. However, we found that styphnate, at a density of 1.56 g/cc, primed with 0.03 g of lead azide, detonated at 2,000 m/sec in a 5-mm i.d. glass tube. Also, when initiated with a spark from a condenser discharge (0.2 microfarad at 800 v), it detonated at 2,600 m/sec in a 7-mm i.d. tube at a density of 1.48 g/cc.

<u>Lead Azide</u>. - Even under the lightest confinement, lead azide detonates immediately upon contact with a hot bridge wire. We have been informed by Bowden(6) that, even with his new image-converter camera of great writing speed and tremendous light-gathering power, he has been unable to observe any deflagration prior to detonation for lead azide.

# Secondary Explosives

We know from previous experience (7) that PETN can be detonated by a high-energy condenser discharge. Since PETN does not burn readily unless it is subjected to moderately high pressures (8), we decided to investigate its transition from deflagration to detonation by obtaining photographs in glass tubes, with initiation provided by the discharge, through a bridge

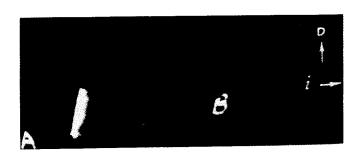


Figure 5 - PETN-7-mm i.d. cellulose acetate foil tube; column height 13.5 cm, density 0.88 g/cc, initiated by condenser discharge 1 microfarad at 10,000 v

wire, of a 1-microfarad condenser. An example is shown in Figure 5. The deflagration is very short lived but quite apparent. The energy threshold for initiation is around 15 joules. At such high initiation energy, confinement and packing density (from 0.8 g/cc to 1.1 g/cc) have no apparent effect on the incidence of detonation.

Several trials with RDX failed to disclose anything but a deflagration trace with discharge energies of up to 50 joules. Bowden(5) was also unable to produce detonation in RDX and tetryl by condenser discharge.

### Smokeless Powder

With E. C. Blank Fire, an uncolloided single-base smokeless powder of great surface area, we obtained our most interesting photographs. Figure 6 shows a matchhead-initiated detonation. This photograph merits some detailed discussion. Deflagration is first visible at "A." Actually there is good evidence that nonluminous processes, if any, are of very short duration, since the vertical height AF corresponds very closely to the powder-column height. Deflagration proceeds at a rate of about 150 m/sec along the outer surface. Because of higher pressures, it is to be expected that in the interior deflagration moves up the powder column at a faster rate. This faster deflagration breaks out to the surface at "B." From Table 1 it is

#### ROTH

apparent that the separation BC decreases with increasing packing density. This is in accord with expectations, since for compressed powders the deflagration encounters more resistance in penetrating into the interior and is forced back to the surface. BD shows a more rapid deflagration - of the order of 300 m/sec. Beyond Dthe deflagration begins to accelerate rapidly. At E it is moving at 900 m/sec, and just beyond E it goes over into a stable detonation. The trace EG indicates that the detonation started below the surface of the powder. For the sake of convenience, we have classified these processes as: initial burning (AB), accelerated deflagration (BD), low-order detonation (DE), and detonation (EF).

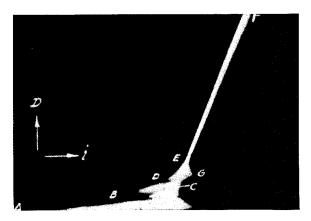


Figure 6 - Uncolloided single-base smokeless powder-8-mm i.d., 2.5-mm thick lucite tube; column height 53.2 cm, density 0.53 g/cc, matchhead initiated

TABLE 1
Time Interval Between First Observable Burning and Breaking Out of Flame from the Interior of the Powder

Density (g/cc)	Initiated by	Time (Milliseconds)					
0.82	M.H.*	0.05					
0.66	M.H.*	0.12					
0.56	M.H.*	0.17					
0.53	M.H.*	0.18					
0.52	M.H.*	0.35					
0.51	M.H.*	0.37					
0.54	M.H.*	0.57					
0.52	C.D.**	- 0.57					
0.46	C.D.**	0.62					

<sup>\*</sup>Matchhead.

Detonations initiated by an exploding bridge wire from a condenser discharge are very similar in nature to matchhead initiations, as shown in Figure 7. The only apparent difference appears to lie in the initial deflagration rate, which is slower for the condenser discharge. This is not unexpected, since the greater area of the fiame front and the higher initial pressure of the matchhead should outweigh the effect of the higher localized temperature of the exploded bridge wire. The energy threshold for detonation is about 10 joules.

The next two illustrations (Figures 8 and 9) show instances where deflagration fails to develop into detonation. The initial phases here are identical with those observed above.

<sup>\*\*</sup>Bridge wire exploded by condenser discharge.

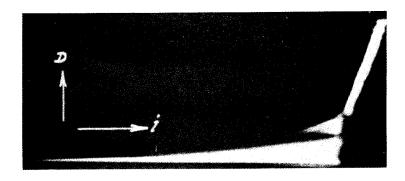


Figure 7 - Uncolloided single-base smokeless powder—density 0.54 g/cc, column height 25.6 cm, initiated by condenser discharge of 1 microfarad at 5000 v

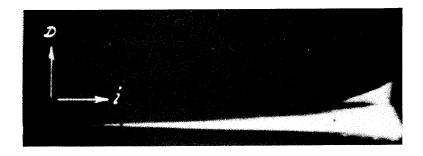


Figure 8 - Uncolloided single-base smokeless powder-density 0.55 g/cc, column height 25.5 cm, initiated by condenser discharge of 1 microfarad at 3800 v



Figure 9 - Uncolloided single-base smokeless powder-density 0.72 g/cc, column height 25.0 cm, initiated by matchhead

TABLE 2

Rates of Various Processes in the Birth of Detonation in Single-Base Uncolloided Smokeless Powder\*

Delay from Initiation to Detonation (M.S.)	0.45	0.45	1	0.31	0.44	0.33	0.40	ı	0.52	1	•	1	ı	69.0	0.63
Detonation (m/sec)	2290	2360	Failed	2430	2380	2520	2770	Failed	2930	Failed	Failed	Failed	2520	2360	2630
Low-Order Detonation (m/sec)	880	920	ı	780	029	1010	880	810(?)	029	490	330	380	099	810	200
Time of Accelerated Deflagration (M.S.)	0.05	90.0	90.0	90.0	0.07	0.08	90.0	0.05	0.08	ı	0.07	1.3	0.07	90.0	80.0
Accelerated Deflagration (m/sec)	360	ca. 300	350	290	305	350	320	270	340	214(?)	300	220	370	360	1.
Initial Burning (m/sec)	100	140	130	1	104	95	100	100	1	78	47	80	52	23	09
Initiated by	M.H.	M.H.	M.H.	M.H.	M.H.	M.H.	M.H.	M.H.	M.H.	2800 v	3800 v	4000 v	4400 v	2000 v	10000 v
Density (g/cc)	0.51	0.53	0.54	0.56	0.56	99.0	0.71	0.72	0.82	0.46	0.55	0.42	0.54	0.52	0.54

\*In 8-mm i.d. tubes.

### CHEMICAL ASPECTS

Table 2 summarizes our observations. As already stated, initial burning rates are generally slower for "condenser-discharge" initiation. They appear to be independent of packing density. The "accelerated deflagration" rate, as well as its duration, appear to be independent of packing density and mode of initiation. For both of these regions, there is no distinction between failures and detonations. It is only in the next region, that of "low-order detonation," that any distinctions become apparent. If stable detonation is to result, the "low-order detonation" must apparently proceed at a rate of over 670 m/sec.

The difference in total delay from start to detonation between matchhead and "condenser-discharge" initiation is due to longer initial burning in the latter case. The observations of nonsteady accelerating deflagration, which goes over into detonation in a continuous manner, are, again, in excellent qualitative accord with Prof. Kistiakowsky's proposals.

### Shock-Wave Initiation

We have made some exploratory experiments on the shock-wave initiation of E. C. Blank Fire. Shock waves of varying velocity were obtained from a piece of Primacord fuse placed at various heights above the powder surface. It is found that, in the packing-density range of 0.4 to 0.5 g/cc, the shock velocity threshold for initiation is around 4,200 m/sec under our experimental conditions. At higher densities no initiation could be obtained even with shock velocities of 6,200 m/sec. In Figure 10 we show a typical rotating-drum photograph. The

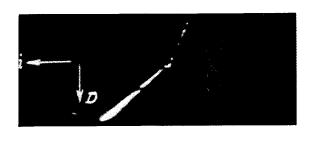


Figure 10 - Uncolloided shock-wave initiation of a single-base smokeless powder-40 cm, column of powder in 10-mm i.d. glass tube of 2-mm thickness, density 0.43 g/cc, spacing 2.5 cm

detonation track of the Primacord is observed at the top. The shock wave is a short, highly luminous portion, which may be detected immediately below the Primacord detonation. The horizontal trace of very high luminosity is due to the collision of the shock wave with the powder surface. To the left of this is a trace of much lesser brightness, which probably corresponds to the initial deflagration. Just below is a weak trace of an accelerating deflagration, and, finally, the detonation of the smokeless powder. This is, of course, quite analogous to the transitions shown previously.

The delay between the impact of the shock wave and inception of detonation of the smokeless powder varies with shock velocity.

Presumably, the high temperature of the powder surface, due to the impact of the shock wave, is a function of the shock velocity. If this temperature can be estimated and related to the observed delay, some very interesting conclusions about the kinetics of the processes leading up to detonation would be possible.

In conclusion, we would like to draw attention to the great similarity of transitions from deflagration to detonation under conditions of weak and strong initiation. Confinement appears to be the most important single factor which determines whether a deflagration shall die out or turn into detonation. In general, with the exception of lead azide and possibly lead styphnate,

### ROTH

our observations of accelerating deflagration which changes into detonation in a continuous manner are in excellent qualitative accord with the theory of initiation presented by Prof. Kistiakowsky.\*

### REFERENCES

- 1. Kistiakowsky, "Initiation of Detonation of Explosives," presented 3rd Symposium on Combustion, Flame, and Explosion Phenomena, at Madison, Wisconsin
- 2. Lawrence, Hercules Powder Company, RI 2073, Progress Report, July 26, 1940
- 3. Bowden, Proc. Roy. Soc. 188A, 392 (1947)
- 4. Bowden, Nature 161, No. 4088, 348 (1948)
- 5. Bowden and Gurton, Proc. Roy. Soc. 350 (1949)
- 6. Bowden, private communication
- 7. Downard, Hercules Powder Company, RI 2082 (Final Formal), p. 16
- 8. Andreev, Doklady 51, No. 1, 29 (1946)

### DISCUSSION

Mr. STRESAU: An interesting experiment was run two years ago. We didn't make any measurements of velocity, but we had some fairly highly confined columns of various explosives which we initiated, and then we observed the deformation. With mercury fulminate it was very easy to observe the transition of deflagration to detonation. The hole would stay the same size until you got to a certain point, and suddenly it got bigger. But with lead styphnate the hole had a very nice taper from one end to the other over a couple of inches.

Some day we intend to make some velocity measurements on this sort of thing. Incidentally, as the density was increased, this taper got more pronounced up to a point beyond which it reduced again, so that there was an optimum density for maximum expansion at the end. The standard column length was an inch and a half. It is probable that with long enough columns the increase in maximum expansion with initial explosive density would continue up to the highest densities.

DR. ROTH: How large a hole did you get with styphnate? Was it considerably smaller than azide or fulminate?

<sup>\*</sup>Note: After the presentation of this paper, Dr. Brunauer made the observation that some of the predetonation burning traces shown appeared to proceed at a steady rate and transition to detonation occurred in a stepwise fashion, which does not fit in with the theory of initiation because of the requirement of nonsteady deflagration and a continuous transition. While it is true that the initial portions of Figures 1, 7, and 8 appear to proceed at a fairly steady rate to within the resolving power of our camera, once the deflagration begins to accelerate, a detailed examination of the originals of these and other photographs shows that deflagration changes into detonation in a continuous manner. The curve traced by the transition is closely represented by a hyperbola with a steep slope on the detonation side and quite a flat slope on the deflagration side. The steady initial portions of these and other records could correspond to burning on the surface, i.e., to burning which has not penetrated into the interior of the powder and, therefore, can remain relatively steady because pressure could increase slowly and in a steady fashion.

### CHEMICAL ASPECTS

Mr. STRESAU: Yes, it was always smaller.

DR. KISTIAKOWSKY: Didn't you also do some experiments with azide? Talk about them.

Mr. STRESAU: We are not sure of the mechanism involved. At high densities, about five or six percent voids or less, a reaction was observed quite different from normal detonation in its effect upon the container. The lower-density explosives, which are assumed to detonate normally, cause an apparent tension failure of the bore of the container. The failure is characterized by longitudinal cracks. Tension failure is to be expected, since the confining medium would be expected to have considerable outward momentum when the detonation wave has passed. The type of failure caused by the high-density explosives was quite different. It can best be described as looking as if it had been beaten out with a ball-peen hammer. As contrasted with the dull black coating left by the normal detonation, the bore had a high metallic luster. The color was white or grey, indicating deposits of lead and mercury on the brass container.

The propagation rate of the reaction which caused this latter type of deformation was measured and found to vary between 1,400 and 1,700 meters per second as compared with 5,000 meters per second for normal detonation of the same explosives loaded at a slightly lower density. It was suggested that the rate of propagations of this type of reaction might be related to the properties of the confining medium. No difference was detected between copper, steel, and aluminum in this respect.

This low-velocity reaction could be achieved only by using a fairly critically defined quantity of explosive. A slightly stronger initiator would cause detonation with a velocity in excess of 5,000 meters per second. A slightly weaker initiator would fail to initiate lead azide and would cause the mercury fulminate to burn at a rate of an inch per second or so. The burning was accompanied by the whistling of the escaping gases.

It was possible to detect the variations in loading density by the change in the note of the whistle. In fact, with care, one could count the increments.

In a similar set of experiments, it was found that, under some conditions, mercury fulminate could be made to burn for a certain distance and finally detonate. Audibly, this was characterized by a whistle followed by a report. In the sectioned containers, it was characterized by a length of hole in which no expansion was apparent, up to a point where a rather sudden change occurred, like a thistle tube. The length of the unexpanded section could be varied by changing either the loading density or the dimensions of the orifice through which the product gasses escaped.

These experiments may cast some light on the phenomenon known as "dead pressing." A "dead pressed" primary explosive has been defined as one which will not effect the transition from deflagration to detonation. Mercury fulminate is said in the literature to be "dead pressed" at 25,000 pounds per square inch loading pressure. In these experiments mercury fulminate, when confined only radially, burned for over a half inch of column length when pressed at only 5,000 pounds per square inch. When well confined in all three dimensions, it built up to detonation in less than 1/16 inch when pressed at 80,000 pounds per square inch. The growth of detonation is apparently a function of both loading density and confinement.

DR. LIDDIARD: How does the stepwise increase in velocity fit in with Dr. Kistiakowsky's ideas on the transition from deflagration to detonation?

DR. KISTIAKOWSKY: I don't see how to understand the step-wise acceleration of deflagration. Personally, I've always thought that the transition from a deflagration to detonation is—well, you might call it continuous or nearly continuous but substantially a sudden process. It may be the result of building a shock wave up to an intensity where it ignites the medium behind it. When it does, you will have sudden detonation. In other words, you will now have,

### ROTH

again, a change-over from a chemical propagation mechanism to a purely physical propagation mechanism caused by shock. But certainly, I do not understand how the deflagration rate should increase continuously.

DR. LEWIS: To what extent do you think that these step-wise changes are influenced by the positional coalescence of the compression wave or shock wave ignited from the containers, simply forming a node at that point and accentuating the building up of the energy at that point, and therefore causing the reaction to go to a larger extent?

DR. KISTIAKOWSKY: I think that's a very interesting point. That's very likely the case.

I might say we are not putting out results at a great rate, because all of this is done by just two graduate students, who are learning as they are progressing. They have been interested, in connection with the transition from deflagration to detonation, in acetylene-oxygen mixtures. And I want to draw a curve which really is a tickler.

If one draws a curve of the detonation velocity against composition of acetylene-oxygen mixtures, the curve rises quite steeply to a very sharp peak at almost exactly a one-to-one acetylene-oxygen mixture. The curve really looks like it has a discontinuity in it. This is an extraordinarily sharp maximum from which the velocity drops down very sharply and then levels off.

Now, we have not finished the Chapman-Jouguet calculations. So we do not know whether this is all consistent with the theory or not. For all I know, it may be. What we do know is this: that the Chapman-Jouguet calculation at this one point, somewhere around 80% acetylene, gives a velocity perhaps only 40 or 50 meters higher than observed under the assumption that the products of combustion are carbon monoxide, carbon, and hydrogen, allowing for hydrogen dissociation into atoms and equilibrium concentration of acetylene—for which there is enough thermodynamic data—not allowing for methane, ethane, and other such things but including solid carbon in the form of graphite. What you actually recover is a very finely divided carbon soot—and quite an active one, too.

So if you assume that this carbon has a few kilocalories higher energy content than graphite, which is certainly not an unreasonable number, then the Chapman-Jouguet calculation and the experiment will agree perfectly.

Now, this means that we have detonation where the chemical reaction zone must be controlled by diffusion processes, because these particles are of such magnitude that they must contain millions, if not billions, of atoms, which must somehow diffuse to these nuclei from the acetylene molecules.

We tried to see what happens if we assume gaseous carbon molecules, and that doesn't fit anywhere with the experiments. Quite recently we made some similar studies on cyanogen-oxygen mixtures, because Doeking and Schoen published a paper about a year ago which pointed out that in the mixture,  $C_2N_2 + O_2$ , according to their calculations, the only equilibrium components are carbon monoxide, nitrogen molecules, and nitrogen atoms. And consequently, the comparison of measured velocity with calculations should permit the calculation of the heat of dissociation of nitrogen, which has certainly escaped a lot of other methods for the last thirty years.

But we have made these first measurements, and we're quite worried that this objective may not be attainable because again we get a curve with a very sharp maximum—almost a singularity at this stoichometric mixture for which the calculations are very simple, because there's very little else present in the thermodynamic mixture.

## SESSION III

12 January 1951

## PHYSICAL ASPECTS OF DETONATION

John G. Kirkwood California Institute of Technology Chairman

### PHYSICAL ASPECTS OF DETONATION

### John G. Kirkwood California Institute of Technology

I notice the title is "Physical Aspects of Detonation," although in looking over the titles it is very difficult to decide just how the distinction between chemical aspects and physical aspects is made. That is one of the things which makes the theory and experimentation in this field very interesting. We have a field in which it is necessary to call on the theoretical and experimental techniques of both chemistry and physics.

Since I'll have the opportunity to make some remarks this afternoon, I'll cut my introductory remarks short at this point and call on Dr. Stuart R. Brinkley of the Bureau of Mines for the first paper.

### THE EQUATION OF STATE FOR DETONATION GASES

Stuart R. Brinkley, Jr. Bureau of Mines, Pittsburgh

### INTRODUCTION

The hydrodynamic-thermodynamic theory of the detonation velocity is based upon integral expressions for the continuity of mass, momentum, and energy across the detonation front formulated by Rankine and Hugoniot and upon the additional condition, stated independently by Chapman and Jouguet, that the stable detonation velocity is the minimum one compatible with the conservation equations. When supplemented by an equation of state and thermal data for the products of the detonation reaction, these relations are sufficient to permit calculation of the detonation velocity and particle velocity of the detonation wave and, in addition, the values of the state variables characteristic of the detonation gases immediately behind the detonation—wave front. 1

Since the combination of high pressures, temperatures, and densities characteristic of the detonation gases from condensed explosives is inaccessible to independent experimental study, it is impossible to establish independently the correct form of the equation of state to be employed in the theoretical description of the detonation wave in such explosives. It has been customary to employ the theory in an inverted form, utilizing experimentally determined values of the detonation velocity to evaluate the parameters of an equation of state of assumed form. The equation of state obtained in this way can then be employed in the prediction of the detonation velocity of additional explosives, the success of such prediction usually being adduced as evidence for the correctness of the assumed form of the equation of state. For this program, several different forms, some of them unreasonable, have been employed, leading to different calculated values of the detonation temperature and pressure.

Knowledge of the equation of state for detonation gases is required in the more detailed theoretical study of the detonation wave and also for computation of the initial parameters of the shock wave generated in the exterior medium by the explosive charge. We shall survey briefly, and not at all exhaustively, several of the forms of equation of state that have been employed for the description of the detonation gases from condensed explosives, and we shall then consider the general problem of the evaluation of thermodynamic state from experimentally determined values of the detonation velocity.

### PROPOSED FORMS OF THE EQUATION OF STATE

Many investigations<sup>2</sup> of the properties of explosives have employed the Abel equation of state,

$$p(v-\alpha) = nRT/M, (1)$$

and H. Bateman, Bull. 84, Nat. Res. Council, p. 557, 1932

2 For example, Cranz, C. J., Lehbruch der Ballistik, 2, 107 (1926); Crow, A. D., and Grimshaw, W. E., Phil. Trans., A230, 39 (1930)

<sup>&</sup>lt;sup>1</sup> A summary of the hydrodynamic theory with references to the original papers has been given by G. B. Kistiakowsky and E. B. Wilson, Jr., OSRD Report 114 (1941) (Report PBL 32715, Off. Tech. Serv., U. S. Dept. Commerce). See also H. L. Dryden, F. D. Murnaghan, and H. Bateman, Bull. 84. Nat. Res. Council. p. 557, 1932

### BRINKLEY

a simplified form of the van der Waals equation of state, where p is the pressure, v the specific volume, T the temperature, n the number of moles of gas contained in mass M, and where  $\alpha$  is an excluded volume, called the covolume. This form of equation has been widely employed in the interpretation of the pressure measured after the explosion of a charge in a closed bomb. The value of the covolume resulting from such studies is usually much less than that determined by considerations at ordinary conditions. When applied to the description of detonation gases, 3 covolumes determined arbitrarily so as to give the observed detonation velocity can have little physical significance. We note that this equation of state requires that the internal energy shall be a function of temperature only, the gas thus being thermodynamically ideal.

A more general form of the Abel equation of state has been assumed by Cook, who employs the relation.

$$pv = nRT + p \alpha(v).$$
 (2)

The function  $\alpha$  (v) is an arbitrary function of the specific volume, evaluated by comparison with experimental values of the detonation velocity. It was found that a single function was adequate for the representation of the detonation velocities of a number of different explosives, and excellent agreement between calculated and observed detonation velocities was obtained. As pointed out by Paterson, the arguments by which Cook justifies the assumption that  $\alpha = \alpha(v)$ instead of the more general assumption  $\alpha = \alpha(v, T)$  appear to be a posteriori in character. An equation of state of form essentially equivalent to Equation (2) has also been assumed by Caldirola. Equation (2) implies that the gas is thermodynamically ideal, the internal energy being a function of temperature only.

Jones and Miller 6 have employed a virial expansion, terminating in the cubic term, explicit in the pressure,

$$pv = nRT (1 + bp + cp^2 + dp^3)$$
 (3)

The virial coefficients, which they point out are properly functions of the temperature and gas composition, are assumed to be constants and are evaluated by a comparison between the theoretical relations and observed detonation velocities. The authors have published the results of calculations for the case of TNT only. Equation (3) implies that the internal energy is a function of temperature and pressure, varying as a power series in the pressure at constant temperature.

Kistiakowsky and Wilson<sup>7</sup> have employed a modified form of an equation originally constructed by Becker<sup>8</sup> on the basis of some theoretical considerations from high-pressure p-v-t data of Amagat on nitrogen. Becker's equation has been employed by Bridgman for the representation of state data at 68°C on nitrogen to pressures of 15 kilobars. The equation is employed by Kistiakowsky and Wilson in the form

$$pv = nRT (1 + xe \beta^{x}),$$

$$x = k/T^{\alpha}v,$$
(4)

<sup>&</sup>lt;sup>3</sup>As, for example, by Langweiler, V. H., Zeit. Techn. Physik, 19, 271 (1938)

<sup>4</sup>Cook, M. A., J. Chem. Phys., 15, 518 (1947). For discussion, see S. Paterson, ibid.,

16, 159 (1948), and Cook, M. A., ibid., 16, 554 (1948)

<sup>5</sup>Caldirola, P., J. Chem. Phys., 14, 738 (1946). For discussion, see Brinkley, S. R., Jr.,

ibid., 15, 113 (1947) and Paterson, S., loc. cit.

<sup>6</sup>Jones, H., and Miller, A. R., Proc. Roy. Soc. London, A194, 480 (1948)

7Kistiskowsky, G. B. and Wilson, F. B. Jr., loc. cit.

<sup>&</sup>lt;sup>7</sup>Kistiakowsky, G. B., and Wilson, E. B., Jr., <u>loc. cit.</u> 8Becker, R., Zeit. f. Physik, <u>4</u>, 393 (1921)

<sup>9</sup>Bridgman, P. W., Proc. Am. Acad., 59, 173 (1924)

where  $\alpha$ ,  $\beta$ , and k are empirical constants. The parameters of Equation (4) have been evaluated <sup>10</sup> by comparison of the theoretical relations with experimental detonation velocities. Equation (4) was employed in calculating values of the state variables for a number of explosives and by Kirkwood and his collaborators in determining the initial parameters of the shock waves in water and air generated by the explosive charge. Equation (4) implies that the internal energy is a function of temperature and density, varying as an exponential in the density at constant temperature.

Calculation of the pressure, density, and particle velocity characteristic of the detonation velocity is relatively insensitive to the form of the equation of state employed for the description of the state of the detonation products, and the different equations of state predict values of the same order of magnitude. However, the calculated temperature is quite sensitive to the form of the equation of state employed. In particular, if the composition of the detonation products does not vary with the loading density of the explosive, the calculated temperature will increase with increasing loading density for equations of state such that the internal energy is independent of the density. If the energy of gas imperfection is significant compared to the internal energy of the ideal gas, the calculated temperature will decrease with loading density. These considerations are illustrated by Table 1, which lists a few calculated results for TNT.

Oniculated Variety of Detonation Temperature			
Loading Density	Cook	Jones	Kistiakowsky and Wilson
1.0	3700	3800	3170
1.5		3400	
		1	1

TABLE 1
Calculated Values of Detonation Temperature

## DETERMINATION OF THERMODYNAMIC STATE FROM DETONATION VELOCITY

4170

It is instructive to consider the general problem of determination of the thermodynamic state of the detonation gases by means of the hydrodynamic theory using an experimental curve U = U ( $\rho_0$ ), where U is the detonation velocity and  $\rho_0$  the loading density. If the particle velocity is eliminated, the Hugoniot equations can be written in the form,

$$p - p_0 = \rho_0 U^2 (1 - \rho_0/\rho),$$

$$H - H_0 = U^2 \left[ 1 - (\rho_0/\rho)^2 \right],$$
(5)

3170

where p,  $\rho$ , and H are the pressure, density, and specific enthalpy of the detonation gases at the wave front, respectively, and where  $p_0$  and  $H_0$ , the pressure and specific enthalpy of the intact explosive, respectively, are assumed to be given. The Chapman-Jouguet condition can be written in the form,

$$c = \frac{\rho_0}{\rho} U, \qquad (6)$$

where  $c = \left[ (\partial p/\partial \rho)_S \right]^{1/2}$  is the Euler velocity of sound in the detonation gases. Although it is customary to employ an equation of state for the pressure explicit in the temperature and density, this choice leads to considerable algebraic complication in the development of the theory.

<sup>10</sup>Brinkley, S. R., Jr., and Wilson, E. B., Jr., OSRD Report 905 (1942) (Report PBL 31088, Off. Tech. Serv., U. S. Dept. Commerce)

### BRINKLEY

A more natural choice is to assume the existence of a relation,

$$\rho = \rho(p, S), \tag{7}$$

where S is the entropy. The usual program for determining an equation of state from experimental values of the detonation velocity is the formal equivalent of the determination of function (7), for given values of  $\rho_0$ ,  $\rho_0$ ,  $\rho_0$ ,  $\rho_0$ , and  $\rho_0$ ,  $\rho_0$ ,

$$J\left(\frac{\rho, H}{p, S}\right) \tag{8}$$

equals zero. This implies that the fundamental relations and given quantities are not sufficient for the unique determination of the thermodynamic state from detonation velocities alone but that the given relations can be satisfied together with any arbitrary function p = p (S).

It follows that the degree to which an equation of state of assumed form reproduces the experimental data employed in the evaluation of its parameters cannot legitimately be employed as a criterion of the correctness of the form of the equation. Assumption of the form of the equation of state provides the additional assumption required to make the theory determinate. Selection of the form of the equation of state must be based upon additional evidence, either experimental or theoretical in nature, or, lacking such information, on considerations of plausibility.

### ENERGY OF GASES AT VERY HIGH PRESSURE

Immediately behind the detonation front, the density is greater than that of the intact explosive, and the molecular volume is less than the excluded volume necessary for the application of an Abel type of equation of state. Under the high compression that exists in the detonation wave, it seems clear that the repulsive forces between the tightly packed molecules must make a significant contribution to the energy. 11

In an important and informative paper, Jones <sup>12</sup>has employed considerations entirely independent of the detonation process to establish an equation of state of the detonation products, and he has employed the resulting equation in an <u>a priori</u> calculation of the detonation velocity for several loading densities of TNT and lead azide. In formulating an equation of state, the limiting case of very high pressure at a fixed temperature was considered, for which it was possible to construct theoretically the form of the equation of state in a way similar to that in which the equation of state of a solid is constructed. The parameters of this equation were fixed, for the particular case of nitrogen, employing Bridgman's data. A virial form of equation was employed to interpolate between high and low pressures. In this way the detonation velocity and values of the state variables were calculated without any reference to explosion experiments. The detonation velocities thus obtained were about 17% higher than the experimental values, but the variation of detonation velocity with loading density was very well reproduced. The calculated detonation temperature was a decreasing function of the loading density. These considerations lead to the prediction that the internal energy of the detonation gases is an exponentially increasing function of the density at very high pressures.

These considerations lend considerable support to the equation of state for detonation gases in the form proposed by Kistiakowsky and Wilson, Equation (4). This equation has the indicated exponential dependence of internal energy on density at high pressures, and at vanishing pressures it has the correct ideal gas form. It may be noted that, by adopting a suitable value of the

<sup>11</sup>H. Jones and A. B. Miller, loc. cit.

<sup>12</sup>H. Jones, Ministry of Home Security (Great Britain) Report RC-166 (1941)

parameter  $\beta$ , this equation can be made to agree closely with Hirschfelder's <sup>13</sup> virial form of the equation of state that has been successfully employed for the description of propellant gases.

### ESTIMATION OF THERMODYNAMIC STATE OF DETONATION GASES

Jones 14 has recently shown that

$$p = \frac{U^{2} \rho_{0}}{(2 + \alpha) (1 + g)},$$

$$\rho = \rho_{0} \frac{(2 + \alpha) (1 + g)}{(2 + \alpha) (1 + g) - 1},$$
(9)

where g = d log U/d log  $\rho_0$  can be determined from an experimental curve U = U ( $\rho_0$ ) and where

$$\alpha (\mathbf{p}, \boldsymbol{\rho}) = \left(\frac{\gamma \mathbf{C}_{\mathbf{v}}}{\mathbf{v} (\partial \mathbf{p}/\partial \mathbf{T})_{\mathbf{v}}} - 1\right)^{-1} . \tag{10}$$

The utility of Equations (9), which do not involve any assumptions as to the form of the equation of state, resides in the fact that  $\alpha$ , which is properly a function of the state, can be shown to be an essentially positive quantity. Equations (9) with  $\alpha = 0$  thus provide rigorous upper limits to the pressure and density. Furthermore, it can be shown to be plausible that

$$0<\alpha<1/4,$$

so that Equations (9) also provide estimates of lower limits to the pressure and density. By applying a previously proposed equation of state, Equation (3), Jones has estimated that  $\alpha$ = 0.20 for the case of PETN. This procedure thus makes it possible to estimate the pressure and density (and, by means of the Hugoniot equation, the enthalpy) and also to give a rigorous upper bound and plausible lower bound to this estimate.

### CONCLUSION

A considerable amount of investigation evidently is required before the appropriate form of the equation of state can be unambiguously established. The direct experimental determination of additional properties of the detonation wave would determine the correct form of the equation. Measurement of the temperature would supplement most effectively experimental detonation velocities for this purpose, since the calculated temperature is the most sensitive to the form of the equation of state. It seems probable that measurement of the time dependence of the velocity of unsteady detonation waves would yield valuable supplementary information. Theoretical studies of the energy of gases at high temperatures and very high pressures might serve to establish the proper form of the equation of state.

At present, it is felt that the Kistiakowsky-Wilson equation of state offers the most plausible description of the state of detonation gases. Unfortunately, the parameters of this equation which are now employed are obsolete, since the velocity data employed in their evaluation have been largely superseded by data of greatly improved accuracy. Since progress is likely to be slow in the various different lines of investigation toward elucidation of the proper form of the

 <sup>13</sup>J. Hirschfelder, D. Stevenson, and H. Eyring, J. Chem. Phys., 5, 896 (1937)
 14H. Jones, Proc. Third Symposium of Combustion, Flame, and Explosion Phenomena,
 The Williams & Wilkins Co., Baltimore, p. 590 (1949)

#### BRINKLEY

equation of state, it is probably desirable that the parameters of this equation be recalculated, using the best available rate data. Because of the formidable numerical nature of these calculations, modern automatic high-speed computational equipment should be employed in this task.

### DISCUSSION

DR. KIRKWOOD: Dr. Brinkley's paper is now open for discussion.

DR. COOK: Following the suggestion of Dr. Brinkley, I would like to say a few things about this Paterson criticism and also my  $\alpha(v)$  approximation. Actually, I agree thoroughly with one of Paterson's points and with Dr. Brinkley on that particular point. Paterson and I really do (and always did) agree, however, in regard to this  $\alpha(v)$  approximation. I don't know whether any of you are familiar with his work, but he started with a completely independent equation of state which includes the  $\alpha(v)$  approximation; that is, an equation of state obtained by evaluating the parameters theoretically and in this particular  $(\alpha(v))$  form. As you know—those of you who are familiar with that work—he was able to calculate detonation properties and to calculate pressures which were in agreement with all of these other methods and velocities which agreed fairly well with experiments. There is one difficulty that I see and that is that his velocity increased a little more rapidly with density than the observed velocities. And his curves crossed over the experimental Dvs.  $\rho$  curve. At about a density of 1.2, it crossed over and it had just a little too high a slope, but when you realize that all the parameters were theoretical, I think Paterson's correlations were very significant. Now, in regard to Dr. Brinkley's statement of Jones' work, I think I agree in some respects with Jones' work but I think the internal energy is going to be negative; the internal pressure is going to be negative at high densities.

Incidentally, I worked out a couple of years ago this same thing that Jones has come up with, but I wasn't resourceful enough at that time to put it out as an upper limit. I realized it was an upper limit, and I have that paper here right now. I never published it. I talked it over with Dr. Kistiakowsky and Dr. Paterson and I had some correspondence on it. I think there are some interesting things about the work of Jones that haven't been presented yet. I would like to show you the calculations of pressures corresponding to that upper limit to compare them to those that we have calculated by other methods, and then I think we can get some information as to the nature of the true equation of state from this, that is, from reasonable considerations bringing in external evidence. For PETN at a density of one, we get 86 kilo atm as the upper limit for the detonation pressure compared with 85 kilo atm obtained from my early work. Also, the upper-limit calculation gives at a density of 1.6 a pressure of 273 kilo atm compared with 225 kilo atm from the earlier work.

These are the values I have calculated from this  $\alpha(v)$  approximation, i.e., the values 85 and 225. The others (86 and 273) are the upper-limit pressures which Jones would calculate, i.e., which I computed from an equivalent equation. This method is identical with Jones', and these are those upper limits. Now, I've been working considerably lately on the solid state, and since Jones' considerations do come from solid-state considerations, I think it is of interest to consider that particular thing from the viewpoint of a familiar potential-energy curve of a molecular crystal. In the solid state, we would expect from the potential-energy curve for a molecular crystal (van der Waals crystal) that at about a density of 1.2 you start to run into a net repulsion instead of attraction. That is, the minimum of the curve comes at this density, and at a greater density your repulsion term exceeds your attractive term in the interaction potentials and I think, then, that this correlation at a density of 1.0 to 1.2 is significant. Also, the fact that one obtains a higher pressure at a density of 1.6 than in the  $\alpha(v)$  approximation and a lower pressure at lower densities is significant. Now, in addition, I calculated a number of other explosives and showed the same situation; in all cases at a density between 1 and 1.2 the upper limit and the  $\alpha(v)$  approximation agree; at a density of 1.6 the upper limit is always much higher, and at the very low densities it is always lower than one computes from the  $\alpha(v)$  approximation. As Dr. Brinkley points out, there are a lot of complicating factors so that it is difficult really to understand what this means, but I feel that it means that we

are passing the  $\alpha(v)$  approximation at about a density of 1 to 1.2. Now the form in which I have this is:

$$\frac{dD}{dv_1} = \frac{D}{v_1} - \frac{D}{2(v_1 - v_2)} + \frac{{v_1}^2}{2D(v_1 - v_2)} \left\{ \frac{dp_2}{dv_2} + \frac{p_2 - p_1}{v_1 - v_2} \right\} \frac{dv_2}{dv_1}$$

where D = detonation velocity, v = specific volume, p = pressure, subscript 1 refers to conditions ahead of the reaction zone, and subscript 2 indicates those immediately behind the reaction zone. If we were dealing with the  $\alpha(v)$  approximation, I think the last term would correspond with the Chapman-Jouguet condition. That is, when the  $\alpha(v)$  approximation is correct, the last term in this equation is zero because then  $dp_9/dv_9$  is the same as  $(dp_2/dv_2)_S$ . This term would be zero. We can then calculate the pressure from the first two terms on the right side of the equation. This (i.e., the equation resulting by dropping the last term) is the equation which is equivalent to the upper limit, so you get your upper-limit pressure from that first part of the equation. When we consider (1) evidence from calculations of numerous explosives, even those with solid residues, and which we have calculated by the  $\alpha$  (v) approximation, and (2) the further fact that the lpha-vs.-v curves are the same curve for all explosives, I still have difficulty in seeing that that doesn't mean this  $\alpha$  (v) approximation is about correct. We have used this same curve, after evaluating it from four explosives, on all types of explosives; and so far as I know, it hasn't failed. Dr. Davis and I worked together on this; he carried out experimental velocity measurements. I know he got great delight out of concocting new types of materials, measuring their velocity, and turning the composition over to me to calculate. We always found agreement. There was no case in which we couldn't calculate the actual velocity within about 200 in./sec from that curve. When you realize the number of different types of explosives that came under our consideration (we have worked out cases with 20 or 30 percent water in explosive mixtures and all sorts of compositions, those with no carbon in them, those with high percentages of  $H_2$ , and various things of that sort) you can look at this  $\alpha(v)$  approximation with consideration.

DR. BRINKLEY: May I make one or two supplementary remarks. In the first place, I am afraid that the result is, of course, negative, but I'm afraid we can't avoid the essential indeterminancy of the theory. I believe that we have to conclude that these things have been a very successful case of curve-fitting and, as such, they have a very high degree of usefulness. Jones' work on the estimation of thermodynamic properties from rate data alone, I think, is a formal statement of the fact that certain of the properties were extremely insensitive to the form of the equation of state employed. Again, those considerations will be extremely useful in a practical sense, but they do not in any way solve the problem of determining the adiabatic temperature of the detonation gases. Yet for the detailed study of the detonation process, and for the study of shock wave associated with the detonation process, it is precisely the adiabatic which we must be able to determine.

DR. PRICE: I would like to make a very brief comment on the upper limit of Jones' value. Dr. Brinkley indicated that this was not absolutely determined at 0.25. If you use the pressure and other parameters computed by Dr. Brinkley, using the Kistiakowsky-Wilson equation of state, you'll find you can obtain alpha values from Jones' expression which are above 0.25. For PETN and TNT they will vary with the loading density of the explosive, and in the case of PETN I think the upper limit was up around 0.36. There are other materials and other explosives for which it is slightly higher, so that I think these values confirm the order of magnitude of alpha but do not necessarily confirm the fact that the upper limit is 0.25.

DR. KISTIAKOWSKY: Since I've already spoiled Von Neumann's contribution to explosions, I would like to destroy another idol. Actually the work was done by R. Halford, but the peculiar (fortunately later revised) rules of NDRC in the very early days required that the names of the official investigators—Kistiakowsky and Wilson—appear on the report.

### CONVERGENT SHOCK WAVES

### Arthur Kantrowitz Cornell University

We were first attracted to the possibility of making convergent shock waves by the very high temperatures and pressures which you might easily expect to reach in this way. Now, the problem of implosion is really not a new one. It exists in various military devices, as you know, and an analysis of a shock wave proceeding toward a center has already been made, in particular by Guderley during the last war. His results are shown in Figure 1.

We have checked Guderley's solution by solving the same problem by the method of characteristics, and you see that we obtain essentially the same result. The line at the top of the figure represents the pressure and temperature after the shock wave reflects from the center, after it goes down to a point, and comes out again, and we obtained some points by the method of characteristics—those I have given here.

Well, this by itself might easily be highly academic, except that it seemed to us that it was really possible to produce such things because shock waves apparently have a tendency to assume certain very simple shapes. For example, if you have a shock wave propagating down a tube in the usual shock-tube experiment, you'll find that the shock is very flat. Hornig has informed me that his experiments on reflection from shock waves indicate that a shock wave such as that found in a shock tube is flat to within about four minutes of angle after it has progressed down the tube a little way. This is a rather remarkable phenomenon, and it indicates some stability mechanism operating to maintain this flatness. Now, I might point out that the assumption of a special shape by a wave is

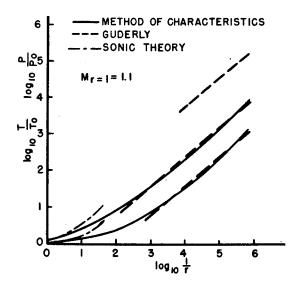


Figure 1 - Comparison between sonic theory, Guderley's solution, and the method of characteristics for spherical converging shock waves ( $\gamma=1.40$ ). The values p/p<sub>0</sub> and T/T<sub>0</sub> are the ratios of pressure and temperature immediately behind the shock to the initial values. The short upper curves correspond to the pressures after reflection from the center.

something that is only possible for a dissipative wave. If you had a reversible process which tended to assume a special shape, this would really be a violation of the second law, but in the case of a shock wave, we have the possibility of a little organization appearing out of the chaos of the dissipation naturally present in the shock wave. The analysis of this stability can best be done, I think, from the point of view of Mach reflection and Figure 2 shows Mach reflection in a schematic form.

Now the characteristic thing about this is that this Mach shock is curved always. Maybe it is best to use a diagramatic sketch of a Mach reflection (Figure 3). If the Mach shock is curved thusly, then the angle between the air immediately behind the triple point and the incident air is much smaller than the angle between the wall flow and the incident air, so that

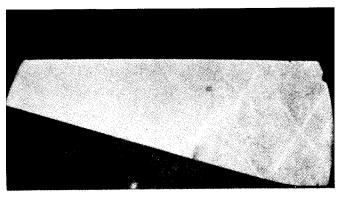


Figure 2 - The entrance of a plane shock wave into a converging two-dimensional channel

when this wave proceeds to the other side and is re-reflected, the re-reflection will be considerably smaller in general than the original reflection. In other words, some of the curvature which was initially concentrated at the corner has been spread out over the Mach shock and this spreading out of curvature is what we term stability of the form.

Now you see if you have a shock propagating in a straight tube, we have a boundary condition that the shock must be normal at the two walls. In other words, there must be equal amounts of positive and negative

curvature, and if that equalizes you get a plane. On the other hand, if we have a shock which is moving in a converging channel and the shock must be normal to the two walls, then you get a circular cylinder for the form where the curvature has been equally distributed.

We have taken the extensive Mach reflection data that was compiled by L. G. Smith at Princeton during the war and plotted up what we call the attenuation of corners. If the attenuation is unity, then it means that a corner disappears in one Mach reflection. If the attenuation is zero, it means the corner propagates out unattenuated and a plot of the attenuation for various incident angles at various Mach numbers is shown in Figure 4. At low Mach numbers you get

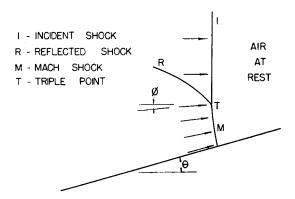


Figure 3 - Sketch of the Mach reflection configuration

very high attenuation in a single Mach reflection, so the corners in a shock wave tend to disappear very rapidly. As you go to higher Mach numbers (Smith data unfortunately gives out at Mach number 2.4) the stability is smaller, and we'll see that this fact plays an important role in what we do from there on.

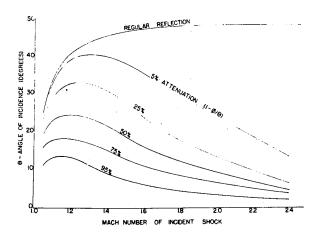


Figure 4 - Attenuation as a function of angle of incidence and Mach number of the incident shock. (From Smith's observations, which were very thinly spaced for the higher Mach numbers of the range shown.)

There is some indication that this rule of a smoothing out of curvatures may not be valid for very high Mach numbers to be found in the linearized theory of Lighthill. Lighthill considers only small corners and he always gets for our attenuation parameter a hundred percent.

### KANTROWITZ

In other words, referring to Figure 4, he derives the bottom contour of very small corners but he finds the shock has an inflection point for Mach numbers greater than 2.5 and this would indicate a possibility of instability at high Mach numbers. There really isn't any way of deciding from a linearized theory, and one of the things we are now attempting to do is to work out a second-order theory which would permit calculations of the attenuation of corners in strong shocks. It would be very nice to extend Smith's measurements to strong shocks. Well, this stability that you get is illustrated in Figure 5, where several Mach reflections have occurred in a converging channel, and you see that you get something

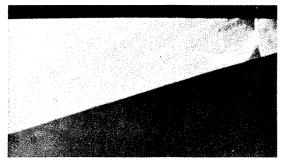


Figure 5 - Same situation as Figure 2 after the shock wave has propagated some distance into the converging channel

which is indeed very close to a cylinder. The Mach reflection, even though it looks quite strong, is a very weak shock as you can see from the fact that it does not bend the main shock appreciably.

Now to get back to our original interest in this problem, in the attainment of high temperatures, if you continued the convergence of Figure 5 until the walls joined, I don't think you would get anything particularly interesting because at the vertex the heat conduction and the diffusion to the walls would be so high as to dominate the phenomena. We have looked around for other ways of producing a converging shock which would not be dominated by heat conduction and diffusion to the walls. We invented the axially symmetric shock tube that is shown in Figure 6. The shock wave comes up to the point and is pierced by the point and forms an

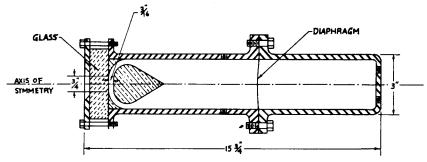


Figure 6 - Sketch of cylindrical shock tube

annulus, and then if it will turn the corner, it will form a converging cylindrical shock wave which has its center of convergence away from surrounding walls. We suspected because of the natural stability of shock waves that, if the shocks were not too strong, it would be possible to produce an angular-ring converging shock wave in this way, but we tested this in a two-dimensional section, and those results are shown in Figure 7.

A cylindrical shock wave is approaching a corner, goes around the corner, and ends up very flat. We built the apparatus shown in Figure 8, and we tried this. There is a glass window to look inside. A camera is in position to take photographs of anything that happens, and the diagram flange is also visible.

I would like to present some photographs that we took of the shock wave on the way in and out. We put a mirror on the end of this thing and the Schlieren system—it was a double-up Schlieren system in which the light went in and out again—and in that way we were able to take Schlieren photographs. You'll notice in Figure 9 quite a weak shock; its stability is very

high, and it forms a beautiful circle. It goes right in as far as you can tell, and it comes out and leaves in the center a hot point where the dissipation was very high. As you might expect, it would form a perfect circle on the way out. If you do the same thing again starting with a little stronger shock, you get the results of Figure 10. Here the stability is not nearly so good, and you don't get quite perfect circles. You get a larger heated region, and the heated region is somewhat irregular, showing that the convergence was not perfect.

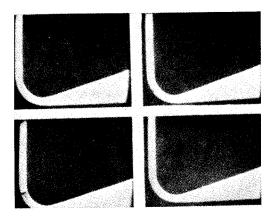


Figure 7 - Schlieren photograph of the progress of a shock wave around a corner in a two-dimensional shock tube

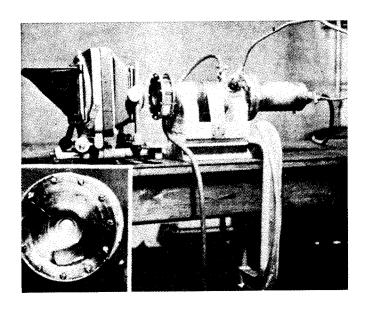


Figure 8 - Original cylindrical shock tube

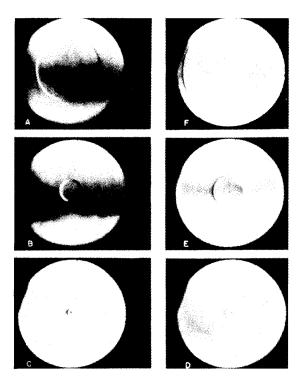


Figure 9 - Schlieren photographs of converging cylindrical shock waves in air (obtained from plane shocks with M=1.1). A, B, C indicate the incident waves and D, E, F indicate the reflected waves. Each photograph is of a different shock wave. The glass window was 1-1/4 inches in diameter

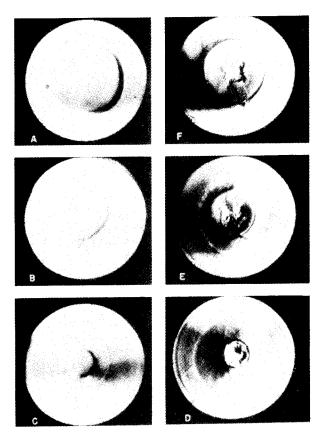


Figure 10 - Schlieren photographs of converging cylindrical shock waves in air (obtained from plane shocks with M=1.8). A, B, C indicate the incident waves and D, E, F indicate the reflected waves. Each photograph is of a different shock wave. The glass window was 1-1/4 inches in diameter

As I said, this convergence drives the shock Mach number up to quite high values. We darkened the room, looked into this shock tube, created a shock with quite a small Mach number, and looked into the glass window at the center. I was willing to bet on our first experiment that you would see a luminous spot. The luminous spots did appear, and we have some photographs of them (Figure 11). This is a three-quarter-inch window, and you see a very tiny luminous spot. Its diameter is limited only by the fact that the optical system we used is quite poor. We don't know how small it is, but it is smaller than a few hundredths of an inch. Now the light that is produced indicates that we are going to at least the temperatures where a certain amount of ionization is present. If you put an electrode some place in this region, you easily establish that the gas becomes conductive for a very short period. Before we could go much further with this type of thing, we really felt that we needed two types of information.

First, we are up against the same kind of problem that has been discussed here this morning of knowing about the state of the gases under these high temperatures and pressures. Well, the pressures aren't high by comparison with what you people are used to, but the temperatures are high. We can use ideal gas laws.

We thought that we could establish that information by experiments easier to interpret than this one. Other information that we need, of course, is about the stability of strong shock waves, but our view

is that the stability will not be high at high Mach numbers. You have to get a good converging shock - get it all smoothed out while the Mach number is low, while it is below two, pressure ratio below five or six—and then let it converge without disturbing it further. We have been doing a little work on the properties of gases at very high temperatures. If you take a garden variety of shock tube with a diaphragm and fill one end with hydrogen and the other end with argon, you can quite easily produce shocks that are strong, even by your standards. For example, if you evacuate this down to one millimeter of pressure and put this in something like ten atmospheres so that you get a 1,000-to-1 pressure ratio, then the theoretical shock which you calculate here is moving at about 4,000 meters per second in a monatomic gas, so it is possible to attain very high temperatures. This gives us an easier method of investigating the properties of gases at high temperatures. First you do a preliminary series of experiments in which you establish that the shock velocity is indeed what you calculate. You'll find it is a little lower than is traditional—ten percent lower or something like that—but its performance is a little different from the low-pressure-ratio shock tube. Then, if you look at the statistical mechanics of argon, you'll calculate that with a pressure ratio you could easily achieve 10,000 to 1. The argon is ionized something like one percent, so it is an excellent conductor of electricity. By that time, theoretically, the gas has other interesting properties that I'll refer

### KANTROWITZ

to briefly later. This is all theoretical. Well, we put a little electrode in the end and the electrical conductivity is shown as in Figure 12.

This is just a measure of electrical conductivity, and the early part of this curve indicates the rise in conductivity as the shock wave covered the electrode and the steep rise corresponds to the reflection of shock wave at the end of the tube. Conductivity that we get decays very rapidly and is far less than you calculate from statistical mechanics by perhaps a factor of a hundred thousand. This I don't understand either. We have examined several of the obvious sources of heat loss. Well, first we eliminated by this experiment the possibility that there is a large relaxation time for the appearance of ionization-by the fact that the curve follows what you would expect in its early phases, which means that some ionization appears immediately. The lags are just a few microseconds at most, but the fact that it doesn't build up to its expected values is somewhat mysterious unless there is some large source of heat loss.

One other experiment which we did which I thought might be of some interest was that we took a spectrogram of the light which is attained in such a shock wave (Figure 13). You see that we get a line spectrum. This

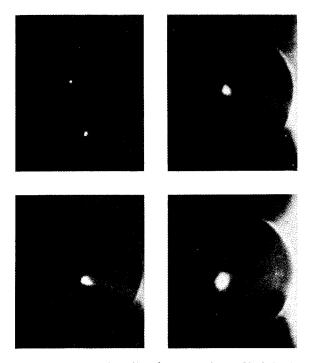


Figure 11 - Luminosity of converging cylindrical shock waves in argon (obtained from plane shocks with M = 1.8). The glass window, rendered visible by double exposure, was actually 3/4 inch in diameter

was just done a few days ago and we haven't had time to analyze this spectrum yet. We get lots more lines than you get from an argon arc with the same exposure, and our immediate intentions are to explore this a little by comparing the spectra of an arc obtained in the shock tube immediately before the shock wave with the light emitted from the shock wave itself to see if there is a real difference when you consider gases of exactly the same composition.

The experiments on shock waves in converging channels were conducted by A. Hertzberg and the author and are reported in the Journal of Applied Physics (Vol. 21, No. 9, 874-878, September 1950). The later converging shock experiments were conducted by R. W. Perry and the author and have been accepted for publication in the Journal of Applied Physics. The most recent group of experiments in straight shock tubes, including the conductivity work and the spectograms, were undertaken by E. L. Resler, S. H. Bauer, and the author and will be reported more fully shortly.

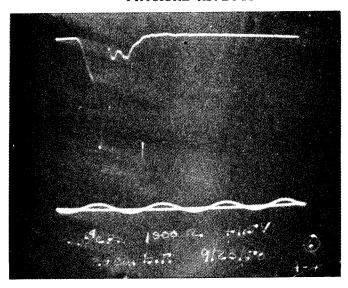


Figure 12 - Oscillogram of the conductivity produced by a shock wave in argon. The low pressure in the argon was 20 cm of Butylphthalate and the high pressure in the hydrogen was 11 atm

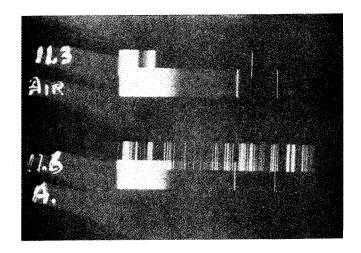


Figure 13 - Spectrograms of the light produced by strong shocks in argon and air. Hg spectra are given for comparison

### KANTROWITZ

### DISCUSSION

- DR. WEYL: I want to ask what the hopes are of using the shock tube to get information about the equation of state of gases at high temperatures by getting another independent measurement in addition to shock velocity? For instance, density behind the shock front.
- DR. KANTROWITZ: One program we have in mind may answer this, and that is to measure the velocity of sound immediately behind the shock. If you know the shock velocity, then the velocity of sound is a nice thing to know. I guess it's about as good as anything. We have done that for low-Mach-number shocks. We intend to do it in ranges where we can get information of interest about the properties of gases. One thing we intend to study in this way is the dissociation of the components of air. Put nitrogen in the shock tube and if you work in a time range, if you adjust the temperature so that the relaxation time is comparable with the time it takes the shock wave to travel across the tube, then you'll see a distortion from the perfect circle which will indicate a subtraction of heat due to the association of nitrogen, so we can measure the association velocity.
- DR. LEWIS: I believe Bleakney is measuring the density behind the shock wave in his shock tubes.
- DR. KANTROWITZ: I would think that that would be good as long as you have good high densities, but if you were trying to work in the range well below atmospheric pressures, it would be difficult, but it might well be that that could be done. He has quite good precision.

## SHOCK WAVES IN SOLIDS

### J. E. Ablard Naval Ordnance Laboratory

Dr. Brinkley has given you a discussion of the hydrodynamic-thermodynamic equations of the detonation process and has pointed out the desirability of being able to measure one or more of the quantities independently. One continually meets the difficulty of lack of information on equations of state at high T and P. Calculations of detonation velocities for example or underwater shock-wave parameters soon lead to difficulties because of lack of such information even for the simple gases that appear as the products of detonation.

Dr. Goranson pointed out in 1946 that certain information obtainable from the study of shock waves in solids could supply some of the data. The argument is as follows:

The three hydrodynamic equations applied to the detonation process are:

$$\rho_0 D = \rho (D - u) = m$$
 (conservation of mass) (1)

$$mD + P_0 = m (D - u) + P$$
 (conservation of momentum) (2)

$$E_0 + mD^2 + \frac{P_0}{\rho_0} = E + m (D - u)^2 + \frac{P}{\rho} - \Delta Q \qquad \text{(conservation of energy)}$$
 (3)

where D = velocity of the detonation front

 $\rho$  = density

u = particle velocity

m = mass flow per sec

P = pressure

E = energy

 $\Delta Q$  = chemical energy released in the reaction.

The subscript zero refers to the state ahead of the front. Characters without subscript refer to a certain condition behind the front. In the detonation process there is one steady-state condition defined by the Chapman-Jouguet hypothesis which states that

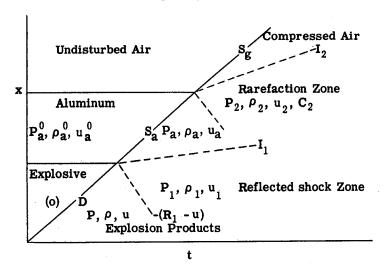
$$D = u + C, (4)$$

where C is the velocity of sound at  $\rho$ , T, and P. In addition to the above equations, there is an equation of state which for our present purposes is best written

$$\mathbf{E} = \mathbf{E}(\mathbf{T}, \boldsymbol{\rho}). \tag{5}$$

A glance at Equation (1) shows that if the detonation velocity can be measured, and in addition one other quantity, for example, u, the rest of the quantities in Equations (1), (2), and (4) can be calculated.

Let us now review the theory of the transmission of shock waves through a solid, and specifically we will choose aluminum for the solid for reasons which will be apparent later. The shock wave is considered to be generated by a detonation wave in an explosive placed in contact with the aluminum. On an x-t diagram, the situation looks like this:



Analysis of the equations for the detonation wave and the two shock waves, together with the reflected waves and the interface conditions yields the relations:

$$\begin{split} &\frac{I_1}{u} = \frac{\rho_0 D + \rho R_1}{\rho_0^2 S_a + \rho R_1} & \tilde{=} & \frac{2\rho_0 D}{\rho_0^2 S_a + \rho_0 D} & \text{if } \rho_0 D = \rho R_1 \\ &I_2 = I_1 + \sigma_a \,, \end{split} \label{eq:interpolation_problem}$$

where

$$\sigma_{a} = \int_{\rho_{g}}^{\rho_{a}} \frac{C_{2} d\rho}{\rho} = I_{1}.$$

Hence

$$u = \frac{\rho_a^0 S_a + \rho_0 D}{2\rho_0 D} (I_2 - \sigma_a) = \frac{\rho_a^0 S_a + \rho_0 D}{2\rho_0 D} \cdot \frac{I_2}{2}$$

These equations have been obtained with the following assumptions:

- (1) that the detonation wave is planar;
- (2) that the shock wave returning into the explosion products has only a small over-pressure;
- (3) that the "escape velocity" of the "free" surface of the aluminum moves with a velocity of  $I_2 = I_1 + \sigma_a = 2I_1$ ,

where

$$\sigma_{a} = \int_{\rho_{g}}^{\rho_{a}} \frac{C_{2} d\rho}{\rho} ;$$

(4) perturbations due to the effect of a peaked front on the detonation wave have been ignored.

We will return to these approximations shortly.

It is possible to measure D,  $S_a$ , and  $I_2$  by an apparatus originally designed by Goranson and altered somewhat to suit our experimental conditions. Briefly, the plane detonation wave is generated in a block of explosive 6x6x5 inches by a plane-wave booster. Aluminum plates of

varying thicknesses from  $0.010\,\mathrm{inchto}\,1.5$  inches have been used. The plates are drilled to allow insulated probes to be inserted at various known depths. These probes make contact with the bottom of the holes as the shock wave passes through the aluminum. Electrical pulses generated by these contacts are brought through coaxial cables and finally appear on a scope as "pips" on the calibrated sweep of a cathod-ray oscilloscope. From the positions of the pins and the times read from the scope, the shock velocity,  $S_a$ , is calculated. Another set of pins set at various known distances from the "free surface" of the aluminum make contact with it as it moves off into the air. By a similar method of recording and computing, the "free" surface velocity,  $I_2$ , is obtained. In most cases the detonation velocity is inferred from the density of the explosive with reference to the literature, but in a few cases we have been able to measure detonation velocities off the side of the charge by a similar, multiple-contact method. Some results of the measurements are given in Table 1.

TABLE 1

Factors	сомр в	TNT
$ ho_0$ (g/cc) D (m/sec) $I_2$ (m/sec) $S_a$ (m/sec) U (m/sec) P (kilobars) U (calc) (m/sec) P (calc) (kilobars) $ ho_0 D \times 10^{-6}$ (gm/sec/cm²) $ ho_a^0 S_a \times 10^{-6}$ (gm/sec/cm²) $ ho$ (g/cc)	1.70 7850 3450 7250 2130 283 1800* 245* 1.33 1.96 2.32	1.58 6880 2500 6880 1690 184 1500 173 1.09 1.86 2.10
$\frac{\rho_{\mathbf{a}}^{0} \mathbf{S}_{\mathbf{a}} + \rho_{0}}{2\rho_{0} \mathbf{D}} \mathbf{D}$	1.237 0.23	1.353 0.16
К	2.68	3.07

<sup>\*</sup>Extrapolated

In lines 7 and 8 are presented the quantities calculated by Brinkley and Wilson in OSRD 1707. The agreement is certainly qualitatively good and in most cases is within 10 percent.

What contributes to the difference between experimental and calculated values is an interesting field for thought. The calculated values, of course, involve some approximations and assumptions mostly arising, as I have previously mentioned, from lack of data at high temperatures and pressures on the simple gaseous products. The "experimental" values involve the approximations listed above plus, of course, the usual experimental variations. Much has been done to improve the apparatus. Considerably more remains to be done.

However, one would like to be able to estimate the errors incurred as a result of the aforementioned assumptions. Let us return to them.

- 1. Plane detonation wave. This is an experimental difficulty. Since the pins must be displaced laterally to avoid the effects of one interfering with the measurements from all the others, they are actually placed so that the contacts form a helix. If the wave is not planar to 0.01 microsecond, the velocities measured will be in error. Only a 2-in. diameter region in the center of the charge and plate is used, hence it is believed that this factor is under control.
  - 2. Shock wave returning into the explosion products is negligible. That is,  $R_1\rho = D\rho_0$

### ABLARD

Actually this can be avoided by matching the impedance of the plate and the explosive so that the reflection is reduced to zero as was suggested by Dr. Kirkwood. We expect to accomplish this by use of alloys of aluminum and magnesium. However, it is possible to show that for aluminum this does not introduce an error of more than 1 percent in the particle velocity. If we assume that the Hugoniot curve is approximated by an adiabatic of the form  $P = A\rho^{\kappa}$ ,

it follows that

$$\mathbf{R}_{1} = \sqrt{\frac{\mathbf{p}_{1} - \mathbf{p}}{\rho \left[1 - \left(\frac{\mathbf{p}}{\mathbf{p}_{1}}\right)^{1/\kappa}\right]}}$$

Hence for Comp B

$$(\rho R_1)' = 1.41 \times 10^6$$
  
u' = 2120 m/sec

compared with 2130, which is well within our present experimental error in determining u.

3. The free surface velocity is twice the particle velocity in the aluminum shock. That is,  $I_2 = \overline{I_1 + \sigma_a} = 2I_1$ .

We borrowhere heavily from the considerations of "Underwater Explosions," by Dr. Robert Cole, who showed by the application of the Tait equation that  $\sigma$  for water is within 2 percent of u for pressures up to 80 kilobars. If we assume that the Tait equation is also applicable to aluminum, it is possible to calculate from the present data a value of  $\sigma$ . This is done in the following way:

The Tait equation is:

$$P_2 = B \left[ \left( \frac{\rho_2}{\rho_g} \right)^n - 1 \right].$$

Assuming B, n, and  $\rho_0$  are only functions of the entropy, we readily calculate that

$$\left(\frac{\partial \mathbf{P}_2}{\partial \rho_2}\right)_{s} = \mathbf{C}_0^2 \left(\frac{\rho_2}{\rho_g}\right)^{n-1} = \mathbf{C}_2^2,$$

$$\mathbf{C}_0^2 = \frac{\mathbf{B}\mathbf{n}}{\rho_\sigma}$$

where

This allows analytical integration for  $\sigma_a$ :

$$\sigma_{\mathbf{a}} = \int_{\rho_{\mathbf{g}}}^{\rho_{\mathbf{a}}} \frac{\mathbf{c}_{2} d\rho}{\rho} = \frac{2C_{0}}{n-1} \left[ \left( \frac{\rho_{\mathbf{a}}}{\rho_{\mathbf{g}}} \right)^{\frac{n-1}{2}} - 1 \right].$$

We were able to fit the Tait equation using n=3 and B=253 kilobars. Checking back for  $C_0$ , we find  $C_0=5330$ , which compares well with 5400, a value obtained by averaging data from various sources in the literature, including the Lazarus data.

Finally  $\sigma$  was calculated from the integrated equation, resulting in a value of 1730 m/sec, compared to the observed  $I_1/2$  =1725 m/sec. A further analysis of the situation allowing variance

in n from 3 to 5 and differences in  $\frac{\rho_a}{\rho_g}$  from 1.3 to 1.5 showed that the maximum error one can expect from the "free surface" assumption is of the order of 3 percent.

4. Perturbations due to the shape of the detonation wave are ignored. I refer here to the Von Neumann picture of the shape of a detonation wave, assuming that the front consists of a shock wave of much higher pressure than at the Chapman-Jouguet condition. The pressure then falls during the subsequent reaction to the Chapman-Jouguet pressure.

Actually, the surface velocity measurements as a function of target thickness have produced a fortunate by-product in the form of confirmation of the essential features of this picture and have allowed estimation of the width of the reaction zone thereby. From measurements on aluminum and other metals, it has been shown that for thin plates the pressure predicted from the surface velocity measurements increases rapidly with decrease in plate thickness to a limiting value some 2.5 times the C-J pressure. Reaction-zone thicknesses were of the right order of magnitude as predicted by Eyring and others. Hence, this experiment shows promise of being a tool to measure the structure of the detonation wave. The picture is fogged, however, by the uncertainty in the above assumption. More work is needed on the theory of the transition of a reactive shock into a pure shock. A recent English publication by Armament Research Estabblishment, No. 22/50, has thrown additional light on the subject. Conditions of transition from detonation in one explosive to detonation in another are discussed. We have not digested this report completely and do not feel qualified to discuss it at the present time. However, it does not appear to be complete enough to settle our present questions.

What value do these experiments have? Which of the many paths will be the most fruitful to pursue?

If I may return now to equation (3), one will remember that, if we accept the assumptions or eliminate them by some means, we will have a knowledge of all the quantities in equation (3) except  $E-E_0$  - $\Delta Q$  and that by making measurements at various initial densities we will be able to calculate this quantity at different pressures and densities. The quantity  $E_0$  is the internal energy of the solid explosive at room temperature and one atm. We can conveniently select our standard state such that  $E_0=0$ , or it would be possible to calculate the difference between  $E_0$  and the internal energy at any other convenient standard state so that  $E_0$  is a known quantity. E is the internal energy of the product gases at the C-J pressure, density, and temperature in excess of what they would have at the same standard state. The quantity  $\Delta Q$  is the heat evolved in the reaction if it could be made to take place at the same standard state, and the products must reach the same equilibrium compositions as they would reach at the C-J temperature. Thus, it is here that most of the assumptions in the calculation methods appear. Suffice it to say here that accurate values of  $E-E_0$  - $\Delta Q$  from the independent surface velocities given as a function of the pressure would permit one to chose between the various assumptions to pick the one which best predicts these additional measurements. As yet we have found it unprofitable to make the calculations because of our uncertainty in U and P.

The adiabatic law assumed for the product gases with exponent calculable from such measurements has good possibilities for application in fragment-velocity theory. Since the experiments also give information on the metals, it is now possible to treat the interaction of explosions on metals with more confidence.

# INTERACTIONS OF DETONATION WAVES WITH MATERIAL BOUNDARIES

R. B. Parlin and H. Eyring Department of Chemistry University of Utah, Salt Lake City

Problems of detonation-wave interactions differ from similar problems involving shock waves in inert materials primarily through the consideration which must be given to the so-called "reaction zone," or the region between the detonation shock front and the Chapman-Jouguet point. The magnitude of this difference is largely determined by the size of this region, and this in turn is primarily a function of the kinetics of the chemical reaction process. Thus, an interpretation of the behavior of detonation waves in nonideal cases would appear to depend in large measure upon methods of analytically introducing the concept of the reaction-zone length into the conventional equations of the thermodynamic-hydrodynamic theory of detonation waves or shock waves.

While there does not at the present time appear to be any universal agreement among workers in the field, either as to the qualitative structure of the detonation wave or as to the general mechanism of chemical breakdown (2, 3, 4, 5), we shall here adopt the point of view previously described by the present authors (2), i.e., the detonation front consists of a <a href="mailto:shock zone">shock zone</a> of width possibly some tens of Angstrom units in which abrupt increases of pressure and temperature occur together with a smaller increase of density, followed by a <a href="mailto:reaction zone">reaction zone</a> in which the heated and compressed explosive reacts to give the equilibrium products at a temperature, pressure, and density as computed by the hydrodynamic-thermodynamic theory at the Chapman-Jouguet point. This reaction zone may vary from 0.1 to some tens of millimeters in length for ordinary condensed explosives. (In explosive dust mixtures reaction zone lengths as great as 10 meters have been reported by (Sir Geoffrey Taylor and others.)

It is convenient in the following analysis to disregard the width of the shock zone itself, together with the complicating effects arising from the lack of equilibrium between external and internal degrees of freedom in this region in an effort to obtain tractable equations. While it is recognized that the Chapman-Jouguet condition strictly applies only to stable plane detonation waves, we shall here effect only a partial correction to this condition following the procedure of Devonshire and others (1, 2), which may be stated as follows: the detonation velocity will be given by the sum of the material velocity and the local velocity of sound, both evaluated at the point in the reaction zone at which reaction is complete, except in the immediate neighborhood of boundaries, in which region these quantities will be evaluated at the point at which the rate of increase of pressure due to the change of chemical composition and entropy just equals rate of decrease of pressure due to the time rate of change of velocity and volume or that due to the curvature of the wave front. It is thus evident that, at least in part, the nonideality of real detonation waves may be ascribed to incomplete release of chemical energy. This effect can be accounted for approximately by assuming the shock front to be curved and such an analysis is used here.

### EFFECT OF CURVATURE ON STABLE DETONATION WAVES

Consider a spherical detonation wave assumed for the moment to be propagating with the stable detonation velocity D. Then the equation of continuity may be written

$$(D-W) dV/dr = -2VW/r - VdW/dr,$$
(1)

where as usual V is the specific volume, W the radial component of the material velocity, and r is measured radially from the detonation front. Letting the radius of curvature be  $\mathbf{r}_0$ , and integrating, one obtains

$$\frac{\mathbf{D}-\mathbf{W}}{\mathbf{V}} = \frac{\mathbf{D}}{\mathbf{V}_0} + 2 \int_{\mathbf{r}_0}^{\mathbf{r}_0} \mathbf{a} \frac{\mathbf{W}}{\mathbf{V}_{\mathbf{r}}} d\mathbf{r}, \qquad (2)$$

or, defining a quantity,

$$= 1 + \frac{2V_0}{D} \int_{\mathbf{r}_0}^{\mathbf{r}_0 - \mathbf{a}} \frac{\mathbf{W}}{\mathbf{V}\mathbf{r}} d\mathbf{r},$$
 (3)

the continuity equation becomes

$$\frac{D-W}{D} = \frac{V}{V_0} \sim V, \tag{4}$$

where a is the reaction-zone length, assumed constant. Using Equations (4) in (3), one may obtain a new form for the equation defining  $\mathcal{S}$ :

$$\gamma^{p} = 1 + 2 \int_{\mathbf{r}_{0}}^{\mathbf{r}_{0} - \mathbf{a}} \frac{\mathbf{V}_{0}}{\mathbf{v}} - \mathbf{v}^{p} d\mathbf{r}$$
 (5)

As a first approximation, it may be assumed that the integrand is sensibly constant through the wave, whence  $\gamma$  takes the form

$$\omega = 1 - 2(V_0/V_1 - 1)(a/r_0), \tag{6}$$

which reduces, for a great many solid explosives, to

$$\mathcal{S} = 1 - (a/2r_0) \tag{7}$$

as previously pointed out (2).

The equation for the conservation of energy is, in differential form, the same as it is for the plane wave:

$$dE + d(PV) + UdU = dQ.$$
 (8)

Integrating, and introducing the Abel equation of state, with a constant covolume  $\alpha$ ,

$$P(V - \alpha) = RT. (9)$$

We obtain then

$$P(\gamma V - \alpha) + \frac{1}{2}(\gamma - 1)(U^2 - D^2) = (\gamma - 1)(\Delta Q + \overline{C}_V T_0).$$
 (10)

In the above,  $\Delta Q$  is the heat of reaction per gram, U is the relative material velocity D-W, and  $\gamma$  is the ratio of heat capacity at constant pressure to that at constant volume.

### PARLIN AND EYRING

The equation of motion is again the same as for a plane wave and may be written

$$VdP + UdU = 0. (11)$$

This may be integrated approximately by introducing for U its value from the continuity Equation (4):

$$dP + (D^2/V_0^2) V dv' + (D^2/V_0^2) J^2 dV,$$
 (12)

which upon integration gives the result

$$P + (D^2/V_0^2) v^2 V + \frac{1}{2} (D^2/V_0^2) \int v^2 dV = Constant.$$
 (13)

For not too strongly curved waves, most of the contribution to the integral in Equation (13) will come from values of s near unity; assigning it this value gives the approximate expression

$$P + (U^2/V) (1 + v^2)/2 r^2 = D^2/V_0.$$
 (14)

In regions far from boundary disturbances, it may be assumed that the Chapman-Jouguet condition may be applied in the same manner as for an ideal plane wave, as discussed above. This leads, as in the traditional equations, to the expression

$$U_1^2 = P_1 V_1^2 \gamma / (V_1 - \alpha), \qquad (15)$$

where the subscript 1 refers explicitly to the values of P, V at the point of complete reaction (hence, approximately, at r = a). Introducing the value of the ideal (plane wave) detonation velocity,

$$D_i^2 = 2(\Delta Q - \overline{C}_V T_0) (\gamma^2 - 1)/(1 - \alpha/V_0)^2,$$
 (16)

Equations (4), (10), (13), (14), (15), and (16) lead to an expression of the form

$$\frac{D_{i}^{2}}{D^{2}} = \frac{\gamma + 1}{(1 - a)^{2}} = \frac{2x\left(1 - \frac{x + 1}{2}a\right)\left(\gamma^{2} + \frac{a}{2}(x - 1)\gamma - ax\right) + (\gamma - 1)\left(\frac{(x - 1)(3x - 1)}{4}\gamma^{2} + x(2ax^{2} - x - 1)\gamma + x^{2}(a^{2}x^{2} - 1)\right)}{\left(\frac{1 + x}{2}\gamma + x\right)^{2}}$$
(17)

or, for values of & not too far from unity, the asymptotic expression

$$\frac{D_1^2}{D^2} = 1 + \frac{(2\gamma - 1)a^2 + 3\gamma(\gamma - 1)a + \gamma(\gamma^2 - 2\gamma - 2)}{(\gamma + 1)(1 - a)^2} (1 - x^2) + O(1 - x^2)^2.$$
 (17a)

For the case in which the reaction-zone length, a, is comparable in magnitude with the radius of curvature,  $\mathbf{r}_0$ , the detonation velocity is not determined by the values of W and C (material velocity and local sound speed) at the point of complete reaction but at some previous point—specificially, at the point where the rate of pressure increase due to reaction is equal to the rate of pressure loss due to curvature, that is, the point at which

$$\left(\frac{\partial \mathbf{P}}{\partial \mathbf{N}}\right)_{\mathbf{V}} \frac{\mathbf{dN}}{\mathbf{dt}} = \frac{2\mathbf{C}^2 \mathbf{W}}{\mathbf{V} \mathbf{r}_0} . \tag{18}$$

Now  $(\partial P/\partial N)_V z P_1$ , and  $dN/dt z 1/\tau$ , where  $\tau$  is defined as the reaction time and is given by the expression

$$\tau = \int \frac{d\mathbf{r}}{\mathbf{U}} z \frac{\mathbf{V}_0}{\mathbf{V}_1} \frac{\mathbf{a}}{\mathbf{D}} . \tag{19}$$

Combining these equations gives, in the case that Equation (7) holds, the result

$$(D_i/D)^2 = 3.88 a_i/r_0,$$
 (20)

with the coefficient 3.88 replaced by a more cumbersome f ( $\mathcal{S}$ ,  $V_0/V_1$ ) in the more general case. In view of the approximations resorted to, it has not seemed profitable to use the more exact expression in this instance.

In general, Equations (6) (or (7) if applicable) and (17) determine the reaction-zone length for a given curvature of the wave front and a known detonation velocity. If the wave front is curved, but does not have uniform curvature, we may make the assumption that small regions of the front are approximately spherical and that the equations above are obeyed for such small regions with a given radius of curvature. If the wave as a whole is propagating at a velocity D and we consider a point on the front whose radius of curvature vector makes an angle  $\phi$  with the axis of the charge, then if the wave proceeds without change in shape the radial component of the detonation velocity is

$$D_{r} = D \cos \phi , \qquad (21)$$

and for a given reaction-zone length the radius of curvature may be obtained from Equation (17) together with the definition of  $\theta$ . (D of Equation (17) and  $D_r$  of (21) are now identical.) By a step-by-step numerical or graphical procedure, the successive spherical arcs may be connected until the angle  $\phi$  between the normal to the front and the axis reaches 90°, or a value somewhat smaller as determined by the shock-wave velocity in the boundary material. Three cases are considered, depending upon the nature of this surrounding medium.

1. When the explosive charge is surrounded by air or other material of very low density, we may assume that the angle between the attached shock wave in the air and the axis of the charge may be taken as essentially zero. Using the analysis above, with  $0 \le \phi \le 90^\circ$ , the values in Table 1 are obtained, where R is the radius of the charge. The values above

TABLE 1

 $D/D_i$ a/R 0.00 1.00 0.11 0.950.200.90 0.29 0.85 0.40 0.80 0.520.750.68 0.70 0.820.65

are appropriate to the detonation of TNT of loading density 1.57 g/cc, covolume  $\alpha=0.422$  cc/g, and  $\gamma=1.24$  for the product gases. Similar calculations for other solid explosives indicate that for moderate deviations from ideality one may use the approximate relation

$$(D/D_i) = 1 - A a/R,$$
 (22)

where A is a function of the parameters above but differs only slightly from the numerical value 0.5.

2. If we assume that the explosive charge of radius R is surrounded by a sheath of material of neglible thickness but of mass  $\sigma$  per unit area, then it may be assumed that the confining action

arises from the inertia of the case. Thus the limiting value of the angle  $\phi$  will be determined by the fact that the elements of the sheathing move with the same velocity as the adjacent particles of explosive in the direction of the normal to the wave front at the point of intersection. Assuming the pressure at this point, approximately  $P_1$ , the value at

### PARLIN AND EYRING

the end of the reaction zone, to be acting for a time  $\tau$ , the reaction time, to produce a momentum  $\sigma W_1 \sin \phi$ , one obtains the expression

$$P_1 \tau = \sigma W_1 \sin \phi. \tag{23}$$

Using ideal wave values for  $P_1$  and  $W_1$ , Equation (19) for the reaction time au, and the definition

$$W_{c}/W_{e} = \frac{2\pi R\sigma}{\pi R^{2}/V_{0}}$$
 (24)

for the ratio of the mass per unit length of casing to that of the explosive, one obtains the expression

$$\sin \phi = 2 \frac{V_0}{V_1} \frac{a/R}{W_c/W_e} \tag{25}$$

Equation (25) defines the value of  $\phi$  at which the shock front reaches the edge of the charge in the procedure sketched in case 1 and hence the value of R, the radius of the charge. Representative values of the quantity  $(a/R)^2/(W_c/W_e)$  are listed in Table 2 for assumed values of  $D/D_i$ , for TNT with properties corresponding to those of Table 1. Empirically, the calculations for a

large number of solid explosives indicate that the relationship between  $D/D_i$ , charge diameter R, reaction-zone length a, and the relative mass of the charge sheathing  $W_C/W_C$  can be expressed by the equation

$$D/D_i = 1 - 2.17 \frac{(a/R)^2}{(W_c/W_e)},$$
 (26)

where, as before, the numeric 2.17 is an approximation to a function of  $V_0$ ,  $\alpha$ , and  $\gamma$ , and has been averaged over a number of substances. It should also be pointed out that the diminution of the detonation velocity for a given a/R ratio is only slightly dependent upon the angle  $\phi$ .

TABLE 2

sin ø	$(a/R)^2/W_cW_e$			
	$D/D_i = 0.95$	$D/D_i = 0.90$	$D/D_i = 0.85$	
0.065	0.017			
0.075	0.017			
0.10	0.020	0.041		
0.15	0.020	0.042	0.066	
0.12	0.020	0.043	0.066	
0.25	0.020	0.044	0.068	
0.30	0.021	0.045	0.071	
0.35	0.022	0.045	0.070	
0.40	0.024	0.047	0.073	
0.45	0.024	0.050	0.076	

3. If, on the other hand, the bounding material is effectively of infinite extent but of considerable density relative to air, it may be assumed that interaction of the shock front with the surrounding medium is due to the setting up of a shock wave in this material. Here we must assume that the pressure and the particle velocity agree at the point of intersection of the detonation shock front and the material boundary. We assume as before that the normal component of the detonation velocity at the intersection is  $D_r$ , and that the normal to the shock front makes the angle  $\phi$  with the axis of the charge. The shock wave in the casing has the normal velocity  $D_c$  at a corresponding angle  $\phi$ . That is,

$$D_r = D\cos\phi_r, D_c = D\cos\phi_c.$$
 (27)

Matching pressures and material velocities at the boundary leads to the condition

$$P_{c} = P_{r}, W_{c} \sin \phi_{c} = W_{r} \sin \phi_{r}. \tag{28}$$

The hydrodynamic conditions in the explosive and in the surrounding material respectively are

$$P_r V_0 = W_r D_r, \quad P_c V_c = W_c D_c. \tag{29}$$

Combining Equations (27), (28), and (29), one obtains for the angle  $\phi$  the expression

$$\tan \phi = (V_{0c}/V_{0}) \sqrt{(D^{2}/D_{c}^{2}) - 1}$$
 (30)

Since the velocity  $D_C$  of the attached shock wave in the case is seldom known experimentally, it must be calculated from the sonic velocity C in the surrounding material and its equation of state; for velocities not too far from sonic, the velocity of the shock wave in a solid may be expressed as

$$D_c = C (1 + AP),$$
 (31)

where A is the compressibility of the solid. Since the pressure is given in the present approximation as

$$P = \frac{D^2 \cos^2 \phi}{V_0} \quad \frac{1-a}{1-\gamma} \quad , \tag{32}$$

it is possible to determine  $\phi$  from the preceding three equations. Again returning to the procedure of case 1, knowledge of  $\phi$ , the angle with which the normal to the wave at the point of contact with the boundary meets the axis of the charge, permits the calculation of the reaction-zone length, a, for any given value of the ratio  $D/D_i$ , the deviation of the actual detonation velocity from the ideal value. Table 3 gives calculated results for a typical case (TNT with constants as before). Again it is possible to average the results for a variety of substances and write

$$D/D_i = 1 - 0.88 (a/R) \sin \phi,$$
 (33)

where the angle  $\phi$  must now be determined from the characteristics of the casing material.

Calculations based upon Equations (22), (26), and (33) give, for the reaction-zone length, a, the values given in Table 4.

TABLE 3

sin ø	(a/R) sin $\phi$ when D/D <sub>i</sub> =		
Sin φ	0.95	0.90	0.85
0.04 0.05 0.065 0.075 0.10 0.16 0.20 0.25 0.30	0.053 0.045 0.042 0.043 0.050 0.050 0.051 0.051	0.109 0.104 0.107 0.111 0.112	0.165 0.164 0.171 0.178
0.35 0.40 0.45	0.054 0.059 0.061	0.112 0.118 0.124	0.175 0.183 0.190
		<b></b>	

### PARLIN AND EYRING

### TABLE 4

Substance	Confinement	Loading Density	Reaction Zone (cm)
Picric Acid	Glass	0.90 g/cc	0.22
<sup>2</sup> RDX	Glass	0.90	0.083
$^{2}60/40$ Amatol	Steel	1.48	0.398
<sup>3</sup> Minol-2*	Lead	1.69	0.538
<sup>3</sup> TNT**	Steel	1.613	0.0346
<sup>3</sup> TNT**	Steel	1.60	0.036

Parisot, A., and Laffitte, P., Congr. chim. ind., Compt. rend. 18me congr.,

### TIME-DEPENDENT DETONATION WAVES

Let us suppose now that a stable detonation wave, either ideal or otherwise, passes from one material into another, where the second medium is characterized by different physical and chemical properties, in particular by a different density and heat of reaction. During the period between one stable regime and the next, an unstable time-dependent detonation wave will exist which may be characterized analytically either by its change in reaction-zone length or by a change in the curvature of the wave front with time. Since it has not been found possible to take into account these factors explicitly, a somewhat different approach has here been followed. It is known that the detonation velocity is determined by the sum  $W_1$  -  $C_1$  at the end of the reaction zone. For a wave whose velocity is changing, the conditions at the Chapman-Jouguet point will not be apparent at the shock front for a time au, where au is the time required for a signal to traverse the reaction zone and is essentially the reaction time. Thus, if

$$C_1 - W_1 = D_{\tau} , \qquad (34)$$

and if, for small perturbations, we may write

$$D_{\tau} = D + \tau (dD/dt), \tag{35}$$

we obtain the expression

$$(dD/dt) = -D - W_1 - C_1 = -U_1 - C_1.$$
(36)

Again, for small perturbations, it may be assumed as a first approximation that the equation of continuity and that for the conservation of energy apply as for a plane wave, without change, whence

$$U_1/D = V_1/V_0 = (\gamma + \alpha/V_0)/(\gamma + 1)$$
 (37)

$$P_{1}(\gamma V_{1} - \alpha) + \frac{1}{2}(\gamma - 1)(U_{1}^{2} - D^{2}) = (\Delta Q + \overline{C}_{V}T_{0})(\gamma - 1)$$
(38)

and, introducing the definition of the velocity of sound, and changing the time derivative to a space derivative,

$$C_1^2 = P_1 V_1^2 \gamma / (V_1 - \alpha)$$
 (39)

$$\tau (dD/dt) = a(V_0/V_1) dD/dx.$$
 (40)

Nancy (1938), 930-6

<sup>2</sup>Copp, J. L., and others, Unpublished reports

<sup>3</sup>MacDougall, D. P., and others, Unpublished reports

\*Angle \$\phi\$ taken as 20° from the velocity in lead of a shock produced by

Pentolite, 2745 m/sec
\*\*Angle \$\phi\$ taken as 8° 10' from the velocity of sound in steel, 5130 m/sec

### PHYSICAL ASPECTS

One finally obtains the result

$$a(dD/dt) = (V_1/V_0)^2 \left\{ \sqrt{D_i^2 - G(\alpha, \gamma, V_0)(D_i^2 - D^2)} - D \right\},$$
 (41)

which, for small  $D_i$  - D, may be approximated by the expression

$$a(dD/dx) = 0.333(D_i - D),$$
 (42)

where the coefficient 0.333 is again a mean value for solid explosives. This approximately logarithmic decay equation has been verified for a few detonation waves decaying from an initially high velocity. It should be pointed out that the quantity D<sub>i</sub> in Equations (41) and (42)—the ideal velocity-may be replaced, in the present approximation, by any stable velocity related to the ideal, plane-wave velocity by the preceding equations. The scattered results presently available are assembled in Table 5.

### TABLE 5

$^{1}2C0 + 0_{2}$ , $D_{i} = 1.76 \times 10^{5}$ cm/sec $^{2}$ Nitroguanidine, $V_{0} = 1.89$ cc/g $^{3}$ TNT, $V_{0} = 1.0$ cc/g, $R = 1.27$ cm $^{4}80/20$ Amatol, $V_{0} = 0.61$ cc/g	a = 1.1 cm 0.88 0.076
$\frac{480}{20}$ Amatol, $V_0 = 0.61$ cc/g	3.9
<sup>5</sup> Ballistite, $V_0 = 0.954 \text{ cc/g}$	0.22

 $^{
m l}$ Bone, W. A., Frazer, R. P., and Wheeler, W. H., Phil. Trans. 235, 29-68 (1935) Photograph number 3141, ERL, Bruceton, Penna. Photograph number 11, ERL, Bruceton, Penna. Photograph number 3737, ERL, Bruceton, Penna. <sup>5</sup>Gurton, O. A., Proc. Roy. Soc., A204, 32 (1950)

## REFERENCES

- (1) Devonshire, A. F., Theoretical Research Report No. 3/43
- (2) Eyring, H., Powell, R. E., Duffey, G. H., & Parlin, R. B., Chem. Rev., 45, 70 (1949)
- (3) Kistiakowsky, G. B., Third Symposium of Combustion, Flame, and Explosion Phenomena, Williams and Wilkins (1949), pp. 560-5
  (4) Ubbelohde, A. R., ibid., 566-571; Proc. Roy. Soc., A204, 25 (1950)
- (5) Von Neumann, J., OSRD Report 1140 (1942)

#### PARLIN AND EYRING

### DISCUSSION

DR. KIRKWOOD: Dr. Parlin's paper is open for discussion.

DR. JACOBS: In connection with the curvature of the wave front, I wanted to make a couple of comments. When Jones proposed his theory, the expansion of the gases in back of the wave front, he said nothing about the shape of the wave front itself, but he used a "Meyer" approximation for the outflow; that is, the flow around a wedge. That is a fairly good approximation, and actually our present knowledge on rarefaction theory gives us a chance to look further into that. I don't think anyone has ever done too much about trying to draw a characteristic net through the reaction zone, but there has been some work done (by the Germans on wedges) of drawing a characteristic net behind a detonation shock. Actually there is a bibliography reference to it in Courant and Friedrich's excellent book on supersonic flow and shock waves. The paper has been translated by Brown University recently. I think it's of interest.

DR. PARLIN: I think it is a useful approximation to assume this region is quite small, and I think this can be small for the wave shapes that people have reported in literature and photographic studies.

# SESSION IV

12 January 1951

# PROBLEMS AND FUTURE DEVELOPMENTS

George B. Kistiakowsky Harvard University Chairman

	•	
1	43	1
9	w	-

## PROBLEMS AND FUTURE DEVELOPMENTS

## George B. Kistiakowsky Harvard University

We started this meeting with remarks by the first chairman on how nice it was to see so many old friends. I'd like to say that after two days it's still nice to see them all here. But at the same time this feeling is slightly moderated by another feeling—that it would have been nice if there were more new faces. I have, somehow, a feeling that maybe the rate of increase of personnel, of scientists who are interested more or less in the field of detonation and explosion, is not quite keeping pace with the needs of this country. And I hope that Dr. Roberts, later on, will talk a little more on this subject.

I have another topic which I will take a few minutes to discuss, and that is in reference to the Zeldovich-Von Neumann priority claim. This fall, having a little more time than I had for several years, I decided it was a good time for me to read some Russian literature in the original, since I am able, with a little difficulty, to do so. And having read, now, about a dozen papers, I got a very uncomfortable feeling that we do not have that order of magnitude of technical superiority over the Russians, at least in the field of explosions, that the newspapers almost convinced me we have generally.

And to give you just an example, here is the Von Neumann discussion of the structure of detonation waves, which was classified, and was terribly important in the development of our thinking. But Zeldovich publishes the same thing in open Russian literature three years earlier. That same paper by Zeldovich contains a reasonably adequate treatment of the charge diameter effect on the detonation velocity as applied to gases—again, something like two years ahead of Jones' discussion applicable to solid explosives.

Once they have the gas theory, there remains such an obvious extension to the solid explosives that one can have no doubt but that they had a full understanding of these phenomena sooner than we had.

During the war, G. I. Taylor developed what quite a few of you have heard referred to as the Taylor instability—what happens when a medium of low density pushes a medium of high density (which is, for instance, applicable, to the expansion of a gas bubble in water). This, again, had rather important, at least military-scientific, applications; but Landau has published the same discussion applied to gases in open Russian literature in '43—a little bit ahead of Taylor's classified report.

That is not all, because, for instance, in '46 I ran across a paper in which delays in initiation of lead azide, measured in fractions of microseconds, were discussed under special conditions. And you see, again in '46 something was published that we're very much interested in right now.

So I'm quite concerned about this and quite interested in dispelling the notion that we are automatically ahead of them. And it seems to me we have to realize that we are not—certainly not in this field—and that we have to make considerable effort to stay ahead, if we are ahead, or to forge ahead if we aren't.

Incidentally, as one minor corollary to that feeling, it seems to me that it would be highly desirable if this Russian literature—which, of course, since it is open literature, largely

# PROBLEMS AND THE FUTURE

concerns gaseous explosions but does contain a lot of interesting thinking applicable generally—were translated into English by competent translators. I've seen one or two translations done by NACA, and at least one of those is completely unintelligible. The man who did the translation knew the English and knew the Russian, but didn't know either kinetics or hydrodynamics.

Well, I hope that ONR or some powers that be elsewhere can take some steps in this direction. It represents the outlay of some money, and finding the right personnel—among whom I'm afraid I can't be counted—to do the job. Well, my time is limited, and I won't steal all the fire from Jack Kirkwood's coming remarks on new developments, but I couldn't resist saying a few things about this general point. After having listened to the discussions, I feel that very interesting and very significant progress is being made but that we don't know everything there is to know about detonations and related scientific areas. And I am talking not from the point of view of military hardware but that of general understanding of the phenomena involved. For instance, we ought to just mention the equation of state, which certainly has been discussed, but which certainly is not settled.

The question of solid residue from an equation-of-state point of view has not been exhaustively treated, and so there are, I think, very important and interesting and challenging problems in the general field of shocks, which are tied in to the effectiveness of explosives—for instance, the impact-loading of solid materials and also shocks in liquid and gaseous media.

I think that the initiation mechanism, thought of broadly, is extraordinarily important. I mean, already as a question of hazards in handling munitions, it has an important practical application which some of us, at least, do know. There were unpleasant catastrophes during the last war which should not have happened if explosives had only the sensitivity which they were supposed to have. In other words, occasionally they seem to have very different sensitivity.

Questions like that have not received really scientific explanation. One thing that occurred to me, of really quite considerable interest, as I was listening to the talks in this conference, was the observations on hydrazine nitrate, where we notice an extraordinary drop in velocity at high density. It was also pointed out that amitol levels off in velocity at high densities. Velocity does not increase with density as it should, according to the normal equation of state. In some dynamites, as I recall, there were very definite maximums observed, just as they were observed in hydrazine nitrate.

Now, it's obviously tied in with the thickness of the reaction zone, because the effect seems to vanish in cartridges of large diameter—or at least is minimized. And that, in turn, suggests that the voids between the solid particles in an explosive have some very important role in propagating detonation. That has never been really sufficiently studied and understood. We know perfectly well that we can make explosives extraordinarily insensitive to detonation propagation by bringing the density nearer the true crystal density. Hence, as we take out the voids from the explosives, it becomes more and more difficult to propagate detonation.

I won't mention, now, the more applied work, but I feel that in that area, also, a great deal can be undertaken. But the problems I mentioned—at least, a good fraction of them—can be undertaken not only in government-organized and—managed laboratories, but even, some of these problems, in colleges and small private laboratories. The more applied work, under present conditions, probably has to be limited to government establishments.

# THEORETICAL DEVELOPMENTS IN DETONATION

# John G. Kirkwood California Institute of Technology

Substantial advances in our theoretical knowledge of the process of detonation in high explosives were made during World War II. New general theoretical approaches were suggested by G. I. Taylor and J. Von Neumann. The structure of the reaction zone was studied in detail by H. Jones and by H. Eyring on the basis of the nozzle theory and the curved front theory, respectively. Systematic calculations of detonation velocities, based on the Hugoniot conditions, the Chapman-Jouguet condition, and empirical equations of state were carried out by H. Jones, by E. B. Wilson, Jr., and by S. R. Brinkley, Jr. In spite of these notable advances, which were of great practical importance in guiding experimental investigations and in providing a basis for decisions on the military use of high explosives, many fundamental aspects of detonation phenomena remain obscure and are in need of further investigation.

Among the general problems requiring further investigation are those of initiation and the propagation of nonsteady detonation waves in solid and gaseous explosives. For this purpose a more detailed study of the structure of the Von Neumann spike, in which the detonation reaction takes place, and of its relation to the Chapman-Jouguet condition, seems to be called for. The dynamical investigations of the Chapman-Jouguet condition by G. I. Taylor and by J. G. Kirkwood and S. R. Brinkley, Jr., provide a starting point for these studies. Such studies should throw light on the mechanism of the transition from deflagration to detonation, which is at present only very incompletely understood.

In the exploration of new explosives of increased power, studies of the kinetics of the detonation reaction with solid reactants, of which aluminum is the representative example, seem to be essential. For underwater use of such new explosives, it is of critical importance to know the distribution of energy between the shock wave and bubble oscillations. This problem should receive special attention both from the theoretical and experimental points of view. It is related not only to the detonation process in the explosive but also to the propagation of the explosion wave in the exterior medium, air or water, in which the weapon is used. For rapid approximate estimation, the propagation theories of J. G. Kirkwood and S. R. Brinkley, Jr., can be used. For an understanding of the finer details of the transmission of the energy of a detonation wave into the exterior medium, more exact integrations of the equations of hydrodynamics with the use of modern computing facilities seem to be called for.

Although the theoretical prediction of detonation velocities has met with considerable success, it frequently fails for explosives leading to products outside of the composition range of conventional explosives. These failures are unquestionably due to inadequate knowledge of the equation of state of the product mixtures. In order to make these aspects of the theory of detonation reliable, a fundamental study of the equation of state of fluid mixtures in the range of thermodynamic variables encountered in explosion products is imperative. On the theoretical side, the best compromise would seem to be to utilize the free-volume theory of Lennard-Jones and Devonshire to the fullest extent, in spite of the approximate nature of this theory. For this purpose it would be necessary to extend the free-volume theory to gas mixtures. Some progress along these lines has already been made by I. Prigogine. On the experimental side the most promising approach appears to be the study of P-V-T relations in gas mixtures, the composition of which simulates that of explosion products, by transient techniques, for example with the pin technique for measurement of particle velocity and techniques involving the observation of the propagation of shock or rarefaction waves in fluid mixtures.

#### PROBLEMS AND THE FUTURE

I will conclude my remarks by elaborating a bit on equation-of-state problems. As Dr. Brinkley pointed out this morning, it is impossible to determine the equation of state of the products of an explosion from a study of detonation velocity as a function of loading density. This was not at first recognized, but it is responsible for the fact that so many different empirical equations of state yielded satisfactory results in representing this particular relationship.

Of course, it is possible to determine the equation of state, using the detonation process as an experimental technique, if one measures certain other variables—for example, particle velocity, which is difficult to measure, or temperature, which is still more difficult. But these approaches to the equation-of-state problem are essentially experimental.

Dr. Brinkley and Dr. H. Jones have proved—Dr. Brinkley outlined the proof this morning—that the equation of state is not determined by the information which one gets merely from studying detonation velocity as a function of loading density. And from the theoretical point of view, it seems rather futile for this reason to explore other empirical equations of state. A number have been used, and used with a certain amount of success. Rather, it would seem desirable to do the best one can with a purely theoretical equation of state. As I have mentioned in my remarks, I believe that the Lennard-Jones-Devonshire equation of state, based on the free-volume theory, provides the best compromise. It is sufficiently simple so that the computations will not be hopelessly involved, and I believe that it is sufficiently accurate from the range of thermodynamic variables encountered in explosion products to give reliable results.

A recent survey of the applicability of the Lennard-Jones-Devonshire equation of state to pure fluids—pure gases and liquids—has been made by Dr. Hirschfelder. He finds that the equation of state is very poor at intermediate densities—densities of the order of the critical density or less—but that at densities of the order of ordinary liquid densities the equation of state is quite reliable.

I could outline certain of the quantitative features of setting up a free-volume theory for mixtures, but I think I will not take our time to do this. I will merely mention some of the assumptions which can be made. One will make the usual assumptions of the free-volume theory for pure liquids, and, in addition, one will assume that in the detonation front the neighbors of any given molecule are randomly distributed, that is, that the fraction of nearest neighbors of a given molecule in a liquid of a given type will be proportional to the gross mole fraction of molecules of that type.

Combining this hypothesis of randomness with the other features of the free-volume theory, one can obtain an equation of state for fluid mixtures which is not especially complicated and which I believe may settle, once and for all, when the appropriate calculations are made, the controversy about what equation of state should be used for explosion products and should allow, I think, for the extension of calculations of detonation parameters with some degree of confidence to explosives yielding products of unconventional composition. And, after all, that is what is necessary if the theory is to be fruitful.

#### DISCUSSION

DR. SNAY: I will make a short remark on the evaluation of the covolume factors of the Kistiakowsky-Wilson equation of state which we have made at NOL. Most of the failures in the prediction of the detonation phenomena mentioned today are probably not due to any inadequacy of this equation of state but to the fact that its covolume factors were incorrect. For instance, the covolume factor for  $\rm H_2O$  was believed to be of the order of magnitude of one hundred. In our investigations this factor was found to be near to the value two hundred and fifty. As long as such discrepancies exist, it is not surprising that unsatisfactory results are obtained. It should be mentioned that this procedure is a straightforward determination of the empirical parameters of an assumed equation of state from measured detonation rates, and it

#### KIRKWOOD

is interesting to note that the values recently obtained are very close to those first published by Kistiakowsky and Wilson in 1941.

As far as the evaluation of the covolume factors is concerned, it is true that this should be done with the use of equilibrium calculations—as pointed out by Dr. Brinkley in his paper today. We did not apply equilibrium calculations but performed the evaluation for two typical product compositions. First, we assumed that all the available hydrogen is completely oxidized to  $\rm H_2O$ . The oxygen left is assumed to combine with the carbon forming  $\rm CO_2$  and  $\rm CO$  in oxygen-rich explosives or  $\rm CO$  and solid carbon in oxygen-deficient explosives. In the other set of calculations it was assumed that  $\rm CO$  is formed first of all. (All this applies to nonaluminized explosives.) These two arbitrary modes of the decomposition of an explosive include a fairly wide range of possible product compositions. The surprising result was that we obtained practically the same covolume factors in both cases. We might, therefore, conclude that the determination of the covolume factors is not too sensitive to the assumed composition of the products.

MR. RUTH: Professor Kirkwood mentioned several problems that still need attention. In that connection, I would like to mention that the matter of sensitivity is still one of the most poorly defined, or at least poorly understood, of the aspects of explosions. And it seems to me that it would be profitable, as the theory of detonation is developed, to attempt to establish a theoretical relationship between sensitivity and detonation.

For example, if we define sensitivity as the ability to propagate the detonation wave stably, we might, by measuring the rate of detonation in two columns—one large and one small—be able to calculate the minimum diameter of a column of a particular explosive which would give stable detonation and use this minimum diameter as a criterion of sensitivity. Following along these lines, we might eventually establish some sort of an absolute criterion on sensitivity.

MR. STRESAU: I might suggest that sensitivity is a more complicated problem than that for the simple reason that, in handling, deflagration might be almost as disastrous as detonation. And we definitely know that some materials, which are rather easy to ignite, are rather difficult to detonate. Materials which are more readily detonated and which are harder to ignite are also well known. For example, in high explosives, PETN is a good bit easier to detonate than tetryl, yet a good bit more difficult to ignite.

Take lead azide and lead styphnate, for example. Lead styphnate is very sensitive to static. It's very easy to get enough of a charge on your body to set off lead styphnate. I've seen it demonstrated very nicely. Lead azide takes much more energy to set it off. But still, lead azide will detonate almost immediately and will detonate in very small columns, whereas lead styphnate is a very difficult material to get to detonate at a high rate.

This is an example of the difficulty in that approach. The difficulty is that sensitivity is so many things it's hard to get any kind of an absolute criterion of sensitivity. This, I imagine, is the big difficulty with sensitivity, anyway — that it's a combination of so many factors.

This, of course, brings up the question of the transition from deflagration to detonation. Perhaps this is a problem that can be expressed in terms of a general relationship which applies to both processes. The rate of propagation of the reaction of an explosive material, whether it is detonation or deflagration, is always a direct function of pressure. We usually consider either stable detonation, which involves very high pressures and velocities, or stable deflagration, which involves much lower pressures and velocities. It is reasonable to believe that these processes are related by a continuous curve in the pressure-mass rate plane. The two processes may not be as different as is usually supposed. As the pressure is increased, a point is reached where it is difficult to determine whether the velocity gradient is due to the improvement in heat conductivity with increasing pressure or the increase in shock velocity with pressure. This point of view is supported by the fact that, with various primary explosives

#### PROBLEMS AND THE FUTURE

under various conditions, we have observed propagation velocities covering nearly the whole velocity spectrum. Thus the point at which deflagration turns to detonation may be rather hard to define.

The transition from deflagration to detonation is usually so sudden because the intermediate reactions are generally extremely unstable. This instability can be traced to rather simple considerations.

In the reaction of any explosive we must consider a system, not unlike that of a solid-propellant rocket, in which both the rate of gas evolution and the rate of gas escape are direct functions of pressure. The rate of gas evolution is directly related to the propagation rate. (In a column which is reacting at the end only, the rate of gas evolution is proportional to the propagation rate.) The velocity in such a system is stable only if the rate of evolution is equal to the rate of escape, and the rate of escape increases more sharply with pressure than does the rate of evolution. If the rate of evolution is less than the rate of escape, the pressure, and hence the propagation rate, will reduce to such an equilibrium point or extinguish. If the rate of evolution exceeds the rate of escape, the propagation accelerates until stable equilibrium is achieved.

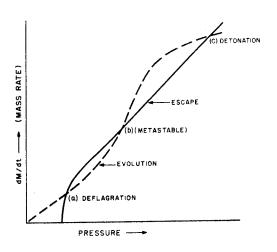


Figure 1 - Mass rates of gas escape and evolution vs. pressure

These ideas are expressed graphically in Figure 1, where dM/dt is the mass rate for both evolution and escape of the gas and P is pressure. The solid curve is the escape velocity versus pressure, and the dotted curve is the rate of evolution versus pressure. The crossings at (a) and (c) are stable equilibria of the kind mentioned above, and that at (b) is a metastable equilibrium above which the reaction will accelerate to (c) and below which it will die out to (a). For the purpose of the present discussion, the shape of the curves is unimportant, except that the three crossings are necessary. The two crossings at (a) and at (c), which correspond to stable processes, are necessary since at least two stable processes, detonation and deflagration, are observable for almost all explosive materials. The crossing at (b) is a necessary condition for the other two.

In general, the shape of the pressure-escape rate curve is determined by the hydrodynamic properties of the surrounding system, while that of the pressure-evolution rate curve is determined by the properties and state of aggregation of the explosive.

All rate phenomena connected with explosive reactions can be described in terms of these curves. In the case of stable plane-wave detonation, high propagation and reaction rates combine to reduce the hydrodynamic system to a one-dimensional system which needs to be considered for only a limited length. Diameter effects in detonation are quite plainly the result of an upward displacement of the escape rate-pressure curve due to the radial components of gas flow. Those concerned with the stability of operation of solid-propellant rockets have applied these concepts quite successfully.

As applied to the growth of detonation, two or three simple cases can be visualized. First, the reaction may be initiated by an external impulse which is vigorous enough to start it at a point on the curve above (b), in which case it will grow to a stable detonation in a very short time. Second, it may start as a stable deflagration (point (a)), but a perturbation of the system, such as a change in loading density with length, may be enough to displace one or the other

#### KIRKWOOD

curve so that they no longer intersect at (a) and (b) but only at (c). Third, it may start as stable deflagration and the discharge system progressively change (as with a lengthening discharge path) in such a manner that (a) approaches (b) until they coincide.

This last case probably explains the results described by Dr. Roth, as well as those which I described earlier, in which a deflagration grew quite suddenly to a detonation after a reasonably reproducible interval.

In all of these cases the rate of growth is determined by the evolution rate-pressure curve and the pressure-time curve. The pressure-time curve is in turn determined by the difference between the rate of evolution and the rate of escape and the free and interstitial volume of the system. In some cases, the elastic or strength properties of the confining system may also be important. Application of these concepts depends upon an extension of our knowledge of propagation rate-pressure relationships over the whole pressure spectrum.

DR. BRUNAUER: Perhaps you will forgive me, now, if I talk about the military angle of the situation. Since we in the Navy, as you so well know, are used to assigning priorities to various projects, I'd like to tell you which, in my opinion, is the most important part of the field to work on. And by that, I mean not from the theoretical point of view—because I guess from the fundamental scientific point of view any problem is as important as any other—but rather from the point of view of what is most urgent for us to know to help us in our further research.

Military explosives have three important properties, none of which are physically definable quantities: power, sensitivity, and stability. There are no units of measurement for these, either physical or chemical. About stability we need not worry. Little was said about it in this conference. That's a chemical problem, and apparently most of our interests, in this particular group, happen to be in physics. But two of the properties have been discussed here—sensitivity and power. The word "power" has not been used, but its manifestations, such as shock waves, have been discussed.

A lot of good and interesting work is in progress in the field of sensitivity, but I'd like to tell you right now that the thing which interests us most is power. I think we can tackle the problem of sensitivity. We know how to detonate explosives. We also know how to avoid detonation of explosives—namely, by careful handling.

So I don't mean to say for a moment that it would not be important for us to know a lot more about sensitivity, but I do believe that that is not the most important thing for us to find out quickly to help us in our research work. What we would like to know more about is how to produce powerful explosives. In other words, explosives which produce a lot of damage — more than our present explosives—by means of shock waves or fragmentation or shape charges.

Even within that field, permit me to specify what I consider as the most urgent for us to find out. I mentioned it, and Dr. Kirkwood mentioned it; Dr. Kistiakowsky mentioned it, and several others, without assigning priority. We so far have mentioned it along with all the other problems.

As I see it, the properties of the shock waves and the detonation velocities are not very sensitive to the form of the equation of state. I'm not sure whether our trouble at present is due to the fact that we don't have the best possible equation of state; it may be that the Kistiakowsky-Wilson equation of state would serve us almost as well as a better equation of state. Our main problem is this: that we encounter, now, explosives which have a much larger fraction of solid products than any explosives with which we dealt in World War II. Within a few weeks, I am going to recommend to the Bureau of Ordnance a new explosive and I expect it will be adopted. It's a modification of an old one, but a more powerful one, and a more damaging one for underwater purposes. It has twice as much aluminum in it as our present explosive. Our present explosive is the best military explosive used at present in the United

#### PROBLEMS AND THE FUTURE

States. This new one will contain twice as much aluminum. In other words, there will be more solid products in the explosion.

Now, since this explosive is already developed, perhaps we don't need any further theory for it. However, we have in the books a whole series of new explosives which have been inadequately tested, or not tested at all, but which appear good on paper. All of them have the common characteristic of having more power, and a much higher percentage of solid products than those used in World War II. So our No. 1 problem is to find out how to handle the theory of these particular types of explosives. The reason why we need it so urgently is because of the shortage of manpower for experimentation.

If Dr. Brinkley could grind out for us the results, after the theoretical considerations have been settled, he could save us a lot of experimentation for which we don't have the manpower. In other words, the progress will be rather slow in the field unless theory helps us out on this score.

If a new equation of state can take care of it, of course it would be a tremendous help. But if there are other considerations necessary to find out what happens to these solids, and to take them into account in the detonation process, then I believe this is a field about which I should like to ask Kirkwood and the others to think seriously, and to help us out in the shortest possible time.

DR. SNAY: At NOL we also made theoretical investigations on explosives which form solid reaction products. A theory is now developed for such cases, and I don't think that the presence of solid particles is the reason for difficulties encountered in calculations on such explosives. The greatest difficulty we have at present is that we do not know accurately enough what the reaction products of an explosive are. For instance, it is still an open question whether the heat of explosion of TNT is 1000 cal/gram or 800 cal/gram, or somewhere between these values, corresponding to the various possible compositions of the reaction products. Our knowledge is even more scanty in the case of highly aluminized explosives. Questions like these, of course, could be attacked by means of equilibrium calculations. Although the determination of the detonation pressure and gas density (and perhaps the evaluation of the empirical parameters of an equation of state) is not very sensitive to the accuracy of the equation of state used, the equilibrium calculations are. Here, we are in particular need of a good equation of state for highly compressed gases.

We made calculations on detonation phenomena assuming the solid particles to be either compressible or incompressible. Comparison of such calculations with experiments have shown that the adiabatic compressibility of the solids can usually be neglected in comparison with that of the gases. However, the actual density of the solids at the Chapman-Jouguet point is an important factor which must be taken into account. This magnitude can be evaluated from measured detonation rates. For carbon we had the interesting result that at high loading densities the assumption of the diamond state leads to a good agreement with the experimental evidence, but the assumption of graphite does not. Perhaps this is a possible way to make diamonds.

DR. BRUNAUER: I'm sorry I'm not entirely as optimistic as Dr. Snay. Just what Dr. Snay said points up one of the difficulties. He stated that there is a considerable discrepancy, unless he assumes that the carbon is in the diamond state. But the point is that it is not a healthy situation if one has to assume such artificial things in order to explain the results where carbon is the product.

Now, as far as aluminum oxide is concerned, there are no two varieties of aluminum oxide of widely differing densities so that we can manipulate between them, and I don't know yet what the results of Dr. Snay are on that. But it seems to me that there are a lot of other things also to be considered. What happens with the solids? I mean, how are they heated up, and do they move or not move in the detonation process, and so on?

#### KIRKWOOD

DR. KISTIAKOWSKY: In the great diamond controversy, the answer, I think, is really this: that the carbon which is formed is not in a state of graphite. I mean, that's come out of our calculations on acetylene-oxygen mixtures. But in the sense of such calculations, you cannot distinguish between diamonds and what I might call an activated carbon—that is, an extremely finely divided soot with a very high surface area, particles only a few hundred Angstroms on the average. The surface-free energy will increase over-all energy content sufficiently so that this finely divided carbon cannot thermodynamically be distinguished from diamonds. It's extremely interesting that this result comes out in the case of solid explosives, because it certainly comes out of our acetylene calculations. I'm rather confident that you can't assume graphite as the product. But if you just say, well, you've got activated carbon, then of course you're a little freer than if you talk about diamonds. And I think you do get good agreement.

DR. SNAY: I would not like to say that the problem of the solid products is completely solved. I'm not so very optimistic about this. But there are probably some more difficult problems from the viewpoint of thermodynamics (for instance, the composition of the gases). But the difficulty is this: the equilibrium composition is very sensitive to the form of the equation of state and there is probably where we actually need a good equation of state.

DR. HIRSCHFELDER: I just wanted to raise the point that when one speaks about an equation of state, in the use of the covolume, he is really getting away with quite a bit. And you get away with it because your equations are particularly insensitive to the equation of state used. However, there's a second place where your equation of state comes in, and this is in your equilibrium constants. In your equilibrium constants you have to deal with it, and you really have to use activities in place of concentrations. And I think this is the place where one is really very sensitive to an equation of state parameter. What are you going to use for the activities of the individual components? And I think this might be the main excuse for further work along equation-of-state lines—to get decent equilibrium constants.

DR. BRUNAUER: First of all, I'd like to state that I stand corrected by Dr. Snay and Dr. Hirschfelder. I see that the equation of state is extremely important. So far, all the discussion was in the direction that it is not too sensitive for calculations of detonation velocities and detonation pressures. But it is true that the equilibrium constant is of vital importance in these calculations, and for that reason we do need the best possible equation of state.

DR. COOK: I don't want to sound like I'm trying to force anything, but if the Navy's willing to stoop to barnyard-type equations of state, the one we use is the one to calculate solids. I mean, we've tried it on lots of explosives in the dynamite industry. We have considered explosives that have very high solid residues—some of these 15-10 percent dynamites—for example, high aluminum compositions. This equation assumes that the covolume  $\alpha$  is the same function of V for all explosives—solids as well as liquids. And I think we have ample proof of this. If you're not too much concerned about theoretical justification of it, the fact that it will work means that we're in business as far as calculating detonation properties and as far as calculating available energy is concerned. That equation has been pretty well demonstrated in our studies of dynamites. I'm not going to tell you any details of that but simply that it does work—so well that I think it might be of interest to apply it.

I might say that, in cases where reactions are incomplete in the detonation wave, all you have to do is increase the diameter, and you'll eventually get to the calculated velocities on those explosives as well as you do on these military explosives. Sometimes you can't go to as high diameters as necessary—that is, to get the theoretical velocity.

In one explosive we figured that we'd have to have a 57-inch-diameter column or diameter explosive to get the theoretical velocity. But we do get theoretical velocities in a 9-incher sometimes, and sometimes even in a 6-incher, or less, in most explosives. And we have a number of velocity-vs.-diameter plots that show that the velocity has leveled off, so that we know that we're dealing with the hydrodynamic velocities. So I think the fact that it's already been tested

## PROBLEMS AND THE FUTURE

is a good justification to use it where it's impossible by other methods to put together the equation of state from the covolumes of the specific products.

In fact, I think that it will be a terrific problem when it comes to trying to put together an equation of state from the component parts, particularly for explosives with solid residues. Lack of heat data and lack of compressibilities, etc., are going to make it almost impossible. But the fact that, in our methods, there seems to be no distinction between completely gaseous explosive products and those with solid residue is, I think, complete justification to use it whenever you need it.

DR. BRUNAUER: Now, could I ask just this question of Dr. Cook, or anybody else? Have detonation velocities been calculated on explosions where there are no gases, for example, aluminum-liquid oxygen where the product is aluminum oxide? Can you tackle it, or can anybody else?

DR. COOK: I think that you'll find that a certain part of it is gaseous.

DR. BRUNAUER: What if you do not have any gas?

DR. COOK: I think you handle it the same way. I haven't gone clear down to a zero amount of gas on these calculations, but I've gone very low, and I don't see any reason why it won't work. If it's true that you have an explosive that will explode and produce a detonation without any gas in it, I'll predict that this method will work on that.

Incidentally, I'd like to say something else in regard to aluminum and in regard to a correlation of fragmentation and things of that sort. Maybe many of you aren't familiar with it, but we did obtain a straight-line correlation between detonation pressure and impulse—that is, the cavity effect in shape charges. Now, that was for a constant charge. And we also found that, if we make a sort of correlation of a detonation head, like Dr. Jacobs talked about, it is a linear correlation. That is, the pressure—or the detonation pressure, as calculated from the Chapman-Jouguet condition—times the size of that detonation head gives you a figure proportional to the impulse in the cavity effect, and things of that sort, e.g., end impulse, booster effects, etc.

I think that's a pretty complete correlation. I don't think there can be much objection to it. Now, as far as aluminum is concerned, those studies showed pretty well that aluminum just doesn't react in a detonation wave (in small diameter charges). This has been discussed by the French and by the Germans and by the Russians, and I think everyone has come to that opinion now. Unless it's very finely divided aluminum, very little of it, if any, gets into the detonation wave.

DR. KIRKWOOD: This has a bearing on the question of reactions yielding solid products. In calculating detonation velocities, when one gets too high a fraction of aluminum, it's possible that one will run into a pathological family of Hugoniot curves—of the kind discussed by Von Neumann—in which they have an envelope. One can express this in a different way, and that must always be taken into account in making such calculations.

DR. JACOBS: I wasn't going to suggest that, but possibly the aluminum acts as inert in small charges. That wouldn't be too surprising if rarefaction set in in a matter of a few microseconds. If the aluminum normally takes 10 or 20 microseconds to react, then for small charges you are really working on a partial-reaction Hugoniot, and you don't have to make it pathological; it could be normal.

DR. KIRKWOOD: Yes, although presumably, in an underwater explosion, you would get full reaction of the aluminum. Your remark had to do with a stick of small diameter, such as would quench the reaction with aluminum.

#### KIRKWOOD

DR. JACOBS: In the case of underwater, where they have spherical symmetry and central detonations, you hold the gases under fairly high temperature for a considerable length of time, behind the detonation, so that they could still react, even though they may not react in the detonation zone.

DR. ROBERTS: The question of personnel came up as I was making a few visits before deciding on the program for the conference, and I tried to influence certain people to attend. Some of them had the opinion that they had made their contributions to the field of detonation and explosion and that it was time that the problems be turned over to younger people with fresh ideas. That stimulated my own thinking about the possibility of getting new men into the field of detonation to consider the problems and perhaps put new ideas and new talents to work.

I think the getting of new manpower into fields of interest to the military establishment can be considered as one of the responsibilities of the Office of Naval Research program. I've always looked at the program as producing two types of products: (1) the scientific papers which are published, and (2) probably more important, the scientific manpower to conduct future research and come out with new ideas for both technological and military development.

Now, I think this is all I really have to say on this subject, but I would like to hear opinions from the people who are in the educational field about how one might go about training new people. If we could influence a few of the real good graduate students into thinking about these problems, it would be worth while.

DR. LEWIS: I would like to see established at one or two, or more if possible, universities courses on the general subject of combustion including of course combustion of solid explosives. To my knowledge there is no university where such a course is being given. I believe this is the only way to get young people—new people—interested in the field.

DR. LAWRENCE: Pertinent to the subject of manpower and personnel, especially in connection with the younger men, is the problem of deferments. We have a young man working on a project which we understand is quite important, and his draft board began to breathe down the back of his neck. So following the practice of World War II, we put in a deferment for him with considerable confidence, and we seemed to be getting nowhere fast. Then he got married, and he was deferred, right off. We have two or three other young men that we need for this program who may be in the same category but who haven't said anything about getting married.

DR. BRINKLEY: I have just a comment to make in line with comments that have already been made on personnel problems and which I'll make in the light of an experience we had at the Bureau of Mines last summer. We found, by a close scrutiny of Civil Service regulations, that it's possible to avoid a lot of the red tape and to hire on a training basis young men who are in the course of their academic preparation. We did so in the case of three individuals last summer, and that experience was exceedingly gratifying. These three people were employed on fundamental research projects that contributed to their own professional preparation, and they were employed on projects that were of benefit to the Bureau of Mines. We were able, that way, to offer them slightly more money than they could have gotten in the usual type of summer employment open to undergraduates and graduates, and I think we were able to contribute to their training.

We had one young man in particular who did quite an extraordinary job in solving a difficult mathematical problem associated with the theory of combustion. He carried it to completion in the time available to him. And I think we had the by-product of having converted a young man of considerable promise from particle physics to continuum physics. That may provide an attractive way to interest promising people in the field, and I suggest that it's worthy of consideration not only by the other government laboratories represented here but by the industry.

## PROBLEMS AND THE FUTURE

I'd like, incidentally, to invite those in this audience who are in academic work to suggest to any very good undergraduate or graduate students that the Bureau of Mines will consider applications for employment of that sort. We wish to expand that program. We're not interested in them unless they're good, but we hope in that way to do our part in interesting more and more people in the general problems of continuum physics.

# Second ONR SYMPOSIUM on DETONATION

February 9 and 10, 1955 NATIONAL ACADEMY OF SCIENCES Washington, D. C.

February 11, 1955 U. S. NAVAL ORDNANCE LABORATORY White Oak, Maryland

> Sponsored by OFFICE OF NAVAL RESEARCH DEPARTMENT OF THE NAVY

### FOREWORD

These papers are to be presented at the Second Symposium on Detonation being sponsored by this Office on 9, 10, and 11 February 1955. Two volumes are being issued, one containing the unclassified and the other the classified papers. Inasmuch as these preprints are receiving a limited distribution they are not to be considered as a substitute for publication in appropriate scientific journals.

The object of this symposium is to bring together scientists from government, university and industry to discuss recent advances in theory, experiment and application in this field of chemical physics.

This Office is of the opinion that the symposium at which these papers will be discussed will stimulate new research in this complex field. The relationship of advances in the knowledge of detonation phenomena to the effectiveness of the use of molecular explosives makes this aspect of science of importance to the Department of the Navy and the Department of Defense.

To all those who are contributing papers and plan to attend this symposium, the Office of Naval Research expresses its appreciation.

F. R. FURTH

Rear Admiral, USN

Work.

Chief of Naval Research

## CHARGE PREPARATION FOR PRECISE DETONATION VELOCITY STUDIES

Edward James, Jr.
Los Alamos Scientific Laboratory
Los Alamos, New Mexico

# INTRODUCTION

High precision determination of detonation velocity in solid explosives presents special difficulties not associated with liquid and gaseous explosives. In particular, the problem of homogeniety with respect to density and composition is peculiar to solids. Particle size distribution also has an effect on detonation velocity which, of course, is not encountered in homogenous explosives. These factors especially must be rigorously controlled in order to achieve the desired confidence intervals in our detonation velocity studies.

To accomplish our aim of the highest degree of homogeneity obtainable, a great deal of development work has been done in the past few years. The various development phases, to mention only a few, have included design engineering, instrumentation, rheological studies, casting techniques, pressing techniques, analytical methods, and data analysis. Obviously, all of this work cannot be treated within the scope of this paper; therefore, this discussion is limited to casting, pressing, machining and inspection techniques.

Some detonation velocity data are presented to show the degree of precision obtained.

# CASTING

A complete description of the casting techniques used on the various explosives studied here at Los Alamos Scientific Laboratory would be needlessly long. I have, therefore, selected "Grade V New Composition B" produced by Holston Defense Corporation as being representative of a typical ordnance explosive and will describe the experimental methods and techniques related to detonation velocity studies on this material in some detail. Other common cast explosive

have been just as thoroughly studied but the techniques involved generally differ only in detail, not in principle.

Melt Preparation

We use 30- or 50-gallon vacuum melt kettles to melt our explosive. For most precise detonation velocity work, smaller kettles introduce an undesirable variability because several melts may be required to prepare enough material to complete an experiment.

Our kettles are equipped with two agitators, each with a variable speed control. One of the agitators, a large anchor-type, conforms to the hemispherical contour of the jacketed kettle bottom and the blades are pitched so as to impart an upward movement to the melt. The second agitator, a smaller turbine-type, is offset and at an angle from center. This turbine stirs in opposition to the anchor.

The temperature of the melt is controlled by a sensitive hot- and cold-water proportioning system supplying circulating water to the jacket and capable of holding the temperature of the melt to + 1°C. During the melting operation the temperature differential between the jacket and melt is kept to a minimum to prevent local overheating.

A vacuum system is used which can maintain the kettle at pressures as low as 25 mm Hg. Figure 1 is a simplified illustration of a melt kettle.

We conduct a series of experiments to determine the optimum melting procedure and, for any subsequent experiment, the different steps and conditions are exactly specified. Attention is paid to the effect of variations in time, temperature and speeds of agitation since they undoubtedly affect the rheology of the melt in a complex fashion. It is known for instance that the particle size distribution of RDX in Composition B and the attendant apparent viscosity is sensitive to the melt procedure. Long periods of unduly high-temperature stirring tend to eliminate the finer RDX crystals, presumably through preferential solubility in the liquid TNT phase and then redeposition on the larger RDX crystals.

Our procedure for melting a 275-lb batch of Composition B in a 30-gallon kettle allows one hour melting time and subsequently 30 minutes of stirring at 25 mm absolute pressure. Jacket temperature is at a maximum of 110°C when melting is started and automatically reduces to 83° by the time melting is completed. The anchor agitator operates at 30 rpm and the turbine at 100 rpm.

Casting

Efforts to cast cylindrical charges of the desired diameter for rate sticks, even with long riser sections, have been abandoned. Our molds are designed with the idea of achieving minimum composition and density spreads within a region of the casting large enough to include a number of rate sticks. The casting is sawed into sections,

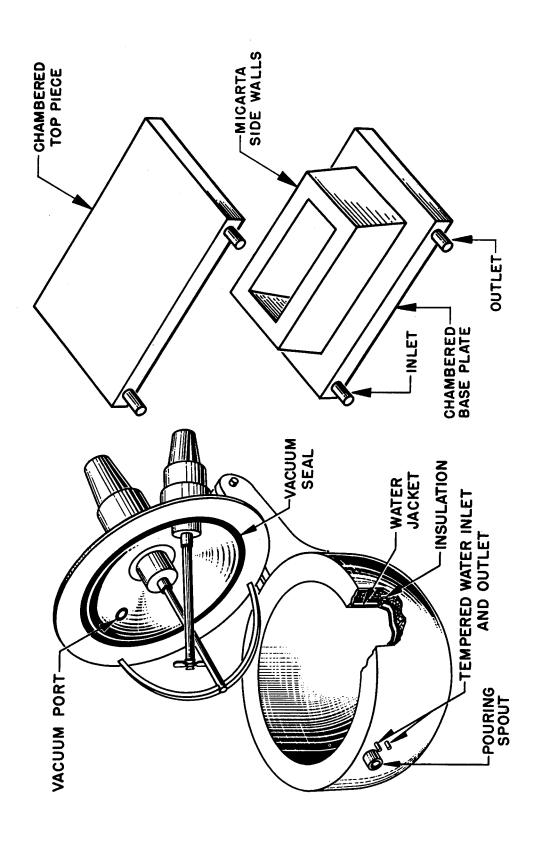


Figure 1 Melt Kettle, Y-3 Design

Slab Mold

Figure 2

121

the poorest sections discarded, and the rate sticks machined out of the high-quality pieces.

The mold used to produce the castings for most of our experiments is illustrated in Figure 2. This mold makes a slab approximately 8-inches high and 12 x 16 inches on a side. Both the top and bottom heat transfer section of the mold are supplied with individually program-controlled circulating water. Temperatures are maintained within + 2°C and cycle timing controlled within + 5 minutes. The side walls are made of a laminated cloth impregnated with phenolic resin (Micarta) which serve more or less as an insulator and prevent freezing from the sides inward. The rest of the mold is made of 245T dural.

In our procedure for Composition B we preheat the mold to 90°C (at least two hours are required for the Micarta side walls). Pouring is done at 83°C and care is taken to insure that little or no air is entrapped. The melt is allowed to settle in the mold for two hours with the top plate at 85°C and bottom plate at 90°C. During this time the RDX settles to its equilibrium packing arrangement in the fluid TNT. At the end of the two-hour settling period, temperature in the bottom plate is reduced to 50°C and freezing from the bottom started. Two hours later temperature in the bottom plate is further reduced to 30°C and held for an additional six hours. During this ten hours the top plate remains at 85°C. Next, the top plate is lowered to 80°C and the two plates held at their respective temperatures for six hours more, at which time the tempered water supply to the top plate is cut off. Temperature of the bottom plate is maintained at 30°C for six additional hours and finally turned off. Three hours later the mold is disassembled, the casting removed, placed in an insulated box and allowed to remain for at least twelve additional hours. The top half of the slab is then sawed off and discarded. The remainder of the slab is now ready for the sawing and machining.

This rather involved procedure is the result of a development program in which various time and temperature cycles were tested and the optimum procedure selected on the basis of the radiographic inspection as well as the results of a statistical analysis of composition and density spreads. Sample plugs were removed from representative castings and subjected to a submersion density check and a chemical composition analysis. Thus we determined that the casting procedure described in the preceding paragraph has a 95% certainty of producing, over the lower four-in. thickness, a casting with maximum density spreads of 0.010 gm/cc and composition spreads of 2.3% RDX.

The procedure described is for Composition B containing 0.1% of an additive which is a 50/50 weight mixture of o-nitrotoluene and p-nitrotoluene. These additives form a cutetic with TMT which apparently contributes a great deal toward making strain-free castings. Similar casting procedures have been worked out without any additive but they are much more time-consuming.

The Micarta side walls play, we believe, a role in making a more or less strain-free casting. Their low heat conductivity allows the liquid/solid interface to move as a plane from the bottom of the casting mold upward during the freezing process. At least this is true for the first four inches. After the first four inches are frozen, we are not much concerned with the upper region except that the upper region, if frozen too fast, can induce strain in the lower section. We deduce this freezing pattern by observing the orientation of the TNT crystals at various levels of the casting. We also observe that when freezing is deliberately induced from the sides inward, a strained casting results. Numerous cracks are invariably present and if the casting is subjected to even minor temperature variations there is a tendency for it to warp.

Our concern with strain-free castings has to do with a desire to produce charges with little or no tendency to develop cracks between the time they are fabricated and fired. It is clear that, should cracks develop after dimensional inspection, the inspection results are no longer the true measure of the dimensions of the test charge.

## PRESSING

At Los Alamos Scientific Laboratory we have studied a number of formulations similar to Composition A but with a variety of other binders. Those with a relatively high softening point seem preferable when the purpose is to produce charges of maximum quality.

Most of these explosives are made by a slurry process similar in principle to the process used in the manufacture of Composition A. When very high melting point binders are used it is convenient to dissolve the binder in a suitable solvent. The solution is then added to a violently agitated aqueous dispersion of RDX. The solvent is then stripped from the slurry by distillation. Subsequently the slurry is filtered and then dried. This process, if properly controlled for the specific wax, produces more or less spherical granules about 1 mm in diameter.

Such explosives are most conveniently fabricated by compression molding in an evacuated die. Certain of the inherent difficulties of cast explosives, such as the settling problem and attendant composition inhomogeniety, either do not exist or are of a much smaller degree in pressed explosives. In fact, we have seldom been able to demonstrate compositional variation within a single pressing. Usually, analytical differences are of the same order of magnitude as the errors of analysis, and statistical tests show no significance in the compositional spreads reported.

The story of density spreads is somewhat different. Large density spreads are observed if pressing is done without evacuating the mold cavity. A considerable amount of development work has gone into various techniques of molding and we have concluded that only vacuum molding will produce the charges of sufficiently high quality

for precision detonation velocity work.

Figure 3 illustrates one of two types of vacuum molds in use here for charge preparation in detonation velocity studies. The molding process is quite similar to conventional compression molding used in the plastics industry, the principal difference being in the additional vacuum feature.

The mold is constructed of 4340 steel except for the punches and the metal immediately surrounding the die cavity. These are made of "Crocar", a high alloy oil-hardening tool steel. The "Crocar" is hardened to Rockwell 57 ± 2C. The mold surfaces are polished to a mirror finish. This high polish contributes to easy ejection. The mold is chambered to permit water circulation through both the top and bottom punch as well as around the die cavity. Vacuum sealing is done with the "O" rings illustrated. Clearances between punches and die are of the order of one mil per inch diameter.

The heat transfer system is similar to the one used in casting and capable of equally precise temperature control. It operates, however, at an input pressure of 95 psia and a suction pressure of 55 psi; therefore, temperatures up to 150°C are attainable.

The mold is installed on an Elmes 300-ton compression-molding press equipped with a semi-automatic control circuit. After loading the mold with molding powder the operator has only to start the cycle. The rest of the operation is automatically controlled by a series of relays and time clocks. In this way, absolute uniformity of timing is insured.

Heating explosives powder in the mold is rather wasteful since the mold is more efficiently utilized in actual pressing. Therefore, we preheat our powder in trays to a temperature depending on the formulation in a steam-heated forced-draft oven. When a fairly rigid binder is used, temperatures as high as 115°C may be necessary. The powder is transferred to the mold at the same temperature and the remotely-controlled pressing cycle begun. The press ram carrying the lower punch and the die advances to a prepress position, thereby compacting the powder slightly. After five seconds, the ram retracts to evacuation position. A poppet valve in the upper punch opens and evacuation begins at a slow rate through a throttled vacuum line. prepressing and throttling are both intended to minimize entrainment of molding powder. At the end of 15 seconds, the density of the residual air being pumped out is sufficiently low so that entrainment ceases to be a problem. At this time, full vacuum is applied and at the end of one minute total evacuation time, the absolute pressure in the mold cavity has been reduced to less than 1 mm Hg. The press now goes on compression stroke simultaneously with the closing of the vacuum valve. Pressure applied is usually around 13,000 psi. Fifteen seconds are required to completely close the press. The leak rate of the mold at 1 mm Hg is about 0.1 mm Hg per minute, so during the fifteen seconds elapsing after the vacuum is cut off and full

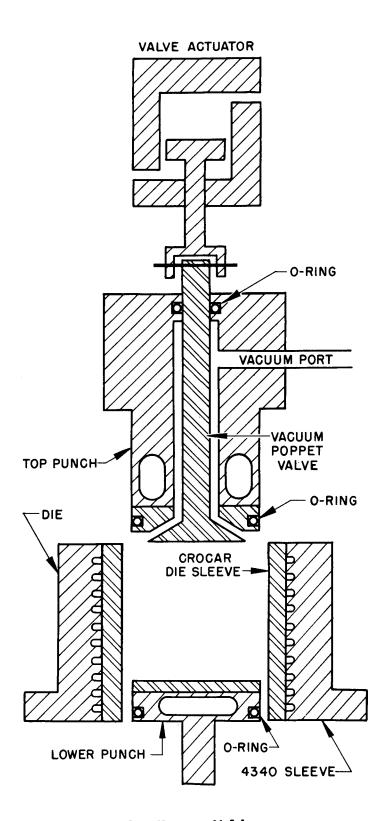


Figure 3 Vacuum Mold

compression occurs, the pressure rise is insignificant. The pressure dwell lasts 20 seconds. At the end of the cycle, the press ram retracts and the molded charge is automatically ejected. If an appropriate minimum molding temperature has been selected the charge is, of course, still at this temperature, but sufficiently rigid to be handled. It is then cooled slowly, either by wrapping in an insulating blanket or placing in an insulated box. Cooling usually takes 12 hours or so. This slow cooling is necessary only when large charges are pressed. Certain compositions are less sensitive than others to thermal shock and therefore even the largest charges do not require any special handling during cooling.

Just as with cast charges, we require that a usable pressed charge shall be free of cracks.

The procedure described above is quite general for most formulations. For example, Composition A with wax of the usual melting point is pressed by exactly the same procedure except the temperature need not be above 70°C and indeed densities of 1.63 gm/cc are readily attained by pressing Composition A at room temperature.

We have had more success in pressing high-quality TNT than we have had with casting. We are able, routinely, to press to a density of 1.62 gm/cc and for us to obtain an equivalent density with cast TNT has been a matter of occasional rare luck. The pressing procedure for TNT is identical to the one outlined above except that we use a 70°C preheat and 70°C mold temperature. In the case of TNT, temperatures must not exceed 75°C or some local melting will occur.

The specific procedure described is by no means the only one which can be used to make high-quality charges. The procedure merely happens to suit our particular equipment and in the interests of reproducibility it is rigorously observed. The procedure works well on very large pressings and has been successfully used on 12-in. dia. x 8-in. high charges.

We do not attempt to use explosives as they come from the pressing operation, but rather we consider our pressings to be machining stock. The various rate sticks are machined from the pressings just as we do with cast explosives; the only difference being that with pressed explosives we have no riser section nor non-uniform region which must be discarded.

Extensive density-spread analyses on individual pressings show typically maximum spreads of 0.005 gm/cc in the six-inch diameter pressings and standard deviation of density about the mean of the sampling-plug density is 0.0023 gm/cc. Between-piece population standard deviation of density runs in the neighborhood of 0.0015 gm/cc. Composition variations within a single pressing and between pressings from the same lot of raw material are less than 0.2%. As stated before, composition analyses usually give spreads which are

statistically indistinguishable from the analytical error.

## MACHINING

Both the rough castings and the pressed blanks are machined to the final dimension. No very special techniques not already familiar to the machine-tool industry are employed, but certain additional safety precautions are observed. For example, before explosives are submitted for routine machining, a high-speed machining test is done on a remotely-controlled drill press with a face milling tool. Speeds as high as 1400 rpm and feeds of 0.045 in. per revolution are employed. On a six-in. dia. charge the linear cutting rate is as high as 2200 ft. per min. at the edge. When a test explosive survives this test without any evidence of decomposition it is considered safe to machine with flat-edged milling tools or the pointed tools common to lathe work at rates up to 200 ft. per min. Cut-off tools and drills are an exceptional case because effective cooling of the cutting edge is difficult. This latter type of machining operation is considered hazardous, and the drilling of small-diameter deep holes especially is avoided.

Most rate sticks are cylindrical. The operation of cutting the cylinder to the correct diameter is usually done first. The cylinder is then sawed to an appropriate length and finished dimension obtained either by milling or facing off on a lathe. Rectangular sticks are prepared by milling alone.

Whenever possible, machining is done while flooding with water. Water-soluble and porous explosives are machined dry. Dry machining, we feel, is justified insofar as the high-speed test is done without water.

The fragility of certain explosives, in particular cast materials, poses a special problem not often encountered in normal machining practice. Securing the piece to be machined on the lathe or mill requires that special vacuum chucks be used with large pieces. Small pieces do not have sufficient area for vacuum chucks to work so we use "Lucite" collets since ordinary metal collets cause excess breakage.

# INSPECTION

Radiographic

Before machining, all charges are subject to radiographic inspection. In this manner cavities and cracks are detected. Should any defects exist the charge is rejected.

Dimensional

Diameter and length measurements are made with conventional measuring devices such as micrometers, dial indicator gauges and, on occasion, a cathetometer is used for cross-checking.

Temperature control during inspection is essential because the explosives under investigation all exhibit the high linear coefficients of expansion characteristic of organic compounds. The value of the coefficient of thermal expansion almost invariably lies in the range of  $7 + 2 \times 10^{-5}$  in./in./°C.

Most cast explosive charges containing appreciable amounts of TNT exhibit an irreversible growth when subjected to temperature cycling. This phenomenon is believed due to certain impurities in TNT; e.g., DNT. The net result is that Composition B and TNT charges, when stored in a magazine for any length of time, will show considerable growth and reinspection is therefore necessary. In order to avoid excessive growth we also make an effort to fire the charges with a minimum delay once they are machined. Also they are protected against excessive temperature variations.

Some explosives may show slight shrinkage on aging. Once the shrinkage has taken place the pieces are dimensionally stable. We therefore allow such sticks to age some time after machining before the final dimensional inspection is made.

Density

A density determination is made on every charge intended for velocity work. The method used depends somewhat on the geometry and size of the piece. The density of small-diameter charges is most easily and perhaps most accurately determined by measuring the volume by the submersion method. We compute the volume of all larger charges from the dimensional inspection data and obtain the density from the volume and weight. We compare the values obtained by each method on a selected intermediate size. Charges are classed according to the density determination and, in the case of pressed charges, only those within + 0.001 gm/cc of the average density are accepted for detonation velocity work. Cast charges for obvious practical reasons cannot be held to this tight a density selection specification; however, a + 0.003 gm/cc tolerance is considered acceptable.

Although each of the density methods give standard deviations which are of the order of 0.0003 gm/cc, when an individual sample is checked a number of times there is some question of the absolute accuracy of the average. For example, the average density of a lot of one-half-inch diameter charges whose density is determined by displacement, is as much as 0.002 gm/cc higher than the density calculated from dimensional data. Just which method gives the more nearly correct answer is not known. The submersion method suffers the disadvantage that when complete wetting is obtained the results may be spurious due to some capillary penetration. On the other hand, insufficient wetting would cause the apparent volume to be too large, just the opposite effect of penetration. The density computed from dimensional inspection data obtained on small charges is undoubtedly in error to some degree since the surfaces are not truly smooth because of tool marks. Density values by each method for pieces of one inch in diameter and larger

check within 0.0005 gm/cc. For a given lot of pieces machined from a single charge we assume that the small-diameter rate sticks (less than 0.500 in.) have the same absolute density as the density determined for the larger pieces cut from the same charge. The standard deviation of the density we ascribe to the series of small-diameter rate sticks is, however, taken from the displacement volume measurement data. We justify this reasoning by the fact that we believe the submersion method gives relatively high precision, even though we suspect its absolute accuracy.

# Composition

Composition analyses on Composition B are done in the usual manner.(1) Our data indicate that the analytical procedure described in the JAN specification produces a standard error of about 0.1%.

Every cast rate stick increment of a composite explosive is sectioned in such a manner that a sample plug is cut from the regions just beyond each end of the stick. By proper arrangement of the sampling pattern, additional data on the composition adjacent to the central region is obtained. Selected charges from the slab are accepted for detonation velocity measurements only if composition spread inferred from the composition analysis adjacent to the specific charge is no more than 0.5 percent RDX. Composition spread analyses are not done on vacuum-pressed charges because of their inherent uniformity; however, lot analyses are performed routinely on the molding powder itself.

Methods of analysis of explosives mixtures vary somewhat with the type of formulation. Except for the use of a solvent picked for the specific components of the explosive, the procedure is similar to the one used for Composition B. Analytical precision of the order of 0.1% is obtained for most mixtures involving RDX.

Detonation velocity measurements are usually corrected to a common density and composition. The velocity correction factor we use for Composition B with respect to density is 3400 m/sec/gm/cc and for composition is 10 m/sec/gRDX. Several other values are used by workers in the field but the exact values are not highly important for small corrections.(2)

# Particle Size

Pressed explosives such as TNT present a problem in describing their particle size distribution. It is a simple matter by conventional wet-screening methods to obtain a distribution characteristic of the molding powder. Whether or not this distribution has any real meaning after the explosive has been highly compressed to almost crystal density is not known. At any rate, we have followed the line of least resistance and we characterize the particle size distribution of a simple pressed explosive by the numbers obtained from the screen analysis on the powder before pressing.

The situation with respect to composite cast explosives is more confusing. In Composition B, solution and recrystallization of RDX during melt preparation as well as during the manufacturing process alters the original distribution, especially of the finer fractions. Extracting TNT from samples of the finished casting and determining the new particle size distribution is perhaps the best approach but the extraction procedure itself also suffers from the same inherent difficulty of probably causing some change in particle size.

The situation in Composition A is not quite as complex as observed for cast explosives. The RDX is relatively insoluble in the wax phase and for those compositions employing a solvent for the wax the process time during which the RDX is subjected to solvent action is quite short compared to the time involved in the Composition B system. Therefore, a determination of particle size distribution of the RDX used in preparation of the mixture is a fair indication of the final particle size in a pressed piece. Some crushing of the RDX particles must occur during pressing but it is to be remembered that the wax probably contributes a cushioning effect.

Some of our formulations include a fine fraction which passes through a 325 mesh screen. The distribution of this fraction is determined by a photometric method.

Particle size distribution of the explosive powder aggregate as distinguished from the particle size of the RDX itself is not believed to have any influence on the detonation process and therefore is only considered insofar as it is related to the practical aspects of pressing.

## DETONATION VELOCITY OF MODIFIED COMP. A.

A special formulation similar to Comp. A, but with a somewhat higher-melting wax was used to press 6-in. dia. by 4-in. high cylinders in our vacuum mold according to the procedure given in the section on pressing. Composition analysis before pressing indicated an RDX content of  $91.8 \pm 0.1$  percent. Particle size distribution of the RDX used in the composition is approximately that given in the table below. Five out of a total of twenty-five of the 6-in. x 4-in. cylinders were sectioned for density spread. The extreme variation found in any one cylinder was 0.004 gm/cc. Average maximum variation was 0.0032 gm/cc.

Two-inch long cylinders of 1 in., 1/2 in., 1/3 in., 1/5 in., and 1/6 in. diameter were machined from the molded blanks. Those pieces falling within the density limit of 1.6874 ± 0.0010 gm/cc were selected for the detonation velocity determination. This density is approximately 9% of crystal density.

James

		PAF	TICLE	SIZE	OF RDX	
Particle	Size	Rang	zе			in Range
Above		300	μ		0.6	$\wedge$
Between	300 -	250	μ		0.6	İ
11	250 -	210	μ		2.8	ļ
11	210 -	177	μ		7.6	18
11	177 -	149	ш		9.7	22
11	149 -	125	H		15.7	ä
11	125 -	105	Ħ		8.0	Ž,
Ħ	105 -	88			6.8	Sieve Analysis
11	88 -	74			3.6	Ž
11	74 -	62			3.8	37.
11	62 -	53			1.4	1
97	53 -		u		4.2	İ
11	44 -	35			3.2	•
11	35 -	30			1.1	不
tt .	30 -	25			5.3	ပ္သံ
11	25 -	20			7.9	Ŧ.
11	20 -	15	•		9.6	ğ
11	15 -	10	•		4.6	Photometric-
##		7.5	ji.		1.7	ğ
Less the		7.5			0.5	_ <u>F</u> _
					98.7	

The velocity data on these rate sticks were obtained by Group GMX-8 using the techniques described by Campbell, Malin, Boyd and Hull.(3) In Table I the data are summarized. The temperature of the rate sticks was observed at the time of firing and corrections made for length and density whenever firing temperature differed by more than 5°C from inspection temperature. The linear coefficient of expansion used in computing the correction was 6.7 x  $10^{-5}$  in./in./°C. An energy correction was also made assuming that the heat capacity of the material was 0.35 cal/gm/°C and assuming that  $D = [0.35 \ (T-25) + 1100]^{-1/2}$  where T is in °C. The heat of explosion of RIX at 25°C is taken as  $1100 \ \text{cal/gm}$ . The net detonation velocity correction for temperature for all temperature effects is thus estimated to be  $-0.35 \ \text{m/sec/°C}$ .

An average velocity and the associated 95% confidence limit of the average was computed at each diameter. In Figure 4 these averages and their 95% confidence limits are plotted as a function of reciprocal diameter.

The data were fitted by the least squares method to an equation of the form

$$D = a_0 + a_1 (1/d) + a_2 (1/d)^2$$

Each average was weighted according to the reciprocal of the square of its confidence limit.

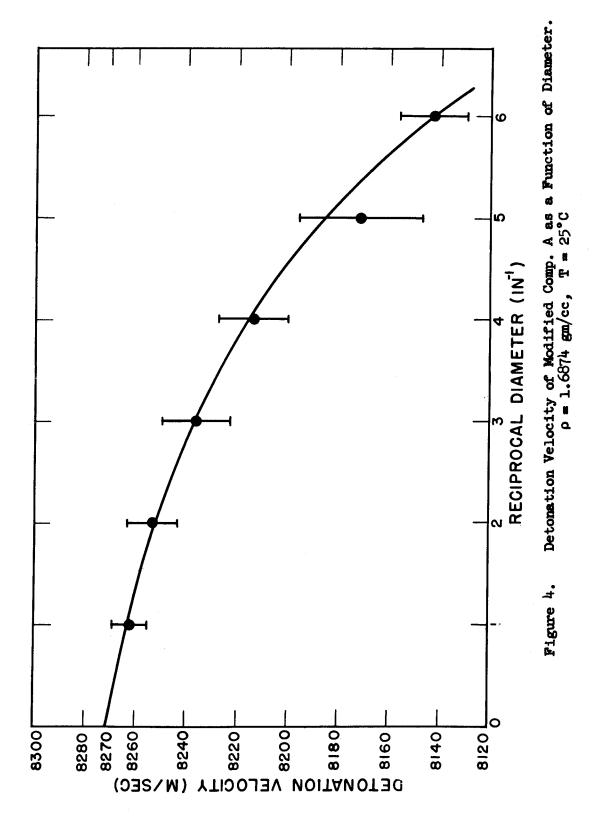


TABLE I
DETONATION VELOCITY - DIAMETER STUDY

MODIFIED COMPOSITION A  $\rho = 1.6874 + 0.0010 \text{ gm/cc}$  (corrected to 25°C)

(corrected to 25°C)							
DIA (in.)	D (m/sec) 8253.7	D	<u> </u>	± <sup>L</sup> 95			
0.999	8267.1 8260.3 8261.7 8283.8 8266.3	8261.8*	5.4	6.7			
0.500	8259.5 8235.0 8263.3 8259.1 8251.5	8253•7	11.3	14.0			
0.333	8218.8 8234.2 8230.8 8231.4 8255.6 8245.7	8236.1	12.9	13.5			
0.250	8223.5 8198.3 8226.6 8227.0 8201.8 8203.1	8213.4	13.5	14.2			
0.200	8195.1 8205.8 8162.7 8161.7 8139.9 8164.4	8171.6	24.3	25.5			
0.167	8140.4 8145.7 8157.4 8127.4 8127.4 8159.2	8142.9	13.9	14.7			

<sup>\*</sup> Fifth increment ommitted from calculation of average.

The standard errors of the coefficients were computed according to an extension of the method described by Birge. (4) Birge's treatment is limited to equally-spaced arguments and if one is desirous of weighing their data the method is inadequate. Members of Group T-1, LASL, however, have extended the method to use points weighed according to the inverse of the square of the confidence limit attached to any one point.

The values for the coefficients so obtained and their standard errors are:

$$a_0 = 8269.8 \pm 1.231$$

$$a_1 = -1.082 \pm 0.885$$

$$a_2 = 3.385 \pm 0.129$$

The standard deviation of the weighted average points about the fitted curve is 2.165 m/sec.

A simple linear fit was also made and the following values obtained:

$$a_0 = 8296.9 + 2.949$$

$$a_1 = -23.72 \pm 0.855$$

The standard deviation of the data about the fitted line in the linear case is 9.463 m/sec.

The two D axis intercepts are 8296.9 and 8269.8 m/sec for the linear and quadratic fits respectively. The quadratic fit is significantly, at the 95% confidence level, better than the linear fit and so, on a purely statistical basis, extrapolation of the quadratic fit may be expected to give a value more nearly correct for the steady state plane wave velocity at infinite diameter. The 95% confidence limit associated with this intercept is 2.5 m/sec.

# ACKNOWLEDGMENT

The author wishes to make it clear that the techniques described in this paper are only in a small part results of his efforts. The combined work of a large number of people over a period of several years has gone into the refinements of techniques described in this paper. The discussion concerning casting is primarily the result of the efforts of Group GMX-3 of the Laboratory. Vacuum-pressing developments have been carried out in Groups GMX-2 and GMX-3. Detonation velocity measurements on the finished rate sticks have all been done by Group GMX-8. Hadiographic inspection development is the result of the efforts of Group GMX-1. Valuable assistance has also been received from the Engineering Department of the Laboratory, and the

machine computations for curve fitting and data analysis have been done by Group T-1.

# REFERENCES

- JAN-C-401, September 25, 1946, par. F-4a (1).
- OSRD Report No. 5611, M. D. Hurwitz et al., "Rate of Detonation of Various Explosive Compounds and Mixtures".
- 3 Campbell, Malin, Boyd and Hull, "Techniques for the Measurement of Detonation Velocity."
- R. T. Birge, Review of Modern Physics, 19, 4 298

#### TECHNIQUE FOR THE MEASUREMENT OF DETONATION VELOCITY

A. W. Campbell, M. E. Malin, T. J. Boyd, Jr., and J. A. Hull Los Alamos Scientific Laboratory Los Alamos, New Mexico

#### INTRODUCTION

Until the last few years most of the measurements of detonation rates have been made with the use of streak cameras, the method of Dautriche, or with the Mettegang recorder. It is the purpose of this paper to describe an electronic method capable of very high precision in the measurement of detonation rates. Commonly referred to as the "pin method", it has been in use at Los Alamos from approximately the year 1944 to date. Recently, Gibson (1) reported a similar technique.

While at first glance the pin method may appear to resemble the Mettegang recorder method, there is a basic difference. The latter depends upon the interruption of the primary circuit of a high voltage transformer to produce a spark which registers on a strip of carbonized paper carried on a revolving drum; the technique to be described here relies upon the conductivity of the detonation wave to discharge a capacitor, forming a pulse which is presented on an oscilloscope trace and photographed.

The pin method offers several advantages over other available methods. Chief among these is that of increased time resolution. In contrast to the Mettegang recorder, the pin technique provides a record of the pulse shape and thus gives evidence of the strength of the detonation wave, i.e., whether the detonation wave may be dying out or is comparatively strong. The pin method also provides a means of observing directly the progress of the wave in the interior of an irregularly shaped piece of explosive; by way of contrast, optical methods for detonation velocity measurement must make observations on the exterior surface of the piece and infer the velocity of the wave from geometrical considerations.

### INSTRUMENTATION

The pin method makes use of electronic circuitry, which may

be divided conveniently into three parts: beginning at the explosive, these include ionization-operated or shock-operated switches, which are inserted into the explosive; a signal mixer circuit and transmission line; and a cathode-ray chronograph, commonly referred to as a "pin machine", which presents the signals on a calibrated time base. For the sake of clarity, these will be discussed in the reverse order.

Chronograph. Many different circuits have been developed by various workers for use with explosives. These have employed a variety of time base presentations including circular sweeps, spiral, linear and raster sweeps, and zigzag sweeps. This discussion will

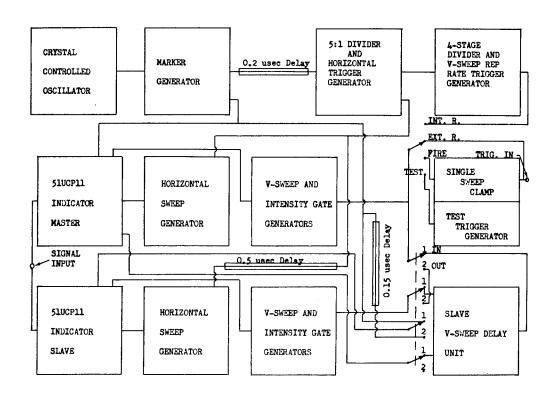


Fig. 1. Block diagram of chronograph circuit.

be limited to a circuit providing a raster presentation, because the authors have found such a circuit to be preferable on the bases of time coverage, attainable precision and ease of maintenance.

The raster chronograph is shown in block diagram in Fig. 1. A typical record from this chronograph is shown in Fig. 2. This apparatus provides two sweep presentations, with a maximum sweep time of 150 µsec. These may be operated in parallel to provide duplicate records and thus increase the precision of observation, or may be operated in tandem to increase the time coverage.

While a detailed discussion of the circuit would be out of place here, a brief description of the functioning of the circuit will be given. Referring to Fig. 1, the output from the crystal-controlled oscillator is shaped by the marker generator to provide

1/2-usec, square-wave timing marks for the indicators. The master indicator, or sweep circuit, receives the timing marks directly. The

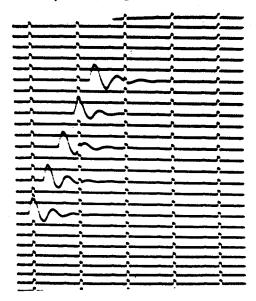


Fig. 2. Sample chronograph record. Pin switch signals are equally spaced at intervals of 7.33 µsec.

slave indicator receives the timing marks after they have passed through a 0.15 µsec delay line, when the indicators are operated in parallel, or receives them directly when the indicators are operated in tandem.

The marker generator also supplies 1/2-usec pulses through a 0.2 usec delay line to a 5:1 frequency divider which, in turn, drives the horizontal trigger generator. The master horizontal sweep generator receives these trigger pulses at 2.5-usec intervals. The slave horizontal trigger generator receives the same pulses after being delayed by one marker interval. By delaying the slave sweep by one marker interval, and by delaying the slave time

markers by 0.15  $\mu$ sec as noted in the previous paragraph, it is made impossible for a signal common to both master and slave records to be adversely affected on both because of coincidence with a marker or with a back-sweep.

The 400 kc horizontal repetition rate pulses are divided by the 4-stage divider to provide an internal, vertical repetition rate of approximately 200 sweeps per sec. By repeating the complete pattern so rapidly, it is made to appear as a steady pattern to the eye to aid in adjustment of the pattern. The vertical sweep and intensity gate generators may be triggered from the internal repetition rate pulses, an external source of repetitive pulses, the single sweep clamp circuit, or the manual test trigger.

The precision which is attainable with these chronographs is derived from close control on the frequency of the crystal controlled oscillator and on the linearity of the horizontal sweeps. The oscillator is a crystal-controlled free-running Miller oscillator having a frequency of 2 Mc ± 50 cps. While this may seem to be greater precision than is necessary, it is easily attained and, for all practical purposes, eliminates the time calibration marks as a source of experimental error.

Sweep linearity is controlled to 1% between adjacent calibration marks ( $1/2-\mu sec$ ). This is accomplished by selecting the 51UCP11 cathode-ray tubes for linearity of deflection as a function of the deflection voltage, and by adjusting the sweep circuit linearity controls. The standard error of measurement, resulting from errors in sweep calibration, linearity, and judgement of the film reader is found to be 3 x  $10^{-9}sec$  for transit times of 25  $\mu sec$  or less.

Mixer Circuits. The mixer circuit is a network of capacitors and resistors which form and send to the chronograph the electrical pulses which mark the passage of the detonation wave through the explosive charge. In Fig. 3 is shown a diagram of the circuit used

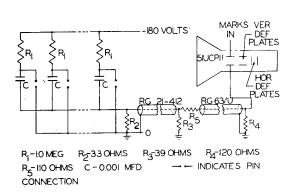


Fig. 3. Mixer circuit.

with most solid explosives. The condensers, C, are charged through isolation resistors, R. When the detonation wave closes a pin switch, one side of the capacitor is shorted to ground. The other side then discharges into the RG 21-412 signal cable, producing a signal pulse. R1 prevents recharging of the condenser during the shot either by other condensers in the mixer, or by the power supply. The characteristic impedance, Rg, prevents reflection of the signals back down the RG 63/U cable. If

pulses are reflected to the left by a faulty connection or other defect, they are absorbed by either  $R_3$ - $R_5$  or  $R_2$ . Because the 51UCP11 display tube has four vertical deflection plates, it is possible to put the signal pulses on a plate separate from that used for calibration pulses and for the vertical sweep. This eliminates the problem of a mixer circuit at this point.

When pin switches must be closely spaced in the charge, the mixer circuit is medified as shown in Fig. 4. With close spacing,

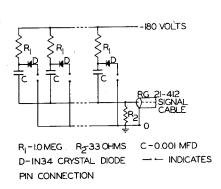


Fig. 4. Mixer circuit for use with closely spaced pin switches.

the conductivity of the detonation wave and of the shock
wave serves to connect the
discharging capacitor with
those which have been discharged. The result is that
the signal rise is affected
adversely. To prevent reverse
current flow into the discharged capacitors, diodes are
inserted as shown. These act
practically as rectifiers,
permitting current flow in the
desired direction only.

A second modification is necessary when the undetonated explosive is moderately

conducting. As shown in Fig. 5, the isolation resistors, R, are replaced with diodes. This permits increased charging current to the leaking pin switches, but prevents the discharged capacitors from drawing current from those still charged via the charging connection. In addition, it is sometimes necessary to increase the discharge time of the capacitors.

For best results all mixers are constructed with shortest leads possible. Parts are staked together, and the finished mixer is

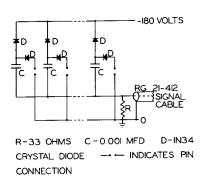


Fig. 5. Mixer circuit modified for use with moderately conducting explosive.

mounted close to the charge. When the latter is detonated, both mixer and the section of RG 21-142 coaxial cable are destroyed by blast. All pin switch leads must be of the same length to within a few inches, or the transit time of electric pulses in the leads must be taken into account for precision work.

Switches. The most commonly used type of pin switch is the one depending upon ionization for clesure. Usually, this is arranged as shown in Fig. 6,

although other arrangements will be discussed later under the section on charge preparation. The switch is made with the thinnest metal

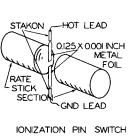


Fig. 6. Pin switch construction.

foils which have at the same time sufficient mechanical strength to withstand the necessary manipulation in preparing the switch. The most commonly used foils are silver, aluminum and copper in 1/8-inch widths and in thicknesses ranging from 0.2 mil to 1.5 mil. Occasionally, gold leaf is used. This has a thickness of appreximately 0.01 mil. However, it is difficult to use because of its lack of mechanical strength, and because it tends to stick to most objects brought near it as a result of electro-

static attraction.

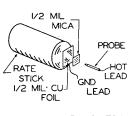
The voltage on the pin switch is dictated by the sensitivity of the indicator circuit. When no signal amplification is required, and when it is unnecessary to mix signals at the indicator by means of cathode followers, a suitable value of the pin voltage is 180 volts.

The gap width on the pin switch is usually held to about 1 mm to 3 mm. For two-component cast explosives or for pressed explosives, the detonation front has been found to be quite irregular, the irregularities being comparable in size to the grains of explosive. Therefore, it is desirable to have the dimensions of the

pin switch gap many times that of the largest grains of explosive, to improve the statistics of switch closure.

Occasionally, the ionization switch is found to be inadequate. One example of such an instance is encountered in the very weak initiation of a solid explosive. Here, the detonation wave may proceed without sufficient ionization to operate the switch described above. In this event, a switch involving mechanical closure may be used. Such a switch is shown schematically in Fig. 7.

The mechanical closure is effected by the motion of a thin metal foil, which is accelerated by the pressure of the detonation



MECHANICAL PIN SWITCH

wave. In order to keep the closing delay as small as possible the metal foil and the insulating foil should be kept very thin, usually less than 1 mil. Typical insulating materials include mica and Mylar or Mylon plastics. Closure times of 10<sup>-8</sup> seconds are easily attained.

Fig. 7. Pin switch construction.

#### ELECTRICAL EFFECTS

Before discussing the method of preparing charges for velocity measurement by the pin technique, it will be well to consider three electrical effects which have been observed to be associated with the detonation of an explosive charge.

The first of these is a difference between the potential of the detonation wave and ground potential resulting from the voltage pulse used to fire the electric detonator. If this potential difference is allowed to persist until the detonation wave reaches the first pin switch, it will be recorded as electrical noise on the chronograph trace. By grounding the detonation wave near the point of initiation, this potential difference can be eliminated.

The second and most important electrical effect, insofar as the pin technique is concerned, is the appearance of a potential difference between the detonation wave and ground, as a result of the detonation process.

This potential difference may be observed by use of the circuit diagrammed in Fig. 8. An uncharged copper wire is placed so as to contact the detonation wave. This wire is connected to ground via a co-axial cable and its termination, R<sub>1</sub>. The electrical circuit is believed to be closed by capacitive coupling between ground and the detonation products. While the probe is in contact with a detonation wave or a conducting shock wave, a potential difference is observed between the terminals of R<sub>1</sub>. This potential is commonly of the order of a few hundred volts, but may exceed 1000 volts under some circumstances.

In Fig. 9 are shown sample oscillograph records taken with the explosive and circuit arrangement shown in Fig. 8. These records

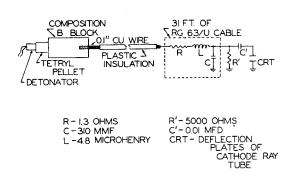


Fig. 8. Experimental arrangement for observing charge separation in detonation wave.

show the effect of changing the gas surrounding the explosive. The signal probe was inserted in the explosive to a depth of one inch. When the detonation wave struck the probe a positive signal (downward deflection) was recorded, which seems to be proportional to the temperature of the shock wave in the surrounding atmosphere. When the shock wave from the end of the stick reached the plastic insulation on the probe, the major signal pulse began. ended with the decay of the shock wave.

It is also important to note that insulation of the pin switch leads from the detonation wave is impossible by ordinary means. Figure 10 shows the signals obtained in an atmosphere of air when the conductor was insulated with plastic, rubber and glass.

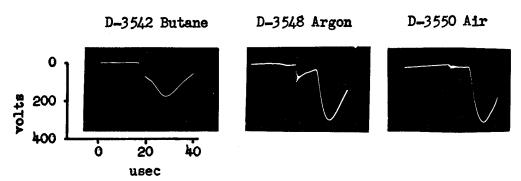


Fig. 9. Effect of atmosphere on voltage recorded by circuit of Fig. 8 using bare copper probe. Time scale: 1.75  $\mu$ sec/mm.

For the purpose of reference, a signal obtained with an uninsulated probe is included. In order to keep the signals within the limits of the oscillograph screen, the signals shown in Fig. 10 were attenuated by a factor of five relative to those shown in Fig. 9.

Perhaps the most plausible explanation of the potential difference between the detonation wave and ground is that involving charge separation. It is postulated that, because of greater mobility, more electrons than positive ions escape from the reaction zone, leaving the latter positive, a condition in agreement with experimental observation. It is further postulated that electrons escaping in the forward direction are soon captured. The presence of the resulting negative region in front of the detonation wave is observed when suitable amplification and time resolution are used in the signal

circuit.

Finally, the charge-separation hypothesis requires that, while a potential difference must exist between the detonation wave and the product gases, the system as a whole must not develope a net charge. Experimentally, no net charge is observed on explosive fired in a Faraday cage.

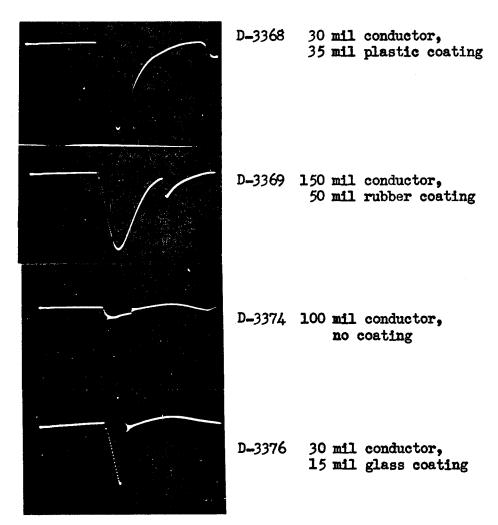


Fig. 10. Effect of probe insulation on voltage recorded by circuit in Fig. 8. The record from a bare probe, showing a 400-volt deflection, is shown for reference, D-3374.

Whether or not the above explanation of the second electrical effect is correct, it is important in using the pin technique to be aware of the phenomenon. Failure to properly ground the detonation wave in the vicinity of a pin switch results in electrical noise intruding on the chronograph record. In Fig. 11 is shown a record on which this has occurred. One pin signal appears at the right end of line 10 measuring from the top of the pattern. In the next section,

methods of grounding the detonation wave so as to eliminate electrical noise will be discussed.

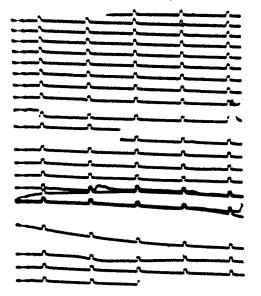


Fig. 11. Sample raster record showing electrical noise on detonation wave.

The third type of electrical effect observed when explosive is detonated is a radiation signal, which may be similar to that observed by Kolsky(2). This radiation does not interfere with the signal circuits described here for use with the pin technique, but is discussed briefly for the sake of completeness. It results from the charge separation mentioned above and/or from the fact that when a piece of explosive is detonated in air, the surrounding shock wave constitutes an expanding, conducting envelope. In the presence of an electric or a magnetic field, e.g., the earth's, this envelope becomes polarized and its surface charge produces effects in external space equivalent to those of

a dipole. It has been experimentally demonstrated that the electrical effects of this dipole can be adequately described by means of quasi-stationary field theory.

If the explosive being detonated is particularly deficient in oxygen, e.g., Torpex, the radiation signal exhibits two maxima: the first is attributed, as mentioned above, to the conducting shock wave, the second to the flame produced by oxidation of the detonation products after mixing with air.

#### CHARGE PREPARATION

The pin technique for measuring detonation velocities, as mentioned above, is capable of very high precision. The standard error of observation can be reduced to better than 0.1% of the rate for charges a few inches in length. Expressed in terms of time, the standard error is, for most experiments, independent of the total time covered, amounting to approximately 3 x 10<sup>-9</sup> sec. This precision is useless, however, unless every precaution is taken in the preparation of charges for rate measurements. Some of the precautions to be discussed here result from the nature of the pin technique, others are necessary to any precise method of measuring detonation

velocity.

Assuming that uniform explosive is at hand and that density and composition are known, the first problem in charge preparation is the insertion of pin switches. In the case of liquid explosives, charged probes may be inserted as shown in Fig. 12. The spacing of

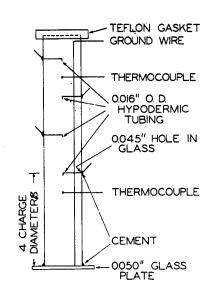


Fig. 12. Pin switch arrangement for liquid explosives.

ment
In high density pressings
and in castings, thin metal foils are
used to form pin switches as explained earlier. The position of the end

of each charged foil relative to the center of the rate stick is kept constant, otherwise the curved detonation front will not short all

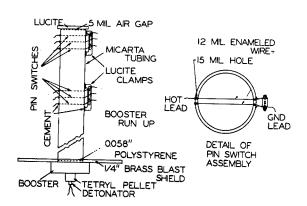


Fig. 13. Pin switch arrangement for granular explosives.

the probes can be measured with a cathetometer to a precision of about 1 mil. By means of the common ground, the detonation wave is maintained at ground potential. The discharge of the pin mixer capacitors takes place via the spaced probes and the detonation wave to ground.

For granular explosives at low loading densities the arrangement used is shown in Fig. 13. Each switch is composed of a pair of fine copper wires stretched taut by means of a clamp on the outside of the containing tube. The spacing between wires is regulated to a few multiples of the maximum grain size. In order to avoid premature operation of the switch by means of photoionization, enameled wires are used. Axial spacing of the wires is controlled by boring the holes for them with a milling machine.

switches in exactly the same manner. To avoid the use of a layer of glue to hold the foils in place the latter are moistened with water. An alternative method of forming pin switches is to use a common ground on the outside of the charge much as is used for liquids, and to use a single charged foil extending in to the center of the stick.

After the method of switch insertion has been decided, in the case of the cast or pressed explosives, some method of assembling the seg-

ments must be devised. The simplest method is to tape them together using a pressure sensitive tape. The use of cellophane tape has, unfortunately, several disadvantages, chief among which is the danger of jetting if the tape is applied loosely. When a small space exists between the lateral surface of the charge and tape, a gas "jet" may be formed. This jet may preced the detonation wave by several tenths of a microsecond and discharge the pin switch prematurely.

A preferred method of charge assembly is that of clamping as shown in Fig. 14. This leaves the sides of the charge free and provides positive contact between charge segments. It is well to point

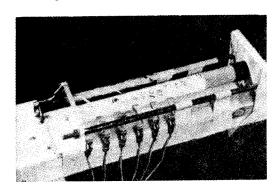


Fig. 14. Method of charge assembly using clamping.

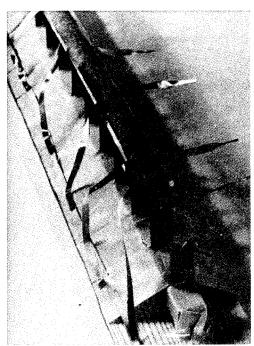
out here again that only the thinnest possible foils are used between segments so as to keep the gap between segments as small as possible. This is necessary because an air gap results in a momentary slowing of the detonation wave, perhaps by dissipating the von Neuman "spike". Quantitatively, a small gap is believed to increase the transit time of a piece of explosive by about 10-8 sec per mil thickness of the gap. Thus, in a two-inch segment of explosive having a deto-

nation velocity of 8000 m/sec, a booster gap of 1 mil would result in a velocity error of approximately 10 m/sec.

In boostering the charge, a single detonator or a plane wave generator is used, followed with 2 to 6 diameters of booster identical with the charge over which rate measurements are to be taken. When using high-energy boosters on rate sticks with low detonation rates, it has been found necessary to impede the expansion of the booster gases by means of a coating of putty or sand, since in some cases the booster gases have preceded the detonation front in the stick, closing the pin switches prematurely.

In making velocity measurement on low energy explosives or on sticks of large diameter it is frequently advisable to provide grounding in addition to that furnished by the grounded side of the pin switch. This results from the resistance of the detonation wave and explosion products—the grounded side of the pin switch fails to ground the wave near the lead from the pin mixer. As a result, the latter begins to respond to the generation of charge on the shock front, introducing noise on the chronograph record to the extent that the latter may not be assessable. It is the practice in such instances to run a ground lead paralleling each charged probe and extending beyond the limits attained by the shock wave during the observation.

A final precaution which must be taken if high precision is to be maintained is the control of firing temperature. The detonation velocity of Nitromethane, for example, has been found to vary with the initial temperature at the rate of -3.7 m/sec/°C . In the



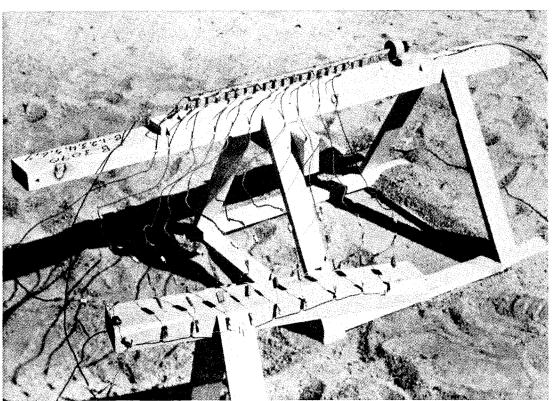


Fig. 15. Above: detail of assembly of 0.500 in. diameter charge on v-notched blocks. Below: fully assembled. Mixer in foreground.

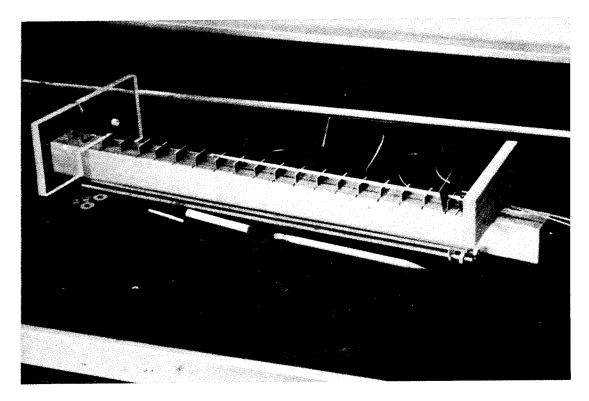


Fig. 16. View of partially assembled charge. Diameter: 0.14 in.

case of Composition B, Mautz<sup>(4)</sup> has found the transit time to vary inversely with the temperature at the rate of 1% per  $100^{\circ}$ C. Taking the linear coefficient of thermal expansion to be  $5 \times 10^{-5/\circ}$ C the velocity variation would be 0.5 m/°C.

It is therefore evident that precision rate sticks may not be exposed to direct sunlight nor fired without suitable thermal insulation if precise data are desired.

#### SAMPLE DATA

In Tables I and II are shown sample data taken with the electronic technique. In taking such data, it is common practice to operate several sweeps in parallel to produce replicate records. This may be done to guard against the failure of a single circuit to operate properly, or several results may be averaged to further reduce the error of analysis.

#### TABLE I

Sample transit time data for pressed TNT. The charge consisted of six sections 1/2 inch in diameter arranged in a column. Transit time data were taken over the last four sections.

Density g/cc	sweep-3	Transit sweep-4	time, µsec* sweep-5	average	velocity m/sec
1.642	7.338	7.330	7.333	7.333	6925
1.642	7.338	7.339	7.336	7.336	692 <b>1</b>
1.641	7.337	7.321	7.334	7.334	6928
1.641	7.338	7.334	7.333	7.333	6929

<sup>\*</sup>The record from sweep-7 is shown in Fig. 3. Shot No. B3243.

#### TABLE II

Sample transit time data for Nitromethane. The explosive was contained in a glass tube 2.570 inches in diameter and 30 inches long. Pin switches were arranged as shown in Fig. 12.

Switch		Transit ti	me, µsec		Detonation velocity
interval mm	sweep-2	sweep-4	sweep-5	average	m/sec
126.27 134.99 129.415	19.903 21.252 20.388	19.893 21.272 20.385	19.896 21.274 20.379	19.897 21.266 20.384	6346 6348 6349

Additional data taken with this technique are presented in other papers given at this conference including: Detonation in

Homogeneous Explosives and Particle Size Effects in One-and-Two-Component Explosives.

#### CONCLUSION

A technique has been developed for measuring transit times in explosives charges which is capable of higher precision than are the methods heretofore used. While it can be used in conjunction with the streak camera, it is not subject to the limitations of the latter. Distortion of the detonation wave at the charge boundaries are not detrimental, nor does confinement of the charge in metal or other opaque materials hamper the measurement of detonation rate. If full advantage is to be taken of the precision afforded by the pin method, great care must be taken in preparing each charge and in controlling the firing conditions.

#### ACKNOWLEDGEMENT

Because so many workers have contributed to the development of the circuitry and the technique of charge preparation, it is impossible to give appropriate credit to each. Recognition should be made here, however, of the important contributions of James L. Tuck and Roy W. Goranson, both of whom were active in introducing variations of the pin method to this laboratory.

<sup>(1)</sup> F. C. Gibson, Rev. Sci. Instr. 25, 226-31(1954) Mar.

<sup>(2)</sup> H. Kolsky, Nature 173, 76, (1954).

<sup>(3)</sup> A. W. Campbell, M. E. Malin, T. E. Holland, Detonation in Homogeneous Explosives. (This Conference).

<sup>(4)</sup> C. W. Mautz, Unpublished Report, Los Alamos Scientific Laboratory.

## A MICROWAVE TECHNIQUE FOR MEASURING DETONATION VELOCITIES

T. J. Boyd, Jr. and Peter Fagan Los Alamos Scientific Laboratory Los Alamos, New Mexico

The measurement of detonation velocities at the Los Alamos Scientific Laboratory is usually accomplished by a pin technique (1). However, this technique often proves unwieldy when applied to nonsteady state studies where the detonation velocity varies with time. In such cases, it has been found practical to employ a microwave technique for measuring these nonsteady velocities. This technique is based on the reflection of microwaves from the ionized detonation front and yields a sequence of detonation velocities which are averages over equal and adjacent intervals along the length of the explosive being studied. In a measurement of the detonation velocity where the pin technique could be employed, the microwave technique would be less accurate and more complicated. There were, however, a sufficient number of nonsteady state studies where the pin technique was impractical to warrant the development of the microwave technique for routine use.

Before the actual microwave system is explained, the basic technique will be illustrated by considering the simplified version shown in Fig. 1. A microwave oscillator is connected to a lossless waveguide section which is terminated by a perfectly conducting, movable piston. In order to isolate the oscillator from any load changes caused by the piston movement, an attenuator is inserted between the piston and the oscillator. A probe is inserted to sample the electric field in the guide. If it is assumed that only one mode, or field configuration, exists in the waveguide, the electromagnetic field in the waveguide can be represented as the sum of an incident and a reflected wave. In the lossless case considered, the sum of the waves is a pure standing wave. The transverse electric field intensity is zero at the piston and at distances which are an integral number of half guide-wavelengths from the piston. As the piston is moved, a periodic signal is recorded by the probe and detector. One cycle of the recorded signal will correspond to a piston displacement of onehalf the wavelength in the guide. If the guide wavelength and the initial position of the piston are known, then the position of the piston as a function of time can be determined.

## Boyd, Fagan

The above analysis assumes the presence of only one mode in the guide. It is possible to choose the dimensions of the guide such

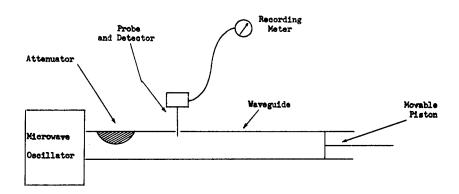


## Figure 1

that only one mode, the so-called dominant mode, can exist in the guide. For a waveguide of circular cross section of radius r, the condition for the existence of only the dominant mode is given by the expression.

$$\lambda/3.412 \le r \le \lambda/2.613$$

where  $\lambda$  is the wavelength of a plane electromagnetic wave in an unbounded volume of the dielectric in the waveguide. The wavelength,  $\lambda$ , can be related to the operating frequency, f, of the oscillator by the expression

$$\lambda = \frac{c_0}{f} \frac{1}{(\epsilon_1 \mu_1)^{1/2}}$$

where  $C_0$  is the velocity of light in free space, and  $\in$ 1 and  $\mu$ 1 are the dielectric constant and magnetic permeability, respectively, of the medium in the waveguide. When the dimensions of the guide and the operating frequency have been chosen, the guide wavelength,  $\lambda$ g, can be computed from the expression

$$\lambda_{g} = \frac{\lambda}{\left[1 - (\lambda/\lambda_{c})^{2}\right]^{1/2}}$$

where the critical wavelength,  $\lambda_c$ , for the dominant mode in a guide of circular cross section is given by

# $\lambda_c = 3.412 \text{ r}$

This simplified version can now be compared with the practical circuit shown in Fig. 2. The piston is replaced by the detonation front and the probe by a waveguide crystal detector mount. A

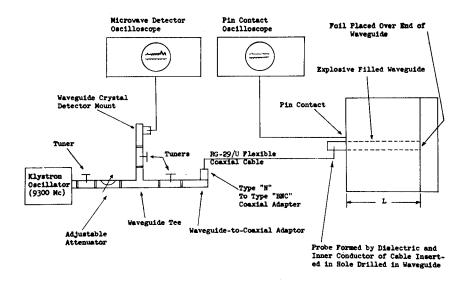


Figure 2 short length of flexible coaxial cable couples the crystal detector to an explosive-filled waveguide which is inserted in the explosive to be studied. This cable permits isolation of the electronic gear from the explosive system, thus minimizing the equipment expenditure per shot. As in the simple model, the signal at the detector should be periodic with a movement of  $\frac{\lambda g}{2}$  of the detonation front, where  $\frac{\lambda g}{2}$  is the guide wavelength in the explosive-filled guide.

Some of the functional details of the circuit shown in Fig. 2 should be explained. The klystron operates at a frequency of 9300 megacycles per second. The tuner adjacent to the klystron is adjusted for maximum power output from the klystron, and the attenuator isolates the klystron from load changes. The detector, together with its tuner, is mounted on the side arm of either an E- or H-plane tee. Both the detector and the waveguide-to-coaxial adaptor are matched to the waveguide before assembly in order to obtain a larger and more reproducible signal amplitude. Since the impedance of the crystal mount may depend upon its power level and external load, it should be matched at its maximum expected power level and normal operating load impedance. The waveguide-to-coaxial adaptor is matched with a long length of the relatively lossy cable, which simulates an infinite length of line attached to the adaptor. The cable is then cut to the desired length (up to 6' lengths have been used and longer lengths may be used if the attenuation of the cable is not objectionable) and the braid at the cut end is folded back over the outer covering of the cable, exposing a short length of dielectric and inner conductor. This short length

## Boyd, Fagan

of dielectric and inner conductor forms a probe, which is inserted in the explosive-filled waveguide.

The explosive-filled waveguide is prepared by machining a stick of explosive, wrapping it with a thin layer of aluminum foil, and drilling a hole near one end for insertion of the probe. The diameter of the stick is chosen to allow propagation of only the dominant, or TE71 mode. For example, at an operating frequency of 9300 megacycles, the stick diameter for Composition B is approximately one-half inch. For this size stick of Composition B at an operating frequency of 9300 megacycles, Ag is approximately 3 centimeters. The stick is made longer than the explosive to be tested to permit insertion of the probe. The hole for the probe is drilled perpendicular to the axis of the stick. This orientation of the probe permits efficient excitation of the dominant mode. The depth of the hole and the distance of the center of the hole from one end of the stick is approximately  $\Lambda g/4$ . The stick is wrapped with two layers of 0.5 mil aluminum foil. This wall thickness is sufficient to confine the electromagnetic fields to the interior of the waveguide but does not measurably affect the detonation in the explosive. Experiments using the smear camera technique have shown that wall thickness of 15 mils could be tolerated.

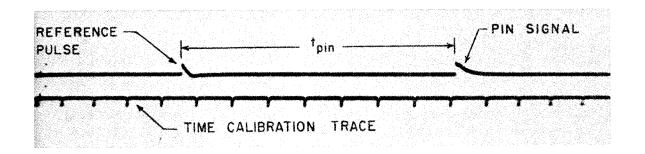
If air spaces exist between the explosive stick and the foil, jetting will occur with resultant distortion of the recorded signal. These air spaces can be eliminated by coating the stick with a thin layer of silicone grease prior to wrapping.

The explosive-filled waveguide is inserted in a hole drilled in the piece of explosive under test. Silicone grease is used again to exclude air spaces between the waveguide and the surrounding explosive. Both the stick and the piece of explosive being tested should be of the same composition and density.

Noise originating in the explosive or in the mechanism used to detonate the explosive (1) can obscure the signal trace received from the detector. It was found that this noise could be effectively eliminated by avoiding any electrical connections between the detonated explosive and the waveguide or external circuits. In particular, when the probe is inserted in the waveguide, the braid of the coaxial cable is separated by a layer of cement from the foil wrapped around the explosive-filled waveguide.

A circular disk of aluminum, 0.2 mils thick, placed over the end of the waveguide shields the microwave circuit from events occuring prior to the time when the detonation reaches the waveguide. The start of the signal trace records the time when the detonation front has reached the waveguide. The arrival of the detonation front at the end of the explosive being tested is detected by a pin contact time. This pin time is necessary since the record does not end until the detonation front arrives at the probe. The microwave detector signal and the pin signal are recorded on separate oscilloscopes. The two displays are correlated in time by a common reference pulse placed on both.

Representative signal traces are shown in Fig. 3. Each signal trace is accompanied by a time calibration trace. These traces, together with a knowledge of the length of the explosive being tested, provide sufficient information to determine the times when the detona-



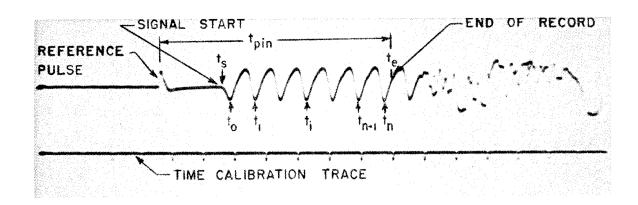


Figure 3.

tion front has reached a sequence of positions in the explosive. Since the detonation front has moved a distance of  $\lambda g/2$  during the time interval between common reference points on any two adjacent cycles of the record, the half-guide wavelength can be found by dividing the length of the explosive by the total number of cycles in the record. Usually, greater accuracy can be achieved by reading the peaks, or troughs, of the record, rather than an arbitrary reference point on each cycle. The incomplete end intervals of the record must be assigned fractions of a cycle. Unless there is additional information on the detonation rate of the explosive, it is assumed that the end intervals have the same periods as their adjacent intervals. With this assumption, the half-guide wavelength for the record shown in Fig. 3 is given by

$$\lambda_g/2 = L / \left[ \frac{t_o - t_g}{t_1 - t_o} + n + \frac{t_e - t_n}{t_n - t_{n-1}} \right]$$

where L is the length of the explosive being studied,  $t_s$  is the time when the microwave signal starts,  $t_e$  is the pin contact time, n is the number of complete cycles, and  $t_o$ ,  $t_1$ , ...  $t_{n-1}$ ,  $t_n$  are the times for the peaks (or troughs),  $t_o$  being the time for the first peak and  $t_n$  the time for the last peak before the pin contact time. At time

 $t = t_i$  (Fig. 3) the detonation front has traveled a distance along the waveguide given by

$$d = \left(\frac{t_0 - t_s}{t_1 - t_o}\right) \frac{\lambda_g}{2} + i \frac{\lambda_g}{2}, (i = 0, 1, 2 ...n).$$

Therefore the position of the detonation front as a function of time can be determined. Detonation velocities can be obtained from this information.

It should be emphasized that the microwave technique should not be used where the pin technique may be employed. The accuracy of the pin technique is 0.1%, (1) and the accuracy of the microwave technique is of the order of one or two percent. The microwave technique is more complicated because of the greater difficulty in fabricating the explosive charge, adjusting the measuring equipment, and interpreting the signal records. In addition, the microwave technique is limited to those explosives which have good dielectric properties. When applicable, the microwave technique provides an almost continuous measurement of the position of the detonation front as a function of time without measurably affecting the detonations. Since the cross-sectional area of the waveguide is small, signal distortion due to side blasts and variations in the waveform of the detonation front is almost negligible.

In the preceding paragraphs, a method involving microwaves has been described for observing the velocity of a detonation wave in the interior of an explosive charge. Circuits for generating and detecting the microwaves together with the display and reduction of the resultant signal have been discussed. The described system is presently being used at the Los Alamos Scientific Laboratory on a routine basis.

<sup>(1) &</sup>quot;Techniques for the Measurement of Detonation Velocity", A. W. Campbell, et. al. (This conference).

## MEASUREMENT OF DETONATION TEMPERATURES

F. C. Gibson, M. Bowser, C. R. Summers, F. Scott, J. C. Cooper, and C. M. Mason

U. S. Bureau of Mines Pittsburgh, Pennsylvania

#### Introduction

The temperature in the detonation front is, at the present time, one of the parameters most urgently needed in the field of solid explosives. Recent surveys (1, 2) show that although the measurement of this parameter has been a matter of active interest for some time, the experimental determination of definitive temperatures has not been very successful. At the last conference, studies (3, 4) were reported on the luminosity emitted from the exterior of charges detonated in air, in water, and in a partial vacuum. The luminosity records obtained at that time were difficult to interpret owing to a multiplicity of peaks, and it now appears that true amplitudes were not observed due to the integrating effect of the field slit. The method described in the present paper, although introducing a foreign material into the explosive powder, provides an interval of time conducive to sampling by one-megacycle circuitry and views the detonation radiation at the core of the charge in solid explosives. It is hoped that temperature data obtained by this method will be of sufficient accuracy to permit its use in developing a single suitable equation of state.

#### Theory

The two-color method currently employed is based on Wien's radiation equation which assumes that the radiation is black or grey body. From the equation

$$E_{\lambda} = c_1 \lambda^{-5} e^{-c_2/\lambda T}$$

it follows that the curve obtained by plotting the logarithm of the ratio of the radiation densities for two wavelengths,  $\lambda_1$  and  $\lambda_2$ , against the reciprocal of the absolute temperature will be a straight line. The slope of the line depends on the frequencies of

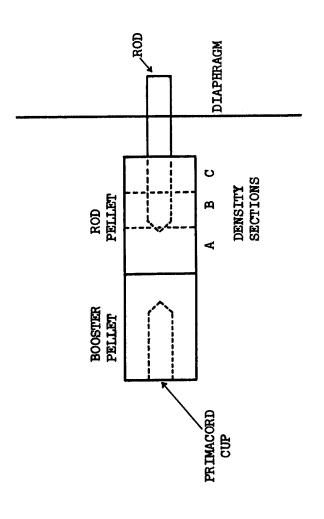
the band pass filters, and its intercept is determined by the relative sensitivities of the electrical equipment which make up each channel.

To determine the nature of the available radiation, spectrograms of detonating tetryl were taken by superimposing the radiation from the axial cavities of twelve charges. It was hoped that radiation from the tetryl charge could be compared with the radiation from the explosive pellets used in the temperature work. However, as the radiation from the former required twelve shots to give a weak spectrum, it has not proved practical to obtain spectra from the charges used for temperature determination. A full investigation of this will be made as time permits. The spectrum obtained is a continuum extending through and well above and below the region of the spectral pass bands of the two interference filters employed.

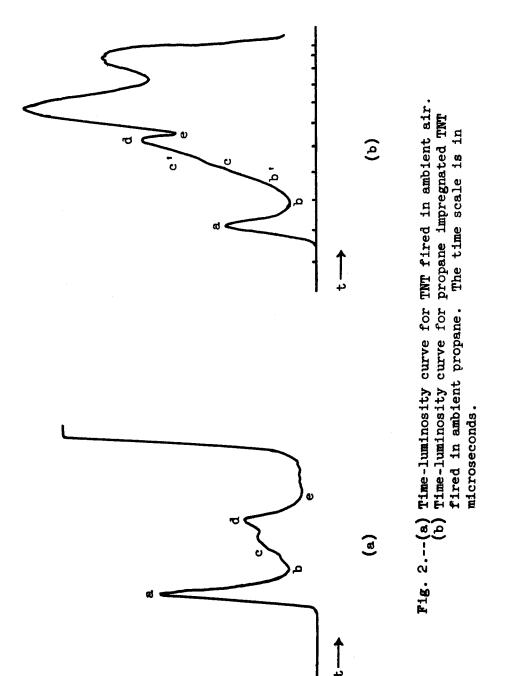
## Method

The novel feature of this method for sampling the radiation which is to be evaluated for quality is the use of a transparent plastic rod imbedded axially in the explosive charge during fabrication of the pellet. This rod (methyl methacrylate) protrudes from the end of the cylinder opposite to the initiated end. In this way, the radiation at the core of the explosive is transmitted along the plastic rod by internal reflection to the aperture of the sensing equipment. The charge confines itself, and the explosion pressures essential to high-order complete detonations are maintained at the zone of measurement as the plastic is completely surrounded by high explosive. The rod is inserted into the charge for a distance of about 2 cm. providing a detonation front transit time of 3 or more microseconds, depending on the velocity of detonation. This interval, which is relatively long with respect to the response times of electronic equipment, permits the temperature to be evaluated after equilibrium conditions have been attained in the system. In addition, refinement of the system may give temperature gradients along the rod due to non-homogeneity in the pellet density, a result of wall friction effects of both the fabricating die and the plastic rod during pressing. A cross sectional view of the charge is shown in figure 1. The end of the rod is pointed to allow powder flow in pressing, thus preventing the pile-up of powder on the end of the rod. Such pile-up would result in undesirable density gradients and rod fracture.

Typical luminosity-time records for TNT are shown in figure 2. Figure 2(a) is the single-channel trace of a TNT charge fired in ambient air. The waveform is analyzed for temperature at points, (a) through (e), each point, except (c), being a maximum or minimum so that the amplitudes of the two channels can be compared accurately at that instant. However, this method makes no allowance for response times of the equipment which may impair the accuracy. Therefore in subsequent analyses, another method was used which is



A, B, and C. Diaphragm is to exclude charge-side radiation from the system during period of passage of the detonation along the rod within the charge. tions were made by dissection of rod pellets into segments Fig. 1.--Drawing of a test charge (scale size). Density determina-



illustrated by the waveform of a propane-impregnated TNT charge (figure 2(b)) fired in ambient propane. In this method, the radiation is sampled after an equilibrium condition has been attained, taking points b', c, and c', at finite times after the first appearance of luminosity from the rod. The points b' and c' were chosen so as to represent the temperatures at the instant when the detonation wave was in the density segments shown in the charge drawing in figure 1. The initial pip, a, may be due to the increased area effect at the rod end as well as to additional luminosity from the shock wave upon impact on the end of the rod. It is believed that the phenomena of opacity due to shock pressure noted by other researchers in plastics of this type may occur here. However this cannot be verified unless charges with detonation velocities lower than the shock velocity in the plastic are tested. The opaque diaphragm shown in figure 1 prevents extraneous radiation from entering the system until after the detonation has passed the charge end and traveled across the gap between it and the baffle diaphragm. Of general interest may be the fact that in this system there is about ten times more radiation from the rod than from a 1.5 kw carbon arc lamp, and that the air-shock radiation amplitude is about ten times as great as that from the rod.

Studies of the pellets were made with the image-converter camera described elsewhere (5), modified to provide streak photography. These tests were conducted to establish the radiation luminosity dependence on the presence of air, propane, and the plastic rod. In air, streak photographs of charges from which the rods had been withdrawn showed strong shock reinforcement due to shock collision within the axial cavity. The same charge fired in ambient propane showed only radiation at the cavity bottom and along the explosive-cavity interface. The luminous zone in this case can be visualized as a doughnut of light traveling at detonation velocity down the cavity wall. Exposures also were made with the rod in place and fired in ambient propane after the charges had been carefully vacuum-impregnated with propane. Here the light was greatly reduced when the detonation reached the charge end, indicating that most of the radiation was not due to shock action on or in the plastic rod but to the explosive material, intergranular voids, or the small space between the rod and the explosive. The actual source of this radiation is still unknown; however the agreement between the experimental results and theory strongly suggests that the radiation is from the detonation zone.

## <u>Apparatus</u>

A diagram of the apparatus is given in figure 3. The explosive charge is positioned as shown in the drawing and during calibration the standard source is placed in the same position as the charge. Accurate positioning is achieved by projecting an image of the hole in the aperture plate through the window into the bombproof. The size of the hole in the plate is such that when it

is enlarged by the field lens it appears slightly larger than the end of the plastic rod (about 3/8 inches). The motor-driven disc acts as a light chopper and is used during calibration to provide a.c. signals from a steady radiation source. A slit on the periphery has a width of about 0.020 inch and scans the aperture hole in about fifty microseconds. The pulse width on the calibration trace can be adjusted by varying either the slit width (a step slit is available) and/or the motor speed (the diameter of the disc is fixed at 16 inches). A lamp-photomultiplier combination, the direct output of which can be switched into the trigger generator or into the oscillographs, allows either single or repetitive sweep operation and is controllable in time by displacing the lamp-phototube assembly with respect to a circular aperture in the disc that has a fixed relationship to the slit. The trigger generator is a simple thyratron circuit which allows single-sweep operation of the oscillograph from either the ionic conductivity probes in the charge or the disc as mentioned. A secondary lens forms a defocused image of the end of the rod on the photomultipliers which are 1-1/2" end-on types so that the entire photocathode surface is employed. At the cross-over point an adjustable slit is used for vernier control of the radiation entering the phototubes. Coarse attenuation is provided by the use of grid attenuators placed to the rear of the field lens and adjacent to it. A half-silvered mirror separates the light into two beams. A transmission filter of the interference type is located in front of each phototube so that the only radiation entering the tube housing is through the filter. The band pass of each is 70 to 100 angstroms at half amplitude.

The electrical circuitry comprises a video amplifier-cathode follower combination and a high-speed oscillograph for each channel yielding a signal proportional to the energy density. Operating levels of the electrical equipment are adjusted by varying the photomultiplier dynode voltages to provide optimum signal-to-noise ratio, and a degree of balance that allows a signal ratio of unity to occur near 4000°K, as the desired temperature for calibration and explosive used lies between 2000°K and 6000°K. As previously mentioned, the light level is adjusted so as not to exceed a maximum amplitude on either oscillograph. This avoids nonlinearity difficulties that otherwise would be encountered since the utilized radiation varies over a factor of several hundred.

The film records (photographic negatives for the explosives tests; Polaroid-Land for the longer sweep calibration traces) are analyzed by means of an optical comparator with the amplitude-time selection as previously described. The time base is furnished by a crystal-controlled oscillator operating at a frequency of 1,2 or 2.5 megacycles.

#### Results

Most of the work to date has been devoted to recognition

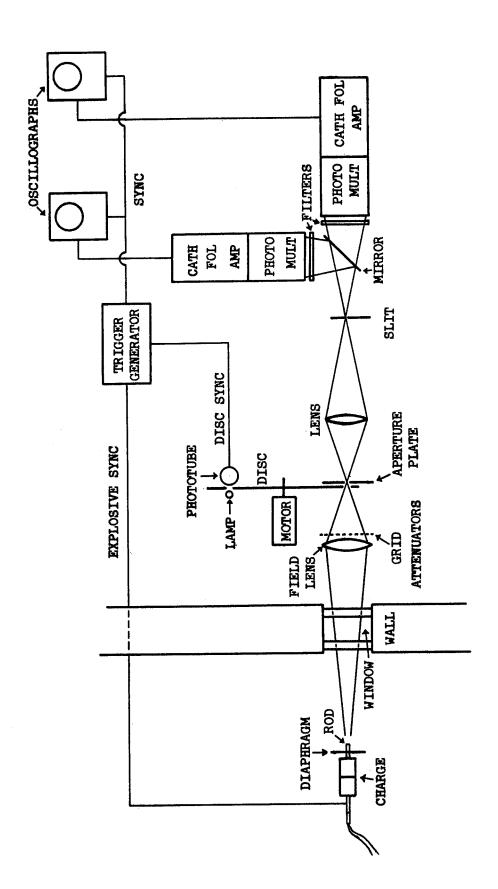


Fig. 3.--Diagram of the apparatus for detonation temperature determination.

of the idiosyncrasies and deficiencies of the system. Preliminary testing of the equipment with rod pellets has been made for tetryl and TNT in both air and propane. The data are considered preliminary, pending complete calibration of the system. Tentative detonation temperature data for tetryl and TNT charges fired in ambient air are given in table 1. The temperature of the TNT is higher because of the influence of the shock temperatures in the air both around the rod and in the intergranular voids. In the tetryl, which has a higher density, air-shock luminosities are minimized. This effect is substantiated when the data are compared with that given in table 2 for similar charges which had been propane-impregnated and fired in a propane surround. Densities of representative pellets of each explosive were determined on three segments (see figure 1). The temperature at b' is considered to be representative of the B segment and being nearer the center of the charge is probably the desirable zone for temperature analysis. The propane effectively reduced the air-shock components in the temperature obtained at point e after the detonation had passed out of the charge. Temperatures of the air shock obtained at point e and given in table 1 may be considered reasonably accurate if detonation spectrograms recently obtained, indicating a continuum for the composite charge radiation, are correct.

These results appear of a reasonable order of magnitude when compared with the theoretical detonation temperatures shown in figure 4 (6, 7, and 8).

Further refinements are being made and it is anticipated that additional data will be available which will support or invalidate these preliminary data.

#### ACKNOWLEDGEMENTS

This work was supported by the Office of Ordnance Research, Department of the Army, Army Project 599-01-004, Ordnance Project TB2-0001.

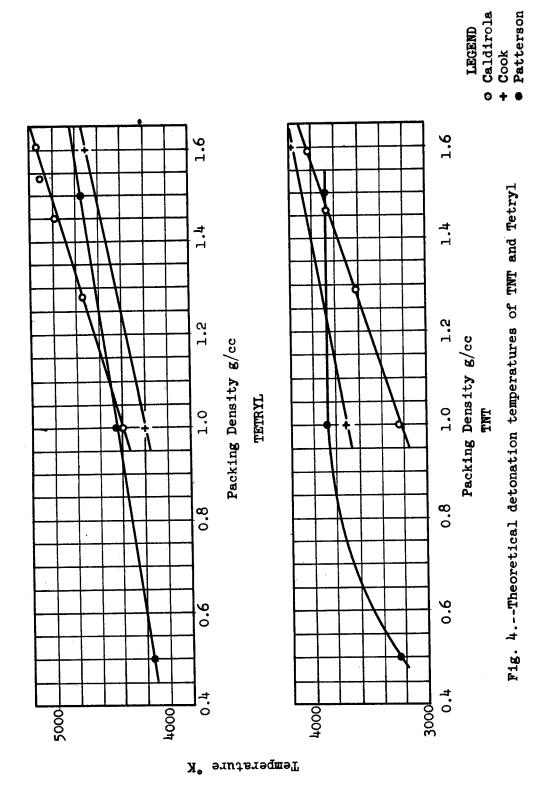


Table 1.--Tentative data on detonation temperatures for two explosives fired in ambient air

Explosive	Representative density a/cm3		Temperature-time profile K *	-time pro	file K° *	
	(Average)	ಥ	Q	υ.	ğ	ψ
Tetryl	1.64		0024		5200	9300
TNT	1.44	9300	5300	ŧ	2700	14000
* This p	This profile is measured at various points along the time-luminosity curve shown in figure 2(a).	d at va (a).	rious points	along the	time-lumi	nosity

Table 2 .- - Tentative data on detonation temperatures for two propaneimpregnated explosives fired in ambient propane

Explosive.	Reps density	Representative density segment g/cm <sup>3</sup>	re g/cm3		Te	mperatu	Temperature-time profile K° *	profile	* \	
	¥	В	D	œ	۵	۵	ပ	້	ರ	ø
Tetryl	19.1	1.68	1.63	4800	4800 5100 5000		2600	5300	5400	1,200
LALL	1.39	1.46	1.47	5400	2400 4400	3900	4500	4300	3800	3800
*					•					

This profile is measured at various points along the time-luminosity curve shown in figure 2(b) with points b', c, and c' taken at finite times with respect to the first appearance of luminosity in the rod.

## LIST OF REFERENCES

- (1) Technical Memorandum, Institute for the Study of Rate Processes, University of Utah, "The Measurement of Temperature in Explosives", August 31, 1953, Contract Number N7onr-45107, Project Number 357 239 (Salt Lake City).
- (2) A Study of Techniques for the Measurement of Detonation Spectra and Temperatures by J. H. Hett and J. B. Gilstein. Final Report from Research Division, New York University, May 14, 1953, Contract DA-30-069-ORD-945, Department of the Army (Restricted).
- (3) Boyer, R. L., "Determination of Detonation Temperatures in High Explosives", Phy. Rev., 74, 1221 (1948).
- (4) U. S. Bureau of Mines Progress Reports, "The Physics and Chemistry of Explosive Phenomena", January 1947 to June 30, 1950, Contract NAonr 29-48, NR 053 047.
- (5) F. C. Gibson, M. L. Bowser, C. W. Ramaley, and F. H. Scott, "Image-Converter Camera for Studies of Explosive Phenomena", Review of Scientific Instruments, 25, No. 2, 173-176, February 1954.
- (6) P. Caldirola, <u>J. Chem. Phys.</u> <u>14</u>, 738 (1946). See also S. R. Brinkley, Jr., <u>ibid.</u> <u>15</u>, 113 (1947).
- (7) M. A. Cook, <u>ibid</u>. <u>15</u>, 518 (1947). See also S. Patterson, <u>ibid</u>. <u>16</u>, 159 (1948).
- (8) S. Patterson, Research 1, 221 (1948).

# A NEW CINE MICROSCOPE AND ITS APPLICATION TO DETONATION PHENOMENA

J.S. Courtney-Pratt, B.E., Ph.D.,
Research Laboratory for the Physics & Chemistry of Surfaces,
Department of Physical Chemistry
University of Cambridge

Abstract

A Microscope has been built using the principle of image dissection that has been applied recently to the optical systems of cameras, so that series of photographs can be recorded at high speed, without complex equipment. (J.S. Courtney-Pratt, J.Phot.Sci.,1953,1,21) A plate embossed with a large number of small lenses is used to dissect the picture into small elements. These are all recorded simultaneously on a plate, but each element is separated from its neighbours by a distance that is large compared with the size of the element. Many successive pictures may be similarly dissected and recorded on the same plate interlaced with the others. The displacement of successive images with respect to the plate need only be as great as the width of a single picture element. In some cameras the displacement was produced by altering the direction in which light fell on to the lenticular plate. In the new microscope the displacement is produced by traversing the photographic plate. The phenomenon may be studied in transmission or reflection and very simple light sources are adequate.

The microscope has been used to take series of 200 pictures at 25,000 per second at magnifications of several hundred X. Higher magnifications are possible but at reduced speeds. Any smaller magnification can be achieved at the same or slower speeds, by simple substitution of longer focal length objectives, and the apparatus may even be used for high speed photography of distant objects. It has also been used to take series of shadowgraphs.

The quality of the pictures is limited by the number of lenslets across the lenticular plate - at present 320 lines across the field - but there is no reason why larger plates might not be used with corresponding improvement of picture quality up to the point at which the resolution is limited by the objective.

The microscope can be used to unscramble the composite record for slow motion viewing and for conventional printing of individual pictures. Separate unscrambling apparatus can easily be made.

#### Courtney-Pratt

The microscope is being used to study the earliest stages of detonation phenomena.

The speed, the range of magnifications, and the simplicity of the apparatus make it suitable for the study of many physical problems.

Introduction In the Research Laboratory for the Physics and Chemistry of Surfaces we have been studying fast reactions (1), and have developed a number of new photographic techniques (2-10). One branch of this work has been a study of the application of the principle of image dissection to cameras (6-9). This makes it possible to record a series of photographs at high speed without complex equipment.

The basic optical layout is shown in Figure 1. The main lens L forms a real image I of the object 0 on the front surface of a plate embossed with a large number of small lenslets. Consider the rays that pass through a small aperture at the centre of the main lens. rays fall on the lenticular plate and each of its lenslets focusses the light that falls on it to a small element on its principal axis. The photographic emulsion is placed in the focal plane of the lenticular plate, and the picture recorded by the emulsion is thus made up of a large number of small dots. In practice this is not a serious disadvantage. Most printed illustrations are similarly made up of dots. Provided the total number of dots is sufficiently large any given amount of information or picture quality can be reproduced. The large number of dots that go to make up a picture are all recorded simultaneously on the photographic plate, but each element is separated from its neighbours by a distance that is large compared with the size of the element. Many successive pictures may be similarly dissected and recorded on the same plate interlaced with the others. The displacement of successive images with respect to the plate need only be as great as the width of a single picture element. The displacement may be produced by altering the direction in which light falls on the lenticular plate or by traversing the photographic plate or the lenticular plate.

In one of the simplest sorts of camera, use was made of the first arrangement - altering the direction in which light falls on the lenticular plate. Consider again in Figure 1 the rays that pass through a small aperture near the outer edge of the main lens L. These rays form a real image I of the object 0 in the same place as before. Again each of the lenslets of the lenticular plate focusses the light that falls on it to a small element in the focal plane of the lenticular plate. However, these rays now fall obliquely on the lenslets so that the picture elements are no longer on the principal axes of the lenslets but are in a displaced peripheral position.

A convenient way of moving an aperture across a suitable lens is to cut the aperture in a disc mounted to run in the iris plane of a camera lens. As the disc rotates the aperture moves across. It is not necessary to restrict the movement of the aperture to a single line, and it is possible to move a series of apertures across different parts of the lens by disposing the apertures as a spiral array around

#### Courtney-Pratt

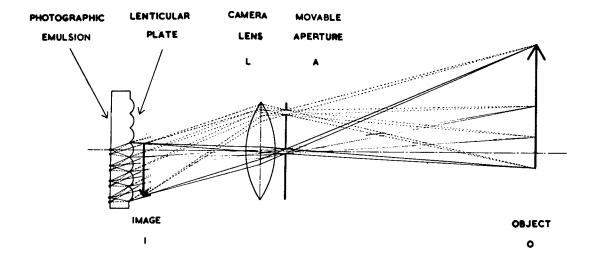


Figure 1: Diagram of the basic optical layout for image dissection multiple frame photography. The camera lens L forms a real image I of the object 0 on the lenticular plate which dissects the picture into a large number of elements each separated from its neighbours by distances large compared with its size, so that considerable numbers of independent pictures can be recorded on the one plate. The displacement of the picture elements for successive pictures can be achieved either by altering the direction in which light falls on the lenticular plate, and this can be achieved by movement of the aperture across the lens; or by traversing the lenticular plate or the photographic plate. Solid lines indicate the light paths when the aperture is in a central position. Dotted lines indicate light paths if the aperture is moved to a peripheral position.

## Courtney-Pratt

the disc.

A number of cameras of this kind have been built in the P.CS Laboratory, and more recently commercial manufacture has been commenced by J. Langham Thompson Ltd. The cameras are able to take series of 200 pictures at rates up to 125,000 per second. None of the mechanical tolerances of manufacture are at all stringent in these Their overall effective aperture is about F6.3 and their resolution, in different examples, 100, 200 or 300 lines across the They can be used equally well for selffield in both dimensions. luminous objects or for objects that are illuminated in reflection or in silhouette. They can be used conveniently for the photography of objects that are relatively distant, that is at magnifications from 1:00 to approximately 1:1: and with some complexity the magnifications can be increased a little beyond this. At magnifications much greater than unity the distance between the lenticular plate and the camera lens is much larger than the focal length of the lens and it is impossible to obtain enough scanning distance across the aperture of the lens to make full use of the photographic emulsion.

The Cine-Microscope It seemed that some of the difficulties of working at high magnification might be overcome if the sequential recording were effected by traversing the photographic plate instead of by moving an aperture across the camera lens. The major disadvantage that had to be faced was that the mechanical tolerances of movement of the photographic plate and of subsequent replacement of the plate after development, and removement were very much more stringent than in the earlier cameras. Figure 2 is a diagram of the optical layout for a simple microscope. Just as before, the main lens forms a real image of the object on the lenticular plate. Each of the lenslets of the plate forms a point image of the aperture of the main lens. As the photographic plate is traversed the bright elements each trace out a line on the photographic emulsion. If the direction of movement of the photographic plate were parallel to either of the axes of the lenticular plate, then after a distance of movement equal to the pitch spacing of the lenslets of the plate the traces drawn out by adjacent elements would begin to overlap. If the direction of traverse is inclined at an angle of, say, 1 in 10 to either axis of the lenticular plate, then the traverse distance can be equal to 10 times the pitch spacing of the lenslets before there is any overlapping of traces. In practice, the size of the image element is less than 1/20 of the pitch spacing and this means that it is possible to record on the photographic plate, traces for each lenslet that could contain 200 separate points. If the illumination is intermittent, these will be discrete points. If the phenomenon being photographed is of slowly varying intensity then there will be a continuous line but of modulated density.

If the distance between the lenticular plate and the microscope objective is large, the geometrical size of each image element is automatically kept suitably small as the angle subtended at the

J. Langham Thompson Ltd., Springland Laboratories, Bushey Heath, Herts.

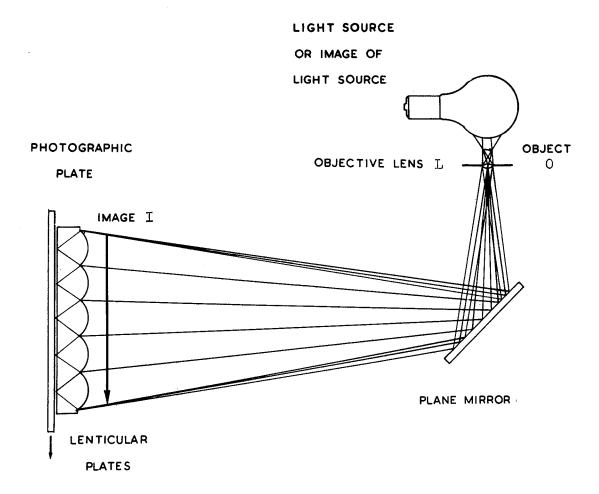


Figure 2: Diagram of the optical layout for multiple frame photography in a simple microscope. The lens L forms a real image I of the object 0 on the lenticular plate. Each lenslet of the lenticular plate forms an image on the photographic emulsion of the aperture of the microscope objective. Sequential recording is effected by traversing the photographic plate.

lenticular plate by the microscope objective aperture is very small. This means that the objective aperture need not be artificially restricted. This is of great importance as full use may then be made of all the light-gathering power that is available with modern microscope objectives.

Again, if the distance between the lenticular plate and the microscope objective is large it is possible to make use of a large lenticular plate and still keep within the field angle of conventional microscope objectives. The resolution of the picture depends on the number of lenslets across the plate and with the plates that we use there are 25 lenslets per cm. The larger the plate the higher can be the picture quality.

The number of pictures that can be recorded in a series depends on the size of the image elements. More strictly the number is proportional to p<sup>2</sup>/e<sup>2</sup> where p is the pitch spacing of the lenslets and E is the width of an image element. The success of the method is thus critically dependent on the quality of the lenticular plates, and I would like to express my thanks for the assistance and co-operation of M.R. Marilhet whose firm has supplied all the lenticular plates that I have used. They were developed primarily for stereoscopic photography by the Bonnet process . A thin sheet of plastic bonded to a sheet of glass is embossed by a die or matrix cut in fine-grained metal with an array of cylindrical lenses. If two such cylindrical lenticular plates are placed together with their embossed faces just touching, the combination acts as though the plate has been embossed with an array of spherical lenses 12. A parallel beam of light is brought to a corresponding array of point foci and the resolution is surprisingly good. The width at half intensity of such point foci is less than p/100. In practice the size of the image element is increased above this because of the grain of the photographic emulsion, and the physical size of the objective aperture. Moreover, image elements to be clearly resolved must be further apart than their widths at half intensity as otherwise there is some interference and ghosting. However, with present apparatus an image width of p/20 can easily be achieved using process plates, and about twice this with fast emulsions.

Figure 3 is a photograph of a microscope made to try out these ideas. A number of pieces from a Vickers projection microscopet have been incorporated. It is possible to use any of the objectives, eye-pieces, illuminators, condensors and any of the attachments to the mechanical stage that are currently available. The box-like structure to which these pieces of the projection microscope are attached simply ensures that the microscope objective (and the projection eye-piece, if one is used) are a long distance from the lenticular plate.

A framework has been built from drawn steel angle to contain the lenticular plate, the photographic plate and the traverse mechanism. This frame is kinematically mounted on the end of the main frame of the

<sup>\* &</sup>quot;La Reliephographie" 152 Av. des Champs Elysees, Paris. + Manufactured by Cooke, Troughton & Simms Ltd., Haxby Rd., York.

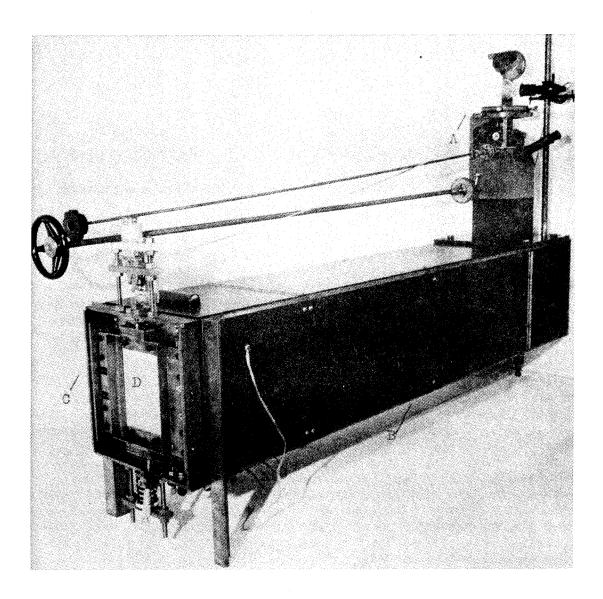


Figure 3: Photograph of the cine-microscope - A. Parts of a Vickers Projection Microscope. B. Main Frame. C. Detachable camera back holding lenticular plate, photographic plate, and traverse mechanism. D. Traversing frame to hold photographic plate. E. Detachable micrometer traverse for unscrambling the composite record.

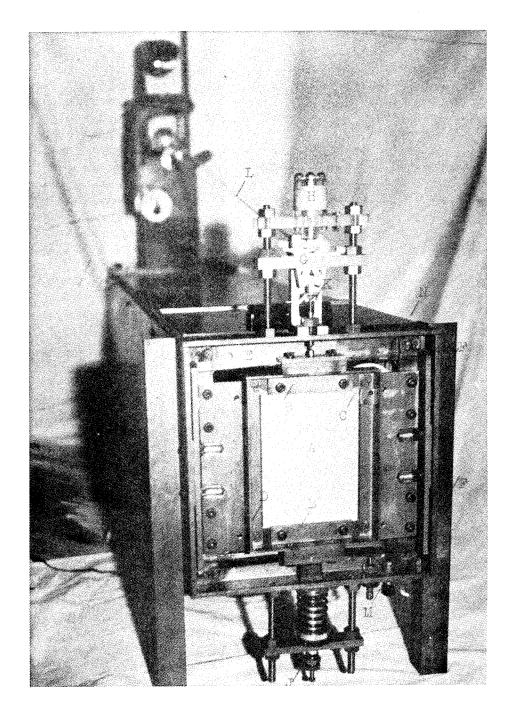


Figure 4: Enlarged view showing traverse mechanism of the cine-microscope. A-The photographic plate. B - clamps. C-Kinematic stops.D-traversing frame to hold plate. E-Elastic steel links. F-Stiff cantilever springs. G-Toggle catch mechanism. H-Release solenoid. J-Accelerator springs and buffers. K-Bell crank. L-Steel tape to operate capping shutter. M-Adjustable synchronising contacts. N- Timing Wheel, 200 teeth, 50 r.p.m. The photographic plate A in the plateholder D can move up and down. The lenticular plate, not visible in this figure, is immediately in front of the photographic plate, and is fixed with respect to the axis of the microscope.

microscope. Figure 4 shows a closer view of the traverse mechanism. The photographic plate A is fastened by clamps B against kinematic stops C in a steel frame D. To avoid any possibility of back lash, this steel frame is mounted on four elastic steel links E. These form an elastic parallelogram linkage but if their outer ends were rigidly fixed they would not allow movement without extension of the links. Accordingly, the outer ends of the steel links E are fastened to four very stiff cantilever springs F. The photographic plate and steel frame D can then be traversed up and down about one centimetre for a force of 15 kilogrammes. A similar force applied in either direction in a horizontal plane produces a deflection which is less than 0.005 cm. As the cross forces need never be greater than a fraction of a kilogramme it is easy to maintain reproducibility of the traverse to a very high order. The variation of force with displacement in the traverse direction is non-linear. The force for small displacements is very small: the force for larger displacements rises very steeply. If the frame D is displaced and then allowed to spring back, the initial acceleration is very high but it traverses. the centre section at nearly constant velocity.

At the top of Figure 4 can be seen a toggle catch mechanism G. It is possible with this to hold the frame displaced and then to release it either mechanically, or electrically by cutting off the current in the solenoid H. At the bottom of this Figure can be seen a system of accelerator springs and buffers J which can increase the working velocity of the plate a factor of  $2\frac{1}{2}$  - from 30 cms/second to 75 cms/second.

Figure 5 is an enlarged view of a small section of a composite plate on which are recorded some 200 pictures of a rotating slotted wheel. Behind each lenslet of the lenticular plate is a track which is alternately dark and light depending on whether or not there was an image of a tooth or a space falling at that moment on that lenslet. It can be seen that the tracks are distinct and separate, and are inclined at an angle of about one in thirteen to the array of lenslets. Figure 6 is an enlargement of a small section of the same composite plate on which fell an image of a second rotating wheel. In this case the small wheel was driven by a synchronous motor at 3000 r.p.m. and had cut in its periphery 200 small teeth. The alternate teeth were cut twice as deep and other sub-multiple numbers of teeth were cut at greater depths. Again, as each slot passed in front of any given lenslet a dot was recorded, and it can be seen that discrete dots have been recorded at 104/second. On occasions on which the additional springs were used to accelerate the plate these timing dots were spaced 21 times further apart so that even at the most conservative estimate it is possible to record pictures at 25,000 per second. This speed could easily be increased a further factor of 3 even using the present elastic suspension system and accelerator springs, if a plate holder of similar design to the present one, but made of light alloy, were substituted for the steel plate holder.

Viewing the Record On some occasions it is valuable to study the

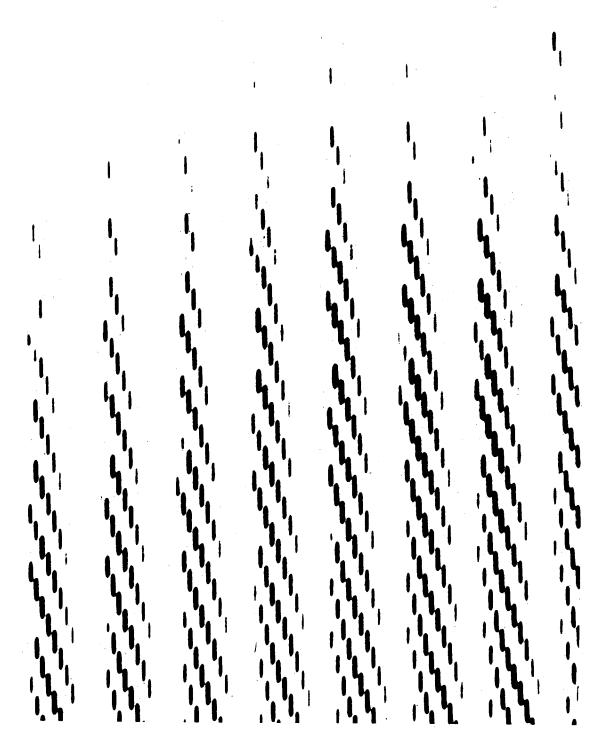


Figure 5: An enlargement at 50X of part of the composite plate on which was recorded a series of 200 pictures at 10<sup>4</sup>/sec. of the rotation of a slotted wheel. The trace behind each lenslet is alternately dark and light depending on whether or not there was falling on it the image of a spoke or a slot of the rotor.

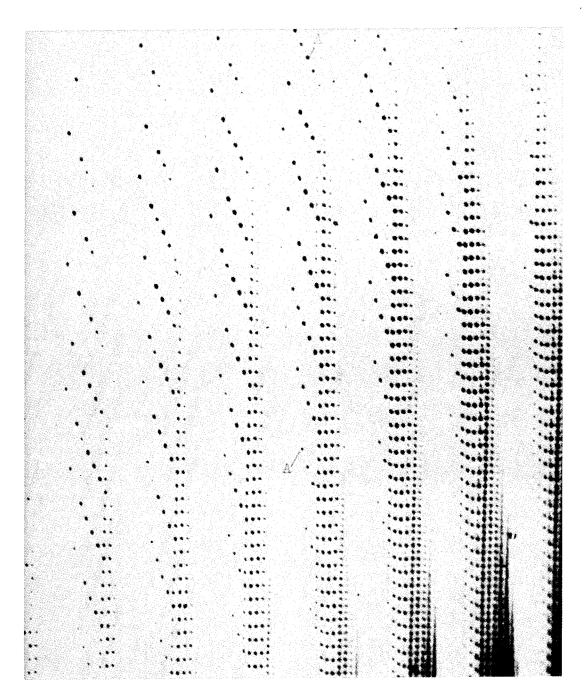


Figure 6: An enlargement at 50X of part of the composite plate on which was recorded a series of 200 pictures at 10<sup>1</sup>/sec. of the rotation of a toothed wheel revolving at 50 r.p.s. In the periphery of the wheel are 200 slots. Alternate slots are twice as deep and other submultiple numbers are deeper still. This wheel silhouetted on each composite plate provides a useful time reference as the dots for the shortest teeth occur at 10<sup>1</sup>/sec. - those seen on the right of the Fig. Other lenslets draw out a series of dots at 1/2, 1/10, 1/20, 1/100 of this frequency - e.g. at AA the dots occur at 10<sup>3</sup>/sec.

composite plate directly. For example, from these last two enlargements it would be possible to determine the rate of rotation of the slotted rotor. More usually, one wishes to examine individual pictures or frames - that is, to unscramble the composite record. There are various ways of doing this. The simplest is to replace the composite plate after processing in the plate holder D, and to illuminate the microscope objective with a steady light source. Light will pass through the apparatus just as during recording and each lenslet of the lenticular plate will concentrate light on to that particular part of the track that was recorded when the photographic plate was in that identical position. The light that falls on any lenslet is focussed to a small dot on the photographic plate. Some of this light is absorbed, depending on the density of the plate at that point, and the remainder passes through the photographic plate and spreads out so that at a distance behind the emulsion about equal to the focal length, f, of the lenslet the light fills an area about equal to the aperture of the lenslet p2. Thus, in a plane distant f behind the emulsion there is a picture of smoother toning but otherwise identical to the single frame made up of the tiny distinct dots that were all recorded simultaneously. This picture can be viewed directly or it can be allowed to fall on a diffusing screen so that it can be more easily seen when looked at obliquely, or alternatively, a photographic printing paper can be placed at this plane for obtaining a direct or 'contact' print.

If the photographic plate is slowly traversed by a micrometer, such as that shown in Figure 3, at E, just below the plate holder D, the phenomenon recorded can be viewed in slow motion. It is possible to copy this slow motion presentation with an ordinary cinecamera for later projection through conventional apparatus. In another method of unscrambling, the direction of the light rays can be reversed. That is, the photographic plate is illuminated from behind and the record can be viewed by placing the eye at the position of the microscope objective or recorded by placing there the lens of a copying camera.

Figure 7 shows four contact prints taken from the same plate, enlargements of parts of which are shewn in Figures 5 and 6. These prints were each taken simply by holding a printing paper against the back of the photographic plate when it was placed in some one of its traverse positions and a light placed over the microscope objective. The second of the prints is similar to the first except that the plate has been traversed forward by .0025 cm. a distance corresponding to  $10^{-4}$  of a second. It can be seen that the timing wheel has travelled forward one tooth in this interval. The third and fourth prints are similar frames but recorded at later intervals. These prints give some idea of the resolution and fidelity of the record.

Applications of the Apparatus The microscope has been used to study a number of things such as the vibration of fibres, the formation of droplets, and the operation of relay contacts.

There is no necessity to restrict the use of this apparatus to photography at enlargement. The whole of the recording mechanism can be used in any camera to take pictures at the same speeds as

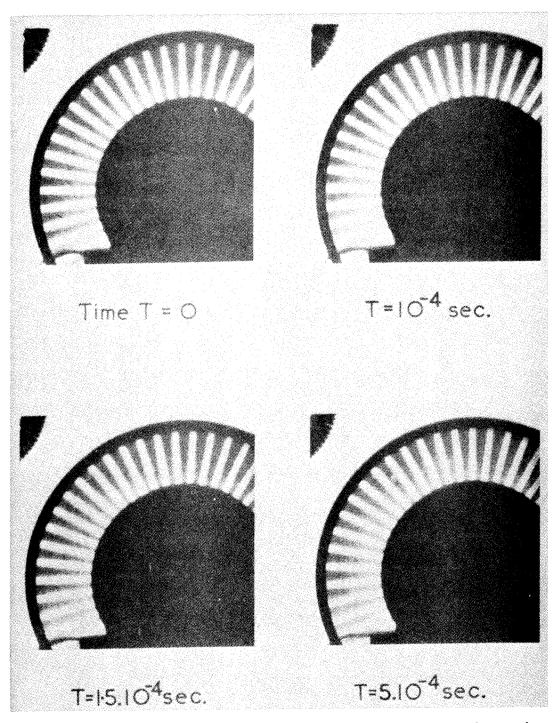


Figure 7: Four prints unscrambled on the microscope from the series of 200 recorded on the composite plate from which Figures 5 and 6 have been enlarged. The slotted rotor and the timing wheel can both be seen to rotate. The measured interval between the first two prints is 10<sup>-1</sup>4 sec., between the second two is half of this, while the last is somewhat later. Both the slotted rotor and the timing wheel have been recorded as shadowgraphs at unity magnification.

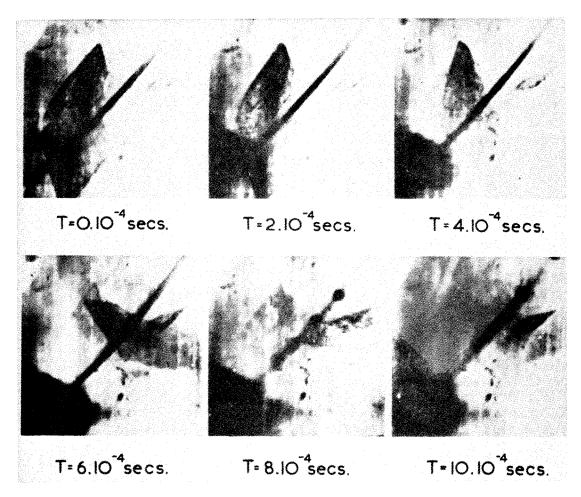


Figure 8: A selection of 6 pictures from the series of 200 recorded at an enlargement of 65X of the ignition of a small crystal of mercury fulminate by a wire heated by a sudden pulse of current. (i) T=0 Two crystals and Platinum Rhodium wire of diameter 0.003" before ignition. (ii) T=2.10<sup>-4</sup> sec. The larger crystal is ignited at the lower left where it is in contact with the wire. (ii) T=4.10-4sec. The crystal begins to move bodily under the reaction from the expansion of the gaseous products of decomposition. The decomposition has formed a crater in the side of the crystal. (iv) T=6.10-4 sec. The crystal has moved further across the field of view and has turned through 90°. Small fragments have broken away from the crystal and are left behind. These fragments do not decrease in size, nor does the crater increase, and presumably reaction has ceased. (v) T=8.10-4sec. The wire has melted and has formed into droplets thinly joined by molten filaments. Severe block cracking of the crystal is evident. (vi) T=10.10-4 sec. Some of the droplets of the melted wire have coalesced and are at this stage oscillating vigorously. It will be noted that the fragments broken from the large crystal are not consumed, and the smaller crystal has remained unaffected throughout.

before (i.e. up to 25,000 frames/second). Simply by the substitution of suitable lenses the apparatus can be used at low magnification - or for the photography of remote objects. These objects, too, can be either self-luminous or separately illuminated. On one occasion, for example, the microscope objective was replaced by a spectacle lens of focal length 1 metre, and an iris fitted to stop it down to an aperture of 1.2 cms. The camera was then used to photograph the cutter of a milling machine running at 600 r.p.m. from a distance of  $2\frac{1}{2}$  metres.

However, the main field of work in which we are using the microscope is the study of the earliest stages of explosive reactions. There are many problems in the mechanism of the ignition of crystals of explosives - How do the crystals burn? Do they break up into blocks? Does detonation proceed uniformly through a crystal? How is the reaction transferred from one crystal to another? Why, sometimes, does a detonation fade? In some cases reaction has been initiated by an intense flash of light, in others azides and fulminates have been ignited by direct contact with a heated wire.

I would like to express my thanks to Dr. A. Yoffe, for the series of six pictures which are shown in Figure 8. These are a selection from the 200 recorded at a magnification of 65X. The illumination was provided by a Philips' Photo-flash bulb, type PF 60E, and an ordinary condenser system was used. The photographic plate was Ilford process type N4O, developed in ID 11 for 2 to 3 minutes. The slow motion record shows the ignition of the crystal of mercury fulminate at one edge by contact with the platinum rhodium wire (dia. 0.003") when it was heated by a sudden 5 amp current pulse. The rapid evolution of gas propels the crystal bodily across the field of view, the part of the crystal that has been decomposed can be clearly seen, and when the crystal has travelled some distance a fragment near this crater breaks off and is left behind, probably because of thermal stresses or due to the evolution of gas within the crystal material. While the crystal is moving across the field of view, the heating wire melts, forms into small droplets, and some of these later coalesce. In the slow motion play-back of the record, the droplets after they coalesce can be seen to oscillate rapidly. It is interesting to note that a second crystal that was originally near the first remained stationary throughout the record, and had not been ignited, although a burning crystal was in close proximity. Indeed it would appear that the first crystal, though it burnt vigorously near the point at which it was heated, did not continue to react at the same rate, and may even have ceased to decompose.

<u>Light Sources and Accessories</u> As mentioned earlier it is possible to make use of the whole of the light gathering power of the microscope objective. Furthermore, all the light which falls on any lenslet of the plate is concentrated to a small picture element which may well be 1/400 of the size of the lenslet. The brilliance of the points that are actually imaged on the emulsion is thus much greater than would be the case in a conventional microscope. Because of this intensifying effect of a lenticular plate<sup>12</sup> and because it is possible to use large numerical aperture objectives, it is possible to take

pictures at high magnification with short exposure times even using comparatively weak sources. A limit to the magnification and speed that is possible with a given photographic emulsion is set by the specific brilliance of the source, provided, of course, that the source is above a certain minimum size. It is possible to use arc lamps, but by far the most convenient sources and, in fact, the ones that I have used for all the illustrations in this paper, are ordinary photo-flash bulbs (magnesium-oxygen). The specific brilliance of these bulbs if of the order of 10th candles/cm2, and is comparable with the brilliance of the crater of a carbon arc. The duration of the flash varies with the different types of bulb, but for the brighter bulbs it is above half intensity for more than 1/100 sec. and usually has a long low-intensity afterglow. The flash from one of these bulbs is sufficient to allow a recording of the whole series of 200 pictures on the one photographic plate, even a process plate, at magnifications up to 500X and more.

It was desirable to reduce the fogging of the film from stray light or from the afterglow from photo-flash bulbs, and a capping shutter has been incorporated in the microscope. A small bell crank K is operated as the plate holder D, Figure 4, moves down and this draws a steel tape L through a slot just below the microscope objective. An aperture cut in the steel tape registers with the microscope objective aperture and allows exposure of the photographic plate for the correct traverse distance, when the plate is in mid-traverse and moving with nearly constant velocity. I would like to express my thanks to G.R.R. Bray for suggestions which, with minor modification, led to the development of this form of capping shutter. Adjustable contacts M have been provided for synchronising light sources or features of the event from movement of the plate holder.

The specific brilliance of flash discharge sources can be higher than that of a carbon arc and some work has been undertaken with D.P.C. Thackeray to produce suitable discharge lamps for use with this cine-microscope. Some of these are described briefly in a paper presented at the recent Conference in Paris on High Speed Photography(10). It was found that enough light could be produced to record pictures at 10<sup>4</sup> frames/second if a current somewhere between 10 and 100 amps was passed between the electrodes in a short gap flash tube. The current could be provided by using a simple contacter on a high-tension supply, or with some difficulty by the use of a number of condensers and chokes arranged as a lumped delay line. Repetitive flashing of the source was also tried, using a rotary brush switch.

The specific brilliance of the spot on the screen of a cathode ray tube is also comparable with the brilliance of the crater of an arc lamp and a good deal of work has been done in the P.C.S. Laboratory on the development of gear for making use of the cathode ray tube as a source of light in high-speed photography (10)

Now in all the uses of the apparatus described above the light that comes through the objective falls directly on the lenticular plate and the physical size of the aperture of the

objective is quite small and fairly distant from the lenticular plate. If any object were placed between the objective and the lenticular plate it would cast a shadow on the plate. The apparatus could thus be used to record a series of shadowgraphs. In fact, use has been made of this for adding a time scale to all of the plates by means of the toothed wheel N, Figure 4, as described earlier; and Figures 5,6 and 7 all relate to a shadowgraph recording of the rotation of a slotted rotor and this timing wheel.

As explained earlier, it is possible to unscramble the composite record by replacing the composite plate, after processing, It would be difficult to make lenticular plates in the plate holder. sufficiently nearly identical to be able to unscramble in one apparatus a record made in another. It is, however, often convenient to have a separate means for unscrambling a record and this can be done quite simply: A graticule plate, such as the Kodak MR plate, is placed behind the lenticular plate and a static picture taken. When this is developed there are small black dots in a clear field. A contact print of this is taken on another graticule plate and when this is developed there are small clear dots in a black field. This array of dots is identical with the array of foci of the crossed pair of lenticular plates. If now a composite plate is aligned on top of this and the two together viewed in transmission, only one of the recorded frames from the composite plate will be visible at a time. By traversing one plate relative to the other it is possible to obtain slowmotion viewing. This provides a much more graphic presentation of an event than the individual examination of successive discrete frames.

Summary A microscope has been built using the principles of image dissection. Without elaborate gear it has proved possible to take series of 200 pictures at 25,000 per second at magnifications as high as 500X, using process plates, and providing the illumination for the whole of each series from one magnesium-oxygen photo-flash bulb. Micrographs have been taken in transmission and in reflection. The resolution of the pictures is 320 lines across the field in each dimension - comparable, that is, with the quality that can be obtained on a standard 16 mm. cine-frame.

It has been shown that, by the simple substitution of long focus lenses, the apparatus can be used equally well for the photography of remote objects at the same high rates. It has also been used for recording fast series of shadowgraphs.

Much higher magnifications (up to 5000X) are possible but at reduced rates. As at these high magnifications the limitation on maximum recording rate is one of light level and plate speed, it is possible to obtain considerable improvement by the use of fast emulsions, but this can only be done at some expense in the number of separate pictures that can be resolved in a series.

It is to be expected that the maximum rate of taking pictures for magnifications lower than 500%, where the limitation is imposed by considerations of mechanical inertia, could be increased by substitution of light alloy components and some attention to design

detail by a factor of 4 at least, so that pictures could be taken at rates in excess of 10 /second without increasing the delay between release and full running speed beyond the present figure of 10 second. This comparatively long delay is a drawback and means that for the photography of many phenomena synchronisation must be from the camera to the event.

The apparatus can be used to unscramble its own record for slow motion viewing or for taking prints of particular pictures. Separate unscrambling apparatus has also been made.

Studies have been made of the initiation and the early stages of reaction in small crystals of explosives, such as azides and fulminates. Records have also been taken of the initiation of reaction by high intensity light flashes.

Timing reference marks at  $10^4/\text{sec.}$  are recorded on the composite plate. Synchronising contacts and a synchronised capping shutter are incorporated.

The speed, the range of magnifications, and the simplicity of the apparatus make it suitable for the study of many physical problems.

## Acknowledgements

The broad principles upon which this cine-microscope and particularly the last design of unscrambler have been built bear considerable resemblance to those embodied in apparatus developed by Fordyce Tuttle (13,14) and by Morton Sultanoff (15,16,17), and I would like to acknowledge the help that I have received from them in discussion and from their papers. I would like to express my thanks to Dr. F.P. Bowden, F.R.S., for his continued advice and encouragement, and to thank the other members of our laboratory for their assistance. I also wish to express my thanks for the support given by the Ministry of Supply (Air), the Royal Society, and Vauxhall Motors Limited.

### References

- (1) F.P. Bowden and A.D. Yoffe, Initiation and Growth of Explosion in Liquids and Solids, Cambridge University Press 1952.
- (2) J.S. Courtney-Pratt, Research 2, 287, 1949.
- (3) J.S. Courtney-Pratt, Proc. Roy. Soc. A204, 27, 1950.
- (4) J.S. Courtney-Pratt, Phot. J., <u>92B</u>, 137, 1952.
- (5) J.S. Courtney-Pratt, Brit. Pat.No. 662,065.
- (6) J.S. Courtney-Pratt, J. Phot.Sci., <u>1</u>, 21, 1953
- (7) J.S. Courtney-Pratt, Fourth Symposium (International) on Combustion, M.I.T., The Williams & Wilkins Company, Baltimore, pp. 508-526, 1953.
- (8) J.S. Courtney-Pratt, Brit. Pat. No. 712,997.
- (9) J.S. Courtney-Pratt, A High Speed Cine Microscope, International Symposium on High Speed Photography, Paris, September, 1954.
- (10) J.S. Courtney-Pratt, and D.P.C. Thackeray, Fast Multiple Frame Photography by Cathode Ray Tube Illumination, International

- Symposium on High Speed Photography, Paris, September, 1954.

  (11) La Reliephographie, Societe pour l'Exploitation des Procedes de Photographie en Relief. Maurice Bonnet. Brit. Pat.No.615,629.

  No. 619,948. No. 622,917, No. 638,551. Brit.Prov.Pat.No.26923/45.
- (12) La Reliephographie, Society pour l'Exploitation des Procedes de Photographie en Relief. Maurice Bonnet. Brit. Prov. Pat. No. 29577/45, No. 29578/45. French Pat. No. 745/942.
- (13) Fordyce E. Tuttle, J. Soc. Mot. Pict. Engrs., 53, 451, 1949
- (14) Fordyce E. Tuttle, J. Soc. Mot. Pict. Engrs., 53, 462, 1949
- (15) M. Sultanoff, Rev.Sci.Ins., 21,653,1950
- (16) M. Sultanoff, J. Soc. Mot. Pict. Engrs., 55, 158, 1950
- (17) M. Sultanoff. Soc. Mot. Pict. Engrs. Convention, October 1952.

### THE MEASUREMENT OF DENSITY CHANGES IN GASEOUS DETONATIONS

G. B. Kistiakowsky and P. H. Kydd Harvard University Cambridge, Massachusetts

### Abstract

An apparatus is described for determining rapid density changes in gaseous detonation waves. Its time resolutions is better than 1/2 usec; quantitative measurements of density changes are possible to about 15%, with an absorbing path of 10 cm and gas densities in the range of 1 g/liter.

Experiments with several explosive mixtures at an initial pressure of one atmosphere have failed to reveal reaction zones (v. Neumann spikes) in detonation waves. Upon resorting to xenon as the X-ray absorbing component, it became possible to study gas density changes in detonation waves produced in mixtures at a small fraction of one atmosphere pressure. Using stoichiometric hydrogen oxygen mixtures with added xenon, the first indications of the spike were obtained at 1/8 Atm. initial pressure. The spike lasted about 3 µsec at 0.1 Atm. and was broadened to 20 µsec at 0.025 Atm. Replacement of xenon with a much higher partial pressure of argon repressed the spike.

Studies of the variation of gas density as a detonation wave passes through an explosive medium should offer a confirmation of the well-known Zeldovich-von Neumann theory of the detonation reaction zone, and yield at least qualitative information on the kinetics of the reactions occurring. The theory predicts a discontinuous rise in density at the wave front to the value expected for a pure shock wave moving at the detonation velocity. The non-isentropic heating of the gas by the shock initiates vigorous chemical reaction, which causes the temperature to rise and the density to fall until chemical equilibrium is reached in the Chapman-Jouguet state (1). One should therefore observe a sharp density peak, whose shape and duration are related to the rate of attainment of equilibrium. In a

typical case the density of shocked but unreacted gas is about five times the initial density, and it decreases to less than twice this amount in the C-J state. The technique of gas density determination by X-ray absorption is particularly well suited to this problem, as it offers instantaneous and continuous measurement of density, and is independent of chemical change or visible light associated with the detonation reaction. An apparatus of this type has been developed (2), and the latest modification of it will be described.

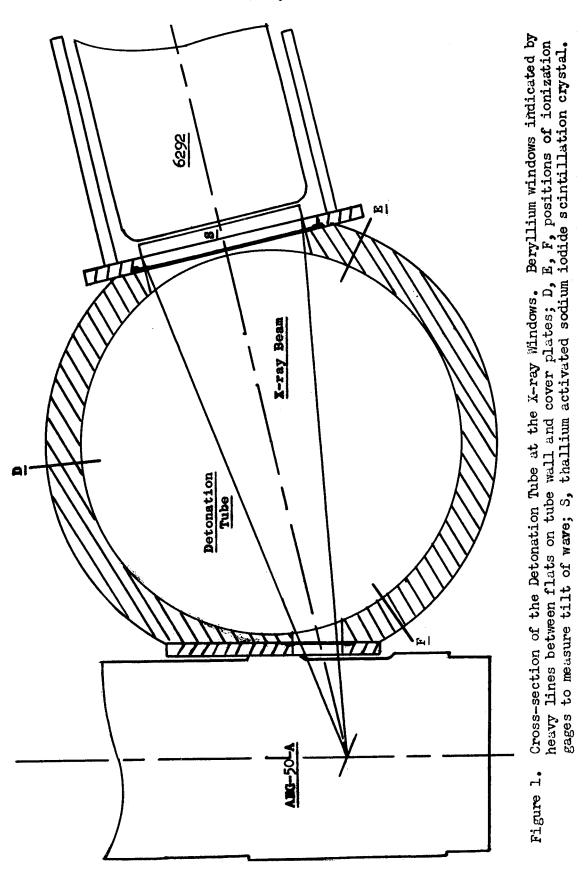
An X-ray absorption photometer with oscillograph recording and suitable calibration equipment has been incorporated into a 10 cm I.D. detonation tube in such a way as to obtain a continuous record of the average gas density along one diameter within the tube. As a detonation wave moves past the photometer slits in a direction normal to this diameter, the changes in gas density in the wave front are displayed on the oscillograph and photographed.

The chief difficulty encountered in the use of this method has been the low signal to statistical noise ratio obtainable with conventional X-ray equipment in the short time intervals of interest. There are two ways of alleviating this; first, to increase the intensity of the primary X-ray beam, since the signal to noise ratio increases as the square root of the total intensity; second, to increase the absorption by using soft X-rays and adding a strongly absorbing component to the explosive mixture.

The most satisfactory type commercial X-ray tube for this application is one with a copper target and beryllium window producing a high intensity of low energy X-rays. The tube in use at present is a Machlett model AEG-50-A. This tube has a grounded water-cooled anode with a focal spot 1.5 mm wide and has been operated at 22 KV DC, 32 ma, supplied by a G.E. XRD X-ray diffraction apparatus transformer and rectifier. The high voltage is filtered by a 1/2 microfarad condenser; the filament current of approximately 4 amps AC is supplied by the same transformer. To increase the intensity without damage to the tube, an automatic switch has been incorporated in the tube filament supply to increase the emission current to 32 ma, somewhat higher than is recommended for continuous operation, for a period of three seconds during which the detonation takes place.

Since the usual explosive mixtures studied do not absorb even soft X-rays to a sufficient extent, it has been found necessary to increase the absorption coefficient by adding a component of high atomic number. Argon and later Xenon have been used successfully, the latter giving sufficient absorption at partial pressures as low as 7 mm.

The X-ray beam is allowed to pass through the 10 cm I.D. detonation tube by two opposing beryllium windows resting on flats milled in the tube wall, see Figure 1. Slits, 3/32" wide in the direction of the wave travel, were milled in the wall under the



windows defining a  $17^{\circ}$  wedge of radiation. The windows are .010" think, supported by 1/8" steel cover plates which carry 1/16" wide defining slits and rubber gaskets to seal the windows. This arrangement leaves the windows free to be removed, and yet is strong and vacuum tight.

The cover plate over the exit window also carries the photomultiplier detector. This is a DuMont type 6292 end-window tube with a photocathode diameter of 1-11/16", coupled with a 1-3/4" diameter, thallium activated, sodium iodide scintillation crystal. The potential divider for the dynode supply voltages and a cathode follower to match the output to the input of the signal amplifier are mounted in a small chassis attached to the tube socket. The tube and socket slip into a brass tube soldered at right angles to the cover plate which provides shielding from light and electrical interference as well as support. The signal amplifier is a Browning video type with a constant and adjustable gain of as much as 650 from 7 CPS to 4 Mc. The amplifier is connected to the vertical plates of an Atomic Instrument Co. single sweep oscilloscope with an adjustable horizontal sweep duration, which can be accurately timed by 20 microsecond pips. The X-ray intensity vs. time traces obtained when the oscilloscope is tripped are photographed.

To relate the vertical displacements of the CRO traces to gas density changes requires two separate operations. The first of these is to determine the change in output of the photomultiplier as a function of the gas density for a given set of operating conditions of the X-ray tube. The output is read directly on the micro-ammeter shown in Figure 2. This corresponds to the observed X-ray intensity, I, and is plotted against gas density as the natural logarithm of the ratio of I to I, the output with the detonation tube evacuated. The slope of this plot is the mass absorption coefficient times the (constant) path length in the absorption equation

$$\ln \frac{\mathbf{I}}{\mathbf{I}_o} = -\alpha$$

The absorption coefficients determined in this manner are not constants due to the non-monochromatic nature of the radiation and are dependent on the X-ray tube voltage and emmission current.

To the accuracy of the present measurements, the slight effects of chemical change on X-ray absorption are negligible. Therefore, the calibration is carried out with a non-explosive gas mixture at room temperature chosen so that the ratio of atomic species is identical to that of the explosive mixture to be used later. The calibration curve determined for this mixture is then taken to be that of the explosive mixture before, during, and after the explosive reaction.

The second step is to relate the vertical displacements on the CRO records of each experiment to changes of X-ray intensity and thus, through the above calibration curve, to changes in density. To accomplish this the X-ray intensity is observed on the microammeter immediately before each experiment. Because of the AC amplifier used, this corresponds to a horizontal line of zero vertical deflection on the oscilloscope record. Immediately after the experiment the photomultiplier supply voltage is turned off. A circuit shown in Figure 3 is connected to the detector chassis which substitutes for the photomultiplier and produces step function traces on a separate film, corresponding to known changes in X-ray intensity from the The mode of operation is as follows. After the initial value. calibration circuit is connected, the initial intensity adjustment is set to reproduce the initial observed current on the microammeter. Then the step intensity selector is set to the first position and the thyratron switch triggered by shorting the grid to the cathode. This raises the potential at A, causing less current to flow through the nitial intensity adjustment resistor, i.e. simulating a reduced X-ray intensity in a stepwise manner. The single sweep oscilloscope is triggered at the same instant and the result is a horizontal trace corresponding to a decreased intensity as might have been caused by a sudden increase in gas density. This decreased intensity is then read on the meter. The thyratron switch is turned off, by breaking the grid-cathode short circuit and breaking the connection in the step intensity selector; the next selector setting is chosen and the process repeated. This is continued until the desired lines are drawn, and a base line corresponding to I, is added by triggering the oscillioscope manually, with the thyratron switch open. By matching the baselines corresponding to  $\mathbf{I}_{\mathbf{i}}$  in this record and the density record obtained in the detonation experiment, it is possible to read the intensity at any point by interpolation between the calibration lines.

To convert the intensity values to gas density, I must first be determined by using I, the known initial density, and the calibration curve. Then values of  $\ln \frac{I}{I}$  can be referred back to the calibration curve and the density determined at any point.

Random errors are introduced during this procedure by the static calibration and the reading of the two films. The total error from these sources is estimated to be 10%. Further random error occurs due to the statistical fluctuations of X-ray intensity. It has proved possible to compensate for this to a large extent by making a number of duplicate runs and averaging the results at each

The systematic errors are more difficult to estimate as well as more serious. Despite the fact that low output currents were drawn from the previously employed 1P21 photomultiplier tube during the static calibration, serious fatigue was encountered, which

time of interest.

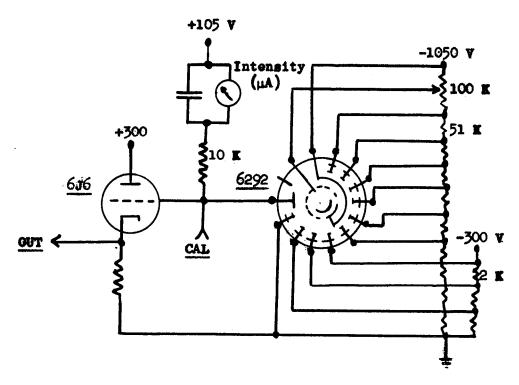


Figure 2. Photomultiplier Detector Circuit.

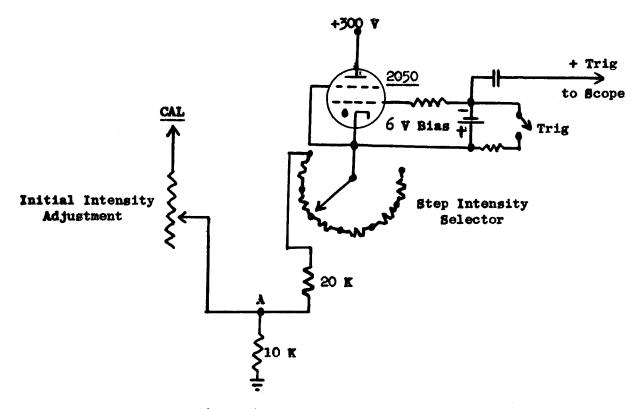


Figure 3. Calibration Circuit.

necessitated corrections. Any change in the characteristics of the oscilloscope and amplifier between the experiment and the calibration could aggravate this. The agreement between theory and experiment to date has been within 15%.

The detonation tube is made up of sections of 10 cm ID steel and brass pipe equipped with flanges and O ring grooves at the ends and bolted together to make up any desired length. A 50 cm length at the initiation end is separated from the remainder by a thin plastic diaphragm and filled with equimolar acetylene-oxygen. This when ignited by spark very rapidly forms a stable plane detonation wave which is transferred through the diaphragm to the experimental mixture. In addition to the X-ray apparatus, the remainder of the tube is equipped with ionisation gages (3), which produce small electrical signals when struck by the detonation wave front. The signals can be displayed directly on a time calibrated oscilloscope sweep and photographed, but more accurate reading is possible by inserting the amplifier-pulse shaper described in (8). Twelve gages are spaced at 10 cm intervals along the top of the tube. The first and ninth serve to trigger the velocity recording scope and the density recording scope respectively, and the other nine determine the velocity. At the tenth and eleventh positions, two additional gages, at the same distance along the tube but at 120 degrees to the first, indicate the tilt of the wave front. The signals from these gages are delayed by 2 and 4 microseconds respectively to distinguish them from the first. The end wall of the tube contains three more gages on a diameter to detect non-planarity of the wave: the signals are delayed in the same manner as the tilt signals. It has been found that at low experimental pressures favorable to X-ray investigation plane and normal waves could only be obtained in relatively long tubes and a length of 3.5 meters from diaphragm to slit system has proved satisfactory. In addition the ionization gages were found to be insensitive to low pressure detonation waves in  $H_2-O_2$ . by using higher voltage on the ionization gap electrodes with very small signal condensers of 15-30 μμf to prevent multiple signals, and especially by using steel wires protruding 1/4" into the tube as the electrodes, this difficulty was overcome down to experimental pressures of 15 mm.

#### Results

The experiments so far performed have been made with an earlier modification of the apparatus herein described which differed only in detail. A number of experiments were made to detect the reaction zone in detonations of both hydrogen-oxygen and acetylene-oxygen mixtures at one atmosphere initial pressure. Under these conditions the reaction zone was undiscoverable within the resolving time of the apparatus of less than 1/2 microsecond. Nothing of interest was determined in this phase of the investigation, and the apparatus was used to verify the hydrodynamic predictions for the

density distribution in the rarefaction region behind the steady state zone (4). This was done for equimolar acetylene-oxygen with 20% added argon at a point 69 cm from initiation. It was found that the manner of initiation was important for the rapid establishment of a normal detonation, and that simultaneous sparks distributed evenly over the initiation end wall gave very satisfactory results. This initiation system has been used since in all experiments. The results were in agreement with the hydrodynamic prediction of an isentropic expansion wave following the detonation wave front, with the gas expanding until its forward motion ceased and then remaining at rest at constant density.

At the completion of this work hydrogen-oxygen mixtures were again studied, this time at reduced pressure with xenon as the absorbing additive. Due to the pressure dependence of the reaction rates, it was now possible to identify the reaction zone and vary its duration by varying the pressure. The highest pressure at which concrete evidence of the reaction zone was obtained was 95 mm of 70% H\_-30% O with 15mm We added, with which a sharp density spike was observed in one experiment. At 85 mm reactant pressure, the reaction zone was observed consistently and five experiments were performed so that the results could be averaged and the statistical fluctuations reduced, as shown in Figure 4. The density does not reach the full shock value by a large margin though measurements were carried out to within 1/2 microsecond of the wave front. This is partly due to finite time resolution of the equipment and perhaps to errors in the static calibration curve. However, since the same behavior was noticed in experiments at lower pressures in which the reaction zone is much longer and in which the C-J density is reproduced accurately. it appears that, contrary to expectation, the reaction starts practically instantaneously at a very high rate which decays rapidly as equilibrium is approached.

Experiments at 65 mm show somewhat longer reaction times and a closer approach to the theoretical density at the wave front but still show no evidence of an induction period.

It was found that detonations would propagate in a normal fashion at reactant pressures as low as 15 mm with 11 mm Xe added, though at a very low velocity of close to 1200 m/sec. At these low pressures the reaction zone is approximately 20 microseconds long, Figure 5, and though the initial portion is often marred by non-planarity of the wave front, it still shows the steady fall of density from the extreme front of the wave to the C-J state.

This is not enough evidence as yet to clearly specify the dependence of the reaction zone length on reactant pressure, but a preliminary estimate is that the duraction of the reaction increases as the inverse square of the pressure.

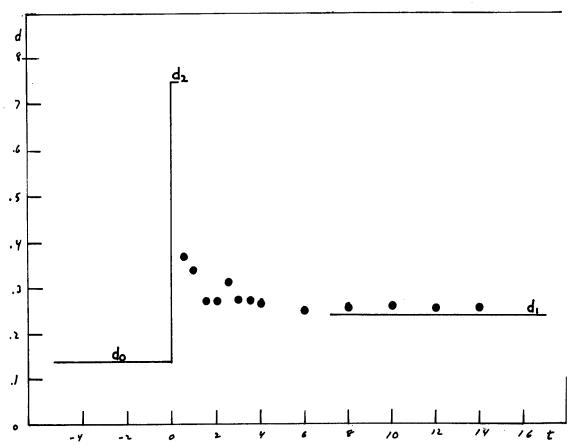


Figure 4. The Reaction Zone in Hydrogen-Oxygen Mixture at 85 mm Total Pressure: Average Density Values for 5 Experiments.

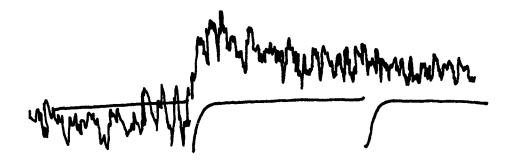


Figure 5. The Reaction Zone in Hydrogen-Oxygen Mixture at 15 mm Total Pressure. Density (Ordinate) vs. Time (Abscissae), Distance Between Negative Timing Markers 20 µsec.

The observed duration of the reaction zone is not identical with the time that a gas volume element spends in passing from the shock front to the C-J state, i.e. with the duraction of chemical reactions in this volume element. Considerations of the reaction zone as a stationary wave form moving by the observer with the detonation velocity lead to the expression:

where  $\tau_o$  is the observed duration of the reaction zone,  $\tau_o$  is the true duration of chemical reactions in a volume element; is the initial gas density, L is the observed length of the reaction zone ( $L = \tau_o/D$ ),  $\Gamma_o$  is the instantaneous density of gas in the reaction zone. If the latter is replaced by the average gas density in the reaction zone,  $\Gamma_o$ , the last form of the equation results which is particularly instructive. Since the actual densities observed average from 2 to 2.5 times the initial density, the actual reaction times appear to be 2 to 2-1/2 times the observed ones. This ratio does not significantly depend on the initial pressure in the above described experiments.

The effect of inert gas is of interest. When a mixture of 13 parts argon and three parts stoichiometric H<sub>2</sub>+O<sub>2</sub> was detonated at a total pressure of 1/2 atm., i.e. a pressure of H<sub>2</sub>-O<sub>2</sub> of 71 mm at which the reaction zone would certainly have been observed had the argon not been present, no trace of a density peak was discernable in two identical experiments. This indicates that added rare gas increases the reaction rate even though it lowers the temperature in the shock wave.

It is a pleasure to acknowledge the support of this research by the Office of Naval Research under Contract N5ori-076, T.O. XIX, NR-053-094, with Harvard University; also the gift of Xenon by the Linde Air Products Co. Some of the electronic equipment described was constructed by Mr. Roger Humberger.

# Bibliography

- 1. J. G. Kirkwood and W. W. Wood, J. Chem. Phys. (in press)
- 2. G. B. Kistiakowsky, J. Chem. Phys. 19, 1611 (1951)
- 3. H. T. Knight and R. E. Duff, Rev. Sci. Inst. (in press)
- 4. G. B. Kistiakowsky and P. H. Kydd, J. Chem. Phys. (in press)

#### THE ATTAINMENT OF THERMODYNAMIC EQUILIBRIUM IN DETONATION WAVES

# G. B. Kistiakowsky and Walter G. Zinman Harvard University Cambridge, Massachusetts

#### Abstract

Detonation velocities were accurately measured in lean acetylene-oxygen mixtures in which unreacted oxygen may be delayed reaching equilibrium in regard to its vibrational heat capacity and dissociation into atoms. Comparison with calculated velocities proves that with all mixtures containing from 50 to 5% acetylene the observed velocities agree with equilibrium calculations. The degree of agreement is such that equilibrium temperatures are determined to better than 1%.

Observed detonation velocities in mixtures containing 53 and 55% acetylene are inconsistent with equilibrium calculations, provided the heat of sublimation of carbon is taken to be 141 Kcal. They agree excellently with similar calculations assuming 170 Kcal as the heat of sublimation. This is regarded as strong evidence for the latter value.

Up to 71% acetylene the observed velocities agree with calculations assuming that no solid carbon is formed in the Chapman-Jouguet state, although total equilibrium demands its presence. With 71% acetylene two velocities are observed in the same experiment. First a slow wave, whose velocity agrees with a calculation not allowing for solid carbon. Then, after an almost discontinuous transition, a faster wave whose velocities is fairly close to a velocity calculated under the assumption of total equilibrium including solid carbon. With still more acetylene only the faster type of wave is observed.

The nature of the transition at 71% acetylene is discussed on the basis of ideas advanced by Doering and by Kirkwood and Wood.

The effect of tube diameter on detonation velocity has been measured in several mixtures and has been found to be of a small constant magnitude.

#### Introduction

Whether or not thermodynamic equilibrium is attained in the Chapman-Jouguet (C-J) state of stationary detonation waves, has been repeatedly considered from the experimental and the theoretical point of view. In more recent times Lewis and Friauf (1) demonstrated that the velocities in hydrogen-oxygen mixtures agreed far better with calculations in which complete thermodynamic equilibrium was assumed to exist among the reaction products in the C-J state, than with those assuming quantitative reaction. Zeldovich (2) came to the same conclusion. The detonation velocities obtained in this laboratory (3) for cyanogen-oxygen mixtures containing at least 50% oxygen agreed within experimental error with the velocities calculated assuming thermodynamic equilibrium in the C-J state. The high value for the heat of dissociation of nitrogen which had been used in these calculations has now been confirmed (4), and the high value for the heat of dissociation of carbon monoxide which had also been used in these calculations seems probable (5). Also in the case of acetylene-oxygen mixtures containing from 25 to 50% oxygen (6) and of the approximately stoichiometric mixture of carbon monoxide and oxygen (7), excellent agreement with equilibrium calculations had been obtained.

From the theoretical point of view, the attainment of equilibrium in the C-J plane is not a necessary requirement. Zeldovich (2) pointed out that an endothermic reaction lagging behind the exothermic processes responsible for the detonation will not be included in the C-J state and will occur, therefore, in the rarefaction wave where it has no effect on the detonation wave parameters.

The rigorous analytical treatment of the problem by Kirkwood and Wood (8) has defined the conditions under which equilibrium may not be attained. The C-J state corresponds to the condition

$$\sum_{j} \sigma^{j} r^{j} = 0$$

where the r<sup>j</sup> are the chemical rate functions of the j reactions, presumed to be involved in the detonation process, while the c<sup>j</sup> describe the effect of each reaction on the pressure of the system, caused by the enthalpy and mole number change. As they point out, the normal case is for the left side of [1] to become zero when all r<sup>j</sup> vanish, because equilibrium has been attained. However, when some c<sup>j</sup> have negative values (i.e. when reactions occur which are either endothermic or are accompanied by a large volume decrease, or both), equation [1] may be satisfied prior to establishment of equilibrium. In this event those residual reactions which occur after the summation in [1] has become negative, occur behind the C-J state and have no effect on the detonation parameters. The authors are unable to decide, on the basis of their steady state considerations, what happens if the summation in [1] becomes positive again after having been negative for some time. A less defined case of a fast and slow exothermic reaction has been qualitatively discussed by Doering (9).

He suggests that while the detonation wave is still "young" and therefore its rarefaction wave is steep, the slow exothermic reaction m must occur in the rarefaction wave. With the progress of the detonation wave, the rarefaction becomes less steep and the delayed reaction develops a shock which must eventually overtake the C-J plane. Thereupon, the slow reaction contributes to the parameters of the wave. In the language of Kirkwood and Wood, Doering's proposal means that in the early stages of a detonation wave its parameters are determined by that thermodynamic state of the system which corresponds to the earliest vanishing of the left side of [1]. With the aging of the detonation, the wave parameters suffer a discontinuous change and become determined by that subsequent state of the system in which eq. [1] is satisfied again.

The experimental evidence on deviations from equilibrium is rather inconclusive, except for one instance. The evidence cited by Zeldovich (2) on the pressure dependence of detonations in hydrogenchlorine mixtures is open to other interpretation. In the light of subsequent experience in this Laboratory on overdrive and the diameter effect, the suggestion (10) that significant deviations from equilibrium were observed in the hydrogen-oxygen mistures does not seem tenable. In cyanogen-oxygen mixtures containing excess cyanogen (3), the observed velocities are appreciably higher than calculated, but the calculations involve simplifying assumptions about the thermodynamic functions of the cyanogen molecule and the experimental data are not altogether trustworthy, as was noted at the time. A few velocities measured in lean acetylene-oxygen mixtures (6) are significantly higher than calculated. The most striking deviation is that observed in acetylene-oxygen mixtures containing between 55 and 70% acetylene (6). The velocities of these mixtures are lower and decrease faster with rising acetylene concentration than is predicted on the basis of calculations performed, assuming that the thermodynamically required amount of solid carbon is formed before the C-J state is reached. Moreover, the velocity was observed to increase from 70 to 80% acetylene to values which are in fair agreement with the complete equilibrium calculations. It was suggested, therefore, that delays in nucleation of solid carbon particles prevent this reaction from occurring within the reaction zone leading to the C-J state until, owing to decreasing temperature and increasing unburned acetylene concentration, the degree of supersaturation becomes great enough to insure adequately fast precipitation of carbon.

The present paper deals with the last two instances of deviations from complete equilibration, since they appeared to be best authenticated by previous work.

# Experimental Details

In general, the equipment and experimental procedures were similar to those described previously (3). The following points of difference should be noted.

In addition to piezoelectric velocity gages previously described, also the ionization gages (11) were used occasionally. They appeared to function at least as well as the others.

In the light of previous experience, it was clear that emphasis should be placed on tests of stability and constancy of detonation velocities. Therefore, seven to eight equidistant gages (10 - 12 cm apart) were mounted in the experimental sections of each of the detonation tubes. Only those runs in which at least six of these gages gave pips on the CRO record were used for velocity calculations. The velocities were obtained by the method of least squares from the time intervals between gage signals. The standard deviations of the velocities so calculated ranged between 3 and 8 m/sec. Once in a great while a gage signal appeared many microseconds too soon or too late. Such signals were not used in the calculations, as they were traced to solid deposits on the gage bodies.

In the course of these experiments the gas mixing and storage system underwent several modifications and, because of explosion hazards, was eventually converted to an all-metal system, with an 0-ring sealed piston pump providing for the mixing and the transfer of gases from stainless steel storage tanks. Airco oxygen containing 0.5-0.6% argon and 0.0-0.1% nitrogen and standard grade Linde argon containing 0.4% nitrogen were used without further purification. Acetylene from a Prestolite tank was passed through Dry Ice traps to eliminate acetone and other high-boiling impurities. It was then analyzed mass spectrometrically and found to be 99.8% pure, the impurity being very largely methane.

### The Results and Conclusions

The results obtained fall into two categories, those dealing with the lean and those dealing with the rich acetvlene-oxygen mixtures. They are considered here in that order.

It has been pointed out by Zeldovich (2) that in branching chain reactions—and most if not all high temperature oxidation reactions are of this type—the last event chronologically is the recombination of free radical intermediates which are first produced in concentrations exceeding thermodynamic equilibrium. As such recombinations, because of large enthalpy decrease, have positive for the summation on the left of [1] should vanish only when equilibrium is attained. The situation is different when a large excess of an inert diatomic gas is added to the system. As it does not participate in the reaction chains, the excitation of its vibrational heat

capacity and its dissociation into atoms might occur largely through random processes of thermal energy exchange. Since the temperature rises monotonically to the C-J state, these processes might be the last to be completed; having negative o, they will recede behind the C-J state, according to the Kirkwood-Wood argument. Unfortunately, the inclusion of a large molefraction of an inert gas leads to instability of detonation waves and so to failure of experiments to test the proposition. But mixtures of a large excess of oxygen with a little acetylene may come close to the above condition because here most of the oxygen does not take part in the reaction and yet they The detonations were initiated in support steady detonation waves. an equimolar acetylene-oxygen mixture, which was separated from the mixture being studied by a thin plastic diaphragm. The detonation in the equimolar mixture ruptured the diaphragm and started a detonation in the mixture being observed. With this technique, it was found that mixtures containing less than 5% of acetylene gave distinctly non-steady waves. No detailed measurements were made on these mixtures. The main source of difficulty with other mixtures has been the overdrive from the initiator compartment. It showed itself as a decreasing velocity in the experimental mixtures. To insure against the results being falsified on this score, interval velocities obtained between gages spaced 10-12 cm apart in the experimental sections of the tubes were analyzed by the usual statistical procedures for significant trends and only those runs accepted which gave no evidence thereof. The following Table 1 gives an example of an acceptable run and of one wherein the wave was overdriven. Further tests were made by using the initiator mixture at different initial pressures, so as to vary the shock pressure acting on the experimental mixture. As the following Table 2 shows, there exists a range of initiator strengths within which the same detonation velocity is obtained in the experimental mixture, which is therefore considered to be the steady velocity.

The magnitude of random errors involved in the present measurements is seen from the following. The standard deviation of measured velocities within 44 pairs of runs made under identical conditions was 4 m/sec. The standard deviation within 7 pairs of runs, identical in all respects except that a separately prepared gas mixture was used for each of the runs comprising a pair, was 7 m/sec. The compositions included in this analysis range from the leanest to the richest studied. Systematic errors due to the time standard used, impurities of gases, their deviations from ideality, not allowed for in making up the mixtures, etc. involve together an error certainly less than 0.2% in detonation velocity. Altogether, it would seem that a probable error of 0.3 to 0.4% in each velocity determination is a conservative estimate.

Earlier work from this Laboratory indicated (3,6) that detonation velocities depend on the tube diameter to such an extent that the extrapolation (3) from the widest diameter used (10 cm) to the velocity of the infinite plane wave adds a significant increment. Quite limited measurements suggested also that this correction is

Table 1. A comparison of steady and overdriven waves.

- Run A: A steady run made with a 7.5% acetylene-92.5% oxygen mixture at an initial pressure of one atmosphere in the 5 cm tube.
- Run B: An overdriven run made with a 6.0% acetylene-94% oxygen mixture at an initial pressure of one atmosphere in the same tube.

Distance from Diaphragm to Start of Interval (cm)	Gage to Gate Interva	al Velocity (m/sec) Run B
68.6	1764	1714
80.1	1763	1693
91.5	1755	1713
102.9	1760	1679
114.3	1761	1679
<b>125.</b> 8	<b>175</b> 8	1671
137.2	1769	1683
Least Squares Velocity	1762	

Table 2. Initiation experiments made with a mixture of 8.2% acetylene and 91.8% oxygen at an initial pressure of one atmosphere in the 5 cm tube.

Pressure of Initiator Mixture (Atmospheres)	Velocity (m/sec) in the Experimental Mixture.	
3/8	1796	
1/2	1793	
<b>5/</b> 8	1792	
3/3	1790	
7/8	1791	
i	1792	

very sensitive to the composition of the mixture. Considerable effort was concentrated therefore now on determining the diameter effect for variously composed mixtures. Figure 1 shows the results for all those mixtures with which experiments were made in three or four different tubes. The data obtained with the smallest (1.3 cm) tube are of doubtful significance because of experimental imperfections but they suggest an only limited validity of the linear relation between velocity and inverse tube diameter. The other data shown give an extrapolation to infinite diameter of about 7 m/sec, which agrees well with the previously determined (6) diameter effect of 9 m/sec for equimolar mixtures. However, the new data show that within the experimental error the diameter effect is independent of composition except possibly for the 75 - 25% mixture. Velocity data in two tubes of different diameters were obtained for several other mixtures. They confirm the independence of the diameter effect from composition, shown by Figure 1. The velocities measured by Guenoche and Manson (12) were obtained in tubes of rather small diameters. Hence extrapolations to infinite diameter are quite uncertain, but the magnitude of the correction appears to be even less on the basis of their data than the 7 m/sec suggested above. In any case, it is certain that this correction is almost within the experimental error of the present measurements.

To compare the experimental extrapolated velocities with those calculated by the thermo-hydrodynamic procedure, it is necessary to make a correction for gas non-ideality in the C-J state. If the Schmidt equation (13) is used for this purpose, as seems entirely legitimate, the correction amounts to ca. -0.15% (14) and thus just about cancels the increase in velocity on extrapolating to infinite diameter. Hence velocities obtained in the 10 cm tube are directly compared below with theoretical velocities.

The hydrodynamic velocity calculations on lean mixtures were kindly performed by Dr. R. E. Duff of the Los Alamos Laboratory, using IBM computing machines. Aside from the uncertainties in the thermodynamic functions used, all taken from the NBS tables (15) or extrapolated therefrom to higher temperatures by standard procedures, the calculations are accurate to better than 0.1% in the composition and temperature of the C-J state. They were obtained by a method of successive approximations, analogous to that employed in manual calculations but adapted for machine operation. The following specie were allowed for: CO2, CO, H2O, OH, H2, H, O2, O. The concentrations of carbon vapor, H<sub>2</sub>O<sub>2</sub> and O<sub>3</sub> are too small to affect the calculations; the chemical potential of the radical HO is not known, but, by analogy with ozone, it may be safely omitted as of no importance in equilibrium calculations. In computing the detonation velocities from the parameters of the C-J state, Dr. Duff assumed that the sound velocity involved in this calculation is that corresponding to mobile equilibrium. Brinkley and Richardson (16) concluded, however, that the velocity corresponding to frozen equilibrium is correct and

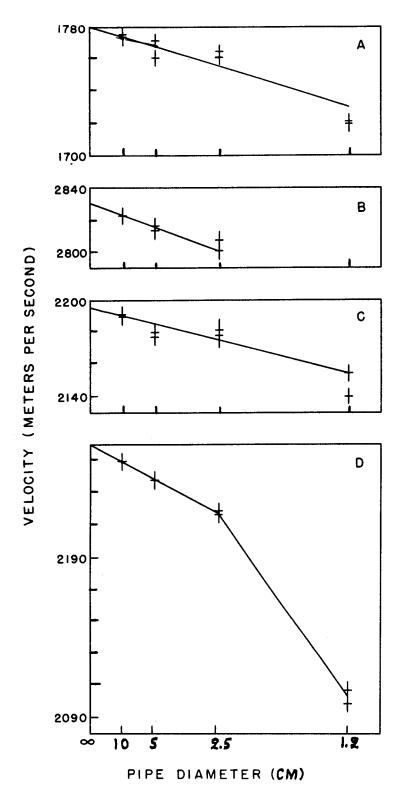


Figure 1. Detonation velocity in acetylene-oxygen mixtures in tubes of different diameter plotted against inverse tube diameter. Graph A: 7.5% acetylene; Graph B: 53% acetylene; Graph C: 70% acetylene; Graph D: 75% Acetylene.

Kirkwood and Wood (8) now confirm this deduction. The corresponding correction to Dr. Duff's velocities amounts, however, to only +4 m/sec in the mixture containing 25% acetylene and is less in leaner mixtures. His values, therefore, were used without correction.

The problem of calculating non-equilibrium detonation velocities has, of course, no single answer because so many alternative assumptions may be made and each suffers from artificiality. At our request, Dr. Duff calculated also non-equilibrium velocities assuming that the vibrational heat capacity of unreacted oxygen was not excited ( $C_v = 5/2$  R) but that its degree of dissociation into atoms was the same as if it has the normal chemical potential. This assumption changed the other equilibria only insofar as it changed the C-J temperature of the reaction products. Rather rough estimates carried out by us indicate that the supression of oxygen dissociation should double deviations from equilibrium velocities, compared with calculations of Dr. Duff.

In Figure 2 the lower curve shows the equilibrium velocities. while the upper curve shows velocities with vibrationally non-excited oxygen. The experimental data are shown by circles. Their position on the diagram is such as to reject definitely the possibility of nonattainment of equilibrium in these mixtures. The earlier results (6) obtained in this composition range undoubtedly were too high because of overdrive, not sufficiently guarded against at the time. We also obtained such high velocities, but they invariably showed downward trends. The earlier results (6) on richer mixtures (with which ours agree at 25% acetylene) have shown that between 50 to 25% acetylene there exists perfect agreement between experiments and equilibrium calculations. Now this agreement has been extended down to 5% acetylene. This is instructive because in mixtures containing nearly 50% acetylene the major dissociation equilibrium is that of hydrogen. In the very lean mixtures, on the other hand, the dissociations of oxygen and water vapor are thermodynamically of greater importance. The kinetic mechanisms by which these dissociations tend to equilibrium are undoubtedly different and yet, as the measurements show conclusively, they all reach equilibrium in the C-J state. It might be noted in this connection that in comparison with the other methods of studying gaseous equilibria at very high temperatures, the technique of detonation velocities is extremely precise. Thus if the entire residual discrepancy between the experiments and calculations is regarded as an experimental error in temperature estimation, the measurements on these acetylene-oxygen mixtures permit the determination of temperatures to better than 1% accuracy in the range from 3000 to 4500° K.

Mixtures of acetylene and oxygen containing excess acetylene are of interest in two respects. In those containing but a small excess of acetylene, the temperature of the C-J state is so high that unburned acetylene must be substantially dissociated into hydrogen and gaseous carbon if the heat of sublimation of the latter is only 141 Kcal (17). Since the alternate value, 170 Kcal, is not as yet

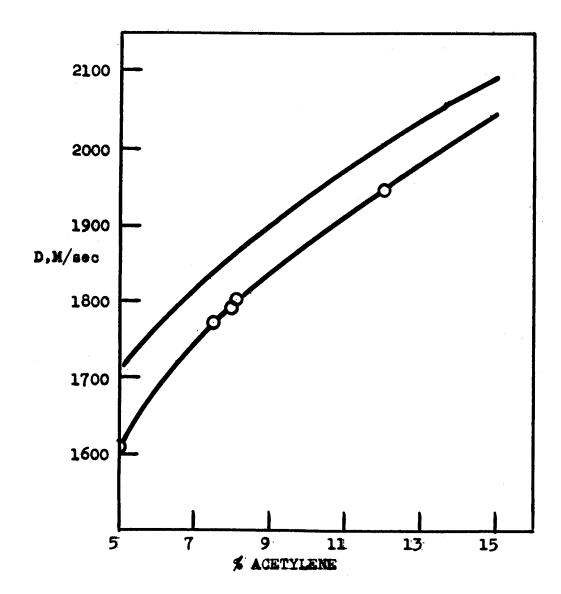


Figure 2. Observed and calculated detonation velocities in lean acetylene-oxygen mixtures. Circles: averages of at least two runs each in the 10 cm tube at 1 Atm. pressure. Lower curve: calculated velocities under the assumption of complete equilibrium. Upper curve: excess molecular oxygen assumed to be non-vibrating but in equilibrium with oxygen atoms.

proven beyond further doubt (5), contributory evidence obtained in the present investigation is of some interest. The experimentally observed velocity in a mixture containing 53% acetylene at 1 atm. initial pressure (cf Figure 1) is 2822 meters, which value should be within 10 m/sec of the true velocity of an infinite plane wave in ideal gases. The calculation of the theoretical velocity was carried out by previously described (3) manual techniques. Thermodynamic functions were the same as previously used (6). Allowance was made in the calculations for the following specie: CoHo, CH, CO, C, H, Having thus determined the equilibrium composition, pressure and temperature of the C-J state, it was found upon their substitution into the appropriate equilibrium equations that the concentrations of the following specie were too small to alter the results of the calculation, had they been allowed for: 0, CO, H2O, CHh, CoHh. The equilibrium concentrations of Co etc. are not known, but if the assumptions of Glockler (18) are accepted, these carbon specie affect significantly the calculated velocity, by lowering it a few tenths of a percent, only if the heat of sublimation is 141 Kcal. Without allowing for them, this heat of sublimation leads to a calculated velocity of 2750 m/sec. With the 170 Kcal value, the result is 2819 m/sec. If acetylene is assumed to be vibrationally excited, but not dissociated, the result is 2830 m/sec. Were it not vibrationally excited, the result would be sufficiently higher to be in significant disagreement with the experimental figure. Finally, if hydrogen left behind when acetylene is oxidized to carbon monoxide is also assumed not to be dissociated, although vibrationally excited, the velocity is raised to ca. 2900 m/sec. The experimental value is consistent only with the equilibrium calculation assuming 170 Kcal as the heat of sublimation and with the non-equilibrium calculation which excludes the dissociation of acetylene but includes that of hydrogen. The second alternative makes it impossible to assert that the high heat of sublimation has been proven. However, in the context of the previously discussed results on lean mixtures, the supposition that hydrogen is dissociated but acetylene (which plays now a role similar to that of excess oxygen in lean mixtures) while vibrationally excited is not dissociated is so improbable that strong evidence for the high heat of sublimation is believed to have been adduced.

With 55% acetylene, the experimental velocity is 2745 m/sec while the equilibrium calculation, with 170 Kcal as the heat of sublimation, gives 2741 m/sec.

Our early experiments with these and richer acetyleneoxygen mixtures suffered from considerable lack of reproducibility,
a fact noted also by other investigators. The cause was eventually
traced to loose carbon black which remained in the tube from run to
run, was stirred into the fresh admitted gases, and slowed down the
detonation wave by the inertia of carbon particles. After the procedure was adopted of removing all loose carbon before each run,
entirely consistent data were obtained up to 80% acetylene. At

still higher concentrations, wave instability was regularly observed, presumably indicative of incipient spin which is strong in pure acetylene (19).

In Figure 3 are shown the results on rich acetyleneoxygen mixtures, obtained at 1 Atm. initial pressure in tubes of
10 cm diameter. Within the experimental error, the velocities
shown in Figure 3 are identical with extrapolated and corrected
velocities. Lines A and B in this figure are interpolations between
calculated velocities, the first for the homogenous equilibrium not
involving solid carbon, the other for complete equilibrium. Had the
heat of sublimation of carbon been assumed to be 141 Kcal, the
calculated velocity curve would have started at the same value as
curve A for the equimolar mixture, dropped about 70 m/sec lower than
the curve shown for the mixture containing 53% acetylene, and then
drawn closer again, to become experimentally indistinguishable from
it when more than 60% acetylene is present.

In the composition range of 50 to 71% acetylene, the experimental points lie quite close to the calculated curve A. The deviations are undoubtedly within the combined experimental and calculational errors because in richer mixtures, in which the C-J temperature is low and much unoxidized acetylene is present, the calculations which allow only for its dissociations into the CH radicals and into  $H_2 + 2 C_g$  (both of which are then entirely insignificant) become rather inadequate, in view of other possible constituents of homogenous equilibrium (CH1, C2H1, H2CO, etc.) and of uncertainties in the thermodynamic functions of acetylene. Figure 3 shows that at 71% acetylene a discontinuous rise in velocity is observed. This we shall consider in some detail later. Above 71% acetylene the experimental points are far from curve A, but still do not fall on curve B. This discrepancy, however, is not a convincing evidence that complete equilibrium is not established in the C-J state. Firstly, the calculations, as noted above, are quite uncertain in this region. Secondly, the calculations assume that graphite is the solid product. Actually formed is extremely finely divided active carbon, whose chemical potential is probably well above that of graphite, so that less energy is released for wave propagation by its formation, as was noted already in the earlier publication (6).

Figure 4 shows the interval (gage to gage) velocities for mixtures containing close to 71% acetylene. Each point is the average of two or more runs. With 70% acetylene a normal velocity is observed all along the tube. The initial velocity with 71% is lower (and hence close to curve A of Figure 3), but some distance down the tube the velocity undergoes a nearly discontinuous change, followed by a more gradual rise. With 72% acetylene only the high velocity is observed. There appears to be a substantial upward trend in velocity which is statistically just significant. The same is true of the upward trend observed with the 75% acetylene mixture.

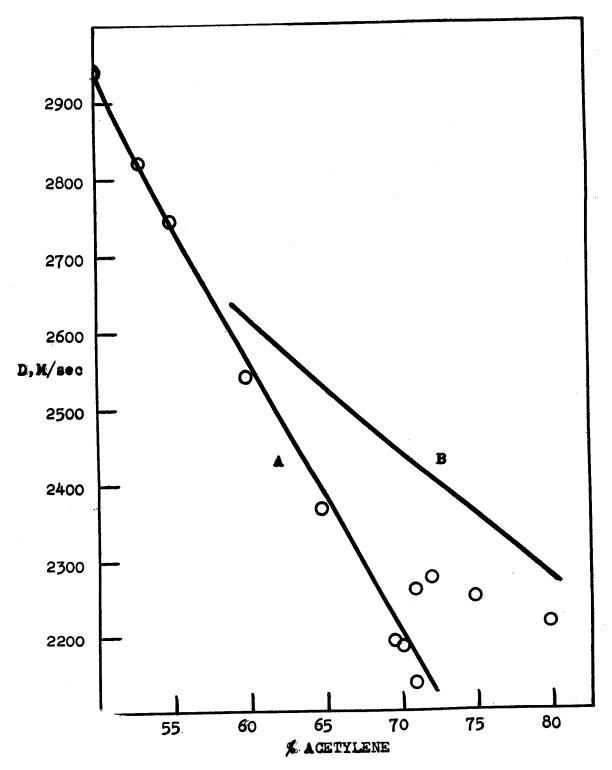


Figure 3. Observed and calculated detonation velocities in rich acetylene-oxygen mixtures. Circles: averages of experimental data except for velocities at 50% and 80% acetylene which are taken from reference (6). Lower curve calculated on the assumption of homogenous equilibrium only. Upper curve includes solid carbon among reaction products.

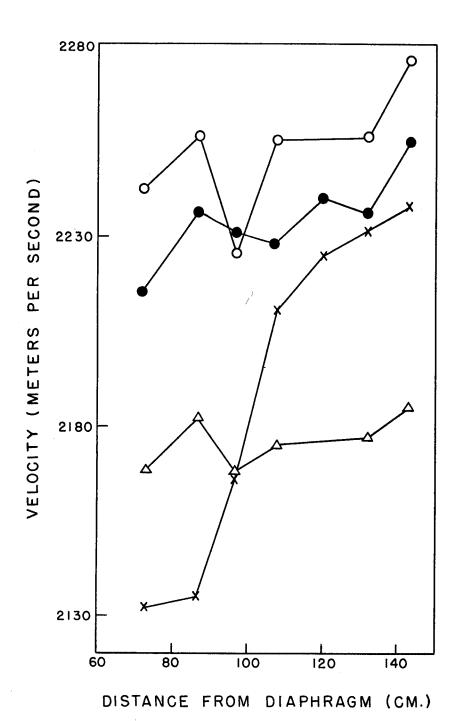


Figure 4. Detonation velocity as a function of distance from the plane of initiation. Triangles: 70% acetylene; crosses: 71% acetylene; dots: 72% acetylene; circles: 75% acetylene.

Thus the limiting steady velocities in these mixtures are probably higher than shown in Figure 3 and lie therefore closer to the theoretical curve.

We believe that these observations represent the first experimental examination of the situation envisaged by Doering and more precisely by Kirkwood and Wood, that equation [1] is satisfied for two consecutive states of the system, with an intervening period of negative values of the function involved. In our case, the function might go negative, after the homogenous equilibrium has been established, because of energy losses to the walls. This is suggested by the observed difference in the behavior of the waves in the 5 and 2.5 cm tubes. In the latter the transition to high velocities occurs much farther from the point of initiation than in the 5 cm tube.

In accord with Doering's general concept, we believe that the condensation of carbon starts a substantial distance behind the shock front because of delays in nucleation, and so it occurs in the rarefaction wave following the homogenous reaction. As the rarefaction wave comes less steep with the progressof the wave down the tube (20), the energy released in the carbon condensation reaction develops a finite pressure wave, which is able to advance toward the C-J state because of its locally supersonic velocity. At some instant it reaches the C-J state, and from this time on the energy released by the carbon precipitation commences to contribute to the wave propagation because, within the entire region from the primary shock to the carbon precipitation zone, the gas is now moving with subsonic velocity relative to the shock front. If the new stationary state is established instantly, the change in the detonation velocity should be discontinuous, but the observed upward trends after the initial rapid change suggests that the transition takes some time. In fact, the velocity trends noted in the 72% and 75% mixtures may be due to similar transitions having taken place too near the diaphragm to be observed. On the other hand, had we had available very long tubes, we might have observed, much farther from the diaphragm, transitions in leaner mixtures.

When the transition to the new C-J plane has been completed and the wave has again attained a stationary character, the structure of its steady state region is probably as follows. Behind the shock front there is a zone of oxidation reactions (von Neumann spike), probably of quite short duration. Thereupon follows a region of substantially constant pressure, in which no rapid reactions take place; finally comes the region of carbon precipitation from residual acetylene with a further drop of pressure, ending in the C-J state. Such structure would be quite analogous to that reported recently for non-spinning detonation waves in pure acetylene by Duff, Knight and Wright (19), except that there the initial reaction zone is absent because of lack of oxygen.

The existence of the second reaction zone and its motion relative to the front of the detonation wave should be observable optically because of probable accompanying changes in luminosity. Experiments with a smear camera are now underway to demonstrate its existence.

It remains to describe some experiments which are perhaps inconsistent with the interpretation advanced above. If one uses identical partial pressures of acetylene and oxygen as in the previously described experiments, but adds some argon, the effect should be first of all a lowering of temperature in the C-J state and therefore an increase in the degree of supersaturation with respect to solid carbon. Therefore, we expected that in such triple mixtures the transition to higher velocities would occur at substantially lower acetylene: oxygen ratios. Upon adding 114 mm Argon to 1 Atm. of acetylene-oxygen mixtures, the discontinuous transition was indeed observed with the acetylene-oxygen ratio varying from 69:31 to 71:29. But the addition of 190 mm of argon did not shift the transition to still lower acetylene concentrations. The experiments were not very reproducible and are inconclusive. Smear camera investigation, now underway, may provide better information on the internal structure of these complex detonation waves and perhaps serve as a technique for a quantitative study of the kinetics of condensation of carbon.

It is a pleasure to acknowledge the support of this research by the Office of Naval Research under Contract N5ori-076, T.O. XIX, NR-053-094, with Harvard University.

# Bibliography

- 1. B. Lewis and J. B. Friauf. J.A.C.S. 52, 3905 (1930)
- 2. Y. B. Zeldovich, Theory of Combustion and Detonation of Gases (translated from Russian), Technical Report No. F-TS-1226-IA (CDAM A9-T-45), Air Material Command, Dayton, Ohio
- 3. G. B. Kistiakowsky, H. T. Knight, and M. E. Malin, J. Chem. Phys. 20, 876 (1952)
- 4. J. M. Hendrie, J. Chem. Phys. 22, 1503 (1954)
- 5. W. A. Chupka and M. G. Inghram, J. Chem. Phys. 22, 1472 (1954)
- 6. G. B. Kistiakowsky, H. T. Knight, and M. E. Malin, J. Chem. Phys. 20, 884 (1952)
- 7. G. B. Kistiakowsky, H. T. Knight, and M. E. Malin, J. Chem. Phys. 20, 994 (1952)
- 8. J. G. Kirkwood and W. W. Wood, J. Chem. Phys. (in press)
- 9. W. Doering, Ann. phys. 43, 421 (1943)
- 10. D. J. Berets, E. F. Greene, and G. B. Kistiakowsky, J.A.C.S. 72, 1080 (1950)
- 11. R. E. Duff and H. T. Knight, Rev. Sci. Inst. (in press)
- 12. H. Guenoche and N. Manson, Rev. de l'Inst. Français du Petrole et Annales des Combustibles Liquides 9, 214 (1954)
- 13. H. Eyring, R. E. Powell, G. H. Duffey, and R. B. Parlin, Chem. Rev. 45, 69 (1949)
- 14. In reference 3, through an arithmatical error pointed out to us by Dr. R. E. Duff, this correction was estimated to be ca. 0.4%.
- 15. National Bureau of Standards, Selected Values of Thermodynamic Functions (1945, 1947, 1949)
- 16. S. R. Brinkley, Jr., and J. M. Richardson, Fourth Symposium (International) on Combustion (Williams and Wilkins Company, Baltimore, 1953), page 450
- 17. Th. Doehaerd, P. Goldfinger, and F. Waelbroeck, Bull Soc. Chim. Belg. 62, 498 (1953)

- 18. G. Glockler, J. Chem. Phys. 22, 159 (1954)
- 19. R. E. Duff, H. T. Knight, and H. R. Wright, J. Chem. Phys. 22, 1618 (1954)
- 20. G. B. Kistiakowsky and P. H. Kydd, J. Chem. Phys. (in press)

ON THE STRUCTURE OF A DETONATION FRONT\*,\*\*

W. R.Gilkerson\*\*\* and Norman Davidson Gates and Crellin Laboratories of Chemistry California Institute of Technology Pasadena, California

### ABSTRACT

An effort was made to observe the structure of the reaction zone for a detenation in a gas. Detenations in a 50%H2:50%O2 mixture at 0.035 atm. pressure containing 1% I2 were initiated by shock waves in a shock tube. Because of ignition delays and the short length of tube available, the detenations did not settle down to a steady state and were of unexpectedly high velocity. The iedine served as a colormetric indicator for the shock front. The light output of the detonation is a step function of time with a front coincident with the shock front within 2-3 n sec. The experiment indicates that the reaction zone is less than 104 collisions thick. A crude theoretical estimate of the reaction zone thickness of 1000-4000 collisions is made. Possible chain initiating steps are also considered.

<sup>\*</sup>Research supported by the O.N.R., Project NR 051-248. \*\*This paper has been submitted for publication to the Journal of Chemical Physics. \*\*\*Present address: Department of Chemistry, University of South Carelina, Columbia, S. C.

The v. Neumann theory of detonation (1) assumes that the front consists of a shock wave which compresses and heats the unburned gas, thereby initiating combustion, and a reaction zone in which the temperature rises and the density falls as the combustion proceeds. The plane behind the reaction zone where the high temperature equiliprium essentially obtains is called the Chapman-Jouget (CJ) plane for an ordinary detonation.

The experiment described herein is an attempt to observe the thickness of the reaction zone for a detonation in a hydrogen-oxygen gas mixture in a glass tube. It has been successful only in establishing an upper limit for the thickness of this zone under certain special conditions. Kistiakowsky (2) has observed the density profile for a detonation in a mixture of oxygen, acetylene, and methyl bromide, presumably at 1 atm. initial pressure, by x-ray absorption, and reports that in this system the reaction zone is less than 1 mm thick.

The basic idea of the experiment is to observe a detonation in a  $\rm H_2-O_2$  mixture containing a small amount of  $\rm I_2$ . Light absorption provides information about the concentration of iodine and therefore about the shock front. This can be compared with the position of the combustion zone as manifested by light emission by the reacting mixture.

The experiment was carried out in a shock tube, and some of its features may be described by reference to figure la. When the membrane breaks, the expansion of the high pressure gas, hydrogen, into the low pressure reaction mixture results in a strong shock wave which initiates combustion. We call the resulting detenation a supported detonation because the "push" by the high pressure driving gas prevents the formation of a rarefaction wave behind the CJ plane, as is characteristic of an ordinary detonation. For the actual pressure ratios used, the detonation is semewhat stronger than is a free detonation. This subject is discussed in detail below.

### EXPERIMENTAL

The shock tube and our general techniques have been described previously (3). The driving section is a 180 cm length of 15 cm diameter steel pipe. The shock wave section is a 140 cm length of 15 cm aluminum pipe and a 150 cm length of 15 cm Pyrex pipe. Cellulose acetate membranes are clamped between the steel and aluminum sections. The shock wave chamber could be evacuated to 0.5 µ pressure and degassed or lagked at a rate less than 0.1 µ min. Tank hydrogen and oxygen (Linde) were passed over Drierite and through flow-meters, mixed, and then passed through the pressure reducing, iodine saturating system described previously (3). After the tube was filled, a sample of the mixture was withdrawn into a one liter bulb and ignited by a hot platinum wire. The water preduced was

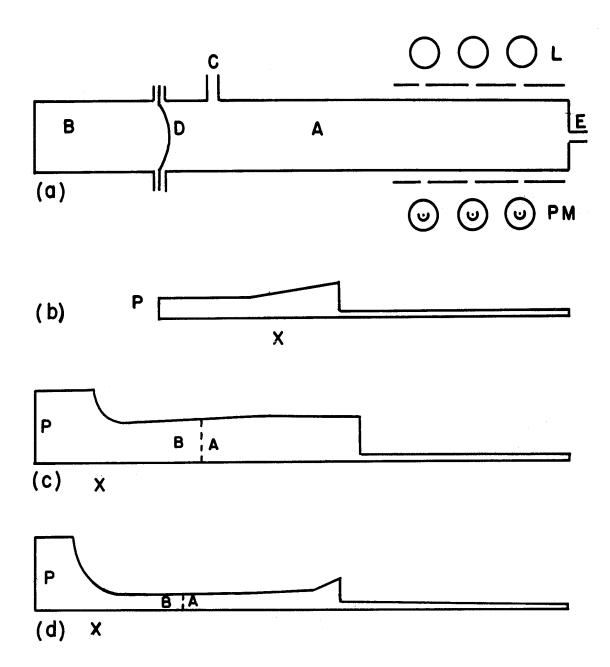


Fig. 1. (a) Schematic diagram of apparatus. B, driving gas  $(H_2)$ ; D, diaphragm; A, driven gas  $(H_2, O_2)$ ; L, lights; PM, photomultipliers; C, to vacuum line; E, gas inlet; (b,c,d) Pressure, P, as a function of distance, x, at sometime after the bursting of the diphragm or the beginning of detonation for a free detonation (b); a supported detonation (c); and an insufficiently supported detonation (d). The dotted lines in (c) and (d) indicate the contact surface between expanded, cold driving gas and shocked, combusted, driven gas.

taken up by Drierite. From the pressure before and after combustion, the ratio of oxygen to hydrogen, L (table II) was computed. This analysis was reproducible and accurate to  $\pm$  0.6%.

## "SUPPORTED" DETONATION

The symbols to be used in this discussion are:  $\underline{P}$  = pressure,  $\underline{W}$  = mean molecular weight of unreacted gas,  $\underline{V}$  = velume per  $\underline{W}$  grams of gas,  $\underline{H}$  = enthalpy per  $\underline{W}$  grams,  $\underline{S}$  = shock velocity,  $\underline{S}_{\underline{f}}$  = velocity of a free detonation calculated using the Chapman-Jouget condition,  $\underline{V}$  = material velocity of gas in laboratory system. Subscripts 1 and 2 refer to unshocked and shocked gas at chemical equilibrium respectively.

As is well known, the P,V behavior of a fluid subject to shock compression is defined by the Rankine-Hugoniet (RH) equation,  $(\underline{P}_2 - \underline{P}_1)(\underline{V}_2 + \underline{V}_1) = 2(\underline{H}_2 - \underline{H}_1)$ . This with the perfect gas law and the thermodynamic conditions for chemical equilibrium between the various components can be used to define the behavior of a detonating mixture, and the RH curve so calculated for  $50H_2:50\%0_2$  at an initial pressure of 0.035 atm. is illustrated in Fig. 2. Useful numerical results are given in Table I. The velocity of any particular shock is  $\underline{S}^2 = \underline{V}_1^2$   $(\underline{P}_2 - \underline{P}_1)/(\underline{V}_1 - \underline{V}_2)$ . The tangent illustrated in Fig. 2 defines the slowest shock possible for the mixture provided it reacts to chemical equilibrium. We refer to this wave as a free detonation; the gas at the CJ plane has a material velocity  $\underline{v}$  and a temperature such that

$$\underline{S} - \underline{y} = V_2 (P_2 - P_1)^{1/2} (V_1 - V_2)^{-1/2}$$

is the local sound velocity. For a shock proceeding to point A of Fig. 2, the velocity is greater than that for a free detonation, the temperature is higher, and  $\underline{S} - \underline{v}$  is locally subsonic. For a shock proceeding to point B, the velocity  $\underline{S}$  is greater than that for a free detonation, the temperature is lower, and  $\underline{S} - \underline{v}$  is supersonic.

Fig. 1b,c,d illustrates pressure profiles for several possible experiments. Fig. 1b is for a free detonation eriginating at the closed end of a tube. A rarefaction originates at the same end and fellows the detonation. In a shock tube configuration with a sufficiently large bursting pressure ratio, the pressure profile will be that of Fig. 1c. The push by the driving gas is sufficient to suppress the rarefaction and give a step function shape to the pressure wave. If the bursting pressure ratio is insufficient for the expanding gas from the driving chamber to reach the velocity  $\underline{\mathbf{v}}$  at the pressure  $\underline{\mathbf{P}}_2$  which obtains at the CJ plane for a supported detonation, then the situation is as depicted in Fig. 1d. There is a rarefaction behind the detonation front and the velocity of the front is the same as that for a free detonation.

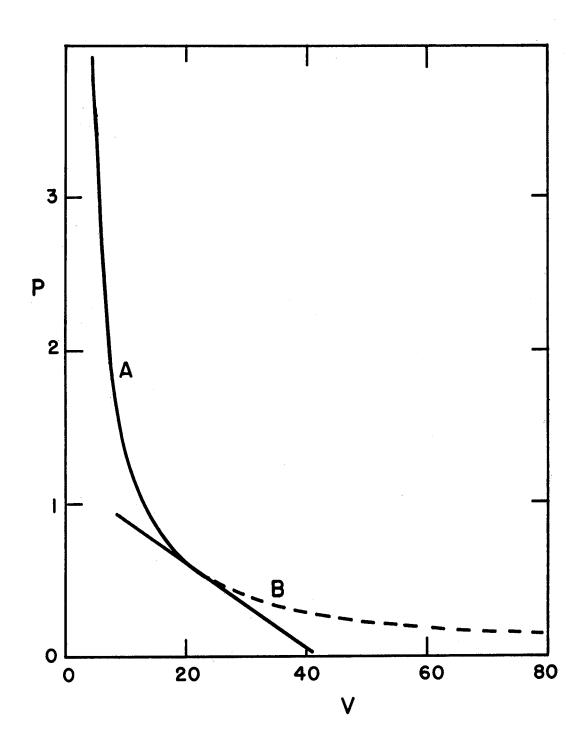


Fig. 2. Rankine-Hugoniat curve for a detonation in  $50\%H_2:50\%O_2$ ; initial conditions, 0.035 atm., 300 %, V = 41.4 liter gram 1; P in atm., V is specific volume, liter gram 1

Table I

Calculated Properties in 50%H2:50%02 Detonations

H <sub>2</sub> 0	0.199	•276	•435	957.	197•
<b>7</b> 0	0.209	.244	•256	•262	•268
H <sub>2</sub> ions	0.0760	•0670	•0545	•0505	•0485
0 H <sub>2</sub> mol fractions	0.205	.153	.0811	•0736	•0702
ш	0.133	•0915	•0492	•0441	•0430
НО	0.179	.168	.124	.114	.104
S cm/sec x 10 <sup>-5</sup>	3.62	3.57	2.20	3.09	1
H 4≱	3750	3500	3000	2900	2750
V <sub>1</sub> /V <sub>2</sub>	8.90	76.9	1.84	1.15	
$P_2/P_1$	211	75.3	16.0	9.50	3.46

(initial conditions, 0.035 atm., 300 °K, thermodynamic data from "Selected Values of Chemical Thermodynamic Properties," National Bureau of Standards, Series III, 1950).

The equation relating the velocity  $(\underline{v}_4)$  and pressure  $(\underline{P}_4)$  of the gas from the driving chamber expanding from the pressure  $\underline{P}_3$ , if the initial velocity of sound be  $\underline{s}_3$  is

$$v_4 = (2A_3/Y - 1) \left[1 - (P_3/P_4)^{(Y - 1)/2Y}\right].$$

By matching  $\mathbf{v_4}$  and  $\mathbf{P_4}$  te  $\mathbf{v_2}$  and  $\mathbf{P_2}$ , the shock velecity vs. bursting pressure graph in Fig. 3 is obtained. The upper arm of the curve is the predicted steady state detonation velocity as a function of bursting pressure for an ideal shock tube. The lower dotted arm of the cruve represents computed velocities for a transition to the detted arm of the RH curve, Fig. 2. Gas on this arm of the RH curve is in an unstable condition in that the velocity  $\underline{S} - \underline{v}$  is supersonic and a shock transition to the upper arm of the RH curve is possible. The transition to the dotted arm of the curve is impossible in the  $\underline{v}$ . Neumann description of a detonation in which combustion is preceded by a shock wave. It is conceivable if the combustion is initiated by the diffusion of free radicals ahead of the shock zone and takes place in the few mean free paths that constitute the shock zone. Very high velocities for rather low bursting pressures are possible for this hypothetical case.

The computed free detonation velocity for  $50\%H_2:50\%O_2$  at 0.035 atm. is 2.20 x  $10^5$  cm/sec. The velocity at an initial pressure of 1 atm. is 2.33 x  $10^5$  cm/sec. it the lower pressure, more enthalpy is absorbed in dissociation precesses.

The experimental results are not suitable for quantitative comparison with Fig. 3. It should be remarked however that the effect of a small amount of iodine on the calculated curve would be quite small.

## RESULTS AND DISCUSSION

Successful detonations occurred with bursting pressure ratios of 87 or greater, but did not occur with bursting pressure ratios (B) below 80. The theoretical B to just support a free detonation is 35, and shock tube experience indicates that a pressure ca. 10% higher might actually be required. Presumably the failure to obtain detonations at low B is because the shock wave resulting when the membrane breaks is too weak to initiate combustion. The calculated temperature for B = 85 for a pure shock tube experiment with no combustion is 1140°K. It may be recalled that Fay (4) observed the surprisingly low shock ignition temperature for stoichiometric H<sub>2</sub>:0<sub>2</sub> of 400°K. It is not possible to say which of the many differences between the two experiments is responsible for the striking difference

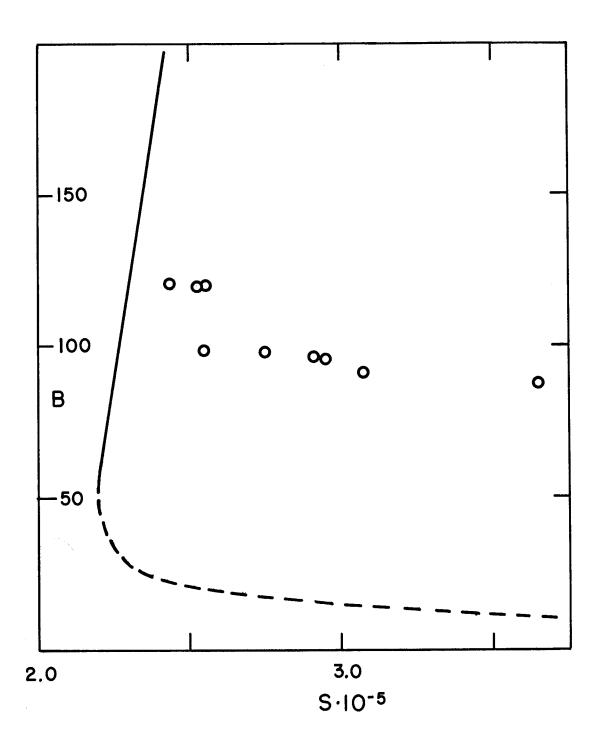


Fig. 3. The bursting pressure ratio,  $\underline{B}$ , vs. velocity,  $\underline{S}$ , cm sec<sup>-1</sup>; —, calculated for the solid arm of the RH curve, Fig. 2; - - -, calculated for the dotted (unstable) arm of the RH curve, Fig. 2; 0, experimental points, stations 1-3, Table II.

in results. One important possibility is that iodine added in our experiments inhibits ignition.

It is the general belief that it is difficult to maintain stable free detonations at low pressures. Mooradian and Gordon (5) report stable free detonations initiated by shock waves in a l" pipe for an initial pressure of 0.125 atm. They also report stable detonations in 1:10 Knallgas:argon at 1 atm. pressure. The low pressure (0.035 atm. initial pressure) detonations achieved here are presumably due to the fact that the detonations were supported, and indeed overdriven, so that quenching by the rarefaction wave is absent, and due to the large tube diameter, which deemphasizes attenuation by the walls.

Photoelectric measurements were obtained at three stations 240 cm (16 tube diameters), 260, and 280 cm from the membrane. Observations were made with light beams defined by 2.5 cm by 1 mm slits. The collimation was such that for perfect alignment of the slits and tube, a 3 mm length of the tube was observed by the photomultiplier for light absorption, and a 5 mm length for light emission. A signal due to absorption of blue green light at station 1 was used for triggering the oscilloscope sweeps. Light absorption measurements were made at station two with blue green light from a projection lamp passed through an interference filter with a maximum at 487 mu and a half-width of 8 mu, and a transmission of the order of 1/2 - 1%through the rest of the spectrum. In some experiments a sharp cut Corning filter (No. 3385) opaque for wavelengths less than 480 mm was also used. In others, this cutoff filter was omitted and the light emission by the detonation, which is principally blue light, was superimposed on the light absorption changes. Light output of blue light (Corning filter No. 5562) was observed at station 3. Time intervals between the several stations were measured on the oscilloscope traces. In some runs, the time interval between the first and third stations was also measured with a Potter 1.6 Megacycle Counter Chronograph; these results agreed with the oscilloscope measurements.

Table II shows quantitative data for most of the experiments. The photoelectric signals of transmission of blue green light (Fig. 4) at station 2 show that (a) for typical experiments, there is no observed compression of the iodine, but that it disappears directly at the shock front; (b) the light output of the detonation is coincident with the shock front within the rise time of either signal (2-3) usec.). The calculated shock temperatures before combustion ( $\underline{T}_S$ , Table II) are sufficiently high so that the thermal dissociation of iodine (3) is sufficiently fast to account for (a), without invoking an increased rate of removal of iodine by the combustion process or by an increased rate of thermal dissociation due to combustion.

Observation (b) is, we believe, the most important result of this investigation. The reaction zone is less than 2 - 3 usec. or 4-6 mm. thick.

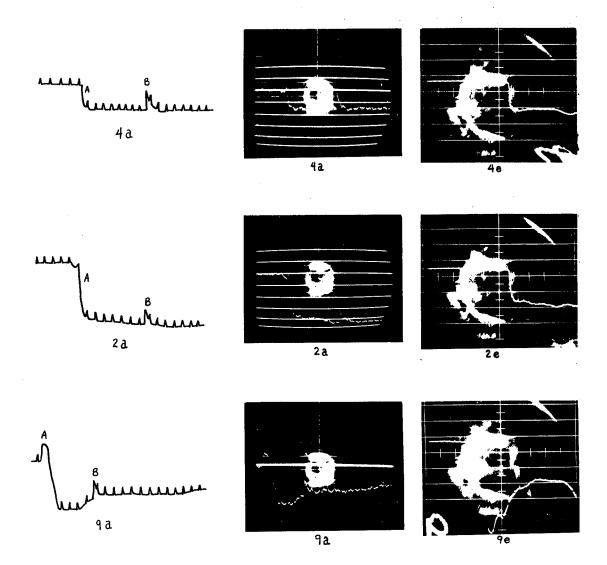


Fig. 4. Oscillograph records of photocurrent for some experiments. 4a, 2a, 9a are principally light absorption records at station 2 for expts. 4, 2, 9 of Table II. A, increase (or decrease (9a)) of light upon passage of the shock front. B, timing pulse from trigger circuit when shock passes station 3. The smudges are cathode glow on the CRO screen and are not significant. The small pips are 10 usec timing markers. The smooth horizontal traces are either voltage calibrations or the cm rulings on the CRO screen. In 4a, the light filter was the 487 mu interference filter plus the 3385 Corning cut-off filter. The increase in light at the shock front is 1.7 times that expected for complete dissociation of the I2, the additional amount being due to light emission. In 2a, the cut-off filter was omitted, permitting more transmission of blue light. The increase in transmission is 3.7 times that expected for complete dissociation of the  $I_2$ . 4e, 2e, 9e are light emission records at station 3 through a Corning 5562 blue filter (360-500 mu). The slit geometry at the two stations was about the same, but the photoelectric sensitivity at station 3 was adjusted to be 1/120 that at station 2.

Table II

Observed Velocities of Supported Detonations

Experiment No.	В	S <sub>13</sub> (cm/sec	S <sub>23</sub> x 10 <sup>-5</sup> )	T <sub>s</sub> ex	p(-17,000/RT)	L
1	121	2•43	2.50	2060	1/62	0.982
2	120•5	2•55	2.69	2130	1/54	0.877
3	120	2•52	2.71			0.989
4	98•9	2•54	2.72			0.902
5	98.0	2.75	3.46			0•958
6	96.7	2.91	2.89	2680	1/24	0.993
7	96•2	2.95	3.06	2760	1/22	0.967
8	91•4	3.07	3.56			0.967
9	87.5	3.65	3.71			0.881

 $\underline{B}$  = bursting pressure ratio;  $\underline{S}_{ij}$  = velocity between stations  $\underline{i}$  and  $\underline{j}$ ;  $T_s$  = computed temperature behind shock for velocity  $S_{13}$ , assuming no combustion, and that  $C_p$  = 7/2 R, L = mole ratio of  $O_2$  to  $H_2$ .

\* Professor G. B. Kistiakowsky, while refereeing this manuscript, has very generously transmitted the following communication to us. "Using the X-ray absorption technique, we have now observed reaction zones (as zones of high initial density) in  $2H_2-O_2$  mixtures at pressures from 85 to 20 mm (with some Xe added to increase X-ray absorption). The waves were not overdriven but steady and of normal velocity; the duration of the reaction zone varies from a couple of microseconds at the highest to 20 usec at the lowest pressure, changing roughly as 1/P2. There seems to be no induction period . . . . I suspect that the overdrive and the presence of iodine must have somehow reduced the duration of the zone in the present experiments; or that the light emission starts as soon as reaction starts, not when it essentially ends, and then continues." These results predict that the time of passage of the reaction zone at the pressure used by us would be 11 usec. for a free detonation. The approximate calculations presented further on in the present paper predict a difference of a factor of about three between a free detonation and the overdriven detonations studied here, so that the time of passage of the reaction zone would be 3-4 usec., which is only slightly larger than the upper limit estimated by us. The possible explanations proffered by GBK for any such differences are eminently reasonable.

The light emission, as observed at station 3, consists principally of blue light and is a step function of time. There is no build-up of the luminosity nor is there a peak due to chemiluminescence of the reaction zone.

Fig. 4c is an atypical record that was obtained only once. One sees compression of the iodine followed by a long delay with very little dissociation (temperature below 1200°K) followed by a detonation front which is luminous and where the iodine rapidly disappears. We believe that this is due to delayed ignition of the gas behind the shock, so that the pure shock (no combustion) has reached the second light station before the detonation catches up with and merges with the shock. (The recorded velocities for this experiment are not significant because of uncertainties as to the optical signal at station 1 which triggered the various timing circuits.)

In typical experiments Table II shows that the shocks are accelerating as they proceed downstream; although for pure shock waves, the velocities are quite steady (3). Furthermore, the velocities are much higher than the theoretically expected value. Unusually high unsteady velocities at the inception of detonation are commonly observed (6,7). Probably in all of our experiments, combustion did not begin immediately when the membrane broke, but was delayed until the shock propagated some distance downstream. When combustion starts, an unsteady very fast detonation moves up and merges with the shock. A longer tube than was available for the present investigation would be required in order for the steady state behavior of the system to be established.

Assuming that the average no. of collisions per sec. per molecule at room temperature at 1 atm. pressure is  $10^{10}$ , an average compression factor of 3.5 for the reaction zone to the CJ plane, and an average temperature of <u>ca</u>. 2700°, the observation that the reaction zone is less than 5 mm thick means that the reaction is complete in less than  $9 \times 10^3$  collisions. Without attempting a complete solution of the flame equations (8), it is possible to make a rough estimate of the time for complete combustion as follows.

Assume	the	diverg	ent	chain	reaction	scheme, AE
		1-				(kcal)
H +	02	$\xrightarrow{k_1}$	ОН	+ 0		17.0
0 +	H <sub>2</sub>	$\rightarrow$	OH	+ H		3.0
OH 4	H <sub>2</sub>	<del>&gt;</del>	HOH	H + H		-15.5

At the temperature of a detonation, the conventional low temperature chain breaking step,  $H + O_2 \longrightarrow HO_2$ , is not of great importance because of the instability of  $HO_2$ . Three body chain terminations like  $H + H + M \longrightarrow H_2 + M$  have k's of the order (3) of  $10^{-32}$  atom<sup>2</sup> cc<sup>2</sup> sec<sup>-1</sup>; even if all of the gas were dissociated into atoms or radicals, their concentration would be ca.  $2 \times 10^{-18}$  cc<sup>-1</sup>, and the half time for recombination of the order of  $10^{-32}/(4 \times 10^{-36}) = 2.5 \times 10^{-5}$  sec. or  $2.5 \times 10^{-6}$  collisions and this type of termination would not affect the reaction kinetics very much.

Reaction (1) is probably the slow step in the divergent chain. One can therefore treat OH and O as intermediates present at low concentration to which the steady state approximation applies and consider the time rate of change of the hydrogen atom concentration. The resulting equation is  $\underline{d}(H)/\underline{dt} = 2 \underline{k_1}(O_2)$ , and the solution for constant  $\underline{k_1}(O_2)$  is  $(H) = (H)_0 e^2\underline{k_1}(O_2)$ . Each chain cycle creates two H atoms and two HOH molecules. In the final mixture, there are  $\underline{ca} \cdot 10^{18}$  molecules/cc. If  $(H)_0 = 1$  atom/cc, the time required for complete reaction is  $18 \times 2.3/(2\underline{k_1}(O_2)) = 20$  chain cycles.

Baldwin and Walsh (9) have argued that at  $520^{\circ}$ C,  $k_1 = 10^{-14}$  atom<sup>-1</sup> cc sec<sup>-1</sup>, although Lewis and Von Elbe (10) recommend  $k_1 = 10^{-17}$ .

The value  $10^{-14}$  equated to PZ exp (-17,000/RT) gives P approximately unity. Referring to the initial temperature of the shocked gas (Table II), the Boltzmann factor for  $k_1$ , at 2060° is 1/62, at 2700° it is 1/22, and at the equilibrium temperature of ca. 3400° it is 1/10. At 1580°, the temperature of the shocked, uncombusted gas in a free detonation, the Boltzmann factor is 1/200. The initial rate of the reaction will always be the slowest and we may

estimate therefore a thickness of the reaction zone of the order of  $20 \times 200 = 4000$  collisions with  $0_2$  molecules for a free detonation and  $20 \times 60 = 1200$  collisions for some of the supported detonations of Table II. These estimates are consistent with the experimental observation that the reaction zone is less than  $10^4$  total collisions thick. If P, the steric factor for reaction (1) were 0.01 or less, the reaction zone would probably be thick enough to be observed in our experiment. Indeed, the arguments presented above indicate that if a decrease by a factor of ten in the number of collisions to be resolved could be achieved, the structure of the reaction zone could be observed, at least coarsely.

The activation energy of 17 kcal for the rate determining step (1) means that this reaction occurs at only a small fraction of the pertinent collisions even at <u>ca</u>. 2000 K and excludes the possibility mentioned previously of the reaction occurring ahead of the shock wave leading to a transition to the lower arm of the RH curve.

It is of interest to make some equally crude calculations about the chain initiating step. Assume that it is  $H_2 + O_2 = 20H$ . Using the approximate rule for reactions of this type that the activation energy in the exothermic direction is 0.25 times the sum of the bond energies,  $E_{\rm ACT} = DH_2 + DO_2 - (1/2)D_{\rm OH} = 70$  kcal. Assuming a steric factor of 0.1 and a rate constant  $10^{-11}$  exp (-70,000/RT) atom<sup>-1</sup> cc sec<sup>-1</sup> and  $(H_2) = (O_2) = 10^{18}$ , the initial rate of production of OH radicals is  $10^{18}$  cc<sup>-1</sup> sec<sup>-1</sup> at  $2000^{\circ}$  and  $10^{16}$  cc<sup>-1</sup> sec<sup>-1</sup> at 1580; in each case the rate is ample to initiate the divergent chain.

The relative importance of chain initiation by diffusion of radicals into unreacted gas may be estimated as follows. Let  $\underline{\ell}$  be the thickness of the reaction zone and  $\underline{c}_0$  the concentration of H atoms (the most diffusible species) at equilibrium, and  $\underline{D}$  their diffusion coefficient. In a system of coordinates sitting on the shock wave, the number of H atoms diffusing upstream across any plane into unreacted gas is  $\underline{D}$   $\underline{c}_0/\underline{\ell}$ . The volume of gas flowing across the same plane is  $\underline{S}(\underline{V}_2/\underline{V}_1)$ ,  $(\underline{V}_1/\underline{V}_2)$  is the compression factor) so that the volume rate of production of H atoms by diffusion is  $(\underline{D}$   $\underline{c}_0$   $\underline{\ell}/\underline{S})$   $(\underline{V}_1/\underline{V}_2)$ . For  $\underline{D}$  = 5 cm<sup>2</sup> sec<sup>-1</sup>, which is reasonable for our experiment,  $\underline{c}$  = 10<sup>17</sup> atom/cc, and  $\underline{\ell}$  = 10<sup>11</sup> cm, this is 10<sup>11</sup> atom cc<sup>-1</sup> sec<sup>-1</sup>, 10<sup>-7</sup> - 10<sup>-5</sup> less than the estimated rate of initiation by chemical reaction.

#### ACKNOWLEDGMENT

We are grateful to Dr. Arthur Bennett and Professor G. B. Kistiakowsky for stimulating advice and discussion.

## LITERATURE CITED

- Referred to, for example, by Berets, Greene, and Kistiakowsky, J. Am. Chem. Soc., 72, 1080 (1950).
- <sup>2</sup> G. B. Kistiakowsky, J. Chem. Phys., <u>19</u>, 1611 (1951).
- 3 Britton, Davidson and Schott, Disc. of the Faraday Soc., in press.
- <sup>4</sup> J. Fay, "Fourth Symposium on Combustion," Williams and Wilkins Co., Baltimore (1953), p. 501.
- A. J. Mooradian, W. E. Gordon, "Gaseous Detonation III. Detonation Limits in Hydrogen-Oxygen Mixtures" ONR report on Contract N7onr-292. Task Order I, with the University of Missouri (1950). See also Ph. D. Thesis by A. J. M.
- 6 Berets, Greene and Kistiakowsky, J. Am. Chem. Soc., 72, 1086 (1950).
- 7 A. J. Mooradian, W. E. Gordon, J. Chem. Phys., 19, 1166 (1951).
- Hirschfelder, Curtiss and Campbell, "Fourth Symposium on Combustion," Williams and Wilkins Co., Baltimore (1953), p. 190.
- R. R. Baldwin and A. D. Walsh, Discussions of the Faraday Soc., in press.
- B. Lewis and G. von Elbe, "Combustion, Flames and Explosions of Gases," Academic Press, New York (1951), p. 59.

# HIGH TEMPERATURE THERMODYNAMICS AND GASEOUS DETONATIONS IN MIXTURES OF CYANOGEN, OXYGEN, AND NITROGEN

H.M. Peek and R.G. Thrap
Los Alamos Scientific Laboratory
Los Alamos, New Mexico

## INTRODUCTION

This paper is a report of experiments concerning the validity of the Chapman-Jouguet theory (1,2,3,4,5,6) in the case of mixtures of cyanogen, oxygen, and nitrogen. There are several reports in the literature of similar experiments (6,7), but due to experimental errors and lack of sufficient calculated results in most of them, the only effective investigation of the experimental and theoretical problems involved is that of Kistiakowsky, Knight, and Malin (KKM) (7). The methods used here are essentially the same as those used by KKM, but these experiments cover a wider range of compositions and the calculations are considerably more extensive than theirs.

The detonation velocities have been measured in tubes of two, three, and four in. i.d. for gaseous mixtures of cyanogen and oxygen in the composition range 30 to 55 mole % cyanogen and for a gaseous mixture of cyanogen, oxygen, and nitrogen of composition 40 mole % cyanogen, 40 mole % oxygen, and 20 mole % nitrogen. The results for mixtures of greater than 50 mole % cyanogen were not reproducible and are not further discussed in this paper.

These experimental results are compared with Chapman-Jouguet values computed on an International Business Machines Type-701 digital computer for which the problem was coded by one of the authors (RGT) using standard methods developed at this Laboratory. (8)

# EXPERIMENTAL DETAILS

# A. Preparation of Mixtures

Oxygen and nitrogen were obtained from commercial cylinders after passage through Drierite to remove water. Mass spectrometric analyses of the dried gases were made and the results were used to determine the

final mixture composition. Typical analytical results are as follows: Oxygen tank - 99.8 mole % O<sub>2</sub>, 0.2 mole % A; Nitrogen tank - 99.7 mole % N<sub>2</sub>, 0.2 mole % O<sub>2</sub>, and 0.1 mole % A.

Cyanogen was prepared by the reaction of Cutt with CN in concentrated aqueous solution at about 50°C and 0.5 atm. The gaseous products from this reaction were first passed through a trap at 0°C to condense some of the water vapor, then through a silver nitrate bubbler to remove HCN, through a second 0°C trap to remove more water, and finally through a three-ft. long column of Drierite to remove the rest of the water before being condensed in a vessel at liquid nitrogen temperature. The crude product was twice distilled and collected at dry-ice temperature prior to the final distillation and collection at liquid nitrogen temperature in a metal storage vessel equipped with a high-pressure, vacuum-tight valve and pressure gauge. Periodic mass spectrometric analyses indicated run-to-run purities of 99.8 to 99.9 mole % CoNo. The remaining constituents were HCN and a small amount of water. The water was removed prior to making a mixture by passage through a Drierite column. No attempt was made to remove the small amount of HCN present. The effects of this impurity are discussed below.

Mixtures of the gases were prepared in a vacuum-tight system of valves and copper tubing which connected together a vessel of constant but unknown volume; a constant-displacement, variable-speed, reciprocating pump; and a mercury capillary manometer. In preparing a mixture, cyanogen was admitted to the mixing vessel of volume V<sub>C</sub> until pressure P<sub>A</sub> was reached. Then by manipulation of appropriate valves, oxygen was admitted to a pressure P<sub>A+B</sub> under conditions that insured no mass flow out of the system. If there was to be a third component, it was added in a similar manner. All pressures were determined to + 0.05 mm Hg by cathetometer readings of the capillary manometer. When all the gases had been admitted, the mixing pump was turned on and the gases were mixed by circulation through a closed loop.

The composition of the mixture was determined by solving the following equations for  $n_A$  and  $n_{A+B}$ , modified as necessary if there were three components:

$$P_A V_C = n_A (RT + B_A P_A)$$
 (1)

and

$$P_{A+B}V_C = n_{A+B}(RT + B_{A+B}P_{A+B}),$$
 (2)

where  $n_A$  is the number of moles of cyanogen in the volume  $V_C$  at pressure  $P_A$  and temperature T,  $n_{A+B}$  is the total moles of gas admitted to the system at pressure  $P_{A+B}$ , and  $P_A$  and  $P_{A+B}$  are second virial coefficients appropriate to cyanogen and the cyanogen-oxygen mixture, respectively. The condition of no mass flow out of the system when introducing the gases means that  $P_A + P_B \neq P_{A+B}$ ; i.e., this is the effect of gaseous imperfection of the mixture. The  $P_A$  and  $P_A$  lead to mole fractions which are then corrected for the deviations from 100% purity according to the mass

spectrometric analyses.

In all of this work the values for  $B_A$  and  $B_{A+B}$  were calculated from data compiled by Hirschfelder, et al. (9)

# B. Detonation Tubes, Velocity Measurement, and Initiators

Detonation tubes of 2.00, 3.00, and 4.00 in. i.d. (± 0.01 in.) were constructed from steel tubing of 1/2 in. wall thickness. The tubes consisted of two flanged sections bolted together and made vacuum-tight by using Neoprene "0" rings. The initiator was located at one end of a 3-1/2 ft-long section and the other 3 ft-long section was used as the velocity measuring section. The detonation tubes could be evacuated and filled by means of copper tubing and appropriate valves attached at the initiator end. The tubes were filled by means of the pump used in making the gas mixture. The final pressure was adjusted by manipulation of appropriate valves, the pressure being determined by cathetometer reading of the capillary manometer.

The detonation tubes were located in a building equipped with heating and ventilation controls such that the tube temperatures were maintained within two or three degrees of 25°C. The time between shots in any given tube was always of sufficient duration to allow the tubes to cool to ambient temperature.

The detonation velocities were measured by ionization gauges and associated electronic equipment similar to that described in detail by Knight and Duff. (10) A gauge consists of two copper wires, 0.020 in. i.d., inserted into a Teflon plug at a separation of 0.125 in., so that the ends of the wires are flush with the end of the plug. The Teflon plugs were machined and drilled, using an appropriate jig to ensure constant plug dimensions and location of gauge wires.

The gauges, seven per tube, were first mounted in modified Amphenol connectors having an appropriate tongue which fixed the orientation of the Teflon plug in the connector. The mounted gauges were inserted into holes in the wall of the measuring section of the tube; the gauges were flush with the inner tube wall and were made vacuum-tight by the use of "0" rings. The gauge-locating holes were carefully machined to ensure a snug fit of the plugs. The great care taken in machining the gauges, inserting the wires, and locating the gauge holes results in a very small error in the determination of gauge distances. As a result of several measurements using a micrometer and standard dowel pins, the gauge distances are known to ± 0.0003 in. The gauge distances were checked from time to time as the tubes were used in making shots.

Across each gauge there is a potential difference of about 200 v which charges a condenser in each gauge circuit; this condenser discharges as the detonation wave passes the gauge. The signal from the gauge nearest the initiating end is used to trigger a Raster-type

oscilloscope on which the remaining six signals are displayed after amplification and shaping. The signals as displayed on the oscilloscope are photographically recorded on Kodak Single Coated X-Ray film which is processed according to the manufacturer's recommendations. The times at which gauges "fired" are determined by reading these records. The average detonation velocity is then computed as the slope of the least squares straight line through the time-distance points. For a given mixture and initial pressure the average detonation velocities from each tube are then used to compute the infinite-diameter velocity required for comparison with the theoretical value. This is done by making a least squares straight line calculation of the velocity as a function of the reciprocal of the tube diameter.

The probable error in the average detonation velocity for any shot was easily determined from the results of the least squares calculation.(11) If this probable error exceeded five or six m/sec, the shot was repeated using a different initiator. It was found, in this way, that the nearly equimolar cyanogen-oxygen mixtures were adequately initiated by a small exploding wire. As the initial cyanogen concentration decreased, it was necessary to use small amounts of PETN; and for the weakest shots, including the mixture with added nitrogen, it was necessary to add a few grams of tetryl.

### EXPERIMENTAL RESULTS

Table I summarizes the results obtained for the cyanogenoxygen mixtures. Table II contains the results for the mixture containing added nitrogen. The error quoted is the probable error in the slope of the least squares straight line through the time-distance points. In computing the infinite-diameter velocities for one atm initial pressure, as shown in Table III, small variations in initial pressure and composition have been ignored. All shots were made at an initial temperature of 25°C.

There are several sources of error contributing to the uncertainties in the infinite-diameter velocities. First, there is the error of 0.001 in the cyanogen mole fraction due to the HCN impurity. Second, there is the effect of record-reading errors; this is probably the largest experimental error. It is, however, less than four m/sec, since the records could be read to at least + 0.2 µsec. Next, there is an effect of no more than + 0.2 m/sec in individual velocities due to gauge distance errors. Finally, the velocity-reciprocal tube diameter points do not lie exactly on a straight line as assumed in making the extrapolation to the infinite-diameter velocity. This leads to errors which are smaller for some mixtures than for others since in some cases several shots of the same mixture were fired at the same tube diameter. The combined effect of all these errors is an uncertainty of about five m/sec in the velocities given in Table III.

TABLE I. Experimental Detonation Velocities in Cyanogen-Oxygen Mixtures

Con	mosition	a 1			D, m/sec	
X <sub>c</sub> <sup>S</sup> N <sup>S</sup>	X <sub>0</sub> <sub>2</sub>	XA	P atm	4 in.	3 in.	2 in.
0.496	0.503	0.001	1.045	2758.3 <u>+</u> 0.5		
0.496	0.503	0.001	1.026	2759 <b>.6<u>+</u>1.</b> 6		
0.500	0.499	0.001	1.0011	2746.9 <u>+</u> 1.2	2752.3 <u>+</u> 2.8	
0.498	0.501	0.001	1.0005	2753.4+2.4	2748.3 <u>+</u> 1.4	
0.499	0.500	0.001	1.0011		2745.8 <u>+</u> 1.3	
0.499	0.500	0.001	1.0003			2740.3 <u>+</u> 1.9
0.499	0.500	0.001	1.0000			2742.7+1.0
0.499	0.500	0.001	0.9985			2743.1 <u>+</u> 1.0
0.499	0.500	0.001	1.0007			2742.3 <u>+</u> 1.0
0.499	0.500	0.001	0.5046			2703.6 <u>+</u> 2.7
0.499	0.500	0.001	0.5040			2703.7 <u>+</u> 1.7
0.484	0.515	0.001	0.9964	2754.3 <u>+</u> 5.0		2733.6+4.0
0.478	0.521	0.001	1.0049	2752.8 <u>+</u> 0.6	2751.4 <u>+</u> 0.8	
0.451	0.548	0.001	1.0001	2687.9 <u>+</u> 2.1	2680.1 <u>+</u> 0.8	
0.448	0.551	0.001	1.0044	2679.8 <u>+</u> 0.1		
0.448	0.551	0.001	1.0005		2676.3 <u>+</u> 0.0	2668.0+1.2
0.401	0.598	0.001	1.0008	2496.1 <u>+</u> 0.3	2492.0 <u>+</u> 0.3	2482.0 <u>+</u> 0.5
0.352	0.647	0.001	1.0002	2368.2 <u>+</u> 0.2	2361.1 <u>+</u> 0.3	2356 <b>.3<u>+</u>0.</b> 4
0.301	0.697	0.002	1.0008	2251.6±0.2	2249.6+0.1	2241.5+0.3
0.300	0.698	0.002	1.0004	2254.7 <u>+</u> 0.0	2251.2+0.0	2241.9 <u>+</u> 0.4

a Superscript zero refers always to the initial mixture composition.

TABLE II. Experimental Detonation Velocities in a Cyanogen-Oxygen-Nitrogen Mixture

X° -	X°	X°.	X°.			D, m/sec	
5 <sub>u</sub> 5	-05		A	P <sub>o</sub> atm	4 in.	D, m/sec 3 in.	2 in.
							2631.8+0.3

TABLE	III.	Infinite-Diameter	Detonation	Velocities

$\mathbf{x_{c}^{2}N_{2}}$	x <sub>0</sub> <sup>5</sup>	X <sub>A</sub>	D, m/sec
0.499	0.500	0.001	2768
0.449	0.550	0.001	2694
0.401	0.598	0.001	2511
0.352	0.647	0.001	2378
0.301	0.698	0.001	2263
0.401 <sup>a</sup>	0.400	0.001	2650

This entry refers to the mixture with added nitrogen; refer to Table II for composition and initial pressure.

The final result for the equimolar mixture is in excellent agreement with the corresponding data of KKM. However, at other compositions the agreement is not very good, the present results being higher. These experiments also show that the detonation velocity is a maximum for a mixture containing about 49 mole \$ C\_N\_0 rather than for a 50% mixture as previously supposed. The data of Table I also show, in disagreement with the results of KKM(7), that the effect of tube diameter on the detonation velocity is practically independent of the composition.

### THEORETICAL DETAILS

In calculating the theoretical results the product gases are assumed to be ideal. With this assumption the Chapman-Jouguet condition (7) and the Hugoniot equation can be written as follows:

$$F = (1 + \frac{1}{4}) + \left\{ (1 + \frac{1}{4})^2 - \frac{4}{8} + \frac{2}{8} + \frac{2}{8} + \frac{1}{8} \right\}^{\frac{1}{2}} - 2\frac{V_0}{V} = 0$$
 (3)

and 
$$G = 1 + \frac{\overline{C}_{p}(T)}{\overline{C}_{p}(T_{0})} \left[ \frac{R_{1}(P-P_{0})(V_{0}+V)}{2 R_{2} T_{0} \overline{C}_{p}(T)} - \frac{T}{T_{0}} + \frac{\Delta H_{f}^{o}(T_{0})_{exp} - \sum N_{1} \Delta H_{f}^{o}(T_{0})_{i}}{T_{0} \overline{C}_{p}(T)} \right] = 0,$$

$$(4)$$

in which F and G are dimensionless functions useful in calculations for numerical convenience. In these equations the subscript zero refers to the initial state of the unreacted explosive mixture, lack of subscript refers to the products in the Chapman-Jouguet state, V is specific volume, T is temperature, P is pressure,  $\gamma$  is the ratio of the constant-pressure to constant-volume heat capacities of the product mixture,  $\sum_{i=1}^{n} x_i$  is the total moles per gram of reactant,  $\sum_{i=1}^{n} x_i$  is the total moles per gram for the products,  $R_1$  and  $R_2$  are the gas constant in units of cal/mole/deg and cc atm/mole/deg, respectively,  $\Delta H_1^{\alpha}(T_0)_{\text{exp}}$  is the heat of formation in units of cal/g for the explosive mixture at temperature  $T_0$ ,  $\Delta H_1^{\alpha}(T_0)_i$  is the heat of formation in units of cal/mole for product component i at temperature  $T_0$ , and the  $T_0$ 's are average constant-pressure specific heats for the mixture between temperature T or  $T_0$  and  $T_0$ . The equation for the Chapman-Jouguet detonation velocity, D, can be conveniently rewritten in dimensionless form

$$\frac{D^2}{P_0 V_0} = \frac{\left(\frac{P_0 - 1}{V_0}\right)}{\left(1 - \frac{V_0}{V_0}\right)} . \tag{5}$$

Except for argon, which is treated as an inert, the n<sub>i</sub> are to be determined by solution of the various equilibrium conditions and mass balance relations among the assumed product components. Then, if the temperature variations of enthalpy and heat capacity are known for these components, Equations (3) and (4) can be solved, using the assumed ideal equation of state of the product mixture, to give the values of T, P, and V at the Chapman-Jouguet plane. The detonation velocity is then computed from Equation (5).

The velocity computed under the assumption of an ideal product mixture must be corrected for non-ideality. The correction used here is that indicated by Schmidt.(12) The Abel "co-volumes" for these mixtures are approximated from the empirically-determined Lennard-Jones "12-6" potential parameters discussed by Beattie and Stockmayer.(13)

In these calculations a total of eleven product components is considered. The most important equilibria are as follows:

$$1/2 \text{ N}_2 \implies \text{N} \tag{6}$$

$$C(g) + 1/2 0_2 \implies CO \tag{7}$$

$$C(g) + 1/2 N_2 \implies CN$$
 (8)

$$1/2 \ 0_2 \implies 0 \tag{9}$$

$$1/2 N_2 + 1/2 O_2 \implies NO$$
 (10)

$$C(g) + O_2 \implies CO_2 \tag{11}$$

$$2C(g) + N_2 \implies C_2N_2 \tag{12}$$

It is not inconceivable that other reactions involving more complicated molecules may be of importance. However, the only reaction that seemed reasonable, i.e., one involving C<sub>2</sub>N, could not be included due to a lack of the necessary thermodynamic data.

For these mixtures the equilibrium problem can be reduced to obtaining the solution of two non-linear equations in two variables; this description is also appropriate to Equations (3) and (4). The method used here was suggested to the authors by W. W. Wood(14) of this Laboratory and is described briefly in the Appendix.

### Thermodynamic Data

Enthalpy data are from the National Bureau of Standards' tables (15) except for CN and  $C_2N_2$ . Data for CN are from the results of Johnston, et al. (16) Data for  $C_2N_2$  were computed by the authors using the harmonic-oscillator, rigid-rotator approximation\* and spectroscopic data summarized by Herzberg. (17) Since the data of the NBS tables (15) do not extend beyond 5000°K, the data from 3000° to 5000°K were used to make least squares quintic fits, i.e.,

$$\overline{C}_{p}(T)_{i} = \frac{(H^{2} + H_{o}^{2})_{i}}{T} = \alpha + bT + cT^{2} + dT^{3} + eT^{4} + fT^{5}$$
(13)

and these fits were extrapolated to the desired temperature where necessary. Similar fits were made for CN and C2N2 using the data mentioned which were available from 3000° to 6000°K. The validity of the fits and extrapolations was checked by comparing selected values with the high temperature values calculated by Fickett and Cowan. (18) The errors were never greater than 0.1%.

<sup>\*</sup> Errors due to the harmonic-oscillator, rigid-rotator approximation in calculating the data for C<sub>2</sub>N<sub>2</sub> turn out to be negligible since, for the mixture studied, there is essentially no C<sub>2</sub>N<sub>2</sub> in the product mixture.

Heat capacities were computed for all components by means of the equation

$$C_{\mathbf{p}}^{\circ}(\mathsf{T})_{i} = C_{\mathbf{p}}(\mathsf{T})_{i} + \mathsf{T} \frac{\mathsf{d}}{\mathsf{d}\mathsf{T}} C_{\mathbf{p}}(\mathsf{T})_{i} \tag{14}$$

using the quintic fits for  $\overline{Cp}(T)_i$ . Equation (14) is exact if  $\overline{Cp}(T)_i$  and its temperature derivative are known exactly at the temperature of interest. Since the  $\overline{Cp}(T)_i$  fits were quite good, it seemed justifiable to compute the temperature derivative from these fits by direct differentiation. Such a procedure has the added advantage of requiring only one fit to compute two quantities.

This method of calculating  $C_p^o(T)_i$  was checked as follows: (1) For C, O, and N, values from Equation (14) were compared with data computed by the authors at a few temperatures using standard procedures and spectrocopic data summarized by the National Bureau of Standards(19); (2) For  $O_2$ ,  $N_2$ , and CO, values from Equation (14) were compared with data computed at a few temperatures by Fickett and Cowan(20), and Wood(21); (3) For CN, values from Equation (14) were compared with the data of Johnston, et al.(16) In every case the disagreement was less than 0.3%, the largest errors being confined to the components present only in small amounts.

Free energy functions,  $-(F^{\circ}-H_{O}^{\circ})/T$ , for CN are taken from the data of Johnston, et al.(16); data for C, O, N, and  $C_{2}N_{2}$  were computed by the authors from spectroscopic data.(17,19) For all other components the data of the NBS tables (15) were used to make cubic fits in ln (T/3000) and these fits were extrapolated to the desired temperature. The extrapolations were checked by comparison with the results of Fickett and Cowan(18) and were found to be very good.

 $\Delta H_0^O$  data for CN and  $C_2N_2$  are from Brewer, et al.(22), and Knowlton and Prosen(23), respectively; data for N and O were computed from dissociation energies,  $D_0^O$ , compiled by Herzberg.(24) All other  $\Delta H_0^O$  values are computed from the data listed in the NBS tables.(15)

Equilibrium constants are computed from  $\Delta H_O^O$  and free energy data in the usual way. For computing convenience the equilibrium constants were then fitted as cubics in T, a separate fit being used for each 1000° interval in the temperature range 3000° to 7000°K.

The thermodynamic functions computed by the authors are given in Table IV. Physical constants are taken from Herzberg. (24)

### THEORETICAL RESULTS

Calculations were made for cyanogen-oxygen mixtures in the composition range 10 to 52 mole % cyanogen and for a mixture of cyanogen, oxygen, and nitrogen containing 40 mole % cyanogen, 40 mole % oxygen, and 20 mole % nitrogen. Table V shows the computed detonation properties for the mixtures, the detonation velocities having been

Peek and Thrap

TABLE IV	. <u>Con</u>	muted Thermody	ynamic Fun	ctions*		
T ok	(H°-H°)	$-(F^{O}-H_{O}^{O})$	T OK	•	(F <sup>O</sup> -H <sub>O</sub> )	
	T	T			T	
	$\mathbf{C_{2}N_{2}}$	C2M2		C(g)	N	0
298.16	10.213	47.444	3000	44.249	43.117	45.052
3000	18.059	80.472	3250	44.653	43.515	45.456
3200	18.210	81.642	3750	45.377	44.228	46.177
3400	18.346	82.750	4000	45.705	44.550	46.502
3600	18.469	83.802	4250	46.015	44.854	46.808
3800	18.581	84.804	4750	46.585	45.414	47.370
4000	18.682	85.759	5000	46.849	45.674	47.630
4200	18.776	86.673	5250	47.101	45.923	47.877
孙00	18.861	87.549	5750	47.573	46.391	48.339
4600	18.940	88.389	6000	47.784	46.612	48.556
4800	19.013	89.197	6250	48.008	46.825	48.764
5000	19.081	89.974	6750	48.411	47.232	49.158
5200	19.144	90.724	7000	48.602	47.427	49.345
5600	19.258	92.147				
5800	19.309	92.823				
6000	19.357	93.479				
6200	19.402	94.114				
6400	19.445	94.731				
6600	19.486	95.330				
6800	19.523	95.912				
7000	19.560	96.479				

<sup>\*</sup> Units are cal/mole/deg.

TABLE V.		"Standar	d" Calcula	ted Detona	tion Prope	erties.	
x <sub>C2N2</sub> b.	٧ <sub>0</sub> ,c	c/g	V,cc/g	P,atm	T, ok	D,m/s	ec
0.5195	572	•7	323.9	54.80	5930	2685	
0.4995	578	3.3	327.4	56.80	6181	2750	)
0.4795	584	.0	331.2	56.15	6133	2750	)
0.4395	595	.8	339•4	50.31	5535	2634	,
0.3995	608	3.1	347.0	44.06	4958	2490	)
0.3595	620	.8	354.0	39.66	4627	2383	,
0.3296	630	.7	359.2	37.00	4454	2316	•
0.2996	640	.9	364.6	34.61	4310	2253	}
0.1997	677	•5	383.6	27.52	3883	2052	!
0.1497	697	·3	394.5	24.05	3631	1938	}
0.0998	718	<b>1.</b> 3	407.1	20.19	3263	1798	ĭ
xc <sup>5</sup> N <sup>5</sup>	*0 <sup>2</sup>	xN <sup>5</sup> c.	V <sub>o</sub> ,cc/g	V,cc/g	P,atm	T, ok	D,m/sec
0.401	0.400	0.198	619.9	351.2	48.84	5771	2637

a. 
$$P_0 = 1.000 \text{ atm.}$$
,  $T_0 = 298.16^{\circ}\text{K}$   
b.  $x_{0_2}^{\circ} = 0.998 (1-x_{0_2}^{\circ})$ :  $x_A^{\circ} = 1-x_{0_2}^{\circ}-x_{0_2}^{\circ}$   
c.  $x_A^{\circ} = 1-x_{0_2}^{\circ}-x_{0_2}^{\circ}-x_{N_2}^{\circ}$ 

corrected for gaseous imperfection of the products. For convenience, these results are called "standard" results. This designation will mean results obtained in which D0 for N<sub>2</sub> is 9.756 ev,  $\Delta$ H0(25°C) for CN is 94.8 kcal/mole, and  $\Delta$ H0(25°C) for C2N<sub>2</sub> is 73.84 kcal/mole. The computed equilibrium compositions of the "standard" product mixtures are given in Table VI. Table VII compares some of the "standard" velocities with values calculated by changing  $\Delta$ H0(25°C) for C2N<sub>2</sub> from 73.84 to 75.84 kcal/mole and  $\Delta$ H0(25°C) for CN from 94.8 to 95.8 kcal/mole.

The only known error in the calculated results, aside from the small errors in thermodynamic data and the imperfection correction, is one due to failure to account for HCN in the experimental mixture; i.e., in the calculations HCN is assumed to be C<sub>2</sub>N<sub>2</sub>. Approximate calculations show that the effect on detonation velocity due to this assumption is to decrease the calculated value by at most 0.2 m/sec; therefore, the calculated results are quoted to only four significant figures.

These results do not agree with the data calculated by KKM (7) for similar mixtures. There seem to be several reasons for the discrepancies. Probably the most important one is failure to allow for excited electronic levels and anharmonicity in computing their thermodynamic data for C, O, N, and CN at temperatures above 5000°K. Their results also contain errors associated with failure to attain convergence of the numerical iterations to better than 0.2% of the temperature; the present calculations were carried out to a convergence of better than 0.01%. Finally, their results seem to have the small errors almost always made when doing such complicated numerical calculations on a desk-type calculator.

# DISCUSSION

In Table IX and Figure I the "standard" velocities are compared with the experimental results. In some cases the calculated result has been computed from a four or five point Lagrangian interpolation of the results given in Table V.

The most important question to be considered is whether a comparison of experimental and theoretical results demonstrates the validity of the Chapman-Jouguet theory. According to a recently developed theory of the detailed structure of the detonation wave(25), it is necessary to consider the kinetic details of the detonation reaction in order to show that the Chapman-Jouguet state is the state of thermodynamic equilibrium. There are no experimental data on reaction kinetics at these detonation temperatures, and for reactions which might be important in these cases there seems to be a dearth of data from which to make even order of magnitude approximations. Consequently, it does not seem possible at the present time to demonstrate conclusively that thermodynamic equilibrium is attained in these mixtures.

Peek and Thrap

0.620(-3) 0.649(-3) 0.676(-3) 0.729(-3) 0.797(-3) 0.882(-3) 0.953(-3) 0.152(-2) 0.172(-2) 0.703(-3) 0.10t(-2) 5.134(-2) 0.225(-4) 0.258(-5) 0.359(-6) 0.486(-8) 0.199(-2) 0.115(-1) 0.214(-5) 0.464(-2) 0.157(-1) 0.161(-1) 0.129(-3) 0.681(-3) 0.409(-1) 0.170(-1) 0.758(-2) 0.123(-3) 0.598(-2) 0.208(-1) 0.424(-3) 0.679(-2) 0.612(-2) 0.714(-5) 0.6 (-7) 0.362(4) 0.277(-5) 0.584(-1) 0.117(-5) 0.282(-2) 0.375(-1) 0.490(-1) 0.546(-1) 0.588(-1) 0.514(-1) 0.363(-1) 0.230(-1) 0.828(-2) 0.423(-3) 0.212(-1) 0.294(-2) 0.106(-2) 0.226(-1) 0.472(-1) 0.376(-3) 0.850(-7) 0.872(-1) 0.672(-1) 0.113(-1) 0.146(-1) 0.356(-2) 0.332(-3) \*c02 0.1620 0.1561 0.7 (-14) 0.2 (-8) 0.1457 0.961(-3) 0.771(-6) 0.241(-6) 0.223(-2) 0.577(-5) i ŀ 0.587(-3) 0.220(-1) 0.526(-1) 0.489(-1) 0.995(-1) 0.1353 0.1728 0.1703 0.1591 0.1711 **6.122** 0.315(-5)<sup>b</sup> 0.480(4) 0.292(-3) 0.421(-2) 0.233(-1) 0.592(-1) 0.223(4) 0.945(-1) 0.1366 0.3320 0.4703 0.6443 0.3070 0.3028 0.2948 0.2458 0.1379 0.4073 0.2071 0.1915 0.1086 0.2721 0.2230 0.0775 0.6141 0.5664 0.3546 0.1889 0.0351 0.5486 0.6227 0.6135 0.1487 0.4022 0.5087 0,1067 **\*** 0.401° 0.2996 0.5195 0.4395 0.3595 0.32% 0.1997 0.4995 0.4795 0.1497 0.0998 0.3995

"Standard" Product Gas Compositions

TABLE VI.

The remaining initial mole fractions, Posmd To are the same as indicated in Table V.

The number in parentheses is the power of 10 by which the entry is to be mailtiplied.

This row gives results for the mixture with added nitrogen; mole fractions of initial mixture listed in Table V.

TABLE VII. Detonation Velocity vs Dissociation Energy of  $N_2$ .

x°	Detonation Vel	Locity, m/sec
0.4995	2750 <sup>a</sup>	2670 <sup>b</sup>
0.4795	2750	2653
0.4395	2634	
0.3995	2490	2455
0.2996	<b>225</b> 3	2246
0.1997	2052	2050

a  $D_0^0$  of  $N_2 = 9.756$  ev

b D0 of  $N_2 = 7.373$  ev, all other data same as "standard" results

TABLE VIII. Calculated Velocities for Various Heats of Formation.

$x_0^{C_N}$	Detonat	ion Velocit	y, m/sec
0.499	2750 <sup>a</sup>	2760 <sup>b</sup>	2763 <sup>c</sup>
0.449	2671	2684	2684
0.401	2494	2507	2506
0.352	2366	2374	2374
0.301,	2256	2263	2263
0.401 <sup>d</sup>	2637	26 <del>4</del> 8	2646

a "Standard" results in this column.

TABLE IX. Experimental vs "Standard" Calculated Velocities.

$x_o^{c^{5}N^{5}}$	D <sub>exp</sub> ,m/sec	D <sub>calc</sub> ,m/sec	Disagreement <sup>8</sup>
0.499	2768	2750	-0.6%
0.449	2694	2671	-0.8%
0.401	2511	2494	-0.7%
0.352	2378	2369	-0.5%
0.301	2263	2256	-0.3%
0.401b	2650	2637	-0.5%

a This column computed as  $\frac{100(D_{calc} - D_{exp})}{D_{exp}}$ 

b "Standard" except  $\Delta H_2^0(25^{\circ}C)$  for  $C_2N_2 = 75.84$  kcal/mole.

C "Standard" except  $\Delta H_2^0(25^{\circ}C)$  for  $C_2N_2 = 75.84$  kcal/mole and  $\Delta H_2^0(25^{\circ}C)$  for CN = 95.8 kcal/mole.

d This row refers to the mixture with added nitrogen.

b This row refers to the mixture containing added nitrogen.

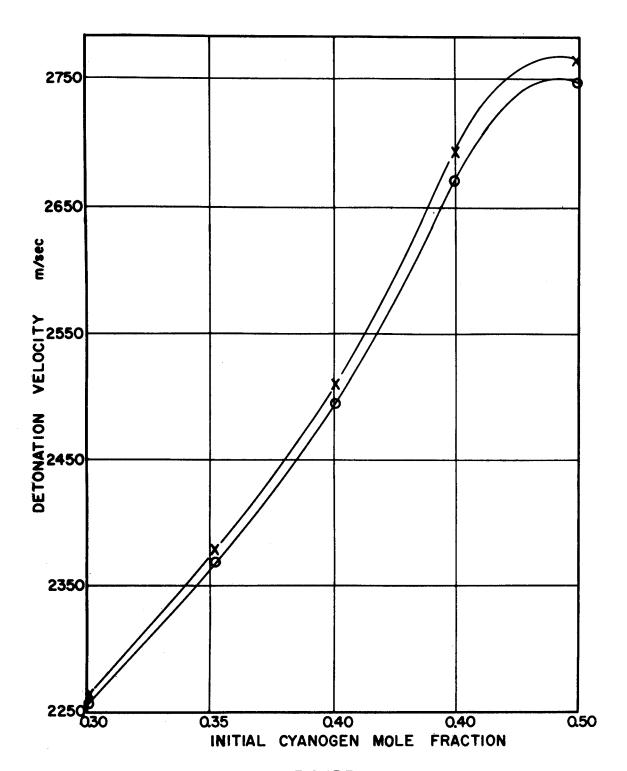


FIGURE | EXPERIMENTAL VS STANDARD CALCULATED VELOCITIES X • EXPERIMENTAL 0 • CALCULATED

However, it is possible to make at least one intuitive argument. This argument was suggested by Kistiakowsky (26) and goes somewhat as follows. Within a very short time after the onset of reaction in any region of interest there are relatively large concentrations of free radicals formed.(6) In the case of the nearly equimolar mixtures of cyanogen and oxygen the latter stages of the over-all reaction would involve the exothermic recombination of these free radicals, resulting in a certain distribution of, say, oxygen molecules among the possible energy states. If thermodynamic equilibrium were not attained, a different distribution among available states would be expected when there is "excess" oxygen present, as in the case of mixtures containing appreciably less than 50 mole % cyanogen. In this case the latter stages of the over-all reaction would be composed of processes involving the endothermic heating and dissociation of the "excess" oxygen ("excess" denoting the difference in concentrations of oxygen and cyanogen). Similar arguments should apply to the question of thermodynamic equilibrium in the case of the mixture containing added nitrogen. If the values calculated by assuming thermodynamic equilibrium are the same, or very nearly the same, as the experimental velocities over a fairly wide range of composition, this is evidence that thermodynamic equilibrium is attained.

On the basis of the above argument and the agreement demonstrated in Table IX it seems reasonable to assume thermodynamic equilibrium was attained in the mixtures studied. It then follows that the thermodynamic data used in the computations are very nearly correct, and it is of interest to inquire if better agreement can be attained by changing some of the more uncertain data.

There are two types of change which may be made. The first is to change thermodynamic data for the reactants and the second is to change the data for a particular product component(s). Changes of the former type would produce an effect for all the mixtures with the magnitude of the effect depending on the composition, but changes of the latter type would affect only those mixtures in which there is an appreciable concentration of the particular component in the product mixture.

With regard to changes in reactant thermodynamic data the only datum subject to change, which also produces an effect of the desired magnitude when changed, is  $\Delta H_{2}^{0}(25^{\circ}C)$  for  $C_{2}N_{2}$ . There are three quantities in doubt in the case of data for the products; namely, D8 for  $N_{2}$  and C0, and  $\Delta H_{2}^{0}(25^{\circ}C)$  of CN. Of these four quantities the dissociation energies are limited by spectroscopic evidence (24,28) to certain well-determined, but widely separated, values, while the heats of formation are subject to possible errors of only a few kcal/mole.

The results of Table VII clearly show that  $D_0^0$  for  $N_2$  is 9.756 ev rather than 7.373 ev. Although there is still some controversy over the value of  $D_0^0$  for CO(24), only one of the disputed values, 11.108 ev, was used extensively in these calculations. However, in a few cases calculations were made using the value

9.605 ev. In these cases the calculated velocity was lowered by about the same order of magnitude as when D8 for  $N_2$  was lowered to 7.373 ev. Consequently, D8 for C0 is 11.108 ev.

The results in the third velocity column of Table VIII are compared with the experimental results in Figure II. Clearly, the agreement between calculation and experiment is better in this case than when the experimental results are compared with the "standard" calculated values. This better agreement is an indication that  $\Delta H_2^2(25^{\circ}\text{C})$  of CN(22) and  $C_2N_2(23)$  are perhaps slightly higher than previously supposed.

In summary, the authors believe that these experiments have demonstrated the validity of the Chapman-Jouguet theory for gaseous mixtures of cyanogen, oxygen, and nitrogen. On this basis the agreement between calculated and experimental detonation velocities shows that  $D_0^\circ$  for  $N_2$  is 9.756 ev and  $D_0^\circ$  for CO is 11.108 ev. There is also some evidence indicating that  $\Delta H_1^\circ$ (25°C) of CN and  $C_2N_2$  are perhaps higher than previously supposed.

#### APPENDIX

Let the two non-linear equations in two variables be written as:

$$f = f(\alpha, \beta) = 0$$
 and  $g = g(\alpha, \beta) = 0$ ,

and suppose that these equations may be inverted to the form:

$$\alpha = F(f,g)$$
 and  $\beta = G(f,g)$ .

Let the solution of the former equations be  $(\alpha_0, \beta_0)$  and expand F and G in a Taylor's series about that point. The result is approximately,

$$\alpha = \alpha_0 + \text{af + bg}, \tag{15}$$

and

$$\beta = \beta_0 + a'f + b'g, \tag{16}$$

where a, a', b, and b' denote the partial derivatives of F and G with respect to  $\alpha$  and  $\beta$ . Equations (15) and (16) are equations of planes, the constants of which can be determined by computing the values of f and g for each of three values of  $\alpha$  and  $\beta$ . The only constant of interest in this case is  $\alpha_0$  or  $\beta_0$ , since these constants can then be used to compute a new f and g and this process can be repeated until the equations have been solved to the desired precision. No proofs of conditions for convergence of this iteration are known to the authors, but Milne(27) cites possible cases to be avoided in a somewhat similar method for one non-linear equation.

Practical experience with this method shows that the three initial guesses for  $\alpha$  and  $\beta$  should be triangularly spaced about the solution. It turns out that if good initial guesses are made the computation of the detonation properties of any given mixture can be

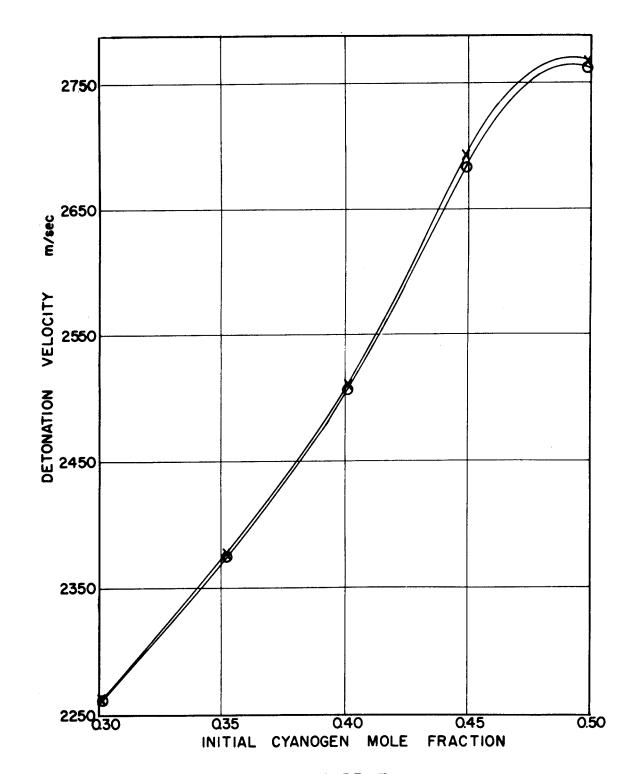


FIGURE II

EXPERIMENTAL VS ADJUSTED CALCULATED VELOCITIES

X\* EXPERIMENTAL 0 \* CALCULATED

completed on the IBM Type-701 computer in 20 to 30 seconds. At the worst, a complete calculation might take 45 seconds.

#### **ACKNOWLEDGMENTS**

The authors wish to acknowledge interest and very helpful discussion on the part of many of their colleagues; in particular, W. W. Wood, W. Fickett, R. E. Duff, H. T. Knight, L. C. Smith, and, especially, Professor G. B. Kistiakowsky. They also acknowledge the assistance of Patricia Fain, W. H. Rogers, and R. J. Kandel who performed the mass spectrometric analyses.

### BIBLIOGRAPHY

- 1. D. L. Chapman, Phil. Mag. 47, 90(1899).
- 2. E. Jouguet, J. Mathematique, 347(1905), 6(1906).
- 3. W. J. M. Rankine, Phil. Trans. 160, 277(1870).
- 4. H. Hugonoit, J. de l'Ecole Polytech. 57, 3(1887), 58, 1(1888).
- 5. R. Becker, Z. Physik. 8, 321(1922); Z. Elektrochem. 42, 457(1936).
- 6. B. Lewis and G. von Elbe, <u>Combustion</u>, <u>Flames</u>, <u>and Explosions of Gases</u>, Academic Press, Inc., New York, 1951.
- 7. G. B. Kistiakowsky, H. T. Knight, and M. E. Malin, J. Chem. Phys. 20, 876(1952).
- 8. S. Schlesinger, Los Alamos Scientific Laboratory, Report LA-1573, 1953.
- 9. J. O. Hirschfelder, C. F. Curtiss, and R. B. Bird, Molecular Theory of Gases and Liquids, John Wiley and Sons, Inc., New York, 1954.
- 10. H. T. Knight and R. E. Duff, Rev. Sci. Instr., in press.
- 11. H. Margenau and G. M. Murphy, <u>Mathematics of Physics and Chemistry</u>, D. Van Nostrand Company, Inc., New York, 1943.
- 12. A. Schmidt, Z. ges. Schiess-u-Sprengstoffw. 30, 364(1935).
- 13. J. A. Beattie and W. H. Stockmayer, A Treatise on Physical Chemistry, Chapter II, Volume II, Edited by H. S. Taylor and S. Glasstone, D. Van Nostrand Company, Inc., New York, 1951.
- 14. W. W. Wood, private communication.
- 15. Selected Values of Thermodynamic Properties, Series III, Mational Bureau of Standards, U. S. Government Printing Office, Washington, D. C., 1947.
- 16. H. L. Johnston, J. Belzer, and L. Savedoff, Cryogenic Laboratory of Ohio State University, Technical Report TR 316-7, May, 1953.
- 17. G. Herzberg, Infrared and Raman Spectra, D. Van Nostrand Company, Inc., New York, 1945.
- 18. W. Fickett and R. D. Cowan, to be published.
- 19. National Bureau of Standards, Atomic Energy Levels, Circular 467, U. S. Government Printing Office, Washington, D. C., 1948.
- 20. W. Fickett and R. D. Cowan, private communication.
- 21. W. W. Wood, private communication.
- 22. L. Brewer, L. K. Templeton, and F. A. Jenkins, J. Am. Chem. Soc., 73, 1462(1951).

- 23. J. W. Knowlton and E. J. Prosen, J. Research National Bureau of Standards, 46, 489(1951).
- 24. G. Herzberg, Spectra of Diatomic Molecules, D. Van Nostrand Company, Inc., Second Edition, New York, 1950.
- 25. W. W. Wood and J. G. Kirkwood, J. Chem. Phys., to be published.
- 26. G. B. Kistiakowsky, private communication.
- 27. W. E. Milne, Numerical Calculus, Princeton University Press, 1949.
- 28. J. M. Hendrie, J. Chem. Phys. 22, 1503(1954). This determination of D8 for N<sub>2</sub> was published during preparation of this paper and constitutes definite evidence for the higher value.

### DETONATION IN GASES AT LOW PRESSURE

Arthur L. Bennett and Henry W. Wedaa U. S. Naval Ordnance Test Station China Lake, California

Preliminary results of an investigation of detonation in gases were reported previously (1). The 2.5 cm square tube used then was not long enough to insure stable detonation nor was it feasible to provide adequate velocity measurement. A new tube of aluminum has been constructed and instrumented. The behavior of detonation in acetylene-oxygen and in stoichiometric hydrogen-oxygen at initial pressures down to 10 mm Hg is reported herein.

The driver section of the tube is 97 cm long and 12 cm in diameter. A diaphragm is normally used to isolate this section from the remainder of the tube. The first part of the experimental section is 215 cm long and 12 cm in diameter. A transition section 46 cm long provides a smooth transition to the final 10-cm square section 183 cm long. This section has a number of 2.5-cm windows flush with the interior surface. The run from the diaphragm to the window used for photoelectric measurements is 398 cm or 33 tube diameters. The run in the square section alone is 137 cm or 13.7 times the tube height.

Valves in both the driver section and experimental section lead to a diffusion pump for evacuation. Storage tanks are used for premixing the various gases. The mixture ratio is established by the pressure increment of each component. The mixture is allowed to stand at least 12 hours for diffusion. Control of the mixture ratio is run on the mass spectrometer.

The position of the detonation is determined by eleven ionization probes along the top of the tube at 36 to 50 cm intervals. The probe design and circuit used at Los Alamos (2) has been modified to suit the recording equipment. The probe consists of a 1.5 mm nichrome wire surrounded by Teflon 4 mm in diameter. The Teflon and wire are pressed tightly into a hole in a tube wall and then smoothed off flush with the interior surface. The signal pulse created by the discharge through the ionized gas of a 100-puf capacitor charged to a potential from 22 to 450 volts (depending on the pressure) is

transmitted through a germanium diode to the coaxial cable connecting all probes to the input of the Time Interval Recorder. The time constant of the circuit depends on the conductivity of the gas and varies from 0.1 us for higher initial pressures to 10 µs for the lowest.

The time scale of the Time Interval Recorder (TIR) is provided by a Tektronix Time Mark Generator (TMG) controlled by a 1-megacycle crystal oscillator which furnishes pulses from 1 µs to 1 second spacing. The duration of the record is 2000 µs at 1.5 mm/µ sec. Two Tektronix type 511 oscilloscopes, each with a 35 mm still camera, are used. The scopes are triggered alternately at 50 µs intervals by pulses from the TMG. The scopes are sweeping alternately, but dark, until the first probe signal is received by the control equipment. This signal brightens the beam of the active scope wherever the beam is at that instant and this scope continues to write for a full sweep of about 60 µs. At 50 µs on the TMG the second scope also begins to sweep providing an overlap in the recording.

Both scopes record three signals mixed in the TIR and fed to the vertical deflection: (a) the probe signals (positive); (b) TMG pulses at 1- and 5-µs intervals (negative); and (c) a sawtooth signal of 2000-µs duration which provides a vertical displacement of about 4 mm between successive lines. The relative times of the probe signals are read by interpolation between the 1-µs markers.

An "ionization profile" is obtained with an auxiliary oscilloscope. The positive side of a 23-volt battery is connected to the probe through a 10 K resistor, the other terminal being grounded to the tube. The probe is connected through coaxial cable to the input of the scope. The zero of the scope is set at the top line of the graticule and the sensitivity adjusted so that shorting the probe gives a deflection of 2 or 4 cm according to the linear range of the scope. Deflection of 1/4 the preset deflection corresponds to an internal resistance of 30,000 ohms, 1/2 to 10,000, and 3/4 to 3333.

A "light profile" is recorded with a separate oscilloscope. Two 0.65-mm slits 2.5 cm high separated 17.5 cm are aligned perpendicular to the axis of the tube in line with one of the windows. The slits exclude all direct light from the tube beyond a width of 1.2 mm at the distant wall of the tube, and hence the time resolution is 0.5 usec for the slowest detonation recorded. Behind the second slit a 10-stage, end-on, S4 photomultiplier type 6199 at 90 v/stage, battery powered, is used. The anode resistor of 1000 ohms with a short, low-capacity coaxial cable gives a time resolution of 0.1 us and a good signal-to-noise ratio. The slit lengths were adjusted to limit the maximum current to 4 mA.

The standard operating procedure is to clean the tube of any diaphragm debris, put in a new diaphragm, and pump a vacuum below 25 microns Hg. A leak rate of 10 microns a minute is considered satisfactory. The two sections of the tube are filled in turn, the

pressure being read on a dial manometer accurate to 0.2 mm Hg. Prior to this the oscilloscopes have been readied so that the tube is fired within 1 to 2 minutes of the completion of filling.

### EXPERIMENTAL RESULTS

The location of the probes relative to the diaphragm is given in Table 1. The measured detonation velocities for acetylene-oxygen are presented in Tables 2 and 3. Only the measurements over the latter part of the tube are given to indicate the degree of uniformity of the velocity. Some runs in Table 2 were made with red zip tape 0.002-inch thick, 0.003-inch acetate film and 0.002-inch copper foil as indicated. No appreciable effect on the velocity is evident at the usual working distance from the diaphragm. It was noted that at 50 mm initial pressure the velocity at the probes near the location of the diaphragm would be above 3200 m/sec without the diaphragm and then would settle down to uniform velocity. With the zip-tape diaphragm, however, the run-up to detonation was smooth and the final uniform velocity was present at the first interval.

The measurements in Table 3 were made to investigate the effect of the transition from round to square section. The ignition spark plug was placed at the end of the square section, 9.3 cm from probe 11, and the velocity was measured in the upstream direction. There appears to be no significant difference. The uniformity of the velocity at high pressure indicates that the measured distances and the timing are highly accurate.

The detonation velocities for stoichiometric hydrogenoxygen are given in Tables 4 and 5. The mean velocities are plotted in Figure 1. The velocity computed by Mooradian and Gordon (3) is shown for comparison. Good agreement of the observed velocities down

TABLE 1
DIMENSIONS OF THE TUBE

Element	Distance (Cm)	Element	Distance (Cm)
Diaphragm Probe 1 2 3 4 5 6	0 22.50 60.58 98.63 136.78 187.46 238.14	7 8 9 10 11 End	288.69 325.25 361.81 398.31 434.82 444.10

to 100 mm initial pressure is evident. The velocity of the one run at 10 mm is high relative to the velocities for 30 to 20 mm. In this case the driver initial pressure, 40 mm  $^{\rm C}_2{\rm H}_2{+0}_2$ , is high enough so that the pressure behind the detonation in  $^{\rm 2H}_2{+0}_2$  may well exceed the Chapman-Jouget pressure.

Figure 2 (a) is the light profile for  $400 \text{ mm } 2\text{H}_2 + 0_2$  taken at the side of the tube at the same distance from the diaphragm as Probe 10. Figure 2 (b) is taken at the same location at a side probe centered in the slits of the photomultiplier. A considerable degree of correlation is noted, even though the probe measures the conductivity of at most a few millimeters of the gas adjacent to the wall, whereas the photomultiplier receives light from the full 10-cm depth of the tube. The local nature of the probe measurement is indicated by the wider fluctuation of the record.

The light and probe profiles at 50 mm initial pressure of  $2H_2+0_2$ , driven by the detonation of 50 mm of  $C_2H_2+0_2$ , Figure 3 (a) and 3 (b), respectively, show a similarity to those of higher pressure. It is to be noted, however, that, following the initial peak and a plateau of 30 usec, there is a progressive increase in intensity, which continues for the whole 150 usec recorded, to a value equal to or exceeding the initial peak.

At 20 mm initial pressure of  $2H_2+0_2$  driven by 35 mm  $C_2H_2+0_2$ , illustrated by Figure 4, there is some fluctuation in intensity over about 50 usec in the five records obtained. In each, however, the increase in intensity beginning about 15 usec after the start of emission leads to a value greater than the initial peak, 150 to 170 usec.

Figure 5 is the record obtained at 10 mm initial pressure of  $2H_2+0_2$  driven by 40 mm of  $C_2H_2+0_2$ . The increase in light after the first peak is striking in this case.

Light profiles of longer duration have not as yet been taken. The many ionization profiles taken at slower recording speed indicate that the maximum conductivity occurs in a rather broad maximum at about 200 psec after the first signal. No marked dependence on pressure of the interval to maximum conductivity is evident at the location of the window near the end of the tube.

Examination of the light profiles shows that the duration of the rise of intensity to the first peak becomes progressively longer as the pressure is lowered. The mean values of the time of rise are: for 400 mm, less than 1 usec (1 run); 50 mm, 3 usec (2); 20 mm, 5 usec (5); and 10 mm, 7 usec (1).

#### DISCUSSION

The observed increase in the time taken to reach the first maximum could be interpreted to be the duration of the reaction zone.

This interpretation must be qualified, however, by the continuing increase in emission lasting some 200 µsec. Even if the radiation is purely thermal, the increase in intensity following the first peak indicates an increase in temperature, contrary to the Chapman-Jouget model of the detonation phenomena, unless one accepts the interpretation that the reaction zone is upwards of 200 usec or some 50 cm in extent.

Our present interpretation of these data is that, even after a run of more than 30 tube diameters, stable detonation has not been achieved. Even though the detonation velocities show little variation over the last three measured intervals, the marked irregularity of the ionization profiles suggest that the detonation is not a single shock followed by chemical reaction, but rather a series of shocks or pressure pulses overtaking the leading shock from the rear. As Brinkley and Richardson (4) have shown, energy released in the rarefaction wave is not lost, but will be delivered, at least in part, upstream. The average velocity will, therefore, be reasonably constant even though the arrival of the pulses must result in fluctuations of short duration.

Is the observed turbulence at low pressure a general phenomenon or is it peculiar to the geometry of the tube used? One should expect the transition from circular section to square section to produce lateral shocks, mild because the maximum angle of the wall relative to the axis is about one degree. A number of runs have been made to investigate this point. Figure 6 is a typical record: (a) is the ionization profile at probe 5, 29 cm upstream from the beginning of the transition section. Figure 6 (b) is the profile at probe 7, 28 cm downstream from the end of the transition. Figure 6 (c) is the profile at the usual measuring location, probe 10. This run was 100 mm 2H<sub>2</sub>+0<sub>2</sub>, driven by 150 mm C<sub>2</sub>H<sub>2</sub>+0<sub>2</sub>. Our interpretation of the group of records is that the irregularities smooth out in the course of the run through the tube without regard to the geometry. The indication is, therefore, that the turbulence is not peculair to this tube, but that detonation initiated by the technique used here will require a run of considerably more than 30 tube diameters to become stable.

### REFERENCES

- (1) Detonation in Gases, Bulletin A.P.S., Vol. 27, No. 6, Dec. 1952.
- (2) Precision Measurement of Detonation and Strong Shock Velocity in Gases. Knight and Duff, Bulletin of the APS, Vol. 29, No. 1, January 1954.
- (3) ONR Contract N7 onr-292. MS provided through the courtesy of ONR.
- (4) Fourth Symposium (International) on Combustion, 1952, p. 450

TABLE 2

		777	TTW///	<b>VIII.</b>	7 7 7 7 7	70.7	WCE1114	ELUNALLON VELOVILL OF U.2 AUBILLENE, U.5 UNIGEN (M/Sec)	OXXCEN	) m/sec	7		
Run No.	189	189 193	196	196 194 205 143	205	143	176	178	195	177	170	8	107
Pressure (mm Hg)	100	100	100	100	92	8	Š	52	52	52	52	50	2 2
Diaphragm	ı	1	ı	zip	zip	1		ı	ı	$z_{ip}$	.003	00.	zip
Probe 6-8	2703	2000	2793	2700	2799	7040	0,40	i i	0,20	ì	tate	ਤ <u>`</u>	2761
9		600	2790	6(7)	73.	2745	2757	2763	5/03	2754 2754	2763	2755	2767
6-10 6-10	7807	1612	2788	76/2	2803	2765	2767	2781	2757	2765	2758	2764	2763
10-11 Mean 8-11	279 <b>7</b> 2801	2791	2806	2795 2792	2797 2798	2768 2759	2761 2762	2764 2769	2755 2756	2759 2759	2685 2769	2745	2767 2766
Component C2H2 (%) Acetone (%) O2 (%) A (%)	<b>%</b>						49.57 .60 49.66 .17	49.42 .60 .49.78	50.17 1.10 48.57 .16	49.57 .60 49.66 .17	49.42 .60 49.78 .20	77.67 .60 .74.67	50.87 .74 48.20

TABLE 3

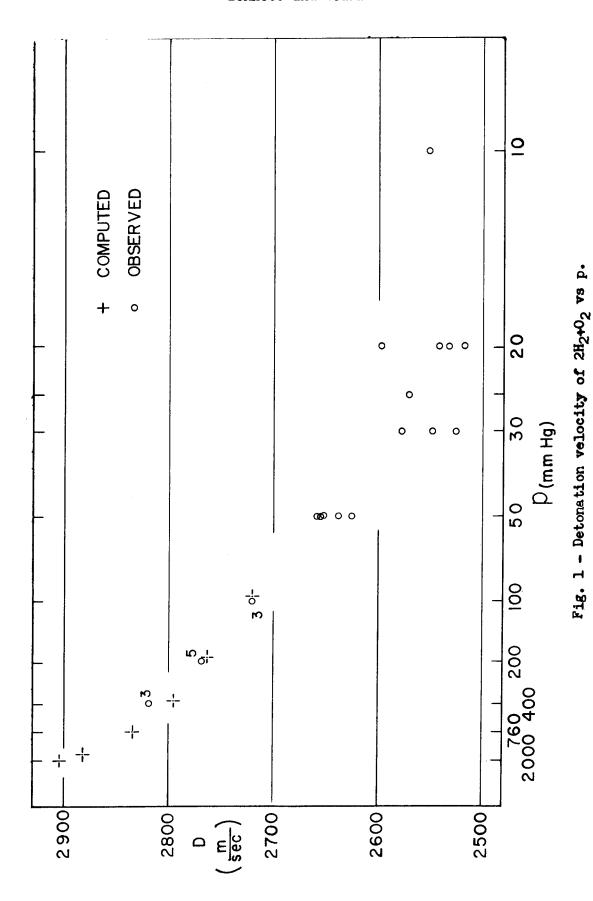
DETONATION	VELOCITY C	F O.5 ACE	TYLENE, O	.5 OXYGEN	(m/sec)
Run No.	141	171	173	174	175
Pressure (mm Hg)	250	100	100	50	50
Diaphragm	-	-	-	-	-
Probe 8-7 7-6 6-5 5-4 4-3 3-2 2-1	2856 2847 2855 2851	2797 2799 2803 2803	2798 2797 2801 2789	2766 2762 2761 2763	2766 2764 2759 2761
Mean (last 3 int.)	2851	2802	2796	2762	2761
Component C2H2 (%) Acetone ( O2 (%) A (%)	<b>(%)</b>	51.48 .03 48.31 .18			49.57 .60 49.66 .17

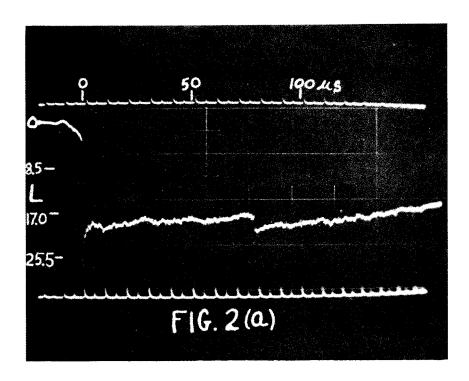
PABLE 4

a	ETONAT	TON VE	COCITY	OF STC	CHIOM	DETONATION VELOCITY OF STOICHIOMETRIC HYDROGEN-OXYGEN	DROGEN	OXYGE	-		
Run No.	139	232	233	200	201	<b>305</b>	203	204	206	506	210
Pressure (mm Hg)											
Driver C <sub>2</sub> H <sub>2</sub> +O <sub>2</sub>	200	170	170	100	100	85	85	85	150	125	100
Exper. $2H_2 + 0_2$	007	007	007	200	200	<b>30</b>	88	200	100	91	8
Probe 6-8		2813		2765	2767	2766	2769	2777	2713	2718	272L
8-9	2819	2812	2797	2761	2752	2769	2769	2773	2708	2728	2708
9-10	2829	2827	2816	2767	2782	2760	2786	2765	2729	2723	2723
10-11	2829	2810	2814	2761	2769	2769	2765	2786	2718	2714	2724
Mean 8-11	2826	2816	2809	2763	2768	2766	2773	2775	2718	2722	2722
Component H <sub>2</sub> (%)				67.39	67.16	67.16	67.16				
00 (8)				31.51	32.29	32.39	32.39				
A~ (%)				0.11	0.09	0.0	0.0				
N <sub>2</sub> (%)				0.99	0.36	0.36	0.36				

TABLE 5

		D	DETONATION VELOCITY OF STOICHIOMETRIC HYDROGEN-OXYGEN	ION VE	LOCITY	OF ST	DICHIO	ETRIC	HYDROC	EN-OX	CEDN			1
Run No.	213	224	225	228	216	185	186	187	217	219	220	221	230	223
Pressure (mm Hg)													,	
Driver $c_2^{\mathrm{H}_2+0}$ 2	8	50	8	5	35	50	52	8	35	8	35	35	07	04
Exper. 2H <sub>2</sub> +0 <sub>2</sub>	20	50	20	50	50	30	30	30	25	80	50	80	80	01
Probe 6-8	2647	2647	2647	2631	2660	2661	2630	2593	2569	2562	2600	2569	2627	2739
8-9 9-10 10-11	2668 2641 2567	2668 2644 2645	2656 2656 2653	2649 2664 2664 2664	2603 2697 2613	2539 2517 2571	2557 2552 2470	2574 2570 2589	2556 2588 2570	2521 2543 2535	2486 2532 2609	2538 2683 2570	2486 2534 2535	2611 2570 2552
Mean 6-11 " 8-11	2631	2651 2652	2653 2655	2652 2659	2643 2638	2572 2548	2552 2526	2581 2578	2571 2571	2540 2533	2557 2542	2590 2597	2546 25 <b>18</b>	2618 2578
Component H <sub>2</sub> (%) 02 (%) A (%) N <sub>2</sub> (%)	65.85 33.71 .10													





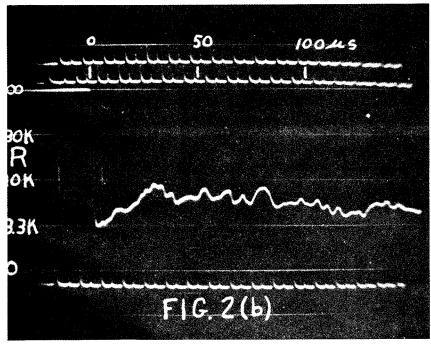
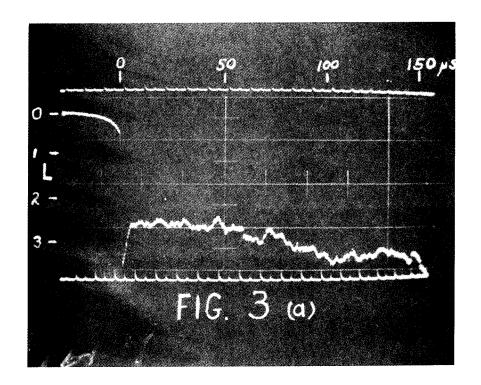


Fig. 2 - (a) Light profile, (b) Ionization profile. 400 mm Hg initial pressure of  $2H_2+0_2$  detonated by 170 mm Hg of  $C_2H_2+0_2$ .



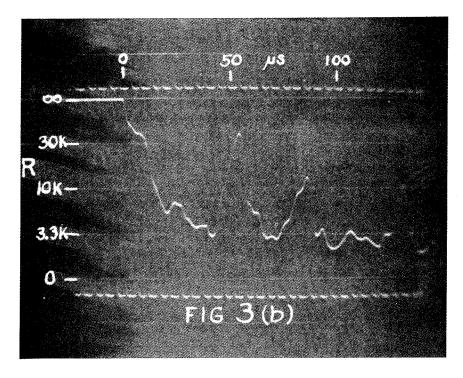
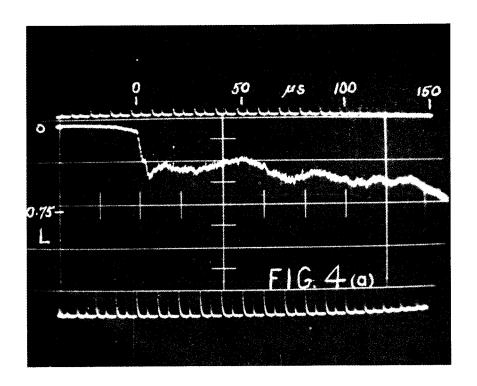


Fig. 3 - (a) Light profile, (b) Ionization profile. 50 mm Hg initial pressure of 2H<sub>2</sub>+0<sub>2</sub> detonated by 50 mm Hg of C<sub>2</sub>H<sub>2</sub>+0<sub>2</sub>.



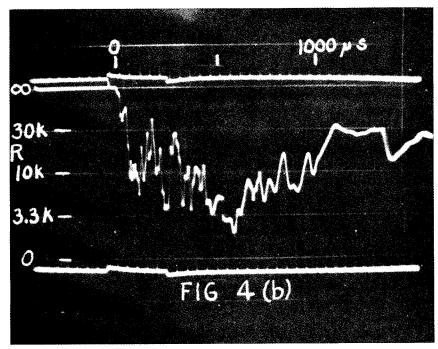
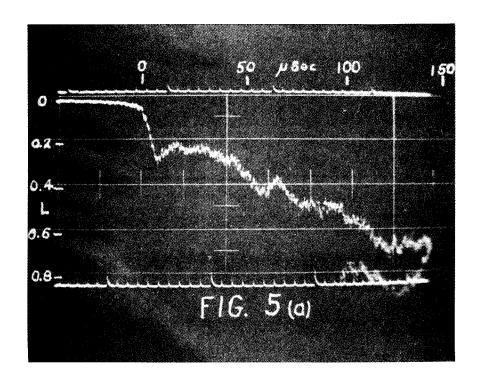


Fig. 4 - (a) Light profile, (b) Ionization profile. 20 mm Hg initial pressure of  $2H_2+0_2$  detonated by 35 mm Hg of  $C_2H_2+0_2$ .



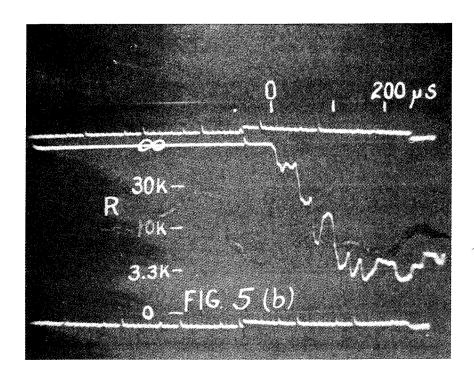


Fig. 5 - (a) Light profile, (b) Ionization profile. 10 mm Hg initial pressure of 2H<sub>2</sub>+0<sub>2</sub> detonated by 40 mm Hg of C<sub>2</sub>H<sub>2</sub>+0<sub>2</sub>.

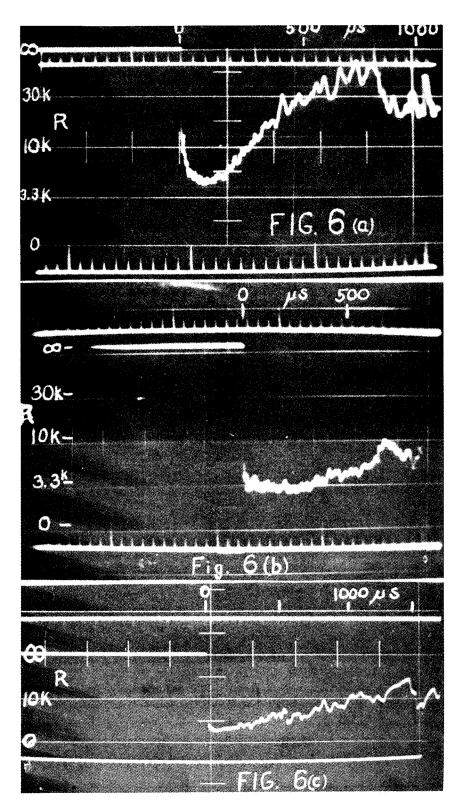


Fig. 6 - Ionization profile development along the tube. 100 mm Hg  $2H_2+0_2$  detonated by 150 mm Hg  $C_2H_2+0_2$ . (a) Probe 5 at 187 cm from diaphragm, (b) Probe 7 at 289 cm, (c) Side probe at 398 cm from diaphragm.

# MEASUREMENTS ON GASEOUS DETONATION WAVES

J. A. Nicholls, R. B. Morrison, R. E. Cullen
Aircraft Propulsion Laboratory
Engineering Research Institute
University of Michigan
Ann Arbor, Michigan

Most analyses of detonation describe the phenomenon in terms of the change in state conditions across the wave wherein Hugoniot curves are utilized (1). Such an approach is of great utility but tends to obscure the dynamic properties of velocity and heat release. Accordingly, it is enlightening to analyze the equations from the latter point of view and then to trace the various possible processes. Despite a number of simplifying assumptions which are necessary to do this readily, the analysis has a very definite qualitative value.

The system to be considered is as shown in Figure 1. The detonation wave is treated as a standing wave so that the unburned mixture is flowing into the wave front at velocity, U<sub>1</sub>, and the burned products recede from the front at velocity, U<sub>2</sub>. Assuming lean fuelair mixtures

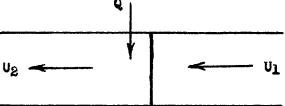


Figure 1. Heat Addition in a Constant Area Duct

so that the process may be treated as an air cycle, the following equations for steady one dimensional flow in a constant area tube may be written:

Conservation of Mass:

$$\rho_1 \quad v_1 \quad = \rho_2 \quad v_2 \tag{1}$$

Conservation of Momentum:

$$P_1 + C_1^{U_1^2} = P_2 + C_2^{U_2^2}$$
 (2)

Conservation of Energy:

$$h_1 + \frac{1}{2}U_1^2 + Q = h_2 + \frac{1}{2}U_2^2$$
 (3)

Equation of State:

$$P = \rho KT \tag{4}$$

where:

P = static pressure

P = density

U = velocity

h = enthalpy

Q = heat addition

T = static temperature

R = gas constant for air

The equations of mass, momentum and state may then be combined to yield an expression for the final temperature. That is:

$$T_{2} = \frac{\overline{v_{2}}}{\overline{v_{1}}} (RT_{1} + \overline{v_{1}}^{2}) - \overline{v_{2}}^{2}$$
(5)

Assuming a perfect gas so that the enthalpies depend on temperature alone, equation (5) along with the energy equation is sufficient to yield a plot of the final state of the mixture as a function of the initial conditions. This curve is shown in Figure 2 where heat release is plotted against velocity with temperature as a parameter.

The path lines, denoted by Tp, represent the transient condition of the stream as heat is added. There are, of course, a number of these path lines but for purposes of discussion only two are shown.

There are also a number of static temperature lines but only one is shown. The line of Q = 0 represents the loci of all points of sonic velocity as heat cannot be added to a sonic stream without a readjustment of the flow. For any path line, such as the ones shown in Figure 2, conditions to the left of points g or h are of subsonic velocity and those to the right are supersonic. The initial conditions of temperature and velocity establish the process on a path line. As heat is added the process follows this path line and whether the velocity be subsonic or supersonic, the heat addition will force the process towards sonic velocity.

### DETONATIVE PROCESSES

The heat release - velocity curves are instructive in describing the various types of detonation possible (2). Consider a combustible mixture at an initial temperature,  $T_1$ , and of velocity,  $U_1$ . This establishes the process on a path line, say at point a in Figure 2. If a shock wave occurs, the process jumps adiabatically to point b, the subsonic branch of the same path line. Suppose that chemical reaction takes place which yields an amount of heat,  $Q_R$ . The process then advances along the path line to point c where  $Q_b - Q_c$  is equal to  $Q_R$  and  $U_c$  is subsonic. Such a process is entirely possible and is ordinarily classified as a strong detonation.

If, in the above case,  $Q_R$ , is just equal to  $Q_b$ , the process will terminate at point g, that is the combustion products will be moving at a Mach number of one relative to the front. This is the Chapman-Jouguet type of detonation and is ordinarily the type observed.

The third possibility for this shock process is that where  $Q_R$  is greater than  $Q_b$ , say equal to  $Q_0$ . The implication of heat addition to a sonic stream requires that there be a readjustment of the flow and hence an unsteady condition exists. Since no solution can exist below  $Q_0$ , the intersection of the lines  $Q = Q_0$  and  $T = T_1$  represents the minimum velocity detonation which will satisfy the hydrodynamic equations. This advances the process from point a to point e and then to f and h which is again the Chapman-Jouguet type of detonation.

The third type of detonation, classified on the Hugonict Curve as weak detonation, is described as a supersonic combustion wave with the combustion products also moving supersonic relative to the front. A process of this type could be visualized as one with an initial state of a and a final state of d. Now there are two possible mechanisms by which this final condition could be attained. First there could be a shock to point b, heat addition to c, and an adiabatic jump to d. This latter path, that from b to c to d is known as a strong deflagration. However, it can be shown that such a path involves a decrease in entropy under adiabatic conditions and is thus

impossible. The remaining possibility is to proceed directly to point d with the stream remaining supersonic throughout the heat addition. In view of the present knowledge of flame propagation it seems very unlikely that this mechanism could ever occur though it may be possible under other forms of energy addition. It appears then, that two types of detonation are possible; that of the Chapman-Jouguet type or a strong detonation. The latter has been evidently experienced but only as a transient phenomenon.

The above discussion is premised on conditions of one dimensional steady flow. Accordingly, it cannot serve to explain such wave structures as shown in Figure 3 (taken from reference 3). The pictures shown are of two separate lean hydrogen-oxygen detonations propagating to the right in a ½ inch by 3/8 inch tube. Assuming that the waves developed identically, it can be seen from the similarity of the two photographs that they are about 180° out of phase. Very possibly this is a case of spinning detonation and calculation of the pitch agrees quite well with the theory of J. A. Fay (4). Also, the pitch is about identical to the perimeter of the tube. From the photographs it is apparent that the assumption of one dimensional steady flow is not entirely valid and the instabilities are time dependent. Needless to say, the chemical kinetics will be altered by such instabilities and it becomes hard to separate the chemical aspects from the hydrodynamics.

### CORRELATION OF DETONATION VELOCITIES

The heat addition - velocity curve has proved valuable in studying qualitatively the phenomenon of detonative combustion. However, its use has been restricted to an air cycle and consequently does not allow for any change in molecular weight across the combustion front. A more rigorous treatment of the equations with appropriate simplifications points to two non-dimensional parameters; namely,

 $\frac{m_1}{m_2} \frac{Q}{C_{p1}T_1}$  and  $M_D$ , where  $m_1$  and  $m_2$  are the molecular weights before and

after combustion respectively,  $c_{\rm pl}$  is the specific heat at constant pressure for the initial mixture, and  $\mathbf{M}_{\rm D}$  is the Mach number of detonation. Such an analysis has been described in an earlier paper (5) and shall not be repeated here. Q is the actual energy added and should, of course, allow for the effects of dissociation.

the detonation velocities of a number of gaseous mixtures have been measured at the Aircraft Propulsion Laboratory and reported earlier (2). These data were reduced to the parameters mentioned above and the results are shown in figure 4. Simplifications on the chemical aspects were made so as to permit ready calculation. It can be seen that the data correlate very well although the slope differs from that of the theory. A few points at the lower Mach numbers are

seen to fall off of the curve. These points correspond to those near the limits of detonation and it is highly probable that the flow was unstable when the velocity measurements were effected.

## SPARK SCHLIEREN PHOTOGRAPHS

A number of spark schlieren photographs of detonation waves have been obtained. For the most part these waves were initiated by a spark in a rectangular tube of  $\frac{1}{2}$  inch by 3/8 inch internal dimensions.

The first series of pictures, Figure 5, represent a time sequence in the initiation of detonation in a 50% (by volume) acetyleneoxygen mixture. Each photograph is for a different detonation, but taken at a different time interval from the energization of the initiating spark. In Figures 5a, 5b, and 5c, the flame front with the preceding shock wave can be seen propagating along the tube. In Figures 5d and 5e the shock front has evidently initiated combustion directly behind it and is now propagating to the right as a detonation. The generated retonation wave has evidently passed through the original flame front and has reflected from the closed end of the tube as a shock wave. It is believed that the inclined shock waves behind the detonation front can be attributed to the spark ignition as numerous photographs of shock initiated detonations do not seem to show this phenomenon. Another spark ignited detonation is shown in Figure 6. This is of a 50% hydrogen-oxygen detonation and was effected with a rectangular tube of  $2-\frac{1}{4}$  inches by  $3-\frac{1}{4}$  inches. Again, the trailing inclined shocks are apparent.

A second series of pictures were taken of a 50% hydrogenoxygen detonation passing over an inclined wedge. The wedge was mounted in the  $2-\frac{1}{4}$  inch by  $3-\frac{1}{4}$  inch tube such that the bottom surface was parallel to and a inch above the lower wall of the tube. In this way part of the detonation could traverse the lower channel and serve as a time reference to clock the portion of the wave passing over the upper surface of the wedge. This, of course, assumes no influence of the collision with the wedge on the characteristic Chapman-Jouguet velocity of detonation for that mixture. The first picture of this time sequence is shown in Figure 7. The wave is moving to the right and it appears as though the upper portion has already accelerated. The curved shock which interacts with the detonation front to form a triple point is originally generated from the apex of the wedge. The rectangular shape near the leading edge of the wedge and the fuzziness along the inclined surface are due to marks on the glass sides of the tube. At later times, Figures 8 and 9, the upper portions of the detonation wave are seen to be definitely accelerating away from the lower Chapman-Jouguet condition. The influence of the bubble undoubtedly accounts for the excess Chapman-Jouguet velocity of that portion of the detonation front which is perpendicular to the wedge. However, it is difficult to understand why the other portion has been accelerated as it has theoretically been unaffected by the

presence of the wedge. Other photographs, along with those shown, have enabled the variation of velocity of the components of the detonation front with time to be determined. This information is plotted in Figure 10.

Spark schlieren photographs of various hydrogen-oxygen detonations have been obtained and are shown in Figure 11. The volumetric mixture ratio is indicated under each photograph. In the case of 19.5% detonation the initial front has passed out of the picture to the right and the combustion lags considerably behind, as much as 4 to 5 inches. As the mixture is enriched this combustion lag is noticably shortened until the combustion is evidently initiated immediately in the shock front as shown in Figure 11-d.

All of the schlieren photographs shown to this point have been limited to one per detonation. This makes it extremely difficult to detect any unsteadiness in the propagation. Accordingly, two spark gaps were designed and fabricated to serve as light sources for two separate schlieren systems. In addition an adjustable time delay was incorporated between the two spark gaps. In order to utilize very small time delays, it was necessary to overlap the two schlieren fields of view. Hence, the two optical paths crossed at the test section of the tube with an included angle of about 7 degrees. This leads to some slight discrepancy between two pictures of the same wave. A few of these dual spark photographs were obtained on lean hydrogen-oxygen aetonations and are shown in rigures 12, 13, and 14. The time delays between photographs in the figures are 7.0, 7.5 and 8.0 microseconds respectively. Apparently there is a rotation or oscillation taking place. The marked difference between these figures suggests that insufficient tube length was used to insure that Chapman-Jouguet detonation was established. It is planned to investigate this aspect further.

### ACKNOWLEDGEMENT

Sincere appreciation is extended to Project Squid which has sponsored a large part of the work and the formulation of this paper. Some of the data presented was obtained and reported under an earlier Air Force contract (References 2 and 3).

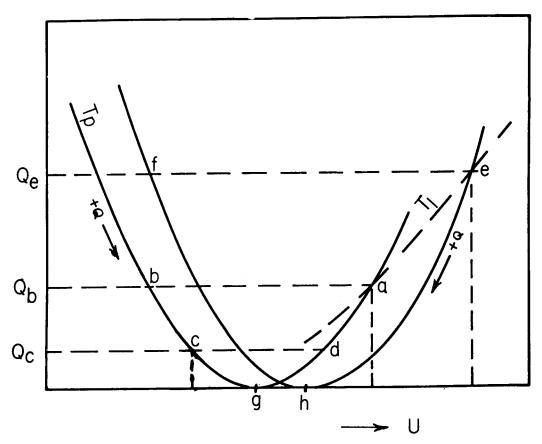
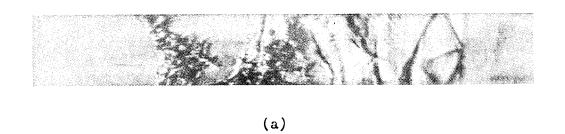


Figure 2 - Heat Release vs. Velocity



(b)

Figure 3 - 24% Hydrogen-Oxygen Detonations

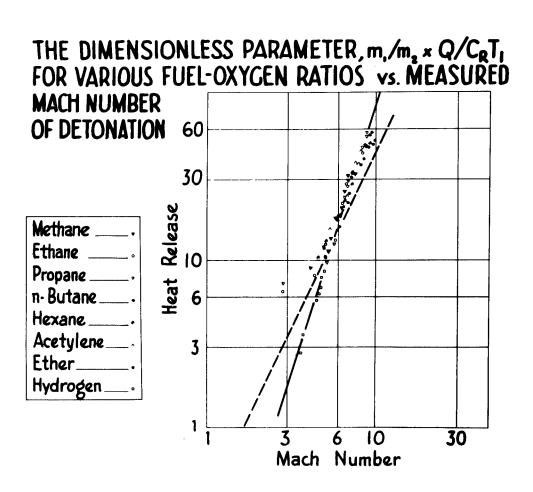


Figure 4 - Correlation of Detonation Velocities

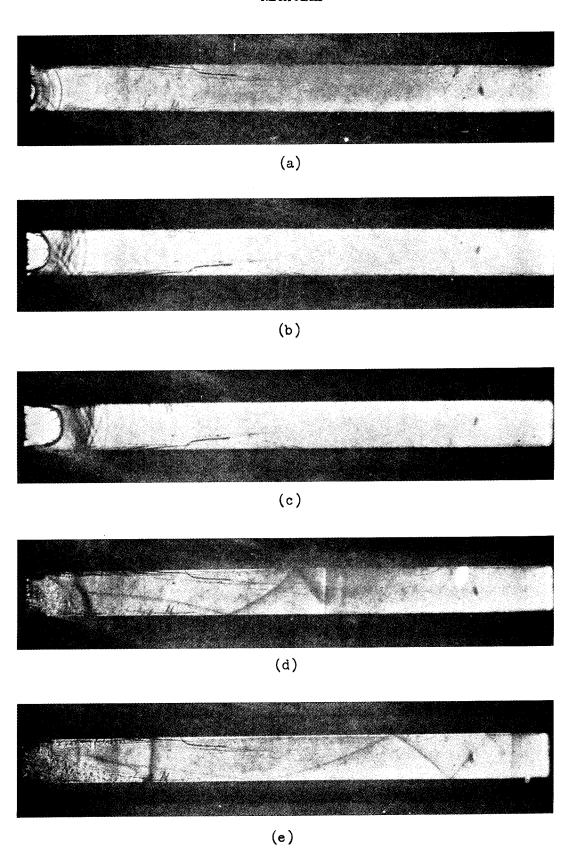


Figure 5 - Spark Initiation of Acetylene-Oxygen Detonation

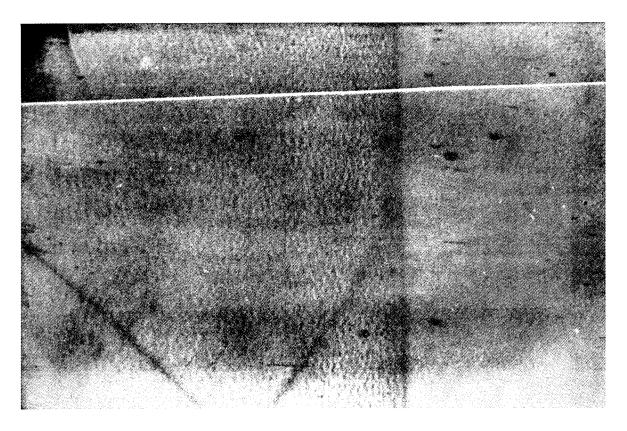


Figure 6 - 50% Hydrogen-Oxygen Detonation

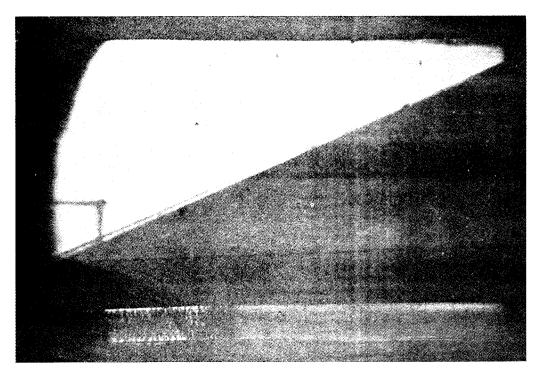


Figure 7 - Detonation Wave over a Wedge

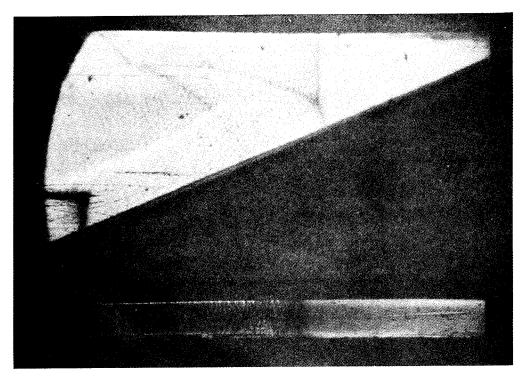


Figure 8 - Detonation Wave over a Wedge

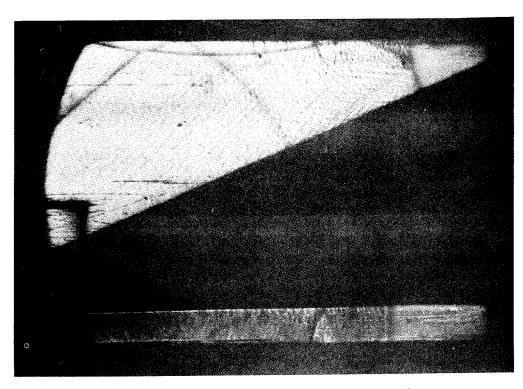


Figure 9 - Detonation Wave over a Wedge

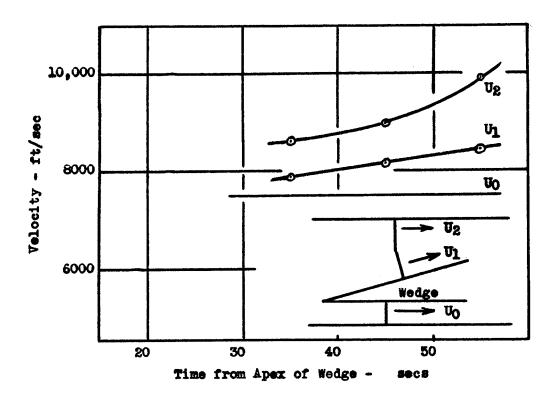


Figure 10 - Results of Wedge Experiment

# Micholls



(a) 19.5% Hydrogen-Oxygen



(b) 40% Hydrogen-Oxygen



(c) 50% Hydrogen-Oxygen



(d) 72% Hydrogen-Oxygen

Figure 11 - Hydrogen-Oxygen Detonations



Figure 12 - Hydrogen-Oxygen Detonation, 7 secs Delay



Figure 13 - Hydrogen-Oxygen Detonation, 7.5 secs Delay

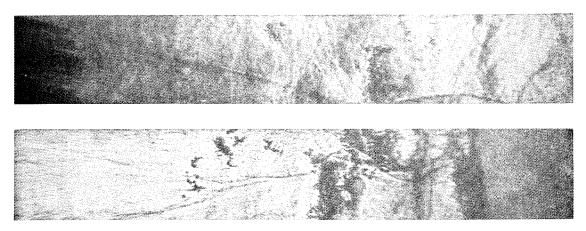


Figure 14 - Hydrogen-Oxygen Detonation, 8.0 secs Delay.

#### Nicholls

# REFERENCES

- 1. Courant, R. and Friedricks, K. U., "Supersonic Flow and Shock Waves," Interscience Publishers, Inc., New York, 1948.
- 2. Morrison, R. B., "A Shock Tube Investigation of Detonative Combustion," University of Michigan, UMM-97, 1952.
- 3. Nicholls, J. A., Morrison, R. B., Reid, F. A., Ong, R., "Final Report on Detonative Combustion," University of Michigan, Engineering Research Institute, August 1953.
- 4. Fay, J. A., J. Chem. Phys., 20, No. 6, 942-950, June 1952.
- 5. Morrison, R. B., "A Study of Detonative Phenomena in Gaseous Mixtures by the Use of Shock Tube Techniques," ASME Paper No. 52-5A-20.

#### STUDIES ON GASEOUS DETONATION

B. Greifer, F. C. Gibson and C. M. Mason U. S. Bureau of Mines Pittsburgh, Pennsylvania

#### Introduction

A photographic investigation of combustion waves in gases was undertaken to observe experimentally the constitution of deflagrations and detonations. Although the principles of the techniques applied were not new, the careful use of precision optical components produced exceptionally detailed and revealing pictures. Photographs obtained for various mixtures of oxygen with hydrogen and/or carbon monoxide support many of the concepts on the mechanism of detonation presented in the literature and permit a choice among several theories of detonation wave structure.

# Experimental Procedure

A diagram of the laboratory set-up is shown in figure 1. The explosions occurred in a steel tube of rectangular cross section with suitable observation ports and were photographed by the schlieren technique. The essential components of the optical system for schlieren photography were a matched pair of parabolic reflectors of 16 inches diameter and 128 inches focal length, a point source of light at the focus of one mirror, a field slit at the detonation tube, a knife edge at the focus of the other mirror, and a rotating-mirror camera immediately behind the knife edge. With this optical system, density gradients were observed readily in the detonation tube placed in the light path between the two mirrors.

As the resolution, i.e. the ability to separate the fine detail in the photographs, depends upon the degree of optical perfection, the fabrication and mounting of the mirrors were subject to rigid specifications. The mirrors were set into heavy cast iron mounts which rested on concrete pillars that passed through the laboratory floor into the ground beneath the building. These mounts were massive enough to assure vibrationless support for the mirrors,

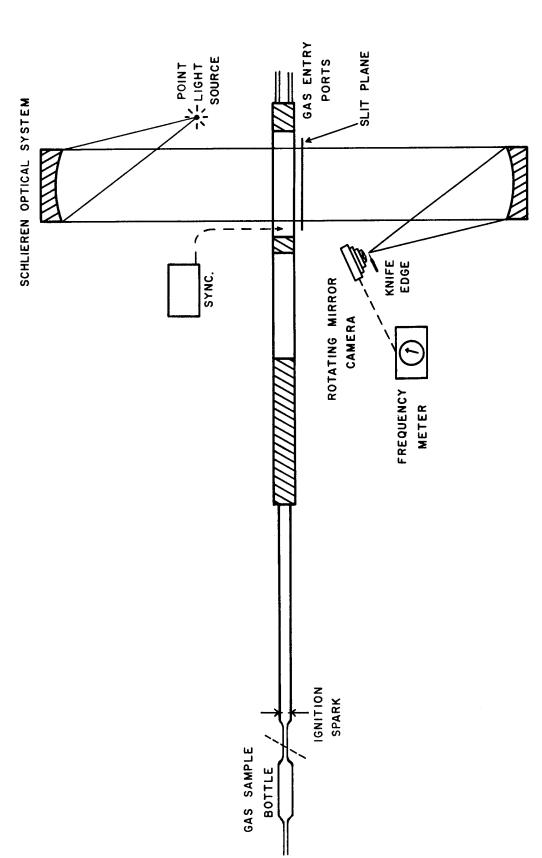


Figure 1 - Experimental arrangement.

yet were precise enough to provide delicate micrometer adjustment in three planes, for focusing and aligning the optical system.

The rotating-mirror camera was simple in design and could be constructed readily from commercially available materials. It has been described in detail elsewhere (1). A steel tube of rectangular cross section, one inch high by 3/4 inches wide and 7 feet long, was used for the hydrogen-oxygen work. To obtain detonation with carbon monoxide, it was necessary subsequently to add enough half-inch copper tubing to increase the over-all length to 55 feet. This change of size and shape is not believed to have any significant effect on the transition from deflagration to detonation, because this transition did not occur until the combustion had progressed well into the rectangular section.

In each experiment, the tube was filled with a gas mixture of known composition which was ignited at the open end of the tube by means of an electric spark. Electronic synchronization activated the schlieren light source while the combustion was in the field of view of the camera. Each print was mounted within a coordinate grid and the various structural features were measured directly.

# Hydrogen-Oxygen Explosions

Figure 2 is representative of the photographs obtained for stoichiometric mixtures of hydrogen and oxygen. It shows a detonation wave traveling across the field of view from left to right and a reflection from a corner of the observation window which projected slightly into the path of the combustion. The group of parallel lines behind the shock front is due to strains in the glass windows. Note that the group is reflected elastically, the speed remaining constant at 3140 m/s. This is to be compared with the reflected shock in the gas which has decelerated from 3140 m/s to 1350 m/s.

An important feature which may be observed in this hydrogen-oxygen photograph (figure 2) is the appearance of striations with a positive slope. These striations indicate the presence of a disturbance traveling 600 m/s in a direction opposite to the movement of the detonation and will be referred to as "retrograde striations". It has been suggested (2) that these retrograde striations are evidence of periodic velocity change of the detonation front or of spinning detonation. This appears to be the first time that such a phenomenon has been observed for stoichiometric mixtures of hydrogen and oxygen (3). The period of occurrence of the retrograde striations in hydrogen-oxygen detonations is 0.4 microsecond, corresponding to a recurrence frequency of 2.5 megacycles.

# Carbon Monoxide-Oxygen Explosions

In the case of carbon monoxide-oxygen mixtures, it was possible to adjust the experimental conditions so as to obtain

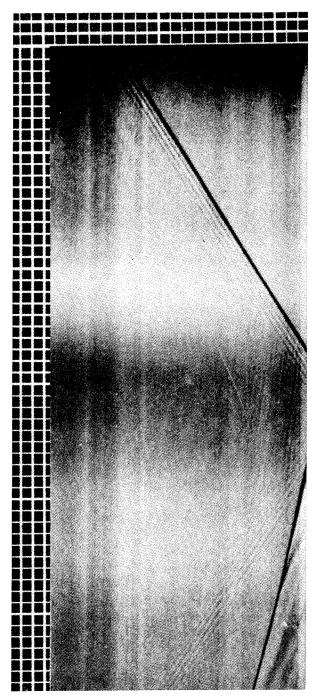


Figure 2 - Streak Schlieren Photograph of Detonation in a Mixture of 70% Hydrogen, 28% Oxygen, 2% Inert Gas. Observe the retrograde striae, the strains in the glass windows of the detonation tube, and the reflections off the end of the observation section. Each horizontal scale division equals 7.06 mm, and each vertical division 1.41 microseconds.

photographs of deflagration and detonation and, in a few cases, of the actual transition from one to the other. Figure 3 is a photograph of a carbon monoxide-oxygen deflagration and figure 4 shows a similar deflagration just before the transition to detonation. Figure 5 is a line drawing of the features of a deflagration to be compared with figures 3 and 4. The transition from deflagration to detonation is photographed in figure 6 and shown diagramatically in figure 7.

One feature of considerable interest is the pronounced hooks or "cusps" shown in figure 5. These are prominent in figure 3, discernible by careful scrutiny in figure 4, and visible in the deflagration region of figure 6. These cusps are located immediately behind the shock wave, well inside the reaction zone. The peaks of the cusps fall 4 to 7 mm. behind the shock wave in the tube. This distance may be compared with the thickness of the shock (0.8 mm.) and the 25-to-50 mm. average thickness of the entire reaction zone. It is possible that the peaks of these cusps represent sites of energy release in the chemical reactions which trail the shock wave. Such sites of energy release would form a cuspshaped pattern on a streak photograph. It has been predicted (4) that a flame front might be overtaken from the rear by weak compression waves and thus be accelerated discontinuously. Sighting along the line of the shock front in figure 4, we see that wherever such a pressure wave strikes the shock front from behind there is such an increase of flame velocity. This is pictorial confirmation of the above prediction.

Figures 6 and 7 show a deflagration becoming a detonation. The deflagration wave changes suddenly to a detonation at point T, the transition point, and a rearward-traveling wave, the retonation wave, marks the sudden release of energy. The fact that point T (figure 7) is not on a linear extension of the deflagration shock front may be due to the initiation of detonation above or below the slit and off center in the tube. Other photographs have located T right in line with S. The close resemblance between the shape of T and the shape of the cusps is to be noted.

Figure 8 is a photograph of detonation in carbon monoxide and oxygen immediately after the transition point T; figure 9 shows a detonation at a somewhat later time. The co-linearity of the shock front in the luminous and schlieren photographs may be noted (figure 8), although the significance of this co-linearity is dimmed somewhat by the consideration that there is a definite parallax between a two-mirror system (schlieren) and a one-mirror simple reflection (luminosity).

The arcs between the detonation and retonation waves in figure 8 are due to multiple reflections of pressure waves from the walls of the detonation tube. The last of these arcs are still visible in figure 9. These pressure waves originate at the moment

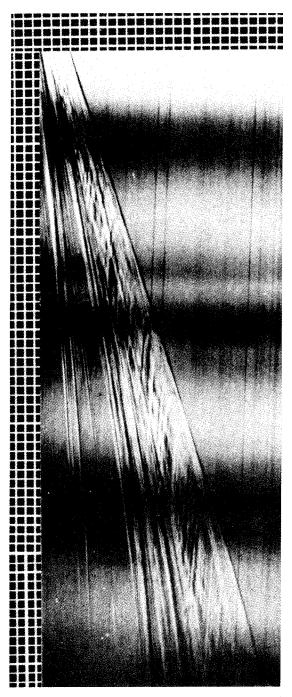


Figure 3 - Streak Schlieren Photograph of Deflagration in a Mixture of: 64.1% Carbon Monoxide, 30.5% Osygen, 2.2% Hydrogen, 3.2% Moisture and Inert Gases. Note cusps immediately behind the shock. Each horizontal scale division equals 7.06 millimeters, and each vertical division is 2.82 microseconds.

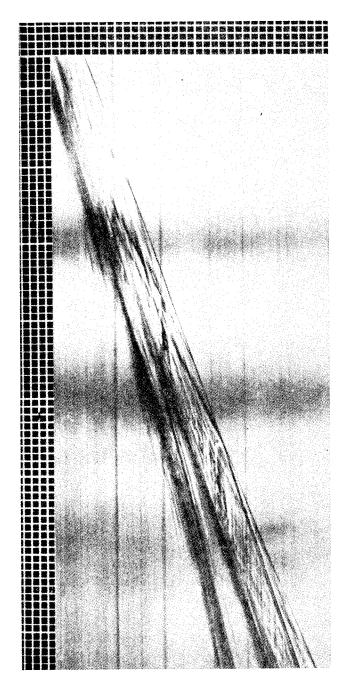


Figure 4 - Streak Schlieren Photograph of Deflagration in a Mixture of: 47.4% Carbon Monoxide, 49.1% Oxygen, 1.1% Hydrogen, 2.4% Moisture and Inert Gases. Note acceleration of shock front by support of pressure waves from behind. Each scale division is 7.06 millimeters horizontally, and 2.82 microseconds vertically.

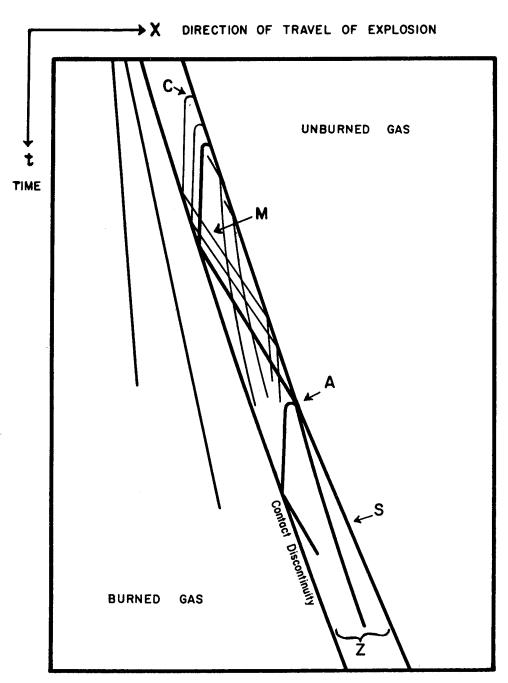


Figure 5 - Deflagration in a  $\text{CO-O}_2$  Explosion.

- C Cusp
  M Multiple reflections of compression waves
  A Acceleration of shock front at this point
- Z Reaction Zone
- S Shock front

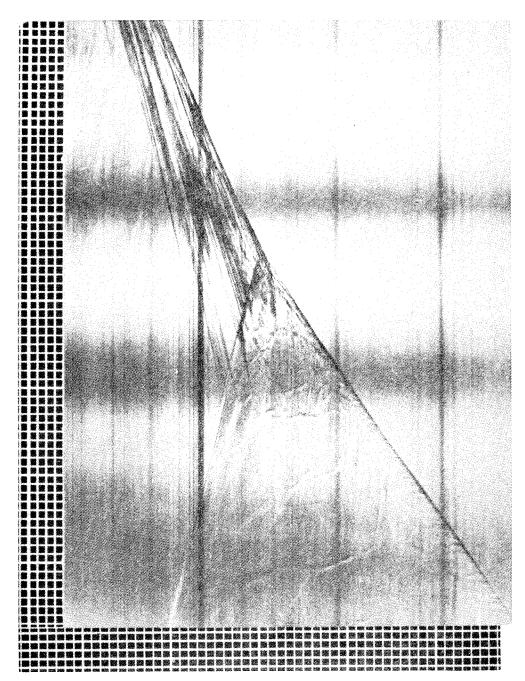


Figure 6 - Streak Schlieren Photograph of the Transition from Deflagration to Detonation in a Mixture Containing 64.5% Carbon Monoxide, 31.6% Oxygen, 1.6% Hydrogen, 2.3% Moisture and Inert Gases. Each horizontal scale division equals 7.06 mm, and each vertical scale division 2.82 microseconds.

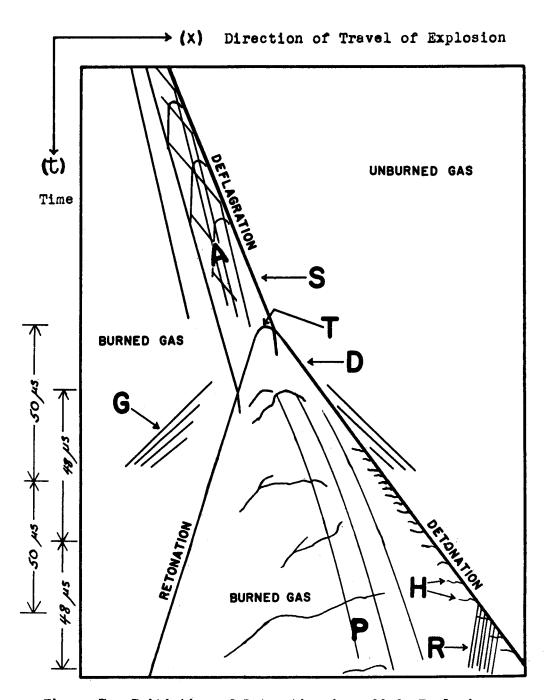


Figure 7 - Initiation of Detonation in a CO-O<sub>2</sub> Explosion

- A Combustion wave reaction zone
- G Shocks in glass windows
- T Transition point
- P Particle paths
- S Shock in gas
- D Detonation front (shock front)
- H Horizontal striae
- R Retrograde striae

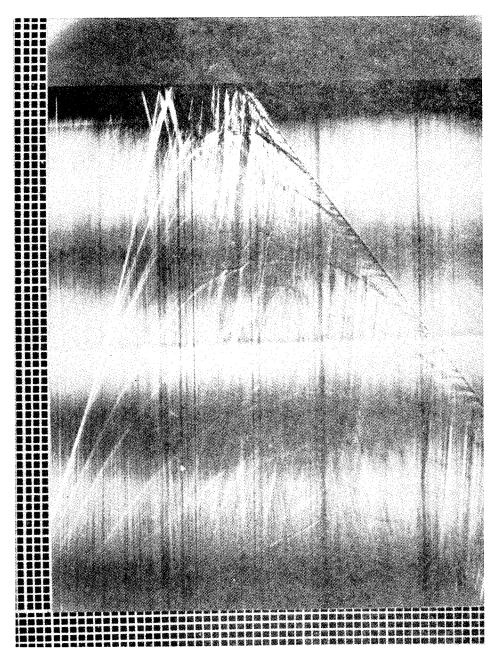


Figure 8 - Streak Schlieren Photograph of Initiation of Detonation in a Mixture Containing 72.2% Carbon Monoxide, 21.6% Osygen, 1.1% Hydrogen, 5.1% Moisture and Inert Gases. Note retonation wave, retrograde striae, particle paths, and arc-shaped foci caused by multiple reflection of the pressure waves inside the detonation tube. Each scale division equals 7.06 mm horizontally, 2.82 microseconds vertically.

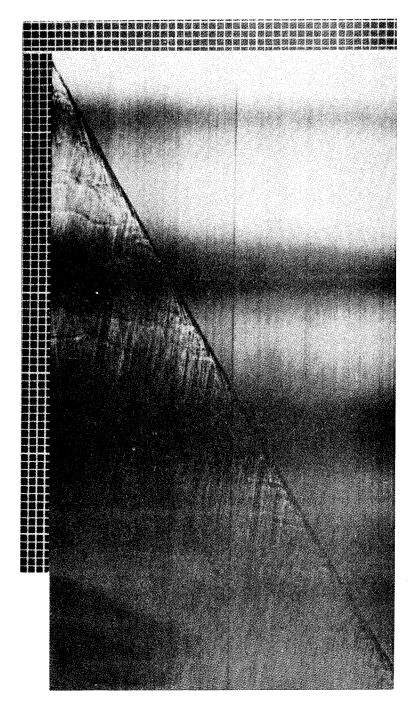


Figure 9 - Streak Schlieren Photograph of Detonation in a Mixture Containing 69.8% Carbon Monoxide, 25.8% Oxygen, 1.9% Hydrogen, 2.5% Moisture and Inert Gases. Note horizontal striae, retrograde striae, periodic velocity change of flame front, and foci due to multiple reflections of pressure waves inside the detonation tube. Each horizontal scale division equals 7.06 millimeters, each vertical division 2.82 microseconds.

of transition T (figure 7) and the frequency of the reverberation as shown on the photographs is sonic and relates to the physical dimensions of the tube.

The retrograde striations are clearly visible in all the carbon monoxide-oxygen photographs. They are indicated by R in figure 7 and are easily seen in figures 8 and 9.

A detailed examination of figure 9 shows that the detonation front consists of a smooth featureless black line-the shock-followed closely by a zone of optical gradients which approaches and recedes cyclically from this shock. One retrograde striation is formed during each cycle and direct measurements on the photographs indicate a recurrence frequency of the order of one megacycle. This frequency seems too high for any kind of mechanical spinning phenomenon in the gases, suggesting that the concept of periodic velocity change developed by Becker (5) and Lewis and von Elbe (6) may apply here.

It is planned in the near future to supplement the present photographs by end-on pictures of detonations to be used in determining whether the analysis developed by Smith and Sprenger (7) for rocket combustion is applicable to the gaseous systems considered here.

# ACKNOWLEDGEMENTS

This work was supported by the Office of Ordnance Research, Department of the Army, Army Project 599-01-004, Ordnance Project TB2-0001.

# LIST OF REFERENCES

- (1) U. S. Bureau of Mines Summary Technical Report No. 3376. Studies on Detonation Phenomena in Gases. 1. Rotating Mirror Camera. B. Greifer, March 31, 1954.
- (2) von Elbe, G. Private communication.
- (3) U. S. Bureau of Mines Progress Report No. 1, "Detonation and Explosives Phenomena", July 1 to September 30, 1953, Army Project 599-01-004, Ordnance Project TB2-0001.
- (4) B. Lewis and G. von Elbe, "Combustion, Flames and Explosions of Gases", Academic Press Inc., New York, 1951, p. 614.
- (5) R. Becker, Z. <u>Elektrochem</u>. <u>42</u>, 457 (1936).
- (6) B. Lewis and G. von Elbe, ibid., p. 624.
- (7) R. P. Smith and D. F. Sprenger, Combustion Instability in Solid-Propellant Rockets, Fourth Symposium (International) on Combustion, Sept. 1-5, 1952, Cambridge.

# CONDENSATION SHOCKS AND WEAK DETONATIONS

S. G. Reed, Jr. and W. H. Heybey U. S. Naval Ordnance Laboratory White Oak, Silver Spring, Maryland

#### INTRODUCTION

Rapid condensation of gas constituents in supersonic nozzle flow leads to shock-like phenomena which have been known for some time (1,9) and have been discussed by various authors. The exothermic character of these processes places them in close relation to flow processes involving chemical reactions. This relationship has been stated speculatively by J. M. Burgers (2) and has been touched on more recently by K. Oswatitisch (3); however, a detailed treatment of these rapid condensation phenomena from this standpoint has not appeared in the literature. Some steps towards such a treatment are taken in the present paper by describing the place the irreversible condensations occupy within the general framework of flow discontinuities induced by exothermic processes. Such a place exists because the laws of conservation of mass, momentum, and energy are the foundation of the treatment of all these flow discontinuities. It then becomes apparent that irreversible condensation processes in supersonic flow are formally identical with weak detonations and may be viewed as examples of such. We call them here "weak condensation detonations."

Chemical weak detonation fronts have never been definitely observed (4). Theoretically, this gap in available experience is commonly linked to the initiation process (5,13). More recently, however, the possible existence of three-dimensional weak detonations has been demonstrated by G. I. Taylor (6) and of one-dimensional detonations by K. O. Friedrichs (7). Taylor gives no hint as to the physical conditions under which his solution might be realized; Friedrichs, however, does discuss the existence problem, linking it with the behavior of chemical reaction rates.

In the following we present, first, a discussion of the normal condensation shocks in a steady supersonic air stream containing

a small portion of water vapor. This enables a comparison to be made with the standard treatment of steady detonation theory.

Next, the case of rapid condensation of a pure substance, e.g., steam, in steady nozzle flow is presented. Both of these examples show that these condensation processes are, in fact, weak detonations. A discussion of the kinematical features of such a process in one-dimensional unsteady flow is then given and compared with shock tube experiments. Finally, the relationship of these processes to the theoretical weak detonation solutions of K. O. Friedrichs is discussed briefly.

STEADY CONDENSATION SHOCKS IN AIR INDUCED BY SUDDEN CONDENSATION OF A SMALL FRACTION OF WATER VAPOR

If a small amount of water vapor condenses in an air stream, the ensuing changes of the mass flow, of the gas constant, and of the ratio of specific heats can be neglected. The simple theory (10) considers the condensation merely as a heat source and deals with the changes wrought upon a uniform air stream by steady injection of heat energy, say of g calories per unit mass, at a fixed station. This addition instantaneously raises the original stagnation enthalpy (from  $h_0$  to  $h_0$  + g calories per unit mass) and, consequently, the sound speed at a fictitious throat from a\* to a\*¹. The discontinuous change of state is governed by the three conservation laws (of mass, momentum, and energy) which permit a complete description of the transition. In what follows the states immediately in front of and behind the shock will be designated by the subscripts 1 and 2, respectively. The dimensionless flow speeds  $v_1 = u_1/a*$  and  $v_2 = u_2/a*$  are related by the conservation laws which yield

$$2Qv_1v_2 = (1 + v_1^2) \pm \sqrt{(1 + v_1^2)^2 - 4Q^2v_1^2}$$
 (1)

where

$$Q^2 = 1 + g/h_0 = (a*1/a*)^2$$

It is seen that the velocity  $\mathbf{v}_2$ -is not determined by  $\mathbf{v}_1$  alone; the quantity g must also be known. Its numerical value is probably connected with the speed with which, at temperature  $T_1$ , undercooled water vapor is condensing. This condensation rate cannot be determined from gas dynamical relations alone, although there is a connection, as we shall see in discussing Friedrich's work at the end of this paper. Thus, the quantity g will be taken here as an indeterminate parameter. In order for  $\mathbf{v}_2$  to be real, however, g obviously cannot be larger than

$$g_{\text{max}} = h_0 \frac{(v_1^2 - 1)^2}{4v_1^2}$$
 (2)

This condition is imposed by the three conservation laws.

The ambiguity in sign appearing in equation (1) can be removed. Since normal condensation shocks have been observed in supersonic flow only, we first take it that  $v_1 > 1$ . Secondly, no change of state can occur in the uniform air stream if no liquid is formed at all, so that  $v_2 = v_1$  if Q = 1. These conditions require the upper sign in equation (1). Once the velocity  $v_2$  is thus established as a unique function of  $v_1$  and g, a simple analysis, omitted here, shows that a normal condensation shock transforms supersonic velocity at the front side into a (smaller) supersonic velocity at the back side, at the same time raising pressure and density. It thus provides for the same change of state as would a one-dimensional weak detonation front separating unburnt gas from burnt gas in a chemical reaction process (5). The part of the air stream containing liquid water obviously corresponds to the burnt gas flow.

# RELATIONSHIP WITH WEAK DETONATIONS

For a mathematical treatment in terms of a Hugoniot diagram, one will first observe that the internal energy, e, per unit mass of air, assumed to be a perfect gas, is the same function of specific volume, 7, and pressure, p, before and behind the front:

$$e = \frac{1}{Y-1} p \tau$$

The equation of the Hugoniot curves then becomes

$$\frac{Y+1}{Y-1} (p_1 T_1 - pT) + T_1 p - p_1 T + 2g = 0$$
 (3)

It is seen that for parametric values of g the curves here are non-intersecting hyperbolas with common asymptotic lines

$$p = -\frac{\gamma - 1}{\gamma + 1} p_1$$
,  $\tau = \frac{\gamma - 1}{\gamma + 1} \tau_1$ 

Adopting now the pattern used in conventional theory to exclude weak detonations (5,14), we replace the ideally sharp shock discontinuity by a narrow reaction zone within which the heat is liberated gradually. In other words, the agglomeration of water molecules into droplets is not supposed to occur instantaneously, since it requires a small but finite time to be completed. It thus extends across a narrow slab, which in turn is subdivided into individual layers, each characterized by the amount of heat liberated up to that layer. The Hugoniot curve, equation (3), with g = g<sub>i</sub> gives the possible p - T relationship in that layer; the values actually prevailing are obtained by the intersection with the Rayleigh line,

$$\frac{p - p_1}{\tau - \tau_1} = - \rho_1^2 u_1^2 = - \gamma \frac{p_1}{\tau_1} M_1^2$$

where  $\S$ , denotes the density forward of the shock and  $M_1$  is the supersonic Mach number at which condensation sets in.

HUGONIOT CURVES AND RAYLEIGH LINE FOR A CONDENSATION PROCESS

The slope of the Hugoniot hyperbola at P1, according to equation (3), is  $-\gamma p_1/\tau_1$ . Since M1>1, it follows that at P1 the inclination of the Rayleigh line is steeper than that of the Hugoniot curve. Hence, the intersection points on Figure 1 will, in chemical reaction processes, correspond to detonations. We denote by gf the final amount of heat liberated by the condensation process, thus assigning a definite value to the parameter g. It is geometrically clear that gf cannot be larger (for a given Rayleigh line) than a certain amount  $g_{max}$  (which is given analytically by equation (2)). The Hugoniot hyperbola  $g = g_{max}$  will have a point of contact with the Rayleigh line on Figure 1. With detonations this point describes a Chapman-Jouguet process (5,14) for which the velocity is sonic in the burnt gas, and behind a condensation shock the velocity u2 is known to be sonic if the maximum amount of heat is liberated (10).

The successive states within the narrow reaction zone are given by a sequence of points on the Rayleigh line. This sequence starts out at P1 and comprises all the intersection points with the Hugoniot curves for  $g = g_i$ , until the point  $T_2$  on the hyperbola  $g = g_i$  is reached. With chemical reactions all these points would characterize the momentary state within a weak detonation zone. Beyond T2 the sequence cannot be continued, because this would call for layers where more than the final amount of heat is liberated. In particular, the strong detonation point To cannot be reached. This reasoning evidently is parallel to that commonly used in excluding strong deflagrations (5) and, therefore, weak detonations, since these are visualized as initiated by a shock setting off a strong deflagration. It appears that this mechanism cannot be upheld for weak condensation detonations; since they are real, they cannot begin with a shock. Measurements by P. Wegener (8) reveal that, although on Schlieren pictures the water condensation in supersonic air flow may have a shock-like appearance, the actual reaction zone, as indicated by nonisentropic gradual pressure variation, can be quite wide (order of magnitude 1 cm). It should also be noted that K. O. Friedrichs (7), in establishing the existence of weak detonations, never makes use of a shock transition in the unburnt gas. The Chapman-Jouguet process appears as a limiting case of weak detonations. One can adapt the arguments usually given (5) for the "stability" of the Chapman-Jouguet point when approached from the "strong" side along a fixed Rayleigh line to show that this point has also an analogous stability when approached from the weak detonation side. A weak detonation cannot proceed past the Chapman-Jouguet point.

It can be fairly objected that the discussion just presented is artificial in the sense that g or  $g_f$  cannot be arbitrarily fixed.

To answer this objection theoretically would require proof of the existence, uniqueness, and stability of the process at hand. Friedrichs (7) has shown the existence and uniqueness, but not the stability, of possible weak detonations. A practical answer is provided by the experimental fact that stable condensation shocks do occur, for fixed starting conditions, at a fixed Mach number.

# CASE OF SUDDEN CONDENSATION OF A SINGLE COMPONENT GAS

There is, of course, only one Hugoniot curve for the final equilibrium state that can be attained in a steady, adiabatic process starting from a given initial state. This can be shown for the case of the mixture of water vapor and air discussed above; for simplicity we give here the Hugoniot diagram for pure water vapor. Using thermodynamic data for steam, Hugoniot diagrams can be drawn for equilibrium conditions downstream of any given point. Figure 2 illustrates the type of result obtained. AA' represents the coexistence line, below which two-phase equilibrium prevails. The dotted curve is a dry-steam isentrope, continued metastably into the shaded coexistence region to the condition Z1. The Hugoniot curve H, corresponding to Z1 and to equilibrium conditions downstream, can be shown to be convex and to exhibit a sharp rise in the absolute value of its slope at its point of intersection with the coexistence line. The Rayleigh line through Z1 intersects H in the two points  $\mathbb{Z}_2$  and  $\mathbb{Z}_2$ ;  $\mathbb{Z}_2$  is the weak detonation solution and is the one that corresponds to the mixture of droplets and vapor observed experimentally. If the expansion continues downstream of Z2, it does so along a mixed phase adiabatic; and if equilibrium of the two phases is maintained, the adiabatic is reversible. To our knowledge, no direct observation has been made that the flow downstream of  $Z_2$  is supersonic in the case of steam; in the case of the irreversible condensation of a small amount of water vapor in air, or of air itself, this has been confirmed by observation of Mach lines (9,11). One can, however, calculate sound speed at Z2 for steam with available thermodynamic data, obtain flow speed from the Hugoniot diagram (knowing the speed at Z2), and establish that the flow is indeed supersonic.\* Jouguet's rule (5) is thus verified. A Chapman-Jouguet process would occur in the special case in which the Rayleigh line was tangent to H at Z2.

Figure 3 shows schematically a one-parameter family of Hugoniot curves representing idealized progressive stages of condensation advancing from the "dry" Hugoniot  $H(\mathbf{\xi}=0)$  towards the equilibrium Hugoniot curve  $H(\mathbf{\xi}=1)$ . It is taken for granted that a single significant parameter  $\mathbf{\xi}$  may be found corresponding to a given mixture of growing molecular clusters (size larger than

<sup>\*</sup>This can be verified for the experiments reviewed by Ruedy (reference (12)). The method of obtaining the sound speed is given in reference (11).

critical) and single molecules. Here the family of Hugoniot curves is a pencil coalescing at the point C because of the single-phase condition above the coexistence line AA'.

This diagram suggests that the sequence of weak detonation from  $Z_1$  to  $Z_2$ , followed by a normal shock from  $Z_2$  to  $Z_2$ , will give the same end result as a "dry" normal shock leading directly from  $Z_1$  to  $Z_2$ . It can be verified easily that this "transitive" relation of the shock solution holds in general.

#### CONDENSATION SHOCKS IN ONE-DIMENSIONAL UNSTEADY FLOW

In two-dimensional steady nozzle flow, normal condensation shocks have been observed only within a limited domain of Mach numbers; in the majority of cases the shocks are X-shaped. There is, however, no reason why, in strictly one-dimensional flow, normal shocks could not arise at any supersonic Mach number. In the following, some considerations are offered to support this view. In order to obtain a variation of Mach number, we deal with unsteady flow as may be produced, e.g., by a piston receding with uniform velocity, U, from a semi-infinite air chamber. The air is first taken as dry; its initial state is denoted by the subscript o. In an x - t diagram the flow process is characterized by a pencil of straight rarefaction lines (Figure (4)), along each of which the flow state is constant. This centered simple wave will be defined by the condition

$$u + \sigma = \sigma_0 = const.$$

where u is the local particle velocity and  $\sigma$  is the Riemann function which, in the case considered here of an ideal gas, is known to be proportional to the local velocity of sound,

$$\sigma = \frac{2}{\gamma - 1} a$$

The equation of any rarefaction (characteristic) line is then given as

$$\frac{x}{t} = u - a = k$$

where 1/k is the slope of the line in the x - t diagram.

Abandoning now the assumption of dry air, we stipulate the presence of a certain amount of water vapor, which may not yet be saturated at stagnation conditions, and thus partakes in the expansion process. Suppose that at  $T_1 \leq T_0$  the vapor is saturated. In general, condensation will not occur at that temperature, since the change of state in the expanding gas column is not infinitely slow. A gas layer that became saturated with water vapor at time  $t_1$ 

will continue to expand at constant entropy until, at some later time t, it attains a temperature  $T \leq T_1$  at which condensation takes place. According to a recent investigation by Kantrowitz (16)\*, the elapsed time and the condensation delay  $T_{sat}$  - T are connected by the approximate relation

$$t - t_1 = \frac{B}{(T_{sat} - T)^4} \tag{4}$$

where the constant B is of order  $10^3$  (degree x sec). Here  $T_{\rm sat}$  denotes the saturation temperature at the pressure prevailing at temperature T;  $T_{\rm sat}$  must not be confused with the temperature  $T_1$ , where the vapor is saturated at the higher pressure  $p_1$ . Obviously,  $T < T_{\rm sat} < T_1$ .

The location taken by the gas layer when it reaches the temperature T evidently indicates the momentary shock location. The ordinate is known to be given by

$$\frac{t}{t_1} = (\frac{T_1}{T})^{\frac{1}{2}} \frac{\gamma + 1}{\gamma - 1}$$
 (5)

whereas the abscissa follows from

$$\frac{x}{t} = u - a = 6 \left( 1 - \frac{\gamma + 1}{2} \sqrt{\frac{T}{T_0}} \right)$$
 (6)

since this is the equation of the characteristic line along which the temperature T prevails.

The Kantrowitz relation can now serve to set up the equation of the shock path. Every individual gas layer is characterized by the time, t<sub>1</sub>, at which the air in it becomes saturated. On eliminating t<sub>1</sub> from equations (4) and (5) we obtain

$$t = \frac{B}{(T_{sat} - T)^4 \left[1 - (\frac{T}{T_1}) \frac{1}{2} \frac{\gamma + 1}{\gamma - 1}\right]}$$
 (7)

This is the ordinate of the shock path in terms of the parameter T which, in the x - t diagram, determines the individual characteristic lines. The abscissa is given by equation (6).\*\*

<sup>\*</sup> Much of our discussion is independent of this explicit relation due to Kantrowitz. See also Oswatitisch (17).

<sup>\*\*</sup> In the presence of the shock the dashed parts of the originally straight rarefaction lines (Figure 4) will alter their course.

It is seen that the shock never can be found to the left of the characteristic line  $T = T_1$  (since t would become negative if  $T > T_1$ ); indeed, as  $t > \infty$ , if  $T > T_1$ , the shock path, coming from the right, approaches asymptotically the "saturation characteristic"  $T = T_1$ . Moreover, it can intersect but once with any characteristic line, since equation (4) is a unique function of T. As a consequence, the shock path, at any point P within the fan, will make a larger angle with the positive x-axis than does the rarefaction line through P. Hence, the shock velocity relative to the tube wall, V, satisfies

at P, as is readily verified from the fact that the slopes of the intersecting lines are 1/v and 1/k, respectively. The Mach number relative to the shock is

$$M = \frac{u - v}{a} > 1$$

If we now follow the shock curve as it approaches the asymptotic line, the difference between V and k=u-a becomes increasingly smaller. It is thus seen that normal condensation shocks can occur theoretically at supersonic Mach numbers as low as we may choose.

Presumably the highest Mach number will be found at the intersection of the shock with the last characteristic line on which any quantity will be given the subscript 2. The particle velocity here is equal to the piston velocity

$$\mathbf{u}_2 = \mathbf{U}$$

The sound speed can be obtained from the simple-wave condition

$$\sigma_0 = v + \sigma_2$$

It follows that

$$a_2 = \frac{Y-1}{2} \sigma_2 = \frac{Y-1}{2} (\sigma_0 - U)$$

The shock velocity  $V_2$  could be computed from the shock path equations (6) and (7). One would have to introduce the explicit dependence on T of  $T_{\rm sat}$  with the use of the Clapeyron-Clausius relationship of saturation pressure and temperature. It was found that, in order to arrive at a closed formula, several simplifying assumptions had to be made and that, even then, the expressions became rather unwieldy. With more ease the velocity  $V_2$  can be obtained from the shock path within the zone of constant state extending between the piston path and the last characteristic line.

In this zone the Kantrowitz relation gives

$$t - t_1 = \frac{B}{(T_{sat} - T_2)^4} = t^* = const.$$

In the idealized expansion process considered here the gas layer immediately adjacent to the piston is saturated at time  $t_1 = 0$ ;  $t^*$  then denotes the time at which condensation occurs in that layer.\* The condensation shock makes its first appearance at  $t = t^*$ ,  $x = Ut^*$ , which is a point on the piston path.

It is not hard to deduce that the path in the constant-state zone of a gas layer that was saturated at  $t = t_1 \neq 0$  is the straight line

Ut - x = 
$$a_2 t_1$$
  $(\frac{T_1}{T_2}) \frac{1}{2} \frac{\gamma + 1}{\gamma - 1}$ 

On eliminating t<sub>1</sub> from this equation and the Kantrowitz relation the shock path in that zone is found to be

Ut - x = a<sub>2</sub> (t - t<sup>1</sup>) 
$$(\frac{T_1}{T_2})^{\frac{1}{2}} \frac{\gamma + 1}{\gamma - 1}$$

This again is a straight line. Its reciprocal slope is

$$\frac{dx}{dt} = V_2 = U - a_2 \quad (\frac{T_1}{T_2}) \frac{1}{2} \frac{\gamma + 1}{\gamma - 1}$$

Hence, the Mach number relative to the shock in the constant-state zone (which includes the last characteristic line) becomes

$$M_2 = \frac{u_2 - V_2}{a_2} = (\frac{T_1}{T_2}) \frac{1}{2} \frac{\gamma + 1}{\gamma - 1} = (\frac{\sigma_1}{\sigma_0 - U})^{\frac{\gamma}{\gamma} + 1}$$

 $\sigma_1$  and  $\sigma_0$  are given quantities. It is seen that the Mach number M2 becomes large if the piston velocity approaches the velocity

$$\sigma_0 = \frac{2}{Y-1} a_0$$

The results of these considerations indicate that the apparent restriction of normal condensation shocks to a limited region of Mach numbers, as suggested by available experimental evidence in two-dimensional nozzle flow, is probably not founded in the nature of the irreversible condensation process.

<sup>\*</sup> Relations such as Kantrowitz' cannot be expected to hold for very small times t'. Gilmore (21) has estimated these induction times; for conditions of interest here they are of the order 10<sup>-3</sup> sec.

Condensation shocks in unsteady one-dimensional flow have been obtained in shock tube experiments made at the University of Toronto.\* Figure 5 gives an example. That the condensation shock should appear as a straight line even within the expansion fan is explained by the fact that the entire path corresponds to a time interval of about 1/2 milliseconds during which the condensation shock velocity is not likely to change noticeably save in extreme cases.

In the experiment from which Figure 5 was obtained the air was saturated initially. Figure 5 seems to raise a difficulty because, from our discussion, the condensation shock should approach, asymptotically, the saturated state, which would be the first rarefaction line in Figure 5. The observed condensation shock seems to diverge from the rarefaction line. The experiments of C. T. R. Wilson (18) may throw some light on a possible explanation. Wilson found that for an expansion which is very slow, as it is in the later stages of an expansion such as Figure 5, and for saturated air relatively free of condensation nuclei, a minimum expansion ratio was required before the onset of rapid condensation. The line  $T = T_0$  then can never be reached. The characteristic asymptotically approached by the condensation shock in Figure 4 may be relabeled the "Wilson line". One can show that, for the time interval in Figure 5, the shock line should be fairly straight and close to the Wilson line if the expansion were an ideal, centered, simple wave. In fact, it is not a centered, simple wave and, although velocity measurements can be made in these experiments, one cannot determine the thermodynamic states because the path of the contact surface is not determinable from the picture.\*\*

It is interesting to remark that T. Lee (20) has observed three-dimensional unsteady condensation shocks due to jet formation when a diaphragm is burst in a shock tube. These would correspond to the weak detonation solution indicated by G. I. Taylor (6).

## DISCUSSION

A more detailed description of the weak condensation detonation processes discussed above may help to clarify their relation to more familiar types of chemical detonation processes.

If one tries to describe the processes occurring in the detonation front itself, the theory of steady detonation waves (see, e.g., von Neumann (14)) gives some support to the notion that

<sup>\*</sup> The authors are indebted to Dr. G. N. Patterson and Dr. I. Glass of the Institute of Aerophysics, University of Toronto, for doing these experiments at our request, and for permission to publish one of the resulting wave-speed camera photographs.

<sup>\*\*</sup> Possibly modification of these experiments is possible in which the gas is allowed to push a piston, the path of which could be measured (11). With this the condensation history from time zero could be observed.

ordinary chemical detonations start from a situation in the neighborhood of a normal shock solution of the conservation equation for the unburned gas and proceed along a sequence of (local) steady states to the Chapman-Jouguet point.

In the case of the weak condensation detonations, we have seen that the analogous sequence of states starts in the neighborhood of the "weak" disturbance solution and remains there.\*

For both sorts of detonation the equilibrium of molecular species or phases is reached in a kinetic balance of forward and reverse reactions. In the usual chemical process, both forward and reverse reaction rates increase with the temperature. In the case of condensation processes the forward reaction rate (the condensation) decreases with increasing temperature while the reverse reaction rate (evaporation) increases. The process may cut itself off (i.e., equilibrium may be established) even if some of the vapor is not yet condensed.

In order to obtain the weak condensation detonation, an unstable condition is brought on by means of a fast adiabatic expansion. Two basic mechanisms are at work in such a condensation process. The first stage, as is well known, depends on the build-up of "critical" nuclei; once these are present in sufficient quantity the rapid stage of condensation commences. The first stage is "hidden" insofar as it is not made manifest by any appreciable alteration of thermodynamic properties. The evaporation (reverse) process depends on the presence of droplets and on the heat release due to their fast initial growth.

This description prepares the way for a comparison with the weak detonation solution found by Friedrichs (7). Friedrichs has treated the one-dimensional model detonation process as governed by a differential equation involving macroscopic viscosity, heat conduction, and a reaction rate. He has shown the possibility of weak detonation solutions of these equations and has shown that these will have an eigenvalue of locally steady propagation velocity for given boundary conditions ahead of the wave and for a given form of the reaction rate. In this these solutions have formal similarity to flame solutions. Assuming a reaction rate increasing with temperature, the weak detonation solutions are characterized as being associated with a reaction rate which he terms "extremely fast". Much of his discussion is independent of this assumption. What is essential to the matter is the behavior of the solutions of his

\*The fact that the disturbance is small in the condensation case indicates that one might compute eigenvalues of the propagation velocity by an appropriate modification of a procedure used for flames (14); inversely, the pattern of solution fields for different assumptions as to the reaction rate indicates more closely what conditions might have to be met to have a chemical weak detonation.

model equations in the  $(\xi, \theta, \tau)$  space, where  $\xi$  is the fraction of burnt gas,  $\theta$  = a reduced temperature, and  $\tau$  = specific volume. To have a weak detonation solution, Friedrichs finds, in accordance with physical expectation, that the transition between the planes  $\xi = 0$  to  $\xi = 1$  must be effected without departing far from the plane  $\theta = \theta$ , where  $\theta$ , is the reduced temperature ahead of the reaction front. This is the reason for the requirement that the reaction rate be fast at a relatively low temperature.

It is known from experience that the weak condensation detonations satisfy the condition of transition from £=0 to £=1 without marked increase in temperature. The reaction rate has two fast stages: rapid growth on nuclei, and the reverse reaction of evaporation moderating the growth of droplets. A second type of weak detonation solution found by Friedrichs involves a shock transition in the neighborhood of the plane £=1, i.e., in the burnt gas. This cannot occur in the condensation case because of the stabilizing conditions of the reaction rate.

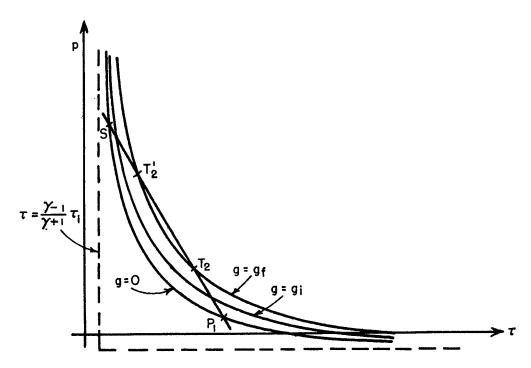


Figure 1 - Hugoniot curves and Rayleigh line for condensation of a fraction of water vapor.

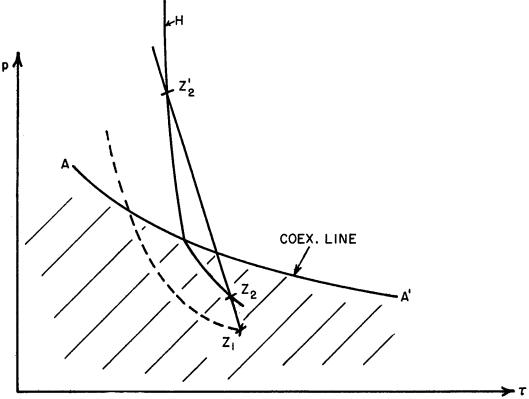


Figure 2 - Hugoniot diagram for steam.

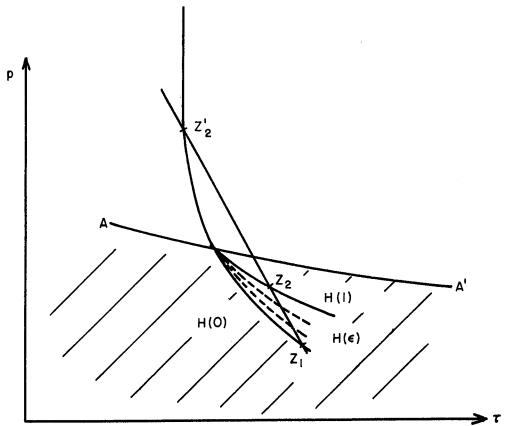


Figure 3 - Schematic drawing of one-parameter Hugoniot curves for steam.

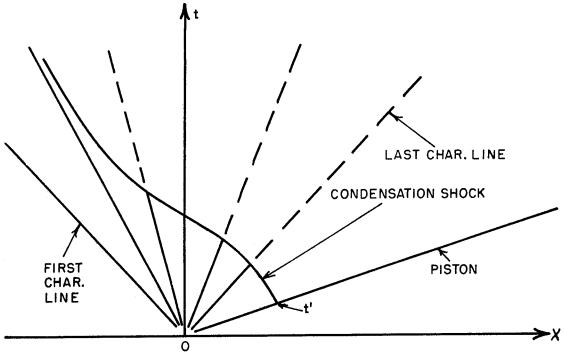


Figure 4 - Condensation shock in a centered simple wave expansion.

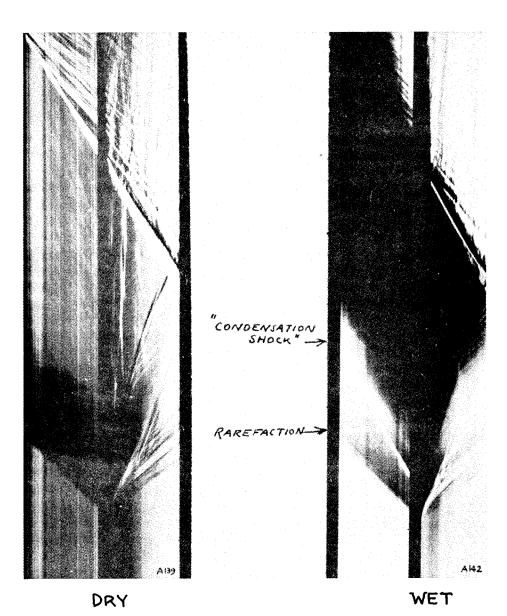


Figure 5 - Wave speed camera photographs of unsteady expansions in dry and moist (wet) air.

#### BIBLIOGRAPHY

- (1) C. Weiselsberger and L. Prandtl, Proc. Volta Conference, Rome 1935 (water vapor in air); C. Robb, Cam. J. Research <u>Al9</u>, p. 87, 167 (1941) (pure steam).
- (2) J. M. Burgers, Address at the dedication of the Naval Ordnance Laboratory Aeroballistic Research Facilities 1949. (NOLR 1130).
- (3) K. Oswatitisch, Gasdynamik (Springer, Wien 1951) p. 59, 65.
- (4) A. R. Ubbelohde, Proc. Roy. Soc. A204 (1950); Proc IV International Conference on Combustion and Detonation (1952) (Williams and Wilkins Co., Balt., Md.).
- (5) R. Courant and K. O. Friedrichs, Supersonic Flow and Shock Waves, (N. Y.; Interscience 1948); Y. B. Zeldowich, "Theory of Combustion and Detonation of Gases" (Acad. Sci. USSR 1944).
- (6) G. I. Taylor, Proc. Roy. Soc. <u>A200</u> (1950) p. 235.
- (7) K. O. Friedrichs, NAVORD Report 79-46.
- (8) P. P. Wegener, To appear in J. Appl. Physics.
- (9) R. Hermann, Luftfahrtforschung, 19, p. 201 (1942).
- (10) W. Heybey NACA TN 1174 (1947).
- (11) D. Coles, Guggenheim, Aero. Lab., Cal. Inst. of Technology, Private Communication (1951).
- (12) S. G. Reed, Jr., J. Chem. Phys. 20, p. 539 (1952).
- (13) R. Ruedy, Can. J. Research A22, p. 77 (1944).
- (14) J. Von Neumann, OSRD Report 549 (1942).
- (15) D. Layzer, J. Chem. Phys. <u>22</u>, p. 222 (1954).
- (16) A. Kantrowitz, J. Chem. Phys. 19, p. 1097 (1951).
- (17) K. Oswatitisch, ZAMM 22, p. 1 (1942).
- (18) C. T. R. Wilson, Proc. Roy. Soc. <u>A61</u>, p. 240; Phil. Mag. <u>189</u>, p. 281 (1897).
- (19) Michels, Slawsky, and Jacobs, Physica XX, p. 223 (1954).

- (20) T. Lee, Dissertation, U. of Toronto (1950).
- (21) F. R. Gilmore, Thesis, Cal. Inst. of Tech. (1951).

# THE STRUCTURE OF A STEADY-STATE PLANE DETONATION WAVE WITH FINITE REACTION RATE

John G. Kirkwood Sterling Chemical Laboratory Yale University New Haven, Connecticut

and

William W. Wood
Los Alamos Scientific Laboratory
Los Alamos, New Mexico

#### ABSTRACT

An analytical elaboration of von Neumann's model of the detonation wave is presented. A hydrodynamic argument for the well-known Chapman-Jouguet condition is advanced, and the sound speed to be used therein is identified as that obtained with frozen chemical equilibrium, in agreement with a recent result of Brinkley and Richardson. Possible situations in which the classical Chapman-Jouguet hypothesis might be incorrect are very briefly discussed.

I

The propagation of a plane detonation wave through a semi-infinite explosive medium has been discussed theoretically by a number of investigators (1-12), beginning with Chapman and Jouguet . The central problem is the selection of a unique detonation process from a one-dimensional continuum of processes all of which satisfy the usual conservation laws for mass, momentum, and energy. The rule by which this selection is made is known as the Chapman-Jouguet (denoted in the following by C-J) hypothesis, after these early investigators. The chemical reaction responsible for the detonation process has been treated as an instantaneous transformation in many of these discussions (1-5, 9, 11). In particular, Brinkley

#### Kirkwood and Wood

and Kirkwood have studied the stability of the C-J detonation under this assumption.

Chemical reaction rates are of course finite, and as a consequence the region in which the chemical transformation takes place must be of non-vanishing dimensions. Certain well known properties of detonation waves in finite geometry afford experimental verification of this, and in fact considerable interest is attached to the determination of such parameters as the reaction time, etc. The classical paper in the discussion of the influence of finite reaction rates on the detonation process is that of von Neumann (7). The present work is essentially an analytical elaboration of his geometrical discussion, which we hope will clarify several points. Brinkley and Richardson (10) have also recently considered this question, and our Section IV is similar in certain respects to their work.

TT

Our model is that of a fluid undergoing one-dimensional, compressible, non-dissipative, adiabatic, reactive flow.\* Shocks are treated as mathematical jump

\*See ref. 12 for a discussion in which dissipative and diffusion processes are considered.

discontinuities in certain of the hydrodynamic-thermodynamic variables. Among the variables specifying the state of the system are certain composition variables  $\lambda^{J}$ ,  $j=1,2,\dots,r$ , corresponding to certain independent chemical reactions, r in number, involving the n components of the fluid, which reactions are denoted by

$$\sum_{\alpha=1}^{n} v_{\alpha}^{j} \chi_{\alpha} = 0, j=1,2,\cdots r$$
 (1

The  $\nu_{\kappa}$  are stoichiometric coefficients, positive for products, negative for reactants, and so chosen that (1 expresses the transformation of unit mass of reactants to products;  $X_{\kappa}$  denotes unit mass of component  $\kappa$ . The  $\lambda$  are progress variables, specifying the increase in mass of the various components within a fluid element of total

#### Kirkwood and Wood

mass m due to the r chemical reactions:

$$dm_{\alpha} = m \sum_{j=1}^{r} \gamma_{\alpha}^{j} d\lambda^{j}, \alpha = 1, 2, \cdots n.$$
 (2)

We assume throughout this discussion the existence of local thermodynamic quasi-equilibrium, such as to permit the definition of local temperature, etc., and to permit the assumption that the various thermodynamic quantities may be regarded as functions of a suitable set of independent thermodynamic variables. We also suppose the Lagrangian time derivatives of the progress variables to be given by

$$\frac{dx^{j}}{dt} = r^{j}, \qquad (3a)$$

$$r^{j} = r^{j} - r^{j}, \quad j = 1, 2, \dots r,$$
 (3b)

where  $\mathbf{r}_f^j$  and  $\mathbf{r}_b^j$  are chemical rate functions for the forward and back directions of reaction j, given as functions of the local thermodynamic state.

In regions of space-time in which shocks are absent the flow is governed under our assumptions by the usual hydrodynamic equations

$$\frac{dQ}{dt} + Q \frac{\partial w}{\partial x} = 0, \qquad (4a)$$

$$\frac{du}{dt} + V \frac{\partial D}{\partial x} = 0, \tag{4b}$$

$$\frac{dE}{dt} + p \frac{dv}{dt} = 0, \qquad (4c)$$

# Kirkwood and Wood

$$\frac{d}{dt} = \frac{d}{dt} + \mu \frac{\partial}{\partial x}, \qquad (4d)$$

$$\frac{\partial}{\partial t} = \left(\frac{\partial}{\partial t}\right)_{x}, \quad \frac{\partial}{\partial x} = \left(\frac{\partial}{\partial x}\right)_{t}.$$

We use Q to denote matter density; u the mass velocity in a coordinate system with x as space variable, t as time variable; p the fluid pressure; v the specific volume equal to 1/0; E the specific internal energy, assumed to be a known function of the local thermodynamic state, say the variables  $\lambda$ , Q, S, where  $\lambda$  denotes the set of variables  $\lambda'$ ; S the specific entropy. The equation of state is also assumed, giving p as a function of  $\lambda$ , Q, and S.

From the alternative form of the first law

in which  $\mu_{\infty}$  denotes the specific chemical potential, we obtain the entropy transport due to chemical reaction:

$$\frac{dS}{dt} = \sum_{j} \frac{\Delta^{j} F}{T} \frac{d\lambda^{j}}{dt}, \qquad (6a)$$

$$\triangle^{j} F = \sum_{\alpha} \nu_{\alpha}^{j} \mu_{\alpha}^{i} \qquad (6b)$$

Corresponding to the classical Riemann analysis of the hydrodynamic equations in the non-reactive case, we now utilize the equation of state, and the entropy transport equation as well, to establish the relation between the substantive derivatives of p,  $\rho$ , and  $\lambda$ . The usual rule for differentiation gives

$$\frac{dP}{dt} = (\frac{\partial P}{\partial e})_{s,\lambda} \frac{de}{dt} + (\frac{\partial P}{\partial s})_{e,\lambda} \frac{ds}{dt} + \sum_{j} (\frac{\partial P}{\partial \lambda^{j}})_{s,e} \frac{d\lambda^{j}}{dt}.$$
 (7

With the definitions

$$C_o = \left(\frac{3p}{3\theta}\right)_{S,\lambda}, \tag{8a}$$

$$\beta_{\circ} = \left(\frac{\partial Y}{\partial T}\right)_{\beta, \lambda}, \tag{8b}$$

$$C_{p}^{\circ} = \left(\frac{\partial H}{\partial T}\right)_{p, \lambda}, \tag{8c}$$

we obtain after some manipulation the relation

$$\frac{d\xi}{d\xi} = \frac{c_0^2}{c_0^4} \frac{d\xi}{d\xi} - 6\sum_i e_{ij} \frac{d\xi}{d\xi}, \qquad (9)$$

where

$$C_{p}^{i} = \frac{Q_{p}^{0}}{Q_{p}^{0}} \left( \frac{\partial E}{\partial A_{i}} \right)_{p, \vee} ;$$

$$C_{p}^{i} = \frac{Q_{p}^{0}}{Q_{p}^{0}} \left( \frac{\partial E}{\partial A_{i}} \right)_{p, \vee} ;$$

$$(10a)$$

$$\triangle_{A} H = \sum_{A} \Lambda_{A} \stackrel{\underline{H}}{\underline{H}} = \left(\frac{9M_{P}}{9M_{P}}\right)^{\perp B}$$
(10p)

$$\triangle^{i} V = \sum_{\alpha} V_{\alpha}^{i} \overline{V}_{\alpha} = \left(\frac{\Delta m Y}{\delta \lambda^{i}}\right)_{T, p}, \tag{10c}$$

here H denotes the specific enthalpy,  $\overline{H}_{\infty}$  and  $\overline{V}_{\infty}$  respectively the usual thermodynamic partial specific enthalpy and volume of component  $\infty$ . It will be noted that the quantities  $C_{o}$ ,  $\beta_{o}$ , and  $C_{p}$  are the sound speed, volume expansion coefficient, and constant pressure heat capacity evaluated with the composition frozen at its instantaneous value. The parameters  $\sigma$  are thermodynamic variables which, as we shall see, determine in conjunction with the rate functions  $r^{j}$  the explosive behavior of the medium.

Use of (9 permits the elimination of the derivatives of the density from the hydrodynamic equations:

$$\frac{d\lambda^{j}}{dt} = r^{j}, j = 1 \cdots r.$$
 (11c)

We note that these equations are similar to the well-known equations for non-reactive flow, the frozen sound speed appearing in the expected place, but with a non-vanishing right hand side in the first equation. We also note that when our reactive system is at chemical equilibrium, the right hand side vanishes, since r<sup>j</sup> becomes zero when the forward and backward rates become equal. The appearance of the frozen sound speed is of some interest.

The differential equations (11 hold in regions of the flow which are free from shocks. Treating the latter as mathematical discontinuities, they are governed by the

well-known Rankine-Hugoniot conditions,

$$e_{s}(U-u_{z}) = e_{s}(U-u_{s}),$$
 (12a)

$$p_2 - p_1 = e_1 (U - u_1) (u_2 - u_1),$$
 (12b)

$$E_{2} = \frac{1}{2} (p_{2} + p_{1}) (v_{2} - v_{1}),$$
 (12c)

in which  ${f U}$  denotes the shock velocity and the other symbols have their usual meaning with the subscripts distinguishing the values on the two sides of the shock. These relations across discontinuities, and the differential equations in regions free from them, supplemented by suitable boundary conditions, determine the flow of our one-dimensional, reactive fluid.

We now apply them to the propagation of a steadystate plane detonation wave through a semi-infinite explosive medium in a direction perpendicular to the plane surface. We suppose the detonation to have been initiated at this surface at zero time, and suppose the boundary condition to be imposed at this rear surface by a prescribed motion of an infinite piston (see, e.g. refs. 7 and 11). We will consider only the steady-state detonation assumed to be approached eventually, at least for some modes of initiation. Here we adopt the model of the detonation wave used by von Neumann, in which the reaction is initiated by a shock wave in the unreacted medium preceding the reaction zone. (The reaction rates r are assumed to vanish in the medium in front of the shock wave.) We denote by D the velocity at which this shock propagates along the x-axis (taken as perpendicular to the rear surface and pointing into the explosive), the unreacted, unshocked medium being stationary in this coordinate system. During the approach to steady state, D may depend on t, but is assumed to approach a constant value as t increases. In addition to this assumption, the notion of a steady state also includes the supposition that there exists immediately following the shock a region of constant length in which the various hydrodynamic variables are independent of time when viewed from a coordinate system moving with the velocity D.

steady-zone is followed by a flow region whose character is determined by the rear boundary condition. In certain simplified cases it may have approximately the form of a centered-rarefaction wave, reducing the pressure and mass velocity from their values at the boundary between this region and the steady zone to their values at the rear surface. We now proceed to discuss these two flow regions separately, beginning with the steady zone.

#### III

We introduce the moving coordinate system mentioned above. For convenience we take as space variable the distance measured backwards from the shock front. The transformation is

With this change of independent variable the differential equations (11 become

$$(D-\mu) \lambda_{g}^{j} + \lambda_{t}^{j} = r_{t}^{j} \quad j = 1, 2 \cdots r_{t},$$

$$\mu_{g} = \left(\frac{\partial \mu}{\partial g}\right)_{t}, \text{ etc.}; \quad \mu_{t}\left(\frac{\partial \mu}{\partial t}\right)_{g}, \text{ etc.}$$

$$(14c)$$

Solving the first two equations for  $\mu_{k}$  and  $\rho_{k}$ , we obtain

$$u_{s} = -\frac{1}{\eta} \left[ \sum_{j} \sigma^{j} r^{j} - \frac{1}{6c_{s}^{2}} p_{t} - \frac{D_{-u}}{c_{s}^{2}} u_{t} \right], (15a)$$

$$\eta = 1 - \frac{\left(D - \mu\right)^2}{C^2}.$$
 (15c)

If we assume a region of steady state behavior, the time derivatives vanish, and the equations reduce to

$$u_{\xi} = -\frac{1}{\eta} \sum_{j} \sigma^{j} r^{j}, \qquad (16a)$$

$$P_{S} = -\frac{e(D_{TL})}{\eta} \sum_{j} \sigma^{j} r^{j}, \qquad (16b)$$

$$\lambda_{S}^{j} = \frac{1}{D-u} \quad r_{J}^{j} \quad j = 1 \cdot \cdots r \qquad (16c)$$

It is easily seen from these equations that the state variables in the steady zone satisfy the Rankine-Hugoniot relations (12, with states 1 and 2 being any points in the steady zone. Since the steady zone point just to the rear of the shock is connected to the medium ahead by these same relations it is clear that we may write

$$e(D-\omega) = eD, \qquad (17a)$$

$$E-E_{a} = \frac{1}{2}(p+p_{a})(v_{a}-v),$$
 (17c)

the zero subscripts denote values of the quantities in the medium ahead; unsubscripted quantities are at any point in the steady zone. Equations (17, coupled with any one of the differential equations (16, determine the state variables as functions of the distance behind the leading shock, for any assumed value of D. The latter is not yet determined.

We note that we will encounter difficulty in integrating (16a or (16b if  $\eta$ ) becomes zero. Since the flow back of a plane shock relative to the shock front is always subsonic,  $\eta$  will be positive at  $\xi = 0$ .

IV

Corresponding to the classical Riemann analysis for the case of non-reactive flow, we anticipate that, for piston motions opposite in direction to that of the motion of the detonation wave, there will be a rarefaction wave of non-steady character reducing the pressure from its value at the end of the steady zone to a lower value, possibly zero, at the piston surface. Consequently we devote this section to a brief discussion of the characteristic curves of the set of differential equations (11. Without reproducing all the steps, we state the results as follows. The set of equations (11 is always hyperbolic. The characteristics in the x - t plane, r + 2 in number, are given by the following equations:

$$\left(\frac{dx}{dt}\right)_{r+1, r+2} = u \pm C, \qquad (18a)$$

$$\left(\frac{d\times}{dt}\right) = \mu, j = 1, 2 \cdot \cdot \cdot \cdot r.$$
 (18b)

The first two characteristics may be thought of as giving the paths of "sound waves" through a given point in the x - t plane. The other characteristics are degenerate, all coinciding with the streamline through the point.

These results are similar to the well-known results for non-reactive flow, coappearing in the place of the ordinary non-reactive sound speed. There is, however, an important difference; equations (ll are not homogeneous, and therefore not reducible, contrary to the case with the non-reactive equations. Thus part of the usual theory of hyperbolic flow fails to carry over into the reactive case. However, certain general properties of hyperbolic equations remain, among them the following: the boundary between two space-time regions in which the flows are of different type (for example, a region in which the flow is steady adjacent to a region in which the flow is steady) must be a characteristic. In the next section we make an important application of this principle.

V

We now proceed to draw certain conclusions concerning the detonation process from the analyses of the preceding two sections. As noted at the end of the last section, the boundary between our steady region and the succeeding flow must be a characteristic curve, assuming that the differential equations remain valid across the boundary i.e. assuming the boundary is not a shock. It then follows that the flow variables are continuous (not necessarily their derivatives); hence the flow variables are constant along the boundary, and it follows from (18 that the boundary characteristic is straight. Since it is clear that it cannot be a streamline, and since in our coordinate system the wave is forward facing, it must be a u + c characteristic. Still further, in order for the x dimension of the steady zone to be constant in time, it is necessary that the slope of this characteristic in the x - t plane be the same as that of the leading shock locus. We obtain as a necessary condition at the end of the steady zone

$$D = \omega + C_{\alpha}, \qquad (19)$$

a result which has also been obtained by Brinkley and Richardson (10).

Returning to relations (16 for the steady zone, we

note that the preceding result makes  $\eta$ , the denominator of the expressions for  $\mathcal{M}_{\mathbf{S}}$  and  $\rho_{\mathbf{S}}$ , vanish. In order to avoid singularities in these space derivatives the numerators must also vanish, which requires as an additional condition at the end of the steady zone

$$\sum_{j} \sigma^{j} r^{j} = 0.$$
 (20)

These two equations, (19 and (20 may be taken as a generalized statement of the C-J condition. That the indeterminacy of (16 is as it should be is readily appreciated from the fact that (16 holds for the space derivatives in both directions at the end of the steady zone. The indeterminacy thus permits these derivatives to be discontinuous at the end of the steady zone, and in particular allows the derivatives on the non-steady side to be time dependent.

Clearly (20 is satisfied if all the rate functions vanish,

$$r^{j}=0, j=1, \cdots r,$$
 (21)

corresponding to instantaneous chemical equilibrium. This, coupled with (19 corresponds to von Neumann's normal C-J condition. It is the one in common use; see, e.g. Lewis and Friauf (13), papers by Kistiakowsky and co-workers (14).\*

We note that (18, (19, and (21, with the equation of state taken as  $E = E(\lambda, \rho, \vee)$ , constitute r + 4 equations for the r + 4 unknowns D, p, v, u, and  $\lambda$ . Thus we may expect to be able to solve them for D and the state variables at the end of the steady-zone. Of course, in actual practice, rather than (21 one uses the ordinary relations for chemical equilibrium

<sup>\*</sup>It may be noted that the C-J condition used by these investigators actually implies the use of c<sub>o</sub>, although it has apparently been regarded as an approximation to a sound speed defined by ( ) s. S. L. L. L. C.

It is also possible for  $\sum_{i}$  or to vanish with some or all  $r^j$  non-vanishing, due to some of the  $6^j$  becoming negative (or conceivably some of the  $r^j$ ); this corresponds to von Neumann's pathological case. In this case we obtain a sufficient number of equations to determine D and the C-J values of the state variables by eliminating from (16c, obtaining r-1 equations

$$\frac{d\lambda^{j}}{d\lambda^{j}} = \frac{r^{j}}{r^{i}}, j = z, 3 \cdots r.$$
 (23)

These may be integrated by use of the initial conditions at the shock front; with (17, (23, (19, and (20 we then obtain r + 4 equations. In general such a calculation requires explicit knowledge of the rate functions r<sup>1</sup>, in addition to the usual thermodynamic data; this is to be contrasted with the normal case, where the latter information suffices. There might even be multiple zeros of

For the special case of a single reaction the analysis can be carried a little further: the particular case in which  $\bullet$  might become negative while  $\eta$  is positive,  $\bullet$  thereafter remaining negative, so that the C-J point would have to correspond to r=0, can be eliminated. It is possible to show under reasonable assumptions concerning the finiteness of certain thermodynamic variables, that it is impossible for  $\gamma$  to vanish under these conditions.

Also, for the case of a single reaction, the relation of our treatment to von Neumann's discussion of the pathological case, in terms of the envelope to the family of partial Hugoniot curves with parameter  $\lambda$ , is readily seen from the third of the equivalent expressions for given in (10a. In this case also, the calculations of detonation velocity can be performed in the pathological case in the absence of detailed knowledge of the rate function, since (20 reduces to 6 = 0, which is a purely thermodynamic relation. It is, of course, necessary to know what reaction is involved.

No example of a pathological detonation is definitely known. From (10a it is clear that a negative or requires either a volume decrement or an endothermic reaction under the local conditions. Thus the possibility of pathological

behavior may arise, for instance, in gaseous detonations not too strongly exothermic involving an over-all mole decrement, or in detonations in which an exothermic reaction is succeeded by an endothermic one, possibly involving a mole decrement. In condensed explosives the situation is considerably obscured by uncertainties in our present knowledge of equations of state, not to mention kinetics. A possible example might occur in the case of aluminized explosives.

#### REFERENCES

- 1. D. L. Chapman, Phil. Mag. 47, 90 (1889).
- 2. E. Jouguet, Compt. rend. <u>132</u>, 573 (190), <u>144</u>, 415 (1907).
- R. Becker, Z. Elektrochem. 23, 40, 304 (1917);
   Z. Physik 8, 321 (1922).
- 4. W. Jost, Z. Elektrochem. <u>41</u>, 183 (1935); Z. Physik Chem. <u>42</u>, 136 (1939).
- 5. R. L. Scorah, J. Chem. Phys. 3, 425 (1935).
- 6. Y. B. Zeldovitch, J. Exptl. Theor. Phys. (USSR) 10, 542 (1940).
- J. von Neumann, OSRD 549 (1942); see also W. Doering, Ann. der Physik 43, 421 (1943).
- 8. H. Eyring, R. E. Powell, G. H. Duffy, and R. B. Parlin, Chem. Revs. 45, 69 (1949).
- 9. S. R. Brinkley, Jr. and J. G. Kirkwood, Third Symposium on Combustion, Flame, and Explosion Phenomena (Williams and Wilkins Company, Baltimore, 1949), page 586.
- 10. S. R. Brinkley, Jr. and J. M. Richardson, Fourth
  Symposium (International) on Combustion,
  Williams and Wilkins Company, Baltimore, 1953),
  page 450.
- 11. R. Courant and K. O. Friedrichs, Supersonic Flow and Shock Waves, (Interscience Publishers, Inc., New York), page 204.
- 12. C. F. Curtiss, J. O. Hirschfelder, and D. E. Campbell,
  The Theory of Flame Propagation and Detonation,
  CM-690, University of Wisconsin (1952).

- 13. B. Lewis and J. B. Friauf, J. Am. Chem. Soc. <u>52</u>, 3905 (1930).
- 14. G. B. Kistiakowsky, H. T. Knight, and M. E. Malin, J. Chem. Phys. 20, 884 (1952); other papers by Kistiakowsky and co-workers.

# THE MEASUREMENT OF CHAPMAN-JOUGUET PRESSURE FOR EXPLOSIVES

W. E. Deal, Jr.
Los Alamos Scientific Laboratory
Los Alamos, New Mexico

#### BASIC PRINCIPLES

A steady-state plane detonation wave has been shown by von Neumann (1) to consist of a shock followed by a reaction zone of decreasing pressure terminating at the Chapman-Jouguet (C-J) plane. The unsteady flow behind this plane of complete reaction has been described by Taylor (2); such flow is essentially a rarefaction wave centered at the rear of the explosive. The generally accepted picture of the pressure profile of a detonation wave is thus much like that of Figure 1.

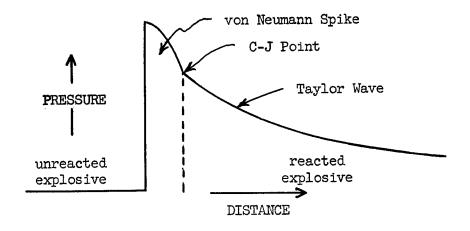


Figure 1 - Pressure Profile of a Detonation Wave

When such a wave impinges upon an inert material in contact with the explosive, the wave transmitted is a shock followed closely by a steep rarefaction which is in turn followed by a more gradual rarefaction. As this wave travels thru the material, the steep rare-

#### Deal

faction overtakes and destroys that portion of the wave corresponding to the von Neumann spike. Then in further travel thru the material the rarefaction corresponding to the Taylor wave gradually reduces the pressure of the remaining shock front. Also, a shock or rarefaction is reflected back into the explosive. If the pressure of the shock front in the inert material is plotted as a function of material thickness, a curve such as Figure 2 results. Pm of this figure corresponds to the pressure at the end of the reaction zone in the explosive (the C-J pressure). Since in these experiments the effects of the von Neumann spike will have become attenuated, we can limit theoretical consideration to a simple wave rising only to the Chapman-Jouguet pressure. If pressure and particle velocities are equated across the interface one obtains the equation:

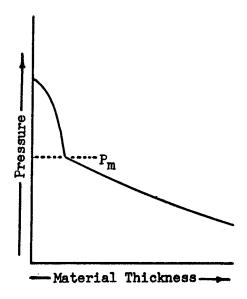


Figure 2 - Shock Front Pressure as a Function of Material Thickness

$$\frac{P_{m}}{P_{c-j}} = \frac{\rho_{t}^{\bullet}D_{t}}{\rho_{t}^{\bullet}D_{t}} \qquad \frac{\rho_{t}^{\bullet}D_{i} + \rho_{r}^{\bullet}D_{r}}{\rho_{t}^{\bullet}D_{t} + \rho_{r}^{\bullet}D_{r}}$$

Here,

Pc-i is the Chapman-Jouguet pressure in the detonation,

Pm is the pressure induced in the inert material.

The p's are densities, and

the D's are shock (or detonation) velocities which are particularized by the subscripts:

- referring to conditions behind the incident front
- r referring to conditions behind the reflected front
- t referring to conditions behind the transmitted front.

Conditions in front of these waves are referred to by a superscript zero accompanied by the appropriate subscript. All velocities are measured relative to the fluid in front of them.

If the further approximation  $p_{p_1} = p_{p_2} = p_{p_3} = p_{p_4} 

$$P_{c-j} = P_m \frac{\rho_t^0 D_t + \rho_i^0 D_i}{2\rho_t^0 D_t}$$

The C-J pressure is then determined since  $\rho_t^0$  and  $\rho_i^0$  are the simply measurable initial densities of the material and explosive,  $D_i$  is the readily measurable detonation velocity (4), and  $D_t$  and  $P_m$  are available from equation of state data if one hydrodynamic variable of the C-J state is measured (5). The quantity established in these experiments was the free-surface velocity corresponding to  $P_m$  in Figure 2.

An alternative method which also ignores the presence of the spike, but tends to minimize the effect of the reflected wave into the explosive is to establish Pm and the corresponding particle velocity for each of several materials of different shock impedance. These define a curve in the pressure-particle velocity plane. This curve must pass thru the C-J point since it is really the locus of all possible shocked and rarefied states (for one direction of wave travel) for the reacted explosive. From the conservation equations one can write:

$$\frac{P_{d}}{V_{o} - V_{d}} = (\rho_{o}D)^{2}$$

where V is specific volume and the subscripts d and o refer to initial conditions and conditions immediately behind the detonation front, respectively. Thus, as shown by von Neumann (1) and illustrated in Figure 3,  $(\rho_0 D)^2$  is the slope in

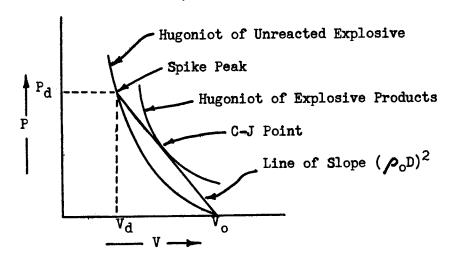


Figure 3 - The Detonation Process in the Pressure-Volume Plane the pressure-volume plane of the line containing both the spike peak point and the C-J point. One may also write from the conservation equations:

$$\frac{P_d}{u_d} = \rho_0 D$$

where u is the particle velocity behind a shock moving into a stationary medium. The straight line in the pressure-particle velocity plane passing thru the origin and of slope  $\rho_0 D$  must then also contain the C-J point. Hence, the intersection of the experimentally defined curve and the  $\rho_0 D$  line must be the C-J point.

#### EXPERIMENTAL TECHNIQUE

The value of free-surface velocity corresponding to  $P_m$  for a given explosive and material is established by measurement of free-surface velocity of an explosive-driven plate as a function of plate thickness. These velocities are measured photographically by the use of a rotating mirror smear camera with a writing speed of 3.2 mm/ $\mu$ sec. A Lucite block assembly like that of Figure 4 is placed with the

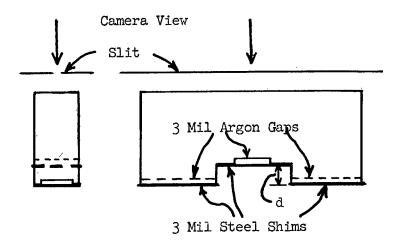


Figure 4 - Lucite Block Assembly

two outer shims adjacent to the surface to be studied. This is then viewed by the camera thru a slit parallel to the long axis of the Lucite piece and swept on the film in a direction perpendicular to the slit image. When the explosive-driven plate on which such an assembly is placed begins to move, the argon gaps near the surface are closed first and yield a brilliant flash of light of short duration. When the free surface moves the distance d, it closes the central gap and yields another flash of light. The gaps and shims are made as nearly identical as possible by machining with a single, shaped cutter and using pieces of shim cut from the same piece of stock. Good contact of shim and plate are assured by holding flatness tolerances over the contact surfaces to 0.0001". Identity of the central and side gaps closure times is readily established by a simple argument.

A print of a resulting camera record is shown as Figure 5.

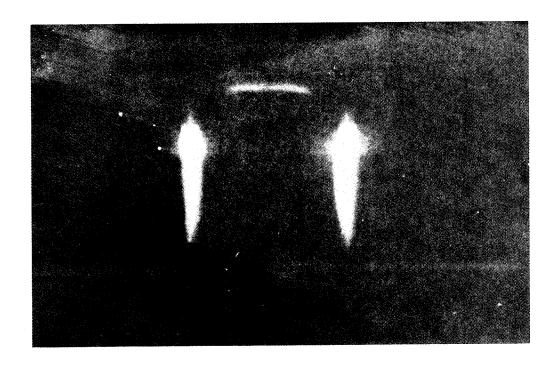


Figure 5 - Smear Camera Record for a Lucite Block Assembly.

Time Increases Downward.

Such records are read with a comparator and plotted; interpolation of the two side traces yields a time of departure of the central free-surface which along with the central arrival trace gives a transit time and hence velocity thru the accurately measured depth of the step. Depths of steps in the Lucite blocks are chosen such that there is not time for the second shock arising from the rarefaction reflection at the explosive interface to return and affect the free-surface velocity. Also the step widths of Lucite blocks are chosen so that the central trace can not be affected by disturbances of the plate motion by parts of the block contacted earlier by the plate. Up to twelve such Lucite blocks  $2\frac{1}{4}$  x 1" x  $\frac{1}{2}$ " may be placed on an appropriately machined plate to get free-surface velocities for twelve plate thicknesses from a single 10" diameter charge.

### DATA AND RESULTS

Charges of TNT, Composition B, 75/25 Cyclotol, and RDX were studied. The TNT charges were in the shape of truncated cones 8" thick with 8 3/8" diameter at the small end and 12 3/4" diameter at the large end. These were pressed without a binder to 99.1% of crystal density from a granular TNT of about 400  $\mu$  median particle size. The TNT charges were detonated on the small end. All charges were detonated by plane explosive lenses of 8" aperture. The opposite surfaces were placed against the test plates with a thin layer of mineral oil filling any gaps due to machining tolerances. The Composition B and 75/25 Cyclotol charges were 8" thick, each made up of two 10"x 10"x4" blocks of cast material. The Composition B was 64.7% RDX with a

#### Deal

spread of 1.5% within a piece. The 75/25 Cyclotol was 77.0% RDX with a spread of 1.5% within a piece. These compositions were based upon samples taken from similar castings. The RDX charges were 6" thick made up of two cylinders 6" in diameter and 3" thick pressed (6) without a binder to 97.7% of crystal density from a granular RDX of  $100\,\mu$  median particle size.

Tables I thru IV are listings of the free-surface velocity and thickness data. These are plotted on Figures 6 thru 9.

Table I. Pressed TNT on Dural Plates

Shot No. 1 charge density 1.640gm/cc. charge density 1.639gm/cc. plate density 2.793

Shot No. 2 plate density 2.793

plate	free-surface velocity	plate	free-surface
thickness		thickness	velocity
.069" .094 .119 .144 .194 .244 .294 .344 .394	2.473mm/ <b>\mu</b> sec. 2.454 2.421 2.419 2.372 2.365 2.360 2.348 2.350 2.334	.069" .094 .119 .144 .194 .244 .294 .344 .394 .444	2.494mm/μsec. 2.466 2.414 2.407 2.373 2.339 2.340 2.309 2.298 2.310 2.309 2.319

Shot No. 3

charge density 1.639gm/cc.

plate density 2.793

Shot No. 4

charge density 1.640gm/cc.

plate density 2.788

<del></del>			
plate thickness	free-surface velocity	plate thickness	free-surface velocity
.074" .099 .124 .149 .199 .249 .299 .349 .399 .449 .474	2.444mm/µ sec. 2.436 2.417 2.400 2.362 2.344 2.307 2.319 2.319 2.317 2.308 2.324	•979" •979 •979 •979 •979	2.287mm/ <b>μ</b> sec. 2.311 2.273 2.285 2.284 2.287

#### Deal

# Table II Composition B on Dural Plates

Shot	No. 5	Shot	No. 6
charge density 1.711gm/cc. plate density 2.793		charge density 1.712gm/cc. plate density 2.793	
thicknéss	velocity	thickness	velocity
.073"	$3.389$ mm/ $\mu$ sec.	.071"	$3.411$ mm/ $\mu$ sec.
.100	3.362	<b>.09</b> 6	3.418
.123	3.358	.125	3.382
.150	3.332	.151	3.366
.197	3.359	.200	3.346
.199	3.320	.200	3.322
.249	3.343	.249	3.299
.300	3.324	.299	3.273
•399	3.293	.400	3.254
.400	3.304	.401	3.253
.500	3.245	.450	3.229
- 2		.482	3.226

Shot No. 7 charge density 1.711 gm/cc. charge density 1.711 gm/cc.

plate density 2.795		
plate	free-surface	
thickness	velocity	
.100"	$3.357$ mm/ $\mu$ sec.	
.143	3.322	
.200	3.321	
.251	3.278	
.296	3.262	
.348	3.236	
.400	3.206	
.450	3.207	
.500	3.174	

Shot No. 9 charge density 1.713 gm/cc. .495 3.229 plate density 2.788

prace den	510y 2.100
plate	free-surface
thickness	velocity
.964"	$3.097$ mm/ $\mu$ sec
.964	3.129
.964	3 <b>.</b> 116
.964	3.172
.964	3.117
.964	3.145
.964	3.161
.964	3.097

Shot No. 8

_plate dens	
plate	free-surface
thickness	velocity
•075"	$3.443$ mm/ $\mu$ sec.
.100	3.411
.125	3.393
.150	3.352
.200	3.324
.250	3.295
.300	3.292
.350	3.265
.400	3 <b>.</b> 267
•450	3 <b>.</b> 263
.475	3.229
1,05	2 01/7

Table III 75/25 Cyclotol on Dural Plates

Shot No. 10 charge density 1.742 gm/cc. plate density 2.793		charge de	No. 11 nsity 1.744 gm/cc. sity 2.793
plate	free-surface	plate	free-surface
thickness	velocity	thickness	velocity
.075"	$3.538$ mm/ $\mu$ sec.	.074"	$3.558$ mm/ $\mu$ sec.
.100	3.528	.099	3.546
.125	3.486	.124	3.513
.150	3.½97	.149	3.517
.200	3.464	.199	3.449
<b>.</b> 250	3.463	.249	3.437
•300	3.449	.299	3.422
.351	3.465	<b>~</b> 349	3.389
.400	3.441	•399	3.390
•450	3.434	•449	3.425
•		.4/4	3·3 <sup>4</sup> 3
		.491	3•35 <sup>1</sup> 4

Shot No. 12

charge density 1.743 gm/cc.

plate density 2.702

Shot No. 13

charge density 1.744 gm/cc.

plate dens	sity 2.793	plate den	
platê	free-surface	plate	free-surface
thickness	velocity	thickness	velocity
.075"	3.538mm/ <b>µ</b> sec.	.100"	$3.496$ mm/ $\mu$ sec.
.100	3.542	.150	3.462
<b>.</b> 125	3.497	.250	3.433
.149	3.501	•350	3.399
.200	3.473	.450	3.421
.250	3.461	.496	3.379
.300	3.441		
•349	3.469		
.400	3.418		
•449	3.417		
.496	3.401		

Shot No. 14 charge density 1.744 gm/cc. plate density 2.788

plate dens	sity 2.700
plate	free-surface
thickness	velocity
.962"	$3.247$ mm/ $\mu$ sec
.961	3.273
.961	3.273
.961	3.291
.961	3.285
.961	3.312

#### Deal

# Table IV. RDX on Dural Plates

Shot No. 15 charge density 1.762 gm/cc. plate density 2.790

Shot No. 16 charge density 1.760 gm/cc. plate density 2.790

plate thickness	free-surface velocity
.101" .201 .301	3.565mm/ <b>μ</b> sec. 3.495 3.473 3.458

plate thickness free-surface velocity

.100" 3.610mm/\mu sec.
.201 3.489
.300 3.454
.401 3.469
.493 3.487

Shot No. 17 charge density 1.764 gm/cc. plate density 2.790

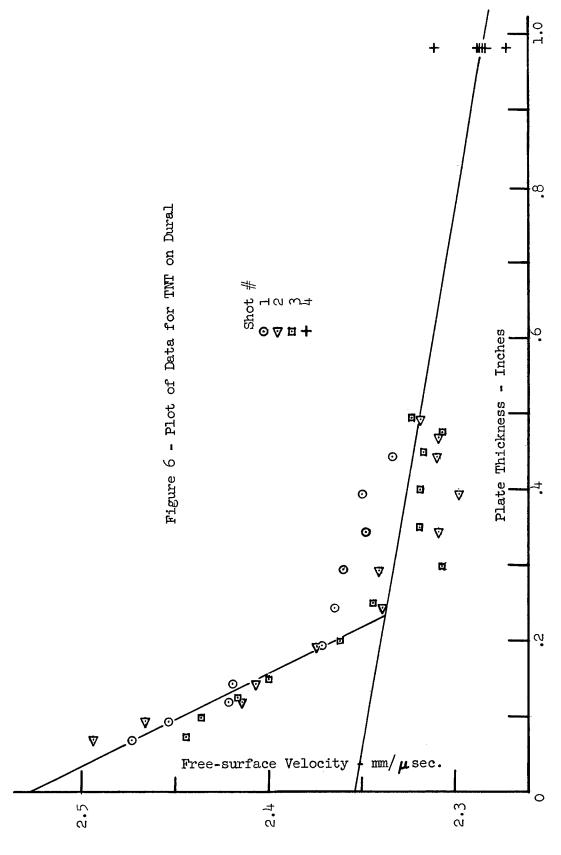
Shot No. 18 charge density 1.763 gm/cc. plate density 2.790

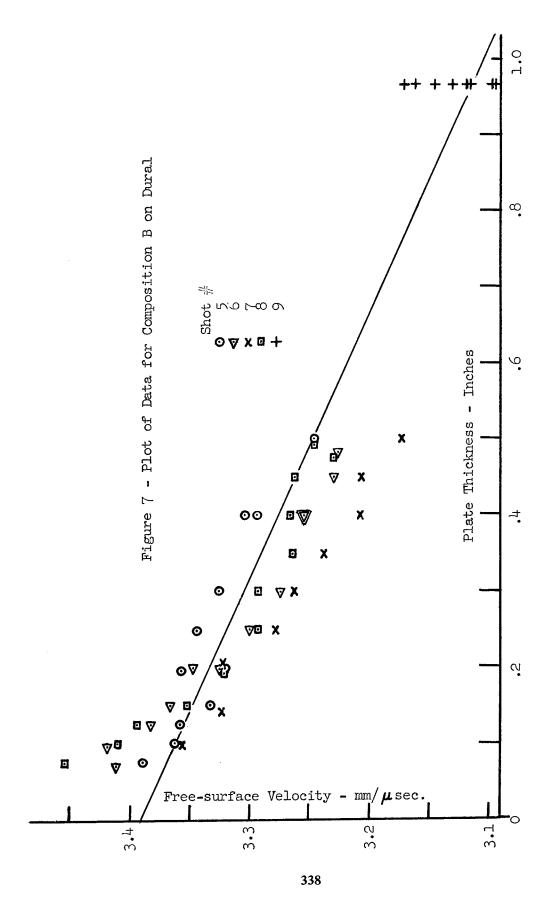
plate	free-surface
.101" .201 .300 .400 .498	velocity 3.593mm/μsec. 3.471 3.483 3.492 3.469

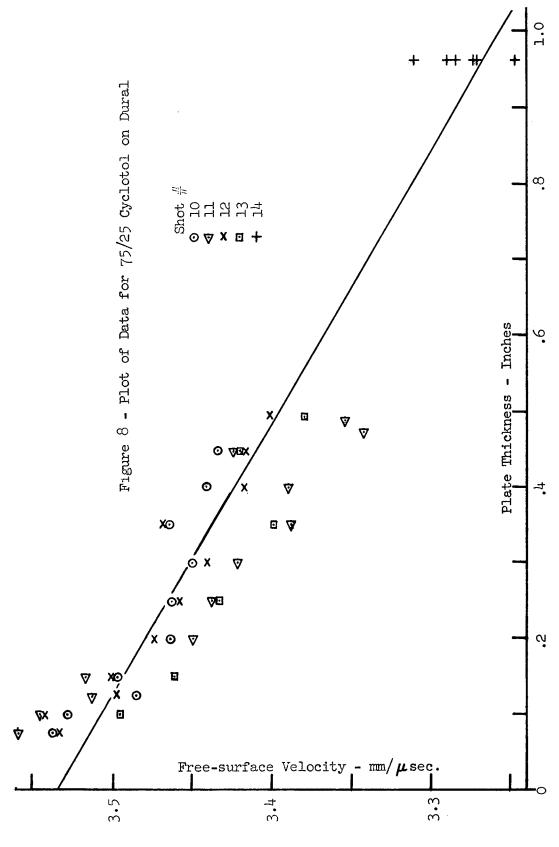
plate	free-surface
thickness	velocity
.100"	3.578mm/ <b>µ</b> sec.
.201	3.481
.300	3.468
.400	3.463
.498	3.449

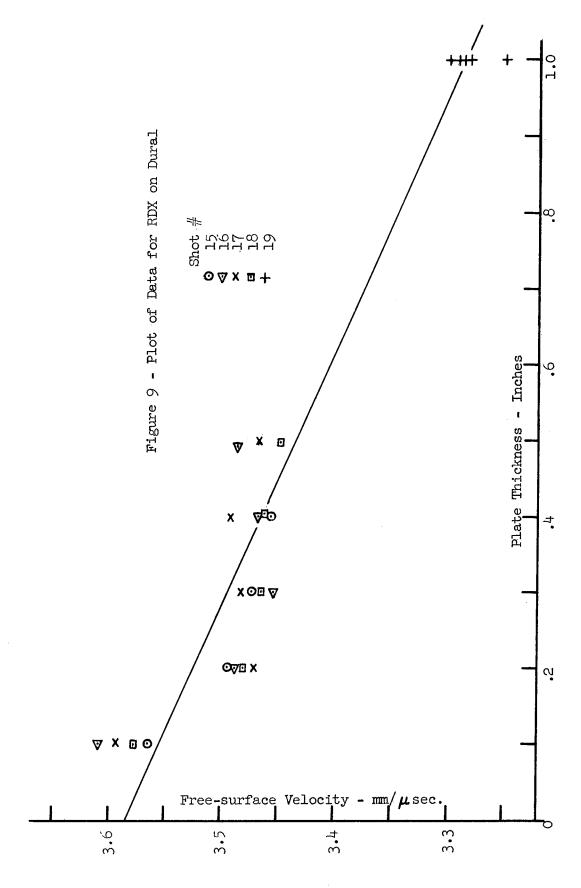
Shot No. 19 charge density 1.759 gm/cc. plate density 2.790

plate thickness	free-surface velocity
.999" .999 .999 .999	3.251mm/μsec. 3.289 3.293 3.307 3.283









The TNT data show definite evidence of the presence of a spike in the explosive. Sufficiently thin plates were not used for the other explosives to show the spike. Linear least squares fits made to the data for plates thicker than 0.2" for TNT and for all data for the other explosives yield the slopes and intercepts of table five. The

Table V.

Explosive	Intercept - mm/ $\mu$ sec.	Slope - mm/ $\mu$ sec-inch
TNT Composition B 75/25 Cyclotol RDX	2.354 ± 0.30% 3.389 0.22% 3.534 0.18% 3.582 0.31%	0.070 <b>±</b> 17.3% 0.287 5.6% 0.276 5.2% 0.295 6.9%

errors quoted are standard deviations. A linear least squares fit to the TNT data for plates thinner than 0.2" gives an intercept of 2.526 mm/  $\mu$ sec. and a slope of 0.819mm/  $\mu$ sec.-inch. This intercept corresponds to a spike pressure of 0.194 megabar. The intersection of the spike line and that of table five for TNT gives a free-surface velocity (Um) from which  $P_m$  can be deduced and C-J pressure calculated. The use of linear fits to the data is justified only by the relatively small deviations of the data (see Figures 7 and 8 ) from straight lines. The use of the extrapolated velocity to get spike peak pressure for TNT is, however, highly in question. Since the spike decay thickness for each of the explosives, exclusive of TNT, is certainly less than 0.1", less than 1% error is introduced by using the intercepts from Table V for the values of Um. Thus the C-J pressures of Table VI follow from the interface equation. Velocities in the

			-	
ጥ»՝	hΊ	6	VT	

1	יליו/וילו	Composition B		ol RDX
U <sub>m</sub>	2.338	3.389	3.53 <sup>4</sup>	3.582
$D_{m}$	6.961	7.646	7.733	7.762
$P_{m}$	0.2244	0.3562	0.3753	0.3817
ьę	2.792	2,792	2.792	2.790
$\rho_i^{\circ}$	1.640	1.712	1.743	1.762
D <sub>i</sub>	6.951	8.022	8.252	8.622
P <sub>c-j</sub>	0.178	0.293	0.313	0.325

table are in mm/ $\mu$  sec. and pressures are in megabars. The metal pressures quoted are thought to be accurate to 1%.

Other work is in progress to obtain these C-J pressures using other materials so as to clear up the uncertainty regarding disturbances reflected back into the explosive.

#### Deal

#### References

- 1. J. von Neumann, OSRD Report No. 549 (1942).
- 2. G. I. Taylor, Proc. Roy. Soc. A200, 235(1950).
- 3. R. E. Duff and E. Houston, Measurement of C-J Pressure and Reaction Zone Length in a Detonating High Explosive, reported at this meeting.
- 4. A. W. Campbell, M. E. Malin, T. J. Boyd, and J. A. Hull; Techniques for the Measurement of Detonation Velocity, reported at this meeting.
- 5. J. M. Walsh and R. H. Christian, Equation of State of Metals from Shock Wave Measurements, to be published in Phys. Rev.
- 6. E. James, Charge Preparation for Precise Detonation Velocity Studies, presented at this meeting.

# MEASUREMENT OF THE CHAPMAN-JOUGUET PRESSURE AND REACTION ZONE LENGTH IN A DETONATING HIGH EXPLOSIVE

Russell E. Duff and Edwin Houston Los Alamos Scientific Laboratory Los Alamos, New Mexico

#### INTRODUCTION

In 1945 Goranson<sup>(1)</sup> suggested that the reaction zone of a detonating solid explosive could be investigated by determining the initial free surface velocity imparted to thin metal plates as a function of plate thickness. In particular he showed that reaction zone length and Chapman-Jouguet pressure could be estimated in this way. Unfortunately, the original results obtained by Goranson are available only in a classified report from this laboratory. This paper describes similar but improved theoretical and experimental results obtained during and since 1950.

#### THEORY OF THE EXPERIMENT

The generally accepted picture of the structure of a steady state, plane detonation wave was proposed independently by Zeldovich(2), von Neumann(3) and Döring(4). The wave is assumed to consist of a non-reactive shock followed by a steady state reaction zone which is terminated at the Chapman-Jouguet surface where the local flow velocity plus sound speed equals the detonation velocity. It can be shown that this condition is fulfilled at the point of tangency in the p-v plane of a straight line from the initial state to the final Hugoniot curve calculated for a fixed composition of the product gases. (More specifically, the C-J point is the tangent point on a Hugoniot curve for the product gases whose composition is assumed fixed at the equilibrium values appropriate for the tangent point. The relation of this statement of the Chapman-Jouguet condition to the usual statement, namely, that the C-J point is the tangent point on a Hugoniot every point of which is in chemical equilibrium, is not clear at the moment because of uncertainties in the equation of state

of the detonation products. The former statement can be derived from a recent theoretical investigation of the structure of a steady state, plane detonation wave by Kirkwood and Wood, J. Chem. Phys., (1954). It should be mentioned that this statement of the C-J condition has been shown to apply to all detonations which are not pathological in the von Neumann sense. Finally, no pathological detonation has yet been observed.) Figure 1 shows a representation of the detonation process in the p-v plane. Reference to the laws of conservation of mass and momentum shows immediately that if viscosity and heat conduction are neglected, the succession of state points assumed by the reacting explosive is represented by the straight line from  $p_1v_1$  to the C-J point. The rate at which an element of explosive passes from  $p_1v_1$  to the C-J state depends on the kinetics of the reactions involved and cannot be determined from hydrodynamic considerations. It follows, therefore, that the pressure-distance profile of a detonation wave consists most probably of a monotone but otherwise unspecified decrease in pressure from  $p_1$  to  $p_{C-T}$  in an unspecified distance. Two profiles often considered are shown qualitatively in Figure 2. They correspond to a reaction rate determined by grain burning and to a rate determined by a first or second order adiabatic reaction of the Arrhenius type. The unsteady flow behind the Chapman-Jouguet plane has been investigated by Taylor (5) This flow may be simply described as a rarefaction wave ending either in cavitation or in a steady state region required to match boundary conditions at the back boundary of the explosive products.

When a plane detonation wave is incident normally on a metal plate, a shock wave is transmitted into the metal which is followed by a rarefaction wave corresponding to the pressure drop in the reaction zone of the explosive. The foot of this rarefaction wave will travel with a velocity equal to the sum of the local flow velocity and sound speed. It will overtake the shock in the metal after the shock has been attenuated by the rest of the rarefaction wave. The strength of the shock wave will decrease relatively quickly as this interaction proceeds because of the small thickness of the reaction zone. As a result, the velocity imparted to a thin metal plate, which depends directly on the strength of the shock in the plate, should change with plate thickness qualitatively as shown in Figure 3.

It has been shown that to a very good approximation the shock particle velocity of a metal in the high explosive pressure range is one-half of the free surface velocity (6). This fact makes it possible to determine the Chapman-Jouguet pressure in the explosive from the free

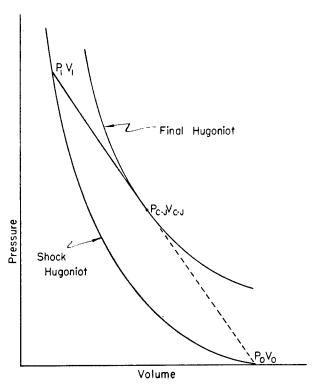


Fig. 1 - A representation of the detonation process in the pressure-volume plane.

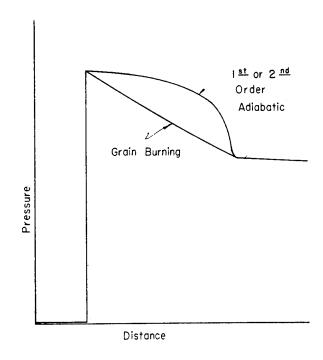


Fig. 2 - Two representative pressure profiles for the reaction zone of solid explosives.

surface velocity of a metal plate corresponding to the end of the interaction caused by the reaction zone. This velocity is v in Figure 3. An immediate consequence of the laws of conservation of mass and momentum is that the pressure behind a shock wave moving into a medium at rest is

$$p = \rho^{\bullet} u D$$
 (1

where  $\rho^{\circ}$  is the density of the unshocked material, u is the shock particle velocity, and D is the shock velocity. In all of the experiments discussed in the next section the metal used was aluminum or dural. For these materials Walsh<sup>(6)</sup> has determined experimentally a relation between shock velocity and free surface velocity in an investigation of the equation of state of the metals. The pressure in the metal can therefore be determined from the measured metal density, the free surface velocity, and this relation.

By applying the usual boundary conditions of equality of pressure and continuity of flow velocity at the interface between explosive and metal, the following expression can be developed relating incident pressure in the explosive to transmitted pressure in the metal.

$$\frac{\mathbf{p}_{\mathbf{m}}}{\mathbf{p}_{\mathbf{x}}} = \frac{\rho_{\mathbf{t}}^{\bullet} \mathbf{D}_{\mathbf{t}}}{\rho_{\mathbf{i}}^{\bullet} \mathbf{D}_{\mathbf{i}}} \left( \frac{\rho_{\mathbf{i}}^{\bullet} \mathbf{D}_{\mathbf{i}} + \rho_{\mathbf{r}}^{\bullet} \mathbf{D}_{\mathbf{r}}}{\rho_{\mathbf{t}}^{\bullet} \mathbf{D}_{\mathbf{t}} + \rho_{\mathbf{r}}^{\bullet} \mathbf{D}_{\mathbf{r}}} \right)$$
(2)

The subscripts i, t, and r refer to properties of the material in which the wave is respectively incident, transmitted, and reflected — in this case the undetonated explosive, the metal, and the explosive products. The superscript refers to properties in front of a shock wave. D refers to shock velocity relative to the medium ahead of the wave. The pressure in the explosive,  $p_x$ , can now be calculated if  $p_r^{\circ}D_r$  is known. An error analysis of this relation shows that

$$\frac{\delta p_{x}}{p_{x}} = \frac{(\rho_{1}^{\bullet}D_{1} - \rho_{1}^{\bullet}D_{1}) \rho_{r}^{\bullet}D_{r}}{(\rho_{1}^{\bullet}D_{1} + \rho_{r}^{\bullet}D_{r}) (\rho_{t}^{\bullet}D_{t} + \rho_{r}^{\bullet}D_{r})} \frac{\delta(\rho_{r}^{\bullet}D_{r})}{\rho_{r}^{\bullet}D_{r}}$$

If the acoustic approximation is made that  $\rho_i^*D_i = \rho_r^*D_r$  and values appropriate for Composition B (nominally 60% RDX - 40% TNT) are inserted, then

$$\frac{\delta p_{x}}{p_{x}} = -.1 \frac{\delta (\rho_{r}^{o} p_{r})}{\rho_{r}^{o} p_{r}}$$

Thus it is clear that the Chapman-Jouguet pressure is

quite insensitive to the value of  $\rho_{rD_r}^*$  assumed. Furthermore, the acoustic approximation is correct insofar as the velocity of the reflected shock can be assumed equal to the velocity of a rarefaction wave in the product gases. Therefore, to a good approximation

$$\frac{\mathbf{p}_{\mathbf{m}}}{\mathbf{p}_{\mathbf{x}}} = \frac{\rho_{\mathbf{t}}^{\bullet} \mathbf{p}_{\mathbf{t}}}{(\rho_{\mathbf{i}}^{\bullet} \mathbf{p}_{\mathbf{i}} + \rho_{\mathbf{t}}^{\bullet} \mathbf{p}_{\mathbf{t}})}$$
(3)

An estimate of the reaction zone length can be made from a determination of the distance required for the end of the rarefaction corresponding to the Chapman-Jouguet plane to overtake the shock wave in the metal. tance is b in Figure 3. If it is assumed that the metal is a perfect impedance match to the explosive so that no wave is reflected back into the explosive, an x-t representation of the interaction will be as shown in Figure 4. The interface is initially assumed to be at x = 0. A detonation wave comes in from the left with a velocity D,. The reaction zone length is a. The velocity of the interface through the reaction zone is d  $D_i$ , the shock velocity in the metal is  $D_t$ , and the velocity of the foot of the rarefaction wave is  $u_t + c_t$ .  $D_t$  and  $\lambda$  will vary as the interaction proceeds. The values used in the formula below and those indicated in Figure 4 are the appropriate average values. As long as the flow behind the shock can be considered isentropic (a good approximation), ut + ct depends only on pressure and is the value corresponding to the C-J state transmitted into the metal. Simple analytical geometry leads to the following relation between the reaction zone length in the explosive and the interaction distance in the metal.

$$a = b \left[ D_{1}(u_{t} + c_{t} - D_{t}) (1 - d) \right] \left[ D_{t}(u_{t} + c_{t} - d) \right]^{-1} (4)$$

The appropriate average value of D<sub>t</sub> can be determined from the free-surface-velocity/plate-thickness relation since at every value of thickness this relation gives the corresponding shock velocity by using the equation of state. It can easily be seen that the appropriate average to be used in the above equation is the inverse average; i.e.

$$D_{t} = \left(\frac{1}{b} \int_{0}^{b} \frac{dx}{D(x)}\right)^{-1}$$
 (5)

Likewise & should be determined from a similar inverse average of the interface velocity.

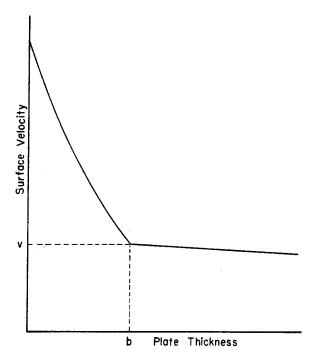


Fig. 3 - Free surface velocity of a metal plate as a function of plate thickness showing the high velocity produced in thin plates by the von Neumann spike in the explosive.

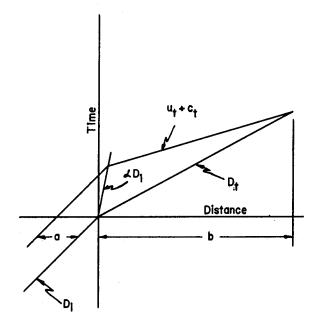


Fig. 4 - Distance-time representation of the interactions between the von Neumann spike in the explosive and the metal plate.

It is possible to calculate in detail the free surface velocity as a function of plate thickness by using the procedure outlined by Courant and Friedrichs (7) under the assumption mentioned above, namely, that the flow behind the shock can be considered isentropic. In particular, if the reaction zone rarefaction and the Taylor wave are both assumed to be centered rarefaction waves, and if a ratio of explosive charge length and reaction zone length is assumed, the ratio of slopes of the free-surfacevelocity/thickness curve for the two waves at the point corresponding to the end of the reaction zone can be calculated. This ratio is about 25 if the charge length is 200 times the reaction zone length and if the spike pressure is 1.5 times the Chapman-Jouguet pressure. practical cases the ratio of charge length to reaction zone length is much greater than 200 so the change of slope would be even larger than indicated above. calculation justifies the sharp change in slope of the freesurface-velocity/plate-thickness curve shown in Figure 3.

It should be remembered that it was assumed in this calculation that the reaction zone rarefaction could be approximated by a centered rarefaction wave. However, most reaction rate expressions show that equilibrium is approached asymptotically in time. If such expressions are appropriate for solid explosives, and there is no experimental evidence that they are, the ratio of slopes could conceivably approach unity. However, the long reaction tail predicted by these kinetic expressions corresponds to a very small percentage of the total detonation reaction, and a rapid rate of change of slope would be expected not at a plate thickness corresponding to the C-J state but at a thinner one, corresponding to essentially complete reaction.

#### EXPERIMENTAL TECHNIQUE

Free surface velocity was measured by recording the time of arrival of the metal surface at a series of metal contactors or pins. The technique used is identical with that described by Minshall(8). In these experiments two or 1. some cases four velocity measurements were made in each experiment by using either two or four groups of pins each consisting of six pins set in a  $\frac{1}{4}$  in. diameter circle. The spacing between pins measured perpendicular to the free surface was 0.003 in. for the thin plates 0.030 in. thick and under, and 0.006 in. for all thicker plates. A cross section through a thin foil experiment is shown in Figure 5.

The electronic circuitry used is indicated in Figure 6. As each pin is shorted to the moving plate, a condenser is discharged through the network producing a signal on the

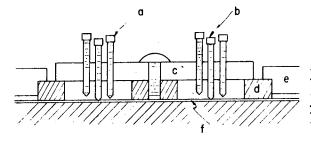


Fig. 5 - Cross-section of an experiment to determine the free surface velocity of a very thin plate or foil.

High Explosive



Explosive Lens

- a. 0-80 pointed steel screws used as surface velocity pins.
- b. Center ground contact pin also used to hold foil against the high explosive
- c. Texalite pin mounting plate.
- d. Aluminum backing plate  $3\frac{1}{4}$  in. O.D.,  $\frac{1}{4}$  in. thick.
- e. Blast shield 8 in. O.D., 3/8 in. thick.
- f. Aluminum foil.

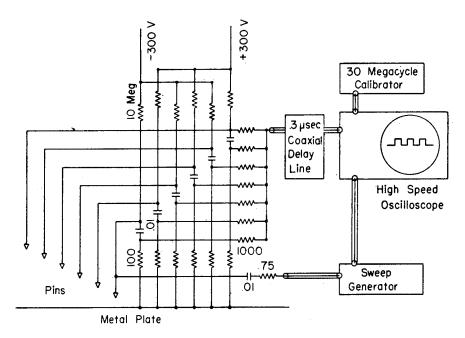


Fig. 6 - Electronic circuitry used to measure free surface velocity. The component values are the same for all circuits. Resistance values are ohms and capacitor values are ufd unless otherwise indicated.

oscilloscope. Successive pins have alternate polarities so that an ideal record would resemble the square wave indicated in the figure. A time base is provided by a trace from an accurately calibrated 30 megacycle crystal oscillator displaced slightly from the velocity record.

The high speed recording oscilloscopes used in these experiments were similar to the system described by the Radiation Laboratory (9). A sweep speed of 10 in./µsec. was used and twenty thousand volts post acceleration was required in order to obtain single traces intense enough to photograph clearly at this high writing speed.

A photograph of a setup ready to be used is shown in Figure 7. The pulse-forming networks are sealed in the plastic blocks located near each pin group.

Precautions were necessary to eliminate two possible sources of error. The shock wave in air preceding the free surface was strong enough to discharge the pin circuits before the arrival of the surface. This difficulty was eliminated by maintaining a methane atmosphere around the pins. If velocity measurements were made on a machined and polished surface, the first several pins were often discharged prematurely by what appeared to be a fine spray of metal jetted out from the surface. This spray was eliminated by using unworked surfaces whenever possible and covering the surface with a very thin, almost invisible coating of light oil.

#### EXPERIMENTAL RESULTS

# Experimental Data

Thirty-three separate experiments were performed in which eighty-seven measurements of free surface velocity were made. In the first twelve of the experiments the metal used was dural and in the remainder pure aluminum was used. Walsh (6) has shown that the particle velocity-shock velocity relationship is identical within experimental error for both metals. The explosive was Composition B which was cast into large blocks and then machined into pieces  $5\frac{1}{2}$ " x  $5\frac{1}{2}$ " x 3". The composition and density of the explosive varied by roughly 2 percent RDX and .01 gm/cc from charge to charge and within a given charge. These charges were prepared in 1950 and are not of as high a quality as those prepared currently.

All of the experimental results were corrected to the following standard conditions: metal density = 2.71 gm/cc; explosive density 1.67 gm/cc; explosive composition 63 percent RDX; and detonation velocity 7.868 mm/µsec. The

following error expression was used in this correction:

$$\frac{\delta u_{t}}{u_{t}} = -0.861 \, \delta \rho_{t} -0.0023 \, \delta \, \% \, RDX + 0.192 \, \delta \rho_{t}$$

In most cases the corrections made velocity changes of less than 1 percent. A random error of  $1\frac{1}{2}$  percent is caused by the composition and density fluctuations within a given charge. The average values of the velocities measured are presented in Table I.

TABLE I

Measured Free Surface Velocity
as a Function of Plate Thickness

Plate	Average	Standard Deviation of the mean (mm/µsec)	Number
Thickness	Velocity		of
(in.)	(mm/µsec)		Measurements
0.0085 0.016 0.021 0.030 0.048 0.057 0.098 0.150 0.198 0.248	3.89 3.60 3.48 3.32 3.20 3.22 3.25 3.04 3.11 3.01 3.02	0.34 0.26 0.25 0.10 0.20 0.02 0.09 0.06 0.07 0.09 0.09	12 15 11 11 10 2 8 4 6 4

These data are also presented in Figure 8.

Two subjects deserve comment before conclusions are drawn from these data. First, the standard deviations reported in Table I are unfortunately large. However, this large standard deviation arises mainly from a systematic source. As discussed above, velocities are determined from measurements of position and time of the metal free surface by means of pins set in a circle. If the metal surface is not perfectly plane and if it does not move perfectly parallel to its initial position, a systematic error in the arrival time of the surface at each pin will be introduced which may be reflected into the surface velocity as determined by least squares techniques. It can be shown that the velocity calculated is related to the

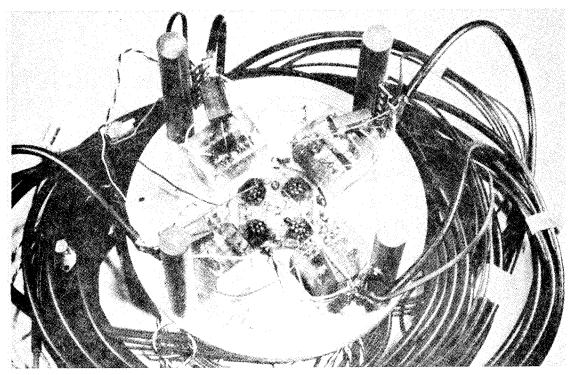


Fig. 7 - A photograph of an experiment ready to be fired.

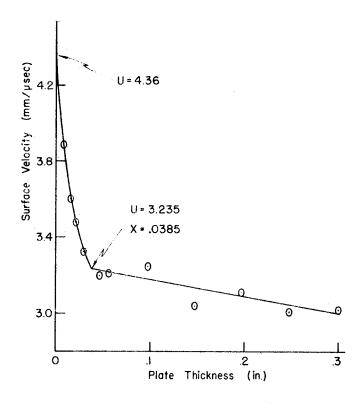


Fig. 8 - Measured free surface velocity as a function of plate thickness.

true velocity as follows:

$$V = Vcalc \left(1 + \frac{R \lambda'}{d} \in \sin \theta\right)$$

where R is the radius of the pin circle, d is the incremental pin spacing,  $\mathbf{J}$  is the angle of tilt of the surface,  $\mathbf{C}$  is a constant =0.11 for the pin geometry used in these experiments, and  $\mathbf{O}$  is an angle which describes the orientation of the pin circle with respect to the tilted wave. A wave tilt of as much as 0.03 radian was observed for some of the charges used. Therefore, this cause alone could produce a velocity error of 15 percent in plates 0.030 in. thick or thinner and  $7\frac{1}{2}$  percent for thicker plates. For this reason many measurements were made, especially on the thinner plates, so as to obtain a reliable value for the average velocity.

Second, it is desirable to place all of the pins close enough to the free surface so that the velocity measurement can be completed before a second disturbance arrives at the surface. This was done for all but the thinnest foil. One might expect a weak shock wave to be the second disturbance to arrive at the surface giving it a small increase in velocity at about the middle of the velocity measurement. Examination of the records does not indicate a noticeable increase in velocity. However, the velocity associated with the 0.0085 in. foil may be slightly high.

#### Explosive Pressure

Two pressures in the explosive can be estimated from the surface velocity plot of Figure 8. A least squares straight line has been fitted to the experimental measurements at thicknesses greater than 0.030 in. Each of the average velocities was given a weight equal to the number of measurements included. A smooth curve was drawn through the remaining four measurements on thin plates. The Chapman-Jouguet pressure can be determined from the free surface velocity indicated by the intersection of these two lines, 3.235 mm/usec.

The equation of state data of Walsh<sup>(6)</sup> for aluminum has been analyzed by Fickett (unpublished communication). An analytic form of the equation of state was derived which agreed with Walsh's data at low pressures and with Fermi-Thomas-Dirac calculations at high pressures. The following fit of shock velocity as a function of free surface velocity is appropriate for the pressure range of interest in these experiments.

$$D = 4.8375 + 1.1235 u - 0.1095 u^2 + 0.0066 u^3$$

Therefore, in the metal

$$p_{m} = t^{u}t^{D}t$$
  
= 2.71 x  $\frac{3.235}{2}$  x 7.55 = 0.3309 megabar.

In the explosive

$$p_{C-J} = \frac{p_m (i_D_i + t_D_t)}{t_D_t} = 0.272 \text{ megabar.}$$

Thus the Chapman-Jouguet pressure in Composition B explosive containing 63 percent RDX at a density of 1.67 gm/cc is 0.272 megabar. This number is thought to be correct to within 2 percent.

The extrapolation of the free surface velocity to zero plate thickness in what is thought to be a reasonable manner gives a limiting velocity of 4.36 mm/µsec. From this number and the extrapolation of the equation of state data for aluminum made by Fickett, a peak pressure in the explosive of 0.385 megabar is estimated for the von Neumann spike. It is interesting to note that the spike pressure appears to be only 1.42 the Chapman-Jouguet pressure. It should be emphasized that the extrapolation to zero thickness is only what appears to be a reasonable one. There is no theoretical justification for the assumed form of the curve because the form depends on the details of the chemical kinetics of the detonation reaction about which essentially nothing is known.

### Reaction Zone Length

The reaction zone length was calculated from Eq. 4 using a value of D2 determined from the experimental results as required by Eq. 5. & was determined from the two values of interface velocity which could be estimated from the experimental data, namely, the initial and final The assumption was made that the interface velocity changed with distance in the same way the shock velocity did. A value of  $u_t + c_t$  was obtained from the equation of state calculation for aluminum made by Fickett. The actual numbers used are as follows:  $D_{i} = 7.868$ ,  $D_{t} = 7.771$ ,  $u_{t} + c_{t} = 9.065$  mm/ $\mu$ sec. and  $\frac{a}{b} = 0.232$ ; giving  $\frac{a}{b} = 0.139$ . b was estimated to be 0.0385 in. Therefore, a = 0.005 in. or 0.13 mm. estimate of reaction zone length of slightly greater than one tenth of a millimeter is probably accurate to within 20 percent except for the possible errors discussed below.

Two assumptions have been made in the estimation of reaction zone length. First, the shock wave reflected from the metal back into the explosive has been ignored. This assumption is questionable because the changes in temperature and pressure caused by the wave may decisively influence the kinetics in the as yet unreacted explosive into which it moves. Therefore, the value of reaction zone length determined is probably best described as a lower limit value.

The effect of this reflected shock wave on the detonation kinetics and reaction zone length could be investigated by varying the metal used in experiments of this type. In particular, the effect could be maximized by using a heavy material like brass which has a large acoustic impedance and minimized by using magnesium which is almost a perfect impedance match for Composition B.

The second assumption concerns the shape of the reaction zone. The experimental results have been represented by a profile similar to that of a rarefaction wave in an inert material. However, as discussed above, there could be a slow reaction tail which would cause the true reaction zone length to be somewhat longer than that indicated.

#### CONCLUSIONS

A conclusion can be drawn from the data presented above which is fundamental to the understanding of the detonation phenomenon. Namely, the experimental results provide powerful confirmation for the hydrodynamic theory of the detonation process proposed by Zeldovich, von Neumann and Döring. In fact, this is thought to be the first experimental evidence published which directly verifies this theory which has, however, attained almost universal acceptance because of its hydrodynamic completeness.

The Chapman-Jouguet pressure in Composition B explosive containing 63 percent RDX at a density of 1.67 gm/cc was measured to be 0.272 megabar. The reaction zone length for the same explosive is 0.13 mm.

# ACKNOWLEDGEMENTS

The authors are indebted to many people for assistance in various phases of this work. In particular, we are happy to acknowledge the help of the following individuals: R. Holbrook, E. Gittings, R. E. Faudree and V. Thurlow for assistance in the actual performance of the

experiments; C. L. Miller for the preparation of the many explosive charges used; C. W. Mautz for the derivation of Equation 4; and W. W. Wood for many valuable discussions of the theoretical problems involved and also for making the detailed calculation of the attenuation of a shock wave in metal by a centered simple rarefaction wave.

#### REFERENCES

- 1. R. W. Goranson, Classified Los Alamos Report LA-487.
- 2. Y. B. Zeldovich, J. Exptl. Theoret. Phys. (USSR) <u>10</u>, 542 (1940).
- 3. J. von Neumann, O.S.R.D. Report No. 549, (1942).
- 4. W. Döring, Ann. Physik, 43, 421 (1943).
- 5. G. I. Taylor, Proc. Roy Soc. A200, 235 (1950).
- 6. J. M. Walsh, Phys. Rev. (in press).
- 7. R. Courant and K. O. Friedrichs, Supersonic Flow and Shock Waves, (Interscience Publishers, Inc., New York, 1948), p. 164.
- 8. F. S. Minshall, J. Appl. Phys. (in preparation).
- 9. M.I.T. Radiation Laboratory Report No. 1001, (1946).

#### THE DETONATION ZONE IN CONDENSED EXPLOSIVES

H. Dean Mallory
S. J. Jacobs
U. S. Naval Ordnance Laboratory
White Oak, Maryland

#### Introduction

The hydrodynamic concept of a steady state detonation with finite reaction time was independently proposed by Zeldovich(1), von Neumann(2) and Doring(3). The theory describes a detonation wave as a non-reactive shock followed by a period of chemical reaction which ends in the well known and generally accepted Chapman-Jouguet condition. This theory shows the pressure level in the non-reactive shock to be higher than at the C-J point and has given rise to the concept of a pressure spike in the detonation head. From the hydrodynamic theory alone one can say only that the pressure decreases as reaction proceeds.

For detonation in gases, some few authors have insisted that reaction does not begin at the initial shock front but rather that it is preceded by a steady induction zone where little or no reaction occurs. Lewis and Von Elbe(4) state "If the reaction rate is exponentially accelerating, (the fraction of explosive reacted) changes initially very little and the pressure profile is very flat for some distance behind the shock front. In then drops sharply as the reaction goes, to completion at a high rate. Finklestein and Gamow(5) and Kistiakowsky(6) present similar views. It is the purpose of this paper to present evidence that the steady state detonation of TNT at various bulk densities confirms the hydrodynamic picture given by Zeldovich, von Neumann and Doring, and that the views quoted above are applicable to condensed explosives also. Within the limitation of experiments to be described, the data show the detonation head to consist essentially of two separable zones, one of induction and one of chemical reaction.

The method employed in this paper is based on the hydrodynamic conditions which apply when a shock crosses a boundary between two media, and after propagating through the second media, causes the nearby free surface of the second to move in an ensuing rarefaction. translational motions of shock propagation and free surface velocity of the second media are measured by a method now referred to as the pin technique. The observations made on the second medium can be made to yield pressure-density data for the explosive. An unexpected result, for low density charges, was that the explosive was not compressed to near crystal density by the shock front prior to reaction. Rather, the boundary conditions at the target interface required modest compression to a value far below crystal density.

# Experimental Details

In the fundamental experiments employed by us, the shock in the first medium is a detonation wave in TNT. Several bulk densities of explosive are used. The second medium is essentially pure (2S) aluminum. It can be shown that the free surface velocity set up in the aluminum is a function of the pressure level appearing at that free surface prior to rarefaction. A range of target thickness is a convenient method for sampling the pressure at given distances from the metal-explosive interface. Since reaction in the boundary layer of explosive is accompained by a pressure fall, a range of rarefaction waves spread from the boundary and overtake the pure shock front later in time. Knowledge of the wave velocities in the metal then permits a reconstruction of the pressure profile of the wave which struck the target. Data from this type of experiment can be interpreted as showing a well defined induction zone preceding the reaction in TNT.

In other experiments, an explosive was used to hurl a massive aluminum "driver" plate across an air gap where it impacted a target plate having one of several thicknesses. Since the first plate unloaded during its passage across the air gap, the shock wave induced in the target was free from reaction zone effects and the data obtained indicate only a smooth decrease in pressure at increasing distances from the impact boundary. The absence of the usual velocity plateau in this case, helps establish the reality of the plateau when TNT alone drives the target.

Yet a third series of experiments were performed in an attempt to produce a pressure spike as distinct

from the steady induction zone pressure observed in the first set. These experiments were identical with the aluminum-aluminum impact experiments except that a thin wafer of pressed TNT was centered on the target plate and initiated by impact of the driver plate after it crossed the air gap. The resulting free surface velocity data again show an initial steady induction zone followed by a sudden decrease in pressure, and demonstrate the effect of chemical reaction on the mass velocity transmitted to the target.

A schematic drawing of the aluminum-aluminum impact experiment with the included TNT wafer is shown in Figure 1. The TNT wafers were not used in the series of pure impact experiments. One set of experiments using TNT pressed to a bulk density of 1 g/cc was performed. In this set the "shock driver" was also removed, allowing the 3 inch diameter charge to rest on the target plate. These charges were 5 inches high.

A fourth series used cast TNT charges 6 inches square and 4 inches high. These also rested directly on the target plates. The fifth and last type described were made up of crystalline TNT at a bulk density of 0.624 g/ca (mean density of all those fired). These were our so-called "snow flake packed" charges which were made by first pinning a 6 inch I.D. aluminum tube to the target plate and sifting in the TNT at the firing site. The charge height was 5 3/4 inches. Over this charge was laid a 1 inch thick slab of cast TNT which rested on the rim of the tube and supported the plane wave booster. Most of the crystals passed a 50 but not a 70 mesh sieve.

The arrangement of the pin contactors for velocity measurements is shown in Figure 1. For the impact experiments, 16 contactors were used for each shot. Eight of these were insulated and set into holes drilled to various depths in the target to be shorted out on passage of the shock wave, while the remaining eight were spaced outside the target in such a manner that the moving free surface would contact each in turn. pins were arranged in two concentric circles, one of 5/8 inches and the other 1 inch in diameter. A plane wave booster was used to initiate the main charge since the circular pin geometry required a plane impact in order to give meaningful data. Wave planeness is a difficult thing to control and for this reason a number of identical shots were made at each target thickness in order to obtain a statistically significant velocity.

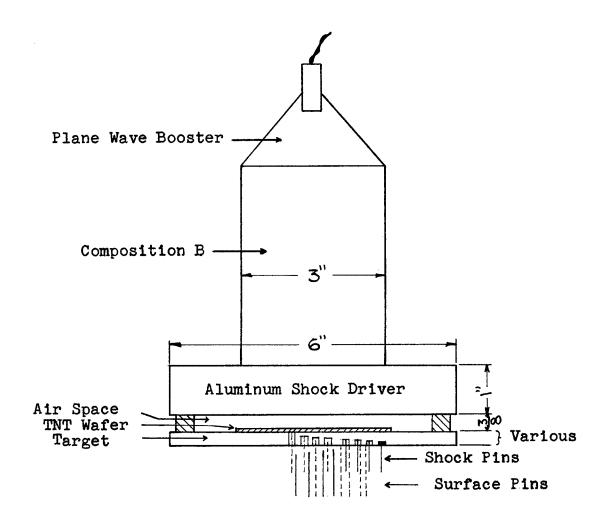


Figure 1. Experimental Arrangement for the Impact Experiments with Included TNT Wafer

Electrical pulses made by contact of the grounded moving target with the charged pins were led through 500 feet of coaxial cable to an oscilloscope where the scope beam deflections were photographed by a still Synchronization with the oscilloscope was achieved by also sending the pulse from the first pin in a set through a second, shorter, piece of cable in a manner such that it started the scope beam in time to record itself and the others as they came through the long cable. The oscilloscope had a 5-10 mc frequency response and about a 2 microsecond time base, single The target plates were coated with a film of vasoline, insignificantly thick, to electrically separate the moving target from the charged pin contactors. External contactors were insulated along their shafts by glyptal resin and spaghetti tubing with their tips bare except for a film of vasoline similar to that on the target plate.

Accurate shock velocity measurements, for any except the impact experiments, were found to be virtually impossible due to violent pressure changes occurring in the detonation head. Free surface velocity measurements were relatively easy for all systems investigated and therefore these were measured while the corresponding shock velocities were computed from the equation of state for aluminum.

# The Measurement of Detonation Pressures

The well known hydrodynamic equation for the conservation of impulse in a shock wave is

1) 
$$p = \rho_0 Du$$

in a coordinate system where  $u_0 = o$ , and  $p_0$  is neglected. The equation is general and applies to a detonating explosive or to an aluminum target being traversed by a shock. It has been shown (7) that u in aluminum is closely approximated by taking 1/2 the first order free surface velocity,  $u_s$ , of the targets and that shock velocity, D, and pressure, p, can both be calculated if  $u_s$  is known.

From the conditions of equality of pressure and continuity of mass flow across a boundary between a detonating explosive and a metal target, an expression relating the incident particle velocity to that transmitted can be derived. The expression is

2) 
$$\frac{u_{\rm m}}{u_{\rm e}} = \frac{(\rho_{\rm o}D)_{\rm e} + (\rho D)_{\rm r}}{(\rho_{\rm o}D)_{\rm m} + (\rho D)_{\rm r}}$$

where subscripts e and m refer to explosive and metal respectively and r refers to the reflected wave sent back into the explosive by the metal interface. Thus if  $(\rho D)_r$  can be approximated, the particle velocity, and therefore the pressure, in the explosive can be determined from the measured free surface velocities of metal targets. Ablard (8) has shown that

$$(\rho_{o}D)_{e} = (\rho D)_{r}$$

for cast Composition B and aluminum targets. His results are not restricted to a given explosive but are determined by the value of the product  $(\rho_0 D)_e$  which is only slightly higher than that for cast TNT reported on here. We have therefore assumed the relation 3) for our cast explosive and computed the peak pressure on this basis. However, this assumption is shown to be in gross error for the case of one of our lowest density explosives where the impedance of the explosive,  $(\rho_0 D)_e$ , is much smaller than that of the aluminum targets,  $(\rho_0 D)_m$ .

# Impedance Mismatched Systems

The conservation of mass and momentum in a reflected wave can be used to establish limits for the reflected shock velocity. The following analysis, which applies to our low density charges describes the method.

Consider a piston driving a shock wave into a unit mass of explosive at pressure and volume  $p_0$ , vobefore compression and  $p_1$ ,  $v_1$  after compression. Further, let the piston be the reaction products produced in a steady detonation wave. Since after establishment of the wave the pressure on the piston is  $p_1$ , the work done by the piston on the unit mass is  $p_1(v_0-v_1)$ . The work done goes to increase the internal energy by an amount of  $\Delta E_1$  and also to give the unit mass a kinetic energy  $\frac{1}{2}$   $u_1^2$ . Therefore

4) 
$$\Delta E_1 = p_1(v_0 - v_1) - \frac{1}{2} u_1^2$$

The Hugoniot equation is

$$\Delta E_1 = 1/2 (p_1+p_0)(v_0-v_1)$$

and if  $p_0 = 0$ , substitution into 4) gives

5) 
$$\Delta E_1 = 1/2 p_1(v_0-v_1)$$
  
= 1/2  $u_1^2$ 

If the shock wave with particle velocity  $u_1$  strikes the boundary of a high impedance medium, a shock wave is reflected which propagates through the unit mass which has the pressure and volume  $p_1$ ,  $v_1$ , after the first shock and  $p_2$ ,  $v_2$  after the second. As in equation 4) we may write

6) 
$$\Delta E_2 = p_2(v_1-v_2) - 1/2 u_2^2$$
  
= 1/2  $(p_2+p_1)(v_1-v_2)$ 

where  $\Delta E_2$  is the change in internal energy due to the reflected wave and  $u_2$  is the particle velocity in the wave referred to a coordinate system moving at velocity  $u_1$ .

The total internal energy change for material behind the reflected shock front is then

$$\Delta E_t = \Delta E_1 + \Delta E_2$$

which by substitution from 5) and 6) becomes

7) 
$$\Delta E_t = 1/2 \sqrt{p_1(v_0 - v_2) + p_2(v_1 - v_2)}$$

But also

$$\Delta E_{t} = p_{1}(v_{0}-v_{1}) - \frac{u_{1}^{2}}{2} + p_{2}(v_{1}-v_{2}) - \frac{u_{2}^{2}}{2}$$

which becomes, on equating to 7) and substituting for  $u_1^2$ ,

8) 
$$(p_2-p_1)(v_1-v_2) = u_2^2$$

The equation of state for aluminum(7) enables us to evaluate  $p_2$  directly from the measured free surface velocity of aluminum targets since pressure is continuous across the metal-explosive interface. The equation just derived enable us to compute  $v_2$  and  $u_2$  (=  $u_1$ - $u_m$ ).

For our lowest density explosive, crystalline TNT at a bulk density of 0.624 g/cc, the highest free surface velocity imparted to the aluminum targets was 1.08 mm/microsecond. This result, along with the corresponding shock velocity from the previously mentioned equation of state, determines the peak pressure in aluminum and therefore the reflected peak pressure in the explosive (p<sub>2</sub> in equation 8). We can choose arbitrary values for  $u_1(=u_e)$  and compute the corresponding values of  $p_1$  from equation 1) since D is known for the explosive. The conservation of mass equation

9) 
$$\rho_{o}D_{e} = \rho_{1}(\mathbf{D}-\mathbf{u})_{e}$$

then determines  $v_1 = \frac{1}{n}$ ) for any  $u_1$ ; since we have an experimentally determined value for  $p_2$ , equation 8) can be used to compute  $v_2$ . In this way we can examine the density behind the shock wave reflected from the metal interface. With values for  $p_1, p_2$  and  $u_2$  at hand, equation 9) can be applied to the reflected wave. The shock velocity so determined is then  $D_r$ , which when multiplied by  $p_1$ , is the impedance of the reflected wave,  $(p_1, p_2, p_3)$  as used in equation 2). Results of these calculations are set out in Table I.

Table I. Consistent Values of the Hydrodynamic Variables for TNT at a Loading Density of 0.624 g/cc Based on  $u_m = 0.54$ 

u <sub>e</sub> (mm/sec)	<b>R</b> <sub>1</sub> (g/cc)	<b>/</b> 2 (g/cc)	(mm/ksec)	$(\frac{\text{dynes/cm}^2 \times 10^{10}}{)}$	$\frac{\rho_1 D_r}{}$
2.1 2.0 1.8 1.7 1.5 1.4 1.3	1.396 1.318 1.249 1.186 1.130 1.078 1.031 0.988 0.949	18.87 4.673 2.817 2.088 1.684 1.439 1.266 1.144 1.053 0.978	1.685 2.034 2.443 2.917 3.525 4.224 5.170 6.308 7.692 9.773	4.975 4.738 4.501 4.264 4.027 3.790 3.554 3.317 3.080 2.843	2.352 2.681 3.051 3.460 3.983 4.553 5.330 6.232 7.300 8.913

For our low density TNT, the acoustic approximation as given in equation 3), estimates  $u_e(=u_1)$  to be 2.1 mm/microsecond As can be seen from Table I, the corresponding value for  $\rho_2$ , the density behind the reflected wave, is impossibly high. Our best estimate for  $u_e$  is 1.46 mm/microsecond as obtained in a

separate report(9). As can be seen from the table, this choice of particle velocity implies that densities in both the reflected and incident waves are below crystal density. It can be seen that even if the reflected density were made to exceed crystal density by another choice of ue, the incident density would still be less than crystal. Since these low density results are also interesting from the standpoint of the kinetics involved, the method used for estimating ue will be outlined after the experiment has been described.

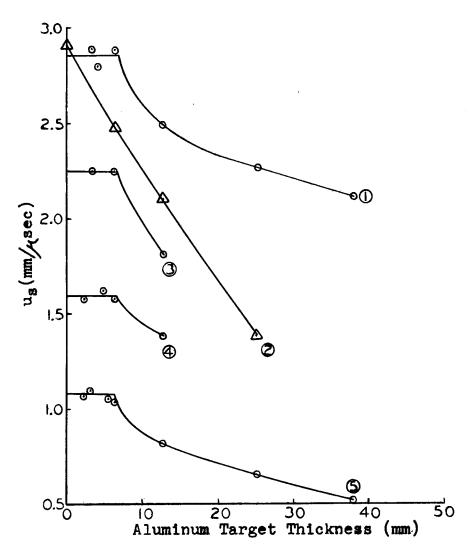


Figure 2. First Order Free Surface Velocities of 2S Aluminum Targets Driven by (1) cast TNT,  $\rho_0$  = 1.58 g/cc, (2) aluminum plate impact, (3) pressed TNT wafers, 1/8 inch thick,  $\rho_0$  = 1.55, (4) pressed TNT at  $\rho_0$  = 1 g/cc (5) TNT at  $\rho_0$  = 0.624 g/cc

# Experimental Results

The experimental results obtained for different density explosives in contact with the targets show striking similarities although the interpretations placed on the data must be very different. Figure 2 is a graph of the free surface velocities obtained in the various experiments, as a function of target thickness. These data are set out in tabular form in Table II.

Table II. Numerical Data for the Curves in Figure 2

Curve No.	Target Thickness (in.)	$\frac{u_s + P.E.}{(m/sec)}$	Number of Targets Fired
1	1/8 5/32 1/4 1/2 1 1 1/2	2892 + 70 2795 + 40 2877 + 72 2497 + 83 2267 + 37 2114 + 20	66 36 36
2	0 1/4 1/2 1	2908 + 59 2475 + 8 2103 + 56 1379 + 40	6 8 6 6
3	1/8 1/4 1	2254 + 56 2234 + 66 1818 + 30	<u>ተ</u> ተ ተ
4	- 3/32 3/16 1/4 1/2	1569 + 64 1619 + 28 1573 + 20 1385 + 24	त त त त
5	- 3/32 1/8	1072 + 42 1080(est.	from reverbera-data)
J	7/32 1/4	1058 ± 18 1034 ± 22	4 6
	1/2 1 1 1/2	816 ± 6 647 ± 3 513 ± 8	7
	ī 1/2	513 ± 8	3

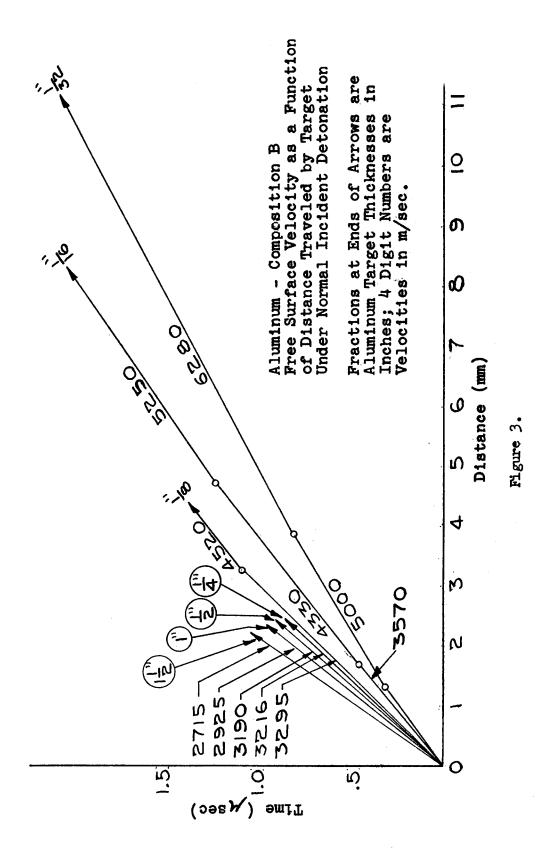
In order that the data be useable in the computation of explosion pressures, it is necessary that they be the free surface velocities present at the start of translational motion. When the unloading wave from the free boundary reaches the metal-explosive interface, a high pressure is still present in the explosion gases. This residual pressure can and does drive a second shock wave into the target. This second wave further increases the free surface velocity. Free surface measurements which include the second or later velocity orders will over estimate us and therefore over estimate the pressure developed in the explosive.

### Wave Reflections in the Target

Figure 3 shows the step wise accelerations which occur in targets of various thicknessess, explosion loaded by Composition B. These data are not to be discussed further in this paper and are included only to illustrate the process of momentum transfer from explosive to target which occurs later in time. They illustrate that the initial or "first order" free surface velocity is far from the terminal velocity which can be obtained. It is emphasized that the data presented in Figure 2 and Table II, are all first order velocities. Unpublished results show that experimental velocity jumps, shown in Figure 3, occur at about the times one would compute by use of the equation of state for aluminum.\*

The velocity plateaus in the TNT data are intriguing since according to equation 1) they imply a steady initial pressure in the detonation head followed by a more or less sudden decrease in pressure level. We have interpreted this initial steady pressure to be an induction zone of finite width which precedes the zone of chemical reaction.

<sup>\*</sup>If the first order free surface velocities for Composition B driven aluminum targets are plotted as a function of target thickness, no plateau is observed as it is for TNT, but rather the curve continues to rise toward the zero target thickness axis. In view of the data obtained with TNT, we conclude that a flat top may be present in the Composition B data but that it occurs in such thin targets that we are unable to observe it with the pin technique.



# The Induction Zone in Cast TNT

Material in a detonation wave propagating through a homogeneous explosive has a high velocity in the direction of wave propagation. If the length of the induction zone is "a", the induction time can be obtained from

10) 
$$\Delta t = \frac{a}{D_e - u_e}$$

where  $D_e$  is the steady state detonation rate (6880 meters/second) and ue is the particle velocity in the induction zone. By use of the acoustic approximation, equation 3) we can immediately obtain ue from equation 2) and the measured plateau velocity for cast TNT. The induction zone length, a, is approximately 0.216 (6.880-1.97) or 1.06 mm. This simple analysis does not apply to low density TNT.

The Induction Zone in TNT at a Bulk Density of 0.624 g/cc

From equations 5) and 7) previously developed, one can compute changes of internal energy which occur behind the incident and reflected shock fronts at the target interface. By assuming the heat capacity at constant volume for the unreacted TNT to be approximately constant and equal to 1/3 cal/g., we can estimate the temperature behind the initial shock front from the expression

11) 
$$T_1 - 300 = \Delta E_1/\bar{e_v}$$

Similarly, for the total change of internal energy due to the incident and reflected shock, we have

12) 
$$T_t - 300 = \Delta E_t / \overline{c}_v .$$

The estimated temperatures which obtain in the explosive before reaction occurs are set down in Table III for arbitrary values of ue. These computations show that, given an induction zone in the detonation wave, the temperature increase behind the reflected shock front may be adequate to initiate a secondary reaction at the metal interface. Despite such a possibility, curve 5 in Figure 2 shows an initial steady pressure extending to nearly the same target thickness as that for cast TNT. Accordingly we can compute the steady pressure time from

13) 
$$\Delta t_1 + \frac{\Delta \ell_1 - u_1 \Delta t_1}{R_1} = \frac{\Delta \ell_1}{D_1}$$

Table III. Approximate Shock Temperatures in TNT vs. Initial Particle Velocity; /o = 0.624 g/cc

(mm/Msec)	$\frac{\Delta E_1}{(ergs/gx10^{-10})}$	$\begin{array}{c} \Lambda E_{t} \\ (\underline{\text{ergs/gx10}} - 10) \end{array}$	(°K)	(°K)
2.1 2.0 1.9 1.8 1.7 1.6 1.5 1.4 1.3	2.205 2.000 1.805 1.620 1.445 1.280 1.125 0.980 0.845 0.720	6.718 5.646 4.736 3.960 3.292 2.721 2.228 1.757 1.456 1.151	1881 1734 1595 1462 1336 1218 1107 1003 906 816	5118 4349 3697 3140 2661 2252 1898 1560 1344 1125

and compare the results at the two density extremes. Equation 13) is obtained by equating two independent statements for the overtaking time in the metal target. The quantities used are obtained from Figure 4 where  $R_1$  is the velocity of the first rarefaction increment and equals  $u_1 + c_1$ .

A comparison between the two TNT density extremes is given in Table IV.

Table IV. Properties of Shocked Aluminum and the Corresponding Steady Pressure Times for the Plateau Region of Figure 2

Cast TNT	TNT at $P_0 = 0.624$ g/cc		
um = 1.43 mm/microsecond	um= 0.54 mm/microsecond		
cm = 7.45 " "	cm= 6.11 " " "		
Dm = 7.12 " "	Dm= 5.94 " " "		
Ali = 6.5 mm	Ali= 6 mm		
Ati = 0.216 microseconds	Ati= 0.117 microseconds		

It can be seen that the steady pressure time for cast TNT is nearly double that for the low density explosive despite a higher temperature in the induction zone of the detonation wave in the cast material. This result makes an hypothesis of a secondary detonation reaction in the low density explosive quite plausible, for indeed if the induction zone were being burned by two distinct flame fronts, then material in the induction zone would be consumed at an extraordinary rate. On this basis, we postulate the sequence of events pictured

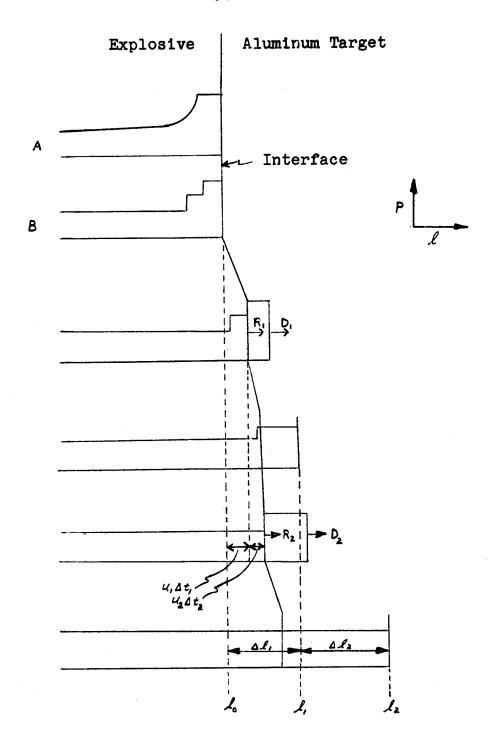


Figure 4. Instantaneous Pressure Profiles During
The Impact of a Detonation Wave With a Stationary
Aluminum Target. A (Probable True Wave Shape), B
(Schematic Step Wave Used in Driving Equations 13
and 18). Reflected Waves Are Assumed to be Negligible

in Figure 5 as occurring at the metal explosive interface for low density TNT. From this figure it can be seen that the steady velocity plateau observed can be associated with a pseudo detonation pressure behind the secondary wave. The high pressure induction peak in the secondary wave would not be observed because its effects would be seen only in extremely thin targets. By assuming the thickness of the secondary induction zone to be negligible in comparison with the primary one, and also that a new C-J condition holds behind the secondary wave, it is possible to compute the length and time of an induction zone undisturbed by a reflected wave. The analysis is as follows:

#### Define

tc = time required for the two flame fronts to
 collide if time zero is the moment of
 contact of the primary induction zone
 with the metal surface

 $u_d = u_e - u_m = particle velocity behind the secondary detonation wave. <math>D_m$ ,  $D_e$  and  $\Delta t$  have their usual meaning.

Let the primary induction zone be of length

$$x = a + b$$

where a is the distance traveled by the primary flame front at the velocity  $(D_e-u_e)$  and b is the distance traveled by the secondary flame front at velocity  $D_d$  during the time required for the flame fronts to collide. The steady pressure time is

$$\Delta t = t_c + t_r$$

Using a coordinate system traveling at the velocity ue, one can quickly visualize the various waves since the induction zone stands still while the metal target impacts it and drives a shock wave into it at velocity Dd. We have then

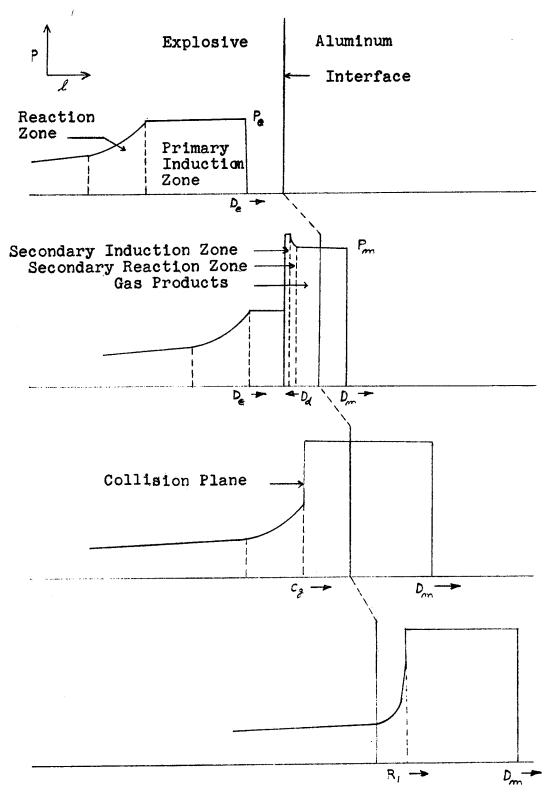


Figure 5. Instananeous Pressure Profiles During the Impact of a Detonation Wave on a High Impedance Metal Surface

14) 
$$t_{c} = \frac{b}{D_{d}} = \frac{a}{D_{e}-u_{e}}$$

$$t_{r} = \frac{b-u_{d}t_{c}}{c_{g}} = \frac{b(1-\frac{u_{d}}{D_{d}})}{c_{g}}$$

therefore

$$\Delta t = \frac{b}{D_d} + \frac{b(1 - \frac{u_d}{D_d})}{c_g}$$

$$= b \left[ \frac{c_g + D_d - u_d}{D_d c_g} \right]$$

If the C-J condition,  $D_d = c_g + u_d$ , approximately holds we obtain

$$\Delta t = \frac{2b}{D_d}$$

Solving equation 15) for b and substituting the result into equation 14) we have

16) 
$$b = \frac{(\Delta t) D_d}{2}$$

$$a = \frac{\Delta t}{2}$$
 (De - ue)

From equations 16) we can compute the length of an undisturbed induction zone if values of ue and the velocity of the reflected detonation, Dd, can be estimated. According to Table I an upper limit for ue is probably about 1.7 mm/microseconds. The density behind the reflected wave is already greater than crystal density under these conditions and the corresponding velocity of a pure shock wave is 3.525 mm/microseconds. However, if the reflected wave went over into detonation, it would be feeding into material at density 1.130 grams/cc, At this loading density, the detonation velocity is greater than 5 mm/microseconds and therefore the pure shock front would be outrun by a detonation wave. Incoming mass at velocity ue would then meet a wave having a velocity higher than the 3.525 mm/microseconds.

It follows then that if a secondary detonation reaction occurs, a value of ue as high as 1.7 is not possible. Continuing in this manner, we have chosen that value of ue where the velocities  $D_r$  of a reflected pure shock and  $D_d$  of a detonation wave are equal. These values are graphed in Figure 6 and yield a value of  $u_e = 1.46$  mm/microsecond. Numerically we have

 $\Delta t$  = 0.117 microseconds  $D_d$  = 5.55 mm/microsecond  $D_e$  = 3.80 " "  $u_e$  = 1.46 " "

and therefore the induction zone length for the steady state wave is

x = a + b = 0.325 + 0.137 = 0.46 millimeters

and the induction time for an undisturbed detonation wave is

$$\gamma = \frac{x}{D_e - u_e} = 0.20 \text{ microseconds}$$

The induction time computed for the low density TNT is very close to the steady pressure time obtained with cast TNT. Since in the later case we assume the acoustic approximation to hold, we then imply that the steady pressure time is approximately the induction time also. Having obtained the result that the induction times in the TNT density extremes are nearly identical, we conclude that an induction time in any intermediate density has a similar value. From equation 1) we can now compute the induction zone pressure in the low density TNT. Thus,  $p = 0.624 \times 3.8 \times 1.46 = 34.6 \text{ kilo-}$ If the postulates leading to equation 16) are correct, it is doubtful that C-J pressures can be obtained from our experimental data on low density TNT since the rarefaction, constituting the reaction zone, has propagated through a burned gas region and spread out to such an extent that the pressure corresponding to the end of the reaction is not clear cut. Fortunately this is not the case with cast TNT and the C-J plane probably arrives at the target interface relatively undisturbed by a reflected wave.

### The Reaction Zone in Cast TNT

The reaction zone front in cast TNT has a rate of  $(D_e-u_e)=4.91$  mm/microseconds relative to the moving particles. Considering the steady state detonation, the C-J plane approaches the metal interface at about this rate also.

Upon arrival a range of unloading waves will have already propagated into the target while the pressure at the interface fell during chemical reaction. Because each successive unloading increment propagates at a lower velocity than the one preceding, the entire range of pressure levels at the interface will propagate into the target and appear at a given distance from the interface.

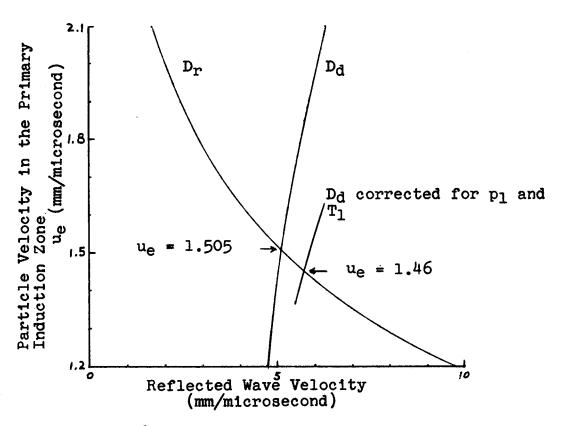


Figure 6. Reflected Wave Velocity as a Function of the Particle Velocity  $u_e$ , Striking the Aluminum Targets. Crystalline TNT at a Loading Density of 0.624 g/cc.

If we assume that reaction zone effects do not extend as far as 1 inch into the aluminum, then the last two data points (for 1 inch and 1 1/2 inch target thicknesses) are characteristic of a smoothly decreasing pressure behind the C-J plane. We can approximate this by assuming the pressure decrease to be of the same type observed in the aluminum-aluminum impact experiments. According to our equation of state for aluminum we can

write the equation u = 0.7705 D - 4.052 over the range of aluminum densities from 3.1 to 3.5 grams/cc. This density range completely covers the data for cast TNT. The equation is consistent to within 10 meters/seconds in D over the restricted range. Since u changes but slowly over the post C-J part of the cast TNT curve in Figure 2, D can be described by a simple quadratic function of time and distance

$$t = b_0 + b_1 \ell + b_2 \ell^2$$

where  $\mathcal{L}$  is the thickness of aluminum penetrated by the shock wave. Therefore we can write

17) 
$$D = \frac{d\ell}{dt} = \frac{1}{b_1 + 2 b_2} \ell$$

Substituting the value of D from equation 17) into the linear relation between u and D and evaluating the constants from the experimental us at the 1 and the 1 1/2 inch target thicknesses, we find for  $\ell$  = 0 that  $D_0 = 6.934$  and  $u_s = 2.581$  mm/microseconds. The computed value of us for zero target thickness is a point on an equation going through the data points for the 1 and 1 1/2 inch target thicknesses. At  $\mathcal{L} = 19.2$  mm the experimental velocity curve deviates from the theoretical curve through these three points. The corresponding free surface velocity, 2.350 mm/microsecond, is interpreted as that due to the C-J pressure in the explosive. The cast TNT curve in Figure 2 is therefore drawn in such a manner that it is somewhat flattened after the point  $\ell$  = 19.2 mm. Thus, the curve shows effects of reaction zone pressures extending from the target thickness  $\ell$  = 6.5 mm to the thickness  $\ell$  = 19.2 mm. Equation 13) can be extended to this portion of the curve by dividing the free surface velocity into equal increments. In general

18) 
$$\Delta t_i + \sum_{\kappa=1}^{m} \Delta t_{\kappa} + \left[ \frac{\Delta \mathcal{L}_i + \sum_{\kappa=1}^{m} \Delta \mathcal{L}_{\kappa} - u_i \Delta t_i - \sum_{\kappa=1}^{m} u_{\kappa, \kappa+1} \Delta t_{\kappa}}{R_{m+1}} \right] = \frac{\Delta \mathcal{L}_i}{D_i} + \sum_{\kappa=1}^{m} \frac{\Delta \mathcal{L}_{\kappa}}{D_{\kappa, \kappa+1}}$$

In this equation,  $u_{k,k+1}$  and  $D_{k,k+1}$  are average slopes for discrete increments of shock front and target interface positions as shown in Figure 7.

In order to estimate the reaction time in cast TNT we have divided the free surface velocity curve

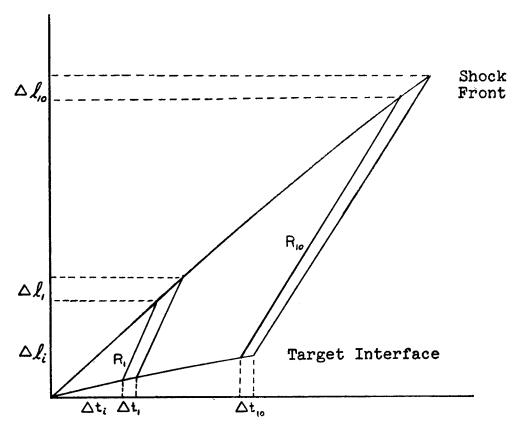


Figure 7. Overtaking of the Shock Front in Aluminum by Rarefactions from the Metal-Explosive Interface

between 1 = 6.5 and 1 = 19.2 mm/microsecond into 10 equal increments of us. Equation 18) was then evaluated by using the data shown in Table V. Our estimate of the reaction time is about 0.29 microseconds and the total time between the shock front and the C-J plane is about 0.51 microseconds. This time compares very favorably with a value obtained by Copp and Ubbelohde (10) by the method of case expansion. These authors have stated that their measured time is that to the "equilibrium of primary processes of explosive decomposition". By interpreting this to mean the induction plus reaction time, the data from the two different experimental methods are in good agreement.

<i>L</i> (mm)	u <sub>s</sub> /2 (mm/4sec)	R <sub>k</sub> (mm/ksec)	wk, k+l (mm//sec)	D <sub>k</sub> , k+l (mm/ksec)	Δt <sub>k</sub> (/rsec)	$ \Delta t_1 + \sum_{k=1}^{\infty} \Delta t_k \\                                    $
0 6.50 6.84 7.26 7.88 8.75 9.90 11.15 12.80 14.70 16.80 19.20	1.430 1.430 1.404 1.379 1.354 1.328 1.302 1.277 1.252 1.226 1.200 1.175	(R <sub>1</sub> )8.885 (R <sub>2</sub> )8.823 (R <sub>3</sub> )8.761 8.700 8.638 8.576 8.514 8.452 8.390 8.329 8.267	1.417 1.392 1.366 1.341 1.315 1.290 1.264 1.239 1.213 1.188	7.098 7.066 7.032 6.999 6.966 6.933 6.899 6.867 6.833	0.21335 0.00888 0.00747 0.01338 0.02059 0.02835 0.02999 0.04089 0.04637 0.04996 0.05611	0.22223 0.22970 0.24308 0.26367 0.29202 0.32201 0.36290 0.40927

Induction time  $\Delta t_1 = 0.213 \, \text{Asec.}$ Time length of detonation head  $\Delta t_1 + \sum_{k=1}^{10} \Delta t_k = 0.515 \, \text{Asec.}$ Reaction time  $\sum_{k=1}^{10} \Delta t_k = 0.302 \, \text{Asec.}$ 

Table V. Numerical Data for Figure 7

# The Chapman-Jouguet Pressures

Since  $u_s=2.860$  at the peak and about 2.350/mm/microsecond for the C-J point, the corresponding particle velocities in cast TNT are 1.979 and 1.626 mm/microsecond respectively. Using a value of 6.880 mm/microsecond for the detonation velocity and 1.58 grams/cc for the density, we find from equation 1) that the pressure in cast TNT is 215 kilobars at the peak and 177 kilobars at the C-J point. Thus, the over-pressure in the induction zone is about 121% of the C-J pressure.

For the snow flaked packed TNT the C-J pressure can be estimated from the Jones equation (11).

19) 
$$\frac{D_{e}}{U_{C-J}} = (2 + \alpha) \left(1 + \frac{\rho_{o}}{De} \cdot \frac{dD_{e}}{d\rho_{o}}\right)$$

Assuming a value for the Jones constant,  $\alpha = 0.25$  one computes  $u_{C-J} = 1.1$  mm/microsecond and  $p_{C-J} = 26.2$  kilo=bars. For the induction zone pressure we find p to be 34.6 kilobars and therefore the over-pressure in the induction zone is about 132% of C-J. In view of the approximations involved, the pressure ratios for the two extreme TNT densities can be considered to be essentially the same.

#### Conclusions

Induction times have been shown to exist in the steady state detonation wave of TNT at various bulk densities. It is approximately the same for all densities, namely 0.2 to 0.25 microseconds. The reaction time has also been measured in cast TNT and amounts to approximately 0.29 microseconds. The total time from the shock front to the C-J plane is therefore 0.51 microseconds in the cast explosive.

The flat top observed in the free surface velocity of aluminum target is not to be interpreted as evidence of no reaction in the induction zone but rather that it is occuring at a negligible rate in comparison with the reaction zone proper. We have drawn the curves in the manner shown because we believe we are not justified in assuming a more detail contour from the data on hand.

The plateau is interpreted as due to a thermal induction period in the initiation of the explosive and is evidence that the reaction in TNT progresses by a thermal mechanism. Grain burning is not necessarily excluded by these results for the reason that time lags in building up to high rates of deflagration can still exist. Mathematically, the data has been treated as though the explosives were shomogeneous fluids. can be readily admitted in the detonation of gaseous and liquid systems, and may also be true for cast TNT. It should be pointed out that the percentage voids in the snow flaked packed TNT is quite large, and although the treatment appears straightforward, it is admittedly difficult to understand how material in the induction zone can be compressed to a value far below the crystal density while sustaining a pressure of at least 35 kilobars.

### Acknowledgements

The authors wish to express their appreciation to the following persons who contributed greatly to the success of these experiments: James Counihan, Halcom Curtis and Donald Danielson who carried out the firing program, Miss Mary Fix by whose considerable effort the results were computed and Keith Mason and Joseph Schleicher who constructed all the target assemblies.

#### REFERENCES

- (1) Y. B. Zeldovich; J. Exptl. Theoret. Phys (USSR) 10 542 (1940)
- (2) J. von Neumann; OSRD Report No. 549 (1942)
- (3) W. Doring; Ann. Physik 43 421 (1943)
- (4) B. Lewis and G. von Elbe; Combustion, Flames and Explosions of Gases, p. 604. Academic Press Inc. New York, 1951
- (5) R. J. Finkelstein and G. Gamow, NavOrd Report 90-46, (1947) Confidential
- (6) G. B. Kistiakowsky; Proceedings of the Conference on the Chemistry and Physics of Detonation, p. 39 (1951) Confidential
- (7) H. Dean Mallory; The Propagation of Shock Waves in Aluminum, J. Appl. Phys. (In preparation)
- (8) J. E. Ablard; ONR Report, Proceedings of the Conference on the Chemistry and Physics of Detonation, p. 82 (1951). Confidential
- (9) H. Dean Mallory; On The Existance of a Binary Reaction Zone at a Metal-Explosive Boundary During Detonation. NavOrd Report 3772.

  July 1954.
- (10) J. L. Capp and A. R. Ubbelohde; The Effect of Inert Components on Detonation, Trans. Faraday Soc. 44 658 (1948)
- (11) H. Jones; The Properties of Gases at High Pressures Which Can be Deduced from Explosion Experiments, Third Symposium on Combustion, Flames and Explosion Phenomena p. 590 Williams and Wilkins Co. 1949

### CALCULATION OF THE DETONATION PROPERTIES OF SOLID EXPLOSIVES WITH THE KISTIAKOWSKY-WILSON EQUATION OF STATE

W. Fickett and R. D. Cowan Los Alamos Scientific Laboratory Los Alamos, New Mexico

#### 1. INTRODUCTION

In an attempt to obtain a working equation of state for the gaseous products involved in the calculation of detonation phenomena, we have investigated a modification of an empirical equation of state first proposed by Halford, Kistiakowsky, and Wilson (1):

$$\frac{PV_g}{RT} = F(x) = 1 + xe^{\beta x}$$

$$x = \frac{k}{V_g(T + \theta)^{\alpha}} \quad k = \chi \sum_{i=1}^{n} x_i k_i$$
(1.1)

Here  $V_g$  is the molar gas volume,  $x_i$  is the mole fraction of component i, and the sum extends over all chemical components of the gaseous mixture. The quantities  $\alpha$ ,  $\beta$ ,  $\chi$ ,  $\theta$ ,  $k_i$  are empirical constants, the  $k_i$  having the nature of covolumes. The values  $\alpha=0.25$  and  $\beta=0.30$ , which were chosen originally to give agreement with experimental data  $\binom{1}{1}$ , have been used in most of the previous work with this equation of state. However, different values of  $\chi$  and several sets of  $k_i$ 's have been determined from experimental data (cf. references 1, 2, 3 and Table III). We have treated all of the parameters  $(\alpha, \beta, \chi, k_i$ 's) as adjustable in an effort to determine a set which would allow the calculations to reproduce a set of experimental data which includes both the variation of detonation velocity with loading density  $(D - P_0)$ , and the Chapman-Jouguet pressure  $(P_{C-J})$  at high loading density for a group of five related explosives (see Table II).

With the value  $\theta=0$  which has been previously used, it may easily be seen that the equation of state has a minimum in P vs. T (for constant  $V_g$  and composition). With  $\alpha=0.25$  and with values of  $V_g$  appropriate to the detonation region this minimum occurs near  $0^{\circ}K$ , but with  $\alpha=0.5$  it moves up to 2000 or  $3000^{\circ}K$ .

We have used the arbitrary value  $\theta = 400^{\circ}$ K for all values of  $\propto$ ; this has proved to be large enough to eliminate the minimum throughout the volume region characteristic of plane detonations, and yet is small compared with the values of T encountered.

The calculations are complicated by the possible presence of solid carbon. We have assumed carbon to be present as graphite and treated its equation of state as known, using a form originated at this laboratory (4):

$$P = P_1(V_S) + a(V_S)T + b(V_S)T^2$$
 (1.2)

where, with P in megabars and T in volts (i.e., in units of  $11,605.6^{\circ}$ K),

$$P_1(V_s) = -2.467 + 6.769\eta - 6.956\eta^2 + 3.040\eta^3 - 0.3869\eta^4$$
  
 $a(V_s) = -0.2267 + .2712\eta$ 

$$b(V_s) = 0.08316 - 0.07804\eta^{-1} + 0.03068\eta^{-2}$$

$$\eta = \frac{V_s^0(T^0)}{V_s} ; T^0 = 25^0C$$

#### THEORY

If solid carbon is considered, expressions are needed for the thermodynamic functions of both gas and solid phases; these are summarized here:

For the gaseous component with equation of state (1.1):

$$E = \sum x_{1}(E^{\circ}-H_{\circ}^{\circ})_{1} + \sum x_{1}(H_{\circ}^{\circ})_{1} + RT \int_{\overline{T}+\overline{\Theta}}^{\times} (F-1)$$
 (2.1a)

$$S = \sum_{i} x_{i} (S^{O})_{i} - R \left[ \sum_{i} x_{i} \ln x_{i} + \ln \left( \frac{P}{P^{O}} \right) \right] + R \left[ \ln F - \frac{e^{\beta x} - 1}{\beta} + \frac{\alpha T}{T + \theta} (F - 1) \right]$$
(2.1b)

$$\mathcal{H}_{1} = (F^{O} - H_{O}^{O})_{1} + (H_{O})_{1} + RT \ln \left( \frac{x_{1}P}{P^{O}} \right)$$

$$-RT \left[ \ln F - \frac{e^{\beta x} - 1}{\beta} - \frac{k_{1}}{k} (F - 1) \right]$$
(2.1c)

where the gas imperfection factor F is defined in equation (1.1) and should not be confused with the free energies  $F^O$  and  $F_S^\prime$ .

For the solid with equation of state (1.2):

$$E = (H^{\circ} - H_{\circ}^{\circ}) + H_{\circ}^{\circ} - (PV_{s})^{\circ} + \int_{V_{s}^{\circ}}^{V_{s}} \{b(V)T^{2} P_{1}(V)\} dV \qquad (2.2a)$$

$$S = S^{\circ} + \int_{V_{S}^{\circ}}^{V_{S}} \left\{ a(V) + 2b(V) T \right\} dV \qquad (2.2b)$$

$$\mathcal{M} = (F^{O} - H_{O}^{O}) + H_{O}^{O} + F_{S}^{\prime}$$
 (2.2c)

where

$$F'_{s} = PV_{s} - (PV_{s})^{\circ} - \int_{V_{s}^{\circ}}^{V_{s}} \{P_{1}(V) + a(V)T + b(V)T^{2}\} dV$$

For chemical equilibrium:

$$\ln \mathcal{N}_{g}(n_{i})^{\gamma_{i}} = \ln K_{p}(T) - \left[\sum_{g} \gamma_{i}\right] \left[\ln \left(\frac{P}{n_{g}P^{\circ}F}\right) + \frac{e^{\beta x}-1}{\beta}\right] - \left[\sum_{g} \gamma_{i}k_{i}\right] \left[\frac{F-1}{k}\right] - \frac{\gamma_{s}F_{s}'}{RT}$$
(2.3)

where

-RT ln 
$$K_p(T) = -\sum_i \vec{y}_i (F^o - H_o^o)_i - \sum_i \vec{y}_i (H_o^o)_i$$

(one such equation for each independent chemical reaction).

In (2.1)-(2.3) E, S, and  $\mu$  are internal energy, entropy, and chemical potential, respectively. A superscript o refers to the reference state (ideal gas or real

solid at pressure  $P^O$  and temperature T)\*, with  $H_O^O$  being the enthalpy of formation from the elements;  $\mathbf{x_i}$  and  $\mathbf{n_i}$  are the mole fraction and number of moles of component i;  $\mathbf{n_g} = \sum_{g} \mathbf{n_i}$ . In (2.3) the  $\mathbf{N_i}$  are the coefficients of the chemical reaction, positive for products and negative for reactants, and the subscript g for a sum indicates it is for gaseous components only.

The thermodynamic state of the detonation products is defined by the Hugoniot equation (6)

$$h = E - E_O - \frac{1}{2} (P + P_O) (V_O - V) = 0$$
 (2.4)

and the Chapman-Jouguet condition

$$\left(\begin{array}{cc} \frac{\partial P}{\partial V} \right) = -\frac{P - P_{O}}{V_{O} - V} \tag{2.5}$$

In(2.4) the subscript o refers to the undetonated explosive, with  $E_{\rm O}$  given by

$$E_o = (\Delta H_f)_e + \sum_j N_j (H^o(T_o) - H_o^o)_j - P_o V_o$$
 (2.6)

where  $(\Delta H_f)_e$  is the molar enthalpy of formation of the explosive at  $T_o$  and  $N_j$  is the number of moles of element j in one mole of explosive.

<sup>\*</sup>In evaluating the thermodynamic functions for the solid we have neglected (PV<sub>s</sub>), and approximated  $V_s^o$  by  $V_s^o(T=25^oC)$ .

<sup>\*\*</sup>In the usual statement of the C-J condition,  $\begin{pmatrix} \frac{\partial}{\partial} & P \\ \frac{\partial}{\partial} & V \end{pmatrix}_S$  is to be evaluated for equilibrium composition. However, Kirkwood and Wood, J. Chem. Phys., in press, have recently shown that this derivative should be evaluated with frozen composition. Our calculations have used the older statement of the C-J conditions, but there is very little difference between the two, at least for our equation of state. Check calculations showed that the use of the correct C-J condition would decrease  $P_{C-J}$  by less than one percent at the lowest loading densities of interest ( $P_{C} = 1.2$ ) and made almost no change at high loading density.

#### 3. CALCULATIONS

The detonation products were assumed to be made up of the following chemical components:

$$1)H_2$$
,  $2)CO_2$ ,  $3)CO$ ,  $4)H_2O$ ,  $5)N_2$ ,  $6)NO$ ,  $7)C(graphite) (3.1)$ 

Oxygen was not included, since none of the explosives considered were more oxygen rich than RDX, which balances to N<sub>2</sub>, H<sub>2</sub>O, and CO. In some preliminary calculations on IBM CPC equipment some of the components considered by Kirkwood, et al., (5) viz. NH<sub>3</sub>, CH<sub>4</sub>, and OH were also included; these were found to be present in small though not negligible amounts.

For the final calculations, however, the set (3.1) was used in order to simplify the solution of the equilibrium equations and thereby reduce the machine time required. Although this set is rather restricted, components of differing size  $(H_2, CO_2)$  and with positive heat of formation (NO) are included.

It was found that with this set of components the determination of the equilibrium composition, given k,  $n_{\rm g}$ ,  $v_{\rm g}$ , and T, could be reduced analytically to the solution of one equation in one unknown. With solid carbon present this unknown was  $n_{\rm CO}$ ; with carbon absent,  $n_{\rm H_2}$ .

The reference-state thermodynamic functions and enthalpies of formation were taken from the tables published by the National Bureau of Standards. (7) The enthalpies of formation of the explosives are given in Table I.

The calculations were done on IBM 701 digital computers. It was found quite feasible to code a single problem to calculate adiabatic or Hugoniot curves, as well as detonation velocities. In order to produce points on these curves Eqs. (1.1), (1.2), and (2.1b), (2.2b) (for an adiabat) or (2.4) (for a Hugoniot) were solved by iteration to obtain values of V and T for the given S or h (=0), with the composition given by Eqs. (2.3) and the mass balance relations. The detonation velocity was determined by finding the point on the Hugoniot where

$$D = V_{o} \left[ (P-P_{o})/(V_{o}-V) \right]^{\frac{1}{2}}$$
 (3.2)

had its minimum value; this is equivalent to satisfying the C-J condition (2.5) with  $(\partial P/\partial V)_s$  evaluated with

equilibrium composition.

TABLE I
Heats of Formation of the Explosives

Explosive	(ΔH <sub>f</sub> ) <sub>e</sub>				
	kcal/mole at 25°C				
RDX <sup>a</sup>	+ 14.71				
$\mathtt{TNT}^{\mathtt{b}}$	- 17.81				
°3.3 <sup>H</sup> 6.2°6 <sup>N°</sup> 5.6	+ 0.49				
<sup>a</sup> E. J. Prosen (NBS), privat	e communication.				
bG. Stegeman, NDRC Division-8 Interim Report PT-7 (1943).					
<sup>c</sup> L. Sitney (LASL), unpublished communication.					
dExplosive presently classified.					

The time required for the calculation of one adiabat or Hugoniot point was about 20 sec.; for a detonation velocity, an average of about 140 seconds.

#### 4. EFFECTS OF THE PARAMETERS

In order to determine the effects of the various parameters on the calculated D-  $\rho_{\rm O}$  curve and P<sub>C-J</sub>, exploratory calculations were carried out for one explosive, 65/35 RDX/TNT. In order to save calculating time, these were carried out under the assumption of a fixed product composition resulting from the following decomposition equation

$$C_q H_r O_s N_t = \frac{r}{2} H_2 O + (s - \frac{r}{2}) CO + (q - s + \frac{r}{2}) C + \frac{t}{2} N_2$$
 (4.1)

A set of geometrical covolume values (Table III) was used, though with fixed composition the individual values of the  $\mathbf{k_i}$  are unimportant. The other parameters were varied from the values

$$\alpha = 0.6, \quad \beta = 0.06, \quad \chi = 30 \quad (4.2)$$

which were found to give approximate agreement with the experimental D -  $\rho_0$  and  $P_{C-J}$ . The results of the calculations are summarized in Figures 1 through 5.\*

Viewed from the standpoint of attempting to reproduce experimental data, the effects of the parameters may be pictured as follows:

The value of  $\chi$  may be changed to raise or lower the D -  $\rho_{\rm O}$  curve without greatly changing its shape (Fig. 1);  $\beta$  may then be used to change its shape and slope while  $\chi$  is varied so as to preserve a given value of D at one point (Fig. 2). Then the calculated C-J pressure may be changed by varying  $\alpha$  -  $\beta$  and  $\chi$  always being adjusted so as to best match D -  $\rho_{\rm O}$  (Figs. 3 and 4). Alpha also has a considerable effect on the C-J temperature (Fig. 3). There exist no accurate experimental data on  $T_{\rm C-J}$ , but it is noteworthy that the T vs.  $\rho_{\rm O}$  curve for  $\alpha$  = 0.45 is similar to that obtained at this laboratory from preliminary calculations with the Lennard-Jones-Devonshire freevolume equation of state. (8)

In order to gain some idea of the effect of the carbon equation of state, calculations were made with the assumption that the carbon retained its normal volume, and also with the two equations of state for carbon mentioned in the footnote below. The results are shown in Figure 5.

#### 5. RESULTS

By assuming a fixed product composition and varying the parameters as described above, a set of values for  $\propto$ ,  $\beta$ , and X was found which gave results in good agreement

\*These parameter studies differed from the final calculations in that they used a more incompressible equation of state for carbon than that which was finally adopted and used in the main calculations. The equation of state for carbon was first based on an interpolation between the static measurements of P. W. Bridgeman, Proc. Am. Acad. Sci., 76, 55-87 (1948), and Thomas-Fermi-Dirac calculations made by R. D. Cowan at this laboratory (unpublished communication). Recently, however, J. M. Walsh has obtained points on the shock Hugoniot of graphite (unpublished communication) by a dynamic method similar to that which he has used for aluminum, Phys. Rev. (in press). The carbon equation of state used in the final calculations, Eq. (1.2), was based on this work and was considerably more compressible than the one described above.

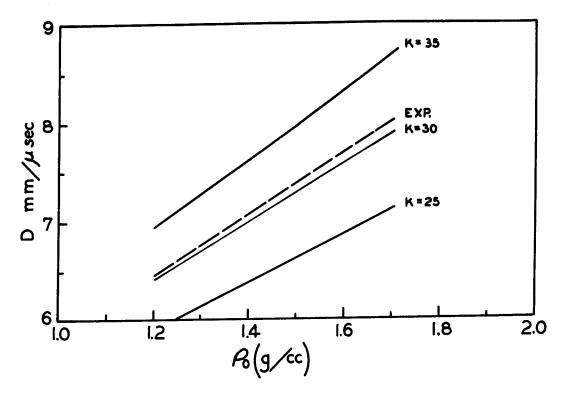


Fig. 1. The Effect of  $\kappa$  on D -  $\rho_0$ .

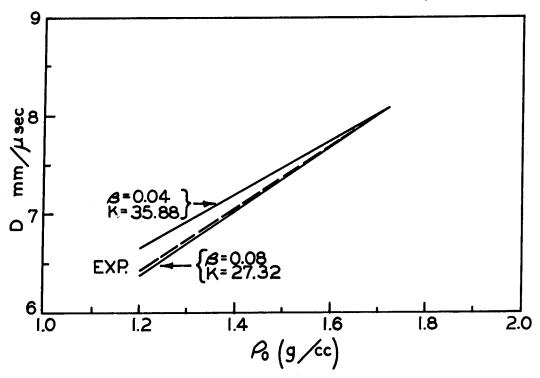


Fig. 2. The Effect of  $\beta$  on D -  $\rho_0$ ;  $\kappa$  Chosen to Match Experimental D at One Point.

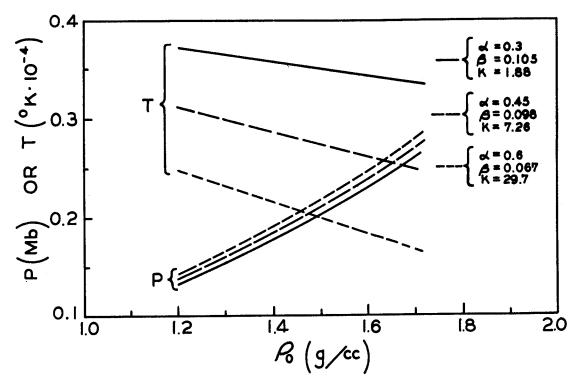


Fig. 3. The Effect of  $\alpha$  on P vs.  $\rho_0$  and T vs.  $\rho_0$ ;  $\beta$  and  $\kappa$  Chosen to Match Experimental D -  $\rho_0$ .

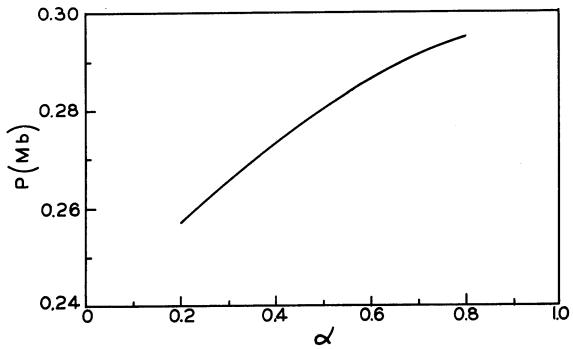


Fig. 4. The Effect of  $\alpha$  on  $P_{C-J}$  ( $\rho_O = 1.715$ );  $\beta$  and  $\kappa$  Chosen to Match Experimental  $D - \rho_O$ .

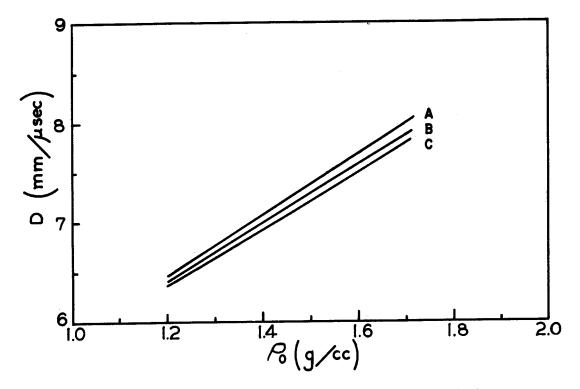


Fig. 5. Effect of the Graphite Equation of State on  $D - \rho_0$ : A - Incompressible, B - Graphite Equation of State used in the Parameter Studies, C - Graphite Equation of State used in the Final Calculations (see footnote on p. 271).

with experiment for 65/35 RDX/TNT. It was found that with equilibrium composition (and the "geometrical"  $\mathbf{k_i}$  discussed below) a not very different set also produced good agreement. The question of how well a single set of parameters could be made to serve for several explosives was then investigated.

The experimental data used were measurements of D -  $\rho_{\rm O}$  and  $P_{\rm C-J}$  at maximum loading density for a group of five related explosives. (9,10,11,12) These data are given in Table II and were obtained as follows:

Measurements of the detonation velocity for infinite diameter,  $D_{\infty}$ , were made for each explosive at two densities,  $\rho_{O}=1.2$  and the highest  $\rho_{O}$  obtainable by pressing or casting. (Values of  $D_{\infty}$  were obtained by firing charges of different diameter d and extrapolating D vs. 1/d). It was assumed on the basis of previous work,

TABLE II

Experimental Data for Explosives

Explosive and	Detonation Velocity <sup>a</sup> $D = A P + B \cdot (m/sec$	tion Velocity <sup>a</sup> (P. + B. (m/sec)	tion Velocity <sup>a</sup> Dural b P + B, (m/sec) Pressure		C-J Pressure <sup>C</sup> (Mb)	o
Density for P <sub>C-J</sub>	<b>A</b>	, , B	(Mb)	Exp.	Calc.	Diff.
RDX (% = 1.800	3466	2515	0.398	0.341	0.3488	+ 2.2%
$c_{3.5}H_{6.2}^{0}e_{N5.6}^{d}$ $\rho_{o} = 1.748$	3233	2785	0.378	0.316	0.3194	+ +
78/22 RDX/TNT Po = 1.755	3193	2702	0.382	0.317	0.3106	2.2
65/35 RDX/TNT Po = 1.715	3127	2673	0.358	(0.286) <sup>f</sup> 0.292	0.2843	8.2
$\mathbf{P}_{o} = 1.640$	2799	2360	0.226	0.177	0.2066	+ 16.6%

d Explosive presently classified

 $^{\rm e}$  More work on the TNT D -  $^{\rm c}$  curve is in progress

f Reference 14

b Reference 10

c See text

a Reference 9

both at this laboratory and elsewhere (13) that over this range of loading density D vs.  $c_0$  could be represented by a straight line within experimental error.

The dural pressures in Table II were obtained by measurements of shock and free-surface velocities in dural plates driven by the appropriate explosive. (10) The explosive C-J pressure P<sub>1</sub> is then given in terms of the metal pressure P<sub>1</sub> by the matching conditions at the H.E.-metal interface: (14)

$$\frac{P_{1}}{P_{t}} = \frac{1 + R \left( \frac{e_{01}D_{1}}{e_{01}D_{t}} \right)}{1 + R} ; R = e_{0r}D_{r}/e_{01}D_{1}$$
 (5.1)

where the subscripts i, r, and t refer to the incident, reflected, and transmitted shocks respectively, and the subscript o refers to material ahead of the shock. All velocities are referred to the material ahead of the shock in question. The value of R need not be known accurately. (14) the so-called "acoustic approximation" R=1 giving results correct to within a percent or so. We have used values of R obtained by calculating shock curves for the detonation products (Table IV).

The measurements of  $P_{C-J}$  and  $D-C_O$  were taken on explosives of slightly differing composition and density, so all the data were corrected to the composition and density values in Table II by means of an error expression obtained by differential analysis of (5.1) with R=1 and making use of the experimental dependence of D on composition and density:

$$\frac{\delta U_{fs}}{U_{fs}} = -0.86 \, \delta \, c_{o} \, -0.0023 \, \delta \, (\% \, RDX) \tag{5.2}$$

in which  $\mathbf{U}_{\text{fs}}$  is the experimentally measured free-surface velocity.

In attempting to determine a set of equation-of-state parameters from this experimental data, we started with a set of "geometrical"  $k_1$  (Table III) based on molecular sizes estimated from both virial-coefficient data and spherical volumes from bond lengths and van der Waals radii. Using these  $k_1$  in preliminary calculations it was found that  $\alpha=0.5$ ,  $\beta=0.09$ ,  $\chi=11.85$ \* would give D -  $\ell_0$ 

<sup>\*</sup>With the  $k_1$  scaled so that  $k_{CO}$  was about the same as that used by Brinkley and Wilson. (2)

and  $P_{C-J}$  close to the experimental values for 65/35 RDX/TNT. However, the agreement for other explosives was rather poor (Fig. 6). A least-squares process was therefore carried out (with this same  $\boldsymbol{\varkappa}$  and  $\boldsymbol{\beta}$ ) to determine a set of  $k_i$  which would give the best agreement with all five explosives. The rather surprising result that the reaction

$$2 CO \rightarrow CO_2 + C \text{ (graphite)}$$

shifts from far left to far right as  $\rho_{\rm O}$  is increased through the range of interest caused us to let points of different  $\rho_{\rm O}$  for the same explosive enter the least squaring on an equal weight with those from different explosives. Accordingly, the least squaring was carried out as follows:

Using a guessed set of  $k_i$ , a value of  $k = \chi \sum x_i k_i$  was determined at four loading densities (1.2, 1.4, 1.6, and maximum) for each of the five explosives by adjusting  $\chi$  in each case until the calculated D was equal to the experimental value. If we designate these values of k as  $k_{obs}$  we then have a set of 20 linear equations for the set of  $k_i$ :

$$\sum_{i} (x_{i})_{r} k_{i} = (k_{obs})_{r}, r = 1...20$$
 (5.3)

These were solved by least squares for a new set of k<sub>i</sub>.\*

Since the determination of so many  $k_{\rm obs}$  is rather expensive in machine time, the final least squaring was started with the  $k_{\rm i}$  from the above trial run and was done only once.

The first result of this process was large negative values for  $k_{\rm H_2}$  and  $k_{\rm NO}$ , probably because  $\rm H_2$  and NO were present in such small amounts. Therefore the equations were solved again with these two covolumes held constant at their original values (multiplied by the average  $\varkappa$  from the determination of all of the  $k_{\rm obs}$ ). Table III contains the resulting  $k_{\rm i}$ , together with our "geometrical" set and

the values obtained by Brinkley and Wilson. The set obtained by Christian and Snay is rather different from any of these. (3)

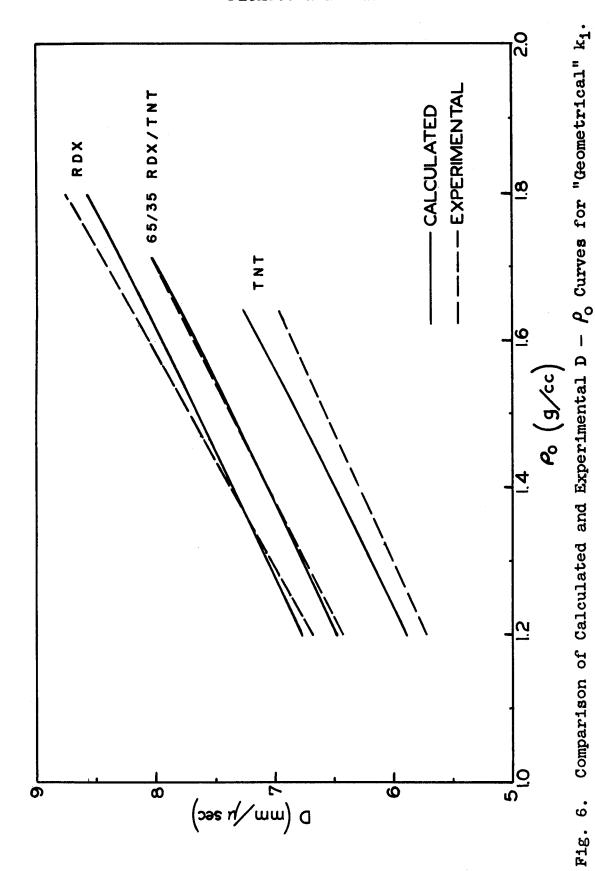
TABLE III Values of k;

Source	ource k <sub>i</sub>						
	$^{\rm H}$	co	CO	H20	$N^{S}$	ИО	
Brinkley- Wilson(2)	153	687	386	108	353	233	
"Geometrical"	<sup>a</sup> 180 <sup>b</sup> 2133	670 7940	390 4622	360 4267	380 4504	350 4148	
Least Square	2133	6407	3383	3636	6267	4148	

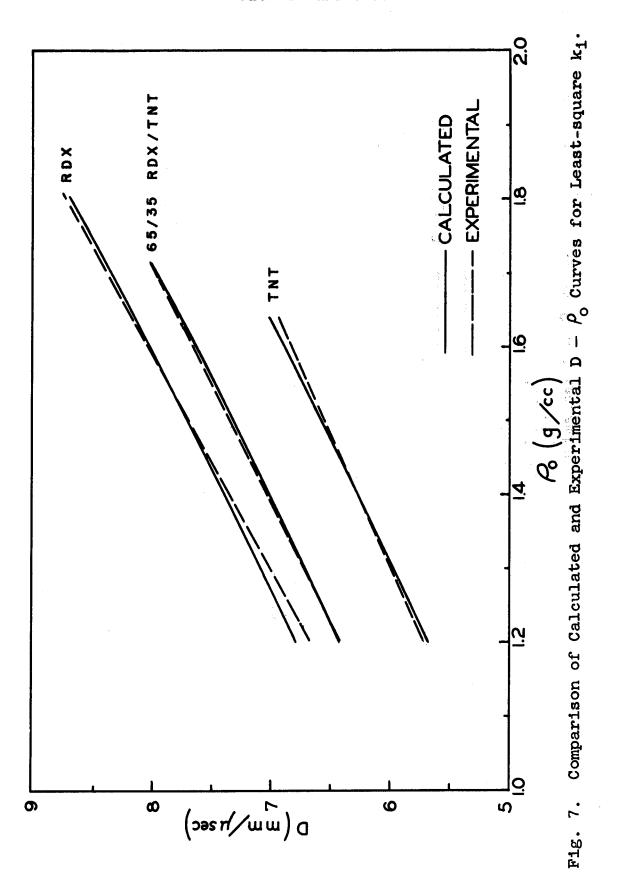
<sup>&</sup>lt;sup>a</sup> Original set chosen so that  $k_{CO}$  would be about the same as that used by Brinkley-Wilson.

In Figures 6 and 7 the calculated results for D -  $\rho_0$  are compared with experiment for both the geometrical and the least-square  $k_i$ . (To avoid confusion, results for only three explosives are shown; the others are qualitatively similar.) It can be seen that with the least-square  $k_i$  fairly good agreement is obtained. The values of the parameters thus determined are

b Scaled by the average X (11.85) from the determination of all of the  $k_{\rm obs}$  (see text).



**397**.



398

k; = least-square set, Table III.

The C-J pressures calculated with this set of parameters are compared with the experimental values in Table II.

The variation of C-J temperature and pressure with loading density for three explosives is shown in Figure 8. In Table IV are given (for 65/35 RDX/TNT) some points on the adiabat passing through the C-J point and also on the shock Hugoniot for the detonation products which originates at the C-J point. It can be seen that for all practical purposes these are identical over the region which can be studied by the interaction of plane detonation waves with stationary metal plates.

### 6. DISCUSSION

As can be seen from Figure 7 and Table II the agreement with experiment is good in the case of D vs.  $\rho_{\text{O}}$ , and, with the exception of TNT, fairly good in the case of  $P_{\text{C-J}}$ . The signs of the disagreement at both extremes of composition may be interesting: The calculated high-density D is low for RDX, high for TNT. For  $P_{\text{C-J}}$ , on the other hand, the calculated values are high for both RDX and TNT.

The disagreement of the calculated and experimental  $P_{C-J}$  for TNT is rather large. Perhaps a more enlightening comparison of theory and experiment can be made with a quantity related to the adiabatic compressibility:

$$\gamma_{C-J}^* = -\frac{V}{P} \cdot \left(\frac{\partial P}{\partial V_S}\right) = \frac{\rho_0 D^2}{P_{C-J}} - 1 \qquad (6.1)$$

This expression can be obtained from Eqs. (2.5) and (3.2) by neglecting  $P_0$ . The values of  $\chi^*$  obtained from the experimental  $P_0$ , D, and P, together with the calculated values of  $\chi^*$  and the fraction of total volume occupied by graphite are shown in Table V.

TABLE IV

Adiabat		ugoniot Thr 65/35 RDX/T	ough the C-J	Point
	•	abat		K Hugoniot
v/v <sub>o</sub>	P	<b>୪*</b>	P	R(Eq.5.1)
0.600 0.625 0.650 0.675 0.700	0.5320 0.4713 0.4198 0.3757 0.3378	2.98 2.96 2.94 2.93 2.91	0.5344 0.4723 0.4201 0.3757 0.3378	1.259 1.202 1.151 1.104 1.063
0.725 0.743(CJ) 0.750 0.800 0.900 1.000	0.3050 0.2843 0.2765 0.2296 0.1643 0.1223	2.90 2.89 2.89 2.85 2.81 2.76	0.3050 0.2843	1.025 1.000
1.2 1.4 1.6 1.8 2.0	0.0743 0.0493 0.0349 0.0259 0.0200	2.69 2.62 2.55 2.50		

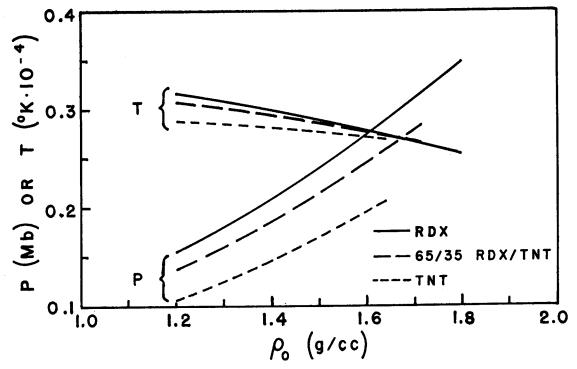


Fig. 8. Chapman-Jouguet Pressure and Temperature Calculated with the Final Set of Parameter Values (5.5).

TABLE V

Explosive	χ* Experimental	%* Calculated	v <sub>s</sub> /v
RDX	3.04	2,908	0.0497
°3.3 <sup>H</sup> 6.2 <sup>O</sup> 6 <sup>N</sup> 5.6	2.93	2.902	0.0633
78/22 RDX/TNT	2.81	2.899	0.0785
65/35 RDX/TNT	2.79	2.887	0.0945
TNT	3.47	2.912	0.1837

It can be seen that both calculated and experimental \*\*'s have a minimum as a function of \*RDX. The former is undoubtedly due principally to the large \*\* of graphite.

(For our graphite equation of state at the TNT C-J point, \*\* = 5.65). Assuming that the usual equilibrium detonation theory applies, there are two possibilities which could explain our low \*\* for TNT: a) the \*\* for graphite is low, or there should be more graphite present; or b) the gas equation of state does not predict a sufficiently large change in \*\* with changes in gas composition, or the gas composition should be different from what it is (probably in the direction of larger components).

In addition to this poor agreement with the experimental  $P_{C-J}$  for TNT, the equation of state (1.1) has other unattractive features. The results obtained with the geometrical  $k_i$  (Fig. 6) and the very different set of  $k_i$  (Table III) required to give agreement with experiment indicate that a priori estimation of the covolumes is likely to be unsatisfactory, and extensive least squaring together with additional experimental data would be required for the introduction of any new chemical components into the detonation products. Also, analytical examination of Eq. (1.1) reveals that as Vg is decreased the minimum in P vs. T at constant Vg will again occur. This unphysical behavior reduces confidence in the equation of state, particularly if it is to be extended to smaller volumes.

This equation of state is probably fairly reliable if its use is restricted to explosives which are similar to those included in a determination of its parameters, and to pressures and volumes not too different from those existing at the Chapman-Jouguet point. There would seem

to be little justification for its use in an extended extrapolation of any sort.

No further work is planned on this equation of state; instead the Lennard-Jones-Devonshire free volume equation of state is being investigated for use along these same lines.

#### 7. ACKNOWLEDGEMENTS

The authors are indebted to Frederick R. Parker for help with the machine computations, and to W. W. Wood for several helpful discussions.

#### REFERENCES

- 1. G. B. Kistiakowsky and E. B. Wilson, Jr., Final Report on the Hydrodynamic Theory of Detonation and Shock Waves, NDRC-Div. B, OSRD Report No. 114, June 1941.
- 2. S. R. Brinkley and E. B. Wilson, Jr., Report on Revised Method of Predicting the Detonation Velocities in Solid Explosives, NDRC-Div. B, OSRD Report No. 905, Sept., 1942; also NDRC-Div. 8, OSRD Report No. 1707, Aug., 1943.
- 3. E. A. Christian and H. G. Snay, Analysis of Experimental Data on Detonation Velocities, NAVORD Report No. 1508, Feb. 1, 1951.
- 4. J. Keller and N. Metropolis, unpublished communication, Los Alamos Scientific Laboratory.
- 5. J. G. Kirkwood, S. R. Brinkley, and J. M. Richardson, The Pressure Wave Produced by an Underwater Explosion, Part V, NDRC-Div. 8, OSRD Report No. 2022, Nov. 1943.
- 6. R. Courant and K. O. Friedrichs, Supersonic Flow and Shock Waves, (Interscience Publ., Inc., New York, 1948), p. 204.
- 7. U. S. National Bureau of Standards, Selected Values of Chemical Thermodynamic Properties, Series III (loose leaf).
- 8. W. W. Wood and W. Fickett, unpublished communication, Los Alamos Scientific Laboratory.
- 9. A. W. Campbell, E. James, M. Malin, C. W. Mautz, and M. J. Urizar, unpublished communication, Los Alamos Scientific Laboratory

- 10. W. E. Deal, The Measurement of C-J Pressure in Explosives, this conference.
- 11. A. W. Campbell, M. Malin, T. J. Boyd, and J. A. Hull, Techniques for the Measurement of Detonation Velocity, this conference.
- 12. A. W. Campbell, M. Malin, and T. Holland, Detonation in Homogeneous Explosives, this conference.
- 13. N. L. Coleburn and T. P. Liddiard, The Rates of Detonation of Several Pure and Mixed Explosives, NAVORD Report No. 2611, Sept. 22, 1952.
- 14. R. E. Duff and E. Houston, Measurement of C-J
  Pressure and Reaction Zone Length in a Detonating
  High Explosive, this conference.

# A SOLID-STATE MODEL FOR DETONATIONS

R. B. Parlin and J. C. Giddings University of Utah Salt Lake City, Utah

#### INTRODUCTION

There are still two fundamental unsolved problems in the analysis of the ideal hydrodynamic-thermodynamic theory of detonation in condensed explosives. One of these is the choice of an equation of state from which to calculate, primarily, the mechanical work done in the Chapman-Jouguet compression. The other involves the question of determining the chemical composition at the Chapman-Jouguet point and from this the change in internal energy. The classical approach employs imperfect gas theory, using equilibrium constants extrapolated from relatively low temperatures, and assumes that the Chapman-Jouguet products are normal, stable molecules. While this is certainly correct for gaseous detonations and probably a good approximation for condensed explosives at very low densities (large void space) there is considerable doubt as to the truthfulness of the basic assumptions at the higher densities. Using an imperfect gas equation of state, for example, it is found necessary to make excessively large fugacity corrections in order to fit experimental detonation velocity data.

The equations of state that have been proposed to cover detonation phenomena are as varied in origin and purpose as in content. Much success has been found, especially in the last decade, in correlating experimental data of many explosives with a common theoretical treatment. The equations developed for this express purpose are capable of approximately predicting results for many explosives. Another line of attack however, has been directed towards predicting detonation velocities without the use of detonation data. The results of such equations do not completely agree with observed values (as might be expected, considering the difficulty of a rigorous derivation of such an equation of state) but they are sufficiently accurate to suggest the essential correctness of the usual thermodynamic-hydrodynamic approach to the detonation process.

In the first class, the methods of Cook (1), Halford, Kistiakowsky and Wilson and others, have led to especially fruitful

results in predicting detonation velocities. An approach by Jones has also been used, but not as extensively. Both Cook and Jones have used a modified Abel equation of state, Cook using the restrictive condition that  $(\partial \alpha/\partial T) = 0$  (where  $\alpha$  is the coverume), whereas Jones has used the condition that  $(\partial \alpha/\partial V) = 0$ . Previous to this the Abel type of equation was quite useful when  $\alpha$  was regarded as a constant dependent upon initial loading density (4). This form of the equation is, of course, convenient for its simplicity.

In the latter class, Jones (5) applied data from high-pressure measurements on nitrogen to a solid state model, and obtained values about 17 per cent above the observed detonation velocities. Kihara and Hikita(6) have derived a virial type of equation with the intermolecular forces assumed to be given by the repulsive term only of a Lennard-Jones type equation. The exponent of the distance was determined from detonation data, and was found to have the value of 9, which agrees quite well with kinetic theory measurements. Cottrell and Patterson(7) have used the values for the compression energy of a hydrogen molecule-ion that were obtained from quantum mechanical calculations. The detonation velocity predicted by their theory was in good agreement with experimental values. Both these workers, as well as Jones, fitted parameters to detonation velocity measurements for the final analysis, although this was not necessary to demonstrate a satisfactory agreement. (8)
Andersen and Parlin have recently derived equations

Andersen and Parlin' have recently derived equations based upon the concept that at high densities the Chapman-Jouguet (CJ) products form a lattice structure, and the corresponding degrees of freedom are vibrational. The primary contribution to their equation of state follows from a term expressing the change of vibrational frequency with volume. The value of a parameter used in their theory was determined from detonation data, and found to be in approximate agreement with solid state theory. The equations derived by these workers are exceedingly easy to apply

in practical detonation velocity calculations.

In what follows, the lattice concept in (8) is retained. The equations are extended to include a very large range of loading densities by requiring the equation of state to reduce to the perfect gas equation at high volumes. Factors other than the equation of state may be expected to vitiate the treatment in the low density region, of course. All parameters are determined by physical data outside the field of detonations, and the results agree to within about 13 per cent with the experimental detonation velocities. The dependence of detonation velocity upon loading density is also in agreement with experimental findings. The equations derived lead very naturally to the concept of universal curves of the reduced variables, velocity, volume, temperature, pressure and material velocity vs. the reduced loading density. Such relationships are particularly simple in application since a single solution of the equation is sufficient for all different explosives under varying initial conditions. Finally the results

of calculations are applied to several actual explosives and the numerical correlation with measured velocities shown.

# GENERAL CONSIDERATIONS

Since the various molecular fragments at the CJ surface are confined by extremely high pressures, they will occupy a volume comparable to that of the solid crystalline explosive itself at room temperature. This volume may reasonably be presumed to depend strongly upon the initial loading density, at maximum loading density the final CJ volume may be seventy-five per cent of the undetonated crystal volume, and as the initial explosive is made to occupy a larger volume, the CJ products also become more voluminous. A theoretical treatment of the detonation process must depend upon the theoretically predicted properties of these high-density CJ products. The properties that are so derived depend upon the model used for interatomic and intermolecular potentials, and the simplifications that are made in the evaluation of the configurational partition function. An exacting semiempiricle approach (the empiricism of which should not depend upon detonation data per se) would employ experimental data from kinetic theory, solid state physics, etc. From the above the form of the partition function is obtainable in principle, but not without considerable difficulty.

Somewhat simplified models may be assumed however, and some of these lead to a prediction of the detonation velocity with considerable accuracy. Thus the Abel equation of state can be derived from the hard-sphere model of a gas; this equation is most successful at low loading densities. However, the correct results for detonation velocities are obtained only if the size of the hard spheres is made dependent upon the initial loading density of the explosive.

The Andersen-Parlin equation of state is derived from a solid state, harmonic-oscillator model, the frequency of which increases as the -nth power of the volume. This equation is successful in the high-loading density region with reasonable values of n. However, n must be made to depend upon the initial loading density in order to predict detonation velocities.

In this region of high loading densities, there is doubtless an advantage in comparing the CJ products to a solid. Certainly the thermal motion of a given molecule will be a periodic vibration within a small confinement space, and not a translation along a path of uniform potential (which latter assumption leads both to the perfect gas and the Abel equations of state). As the loading density is greatly decreased, however, the perfect gas law must certainly eventually become applicable.

In this paper a simplified model of a vibrating solid leads to a partition function, from which the equation of state is derived. In this partition function are three fundamental parameters. At very low specific volumes the only important forces are repulsive, and the value of one parameter is determined by the exponent of the repulsive term in a Lennard-Jones

type of potential equation. The condition that the perfect gas equation of state is adequate at large specific volumes fixes the second parameter. The obvious condition that the repulsive and attractive forces must equilibrate at some density fixes the last of these parameters. The partition function that we intend to use is, as in the previous discussion, that of a harmonic oscillator model. At high temperatures the oscillators are classically excited, and the partition function goes over into the form:

$$\mathbf{F} = \left(\frac{\mathbf{k}\mathbf{T}}{\mathbf{h}\mathbf{v}}\right)^{3\mathbf{N}} \otimes \varepsilon/\mathbf{k}\mathbf{T}$$

$$\varepsilon = \varepsilon (\mathbf{V}) , \mathbf{v} = \mathbf{v} (\mathbf{V}). \tag{1}$$

The Einstein vibrational frequency is made to depend upon the volume, and this dependence is chosen such that the perfect gas law results at high volumes. Since it has been the object to choose a highly simplified partition function, there are a number of shortcomings which must be corrected for in a more elaborate theory. It is proposed to discuss these now:

- i) At low volumes and high temperatures, an anharmonic correction may add important terms to Eq. 1. The potential energy of a vibrating molecule is usually expanded in a power series about the point of minimum energy. Only the quadratic term is retained for low amplitude vibrations, and this term leads to the factor kT/hy of Eq. 1. In the high temperature region, the higher order terms of the expansion should be kept (because of the large average amplitudes) and the configurational integral re-evaluated.
- ii) Although the frequency, v, depends upon volume in such a way that the perfect gas law results at large volumes, the partition function above is obviously not correct at the higher volumes. It is important to note that Eq. 1 predicts a specific heat of k for every degree of freedom for all volumes. At large volumes many degrees of freedom will actually be translational and rotational and thus will contribute only 1/2 k to the specific heat At intermediate volumes, some intermediate specific heat will result. Because of this dependence of specific heat upon volume, the temperature dependence predicted by Eq. 1 will necessarily be unreliable.
- iii) The equation of state at low volumes is that obtained by assuming repulsion energy between atoms that varies as some inverse power of the distance between the atoms, where this power is probably something of the order of from nine to twelve. On the other hand, the equation of state at high volumes is just that of a perfect gas. The region between these extremes is joined smoothly but in a somewhat arbitrary way. There is not a

definite, well established model used for this "imperfect gas" region. Among other factors is the communal entropy contribution, which would increase from zero to R as the volume increases. The proper correction would add this contribution in the region in which the non-localization of molecules becomes important, but the partition function would otherwise be unaffected.

That these and other difficulties exist is a primary reason for the difficulty experienced in predicting detonation parameters on a purely theoretical basis. It is likely that all of the corrections demanded by the remarks above would be insurmountably difficult to formulate at the present time, and it is equally probable that any such formalism would be so cumbersome that it would demand extremely laborious methods to solve for final detonation properties. Thus we propose Eq. 1 for its simplicity, and it is of interest that both the detonation velocity and its dependence upon loading density are found to be predictable within reasonable limits without the use of detonation data as such.

#### THEORY

In the following discussion we will use as the partition function Eq. 1, for the species characteristic of the CJ plane or surface. The equation of state and the thermal equation which follow from this partition function are then given as

$$p = kT(\frac{\partial \ln F}{\partial v})_{T} = -3RT \frac{d \ln v}{dv} - \frac{d\varepsilon}{dv}$$
 (2)

$$E = kT^{2} \left( \frac{\partial \ln F}{\partial T} \right)_{v} = 3RT + \varepsilon(v)$$
 (3)

As usual we assume the customary hydrodynamic-thermodynamic conditions: the thermodynamic properties of the system are determined by the partition function above. The nature of the thermodynamic quantity  $(E-E_0)$  in the Hugoniot equation,

$$E - E_0 = \% p \left( V_0 - V \right) \tag{4}$$

must be discussed from the point of view of the particular model

chosen. Since energy is a property of a system's state, and is independent of the path through the reaction zone, the energy difference in Eq. 4 will be a function of the initial state and the Chapman-Jouguet state of the explosive, and we may choose any convenient path between these. We have considered the final state as a lattice structure with each atom confined by its neighbors to a certain small region in which it may move. The composition of a substance is usually described by stating the number of atoms of a particular type that are bonded to each of the other types of atoms. (thus the composition is specified when we know how many oxygen atoms are free, and how many are bonded to another oxygen atom, how many to a carbon to form CO, etc.). In the case of a lattice

<sup>\*</sup> We neglect poin comparison with p, as we deal only with condensed explosives.

# Farlin

structure, the composition is determined by the number and type of nearest (to a first approximation) neighbors for any representative atom. In both cases the composition is determined by temperature and volume. In particular, at high temperatures a given atom may roam to a position of higher energy with a corresponding increase of entropy. Thus with a free gas as a model, a certain atom will be found dissociated for a fraction of the time. At very high temperatures there will be a large concentration of free atoms. The lattice model is exactly analogous: at high temperatures an atom may be found in a lattice site of high energy (perhaps surrounded by atoms whose valences are completely saturated). No matter what its position, the atom will still undergo periodic vibrations around a point of minimum energy.

The composition that we are interested in is that appropriate to the final CJ temperature and volume. Now let the following process take place: the initial explosive is transformed into the CJ composition at constant volume and temperature. The energy of the CJ composition is an amount  $\Delta Q$  below the energy of the initial explosive; thus an amount of energy  $\Delta Q$  is released in this process. We write

$$\mathbf{E}_{\mathbf{O}} - \mathbf{E}_{\mathbf{i}} = \Delta \mathbf{Q} \tag{5}$$

where  $E_1$  is the energy of the CJ composition at the initial temperature and density. Next the substance is compressed and heated to the final CJ temperature and volume. This brings us to the final state of energy, E. Equations 4 and 5 can be combined to eliminate  $E_0$ :  $E - E_1 = AQ + p(V_1 - V) \qquad (6)$ 

Inasmuch as the CJ composition depends upon the CJ volume and temperature, and the CJ volume and temperature depend upon AQ, and AQ depends upon final composition, normally one requires iterative methods to obtain any of these variables. Of course they will depend upon initial density, temperature, etc., as well. Application of such methods using imperfect gas model seems to indicate, however, that AQ varies only a few per cent with rather wide changes in loading density, in most cases. As a first approximation, we will therefore assume in the following AQ is constant for a given explosive.

From Eqs. 3 and 6 we obtain
$$3R(T-T_0) + \epsilon - \epsilon_0 = \Delta Q + p(V_0 - V)$$
(6)

since  $T_i = T_0$  and  $\epsilon_0(V_0) = \epsilon_0(V_1)$ . The equation of state Eq. 2, can be arranged into the form,

3 R T = A + B p  

$$A(V) = - (d\varepsilon/dV)(dV/d \ln v), B(V) = -(dV/d \ln v) (8)$$

from Eqs. 7 and 8, solving for the pressure, we obtain:

$$p = \frac{\Phi - \psi(v)}{2(v - v_0) + B}$$

$$\Phi = \Delta Q + 3RT_0 + \epsilon_{0} \psi = A + \epsilon \qquad (9)$$

This can be combined with the equations of momentum and matter conservation in the usual way and lead to the following expression for the detonation velocity:

$$D^{2} = \frac{\Phi - \Psi(V)}{\Theta(V)}$$

$$\Theta = (1 - \frac{V}{V_{O}})(\frac{B}{V_{O}} - \frac{1}{\lambda} + \frac{1}{\lambda}\frac{V}{V_{O}})$$
(10)

Now there is a value of the variable v such that the detonation velocity is a minimum, and for which the actual detonation velocity is given. This is a form of the Chapman-Jouget condition, and is the most convenient way to determine the stable detonation velocity from our equations. For certain combinations of the functions B(V), E(V) and A(V), the detonation volume and velocity can be easily determined, but these rather special situations will not be discussed now. Suffice it to say that if E(V) is taken proportional to E(V), the function E(V) must vanish and the resulting algebra is greatly simplified.

sulting algebra is greatly simplified.

Taking  $y = aV^{-n}$  and consequently  $\epsilon = (3/2)NahV^{-n}$ , it has already been shown (8) that one is led to the result

$$p^2 = n(n+2)\phi \tag{11}$$

and

$$V = (n+2)/(n+1) \cdot V_0$$
 (12)

We now consider the general case, using the equation of state given in Eq. 2. The detonation velocity will depend upon the initial loading density according as the average frequency depends upon the volume V. The latter dependence we take as

$$y = (a/V^m) + (b/V^n) \tag{13}$$

for the following reasons. If the detonation products were compressed from some greater volume the molecular vibrational frequency would at first depend very little upon the volume. At a volume V\*, the specific volume of the molecules (without void space) a given atom will be in "contact" position with its neighbors. At a volume slightly smaller than V\* the rapidly mounting repulsive forces will determine the nature of each atom's motion. With increase of repulsion, there is an increase of force constant, and of average vibrational frequency.

The pressure of a confined substance is the outwardly di-

The pressure of a confined substance is the outwardly directed momentum transferred to a unit of area per unit time. At high specific volumes, when groups of atoms tend to have an independent existence, the interatomic vibrations are not important in determining the pressure, since these vibrations tend to cancel out in the average, as regards their contribution to a directed

momentum. In this region of densities, translations are allimportant: a translating group transfers net outwardly-directed
momentum to its neighboring molecules. As soon as the CJ products
are confined to a volume less than V\*, however, all degrees of
freedom are vibrational, and since the important forces are repulsive there will be a net outward momentum transfer. Another way
of stating the same principle is to remark that molecular rotations tend to disapear at about the same time that molecular
translations do, namely when molecular identities become submerged
into a general lattice. Since frequency is an inverse function
of volume (cf.Eq. 13 above), pressure likewise will be an inverse
function, as will be shown when we write the equation of state.

It has been shown previously (8) that if the potential energy between atoms depends upon the distance separating them as an inverse power, c/ra, the low amplitude (harmonic) frequency depends upon volume as c'/V(a+2)/6. The best fit to kinetic data is found for a value of the exponential parameter of a 12. Thus the larger exponential in Eq. 10 will be approximately m=7/3. To determine a value of n, we must examine the thermal equation. It may be mentioned that if every atom acted as a free translater at high volumes  $\nu$  could be considered as the number of collisions with a containing wall, and would be proportional to the reciprocal of the translation length, or the reciprocal one-third power of volume. In that case, our value of n would equal 1/3.

Before writing the equation of state we will determine the values of <u>a</u> and <u>b</u>. When  $V = V^*$ , the vibrational frequency  $v^*$  will be something like a normal solid vibrational frequency which may be assumed to be known. Since at volumes less than  $V^*$  the first term on the right of Eq. 10 will be important, and for greater volumes the second term will predominate, we will let these terms equal one another at  $V = V^*$ . These conditions determine a and b:

$$a = v^*V^{*m}/2$$
,  $b = v^*V^{*n}$  (14)

As a close approximation to  $\nu^*$  and  $V^*$ , we will let these be the Einstein vibrational frequency and the specific volume of the undetonated crystal explosive, respectively.

Defining  $y = V/V^*$  as the reduced volume, Eq. 13 becomes  $v = v^* V^{*m}/yV^{*m} + v^* V^{*n}/yV^{*n}$   $= \frac{v^*}{2v^m} (1 + y^{m-n})$ (15)

The equation of state, Eq. 2, becomes

$$p = -(3RT/V^*)\frac{d nv}{d y} - (1/V^*) \frac{de}{d y}$$

$$\frac{d \ln v}{d V} = -\frac{1}{V^* y} \cdot \frac{m + ny}{1 + y} \cdot \frac{m^{-n}}{1 + y}$$

$$\frac{d \varepsilon}{d V} = -\frac{Chv_*}{2V_*} \cdot \frac{(m + ny^{m-n})}{(m + ny^{m-n})}$$
(16)

The last equation is the result of assuming the proportionality,

$$\xi(V) = \operatorname{Nch} \nu(V) \tag{17}$$

Finally, the equation of state is written in terms of the compressibility:

$$PV/RT = \frac{c}{2\gamma^{m}} \left(\frac{h\nu^{*}}{kT}\right) (m+ny^{m-n}) + \frac{3(m+ny^{m-n})}{1+y^{m-n}}$$
 (18)

At very large volumes, Eq. 15 becomes

$$P_{RT} = 3m \tag{19}$$

In this region the ideal gas law approximately holds and we have

$$pV/R^{\dagger}T = 1, \qquad (20)$$

where  $R^i = N^i k$  and R = N k, and

N' = number of translating groups per gram at low density, and

N = number of atoms per gram of explosive.

If the arbitrary decomposition scheme used previously (8) is followed to obtain the number of translating groups (molecules) divided by the number of atoms, an average fraction equal to N'/N 0.457 is obtained and hence n = N'/3N = 0.152. If N' equal ed N then, as shown previously, n would be 1/3.

As a final result of using the frequency dependence of Eq. 15, we substitute it into the detonation equation, Eq. 10. Defining g as  $V/V_0$  whence  $gy = V/V_0$ , and using the definition of B(y) one obtains the result

$$D^{2} = \frac{2 \cancel{6}}{(1-\cancel{6}\cancel{9})[\cancel{9}\cancel{9}(2f(\cancel{9})+1)-1]}$$
 (21)

where

$$f(y) = \frac{1 + y^{m-n}}{m + n y^{m-n}}$$
 (22)

To find the hydrodynamic velocity, we differentiate and set the derivative of the detonation velocity with respect to the volume equal to zero. This gives

$$\frac{dD}{dy} = -\frac{\phi}{\partial D\theta^2} \frac{d\theta}{dy} = 0 \tag{23}$$

The quantities  $\emptyset$ , D and  $\partial$  (y) must be finite if the detonation velocity is to be finite so that we must have

$$= \frac{(1-29y)(1+y^{m-n})}{m+hy^{m-n}} + \frac{(1-9y)(m-n)^2y^{m-n}}{(m+hy^{m-n})^2} + (1-9y) \quad (24)^{-1}$$

Since we have fixed the values of  $\underline{m}$  and  $\underline{n}$ , the reduced volume  $\underline{y}$  depends only upon the reduced loading density,  $\underline{g}$ . For a given value of  $\underline{g}$ , Eq. 24 is solved by graphical methods to obtain a value of  $\underline{y}$ . Values of  $\underline{g}\underline{y}$  as a function of  $\underline{g}$  are given in Fig. 1.

Values of D are obtained from Eq. 21 when a value of  $\phi$  is known.  $\phi$  depends upon  $\epsilon$  and thus on the value of  $\epsilon$  of Eq. 17. We shall rather arbitrarily give  $\epsilon$  the value of  $\frac{1}{2}$  so that  $\epsilon$  (V) is the zero-point vibrational energy. This latter could be made larger to correspond to a higher potential energy at low volumes but the average potential energy is a function of temperature as well as volume; hence this procedure would not be consistent with the model demanded by the partition function itself and the results would be doubtful value. It has been shown that none of the CJ properties would be changed more than about five per cent by changing  $\epsilon$  from zero to one half. Thus a new condition is introduced that will simplify the calculations of all of the CJ properties. To facilitate this procedure we abreviate Eq. 9

$$\Phi = \Delta \mathbf{Q} + 3RT_o + \mathcal{E}_o = \mathcal{Y} + \mathcal{E}_o \tag{25}$$

and then assume that  $\mathcal{E}^*$ , the vibrational zero point energy at y=1 is equal to

$$\boldsymbol{\epsilon}^* = \mathbf{K} \, \mathbf{Y} \tag{26}$$

where K is a constant, equal for all explosives. If K is set equal to 0.1,  $\underline{c}$  equal to  $\frac{1}{2}$  and N, the number of atoms per gram equal to 6.03 x  $10^{22}$ , then  $\mathcal{V}^* = 2.73$  X  $10^{13}$  ( $\omega = 910$ ) when  $\mathcal{V}$  is taken to be 1300 cal/g. The values of  $\mathcal{V}$  and  $\mathcal{V}^*$  are about what one might expect for an average explosive. Now by combining Eqs. 14, 22, and 23, we obtain the important result

$$\Phi = \chi \left( 1 + K \frac{\gamma_{+}}{\gamma_{+}} \right) \tag{27}$$

Every property of the CJ surface depends in some way upon parameters which characterize the explosive and upon the initial conditions. The parameters that we consider to be important are  $\Delta Q$ , N and V\* (properties of the explosive) and  $T_0$  and  $V_0$  (initial thermodynamic conditions). The quantities  $\underline{m}$ ,  $\underline{n}$  and  $\underline{K}$  are assumed to be approximately independent of explosive type and of the initial conditions, and  $\underline{p}_0$  is neglected. The parameter  $\underline{g}$ , of course, is a useful combination of  $V_0$  and  $V^*$ . Now if a particular quantity is dependent upon a number of these parameters, such parameters will be designated in parentheses after the quantities symbol. Thus in Eq. 24,  $V \equiv X(Q, T_0, N)$ . The quantity  $\Theta$ , which before has

been explicitly designated as a function of the variable y, will now be considered as a function of g alone, since y is determined as a function of g through Eq. 24. Two other quantities along with their parametric dependence are now defined.

$$F(g) = (1 + K \stackrel{?}{\Rightarrow}) \tag{28a}$$

$$\sigma(q) = \frac{(1 - q \gamma)q}{\Theta(q)} \tag{28b}$$

We now examine the dependence of detonation velocity upon these parameters. From Eq. 21 we obtain

$$D^{2} = \phi(\Delta Q, N, T_{o}, g) \theta(g)$$

$$= \chi(\Delta Q, N, T_{o}) F(g) \theta(g)$$
(29)

The reduced detonation velocity becomes

$$\left(\frac{D}{D}\right)^2 = \frac{F(q)\bar{\theta}}{\theta(q)F} = \delta^2(q) \tag{30}$$

where  $\overline{D}$  (and all other barred quantities) refers to the resulting value of that variable when g=1. The reduced detonation velocity is seen to be a function of the reduced loading density only. The value of  $\overline{D}$  is, of course,

$$\overline{D}^2 = Y(\Delta Q, N, T_0) \overline{F} = \overline{D}(\Delta Q, N, T_0)$$
 (31)

Equation 30 specifies a universal detonation curve (against loading density reduced by the parameter  $V^*$ ) independent of the nature of the explosive or the initial conditions. It was to obtain the result, Eq. 30, that the condition Eq 26 was introduced.

The pressure is a detonation property amenable to similar treatment. Solution of the hydrodynamic-thermodynamic equations leads to the expression,

$$P = Y(\Delta Q, T_0, N) F(q) \sigma(q)$$
 (32)

$$\frac{\mathbf{P}}{\overline{F}} = \frac{F(q)\sigma(q)}{\overline{F}\overline{\sigma}} = \pi(q) \tag{33}$$

$$\overline{p} = \frac{Y(\Delta Q, T_0, N) \overline{F} \overline{\sigma}}{V^*} = \overline{P}(\Delta Q, T_0, N, V^*)$$
(34)

Substituting into the equation of state, Eq. 8, and using Eqs. 15 and 17 we get an expression for temperature,

$$T = (pV - \epsilon)/3R \tag{35}$$

Also, from Eqs. 17 and 26,

$$\mathbf{\varepsilon} = \frac{\mathbf{v}}{\mathbf{v}^*} \ \mathbf{K} \mathbf{y} \tag{37}$$

whence, finally, we obtain for the temperature the expression,

$$T = \frac{Y(\Delta Q, T_0, N)}{3NR} \left[ \gamma(g) f(g) \sigma(g) - K \gamma y \gamma^4 \right] \qquad (38)$$

or, in reduced form,

$$\frac{T}{T} = \left[\frac{\gamma(g)R(g)\sigma(g) - KV(g)/v^*}{\left[\bar{\gamma}\bar{k}\bar{\sigma} - K\bar{\nu}/v^*\right]} - \gamma(g)$$
(39)

where

$$\overline{T} = \frac{8(\Delta Q, N, T_0)}{3NB} \left[ \overline{S} \overline{S} \overline{S} - K \overline{V} / y^* \right]$$
 (40)

Volume could be treated just as detonation velocity, pressure and temperature, but it is more convenient to express gy as a function of g, (since gy does dot differ from unity by a large amount at any value of g, while the reduced volume goes to infinity as g approaches zero). Likewise, the material velocity, W, can be treated as those above: the pertinent equations follow.

 $\frac{\left(\mathcal{W}\right)}{\overline{F}} = \frac{F(g) \, \Theta(g) \left[1 - g \, \mathcal{G}(g)\right]}{\overline{F} \, \overline{\Theta} \, \left(1 - g \, \overline{\mathcal{G}}\right)} = \omega^2(g) \tag{41}$ 

 $\nabla^2 = \gamma(\Delta Q, N, T_0) \neq \delta(1 - \gamma \gamma) \tag{42}$ 

The above treatment leads to the formulation of universal loading density curves for all detonation properties. We do not imply that our particular dependence upon loading density provides the best possible reduced curves (since we have fitted no parameters), nor does it imply that such curves are a rigorous consequence of detonation theory. However it is shown that to a good approximation such curves can be derived. A more exact dependence on loading density can be obtained by considering m , n,  $V^*$ , and K as free parameters, rather than as quantities previously determined from physical data.

# RESULTS

Figures 2 and 3 give a representation of the various deteration properties discussed above as functions of the quantity g, which is essentially the loading density. It will be noticed from Figure 2 that the detonation velocity according to this treatment is essentially linear in loading density over a wide range of the latter. The pressure increases fairly rapidly with density as is the case in most treatments. The temperature appears nearly independent of density in the high density region, but is an increasing function over most of the range. The fall in temperature at low values of g probably occurs in a region of density in which the theory is not applicable, for reasons discussed above.

The equation of state and the consequent detonation properties depend upon the quantities m, n, V and K. The detonation velocity is sensitive to these quantities to the following approximate extent. Increasing m by unity, in the range in which we are working increases D by about thirty per cent. The reduced detonation velocity of g = .5 will decrease by about sever per cent (thus a change in m affects the magnitude of the detonation velocity more strongly than it does the shape of the detonation curve). An increase in n by one-tenth increases D by about one to two per cent, and increases  $\delta$  at g = .5 by about 3 or 4 per cent. A given increase in V causes about the same percentage decrease in D at any velocity. Of course the ratio of  $\Delta$  to D at  $g = \frac{1}{2}$  remains unchanged. It has been previously mentioned that K does not affect the detonation velocity strongly in the region of interest.

Calculations have been made for the following five explosives - TNT, tetryl, picric acid, PETN, and RDX. The results of the calculations are shown in Table I. The difference between theory and experiment amounts to about 13 per cent as an average for all compounds. The agreement is seen to be particularly satisfactory for RDX and PETN. The oxygen negative compounds especially TNT, lead to a predicted detonation velocity much too high. This is a consequence of the choice of AQ, which was taken as the high density value 1296 cal/gm in the case of TNT (4).

In Figure 4 are plotted the experimental points for velocity over a wide range of loading density for PETN. It is seen that the calculated values run generally above the experimental velocities at high loading densities. However if the density,  $f^*$ , is taken to be 2.00, instead of the crystal density 1.77, the agreement is found to be good at all loading densities. Likewise, calculated velocities for other explosives agree quite closely with experimental values when  $P^*$  is taken as slightly larger than the crystal density (except for RDX, for which the crystal density appears to be a very good approximation to  $P^*$ ). The value of  $P^* = 2$  was selected for PETN in such a Way that the linear D vs.  $P_0$  equation:  $P^* = P^*$  is taken as 3500(1). This

straight line is also shown in Figure 4.

Table II presents a comparison of several well known treatments of the detonation process with that of this paper, using the pressure as a typical variable. It will be noted that in general the present treatment and that of Ref. (8) give somewhat higher pressure values at high densities, falling off somewhat at the lower densities. However, Cottrell and Patterson as well as Jones also tend to calculate rather higher pressures than are obtained from the conventional thermodynamic treatment.

Finally it may be mentioned that  $\gamma$ ,  $V^*$ , and N must be known to obtain  $\overline{D}$ ,  $\overline{P}$ ,  $\overline{T}$ , and  $\overline{W}$ . The numerical values that we have obtained are  $\overline{D}=3.53~\sqrt{\gamma}$ ,  $\overline{P}~V^*=2.91$ ,  $3RT=1.16~\gamma$ , and  $W=.826~\sqrt{\gamma}$ .

TABLE I

The calculated and observed (4) detonation velocities of Picric acid, PETN, TNT, tetryl, and RDX. (m/sec)

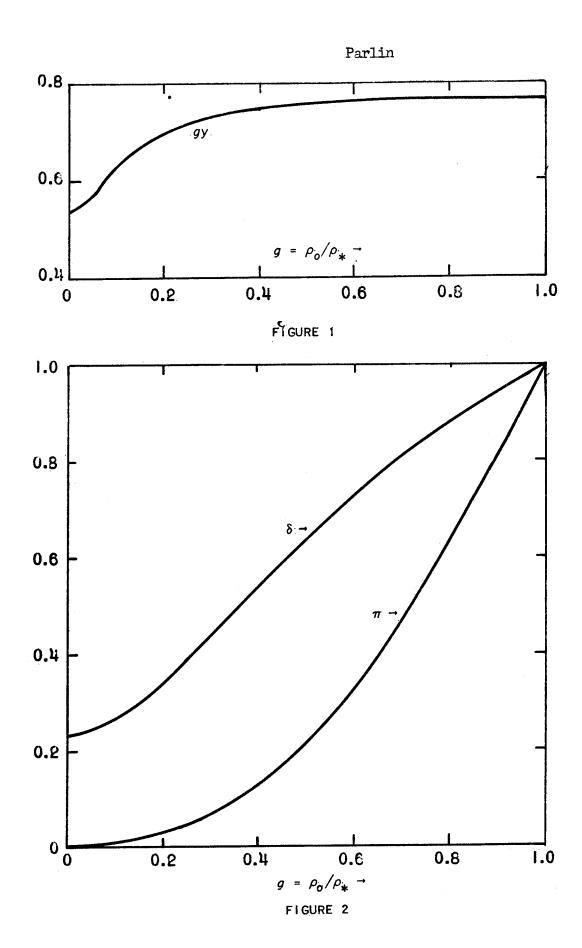
EXPLOSIVE	B	D(calc)	D(obs)
Picric Acid	1.50 1.00	7970 6090	6900 <b>51</b> 00
<b>5 -</b> 8710	•50	3700	3350
PETN - <b>D = 91</b> 00	1.50 1.00 .50	8290 6360 3850	7600 5500 3850
TNT D = 8760	1.50 1.00 .50	8320 6430 3900	6700 4900 3200
Tetryl <b>D =</b> 9040	1,50 1.00 .50	8350 6420 3890	7300 5500 38 <b>5</b> 0
RDX D = 8660	1.60 1.20 .80	8080 6750 5050	8042 6614 5186

TABLE II

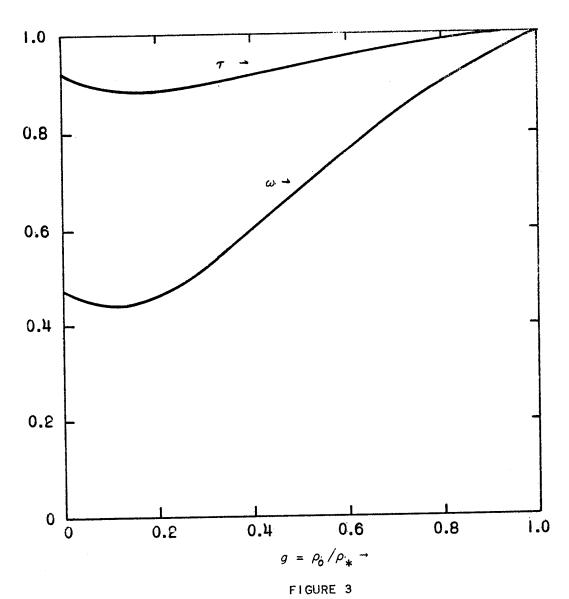
Chapman-Jouguet Pressure for PETN obtained by present Theory compared with that of Jones (3), Cook (1), Brinkley and Wilson (2), Cottrell and Patterson (7), Anderson and Farlin (8), and Kihara and Hikita (6).

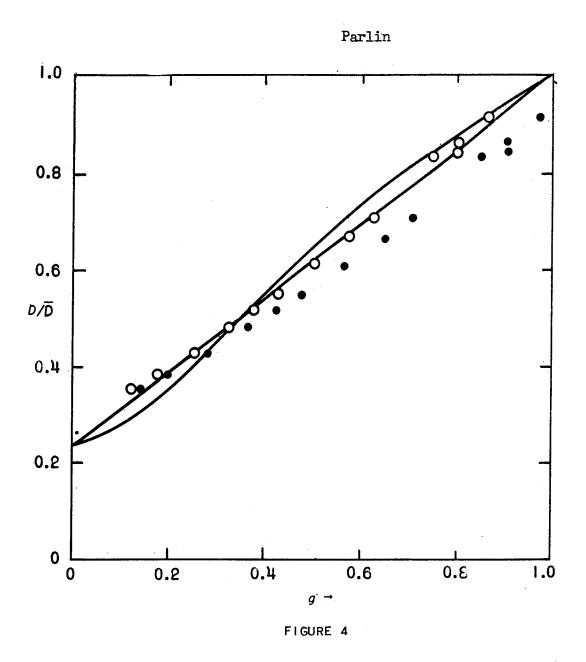
 $P \times 10^{-3}$  atm.

P	This Pap <b>er</b>	Jones	Cook	B-W	C-P	A-P	КН
1.727 1.69 1.6 1.5 1.4 1.25 1.15 1.0 .85 .8 .75 .65 .40 .35 .25	286 273 243 210 179 139 126 114 82 52 50 42 31 18 11 9 5	136 114 86 62 50 39 25 15	255 225 125 85	218 117 83	285 186 88 53 19	282 155 68	239 131 118 83 47









THE REDUCED DETONATION VELOCITY OF PETN.

- EXPERIMENTAL POINTS WITH  $\rho*$  = 1.77
- O EXPERIMENTAL POINTS WITH  $\rho^* = 2.00$

### BIBLIOGRAPHY

- 1. Cook, M. A., J. Chem. Phys., 15, 518 (1947).
- 2. Kistiakowsky, G. B., and Wilson, E. B., O SRD Report 114 (1941).
- 3. Jones, H., Third Symposium on Combustion and Flame and Explosion Phenomena, p. 590, (Williams and Wilkins Co., Baltimore, 1949).
- 4. Taylor, J., <u>Detonation in Condensed Explosives</u>, (Oxford University Press, London, 1952).
- 5. Jones, H., 1941. See Cole, R. H., <u>Underwater</u> <u>Explosions</u>, p. 81, (Princeton Univ. Press, 1948).
- 6. Kihara, T. and Kikita, T., Fourth Symposium on Combustion, Flame and Explosion Phenomena, (Williams and Wilkins Co., Baltimore, 1949)
- 7. Cottrell, T. L., and Paterson, S., Proc. Roy. Soc. A213, 214 (1952).
- Anderson, W. H., and Parlin, R. B., Technical Report 28, Institute for the Study of Rate Processes, University of Utah, Salt Lake City, Utah, (1953).

DIAMETER EFFECT IN CONDENSED EXPLOSIVES. THE RELATION BETWEEN VELOCITY AND RADIUS OF CURVATURE OF THE DETONATION WAVE

> William W. Wood Los Alamos Scientific Laboratory Los Alamos, New Mexico

> > and

John G. Kirkwood Sterling Chemical Laboratory Yale University New Haven, Connecticut

#### ABSTRACT

The limiting slope of the detonation velocity-wave front curvature locus for small velocity deficits is obtained under an assumption concerning the "reaction zone length" as related to the charge diameter and the radius of curvature of the wave front. The model is an extension to two dimensions of von Neumann's classical theory of the plane wave detonation.

I

The relationship between the velocity with which a detonation wave propagates axially along a cylindrical charge and the finite radius of the charge has been studied theoretically by Eyring, Powell, Duffey and Parlin (1) and by Jones (2). Our objective in the present work is somewhat different, namely, to give an account of the relation between velocity and radius of curvature of the wave front, rather than the charge radius. It happens that it is possible to derive such a relation under considerably more straightforward assumptions than have been needed by the investigators mentioned. The theory of Eyring, et al, is commonly called the curved front theory; the present work is closely related to it in many of its details, although the basic model, as well as the

objective, is considerably different. In the following we will use certain results from the preceding paper on the structure of the steady-state plane detonation wave, which we shall abbreviate as SSPD.

II

Our model is once again a compressible, non-dissipative, adiabatic, reactive medium into which a detonation wave is propagating in steady-state. Here, however, the medium is a cylinder of indefinite length, but finite radius. We introduce a system of cylindrical coordinates with z-axis along the charge axis in the direction of propagation, and with r denoting the radial distance from this axis. The origin of z is conveniently taken as the position of the intersection of the wave front and z axis at time t = o. We assume cylindrical symmetry throughout, so that none of the variables depend on azimuthal angle, and all velocities lie in planes containing the z-axis. Under these conditions the equations of hydrodynamics, including the first law and the reaction rate law, become

$$\frac{d\ell}{dt} + e\left(\frac{\partial \mathcal{L}}{\partial z} + \frac{\partial \mathcal{L}}{\partial r}\right) + e\frac{\mathcal{L}}{r} = 0,$$
 (1a)

$$e \frac{du}{dt} + \frac{\partial P}{\partial z} = 0, \qquad (1b)$$

$$e \frac{d\omega}{dt} + \frac{\partial P}{\partial r} = 0, \qquad (1c)$$

$$\frac{d\lambda}{dt} = R$$
, (le

$$\frac{d}{dt} = \frac{\partial}{\partial t} + \mu \frac{\partial}{\partial z} + \omega \frac{\partial}{\partial r} . \tag{1f}$$

The notation is the same as in SSPD, except that u now denotes the axial component of mass velocity,  $\omega$  the radial component, and R the rate function. For simplicity in notation we consider here the case of a single reaction; there is no difficulty in extending the argument to the case of several reactions.

As in SSPD we suppose the reaction zone to be preceded by a (curved) shock, across which we apply the (vector) Rankine-Hugoniot conditions. We assume the medium ahead of the detonation front to be at rest. With D denoting the detonation velocity along the z-axis, U the vector mass velocity at any point on the back side of the shock, n the unit normal to the shock at the same. point drawn in the forward direction, L any unit vector perpendicular to n, variables behind the shock by unsubscripted symbols, and zero subscripts for values in the medium ahead of the shock, the Rankine-Hugoniot conditions are

$$e(\underline{D}-\underline{U})\cdot\underline{n}=e_{0}\underline{D}\cdot\underline{n}, \qquad (2a)$$

$$(p-p)/(v_0-v) = e_0^2 D^2,$$
 (2b)

$$E - E_o = \frac{1}{2} (p + p_o)(v_o - v),$$
 (2c)

$$U \cdot L = 0, \tag{2d}$$

$$\lambda = 0.$$
 (2e)

For any assumed initial shape and velocity for the leading shock the preceding equations determine the state immediately behind the shock. Thereafter the differential equations (1, coupled with the jump conditions determine the flow, which would not be steady in general. Our next step is to ascertain what shock front shapes and detonation velocities are compatible with the steady-state assumption. According to the latter, the flow region behind the shock should be steady when viewed

from a coordinate system moving with velocity  $\mathbf{Q}$ . Introducing such a coordinate system by the transformation

$$\xi = Dt - z$$
, (3)

 being the axial distance measured backwards from the shock, and putting derivatives with respect to t at constant \$\frac{1}{2}\$ and r equal to zero, we obtain

$$(D-u)e_{z}-eu_{z}+\omega e_{r}+e(\omega_{r}+\omega/r)=0$$
, (4a)

$$e\left(D-u\right)u_{\xi}-p_{\xi}+\rho\omega u_{r}=0, \tag{4b}$$

$$e(D-u)\omega_{z}+p_{r}+e\omega\omega_{z}=0, \qquad (4c)$$

$$\frac{dE}{dt} + p \frac{dv}{dt} = 0 \tag{4a}$$

$$\frac{d\lambda}{dt} = R,$$
 (4e)

$$\frac{d}{dt} = (D - u)\frac{\partial}{\partial \xi} + \omega \frac{\partial}{\partial r}; \qquad (4f)$$

$$u_{\xi} = (\frac{\partial u}{\partial \xi})_{r}, \quad u_{r} = (\frac{\partial u}{\partial r})_{\xi}, \text{ etc.}$$

To eliminate the derivatives of Q from these equations we use equation (9 from SSPD,

$$\frac{d\ell}{dt} = \frac{1}{C^2} \frac{dP}{dt} - \sigma \rho R, \tag{5}$$

where the thermodynamic parameter of is defined in SSPD, equations (10a. Use of (5 in (4 then gives

$$-\rho c^2 u_s + (D-u) p_s = \rho c^2 \phi,$$
 (6a)

$$\phi = \sigma R - \omega_r - \frac{\omega}{e c_o^2} p_r - \omega/r, \qquad (6b)$$

$$(D-u) w_{r} + w w_{r} = -\frac{1}{2} p_{r},$$
 (6d)

$$(D-\mu) \lambda_r + \omega \lambda_r = R, \qquad (6e)$$

$$(D-M)(E_s+pv_s)+\omega(E_r+pv_r)=0.$$
 (61)

#### III

The explicit solution of the set of partial differential equations (6 would be an extremely difficult task. Here we follow a different procedure, and begin by specializing them to the axis.\* From obvious conditions

of symmetry the radial component of velocity  $\omega$  vanishes on the axis:

$$\omega\left(\xi,r=o\right)=o\,,\tag{7a*}$$

<sup>\*</sup>In the following we designate equations valid only on the axis with an asterisk.

$$\mathcal{L}(\xi, o) = \mathcal{U}(\xi, o). \tag{7b*}$$

Equations (6 specialized to the axis give

$$-\rho c_{s}^{2} U_{s} + (D-U) P_{s} = \rho c_{s}^{2} (\sigma R - 2 \omega_{r}),$$
 (8a\*

$$\rho(D-U)U_{\xi}-p_{\xi}=0,$$
 (8b\*

$$p_r = 0$$
, (8c\*

$$(D-U) \lambda_{\mathbf{g}} = \mathbf{R}, \tag{8d*}$$

$$E_{z} + pv_{z} = 0,$$
 (8e\*

where all variables are to be evaluated at any  $\xi$  with r = o. Solving (8a and (8b as linear equations for  $\mathcal{M}_{\xi}$  and  $\mathbf{p}$  we obtain

$$u_{\xi} = -\frac{1}{\eta} \left( \sigma R - 2 \omega_r \right), \tag{9a*}$$

$$p_{\xi} = -\frac{e(D-U)}{\eta} (\sigma R - 2 \omega_r), \qquad (9b*)$$

$$\eta = 1 - (D - \mu)^2 / c_o^2$$
 (9c)

Since the flow behind a shock propagating in the direction normal to itself is subsonic (the curved shock in question clearly satisfying this condition because of symmetry), it is clear that  $\gamma$  ( $\xi$  = 0, r = 0) > 0. Furthermore, it is clear that in steady state the flow behind the shock must be similar to that of Prandtl-Meyer steady state expansion, in which the flow becomes supersonic (see ref. 2). Consequently we expect  $\gamma$  to vanish at some point in the steady zone, and therefore the numerators in (9a and (9b must vanish at the same point. Thus we obtain a generalized "Chapman-Jouguet condition" for detonation in a finite stick:

$$D = \mu + C_0$$
 (10a\*

This result is similar to that of Eyring, et al, equation B-12, which is attributed by them to Devonshire(3). Equation (10b may be interpreted as relating the degree of reaction at the sonic point to the radial flow divergence at this point.

In the plane wave theory, the Rankine-Hugoniot relations are integrals of the differential equations of steady-state motion. We now proceed to derive analogous relations for the steady zone of the present theory, where, however, the flow divergence introduces certain correction terms.

For this purpose we return to equation (4a, specializing it to the axis, obtaining

$$(D-U) e_{\xi} - e_{U} = - e_{\xi} = - e_{\xi}.$$
 (11\*

This may be integrated immediately, with use of the Rankine-Hugoniot condition (2a at  $\xi$  = o to give

$$\frac{\varrho}{\varrho_0} \left( 1 - \frac{U}{D} \right) = 1 - 2L \left( \frac{\varrho}{\varrho} \right) , \qquad (12a*)$$

$$L(s) = \int_{0}^{s} \frac{e(s')}{e_{o}} \frac{w_{F}(s')}{D} ds'$$
(12b\*

It will be noted immediately that this is the usual plane wave relation for mass conservation with the divergence perturbation given by (12b added.

In a similar way, (8b may be integrated with use of (12a and (2b to give\*\*

$$b = 60 D \left( 1 - 5 \left( 1 - \frac{\Omega(\xi)}{\Omega(\xi)} \right) \frac{60}{6(\xi)} \frac{D}{M^{2}(\xi)} q \left( 1 - \frac{1}{2} \right)$$
 (13\*

\*\*We have neglected  $p_o$  in the customary fashion.

With neglect of terms in  $\omega_r^2$ , this may be reduced to

$$\Omega(\xi) = \int_0^{\xi} \frac{\omega_r(\xi')}{D} d\xi'.$$
 (14b)

We again obtain a plane wave relation with added perturbation. In similar fashion, equation (4d, specialized to steady-state flow on the axis, may be integrated to

E-E<sub>0</sub> - 
$$\frac{1}{5}$$
 p (%-v) = D<sup>2</sup> {(1+\%) \( \Omega \) \

again with neglect of terms in  $\omega_r^2$ . With the equation of state, (10a, (10b, (12a, (14a, and (15 constitute a sufficient number of equations to determine D and also the axial values of p, U, Q, and  $\lambda$  throughout the steady zone, providing we are able to determine  $\omega_r(\xi)$ . In the

following we designate the C-J point by  $\xi = \xi^*$ , which is determined by

$$\xi = \int \frac{D - U(\lambda')}{R(\lambda')} d\lambda'$$
 (16\*

obtained from (8d.

IV

In order to determine  $\omega_r(\xi)$  we first return to (6d, differentiate it with respect to r, and then specialize to the axis, obtaining

$$(D-U)\frac{\partial w}{\partial S}r + w_r^2 = -V p_{rr}$$
 (17\*

With neglect of  $\omega_{r}^{2}$  and use of (12a this may be integrated to give

$$w_{r}(\xi) = w_{r}(0) - \frac{1}{20} \int_{0}^{\infty} p_{rr}(\xi) d\xi'.$$
 (18\*

The value of  $\omega_r$  at  $\xi$  = 0 can be obtained from the Rankine-Hugoniot conditions, in terms of the radius of curvature S of the shock front at its intersection with the axis:

$$\omega_r(o) = U(o)/S. \tag{19*}$$

It remains to estimate  $p_{rr}(\xi)$ . For this purpose we introduce an assumption concerning the geometry of the reaction zone. We assume the plane  $\xi = \xi^*$  intersects the shock front in the explosive, and that the portion of the shock front for  $\xi < \xi^*$  can be adequately represented by a sphere of radius S; i.e. we neglect the variation of radius of curvature over this part of the shock wave; see Fig. 1. Our procedure is to use the shock relations to

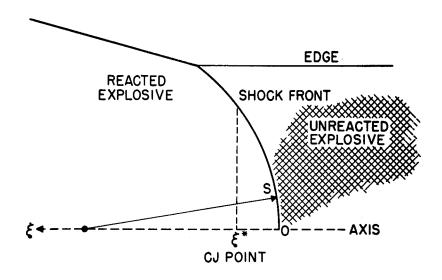


FIG.1

obtain the pressure at any point on the shock front for \$<\xi\*. Then expanding the pressure into a power series in r for fixed \$\xi\$, and retaining only the quadratic term (the linear term vanishes because of (8c) we obtain an approximation to the second radial derivative of p,

$$p_{rr}(s) = (p_s(s) - p(s))/ss,$$
 (20\*

where  $p_s(\xi)$  denotes the pressure at the point  $\xi$  on the shock front. In (20 we have approximated the equation of the spherical front as

$$r^2 = 2 S S$$
. (21)

Furthermore, with neglect of terms of order 1/S,  $p_s(\xi)$  is equal to p(o), the axial shock pressure. Thus we finally obtain an expression for  $p_{rr}(\xi)$  correct to terms of order 1/S,

$$p_{rr}(\varsigma) = \frac{p(o)}{5\varsigma} \left( i - \frac{p(\varsigma)}{p(o)} \right). \tag{22*}$$

Substitution of (22 and (19 into (18, with use of (12a, yields

$$\frac{\omega_{\tau}(\dot{\xi})}{D} = \frac{U(0)}{D} \frac{1}{S} b(\dot{\xi}), \qquad (23a*)$$

$$b(\xi) = 1 - \int_{0}^{\xi} \left(1 - \frac{b(\xi')}{b(0)}\right) \frac{d\xi'}{\xi'}$$
 (23b\*

With the preceding expression for  $\omega_r$ , we may summarize the important equations as follows:

$$\frac{\mathcal{E}}{\mathcal{E}}\left(1-\frac{U}{D}\right) = 1-\alpha(\frac{\xi}{2})/S, \qquad (24a*)$$

$$\alpha(\xi) = 2 \frac{U(0)}{D} \int_{0}^{\xi} \frac{\varrho(\xi)}{\varrho} b(\xi') d\xi'; \qquad (24b*)$$

$$p = e_D^2 (1 - \frac{1}{6}) (1 + \theta(\frac{1}{6}) / 5),$$
 (25a\*

$$E-E_0-\frac{1}{2}p(v_0-v)=D^2\delta(\xi)/s$$
, (26a\*

$$\delta(s) = (1 + \frac{\vee}{\vee_0}) \int_0^s b(s') ds' - 2 \frac{\vee}{\vee_0} \int_0^s \frac{e(s')}{e} b(s') ds', (26b*)$$

$$\sigma(\S^*) R(\S^*) = 2U(0) b(\S^*)/S$$
, (27a\*

$$(D-U(\S^*))^2 = G(\S^*)$$
, (27b\*

$$G \equiv C_{\circ}^{2} \qquad (27c*$$

$$\lambda = \int \frac{\hat{s}}{D - U(\hat{s}')} d\hat{s}' \qquad (28)$$

Equations (24, (25, (26, and (28 hold throughout the steady zone; equations (27 hold only at the C-J point. Equations (24a, (25a, and (27b may be manipulated to obtain

$$\frac{p_{V_{0}-V}^{2}(1-\frac{2\alpha+\theta}{S})=G^{*},$$
 (29a\*

$$D^{2} = \frac{\sqrt{^{2}p}}{\sqrt{-V}} \left( 1 - \frac{9}{5} \right). \tag{29b*}$$

We may conveniently regard (26a, (27a, (28, and (29a as determining the C-J values of p,  $\vee$ , and  $\lambda$ , with (29b then determining D.

V

The theory at this point is formally complete, since the solution of the above equations will yield the desired relation between D and S, correct to order 1/S. To actually proceed further we require explicit information concerning a), the equation of state in the reaction zone and b), the rate function R. Here we shall limit ourselves to a very brief and preliminary discussion which may be appropriate to the detonation of liquid explosives.

With respect to the chemical kinetics problem, a model often used is that of a homogeneous, self-heating

reaction with a rate

$$-\Delta E/RT$$
 $R \sim f(\lambda) e$  (30)

where  $f(\lambda) \sim (1-\lambda)^n$  with n a number of order of magnitude one or two;  $\Delta E$  is a molar activation energy. The appearance of the temperature in the exponential results in a rate of reaction which is initially small behind the shock front (assuming the temperature at this point to be appreciably lower than that near complete reaction, as is almost surely the case), at first increases very slowly, rises to a sharp maximum very close to complete reaction, then falls to zero (asymptotically, for most  $f(\lambda)$ ). If this be true, it is plausible to expect the von Neumann pressure spike to be quite flat-topped during the induction period, then fall rather rapidly to its C-J value. In the following we idealize this pressure spike into a square wave:

$$p(\xi) = \begin{cases} p^{(\phi)}, & \xi < \xi^*, \\ p(\xi^*), & \xi = \xi^*. \end{cases}$$
 (31)

Furthermore, the above discussion suggests that the rate R will be very large for some  $\lambda$  close to complete reaction, then will decrease as  $\lambda$  increases. This suggests that for large radii of curvature the value of  $\lambda$  obtained from (27a will be very close to its plane wave C-J value. In the following we assume this to be true. The same assumption has been made in other discussions of diameter effect<sup>(1, 2)</sup>

We now perform a simple perturbation calculation on equations (26a and (29a to obtain the increments

$$\triangle \vee = \vee (5) - \vee (9), \qquad (32a)$$

$$\triangle p = p \left( \varsigma^{\dagger} \right) - p \frac{\langle o \rangle}{2} \tag{32b}$$

where Vo and po denote the plane wave C-J values. The

result is two linear equations for the determination of  $\Delta p$  and  $\Delta v$ ,

$$\left\{\frac{PE_{p}}{D^{2}} - \frac{1}{5}\left(1 - \frac{1}{5}\right)^{2}\right\} \stackrel{\triangle}{\Rightarrow} + \left\{\frac{VE}{D^{2}} + \frac{1}{5}\frac{1}{5}\left(1 - \frac{1}{5}\right)\right\} \stackrel{\triangle}{\Rightarrow} = \frac{8}{5} . \quad (33a)$$

$$\left(1 - \frac{pGp}{G}\right) \stackrel{\Delta p}{=} + \left(\frac{z - \frac{\vee}{\vee}}{1 - \frac{\vee}{\vee}} - \frac{\vee G}{G}\right) \stackrel{\Delta V}{=} = \frac{z \times + p}{s}$$
(33b)

where 
$$E_p = \left(\frac{\partial E}{\partial P}\right)_V$$
,  $E_v = \left(\frac{\partial E}{\partial V}\right)_p$ , etc.

From (29b we obtain the detonation velocity deficit

$$\frac{\underline{D^{(o)}} \underline{D}}{\underline{D^{(o)}}} = \frac{1}{2} \left( \frac{\beta}{S} - \frac{\Delta \beta}{P} - \frac{1}{\frac{\sqrt{o}}{\sqrt{o}} - 1} - \frac{\Delta \sqrt{o}}{\sqrt{o}} \right). \tag{34}$$

We have used (31 to estimate the plane wave values of the quantities  $\alpha$ ,  $\beta$ , and  $\delta$ , and a free volume equation of state\* to estimate the values of the various thermodynamic

\*The equation of state is based on an intermolecular potential energy of the Buckingham type.

variables under conditions which may be representative for the C-J point of liquid explosives. We assumed  $\frac{1}{\sqrt{6}} = .7$  at the C-J point,  $\frac{1}{\sqrt{6}} = .55$  at the shock. The result for velocity deficit is

$$\frac{D^{(0)}-D}{D^{(0)}} = 3.5 \text{ s}^{*}/\text{s}$$
 (35)

The exact value of the coefficient is quite sensitive to the C-J and spike compressions, especially the former, as well as depending also on the equation of state. The above value should be regarded as only approximate. We hope in the near future to apply the present theory to specific explosives.

#### REFERENCES

- 1. H. Eyring, R. E. Powell, G. H. Duffey, and
  R. B. Parlin, Chem. Revs. 45, 69 (1949; see also
  R. B. Parlin, C. J. Thorne, and D. W. Robinson,
  Tech. Report No. 1, Institute for the Study of
  Rate Processes, University of Utah, Salt Lake City,
  Utah.
- 2. H. Jones, Proc. Roy. Soc. (London) A189, 415 (1947).
- 3. A. F. Devonshire, Theoretical Research Report No. 3/43.

## THE DETONATION BEHAVIOR OF LIQUID TNT

E. A. Igel and L. B. Seely, Jr. Los Alamos Scientific Laboratory Los Alamos, New Mexico

Early results on the detonation characteristics of nitromethane by Campbell et al (1) showed a number of unusual phenomena which led to the work on liquid TNT reported here. TNT above its melting point (about 80°C) is a liquid less sensitive (2) than nitromethane, with a presumably longer reaction zone, in which the same peculiarities of behavior exhibit themselves.

#### Materials

Triple-recrystallized TNT with a melting point of 80.75 ±0.02°C and light transmission of 65%/cm relative to distilled water\* was used for all the work reported here. This material was specially prepared at Picatinny Arsenal as Lot PA-48-1-3 by treatment of USA Grade 1 TNT with sodium sulfite, followed by recrystallizations from alcohol and from an ethylene dichloride-carbon tetrachloride mixture, with appropriate washing after each step.

The liquid TMT was fired in glass tubes which were made of Pyrex brand glass with walls 0.1 inch thick. This thickness was believed to constitute "infinite" confinement as far as Pyrex was concerned, a belief which was consistent with the results of others (1) (2) on confinement in other liquid explosives. It was further supported by several shots at 0.31 inch wall thickness which showed a behavior consistent with other shots at 0.1 inch wall thickness.

Samples of the Pyrex tubes were tested by immersion and the density was found to be 2.212 gm/cm<sup>3</sup>. Individual tubes were measured for wall thickness and diameter. The wall thickness ranged on each tube from a maximum of 0.10" to some lower extreme depending on the tube, but always above 0.08" for these firings. Since both these thickness values were believed to be "infinite", no attempt was made to achieve better control.

<sup>\*</sup>Melting points and transmission values were obtained with the aid of A. Popolato and W. Barry.

The diameters of the tubes varied slightly from tube to tube, along each tube and with the orientation of the diameter being measured. All these variations, however, were limited to ±0.01". Since the detonation velocity of liquid TNT was found to be insensitive to diameter, these variations did not produce detectable velocity variations.

Detonations were also studied in Dural tubes (24ST). Dimensions were much more closely controlled than for glass, and the effect on the velocity of such variations as existed must have been entirely negligible.

#### Method of Velocity Measurement

The liquid TNT problem puts high requirements on the accuracy of detonation velocity measurement. Early in the work it became clear that the total velocity decrement in glass tubes was quite small. It was necessary to keep the error to a few percent of the decrement (rather than of the velocity itself) in order to be able to determine the detailed dependence of the decrement on charge radius.

In the case of liquid TNT the problem of measuring detonation rates by optical means is more than ordinarily difficult, because of low light intensities. Therefore it was decided to use the pin method for velocity determinations. The camera method was used for diagnostic work. The camera was also used for measurements of the radius of curvature of the detonation wave. Here extreme accuracy was not necessary, because the detonation velocity of TNT is not extremely sensitive to the radius of curvature of the wave front.

#### Pin Method

The so-called "pin" method of velocity determination consists of recording the time of arrival of a shock or detofiation wave at two precisely determined points by means of the electrical conductivity of the wave (3). When the detonation wave reaches a conductivity probe a small condenser discharges to ground through the detonation wave by means of a ground probe with which the wave has made contact earlier. In general it is not clear what part of the detonation wave causes the signal. The situation is particularly questionable in the case of a shocked homogeneous material, for which the temperature is much lower than in the interstices of a particulate explosive. In liquid TNT we do not know whether the original shock front triggers the probe or whether a certain amount of chemical reaction is necessary before the discharge can be started. From the point of view of obtaining measurements all that is necessary is that the wave trip the pins in the same manner at both ends of the measurement interval. One can perhaps believe that this is so if a truly steady wave has first been developed. The final consistency of the data is a fairly good indication that the method of triggering was always the same.

The pin signals were recorded on the "Cable Delay Timing System". This is a system by which signals generated early in the travel of the wave are delayed and presented on the same fast oscilloscope sweep with the later signals. Readings can be made quite accurately because of the speed of the sweep. To the time differences as seen on the sweep must be added the times spent by the delayed signals in traveling through the delay cables.

The delay cables were RG-18/U of various lengths up to 10 microseconds which could be connected together by lengths of more flexible cable at a connection panel. We believe the system would be practical for delays up to about 15 microseconds. At some time beyond this the signals would become degraded and reading accuracy would fall off. The advantages of the cable method are ruggedness and electronic simplicity. The cable transit times do not vary with aging or external conditions, but depend only on the dielectric constant of the insulating material. On the other hand the cable delay system is inferior to a raster scope system in flexibility and simplicity in forming the signals.

The results of cable calibrations are shown in Table I. Short cables were calibrated by presenting test pulses on a calibrated sweep before and after travel through the cable in question. Long cables were calibrated by comparing a signal through the cable in question with a simultaneous signal, either direct or reflected, through a previously calibrated cable or collection of cables. This led to a somewhat complicated multiplication of errors for the longer cables, as can be seen from the trend of the standard deviations in Table I.

#### Absolute Accuracy

The cable calibration values given in Table I are the predominant factor in determining the absolute error of the liquid TNT measurements. We have calculated the 95% confidence limits for these values and prefer to use these as an index of absolute accuracy. In the arrangement of cables used for the liquid TNT studies the accuracy of the longest cables was most important so that the absolute accuracy of the final results was about ±0.1%.

## Relative Accuracy

The relative accuracy was something quite different. In the liquid TMT work reported here the cable arrangement was the same for all shots, and under these conditions the relative accuracy was considerably better than the absolute accuracy. The random scatter of the final data results from reading and instrumental errors, from errors in placement of the pins, variations in the explosives and poor control of conditions. As will be seen later in this paper the final velocity results are characterized by a population RMS deviation,  $\sigma_p = 0.1\%$ . Thus by using a sample size of 10, the  $\sigma$  for the average can be reduced to 0.03%.

TABLE I
SUMMARY OF CABLE CALIBRATIONS

Cable Designation	No. Samples	Mean Time	σ <sub>p</sub> (population)	of Mean)	95% Confidence
2	N	usec.	microsec	conds $x 10^{-3}$	
0.1 0.2B 0.2A 0.5 0.6 1.0 2.0A 2.0B 5.0	14 10 11 10 10 11 8 11 10	0.1268 0.2019 0.1968 0.4948 0.6179 0.9702 2.0033 2.0544 4.9521 9.9441	1.06 1.00 1.75 1.20 1.60 3.30 3.26 7.56 15.20	.14 .36 .30 .55 .38 .48 .97 .93 2.27 4.58	2 0.30 2 0.38 2 0.33 2 1.24 2 0.86 2 1.07 2 2.3 2 2.1 2 5.1 210.4

## Temperature Control

The first attempts to obtain detonation velocities for this program yielded spreads much too large to define the details of the velocity decrement. Studies of the detonation wave shape with the camera showed great variability as well. Therefore, a number of investigations were made at that time to study various possible reasons for this instability. The measurement system, explosives purity, presence of dissolved or dispersed gases and other factors were looked into. No positive evidence was encountered to indicate that these particular factors were responsible for velocity variations of the size observed.

The detonation velocity dependence on density for solid TNT is about 350 m/sec. per 0.1 gm/cm<sup>3</sup> according to OSRD 5611 (4). The variation of the density of liquid TNT with temperature is approximately linear with a slope of 0.001 gm/cm<sup>3</sup> per degree C.\* Thus the detonation velocity varies about 3.5 meters/sec. per degree C. On this basis one would not expect that uniform deviation of the temperature from charge to charge was responsible for the spreads observed, since the temperature could be controlled to within a few tenths of a degree from charge to charge. However, the variable wave shapes that were observed suggested that there may have been temperature gradients within each charge.

In order to develop satisfactory control, measurements of the temperature were made in twelve positions in the charge by means of thermoccuples monitored by a Leeds and Northrup automatic recorder. With the original techniques of cooling and stirring by bubbling nitrogen through the liquid, differences in temperature of as much as a 3°C were observed at firing time. By means of such tests several tech-

<sup>\*</sup> Variation of density of liquid TMT with temperature was measured by W. H. Stein, LASL.

niques were developed for holding the temperature constant throughout the charge. Two of these have been used for the shots reported here.

Apparently the key to maintaining uniform temperature was to circulate the liquid, either by means of a twisted-blade stirrer or an exterior circulating pump. This was effective with both a heated-sand jacket and with a pre-heated-circulating-air jacket. When stirring was stopped, before firing, it took several minutes for the gradients to become apparent--long enough for preparations to be made for firing.

## Probe Arrangement

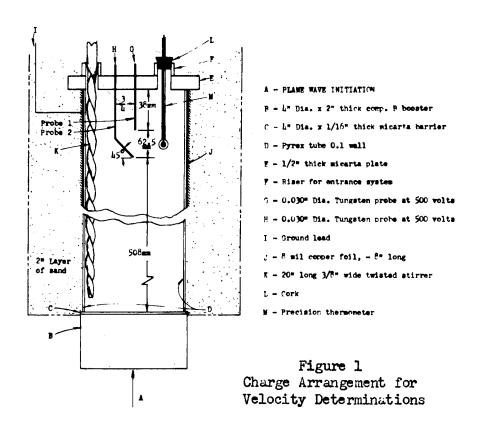
Conductivity probes should be rugged enough to hold their position but yet small enough to avoid perturbing the detonation wave. For work in glass tubes and large diameter metal tubes, .030" tungsten rods were chosen, since they were quite rigid for the diameter. It was also believed that high density would be advantageous in avoiding perturbations. There were, however, serious reservations about their use near failure diameter where the introduction of this foreign material might be expected to affect propagation of the wave. The probes were glued with plastic cement in Micarta caps as shown in Fig. 1.

To test the suitability of this style probe assembly, a number of caps were mechanically vibrated to simulate possible abuse prior to shot time. Measurements of the inter-probe-point distance were also made in water at 93°C behind plate glass windows. These tests showed no effect of vibration or temperature provided strains were first relieved by holding the probes in an oxygen-butane flame for two minutes. Repeated cathetometer readings of the distance between a pair of probes to be used for firing showed a range of ±0.01%.

For metal tubes smaller than 2" in diameter the 0.030" probe was thought to be too large. Instead a 0.005" tungsten wire was strung across a diameter of the tube. This required mounting in 1/8" diameter plastic plugs for insulation in the metal wall. Furthermore close-fitting removable plugs of metal had to be made in the wall at right angles to each wire so that the position of the wires could be measured by means of a cathetometer after installation.

#### Method of Wave Curvature Measurement

Two closely related techniques were developed for observing the shape of the detonation waves. In the first the wave was allowed to collide with a thin aluminum foil against a ground plate of glass. This assembly was held perpendicular to the axis of the tube by the fit of the glass against the tube end, which was ground accurately perpendicular. The aluminum was flat because it was held against the glass by the liquid TNT. In order to increase the light intensity, the small spaces between the ground glass and the aluminum were flushed with argon. The Rotating Mirror Camera then viewed the light through the unground side of the glass.



There was some difficulty with this technique in reproducing intensities, probably because of variations in sand-blasting the glass. Further irregularities in the trace were produced by wrinkling in the foil at 100° C., caused by the difference in the coefficient of expansion between glass and aluminum.

In order to overcome these difficulties, the tube-end was constructed of brass and the joint to the glass made with a circumferential "O"-ring seal. A piece of .005" thick brass shimstock could then be firmly fastened to the brass tube-end, and difficulties caused by differential expansion avoided. A smooth piece of plate glass was held .005" above the brass shimstock by soft aluminum shims, providing a narrow space for argon.

#### The Charges

A number of charge designs were tried in the preliminary shots without any definite specification of the optimum length or mode of initiation. One would like to keep charge weight at large diameters as low as possible and yet it is clear that the detonation must be positively initiated and reach a steady state before measurements are made. The final charge design is shown in Figure 1. The liquid TNT was over-driven by the Comp. B with only 1/16" Micarta between the two explosives. A plane wave generator was used because it was thought better always to have an initiating wave curvature less than the final stable one. By this means some of the possible

initiation trouble at diameters near failure could be avoided.

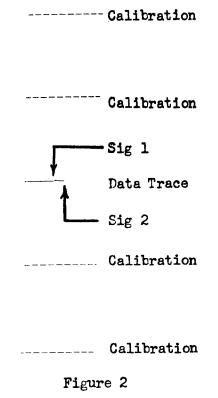
It was never shown in this work just what the minimum satisfactory charge length was. In all velocity measurements in glass tubes we allowed 20" of free run in liquid TMT before starting the measurement. This gave somewhat over three diameters of length at the largest diameter studied (where, incidentally, the least alteration from the original plane wave shape was necessary) and a more generous situation in the small diameters. For other shots in metal tubes involving determination of wave shapes we allowed always more than four diameters of free run before starting measurements.

With either sand jacket or air jacket the total charge assembly was quite bulky. In both cases the signal forming components were mounted as close to the probes as possible and connections made in such a way as to form as small loops as possible. The metal tubes themselves served as electrical grounds. In the case of glass tubes the electrical ground at the charge was an 8 mil copper sheath surrounding the tube in the vicinity of the probes. It was found that this sheath (instead of a simple wire) increased the sharpness of the signal making reading of the films easier.

## Data Analysis

Velocity Data. A typical velocity data film, reproduced in Figure 2, shows five traces. The first two are marked calibration sweeps which were recorded after an hour's warm-up for the scope and as close to firing time as possible. The last two traces are also calibrations, but taken immediately after firing. The middle trace is the data trace taken with no markers. All four calibration traces were read on the comparator and the sweep curve plotted. The data trace was then read and the sweep speed corresponding to the signal interval applied to reducing the data.

Wave Curvature Data. A wave trace of the type shown in Figure 3 was produced when glass tubes were used. The film was placed on the comparator and the stage rotated until the static image of the slit and the horizontal traverse of the comparator agreed. Thus we at this point assumed that the camera slit was truly perpendicular to the direction of writing, in practice an extremely difficult adjustment to make accurately.



Cable Delay Timing Film

By means of the edges of the trace, or markers, if provided, the magnification factor could be computed and the center of the charge determined. Five sets of readings were made of the time displacements relative to the position of the center of the wave at intervals across the face of the trace.

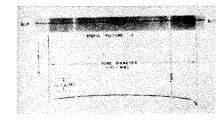


Figure 3
Typical
Wave-Curvature Film

The data were reduced by fitting an ellipse to all but the lagging outer edges of the trace. The central curvatures of these ellipses have been reported as the pertinent data.

We are indebted to W. W. Wood for devising this scheme and adapting it for the IBM 701 Computer, and to F. R. Parker for coding and machine operation. The method assumed that an axis or the ellipse fell on a line parallel to the camera slit. In some of the earliest work this introduced a slight error, since the camera slit was not quite perpendicular to the direction of writing. However, comparison with hand calculations in which radii of curvature were computed for various groups of three points on the wave trace showed that the skewness was very small and that the error thus introduced in the radius of curvature was negligible.

#### Results

<u>Velocities</u>. Shots at various diameters in glass and aluminum were fired over a period of months. The individual results with averages and RMS deviations are shown in Tables II and III. From the results in glass tubes for which a large number of shots were made under identical conditions it is concluded that the population RMS deviation,  $\sigma_p$ , is about 6 m/sec.

The point at the largest diameter (1/R = 0.132) for glass is the average of only three shots. We believe that these shots are part of a population which has the same characteristics as those revealed by the larger number of shots made at other diameters. On this basis we have conservatively assumed that the true  $\sigma_p$  is 6 m/sec. Clearly then the  $\sigma$  for the average of three shots is 3.5 m/sec. rather than the smaller value which can be calculated from the variations of the three shots themselves.

These results for glass tubes, with the proper  $\sigma$ 's indicated, are shown plotted against 1/R in Figure 4. It is seen that the data are adequately satisfied by a straight line with intercept at R =  $\infty$  of 6574 m/sec. Failures occurred invariably at R = 3.0 cm. Thus the lowest point at which measurements were made was R = 3.25 cm, where the velocity was 6515 m/sec. The decrement in velocity, from the extrapolation at infinite diameter to the point nearest failure was 60 m/sec.

TABLE II

Detonation Velocity of Liquid TNT
100° C Pyrex Glass Tubes

	200 0		
Film No.	Detonation Velocity D, m/sec.	Average Detonation Velocity D, m/sec.	Standard Deviation of Mean of . m/sec.
Radius = 3.	25  cm.  (1/R = 0.308)		
15-399	6521		
15-402	6508		
15-403	6516		
15-404	6512	/ 42 4	٦
15-405	6516	6515	1.6
15-408	6515		
15-409	6516		
15-410	6522 6509		
15-411			
Radius = 3.	$50 \text{ cm} \cdot (1/R = 0.286)$		
15-382	6529		
15-383	6528		
15-413	6515		
15-414	6511	4500	2.0
15-415	6521	6520	2.0
15-416	6515		
15-427	6525 6520		
15-428 15-429	6513		
15-429	6524		
	75 cm. $(1/R = 0.210)$		
15-346	6537		
15-348	6541		
15-350	6535		
15-352	6531	6534	1.3
15-354	6534 6531	0994	1.7
15-356	6534		
15-360 15-361	6539		
15-379	6528		
	.56 cm. (1/R = 0.132)		
15-449	6553		
15-449 15-450	6549	6549	3.5
15-451	6547	~ ) <del>**</del> /	
±J~4/±	~ / <del>~</del> /		(op assumed 6)
			· P

TABLE III

Detonation Velocity of Liquid TMT

100° C Dural (24ST) Tubes

Film No.	Detonation <u>Velocity</u> D, m/sec.	Average Detonation Velocity $\overline{D}$ , m/sec.	Standard Deviation of Mean of, m/sec.
Radius - 3.18 c	m. (1/R = 0.315)	$\frac{\text{cm}^{-1}}{}$	2
15-458	6543		
15-4 <i>5</i> 9	(6500)	6537	3.6
15-460	6534		·
15-461	6533		
Radius = 1.59 c	m. (1/R = 0.630)	$cm^{-1}$	
15-485	6515		
15-486	6515	6515	4.3
	4-4	_7.	(op assumed 6)
Radius = $0.95$ c	m. (1/R = 1.05 c)	<u>m-+)</u>	
15-492	6462		••

The velocity data presently available for aluminum confinement are listed in Table III. Although the number of shots is less the accessible range in 1/R is greater than for glass, and the (presumed) straight line can be adequately determined, using, as seems reasonable, an extrapolation point common with that for the glass curve.

There is one shot at the largest diameter among the data for aluminum which is apparently subject to a large error. This point has not been averaged with the others.

The data for aluminum confinement are plotted in Figure 5. In the large-diameter region the data can be represented by a straight line of smaller slope than the line for glass, as one might expect for the denser material. The data are not complete enough to show the form of the curve as failure diameter is approached. However, it appears that the maximum velocity decrement for aluminum is about three times that for glass.

#### Wave Curvatures

The wave curvatures obtained from the IBM 701 Computer are listed in Table IV. At the largest diameter in glass there are enough determinations so that a reasonable estimate of the experimental error can be made. For the other conditions there is really no basis for assigning an estimate of accuracy but we have nevertheless tried to assign one. This should be considered not so much as a guarantee of accuracy as a warning lest the data be used for more than they are worth.

Igel and Seely

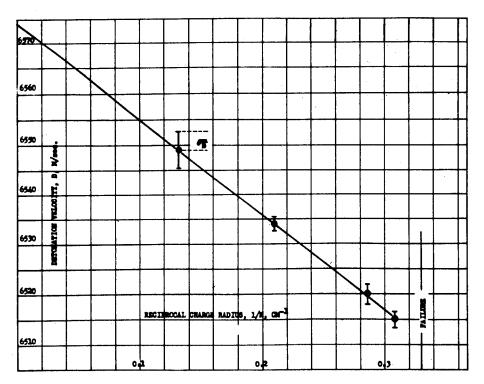


Figure 4
Diameter Effect in Liquid TNT 100°C Pyrex Confinement

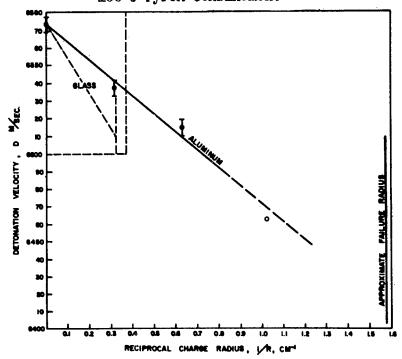


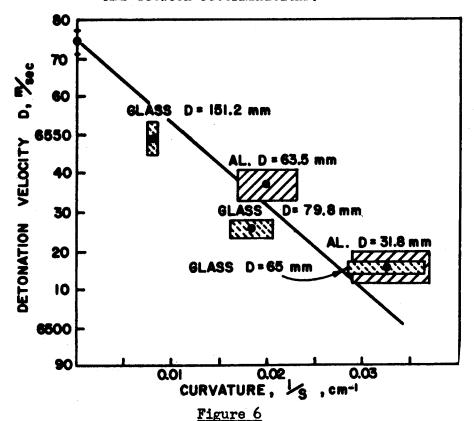
Figure 5
Diameter Effect in Liquid TNT
100°C Dural Confinement

Igel and Seely

Radius of Curvature of Detonation Waves in Liquid TNT at 100° C

	=		<u></u>		
Tube <u>Dia.mm</u>	Detonation Velocity	Rad.Curv. S,mm	<b>%</b>	S mm	Error mm
151.2	6549	1253		1	
151.2	6549	1221		·	
151.2	6549	1203		1255	40 <del>*</del>
151.2	6549	1272			•
151.2	6549	1314		1	
79.8	6526	546	1.4		55
65.0	6515	308	2.2		40
m:					
63.5	6537	575		506	770
63.5	6537			200	70
31.8	6503	306	3.8	'	40
	Dia.mm  151.2 151.2 151.2 151.2 151.2 79.8 65.0 m: 63.5	Dia.mm Velocity  151.2 6549 151.2 6549 151.2 6549 151.2 6549 151.2 6549 79.8 6526 65.0 6515  m: 63.5 6537 63.5 6537	Dia.mm         Velocity         S,mm           151.2         6549         1253           151.2         6549         1221           151.2         6549         1272           151.2         6549         1272           151.2         6549         1314           79.8         6526         546           65.0         6515         308     ***  63.5  6537  575  63.5  6537  437	Dia.mm         Velocity         S,mm         %           151.2         6549         1253           151.2         6549         1221           151.2         6549         1203           151.2         6549         1272           151.2         6549         1314           79.8         6526         546         1.4           65.0         6515         308         2.2    m:  63.5  6537  575  63.5  6537  437	Dia.mm         Velocity         S,mm         %         mm           151.2         6549         1253         121         121         1255           151.2         6549         1203         1255         1255           151.2         6549         1272         1314         1272         1314         1272         1314         1272 </td

\*RMS between determinations.



Effect of Wave Curvature on Detonation Velocity of Liquid TNT

Some of the radius of curvature values have associated of s quoted in per cent. These o's express the uncertainty in the radius of curvature resulting from the scatter of the experimental readings and the failure of the series of points to fit the ellipse perfectly. It is believed that the experimental accuracy is better indicated by the variation in the radius of curvature from shot to shot, since there are a number of factors which can affect the shot-to-shot scatter, and not be evident in any one shot.

The velocity data of the preceding section are shown plotted against the reciprocal of the radius of curvature in Figure 6. According to the Wood-Kirkwood theory all the points, whether with glass or aluminum confinement, should lie on the same straight line. Within the limits set by the rather large experimental error this is the case. At the same time it is possible that more extensive and more accurate data will indicate shortcomings of the theory.

## Discussion

The small velocity decrement of liquid TNT in glass confinement is unexplained. No theory in its present form treats the mechanism of failure, and it is perhaps unjustified to consider failure as a case in which the divergence of material postulated in theories of the diameter effect is carried to its ultimate. As the wave curvature plot now stands, failure occurs in glass and aluminum at different degrees of divergence. The shape of the wave front in glass, characterized by a rapid increase in curvature as the wall of the tube is approached, (see Fig. 3) is not duplicated in the same diameters for metals (very small diameters in metals have not been investigated). For metals the wave front intersects the tube wall with a smooth curvature, almost unchanging. The wave front with magnesium ( $\rho = 1.7 \text{ gm/cm}^3$ ) confinement is of the typical metal type. The failure diameter in cellulose-filled plastic ( $\rho = 1.35 \text{ gm/cm}^3$ ) is approximately that in glass  $(\rho = 2.2 \text{ gms/cm}^3)$ . All this tends to suggest that failure in glass is governed by a unique property of the glass, perhaps its inability to withstand circumferential tension without cracking.

In attempting to treat the data according to earlier theories such as those of Jones and of Eyring et al., one is confronted with immediate experimental contradiction of the theories. As far as the Jones theory (8) is concerned there are two contradictions. First, Jones has ignored the presence of wave-front curvature. Second, the wave shapes observed in glass suggest that flow is not normal at the boundary as assumed by Jones.

In spite of this, one can go ahead, ignore the contradictions, use the angle of expansion calculated by Jones and Strickland for TMT in glass together with charge-radius versus detonation-velocity data reported here, and calculate a reaction zone length. The answer thus obtained is a reaction zone length 0.9 mm.

A similar calculation for the aluminum data gives a value of 1.1 mm for the reaction zone length, the difference between the two calculations probably being due to inconsistency in estimation of the expansion angle.

Eyring's theory assumes a curved detonation wave front with which our experimental findings are more nearly in agreement. However, the wave shape in glass has not been found to agree with the spherical surface assumed by Eyring, but has been found to curve sharply at the edges. The Eyring theory for "infinite" confinement calls for an angle of which the wave makes with the confining wall. We have assumed that the most sensible angle to take is not the actual angle but the angle that the "normal" central part of the wave would make with the case if extended to it. On this basis the results in glass give a reaction zone length of 0.3 mm. The aluminum results indicate a reaction zone length of 0.25 mm.

Finally, the Wood-Kirkwood theory relates the radius of curvature of the detonation wave to the detonation velocity. Our data present no obvious contradictions with the assumptions in this theory. The theory assumes a spherical wave in the center, and this is approximately true. According to the theory this constant curvature should extend radially at least to a point where the wave front has dropped one reaction zone length behind its position at the center of the charge, and this also seems to be approximately true at least at the large diameters. In small diameter metal tubes it is clear that it is not true. There are in the theory certain assumptions necessary for mathematical tractability or concerning the equation of state which have to be put up with. In no case do these appear unreasonable, but in no case do we have an experimental check. Accepting them, we have calculated a reaction zone length of 1.2 mm.

It is probably fruitless to speculate as to which value of the calculated reaction zone lengths lies nearest the actual one. However, by obtaining additional information on the properties of liquid TNT and on the products of its detonation the theoretical idealizations in the Wood-Kirkwood theory can be made more realistic. There is some hope that the detonation process can in this manner be taken apart and described in greater detail than now possible. As a check on these possibilities great interest is focused on experimental techniques for studying the details of the reaction region.

### REFERENCES

- (1) T. P. Cotter, A. W. Campbell, T. E. Holland, M. E. Malin and H. W. Schmitt, unpublished communications, December 20/1950, August 20, 1951. More exact and complete data are given in "Detonation in Homogeneous Explosives", this conference.
- (2) L. C. Smith, E. James, Jr., M. J. Urizar, unpublished communication, August 15, 1951, giving approximate failure diameters for liquid TNT.
- (3) James L. Tuck, Private communication.
- (4) D. P. MacDougall, G. H. Messerly, et al, OSRD 5611.
- (5) H. Eyring, R. E. Powell, G. H. Duffey and R. B. Parlin, Chem. Rev. 45, 69-181 (1949).
- (6) S. J. Jacobs, paper presented at 1st ONR Conference on Detonation.
- (7) W. W. Wood and J. G. Kirkwood, Jour. Chem. Phys. in press, also presented at 2nd ONR Conference on Detonation.
- (8) H. Jones, Proc. Roy. Soc. A-189, 415-426 (1947). Additional work of Jones is quoted in Ref. 5.

#### DETONATION IN HOMOGENEOUS EXPLOSIVES

# A. W. Campbell, M. E. Malin, and T. E. Holland

Los Alamos Scientific Laboratory
Los Alamos, New Mexico

#### INTRODUCTION

The work to be discussed in this paper began as an attempt to obtain precise data for comparison with the predictions of the Eyring (1) and the Jones (2) theories of the diameter effect. The use of liquid explosives seemed to offer a ready means of preparing homogeneous charges. Of the many liquid explosives known, Nitromethane seemed the most desirable for many reasons, among which were its ready availability, cheapness, low toxicity and low sensitivity. Soon after the work was begun on measuring detonation velocities and failure diameters, scatter appeared in the data to a degree which was not explainable on the basis of measuring error. Further investigation, aided by high-performance optical and electronic equipment, revealed several new aspects of the detonation process, some of which appear to be peculiar to liquids, others to homogeneous explosives whether liquid or solid.

#### MATERIALS

The Nitromethane used in this work was obtained in 55 gal drums from Commercial Solvents Corporation. It was specified as having the following composition:

Nitromethane, % by weight, minimum	95
Nitroparaffin, total, % by weight, minimum	9 <b>9</b>
Specific gravity, 25/25°C	1.1283
Acidity as acetic acid, % by weight, maximum	0.01
Water, % by weight	0.052

To further guard against the presence of alkaline materials which might act as sensitizers, the Nitromethane was redistilled at reduced pressure from sulfuric acid and stored in glass bottles.

The Ethyl Nitrate used was White Label grade obtained from Distillation Products Industries. The PETN used was obtained from the Hercules Powder Company.

## EFFECT OF TEMPERATURE ON DETONATION VELOCITY OF NITROMETHANE

The first experiments on the effect of confinement on the detonation velocity of Nitromethane were done in dural and steel tubes at constant charge-weight/casing-weight ratio. Subsequent observations on the effect of metal confinement on Nitromethane have led us to regard the confinement employed here as equivalent to infinite confinement. The detonation velocities were measured using the pin technique (3) and are shown plotted in Fig. 1. These results indicated

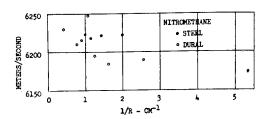


Fig. 1. Detonation velocity of Nitromethane confined in metal tube. No temperature control.

that very little diameter effect was to be expected from Nitromethane in metal tubes, and that some uncontrolled factor was causing bad scatter in the observed velocities. Temperature variations in the explosive at the time of firing were suspected. Such variations could have two effects: raising the temperature of a liquid explosive tends to increase the detonation velocity; the accompanying decrease in density tends to lower

the velocity.

The second of these two effects is the easier to examine. The temperature dependence of the density is given for Nitromethane by the following (4):

$$d_T = 1.1645 - 1.337 \cdot 10^{-3} T - 1.15 \cdot 10^{-6} T^2 + 3.8 \cdot 10^{-9} T^3$$

where  $d_T$  is the density at T  $^{\circ}$ C. Since the Nitromethane used in these experiments contained some impurities, as shown in the above analysis, a set of temperature—density data was taken on it with the result as shown in Fig. 2. The temperature—version of the statement o

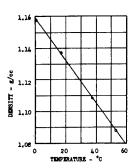


Fig. 2. Density-temperature plot for commercial grade Nitromethane

ture coefficient was found to be 1.33 10<sup>-3</sup> g/cc/°C, in good agreement with the value given in the above equation. Since the velocity dependence on density for most solid explosives, where the density can be varied independently of the temperature, lies in the range 3000 - 4000 m/sec/g/cc, one might expect Nitromethane to show a velocity dependence on temperature of approximately -4.7 m/sec/°C due to the change in density alone.

To determine whether Nitromethane did, indeed, show such a temperature effect, a series of six rate measurements was made

including two at ambient temperature, two just above the freezing point and two at as high a temperature as was deemed safe with our equipment. The experimental arrangement is shown in Fig. 3.

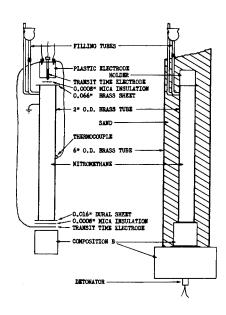


Fig. 3. Charge arrangement used to determine the effect of temperature on the detonation velocity of Nitromethane

The explosive was contained in a brass tube 2.000 in. o.d. with 0.125 in. wall. The tube was sealed at the top by a 0.066-in. brass plate which was soldered into place. The tube was sealed at the bottom with a 0.016-in. dural plate after experiments had shown that adequate initiation could be obtained through such Two holes were drilla plate. ed through the container near the top and two copper tubes were soldered into position. A thistle tube was cemented onto one of these tubes using Armstrong cement\*, which was found to be one of the few plastic materials not attacked by Nitromethane. The thistle tube served as a funnel during the filling operation and as a reservoir in the heating or cooling process.

After assembly, but

before the top and bottom plates were attached, the height of the container was measured with a vernier height gauge which could be read directly to 1 mil. The thicknesses of the brass and dural plates were measured with a micrometer.

Detonation velocities were determined, as before, with the pin technique. The lower pin switch was made of a copper strip, 2 mils thick, insulated with a thin sheet of mica as shown in Fig. 3. The upper switch was a 10-24 brass screw the end of which was turned to a point with a very small flat left at the tip. This was threaded into a Lucite block which was cemented into place with Armstrong cement. The signal circuit ground was formed by a wire soldered to one of the copper filling tubes.

Temperature measurements were made by means of an iron-constantan thermocouple. Two 12-mil holes were drilled near the center of the container part way through the wall, and the thermocouple leads were peened into them. A Leeds-Northrup Portable Indicator Millivolt Potentiometer, Model 8662, was used on which voltage could be read directly to one hundredth of a millivolt and estimated to a thousandth. In the range used, the sensitivity of the iron-constantan thermocouple is about 0.03 millivolt per degree F so that temperature

<sup>\*</sup>Adhesive type A - 1 manufactured by Armstrong Products Company, Warsaw, Indiana.

could be read to one-third degree F.

Since there was an appreciable time lapse between the removal of a charge from the thermostat and the firing instant, it was desirable to use a setup with a large heat capacity to minimize temperature changes. For this purpose a brass container, 6 in. o.d., 1/16 in. wall. 18 in. height, was used as an outside container for the charge, and the space between the two was filled with sand. High temperatures were obtained with an oven, low temperatures with a deepfreeze unit. In the heating and cooling processes, the temperature of the sand alone was adjusted to approximately the value desired and the sand was then poured into the container. The temperature was followed until it became reasonably constant, and the shot was then fired. It was assumed that by the time the temperature appeared to be constant the conductivity of the walls of the charge container and convection currents in the Nitromethane would have served to produce a satisfactorily uniform temperature throughout the charge. In the first shot there was a 22-minute wait before the shot was fired, with the temperature being constant for the last 4 minutes. Other charges behaved in a similar manner. All of the six charges were completed within a period of five days, using Nitromethane taken from a single lot so as to ensure uniformity in the explosive.

Experimental results are given in Table I and are presented in Fig. 4.

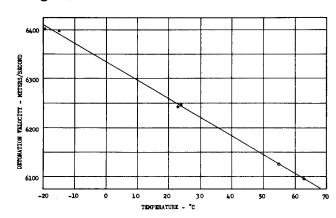


Fig. 4. Effect of temperature on detonation velocity of Nitromethane in brass tubes. 0.125-in. wall, 1.75 in. i.d.

An examination of the data shows that under the conditions of the experiment, Nitromethane exhibits a velocity dependence on temperature of - 3.7 m/sec/°C. This is smaller than might be expected from the density effect produced by temperature change as mentioned earlier. A part of this discrepancy results from the tendency for the detonation velocity to increase with an increase in the initial temperature, density held constant; a-

nother part is due to the finite diameter of the test charges, as will be shown in the next section.

THE DIAMETER EFFECT IN NITROMETHANE AS AFFECTED BY TEMPERATURE

After determining the effect of temperature on the detonation velocity of Nitromethane, experiments were performed to measure the diameter effect in glass tubes. The results of this series of shots and also of observations made during a study of "failures"

Table I

Shot Number	2736	2737	2738	2739	2740	2747
Overall Length (in.)	12,072	12.070 12.044		11,939	12,011	12,079
Thickness of Tube Caps (in.)	0,066 Br	ass; 0.0	0.066 Brass; 0.016 Aluminum - same for all runs.	m - seme	for all	mns.
Nitromethane Path Length (in. mm.)	11,990" 11,988" 304,546 304,495		11.962" 303.835	11.857" 301.168	11.929" 302.997	11.997" 304.724
Transit Time Overall (µsec)	651.67	49.130	49.159 49.130 50.000 49.812 47.708	76,812	47,708	976°27
Time through Al. and Brass Caps (µsec) *	0.377	0.377	0.377 0.377 0.377 0.377	0,377	0.377	0.377
Transit Time for Nitromethane (µsec)	782.87	48.782 48.753	49.623	49.623 49.435 47.331	47.331	47.569
Correction for Brass Expansion ** (mm.	** (mm.) No correction	rection	+•164	+,164 +,205	218	244
Corrected Velocity	6,2429	6,2429 6,2456		6.1262 6.0963 6.3971	6,3971	8007°9
Temperature (°C)	23,09	23.09 24.09		55.04 62.80 -15.01	-15.01	-19.42
Density	1,1283	1,1270	1,1283 1,1270 1,0862 1,0757 1,1788	1.0757	1,1788	1,1848
* Shock wave velocity in Al. taken as 7.1 mm/ $\mu$ sec. (0.016" = 0.056 $\mu$ sec). Shock wave velocity in Brass taken as 5.3 mm/ $\mu$ sec. (0.066" = 0.321 $\mu$ sec).	Al. take Brass ta	n as 7.1 1 ken as 5.	mm/µsec. 3 mm/µsec	(0°016" = (0°066"	0.056 µs = 0.321	ec). usec).

<sup>\*\*</sup> Taking 1.8 x 10-5/0c as linear coefficient of expansion of Brass

(to be discussed later) suggested that the diameter effect might be a function of temperature. Consequently, another set of experiments was designed to investigate this point.

The experimental arrangement used is shown in Fig. 5.

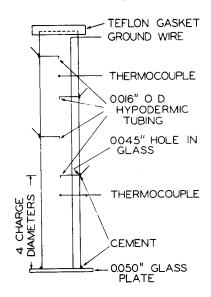


Fig. 5. Charge arrangement for measuring detonation velocity as a function of charge diameter

The containers were made of standard-wall Pyrex brand glass tubing. Holes for pin switches were made in the glass at 5-in. intervals using a hot The tubes were tungsten wire technique. then ground flat on each end, and glass plates were sealed on with Armstrong cement. The pin switches were made with steel hypodermic tubing 16 mils o.d., 4 mils wall, this material being used because of its stiffness. The lower end of each piece of tubing was collapsed and ground flat. After the probes had been inserted and cemented in place with Armstrong cement, the spacing of the probe tips was measured with a cathetometer to an accuracy of about 1 mil.

After each glass tube was assembled and filled with Nitromethane, it was placed in a wooden box and insulated with vermiculite. This assembly was then placed in an oven or a deep-freeze and brought to the desired temperature. The temperature of the Nitromethane was as-

sumed to correspond with the temperature of a piece of brass shim stock taped to the middle of the charge tube and monitored by means of a thermocouple. After the charge had come to the desired temperature it was removed from the thermostat and fired within ten minutes.

Following the above procedure for charge preparation and firing, two sets of diameter-velocity data were obtained — one at 22.5°F and one at 91.3°F. Each series contained four shots, and each shot contained three rate intervals. Between the booster and the first rate interval, a minimum of four diameters of charge was allowed for stabilization of the detonation process. The resulting data are given in Table II and are plotted in Fig. 6.

The straight line drawn through the data taken at 91.3°F was obtained by the method of least squares; the straight line at 22.5°F was simply drawn through the points and found to be adequate. The equations of the two curves are:

$$(22.5^{\circ}F)$$
 D = 6374.5 - 170.5 (1/d)

$$(91.3^{\circ}F)$$
 D = 6212.5 - 51.7 (1/d)

In these equations D is the detonation velocity, expressed in meters per second, at a stick diameter of d cm.

Because the slope of the diameter-effect curve at the lower

Table II

Firing temperature approximately 91.3°F

Shot Number	I.D. Average (inches)	O.D. Average (inches)	1/I.D. (cm-1)	Velocity Uncorrected (m/sec)	Average Velocity Corrected to 91.3°F. (m/sec)
B <b>-</b> 3261	0.974	1.097	0.404	6192 6194 6195	6194
B <b>-</b> 3265	1.247	1.415	0.316	6192 6193	6194
B <b>-</b> 3266	1.749	1.900	0.225	61 <b>99</b> 6200 6201	6199
B-3267	4.055	4.289	0.0971	6203 6218 6207	6209

Firing temperature approximately 22.5°F.

Average Velocity Corrected to 22.5°F. (m/sec)

D-4723	1.330	1.460	0.296		Failed
D-4741	1.742	1.890	0.226	6335 6334 6337	6336
D-4748	2.571	2.769	0.153	6346 6348 6349	6348
<b>D-4</b> 750	4.059	4.295	0,0970	6361 6363 63 <i>5</i> 4	6358

temperature is steeper (with relatively little change in the infinite medium velocity), it may be assumed that the decrease in the initial

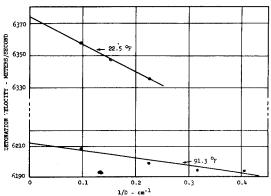


Fig. 6. Effect of temperature on the diameter effect. Nitromethane confined in glass tubes.

The results of the calculations are:

temperature has caused an increase in the reaction zone The thickness of thickness. this zone at each of the two temperatures in the experiment may be estimated by applying the Eyring equation for unconfined charges (which should be a good approximation for Nitromethane in glass tubes):

$$D/D_{i} = 1 - 0.5 (a/R)$$

D: detonation velocity of stick with diameter R.

D<sub>i</sub>: detonation velocity in infinite medium.

reaction zone length.

 $(22.5^{\circ}F)$  a = 0.08 mm

$$(91.3^{\circ}F)$$
 a = 0.27 mm

The value, of a obtained at 91.3°F corresponds closely to that obtained by Cotter (5) at approximately 75°F using a streak camera technique.

It is also of interest to note that the temperature coefficient of the detonation velocity is greater for infinite medium than it is for small diameters. Using the two infinite medium extrapolations given above, a value of -4.2 m/sec/°C is obtained. At a charge diameter of 1.75 in. the value of the temperature coefficient of the detonation velocity is found to be  $-3.5 \text{ m/sec}/^{\circ}\text{C}$ . This is in good agreement with the value -3.7 m/sec/°C found for brass confinement at this diameter, reported in the preceeding section.

#### EFFECT OF TEMPERATURE ON FAILURE DIAMETER

The effect of temperature on the failure diameter of Nitromethane was determined with the use of the charge arrangement shown in The charge of Nitromethane was contained in a Pyrex brand glass tube approximately 12 diameters long. It was poured into the tube through a small hole in a thick dural plate; damage to the latter was used as a criterion for deciding whether detonation or failure had occurred (Fig. 8). Initiation of the Nitromethane was accomplished by use of a heavy booster of Composition B acting through a 50-mil glass plate, this combination resulting in slight overboosting. As in the previous set of experiments, the temperature of the charge was

maintained constant by means of substantial insulation.

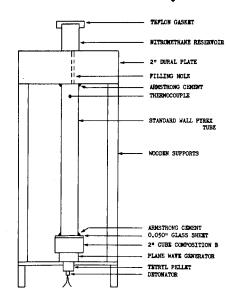


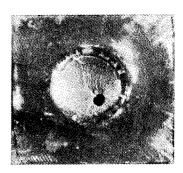
Fig. 7. Charge arrangement used to determine failure diameter

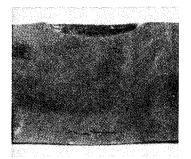
The results obtained at three temperatures are shown in Fig. 9 and are listed in Table III. While there is some overlap apparent at a given temperature, the failure diameter is defined to about 2-3 mm. Over the temperature range covered in these experiments the failure diameter varied from approximately 15 mm to 35 mm, increasing as the initial temperature was lowered.

### FAILURE PROCESS IN LIQUID EXPLOSIVES

Early work on the diameter effect in Nitromethane was directed to finding the failure diameter of this explosive in tubes of glass and various metals. Plastic tubes were not used because of the possibility of contamination of the explosive by solvent action. It soon became evident that Nitromethane

would propagate (at about 75°F) in brass tubes of 3 mm i.d. and 1.6 mm wall and in dural tubes of 4.8 mm i.d. and 1.6 mm wall, but would fail in glass tubes below 17 mm i.d. Subsequent examination of the process





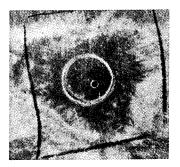


Fig. 8. Photographs A, B show the damage to dural plates resulting from propagation of detonation in charges as sketched in Fig. 7. Photograph C shows the result of detonation failure.

of failure using a streak camera showed non-luminous areas spreading inward from the confining walls and choking off the detonation process. These "failures", first observed in connection with other experiments by T. P. Cotter (5), appear to be characteristic of homogeneous explosives.

A rotating-mirror camera record of the failure of detonation in Nitromethane is shown in Fig. 10. In this figure and in Figs. 11-19 the camera has been directed to look along the axis of the charge. Time proceeds to the right at the rate of 0.39 µsec/mm. In

Table III

I. D. Average (millimeters)	Tube Length / (inches)	Temperature (degrees F)	Result*
30.9	18	<b>-8.</b> 5	F
33.9	17	-9.0	F
33.5	16	-10.5	F
34.5	17.5	-6.5	
36.5	17.5	-7.0	P
38.4	18	-12.0	F P P P P P P
40.4	18	<b>-9.</b> 8	P
22.3	12	17.0	F
27.3	14	17.0	P
31.0	15	20.0	P
40.5	17.8	30.0	P
23.9	12	19.9	F
26.0	15	19.5	F
27.2	16	20.0	f F F
28.2	15.8	18.5	F
28.8	16	19.3	P
30.9	16	21.8	P
31.3	16	17.5	P
33.4	16	19.8	P
12.7	12	96.7	F
14.9	12	98.0	P P P F P
15.5	12	90.4	F
16.7	11.8	95.9	P
17.5	12	92.2	P P

\*F\_Failure

P-Propagation

Note: All tubing was standard wall Pyrex glass tubing.

Fig. 10 the explosive was contained in a glass tube 17 mm i.d. Detonation ceased after a travel of approximately 50 mm in the Nitromethane. Similar behavior was also observed for Ethyl Nitrate (Fig. 19)

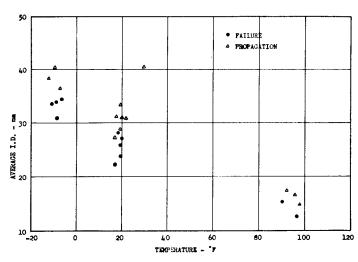


Fig. 9. Effect of temperature on the failure diameter of Nitromethane confined in glass tubes

and for large single crystals of PETN as will be described in a later section of this report.

Figure 11 shows the streak record from a charge similar to that which produced the record in Fig. 10, except that the glass was replaced by dural. No failures are evident. This difference in the effects of glass and dural on the occurrence of failures was at first quite puzzling. Since the charge-weight/casing-weight ratios for the two charges were essentially the same, and

since the densities of the two materials were nearly equal, the intuitive feeling arose that the observed difference was, perhaps, not



Fig. 10. Nitromethane in glass tubing. Booster flash at left end of trace. Tube i.d.: 17 mm. Time increases to the right at 0.39 μsec/mm.

the result of confinement in the usual sense, but came about through some difference in surface effects. This feeling was strengthened by the shot record shown in Fig. 12. This was produced by Mitromethane detonated in a glass tube close to failure diameter. The wall thickness of the tube was about 1 mm. Lead tape was wrapped to a thickness of 1/8 in. about the first two inches of the tube. The second two inches were lined loosely with one layer of 2-mil aluminum foil. Thus, the mass of the first part of the tube was increased substantially over that of the glass alone; the mass of the second part was essentially unchanged, but the inner surface was now aluminum. From the camera record it is evident that the increased confining mass in the first interval was relatively ineffective in eliminating failures

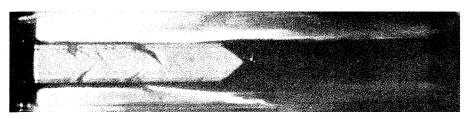
when compared to the action of the aluminum foil.

Referring again to Fig. 12, it should be noted that the detonation process appears to cease abruptly after reaching the end of the aluminum foil. A more direct illustration of the action of failures to choke-off the detonation is presented in Fig. 14. This is a



Fig. 11. Nitromethane in dural tubing. Time scale:  $0.39 \,\mu sec/mm$ .

succession of pictures of a single charge undergoing failure. The experimental arrangement is diagrammed in Fig. 13. A glass tube filled with Nitromethane was arranged to extend into a small glass-walled box, also filled with Nitromethane. The diameter of the glass tube was chosen to be considerably below failure diameter at the temperature of firing. Propagation of detonation in the glass tube was made possible by a lining of 2-mil stainless steel foil. During detonation, the box was illuminated from the rear with argon shock light.



Lead foil | Aluminum | Glass

Fig. 12. Nitromethane in glass tubing. Lead foil wrapped outside tube over first 2 in. of tube length; 2 mil aluminum foil used to line tube for second 2 in. of length

Picture frames were taken with exposures of  $0.3~\mu sec$  and were spaced at intervals of  $1.5~\mu sec$ .

In Fig. 14, the approach of the detonation wave to the upper end of the tube is shown first in frame No. 2. As the wave emerges from the end of the tube, a rarefaction spreads inward from the periphery, giving the wave the appearance of a truncated cone. (Frame No. 3). In frame No. 4 the detonation process has ceased, and a simple shock wave is passing out into the Nitromethane filling the box.

Reverting to the thought that the effectiveness of aluminum foil in suppressing failures might be due to some surface character-

istic not possessed by glass, three experiments were tried to investigate obvious differences. These tests did not constitute an exhaustive examination of the problem, but were performed in the hope of uncovering clues which might suggest more detailed experiments. Although the results were negative, they are offered here because they

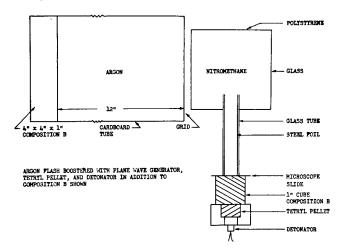


Fig. 13. Charge arrangement used to illustrate failure of detonation in Nitromethane

contribute to limiting the possible explanations of the effect of metal foils in repressing failures.

The first surface effect tested was that of smoothness. The glass tubing used had always had a fire-polished inner surface, whereas the metal foil had been relatively rough. To exaggerate this difference in smoothness, a 35 mm i.d. glass tube was prepared with the latter half of the inner surface roughened with No. 54 Carborundum. The firing trace, Fig. 15, shows little or no difference be-

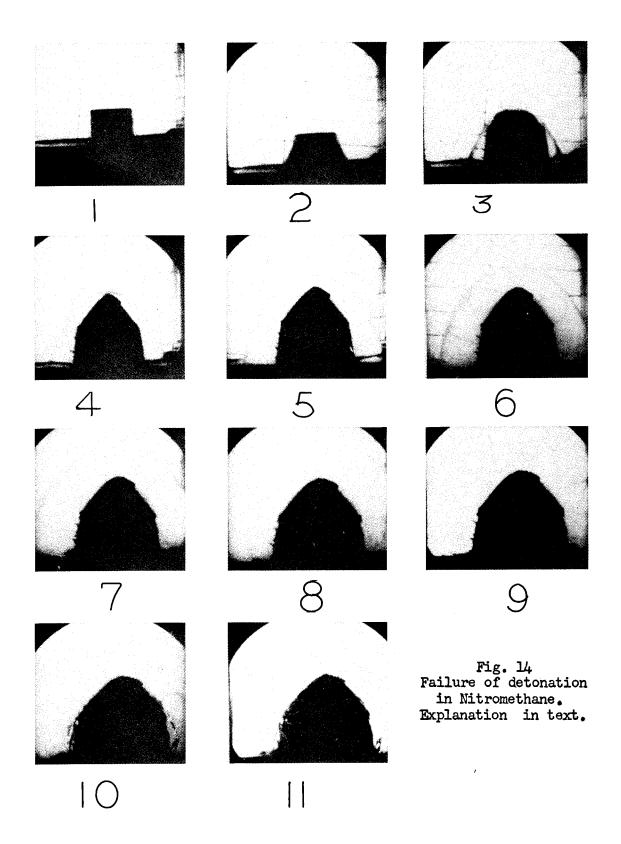
tween the effects of the smooth and the roughened portions. In passing, it should be noted that increase of the tube diameter resulted in the production of smaller failures than those in Fig. 10.

The next surface effect investigated was that of chemical reaction. It was argued that, contrary to the action of glass, the aluminum might react with the Nitromethane to produce decomposition products of the latter which would sensitize the explosive near the confining walls. To test this possibility, aluminum foil was immersed in Nitromethane for 19 hours. The explosive was then decanted into a glass tube. For purposes of reference the first inch of the tube was lined with 2-mil aluminum foil. The firing record, Fig. 16, shows that the Nitromethane was not sensitized to any appreciable extent.

The third surface effect to be studied was that of catalytic activity by the metal foil. A 2-mil platinum foil was poisoned with hydrogen sulfide. This was then used to line a portion of a glass tube, the remainder of which was lined with untreated platinum foil. The firing test showed the two foils to be indistinguishable in regard to the repression of failures.

In the hope of finding some difference between various metals which might furnish a hint of the mode of action of the aluminum in repressing failures, several metals were tried as foils in glass tubes. Because of ready availability, the metals tested included steel, copper, tungsten and platinum. All proved effective in thicknesses of a few mils.

One of the first clues to the true mode of action of foils was obtained in the firing record presented in Fig. 17. In this shot the diameter of the glass tube was less than failure diameter. The



first two inches were lined with 2-mil aluminum and the second two inches were lined with 1/4-mil copper. The firing record shows that

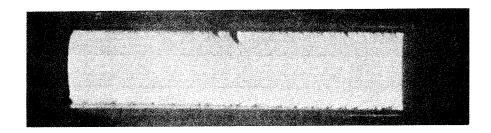


Fig. 15. Nitromethane in glass tubing. Right half of tube ground with Carborundum on inner surface. Time scale:  $0.39 \, \mu \text{sec/mm}$ .

the detonation failed on reaching the copper foil. Since thicker copper foil had been found to be effective in preventing failures, it was suggested here that the thickness of the foil was important.

To investigate further the effect of foil thickness a glass tube with a diameter less than failure diameter for unlined glass was lined with three platinum foils of differing thicknesses. The first foil encountered by the detonation wave was 1 mil thick, the next was 1/2 mil thick and the third was 1/5 mil thick. Each foil occupied two inches of the length of the tube. The firing trace, Fig. 18, shows that only the 1/5-mil foil was ineffective in preventing failure. A

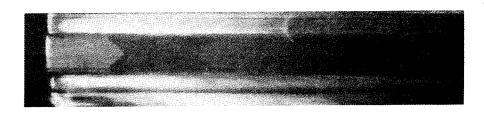


Fig. 16. Nitromethane in glass tubing. The explosive was maintained in contact with aluminum for 19 hours prior to firing. First 2 inches of tube lined with 2-mil aluminum foil. Time scale:  $0.39~\mu sec/mm$ .

similar shot in which the foils were made of copper gave a similar result. Here, then, was a method of differentiating the action of foils which differed by only 0.3 mil in thickness. Additional experiments suggested that for a given foil thickness, steel was more effective a confining material than aluminum, and tungsten was more effective than steel. The effectiveness was evidenced by the minimum diameter glass tube in which propagation was made possible by the presence of the foil.

On the basis of the experimental evidence presented above and from the results of other similar experiments, it may be concluded that the action of metal foils in repressing failures in Nitromethane

is one of confinement of the detonation wave. Such parameters as the density, compressibility and thickness of the confining material are the important ones, and the specific nature of the surface seems to be without effect. Glass may be anomalous, but not enough is known about

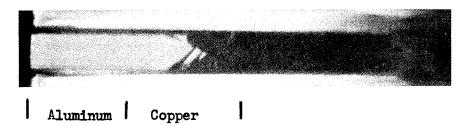


Fig. 17. Nitromethane in glass tubing. First two inches of tube lined with 2-mil aluminum foil; second two inches lined with 1/4-mil copper foil. Detonation failed before reaching end of copper foil. Time scale: 0.39  $\mu$ sec/mm.

shock processes in this material to be certain of this. Because of the surprisingly thin layers of metals which are effective, it may be that confinement of the reaction zone until some initial stage of the reaction is completed is sufficient to prevent the occurrence of failures.

#### DETONATION PHENOMENA IN LARGE CRYSTALS

Work on large, single crystals of high explosive was begun partly because so little was known about the behavior of such crystals and partly because of some unique properties which had been suggested

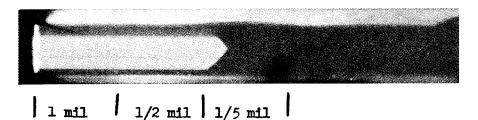


Fig. 18. Nitromethane in glass tubing. Tubing lined with three 2-in. platinum foils in series. Foil thickness: 1 mil, 1/2 mil and 1/5 mil. Detonation failed on encountering the 1/5-mil foil.

Time scale: 0.39 µsec/mm.

for them. There are those who are of the opinion that it is not possible to produce a stable detonation in a single large crystal. This view follows from the belief that the compressional heating in the shock front, in the absence of air voids, is insufficient to account for the rapid rate of reaction associated with detonation. On the other hand, there is a commonly-held view that large crystals of explosive may be much more sensitive to mechanical shock

than the smaller crystals normally encountered.

These questions have been investigated for such different materials as PETN, Tetryl, RDX and TNT. Large crystals of any given explosive studied have been found to be markedly less sensitive to initiation by mechanical shock than the powdered form. However, under

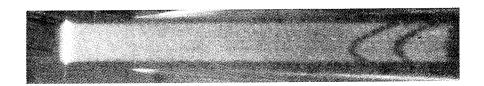


Fig. 19. Ethyl Nitrate in glass tubing 27.2 mm i.d. Tubing lined with 2.5-mil stainless steel foil. Time scale: 0.17  $\mu$ sec/mm.

suitable conditions of boosting, large single crystals may be caused to detonate. It is important to note that the crystals used for detonation studies were in most cases optically clear and free from visible defects, but there was always the possibility that small-scale lattice defects throughout each crystal may have served as centers of reaction, fulfilling the requirements of the "hot spot" theory. Although this possibility may have obscured the main issue here, other equally interesting phenomena have been observed which relate the behavior of large, single crystals to that of liquids.

# Preparation of Crystals

The crystals used were grown from saturated solutions by two methods: by evaporation of solvent, and by lowering the temperature of the solution. In both methods, seed crystals were used. The solvent principally employed was acetone.

Many difficulties were encountered in growing flawless crystals to a size of one inch or larger. PETN crystals in particular, but all of them to some extent, were found to be extremely fragile when exposed to thermal shock. Merely touching the crystal with the fingers was sufficient to produce cracking which was both visible and audible. Evaporation of solvent from the crystal surface when the crystal was removed from the growing solution produced disastrous effects on the clarity of the crystal. This sensitivity to thermal shock increased rapidly with crystal size.

The quality of the crystals was quite variable. Some crystals were grown which were almost optically clear, while others had clear sections which were cut out for use in the experiments to be described below (Fig. 20). The very large crystals used in the rifle bullet tests were quite cloudy. An index of the quality of the better crystals is furnished by the data in the following table.

Explosive	Appearance of Crystal	Density Observed g/cc (25°C)	Density Reported in Literature g/cc		
PETN	Clear	1.777	1.773(6)		
TNT	Cloudy	1.651	1.654 <sup>(7)</sup>		
Tetryl	Clear	1.734	1.73 (8)		
RDX	Cloudy	1.802	1.82 (9)		

The observed density values reported above were determined by preparing a zinc chloride solution in which the crystal could be suspended. The density of the solution was then measured with a hydrometer which had been calibrated with a pycnometer.

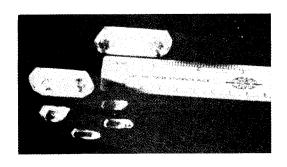


Fig. 20. Unpolished crystals of PETN

Crystals were found to be much easier to cut and shape than to grow. They could be chipped to shape with a razor blade and polished in a manner reminiscent of optical polishing methods. A more elegant way of shaping them was that of grinding with high speed grinding equipment, using kerosene as a coolant and dust allayer. The process of fabricating a cylinder from a PETN crystal was as follows: the

rough crystal was cemented to a short section of wood dowel, using Armstrong cement. Only a thin layer of the cement was used because of the heat evolved in the polymerization process. When the cement had set, the dowel was mounted in a lathe and rotated slowly. The cylinder was formed by taking fine cuts with a 5-in. Alundum wheel (Norton No. 38 A 120 LV) mounted in a tool post grinder and rotated at 5000



Fig. 21. Cylinder ground from PETN crystal

RPM. When the cylinder had been ground to the correct diameter, the ends were cut off (Fig. 21) using a rubber-bonded Alundum wheel 4 inches in diameter and 8 mils thick (Norton No. A-240-x-10R30), also rotated at 5000 RPM.

#### Rifle Tests

At the time work was begun on crystals, there seemed to exist a widespread apprehension that large crystals of explosives were more sensitive than the same materials in any other physical state. This apprehension may have originated from a knowledge of

the great sensitivity of large grains of lead azide. Crystals of this explosive 1 mm in length have been reported to explode spontaneously (10). It was desirable, therefore, to obtain some information on the sensitivity of the large crystals of PETN being grown.

The test decided upon was a rifle test. A rifle chambered for the .220 Swift cartridge was employed; the type of bullet used in the tests was a soft-point one weighing 48 grains. It had a muzzle velocity of 4000 ft/sec and a muzzle energy of 1800 ft-lbs. In each test, with the exception of one, the crystal was mounted on plywood or corrugated paper board at a distance of 50 ft from the muzzle of the gun. The crystal was oriented with the minimum dimension in a direction parallel to the path of the bullet.

The result of each rifle test was determined from the damage to the crystal support and from the manner in which the crystal disintegrated. In all, 25 tests were made with crystals varying in thickness from 3/4 in. to 3 1/4 in. It was found that PETN crystals less than 1 1/4 in. thick did not detonate to any detectable extent; crystals approximately 1 3/8 in. thick sometimes detonated partially; and crystals more than 1 3/8 in. thick always detonated with accompanying loud noise, bright flash and thorough destruction of the backing and supporting stand.

Figure 22-A shows a PETN crystal mounted for testing on a sheet of plywood, and the damage to the backing as a result of the disintegration of the crystal is shown in Fig. 22-B. In Fig. 23-A, a

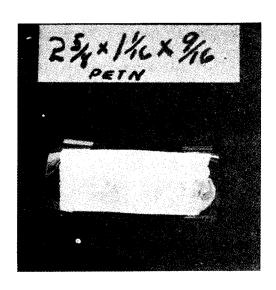


Fig. 22A. PETN crystal mounted on plywood for rifle test

3/4 in. thick PETN crystal is shown mounted on a steel plate. The only damage to the plate as a result of the rifle test was a pit due to the impact of the bullet. Later, a similar crystal was mounted on the same plate at the lower right corner and was initiated with an electric detonator to produce damage for comparison with the result of the rifle bullet test. It is apparent that the crystal struck by the bullet did not detonate.

The relative sensitivity of powdered PETN was illustrated by the results of thirteen additional rifle tests. In each of these tests, the powdered material was poured onto a sheet of cardboard to

form a thin, uniform layer of explosive. Thin strips of wood were used to support the edges of the layer, and a thin cellophane sheet was placed over the top to hold the explosive in place when the assembly was turned on edge. The thickness of the PETN layer was 0.148 in. in the first test. Since this charge detonated, the thickness was reduced in each of the succeeding tests until on the last test a

thickness of 0.092 in. was reached. All tests resulted in detonation. Thus, it became apparent that powdered PETN was much more sensitive

than large crystals of the same explosive.



Fig. 22B. Damage caused by disintegration of crystal under bullet impact

making an angle of 45° with the base. The crystal was separated from a Composition B booster by a distance of 0.3 in. When the charge was

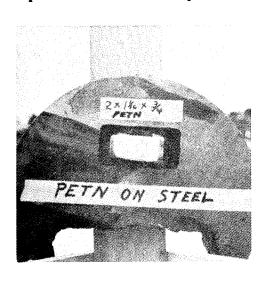


Fig. 23A. PETN crystal mounted on steel plate for rifle test

Detonation of Single Crystals

Observations on the detonation of single crystals were made both with rotating mirror cameras and with the pin technique. Unfortunately, the work on the measurement of detonation velocity was interrupted before satisfactory data could be obtained. Nevertheless, many interesting qualitative details of the detonation process were discovered and these will be discussed here.

In Fig. 24-A, a PETN crystal .616 in. thick is shown mounted above a plane wave generator. A flat face was ground on one side of the crystal, The crystal was separated from

fired a plane detonation wave was produced in the plate of Composition B. This in turn produced a plane shock wave in the air space above the plate, which initiated the PETN crystal weakly. The detonation wave proceeding up the crystal gave evidence of its position by a luminous shock in the narrow air space under the plastic cover.

The firing trace from this shot is shown in Fig. 24-B and is explained by means of the sketch in Fig. 24-C. In the latter figure, interval I shows the shock traversing the air space between the Composition B and the crystal. In interval II, a detonation wave proceeds at low velocity and with low luminosity

through the crystal. At the beginning of interval III, the detonation wave undergoes an abrupt increase in velocity and brightness. The velocity actually exceeds the steady-state value for a short space, then drops to that value. In interval IV, the shock wave in air

beyond the crystal is evident. The details of this record were found to be repeated in many similar experiments. Besides the interesting

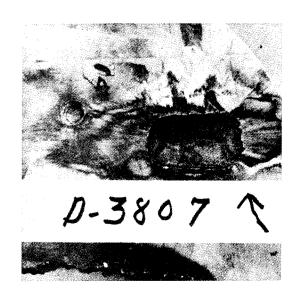


Fig. 23B. Circular pit at left is due to bullet impact in rifle test of crystal shown in Fig. 23A. Rectangular pit at right is damage which resulted from the initiation of a similar crystal with an electric detonator.

phenomenon of overshoot in the velocity, which has also been observed for detonation in gases (11), the experiment shows that with underboosting, the detonation rate increases to the final, steady-state condition, proving that stable detonation in single crystals is possible.

Actual detonation velocities in the above experiment were difficult to measure with accuracy, because of the problem of accurate space measurement. The estimated values of the detonation velocity were 5560 m/sec for the initial phase, 11,120 m/sec for the overshoot and 7240 m/sec for the final state.

In another type of experiment, crystals were ground into rods and stacked to make rate sticks as shown in Fig. 25. The purpose of the two experiments of this type which were completed was to estimate the

failure diameter, and to measure the detonation rate, if detonation occurred, using the pin technique. In the first shot, the crystals were ground to a diameter of 1/4 in. and a length of approximately 1 in. Boosted with a cube of Composition B 1/2 in. on a side, this charge failed to detonate. In the second experiment, the crystal diameter was 1/3 in. and the lengths of the two sections were 0.929 in. and 0.763 in. Measured velocities were 7973 m/sec over the first piece beyond the booster, and 6083 m/sec over the second piece. Since the diameter of the stick may still have been near the failure value, failure might have occurred in the second interval and the final pin signal could have been due to closure of the pin switch by air blast.

### Failures and the Foil Effect for Crystals

The fact that crystals exhibit "failures" and the foil confinement effect is demonstrated in Fig. 26. This is the record obtained from a PETN crystal cut in the form of a parallelepiped measuring 0.25 x 0.25 x 0.40 in. A 2-mil copper foil was glued around the crystal, extending 0.2 inch in the long direction. The end of the crystal which was thus wrapped with foil was initiated with a 1/2-in. cube of Composition B. A rotating mirror camera was directed to look down the long axis of the crystal. From the firing record, Fig. 26,

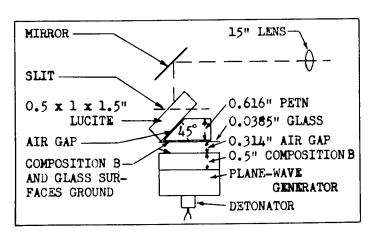


Fig. 24A. Charge arrangement for shot to measure detonation velocity in a single crystal of PETN

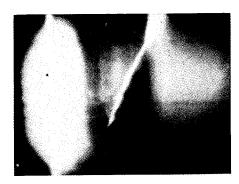


Fig. 24B. Firing trace

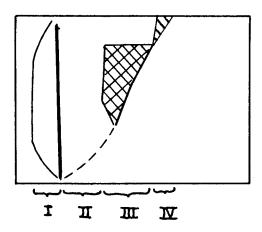


Fig. 24C. Sketch of firing trace

it is evident that while the cross section of the crystal was quite small, no failures occurred until the detonation wave passed beyond the copper foil confinement, at which time failures appeared and

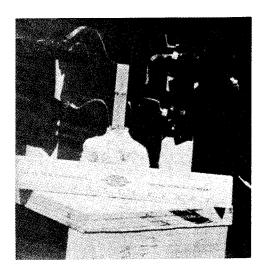


Fig. 25. Rate stick made of PETN crystals ground to cylindrical shape. Putty was placed over the booster to hold back air blast.

rapidly choked off the detonation. Many similar records were obtained in other experiments.

#### CONCLUSION

In the foregoing sections, data have been presented to show that initial temperature has a pronounced effect on the detonation velocity of Nitrome-The velocity was found thane. to increase with decrease in temperature, as was also the diameter effect and the failure diameter. The curves of detonation velocity as a function of the diameter were, for Nitromethane lightly confined in glass, essentially straight lines out to failure diameter.

When detonation fail-

ure occurs in liquid explosives and single crystals, the failure process begins abruptly at the periphery of the detonation wave and spreads inward to engulf the entire wave. For glass confinement above

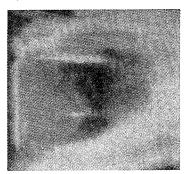


Fig. 26. Single crystal of PETN showing failures. Time increases to the right.

failure diameter, small failures were shown to occur at the walls with high frequency, but each of these persisted for only a brief time.

For explosives in the form of liquids and single crystals, thin metal foils were shown to be effective in suppressing failures and in reducing the failure diameter substantially. The density and the thickness were of importance in determining the confining effect exerted by a foil.

Lastly, work on the growth and fabrication of large crystals of various explosives was reported. Crystals of PETN were tested with rifle bullets and found

to be relatively insensitive when compared to powdered PETN. Incomplete experimental work on measuring detonation velocities in single crystals was described to show that detonation will propagate under the conditions prevailing in these crystals.

#### REFERENCES

- 1. H. Eyring, R. E. Powell, G. H. Duffey and R. B. Parlin, Chem. Revs., 45, 69(1949).
- 2. H. Jones, Proc. Roy. Soc. (London), A189, 415(1947).
- 3. A. W. Campbell, M. E. Malin, T. J. Boyd, Jr. and J. A. Hull, "Technique for the Measurement of Detonation Velocity". (This Conference).
- 4. International Critical Tables (MCGraw-Hill Book Company, Inc., New York, 1928), first edition, Vol. III, p. 28.
- 5. T. P. Cotter, Jr., "The Structure of Detonation in Some Liquid Explosives". (Dissertation, Cornell University, 1953).
- 6. C. D. Hodgman, Handbook of Chemistry and Physics (Chemical Rubber Publishing Company, Cleveland, 0., 1951). 33rd edition, p. 1150.
- 7. N. A. Lange, Handbook of Chemistry (Handbook Publishers, Inc., Sandusky, 0., 1952), eighth edition, p. 693.
- 8. I. M. Heilbron, Dictionary of Organic Compounds (Oxford University Press, New York, 1943), Vol. III, p. 740.
- 9. W. C. M<sup>C</sup>Crone, Analy. Chem., <u>22</u>, p. 954(1950).
- 10. T. L. Davis, The Chemistry of Powder and Explosives (John Wiley and Sons, Inc., New York, 1943), p. 425.
- 11. D. J. Berets, E. F. Greene and G. B. Kistiakowsky, J. Am. Chem. Soc., 72, 1086(1950).

## PARTICLE SIZE EFFECTS IN ONE- AND TWO-COMPONENT EXPLOSIVES

M. E. Malin, A. W. Campbell and C. W. Mautz Los Alamos Scientific Laboratory Los Alamos, New Mexico

#### INTRODUCTION

The subject of particle size effects is an important one in many military and commercial explosives. With the exception of liquid explosives and the blasting gelatins, every explosive in common use is composed of material whose state of subdivision has a bearing on its detonation properties. From a practical viewpoint, then, particle size effects warrant attention.

Aside from practical consideration, it appears that those theories which do not inquire into the details of the reaction kinetics, e.g., early diameter effect theories, do not correctly predict the behavior of at least some heterogeneous explosives at finite diameters. Further, the apparent persistence of particle size effects to infinite diameter opens speculation concerning the location of the Chapman-Jouguet surface under infinite-medium conditions. It seems, therefore, that a better understanding of these effects will require additional theoretical and experimental inquiry into reaction zone structure and also into the mechanism of detonation propagation under conditions of varying particle size and geometry; reaction rate considerations have been introduced by Kirkwood and Wood (1) into their theory of the structure of a plane detonation wave, and this theory does indeed offer possible explanations for certain of the observed infinite diameter effects, as will be seen later in the paper.

The importance of particle size effects in one-component explosives has been well-demonstrated by various workers. MacDougall, Martin, Boggs and Messerly<sup>(2)</sup> have shown that in low density ammonium picrate charges the addition of a small percentage of coarse material to fine particles markedly lowers the detonation velocity (all charges corrected to the same density). More surprisingly, in their experiments the addition of a small amount of fine material to coarse particles also lowers the velocity, while mixtures in the vicinity of 70% coarse, 30% fine (under their conditions of particle size, charge diameter and confinement), could not be detonated. Explanations for this

behavior have been offered by Gamow<sup>(3)</sup> in terms of numbers of loadbearing contact points, but the effect is still not completely understood.

Jones and Mitchell (4) have shown that, within certain particle size ranges, low-order detonation is possible in low density TNT

charges and in Tetryl charges.

Tranter(5) and others have shown that particle size effects are also important in high density, cast explosives. In their experiments, they demonstrate a marked effect of the rate of cooling of cast TNT charges on the detonation velocity.

Although the above is far from being a complete survey of the particle size effect literature, it indicates that in the past much attention has been devoted to one-component systems, and understandably so, since these are already sufficiently complex. Nevertheless, there are many two-component heterogeneous explosives in use in which particle size effects appear to be important, in a manner perhaps different from the case of one-component systems, and this paper is primarily concerned with a discussion of such two-component systems.

The work described here has been done principally with Composition B, a cast explosive containing approximately 60% RDX and 40% TNT. In the casting of this material, the temperature is raised sufficiently to melt the TNT, the RDX is then added, and the TNT is allowed to slowly solidify to form a continuous matrix in which the RDX particles are embedded. Under these casting conditions there is some solubility of RDX in TNT (4 to 8% by weight), the dissolved RDX precipitating as the TNT solidifies. The size of these precipitated RDX particles is not known and probably varies with casting conditions.

The reasons for the choice of Composition B for this work can be stated briefly: Composition B is a relatively inexpensive and available material of intermediate sensitivity and high energy. It is characterized by a short reaction zone length and an accompanying convenient range of working diameters. The failure diameter is approximately 1/6", and sticks 1 1/2" in diameter have a detonation velocity which is lower than infinite medium velocity by about 40 m/sec. Perhaps most important, it is a high density explosive, readily machinable to tolerances of 0.001".

Along with other two-component cast explosives, charges of Composition B have the disadvantage of particle size, density and composition segregation. These are compensated for, to some extent, by well-developed sampling and analytical techniques. Composition B also contains a variable amount of wax and other additives (1 to 1.5%), and for precise work these must be quantitatively determined.

The paper will be divided into two parts; Sections I - III will be concerned with particle-size effects at finite diameter and IV - V with particle-size effects at infinite diameter.

## EXPERIMENTAL I

The detonation velocity of a species of Composition B, which

will be called Type 1, was determined as a function of diameter. The general technique of charge assembly is discussed in another paper (6), so that only the more important details need be given here. The charges were assembled vertically with 0.0002" aluminum ionization foils inserted between sticks. Duco cement was used to keep the sticks in place, and care was taken in the cementing process to avoid introducing any glue between the joints. In each case, before velocity measurements were taken, the detonation wave ran at least four charge diameters in a section of the booster which was the same diameter as the rate stick. The rate sticks were each approximately 2" long. Plate 1 shows a typical charge assembly.

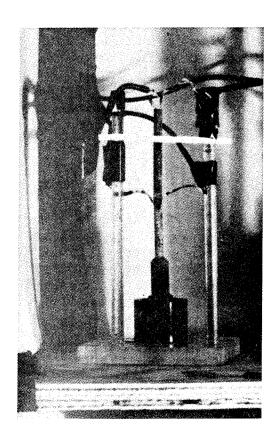


Plate 1. Composition B Charge Assembly

The charges fired were of two types: those including only one rate stick section and those including three rate stick sections. The velocities obtained in a three-rate-stick charge are designated in Table 1, below, as A, B and C.

The casting from which these charges were obtained had been sampled and analyzed throughout for composition and density. It was therefore possible to correct the velocity of each rate stick to a common composition and density, 63.00% RDX and 1.700 g/cc. The correction factors used were +32 m/sec for +0.01 density unit and +13.4 m/sec for +1.00% RDX. These numbers have been obtained from other experiments, involving pressings and castings, in which the density and composition were varied separately.

#### DISCUSSION I

The data given in Table 1 are shown plotted in Figure 1. A plot of detonation velocity versus the reciprocal of charge radius (hereafter referred to as D versus 1/R) is a significant one for comparison with theory.

According to the general diameter effect theory developed by Eyring et. al. (7), which includes certain specific assumptions to extend the theory to the range of small radii of curvature, the D versus 1/R plot for values of a/R from 0 to 0.5 should be very similar to a straight line of the form:

Malin, Campbell, Mautz

	Corrected Velocity (m/sec)	7851 7859 7858 7852 7810 7777 7777 7712 7712 7712 7712 7712 77
	Experimental Velocity (m/sec)	7869 7869 7863 7863 7863 7863 7820 7782 7774 7745 7745 7747 777 777 777 777 777
Table 1	Transit Time (microseconds)	6.456 6.438 6.438 6.433 6.533 6.533 6.533 6.533 6.533 7.14 7.184 7.184 5.014 9.014
Table 1 Type 1 Composition B	Length (cm)	3.5070 3.5070
	1/Radius (cm-1)	00000111199999999999999999999999999999
	Charge Diameter (inches)	1.003 1.002 0.975 A 0.975 B 0.394 C 0.394 O 0.396 O 0.108 O 0.

$$\frac{D}{D_4} = 1 - 0.5 \text{ a/R},$$
 (1)

where D = detonation velocity,

D; = infinite medium detonation velocity,

a = reaction zone length, (assumed constant).

R = charge radius.

It is clear from Figure 1 that this equation does not represent the experimental data over the entire range covered, although

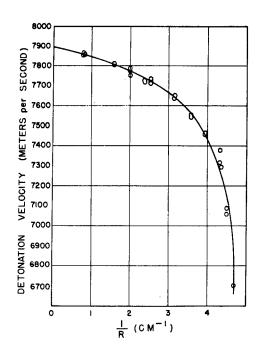


Fig. 1. Detonation velocity versus reciprocal of charge radius, Type 1 Composition B.

at diameters above 0.25" a straight line fits the data well. Below 0.25", the detonation velocity falls markedly with decreasing charge diameter, the slope reaching a value as high as 50 m/sec velocity decrease per 0.001" diameter decrease. The Eyring theory as given in (7) does indeed predict that the D versus 1/R plot will deviate from a straight line at values of a/R above 0.5. It is thought, however, that in the experimental data presented a/R is below 0.5. Further, the deviations from a straight line that we observe at small diameters are in the opposite direction to those predicted by the theory.

If the Eyring theory is applied to the section of this graph above 0.25" one obtains a value of 0.2 mm for the reaction zone length.

An extension to this diameter effect theory has been proposed by Parlin, Thorne and

Robinson<sup>(8)</sup> which gives somewhat different conclusions. This extension still does not allow for the sharp drop in velocity at the smaller diameters, but, in general, is more successful in predicting the overall shape of the D versus 1/R plot.

To compare the diameter effect theory of Jones (9) with the experimental data, a more complicated procedure is necessary. From the Jones theory one obtains the equations:

$$\frac{D_{1}}{D^{2}} = 1 + c(r^{4} - 1)$$
 (2)

$$\mathbf{r} = 1.85(1 - a/R \cot \theta) \tag{3}$$

$$a/R = 0.919 \quad \frac{\sin \theta}{1 + \cos \sqrt{2} \theta} \tag{4}$$

where D = the detonation velocity at charge radius R,

- D<sub>1</sub> = the detonation velocity at infinite charge radius,
- a = the reaction zone length (assumed constant as the radius is varied),
- r = the relative expansion of the stream tube at a distance equal to the length of the reaction zone,
- (90 θ) = the angle between two lines drawn from the inner Meyer streamline, a reaction zone length behind the edge of unreacted explosive, one parallel to the charge axis, and the other drawn to the outer edge of the unreacted explosive,
  - c is a constant, taken to be 2.0 for many cast explosives.

To obtain D/Di for values of a/R smaller than those calculated by Jones (so as to be in our working range), the following was done: an assumed value of a/R was placed in equation (4), and the equation solved for  $\theta$ ; this value of  $\theta$  was placed in equation (3), which was solved for the value of r. This value of r was then placed in equation (2), and the process was repeated for each value of a/R. The results are given below in Table 2.

Table 2

Jones Nozzle Theory for Unconfined Explosives

a/R	<u>r</u>	<u>D/D1</u>
0.1	1.0003	0.9987
0.2	1.0011	0.9956
0.3	1.0044	0.9827
0.4	1.0120	0.9545
0.5	1.0245	0.9116
0.6	1.0418	0.8587
0.7	1.0626	0.8032
0.8	1.0869	0.7474
0.9	1.1192	0.6840

From Table 2, we obtain a plot of D/Di versus a/R, according to the Jones theory. Next, by taking the experimentally extrapolated value of Di (7895 m/sec), we can plot our experimental data in the form of D/Di versus 1/R as shown in Figure 2. If we then take one

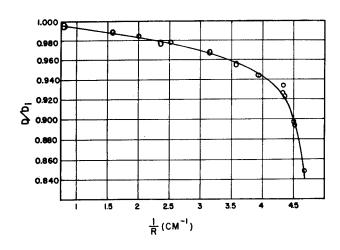


Fig. 2. Experimental velocity/infinite medium velocity versus reciprocal of charge radius. Type 1 Composition B.

dure is a test for the applicability of the theory. Using this method of comparison, the results obtained were:

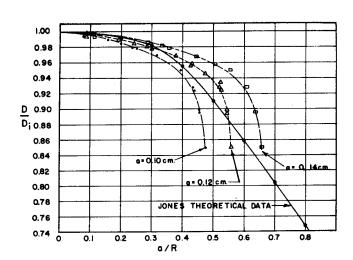


Fig. 3. Experimental and theoretical plots according to the Jones theory.

value of D/Di on this experimental curve, we obtain a corresponding value of 1/R. If we takethe same value of D/Di on a plot of the data of Table 2, shown as a solid curve in Figure 3, we obtain a corresponding value of a/R, thus leading to a value of a for this value of D/Di. Next, taking another value of D/Di and repeating this process, another corresponding value of a is obtained, and so on. Since the Jones theory postulates a constant value of a, this proce-

<u>D/Di</u>	a (in mm)
0.990	1.79
0.970	1.20
0.950	1.09
0.930	1.08
0.910	1.13
0.890	1.19
0.870	1.24
0.850	1.31

The value of a obtained here is greater by a factor of 5 or 10 than the value obtained by applying the Eyring theory at the larger diameters.

Next, assuming respectively values of  $\underline{\mathbf{a}}$ 

= 1.0 mm, 1.2 mm, 1.4 mm, a plot of the experimental data in the form of D/Di versus a/R is obtained. These are shown as the dotted curves in Fig. 3.

It appears that the Jones theory at least predicts the general shape of the experimental curve, although the agreement is not exact over the entire experimental range.

#### EXPERIMENTAL II

Having established a reference curve for a particular type of Composition B, i.e., a particular RDX particle size distribution, the next point of interest is the effect of a change in the particle size on the D vs 1/R relationship. In Type 1 Composition B, 80% of the RDX particles were less than 400 microns and 20% were 400 microns or greater. The first alteration introduced was an increase in the RDX particle size: a Composition B casting was prepared using spherical grain RDX of particle sizes ranging from 20 to 35 mesh (833 microns to 417 microns). Since this RDX of large particle size had a tendency to segregate in the bottom of the melt, it was necessary to add the RDX when the TNT was quite viscous. This resulted in the entrapping of air bubbles, so that the casting was not as free from voids as was the Type 1 casting.

The casting was sectioned into five slabs, the top, bottom and center sections being used for analyses and the two remaining sections for the experimental work.

The charge assembly technique was the same as that described in connection with Type 1 Composition B. The experimental results are given in Table 3, in which this Composition B of large RDX particle size is designated as Type 2. The velocities have been corrected again to 63.00% RDX and 1.700 g/cc.

#### DISCUSSION II

The data obtained in this experiment are neither so consistent nor so reliable as the Type 1 data because of the lack of uniformity of the casting previously discussed. It can be observed in Table 3 that two sticks of the same diameter may differ in velocity by as much as 100 m/sec. In spite of this large scatter at several diameters, the trend remains clear.

The experimental results are shown in Figure 4, where the circles indicate the mean of the velocities obtained at each diameter for Type 2 Composition B. Also shown in the same figure for comparison is the curve obtained for Type 1 Composition B. The curve for the Type 2 material is similar in form to that for Type 1, a relatively straight line section at the smaller values of 1/R, followed by a sharp decrease in velocity at larger 1/R. If the Eyring theory for unconfined charges (equation 1) is applied to the straight line portion of the Type 2 curve, one obtains a value of 0.4 mm for the reaction zone length, compared with the 0.2 mm obtained in the same way for Type 1.

The value of 1/R above which the rapid decrease in velocity occurs is smaller for the Type 2 material than for the Type 1. The failure diameter of Type 2 Composition B is also significantly greater than that of Type 1.

Malin, Campbell, Mautz

Table 3
Type 2 Composition B

Average Corrected Velocity	7773	9492	7501	7438	7415	7263	7321		
Corrected Velocity (m/sec)	7743 7789 7787	7631 7643 7664	7516 7485	7394 7481	7372 7458 7933	7268 7360	7273		
Experimental Velocity (m/sec)	77 <sup>4</sup> 7 7793 7809	7615 7646 7648	7538 7457	7372 7459	7344 7430 7233	7244 7244	7242		
Transit Time (microseconds)	8.541 8.451 8.376	8.621 8.616 8.547	8.878 8.878	8.949 8.887	6.236 6.174 0.003	9.135	9.104 Failed	Failed Failed	Failed Failed
Length (cm)	6.617 5.586 6.541	6.565 6.537 6.537	6.565 6.565 6.80	6.597	+ + 7 1.587 1.587	6.617	6.593	6.602 4.816	4.811 4.098
1/Radius (cm-1)	0.803 0.805 0.803	1.57	v v v v %. v %.	2.56 56	2.67 2.67	 	2.81 2.87	3.90	3.92
Charge Diameter (inches)	0.980 0.979 0.980	0.501 0.501 0.500	0.334 0.334 0.334	0.308	0.295 0.295 0.895	0.283	0.274	0.265 0.202	0.201 0.192

The difference in detonation velocity between these two materials is greater the smaller the diameter.

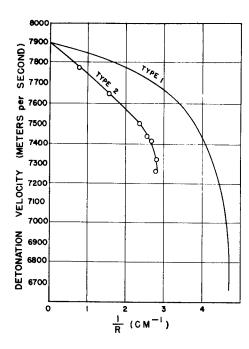


Fig. 4. Detonation velocity versus reciprocal of charge radius, Types 1 and 2 Composition B.

#### EXPERIMENTAL III

Since it has been shown that in Composition B variations in the RDX particle size distribution influenced the detonation velocity at finite diameters, it was thought interesting to inquire into the effects of variations in the TNT crystal size. For a preliminary investigation, the simplest method of introducing variations in the TNT crystal size is by preparing several castings which differ only in cooling time.

Two cylindrical castings were prepared using Type 1 Composition B. These castings were 12" in diameter and 20" high. One of these castings, designated "fast-cooled", was allowed to settle for five hours so that no further settling would take place dur-

ing the cooling period, and then cooled using circulating water at 30°C. The cooling was from the bottom and from the sides half way up to the top. The top section was insulated to prevent air-cooling. It is estimated that the time required for the entire casting to solidify was 5 to 6 hours.

The other casting, designated "slow-cooled", was allowed to settle for 3 hours and then cooled, using water at 70° C. It is estimated that the total cooling time for this casting was at least twice as long as for the fast-cooled, possibly as long as 14 hours.

The bottom section of each charge was then sectioned into rectangular pieces, density and composition analyses spotted through the sections, and the remainder used for rate sticks.

The shots were assembled and fired, using the same method described in connection with Type 1 Composition B. Each shot consisted of a booster, machined to the same diameter as the rate sticks, and two rate sticks. The booster section had a minimum length of five charge diameters.

In Tables 4 and 5, the detonation velocities for each of the two rate sticks in each charge are given. The velocity of the lower rate stick is given first in each case. The velocities have been corrected to 69.00% RDX and 1.700 g/cc.

Type 3 is the fast-cooled Composition B, and Type 4 is the slow-cooled.

	Corrected Velocity (m/sec) 7914 7908 7806 7815 7717 7717 7717 7758 7566 7584 7567 7593 7593 7593 7593	7883 7875 7775 7747 7562 7610 7516 7462
Table 4 Type 3 Composition B	Experimental Velocity (m/sec) 7940 7934 7841 7701 7755 7701 7592 7621 7529 7621 7529 7529 7529	7796 7788 7672 7487 7487 7435 7436 7389
	Transit Time (microseconds) 9.018 8.015 6.716 6.694 4.268 5.141 4.473 3.657 4.335 5.313 4.192 4.108 position B	6.607 6.578 8.232 7.659 5.304 5.110 4.785 4.785
	Length Transit (microsec (5.359 (5.249 (5.249 (5.249 (5.249 (5.424) 5.249 (5.424) 5.249 (5.424) 3.396 (5.424) 5.31 (5.424) 5.34 (5.424) 5.31 (5.424)	5.151 5.123 6.339 5.876 3.971 2.668 3.980 3.524 3.526 3.526 3.533 Failed
	1.78 1.58 1.58 3.15 3.15 3.92 4.71	11998.65.65.65.65.65.65.65.65.65.65.65.65.65.
	Charge Diameter (inches) 0.499 0.334 0.250 0.250 0.223 0.201 0.201 0.185 0.185	0.499 0.334 0.251 0.253 0.222 0.222 0.202 0.186

#### DISCUSSION III

The experimental data are shown plotted in Figure 5, again as D vs 1/R. As is anticipated with any preliminary casting in which

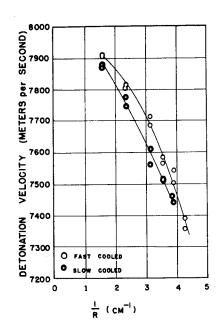


Fig. 5. Detonation velocity versus reciprocal of charge radius, Types 3 and 4 Composition B.

unusual requirements of particle size or cooling procedure are imposed, the points at any one diameter and among the several diameters show a certain lack of uniformity.

It can be seen in Figure 5 that at every diameter fired, the fast-cooled material has a higher velocity than the slow-cooled, so that there is clearly an effect of cooling rate on detonation velocity. Also, the fast-cooled material (on the basis of only a few shots) has a smaller failure diameter than the slow-cooled. We did not have enough material to complete the curve at the larger diameters; and, indeed, if the velocity difference becomes smaller at larger diameters the effect might have been masked by the lack of uniformity of the castings.

One can safely say that there is an effect demonstrated here, but the data are not sufficiently precise (in relation to the extent of the effect) to specify, for example, the dependence of the velocity difference on charge

## diameter.

In addition to the effect of cooling time on TNT crystal size, there is also the 4 to 8% RDX dissolved in the TNT, whose final particle size very likely depends on the cooling time, and may contribute to the effect observed here.

In spite of the advantages of Composition B discussed before, this experiment clearly indicates the need for a more precise method of controlling and varying the RDX and TNT particle sizes than is attainable in a casting.

#### EXPERIMENTAL IV

Although in Figure 4 the curves for Type 1 and Type 2 Composition B are shown extrapolated to the same infinite diameter velocity (for want of conclusive evidence indicating otherwise), the data could be so interpreted as to indicate that Type 1 actually extrapolated to a slightly higher velocity than Type 2. To inquire further into this point, a diameter effect experiment was designed to determine

the infinite diameter detonation velocities of three types of Composition B with sufficient precision (in terms of the expected effect) to draw conclusions.

Our previous data indicated that if we fired of the order of ten 2" long rate sticks at each diameter, the average deviation would be approximately 10 m/sec, which was thought to be adequate. The diameters selected were 0.500", 0.645", 0.902", 1.500", which are equally spaced on a reciprocal radius plot.

The data previously given for Composition B, as described above, had been obtained from sticks which were placed vertically on top of each other with only a thin ring of cement at the joints for rigidity. Since this is a slow and laborious assembly procedure, we decided in this experiment to use a pair of thin angle-iron rails and place the charge horizontally on these rails (the rails having been ground previously, so as to give a minimum of contact), using Scotch tape to fasten the sticks in place. Later in the experiment, the rails were replaced with the V-notch assembly shown in Plate 2, which

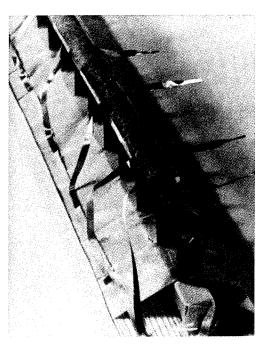


Plate 2. Improved Composition B Charge Assembly.

can be more economically machined.

As described in another paper (6), precautions must be taken with the use of Scotch tape to avoid jetting which can cause premature tripping of the ionization foils. As can be seen in Plate 2, the tape is always placed posterior to a stick junction (where the foils are located), never immediately anterior.

The castings used were well analyzed throughout, and they were of uniformly high quality.

As in previous experiments, a minimum of four charge diameters was allowed for booster run-up.

The three species of Composition B investigated will be designated respectively as Type 5, Type 6, and Type 7. The results from a typical charge are given in Table 6. The velocities have been corrected to 63.00% RDX and 1.715 g/cc.

Table 6
Type 5 Composition B, Diameter = 1.500"

Stick	Length	Transit Time	Uncorrected Velocity	Velocity
Number	(cm)	(microseconds)	(m/sec)	(m/sec)
1	4.798	6.050	7931	7947
2	5.032	6.362	7909	7928
3	5.067	6.396	7922	7941
4	5.077	6.409	7922	7937
5	5.004	6.303	7939	7939
5 6	5.047	6.343	7957	7965
7	5.014	6.325	7927	7937
Ė	4.973	6.252	7954	7968
9	4.902	6.184	7927	7937
10	5.075	6.405	7923	79 <b>2</b> 9
11	5.050	6.354	7947	7948
			ì	Mean - 7943 m/sec

Standard Deviation = 13.1 m/sec

The summarized results are given in Table 7 where the velocities are corrected to 63.00% RDX and 1.715 g/cc.

Types 5, 6, Table 7/7, Composition B

Type 5 Compos	<del></del>		
Stick	Mean Corrected		Standard
Diameter	Velocity	Number of	Deviation
(inches)	(m/sec)	Observations	(m/sec)
1.500	7943	11	13.1
0.902	7928	8	8.3
0.645	7902	8	9.6
•	7884	10	12.0
0.500	1004	10	12.0
Type 6 Compos	ittion B		
1.500	7970	10	17.9
-	7941	10	14.7
0.902	7917	10	12.2
0.645	7890	9 .	17.8
0.500	1030	<b>y</b> .	11.0
	didan D		
	sition B	10	10.0
1.500	7936		6.7
0.902	7918	10	11.8
0.645	7904	9	10.6
0.561	7874	11	
0.500	7854	<b>9</b> 8	11.8
0.250	7620	Ø	8.0

These data are shown plotted in Figure 6.

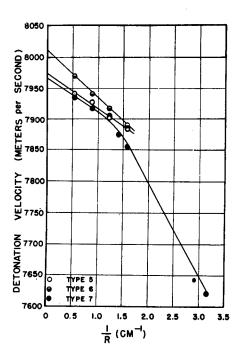


Fig. 6. Detonation velocity versus reciprocal of charge radius. Types 5, 6, and 7 Composition B.

#### DISCUSSION IV

Types 5 and 6 Composition B differ in RDX particle size as indicated in Figure 7. Shown in this bar diagram is the weight percent of RDX as a function of RDX particle size. For example, 3% by weight of the RDX particles in Type 5 Composition B are between 350 and 500 microns in size. This particle size analysis was reproducible to about 1.5%.

Least-squared lines have been obtained for the Types 5 and 6 data and are given below:

Type 5 D = 
$$7975.1 - 57.99 1/R$$
 (5)

Type 6 D = 
$$8008.6 - 75.42 1/R$$
 (6)

where: D is the detonation velocity in m/sec.

1/R is the reciprocal of charge radius in cm<sup>-1</sup>.

The fit of these equations to the experimental data is displayed in Table 8, where the entries show the m/sec difference obtained by subtracting the experimental point from the calculated point at each diameter.

Table 8

Types 5 and 6 Composition B

Diameter (inches)	1.500	0.902	0.645	0.500
Type 5	1.7	-3.7	2.1	-0.2
Type 6	-1.0	1.6	-0.7	-0.1

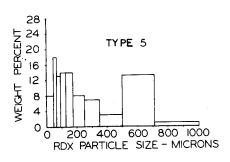
In equations (5) and (6) the infinite medium extrapolated velocity is, of course, the constant immediately to the right of the equality sign. The difference, then, in the infinite-medium velocities for these two types of Composition B is 33 m/sec.

An estimate of the 95% confidence interval for the difference between the two infinite-medium extrapolations is  $\pm$  15 m/sec. This estimate was obtained by doubling the interval obtained from the

following equation:

$$\mu_1 - \mu_2 = A_1 - A_2 \pm 2 \sqrt{\frac{G_1^2 + G_2^2}{N}}$$
 (7)

Here,  $\mu_1$  and  $\mu_2$  are the true extrapolations,  $A_1$  and  $A_2$  are the experimental extrapolations,  $\sigma_1$  and  $\sigma_2$  are the standard deviations of the two sample populations, and N is the number of observations in each sample. Since, strictly speaking, this equation applies



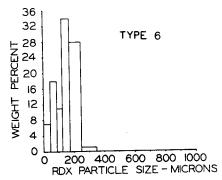


Fig. 7. RDX particle size analysis, Types 5 and 6 Composition B.

to sample means and not to extrapolations, the result calculated from it is an underestimate of the width of the confidence interval. It is believed, however, that doubling the width gives a conservative estimate.

Referring to Figure 7, it can be seen that the Type 5 material is characterized by a bimodal weight distribution of RDX particles while the Type 6 material contains essentially all fine particles. It is not yet clear in detail why such a difference in particle sizes should lead to a difference in infinite medium velocities, but the Kirkwood-Wood theory, referred to before, offers the following interesting possible explanation for this type of behavior.

From this theory one obtains the following important generalized statement of the Chapman-Jouguet condition for the case of a plane detonation wave:

$$D = u + c_0, \tag{8}$$

$$\leq 6^{j} r^{j} = 0 , \qquad (9)$$

where: D = detonation velocity,

u = mass motion velocity,

co = sound speed with the composition frozen at the values characteristic of the end of the steady state region,

 $r^{j} = \frac{d\lambda'}{dt}$ , where j indicates a particular chemical reaction,

λ is a progress variable, indicating the extent of a particular reaction j,

t = time,

 $\rho$  = density,

$$\beta_0 = \left(\frac{\partial v}{\partial T}\right)_{P,\lambda}$$

 $\mathcal{E}$  = specific internal energy (so defined that for an endothermic reaction  $\left(\frac{\partial \mathcal{E}}{\partial \lambda}\right)_{\mathcal{E},\mathcal{V}} > 0$ ,

v = specific volume,

$$c_{\rho}^{\circ} = \left(\frac{\partial H}{\partial T}\right)_{P,\lambda}$$
, i.e., the frozen heat capacity.

If one now thinks of the condition for the Chapman-Jouguet surface at infinite diameter for a two-component explosive as being that given by equation (9), namely:

$$G'r' + G^2r^2 + \cdots + G^n = 0$$
 (10)

where: 1, 2, ... n indicate specific chemical reactions postulated as occurring in the reaction zone and the normal Chapman-Jouguet
condition occurs when r<sup>j</sup> = 0, j = 1,
2, ... n. (i.e., the point of chemical
equilibrium),

then this condition, contrary to the diameter effect theories of Jones and Eyring, does allow for the possibility of particle size effects persisting to infinite diameter. For example, Kirkwood and Wood (and also G. B. Kistiakowsky in a qualitative plausibility argument) have suggested that the normal exothermic reaction might be followed by an endothermic one. In such a case the C for that reaction would become negative and the rj's might not be zero at the Chapman-Jouguet surface. If one further postulates that in at least one of the n reactions above the rate is dependent upon the initial state of subdivision of at least one of the explosive components, then a difference in infinite diameter velocities would be expected for two such explosives differing only in particle size. The important point here is that Equation (10) shows that the location of the C-J surface can be influenced by the rates of reaction, even at infinite diameter.

Although the above is offered as a possible explanation, there is no evidence that such is the case. Further conclusions must await detailed calculations involving reaction mechanisms and reaction rates for the particular explosives and these will be made difficult by the lack of sufficient data.

Considering next Type 7 Composition B, particle-size analyses of the type shown in Figure 7 indicate no detectable difference between Types 6 and 7 Composition B, in spite of the 40 m/sec difference in infinite diameter velocity indicated by the data in Figure 6. Also indicated in the plot in Figure 6 is the fact that the Type 7 Composition B material shows curvature at diameters above 1/2", unlike the Types 5 and 6 materials.

As a possible explanation of the different infinite diameter velocities of Types 6 and 7 Composition B, we inquired in detail into the nature of the small amounts of additives in the castings. The data are given below in Table 9.

Table 9
Chemical Analysis of Types 5, 6, and 7 Composition B

	Type 5	<u>Type · 6</u>	Type 7
TNT	33.87%	35.82%	33.79%
RDX	64.87%	62.89%	64.79%
Wax	0.96%	0 <b>.9</b> 9%	0.92%
Casting Additive 1	0.30%	0.30%	
Casting Additive 2			0.50%

In the above table, the RDX and wax were determined directly and the remaining components obtained either from a knowledge of casting additives or by subtraction. These analytical results are precise to about 0.1% in each case.

Heats of combustion were also experimentally measured for these three types of Composition B, and the agreement on the basis of compositions indicated by Table 9 is within the combined experimental calorimetric and analytical errors.

Considering Types 5 and 6 Composition B, Table 9 indicates that the additives to each are almost identical. (The difference in TNT and RDX composition is corrected in Table 7.)

Considering Types 6 and 7, the two types which have similar RDX particle sizes and yet an infinite diameter detonation velocity difference of 40 m/sec, it can be seen in Table 9 that the additives are somewhat different. However, a detonation velocity calculation made according to the Kistiakowsky-Wilson equation of state indicated that these differences in additives could amount to no more than 2 - 3 m/sec difference in velocities.

On the bases of chemical analysis for additives, heats of

combustion and detonation velocity calculations, it is felt that the difference in infinite medium velocity is not due to the effects of additives but is actually a result of particle-size effects persisting to infinite diameter.

Considering Types 6 and 7, there were differences in the casting procedures used, involving different settling times and a different cooling procedure, but these differences do not enable one to predict the final effect on the TNT crystal size. Here again the difficulties involved in the use of cast explosives become evident.

It may also be that the very small particles, i.e., those of the order of microns are of some importance. Since the particle-size analyses shown in Figure 7 only go down to 44 microns, a difference between Types 6 and 7 Composition B may exist without having been shown.

These difficulties which occur with the use of cast explosives have led us to search for a two-component explosive in which the particle size of each component can be varied more systematically and precisely. Pressing techniques have been developed to the point where it is possible to produce charges which are lower than crystal density by only 1 or 2%, thereby retaining the machinability and other advantages of high density material. The use of pressed material for experiments investigating particle size effects in two-component systems introduces additional problems involving segregation of particles and alteration of particle sizes during pressing. Nevertheless, at the moment, this seems the most fruitful method for further investigations.

#### EXPERIMENTAL V

Another interesting case of particle-size effects persisting to infinite diameter has been demonstrated. Bagley (10) investigated the relation between detonation velocity and charge diameter for different sieve cuts of spherical-grain RDX, at a density of 1.200 g/cc. The separate cuts used were: 1190 to 840 microns; 840 to 710 microns; 710 to 590 microns, 500 to 350 microns. The straight line relationships obtained (on a D versus 1/R plot) for each of these cuts all extrapolated to a detonation velocity of 6850 m/sec at infinite diameter, at density 1.200 g/cc.

Urizar(11) established the D versus 1/R relationship for a single type of RDX, considerably finer than the above. This RDX was ball-milled and varied in size from 5 to 40 microns. The infinite diameter velocity at a density of 1.200 g/cc obtained from an extrapolation of this relationship, is approximately 100 m/sec below the

value obtained by Bagley in his experiments.

This difference in infinite diameter velocities of 100 m/sec is thought to be considerably larger than the combined experimental errors, so that here again, particle-size effects exist at infinite diameter. It is thought, however, that the effect here is of a different nature from that previously observed in Composition B.

An experiment which may shed some light on the situation in

the RDX experiments has been done using spheres of Composition B. Spheres of two sizes were used, 5/8" and 1/4" diameters. The spheres were prepared from rough-sawed cubes by means of a device which abraded the corners off the cubes in a random manner. The device consisted of a hollow cone, attached with its apex downward to the shaft of an electrical motor, rotating inside a stationary, vertical, hollow cylinder. Both cone and cylinder were lined with a coarse abrasive cloth, so that cubes of explosive placed in the rotating cone were thrown violently and randomly about, from the cone to the cylinder and back, being quickly reduced to near spheres. This operation was carried on outdoors with a large centrifugal blower continually removing the dust. Plate 3 shows samples of both sizes of spheres.

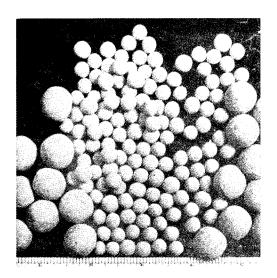


Plate 3. Composition B Spheres Diameters Approximately 1/4" and 5/8".

Three shots were fired which will be discussed in the following order:

Shot No. 1 consisted of 5/8" spheres fired in an octagonal wooden tube 36" long and 7-1/2" in diameter (across flats). Ionization pins were supported by four 1/8" brass rods spaced at 10" intervals, beginning 4" from the booster end. Each rod was drilled with four holes 1" apart, which carried the pin wires. Plate 4 shows this charge assembled.

Shot No. 2 consisted of a single row of 5/8" spheres held directly one above the other in a paper tube.

Shot No. 3 consisted of 1/4" spheres in a tube 24" long and 3-1/4" in diameter

(across flats). The ionization pins consisted of 0.040" o.d. hypodermic tubing inserted 4" apart, starting 4" from the bottom, with a common ground wire running the length of the charge.

#### DISCUSSION V

The overall density of Shot No. 1 was 1.0 g/cc. Its detonation velocity was 7050 ± 100 m/sec. According to the usual ideas about the dependence of detonation rate on charge density mentioned in Experimental I, an infinite diameter Composition B stick of density 1.0 g/cc should detonate at about 5600 m/sec. It is thought that in Shot No. 1 the detonation wave traveled at a velocity close to that characteristic of casting density from contact point to contact point, with perhaps some initiation delay at each junction.

Shot No. 2 gave a detonation velocity of 7520 - 31 m/sec.

This stacked single-row shot therefore, gave an increase in velocity over Shot No. 1 of 470 m/sec. This appears to be in accordance with

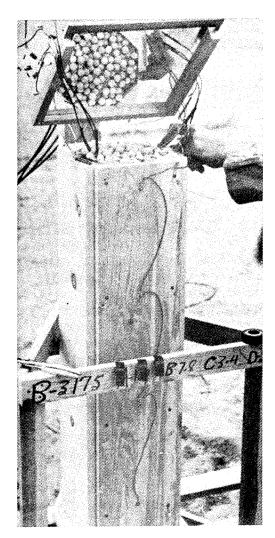


Plate 4. "Composition B Spheres" Charge-Assembled.

the hypothesis given above since there are fewer contact points and a more direct path is available when the balls are stacked as in Shot No. 2, compared with Shot No. 1.

Shot No. 3 had an overall density of 1.0 g/cc and detonated at a velocity of 6020 ± 100 m/sec. In this shot the number of contact points per unit length is greater than in Shot No. 1 and it also seems probable that the initiation delay at each contact point increases somewhat as the sphere diameter is decreased.

On the basis of our present knowledge, it would appear that the large sphere Composition B shots are an extreme case of the effect mentioned before. It is not clear whether jetting was important in the large RDX particle shots (as it might be for a sensitive material) or whether the detonation proceeded in a manner analagous to that postulated in the case of the Composition B spheres.

## SUMMARY

It has been shown in Discussions I, II, and III that particle-size effects are impor-

tant in two-component explosives at finite diameters. Variations in the RDX particle sizes in Composition B greatly alter the shape of the D versus 1/R curve and also the failure diameter of the material. Variations in the cooling pattern of the casting, through a mechanism not yet completely understood, also affect the detonation properties of Composition B.

It has been shown in Discussion IV that particle-size effects appear to lead to different infinite diameter velocities for materials otherwise chemically similar. A plausibility argument, in terms of the Kirkwood-Wood theory, is offered.

It has been shown in Discussion V that even at infinite diameter the presence of large crystals in low density, sensitive explosives may lead to velocities greater than those characteristic of fine

crystalline material. An experiment has been performed using large spheres of Composition B, which may represent an extreme case of these effects.

Further work is planned on these particle-size effects, using pressed materials which may offer greater opportunities for particle-size control and variations than have cast material.

We would like to acknowledge our gratitude to following members of the Los Alamos Scientific Laboratory for assistance in these experiments:

M. J. Urizar, who prepared the Types 2, 3 and 4 Composition B castings.

A. Popolato, who directed the particle size, composition and density analyses for Types 5, 6 and 7 Composition B castings.

L. R. Sitney, who performed the heats of combustion experiments.

W. Fickett, who performed the detonation velocity calculations for Types 6 and 7 Composition B.

F. W. Kramer, for assistance in the preparation of graphs.

#### REFERENCES

- (1) Kirkwood, J. G. and W. W. Wood, "The Structure of a Steady-State Plane Detonation Wave with Finite Reaction Rate". (This conference).
- (2) MacDougall, D. P., F. J. Martin, E. Boggs and G. H. Messerly-work described in Reference (7) below, pages 154-156.
- (3) Gamow, G.-work described in Reference (7) below, page 155.
- (4) Jones, E. and D. Mitchell, Nature, <u>162</u>, 98(1948).
- (5) Tranter, T. C., Nature, <u>174</u>, 81(1954).
- (6) Campbell, A. W., M. E. Malin, T. J. Boyd, Jr. and J. A. Hull, "Technique for the Measurement of Detonation Velocity". (This conference).
- (7) Eyring, H., R. E. Powell, G. H. Duffey and R. B. Parlin, Chemical Reviews, <u>45</u>, 69(1949).
- (8) Parlin, R. B., C. J. Thorne and D. W. Robinson, Technical Report Number 1. Institute for the Study of Rate Processes, University of Utah (1952).
- (9) Jones, H., Proc. Roy. Soc. (London) <u>A189</u>, 415(1947). (10) Bagley, C. H., Unpublished Report.
- (11) Urizar, M. J., Unpublished Report.

# DETONATION WAVE FRONTS IN IDEAL AND NON-IDEAL DETONATION

Melvin A. Cook University of Utah Salt Lake City, Utah

#### ABSTRACT

The experimental wave shape measurements for a number of ideal and non-ideal explosives in cylindrical charges at various charge lengths L and diameters d are summarized. These results show the following:

- (1) The wave fronts are in general spherical.
- (2) The radius of curvature R increases at first directly as L (R = L), but at a value of L between 0.5 d and 3.5 d depending on the explosive it suddenly becomes constant at a value  $R_{\rm m}$  which maintains for all larger values of L.
- (3) The steady state value of wave curvature  $R_m$  varies with diameter and density from a minimum value of 0.5 d at the critical diameter to a maximum value never exceeding 3.5 d 4.0 d in large diameters.
- (4) Values of  $R_m/d$  less than 3.5 4.0 appear to be determined simply by finite reaction zone lengths. The maximum value of 3.5 4.0 maintains in explosives in which the reaction zone length is negligible in comparison with the charge diameter.

The experimental results show that wave curvature is not associated with pressure gradients across the front of the detonation wave. Instead, they are apparently determined simply by the geometry of the detonation head and the tendency for pressure to remain substantially constant in the detonation head. The wave shape results are not only explicable in terms of detonation head concepts but appear to provide strong evidence for this theory.

#### Cook

#### INTRODUCTION

Aside from the extensive wave shape studies conducted in this laboratory, very little data have been published concerning the characteristic features of the fronts of detonation waves. One reason for the previous lack of information on wave shape was the lack of suitable methods for accurate measurement of wave shape. Developments of high speed rotating mirror cameras which have taken place at an accelerated pace during the past ten years, however, have placed into availability excellent precision methods for wave shape study. In spite of the availability of high speed cameras, wave shape studies are still beset with some difficulties, especially as a result of restrictions as to total charge size. Restrictions in charge size are particularly troublesome in studies of cast and pressed explosives of small reaction zone length a where the difference in time of arrival of the wave front at the end of the charge on its central axis and at the periphery of the charge is exceedingly small in small diameter charges. any laboratory restricted to the use of small size charges and concerning itself only with cast and pressed ideal explosives might easily fail to observe many important characteristic features of the wave front even with the use of the best modern rotating mirror streak cameras owing to the high resolution and charge reproducibility required in studies with small diameter charges. Large diameter shots with lowdensity, ideal, and non-ideal explosives, however, may be used without difficulty in wave shape studies.

Eyring and co-workers (1) called attention in their development of the "curved front" theory to the possibility that reaction rate and wave shape may be intimately related. In addition, wave shape is important in the design of many devices. A systematic study of the characteristics of the detonation wave fronts for various types of explosives were therefore undertaken here both in ideal (detonation velocity D equal to the theoretical maximum or hydrodynamic velocity D\*) and non-ideal (D<D\*) detonation. The location and laboratory facilities developed proved to be ideal for the study of wave shape. An excellent high speed, rotating mirror camera was constructed with film writing speeds up to 5 mm/usec. By use of this camera in an inside-out bombproof (camera and investigators inside, explosive outside) in a remote area, it was possible to study charges of almost any desired diameter (d) and length (L). Indeed charges of  $L/d \ge 6$  have been fired in diameters up to 25 cm in many cases, and in one explosive a diameter as high as 46 cm was used. With this instrumentation and by use of explosives of various types and under various physical conditions, many of the characteristic features of the detonation wave front have been elucidated. This paper summarizes the extensive experimental data obtained in these wave shape studies. Also presented is a discussion of the results from a largely geometrical viewpoint employing the concepts of the detonation head model.

#### Cook

#### EXPERIMENTAL

Three types of charges were used in this study, namely loose packed, pressed, and cast charges. Finished charges were either bare charges (in some cast explosives) or were contained in thin-walled paper, cellophane, or plastic tubes. Except perhaps for measurements made in diameters of 5 cm or less where measurements were unreliable anyway, the confinement provided by these tubes was probably quite negligible. Except for determinations of the influence of charge length, photographs of the detonation wave front were made for the most part at  $L/d \ge 6.0$ . To conserve explosive, shots of DNT at d = 25 cm and ammonium nitrate at d = 46.0 cm were made at L/d = 4.0 to 4.5. Since, as will be shown later, the wave shape became steady at L/d < 3.5 in all cases studied, the shots at L/d = 4.0 to 4.5 gave the steady state curvature. Pressed tetryl or cast pentolite boosters having preformed axially centered cap wells were used to detonate the charges requiring boosters. In measurements of the influence of charge length the booster was one inch in thickness with a preformed cap well 3/4" deep. Less care was needed in regulation of the exact position of the cap in steady state wave shape measurements. For cap sensitive explosives the charges were fired directly by caps axially centered at one end of the charge by means of wooden forms placed on this end of the charge. In measurements of the influence of charge length the cap was butted against but not inserted into the end of the charge.

The loose-packed charges were all vibrated to provide density uniformity. In some of the loose mixtures studied such as RDX-salt, RDX-glass beads, etc., however, vibration of the charges may have caused some segregation as indicated by some poorly reproducible results obtained for these mixtures. Cast charges were poured in lengths enough greater than the desired one to provide a 6 to 10 inch head to minimize cavitation in the finished charge. This head was then removed and only the bottom part of the charge used in the test. The pressed charges were made in 1 inch thick wafers, and the charge was made up by placing enough wafers end to end to give the desired length.

The wave was photographed in each case as it emerged from the end of the charge. This end of the charge was made perfectly perpendicular to the charge axis by cutting the tube on a lathe and covering the end with a flat piece of wood during charge preparation. Just before firing, this wooden form was removed and either replaced by a glass plate, or the charge end was left bare depending on the nature of the explosive. The slit of the camera was focussed on the end of the charge across a diameter after a suitable static image of the charge, and a 10 cm grid was taken for determination of the magnification factor. A static image with the slit in was also taken defining the line of view of the camera to show that the slit actually crossed a diameter of the charge. In some of the lowest velocity, non-ideal explosives it was necessary to use a thin (about 1 mm) layer of tetryl at the end of the charge along the line viewed by the camera through the slit in order to produce enough luminosity to observe the emerging wave.

The mirror of the camera was usually operated at or near maximum speed (600-700 r.p.s.) in wave shape measurements in order to reduce errors in measurement of the trace to a minimum. All traces were read on a Cambridge Universal Measuring Machine with a least count of 0.01 mm. The distance across the charge diameter was determined from the measured distance (x¹) multiplyed by the magnification factor M obtained from the static image. The y component parallel to the charge axis was obtained by measuring the perpendicular (y¹) distance from an arbitrary x¹-axis to the trace and multiplying the measured value by the factor  $\rm D/W_S$  where D is the velocity at the terminal end of the charge and W<sub>S</sub> is writing speed of the camera. Thus the measured co-ordinates were converted to real coordinates by the relations

$$x = M x'$$

$$y = y' D/W_{s}$$
(1)

where x' and y' are the values measured with respect to a given set of coordinates on the film itself, and x and y are the actual distances (with respect to the coordinate system) defining wave shape. The velocity D was generally measured on the same charge as was used to measure wave shape for charges long enough that this could be done by means of a pin-oscillograph. (2) In cases where this was not possible and where velocities were not known, velocities at the end of the charge needed in this study were obtained from measurements made in systematic studies of the variation of velocity with charge diameter and length.

Much of the data obtained in the wave shape studies in this laboratory have been presented in various previous technical reports on this project. Additional data used here not previously reported are available upon request. The data are plotted as average values with smooth curves drawn through these average value data. Each point in each of the graphs of Figs. 1 to 9 inclusive, represents usually an average of two or more shots. Sometimes a given point is an average of as many as ten shots. In a few cases, however, a point may represent only one shot. The reproducibility of data in wave shape studies depended on the type of explosive involved and the diameter. Loosepacked shots of pure granular explosives usually gave R/d values reproducible within about 10 percent in diameters above 5 cm. With present techniques this is true also of pressed charges, although in early studies less reproducibility was obtained owing possibly to small air gaps between individual wafers of 1 inch thickness used in making up the charge. In come cast explosives reproducibility has not been as satisfactory, the scatter of results indicating a spread of about 30 percent. Cast mixtures of amatol, baratol, and sodatol, however, have given excellent reproducibility. The difficulty in the reproducibility of measurements of R/d in some cast charges is the tendency toward cavitation and small density fluctuations both of which show up in exaggerated form in wave shape studies. Further work on cast charges is in progress. Other studies will include a plastic, a liquid, and a gaseous explosive.

#### Cook

#### RESULTS

# Spherical Wave Fronts

A very striking result of the wave shape studies carried out in this laboratory is the fact that the wave fronts showed a constant radius of curvature (spherical) across practically the entire wave front. In some cases something similar to the edge effect anticipated from shaped charge studies could be seen as a sharp increase in curvature on the outer edges of the trace. However, in no case did this edge effect amount to as much as expected, namely 3 mm, the maximum observed edge effect not exceeding 2 mm in any case. In many cases, however, the wave remained spherical right out to the edge of the charge. In some cases wave irregularities, usually tipped or asymmetrical wave fronts were observed. These were traced to density and sometimes compositions fluctuations in the charge. When results were repeated with more accurately controlled charges, spherical waves were found. tion near the end of the charge in cast explosives always distorts the wave. Cast charges in which density along the axis is reduced by poor casting tend to give excessive curvature, or if exaggerated, inverted waves. These effects are, however, not reproducible. The wave shape, except for the edge effect, may be expressed in each case except for these irregularities by a single value R, the radius of curvature of the wave front. All wave shape data in this paper are presented in this manner.

# Influence of Charge Length

Fig. 1 shows results of measurements of the radius of curvature of the wave front as a function of charge length in some ideal explosives (D = D\*). For L/d < 3 in low density TNT, R increased almost directly with L until a value of 1.8 d was reached after which it settled down quickly to the constant value  $R_{\rm m}/d$  = 1.8 and remained at this value up to the maximum length studied (L/d = 18.5). In EDNA a similar situation prevailed; R/d increasing almost directly with L/d to L/d = 2.5 after which it remained constant at  $R_{\rm m}/d$  = 2.6. Wave shape with pure granular RDX, 40/60 RDX-salt, and cast pentolite was also studied (as a function of charge length) and the results showed that the wave in these cases expanded geometrically (R = L) for values of L < 3.5 d, but at L > 3.5 d, R remained constant at  $R_{\rm m}/d$  = 3.5.

Striking results were obtained in studies of wave shape at large L/d using various types of initiators. It was found that the same steady state wave shape maintained at large L/d independent of the mode of initiation of the charge. In these studies plane wave initiation, peripheral initiation, irregular wave shape initiation, and inverted wave initiation were used. In all cases the same steady state wave shape resulted as was found in the R vs. L/d studies showing that steady state wave shape is a function only of the explosive and its physical state and not of conditions of initiation.

Fig. 2 shows the results obtained with two non-ideal explosives for which  $D/D^*$  was appreciably less than unity in the particular diameters studied. These explosives were coarse (-6 + 8 mesh) TNT in diameters of 5 and 10 cm, and a simple mechanical mixture of 50/50 TNTsodium nitrate (SN) employing -28 + 48 mesh SN in diameters of 5 and 10 Measurements were made at charge lengths ranging from 1 d to 6 d. They showed that R/d increased directly as L/d for L/d not exceeding  $R_m/d$ . Significantly the steady state value  $R_m/d$  in these non-ideal explosives was established at smaller values of L/d than in the ideal explosives shown in Fig. 1. In fact, the wave appeared to change suddenly from geometrical expansion (R = L) to steady state wave shape  $(R = R_m)$  at  $L = R_m$ . The establishment of a steady state wave front of  $R_m/d \leq 3.5$  even in ideal explosives of very short reaction zone length shows that other factors besides reaction rate influence wave shape. However, the lower values of R<sub>m</sub>/d found for non-ideal explosives show that reaction rate influences wave shape at least to some extent in accord with the suggestion of Eyring. Other factors not taken into account are of sufficient importance, however, to require modifications of the "curved front" theory.

# Influence of Diameter on Wave Shape in Ideal Explosives

Since the results shown in Fig. 1 and 2 show that steady state curvature is established at L/d  $\approx$  3.5, values of  $R_m/d$  as a function of d and  $\rho_1$  were measured in a number of ideal and non-ideal explosives at  $L/d \ge 6.0$  except as indicated above for DNT and AN where L/dwas 4.0 to 4.5 at maximum d. The results are shown in Figs. 3 to 9, inclusive. Results for cast TNT, 50/50 pentolite, and composition B at  $L/d \ge 6.0$  are shown in Fig. 3. As mentioned above, wave shape is extremely sensitive to slight charge fluctuations. Unfortunately cast charges are difficult to prepare without such fluctuations. Hence R<sub>m</sub>/d values were reproducible only to within about  $\pm$  0.5 in these three explosives. Within these limits the results shown in Fig. 3 show that the upper limit of  $R_m/d$  found at large diameters in these ideal explosives was about 3.5 to 4.0. It is significant that the maximum effective charge length in shaped charge phenomena and other phenomena employing "end effect" such as lead block compression and sympathetic detonation is also about 3.5 d to 4.0 d. While R/d and the total end impulse increase uniformly with charge length for values of L/d between zero and 3.5 to 4.0 results for these explosives showed that D did not vary appreciably with charge length in the region 0 < L/d < 3.5. It appears, in fact, that velocity in ideal explosives at diameters well above dm\* (minimum diameter for ideal detonation) is independent of wave shape. In non-ideal explosives, however, velocity transients have been observed to occur over the entire range 0 < L/d < 3.5, but D/D\* is constant at less than unity for L/d > 3.5. Similar transients have been observed in ideal explosives in diameters near d\_\*.

Fig. 4 shows plots of  $R_m/d$  vs. d for some loose-packed, granular ideal explosives including TNT, EDNA, tetryl, RDX, and coarse 50/50 pentolite, all at  $L/d \geq 6.0$ . These results showed  $R_m/d$  to increase with diameter for  $R_m/d < 3.5$  although only quite slowly for 50/50 pentolite.

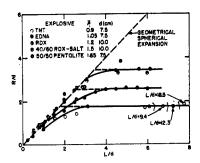


Fig. 1 - Variation of Wave Shape with Charge in Ideal Detonation

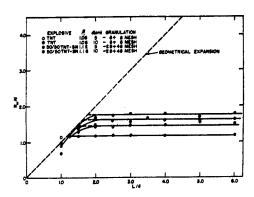


Fig. 2 - Variation of Wave Shape with Charge Length in Non-Ideal Detonation

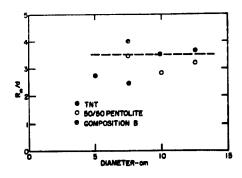


Fig. 3 -  $R_m/d$  vs. d in Some Cast, Ideal Explosives

Only in the cases of RDX and EDNA did the value of  $R_{\rm m}/d$  reach the limiting value 3.5. These results might indicate that the maximum value of  $R_{\rm m}/d$  even at large diameter may be lower than 3.5 for explosives of sufficiently low density, indicating possibly a purely density effect on curvature. However, it is more probable that this effect is simply a reaction rate effect and that  $R_{\rm m}/d$  would approach 3.5 at large enough d. While these explosives were ideal, it is possible (as predicted by the detonation head model) that the reaction zone length may still be appreciable and that this may be responsible for the low  $R_{\rm m}/d$  values in low density, ideal explosives. It has been shown that a is much longer for a given explosive at low density than at high density apparently simply because the temperature increases quite markedly with density (e.g., at least as rapidly as that predicted by the  $\alpha(v)$  equation of state).(3)

# Influence of Density on $R_m/d$ in Ideal Explosives

Numerous measurements of  $R_m/d$  were made as a function of density with fine-grained TNT, EDNA, 50/50 pentolite, and various pentolite salt and TNT-salt mixtures in a diameter of 5.2 cm and with tetryl in 2.5, 5.0, 8.5, and 10.4 cm diameter charges all at  $L/d \ge 6.0$ . These results are shown in Fig. 5. They show that R<sub>m</sub>/d increased with density  $\rho_1$  in all cases as long as  $R_m/d$  was less than 3.5 to 4.0. (In the initial series of  $R_{m}/d$  vs.  $\rho_{l}$  measurements made with TNT a maximum value of 4.5 for  $R_m/d$  was obtained at  $\rho_1$  = 1.51. It was suspected that this high value might be associated with small air gaps between the individual 1 inch thick wafer used in these charges. Hence in later work care was exercised to avoid an air gap by dusting off each pellet carefully and making sure that good contact was obtained between them.) The maximum value of  $R_m/d$  did not exceed 4.0 with the explosives tetryl, EDNA, and 50/50 pentolite, all of which would be expected to give at least as large maximum values of  $R_m/d$  as TNT. The fact that the maximum value obtained for  $R_m/d$  with cast TNT at  $\rho_1$  = 1.59 was between 2.5 and 3.9 in all cases at diameters between 5 and 12.7 gives further evidence that the true limiting value of  $R_{\rm m}/d$  may not exceed 3.5 to 4.0 in this as well as other explosives.

# Influence of Inert Additives on $R_{\rm m}/d$ in Ideal Detonation

values below 3.5 at least at the maximum diameters studied, questions arose regarding  $R_{\rm m}/d$  in explosives with inert additives. Theoretically the temperature would be higher for a given explosive if the voids were filled with inert solid than if these voids were filled with air because of the covolume effect on temperature shown in previous studies. Assuming therefore that the explanation of low  $R_{\rm m}/d$  values in low density, ideal explosives is an appreciable reaction zone length, measurements of  $R_{\rm m}/d$  were made in various loose-packed pressed and cast TNT-salt, pentolite-salt, and RDX-salt mixtures. The results are shown in Fig. 6. In loose-packed TNT-salt mixtures at d = 10 cm,  $R_{\rm m}/d$  decreased appreciably with salt content from 2.1 at zero percent salt to 1.3 at 60 percent salt. This suggested that the density effect

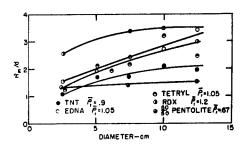
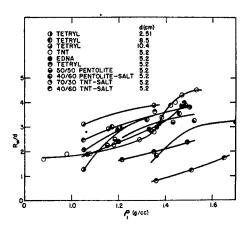


Fig. 4 -  $R_{\rm m}/d$  vs. d for Some Loose-Packed, Ideal Explosives



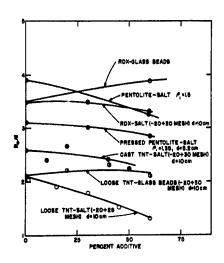


Fig. 6 - Influence of Inert Additives on Wave Shape

described above might not be a reaction zone length effect, although the possibility remained that some of the salt might have vaporized to cause lower temperature and longer a<sub>0</sub>. Hence measurements were repeated using glass beads of -20 + 30 mesh. In this case the influences of inert additive disappeared completely lending credence to the suggestion that the effect is actually a reaction zone length effect.

Cast TNT-salt mixtures showed very little effect of salt on curvature, the  $\rm R_m/d$  values decreasing only from 2.6 at zero percent salt to about 2.2 at 50 percent salt. The smaller effect of salt on  $\rm R_m/d$  in cast compared with loose TNT may be associated with the fact that the exposure time of salt to the detonation head in the cast charge is only about half that of the low density mixture so that less vaporization occurred in the reaction zone. It is clear that vaporization of salt in the reaction zone was not large in either case, since vaporization of only a small percentage of the salt would quench detonation in cast and loose-packed TNT. Powdered salt in small amounts quenches detonation even in very sensitive dynamites.

Results obtained with RDX-salt and RDX-glass bead mixtures showed very little change of  $R_{\rm m}/d$  with percent inert. This may be simply the result of the fact that  $R_{\rm m}/d$  was already at 3.5.

In the RDX-inert and TNT-inert mixtures the density increased with inert content because of the higher density of the inert. To determine the influence of inert at constant density, pressed charges of 50/50 pentolite and salt were prepared in a diameter of 5.2 cm. These results are also given in Fig. 6 and show that the salt additive influenced  $R_{\rm m}/d$  very little at  $\rho_1$  = constant. The conclusions to be drawn from these studies therefore appear to be (1) that additives which are strictly inert do not influence wave shape appreciably for a constant free space inside the charge and (2) that the density effect noted in Fig. 5 may be simply a reaction zone length effect.

# Influence of Reaction Zone Length on $R_{\underline{m}}/d$ in Ideal Explosives

Some additional studies were carried out to provide evidence for the suggestion that only reaction zone length influences wave curvature in ideal and non-ideal explosives when  $R_m/d < 3.5$ . One will note that cast TNT at d = 5 to 7.5 cm showed a relatively low  $R_m/d$ , whereas the pressed charges at d = 5 cm showed normal (or slightly too large)  $R_m/d$  values at densities from 1.38 to 1.5. Moreover, there was a rather rapid increase in Rm/d with density in pressed TNT between  $\rho_1$  = 1.35 and 1.40 g/cc. In the first place cast TNT is coarser than the fine pressed TNT, and at the same density its reaction zone length should therefore be greater. This would explain the higher  $R_{m}/d$  for the pressed compared with the cast TNT. On the assumption that the density effect in the pressed TNT is a reaction zone length effect, there are two factors to consider, namely (1) the increase in the detonation temperature  $T_2$  with density, and (2) the fact that pressing breaks down the particles and should therefore decrease the reaction zone length. The temperature effect would be expected to be continuous with increasing  $\rho_1$  with no abrupt change in the slope of the  $R_m/d$  vs.  $\rho_1$  curve. However, the particle size effect would produce a sudden change at the density where the particles are crushed by pressing. Particle size studies of pressed TNT charges showed that the particles did not crush appreciably due to pressing until a density of 1.35 is reached. But between  $\rho_1$  = 1.35 and  $\rho_1$  = 1.40 g/cc considerable particle breakdown was found. This is precisely the density range at which a sharp increase in  $R_m/d$  was encountered.

Average wave shape vs. diameter measurements of loose-packed tetryl and PETN of particle sizes -20 + 28 mesh and -35 + 48 mesh for tetryl and -35 + 48 mesh and -65 + 100 mesh for PETN made in plastic tubing of 1.6 mm wall thickness are plotted in Fig. 7. These measurements were made at diameters at and above  $d_m^{\,*}$ , the minimum diameter at which D/D\* = 1.0. While results in such small diameters are questionable owing to poor reproducibility, one will note that  $R_m/d$  not only continued to increase with d in the ideal detonation region, but that an apparently definite particle size effect also occurred, the values of  $R_m/d$  for the finer tetryl and PETN always being greater than those of the coarser granulation of tetryl and PETN. The fact that particle size effects on wave shape are pronounced in the ideal detonation region near  $d_m^{\,*}$  as well as in the non-ideal detonation region seems clearly to show that  $a_0/d$  is appreciable in the ideal detonation region near  $d_m^{\,*}$ .

It is concluded from density and diameter studies in ideal explosives with and without inert additives that values of  $R_{\rm m}/{\rm d}$  lower than 3.5 are associated with reaction zone lengths of appreciable magnitude but not long enough to reduce D/D\* below unity. According to the detonation head model D/D\* will not drop below unity until  $a_{\rm o}/{\rm d}$  (the reaction zone length/diameter ratio) is greater than about unity. However, it appears obvious that  $R_{\rm m}/{\rm d}$  will be lower than the maximum value 3.5 as long as the ratio  $a_{\rm o}/{\rm d}$  is appreciable. Apparently only when  $a_{\rm o}/{\rm d}$  approaches zero will  $R_{\rm m}/{\rm d}$  attain the maximum value of 3.5. The above evidence thus substantiates the detonation head model in this regard.

# $R_{m}/d$ vs. Diameter in Non-Ideal Detonation

Fig. 8 presents plots of  $R_m/d$  vs. d for several loose-packed, non-ideal explosives. In all cases except ammonium nitrate (AN)  $R_m/d$  increased with diameter but was considerably below the limiting value of 3.5 to 4.0 at the maximum diameters used. With the -4 + 6 mesh TNT product the velocity was at the maximum value D\* at the largest diameter studied. However,  $R_m/d$  was still only 1.9. D/D\* was just slightly below unity, but  $R_m/d$  was only 1.6 for DNT. In both 50/50 TNT-SN and 50/50 TNT-AN D/D\* was still considerably lower than unity at d = 25 cm, where  $R_m/d$  was 2.5 and 1.6, respectively.  $R_m/d$  was very low for AN (about 0.8 to 1.2) but did not increase appreciably with d even up to d = 46 cm. This is probably simply because D/D\* was considerably lower than unity (theoretically about 0.45 at d = 17.5 cm and 0.65 at d = 46.0 cm) over the range of diameters studied. Except possibly for

the relatively high value for the TNT-SN mixture these results are consistent with the concept that  $R_m/d$  is a function of reaction zone length at values of  $R_m/d < 3.5$ . Even in coarse TNT and fine DNT at d = 25 cm,  $a_{\rm O}/d \sim 1.0$  according to the detonation head model. Hence, in accord with observations,  $R_m/d$  should be appreciably lower than the limiting value of about 3.5 attained for  $a_{\rm O}/d \ll 1.0$ .

Results of  $R_m/d$  vs. d for some cast explosives, non-ideal in small diameters and ideal in some cases and non-ideal in others in large diameter are shown in Fig. 9. Only in the composition B-AN cast charges did  $R_m/d$  reach the approximate limiting value (3.8 in this case). This explosive, however, was ideal under conditions at which  $R_m/d=3.8$ . In all the others except cast amatol,  $R_m/d$  seemed to attain approximately a constant or slowly rising value at  $d \ge 10$  cm.

All of these explosives except the baratols were ideal at the maximum diameter studied. Even the milled barium nitrate product, however, was non-ideal at d = 25 cm. Of particular interest is the fact that 70.7/29.3 cast composition B-AN exhibited an  $R_{\rm m}/d$  vs. d curve which reached the maximum value (3.8) at about the same diameter at which D/D\* became unity. This is probably associated with the small percentage of the slowly reacting component, AN, and a very short reaction zone for the faster one, composition B.

#### THEORETICAL CONSIDERATIONS

Phenomenology allows one to write the following equations pertaining to wave shape:

$$R_{i}(y_{i}) = constant; y < y'$$
 (2)

 $R_i$  = radius of curvature of the wave at a particular charge length and at a point on the wave front a distance  $y_i$  perpendicular to the charge axis, y' is the effective radius of the charge, defining effective radius to exclude the slight edge effect which did not exceed 2 mm in any case. Equation (2) simply expresses the experimental fact that the wave front is in general spherical in shape.

$$R \cong L; L < R_{m}$$

$$R = R_{m} = constant; L > R_{m}$$
(3)

Equation (3) expresses the facts shown in Figs. 1 and 2 that the spherical wave front expands geometrically for a length nearly up to  $R_m$  and then settles down rather suddenly to the steady state value  $R_m$ . For theoretical purposes it is evident that the assumption of a sharp, discontinuous change from spherical expansion (R=L) to the steady state wave front  $(R=R_m)$  is reliable almost within experimental error as indicated by the dotted horizontal lines in Figs. 1 and 2.

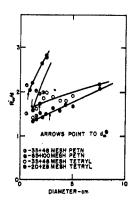


Fig. 7 - Wave Shape vs. Particle Size in Tetryl and PETN at Diameters near  $d_m \rlap{+} \rlap{+}$ 

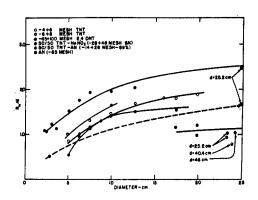


Fig. 8 -  $R_{\rm m}/d$  vs. d for Some Loose-Packed, Non-Ideal Explosives

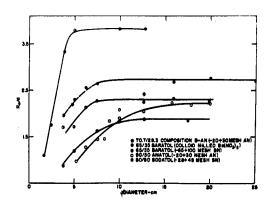


Fig. 9 -  $R_m/d$  vs. d for Some Cast, Non-Ideal Explosives

$$R_m/d \approx 3.5$$
;  $a_o/d \ll 1$   
 $R_m/d = f(a_o/d, X)$ ;  $a_o/d$  finite (4)

Here X represents a yet unknown factor determining wave shape in the region of finite a possibly involving detonation pressure  $p_2$  and perhaps also D. Equation (4) expresses the extensive  $R_m/d$  vs. d results obtained in the studies in this laboratory, evidence that  $R_m/d$  is not the same in all cases at a given  $a_0/d$  being ample. The problem in the interpretation of wave shape results thus involves (1) the elucidation of the factors included in X and (2) the determination of the function f. These functions have not yet been formulated. However, the nature of the unknown variable X may perhaps be implied from the following considerations.

In the geometrical expansion stages of the wave during which R = L, one has no indication that the edge of the charge or the reaction zone length a influences wave shape at all. Moreover, in this region all explosives seem to be alike as to wave shape, whether ideal or non-ideal even though they exhibit widely different velocities or velocity transients as the case may be. One might interpret this result therefore to indicate that nothing occurring at the edge of the charge or in the reaction zone influences conditions determining wave shape in region of geometrical expansion. The only alternative explanation of this fact is that edge effects influence all explosives in exactly the same way in this region of wave propagation. This explanation, however, seems heavily strained, particularly in view of the observed spherical wave fronts.

The influence of explosive characteristics suddenly come into play at the limit of geometrical expansion, L = Rm. At this limit the only effect of explosive characteristics is apparently simply to prevent any further change in wave shape; the differences between explosives regarding wave shape reside simply in the value of L at which steady state conditions are established. Values of Rm/d and therefore also L/d at the (apparent) discontinuity in transfer from spherical expansion to steady state wave propagation fall in the range 0.5 <  $R_m/d < 3.5$ . The lower limit corresponds to the critical diameter  $d_c$ ; the wave front is a hemisphere at  $d_c$ .  $R_m/d$  obviously cannot be less than 0.5. From the geometrical arguments presented here, the facts seem quite significant that values of  $R_{\rm m}/d$  approaching 0.5 have been observed quite frequently as one approaches de, although no values of R<sub>m</sub>/d less than 0.5 have been observed. On the other hand, the upper limit of 3.5 is precisely the value of L/d at which the detonation head attains in unconfined charges its maximum size or that end impulse is optimum as shown, for example, by extensive shaped charge and other studies. The maximum effective length Im for optimum end impulse is approximately the same in non-ideal detonation as in ideal detonation, namely 3-4. This may be shown, for example, by determinations of "end effect" by means of the lead block compression method using a non-ideal explosive. One finds that the compression of the block for a charge of constant composition, density, and diameter continues to

#### Cook

increase with charge length up to L/d = 3 to 4 about which it remains constant. Moreover, when plotted in reduced units ( $\delta/\delta_0$  vs. L/d, where  $\delta$  is the compression at length L and  $\delta_0$  is that at L/d > 3 to 4), all curves of this sort may be approximately superimposed; they would all apparently superimpose at least within experimental error except for the effect of the small "edge effect" mentioned above which is approximately a constant and therefore causes deviations at small L which increase as d is reduced. Wave shape in non-ideal explosives is thus not determined by the total end impulse. However, when  $a_0/d$  is negligible, the same factor or factors which limit end impulse also limit R so that  $L_m$  and  $R_m$  then and only then coincide.

The detonation head model gives a ready explanation for the upper limit value  $R_m$  = 3.5 d, as well as a quantitative explanation of the  $\delta/\delta_0$  vs. L/d curves obtained in end impulse studies. Rarefactions from the sides reach the charge axis (at a distance about d behind the wave front) only after the wave has traveled the length  $L_m$  = 3.5 d. For L/d > 3.5 the detonation head propagates in steady state. Wave shape is also steady in all cases at L/d > 3.5 simply because at L > L all effects of the point of initiation have been erased by the influence of lateral rarefactions.

# Possibility of Pressure Gradients Across Wave Front

The fact that detonation wave fronts propagate in steady state in all cases with appreciable curvature would seem to imply a pressure gradient across the detonation wave front. However, simple arguments based on the experimental facts show that this is not the case, but that the pressure at the wave front is always approximately constant over the entire front except in the region of the edge effect mentioned above which does not exceed 2 mm.

During geometrical expansion (R = L) it is obvious that no pressure gradient exists across the wave front; otherwise expansion would not be geometrical. It follows that at the limit of geometrical expansion (L = R<sub>m</sub>) no pressure gradient should exist across the wave front. But wave shape remains unchanged for  $L>R_{\rm m}$ ; it maintains the same spherical shape for  $L > R_m$  that it had at  $L = R_m$ . Hence no appreciable pressure gradient occurs across the wave front at any stage of propagation since the appearance of a pressure gradient beyond  $L = R_m$  would obviously change the wave shape. This conclusion is in accord with the detonation head model for explosives of  $a_0/d \ll 1.0$ ; as mentioned, this model shows a rarefaction front which moves in from the sides at lower velocity than the wave front velocity D and such rarefactions cannot, therefore, influence the pressure at the front. The pressure all across the front will, therefore, be determined by the C-J condition which occurs (for a  $\ll$  d) a distance small with respect to d behind the wave front.

That no pressure gradient exists across the wave front when  $a_0/d$  is appreciable is not a priori as obvious as it is when  $a_0/d \ll l$ . However, the experimental fact is still the same, namely that the wave

front is spherical at L > R<sub>m</sub> with the same radius of curvature that it had at the limit of geometrical expansion (L = R<sub>m</sub>) at which point there could have been no pressure gradient. This fact still seems to require that no pressure gradient exists across the wave front at L > R<sub>m</sub>. Again if a pressure gradient were to develop as L increases above R<sub>m</sub>, the wave would change shape and would hardly remain spherical in all cases since this pressure gradient if it were to develop would be a function of  $a_{\rm o}/d$ , the total pressure, and other factors the combination of which could hardly produce invariably spherical wave fronts.

# Qualitative Interpretation of Wave Shape by Detonation Head Model

The mere fact that detonation with finite ao/d values is possible shows that there is a strong tendency for microscopic shocklets carrying the energy and impulse generated by chemical reaction to move forward more rapidly than the wave front itself. In ordinary shock waves this effect causes the rarefactions that move forward from behind to eat into the wave front. A normal shock wave exhibits, therefore, rapidly decreasing density-distance  $(\rho(x))$  and particle velocity-distance (W(x)) characteristics from the wave front backward. Detonation waves are apparently, however, not simple shock waves. They differ from simple shock waves at least in the one important respect that they are supported continuously by chemical reaction whereas simple shock waves are not. Conventional theoretical discussions of detonation waves (4,5) have assumed that this effect of chemical reaction in the detonation wave is simply to cause the wave to grow in such a way that  $\rho(x/x_0)$  and  $W(x/x_0)$  remain constant ( $x_0$  the distance from the point of initiation to the wave front and x the distance from the point of iniation to a particular characteristic ρ and W plane behind the wave front). One may, however, question this hypothesis at least in cases where  $a_0 \ll d$ , and chemical reaction appears at the front instead of at the rear of the wave. In this case impulse generated by chemical reaction would not only be sent forward but also to an equal extent backward into the rarefaction region. This effect should surely modify the shape of the  $\rho(x)$  and W(x) curves; it would tend to flatten them. This should be true also in the cases where ao/d is appreciable, since at least part of the chemical reaction will appear at the wave front.

The experimental evidence of reaction rate studies shows that reaction zone lengths are much longer than can be accounted for by  $\rho(x)$  and W(x) contours which commence to decline immediately behind the wave front. A  $\rho(x)$  contour flat at the front and for a distance (for L  $\geq$  L<sub>m</sub>) about d behind the front, and showing rarefaction or a declining  $\rho(x)$  contour for  $x=x_0$  - d seems to be required to account for observed reaction rates. Fig. 10 shows a comparison between the  $\rho(x)$  contour observed by Kistiakowsky and Kydd(5) and the theoretical one of the detonation head model which on the charge axis has a  $\rho(x)$  flat for a distance d followed by a normal rarefaction. The experimental  $\rho(x)$  contours of Fig. 10, however, have been questioned by the authors on the basis of a possible excessive time constant in the electronic equipment used to measure them. Still, other evidences for a  $\rho(x)$  flat region have been found, some of which are discussed by the author. (6)

The detonation head model assumes a steady state flat  $\rho(x)$  region varying in length from zero at the edge to about d on the charge axis in unconfined cylindrical charges of  $L \geq L_m$ . The  $\rho\text{-flat}$  region of the detonation head model undergoes change only in the region  $0 < L < L_m$ . Fig. 11 indicates the development of the detonation head in a cylindrical unconfined charge for a << d.

In the detonation head model rarefactions from the sides and the rear have rather definite fronts of the type indicated in Fig. 11. For L < 0.5 d, there is a tendency only for the wave to remain spherical since no lateral rarefaction occurs in this region, and the effective reaction zone length supporting each element of the wave front is the same for all elements. For L>0.5 d, however, the region of the wave front falling in the annulus of the charge of thickness about  $a_0/2$ (which for a<sub>0</sub> > d would be the entire charge), in which the lateral rarefaction cuts into the reaction zone, there is a tendency toward weakening of the detonation head and perhaps curvature also, owing to the fact that the energy developed by reaction behind the rarefaction front cannot be fed into this region because of the sharpness of the pressure and density gradient at the rarefaction front. The effective reaction zone length will thus fall below ao (or d' whichever is smaller) starting at the inside of the annulus and finally reaching zero at the edge. This effect, however, does not at first (L = 0.5 d) influence the curvature of the wave front because of the tendency for energy and impulse to move forward from the rear of the detonation wave. tendency toward pressure loss in the annulus is thus quickly overcome simply by drawing momentum from the rear of the wave and the effect is merely to increase the ratio  $V_{l,r}$  /D where  $V_{l,r}$  is the lateral rarefaction velocity. In other words, the loss in energy and pressure due to incomplete reaction in the annulus (or over the entire wave front if a<sub>0</sub> > d) may be offset by impulse being fed into the region of the detonation head falling inside this annulus from the rear of the head itself both inside and outside the annulus if a < d and only inside if  $a_0 > d$ . Assuming that this momentum transfer is fast enough (which it must be since the wave remains spherical) the pressure in the entire head may then be held at the same value as that on the charge axis as long as the angle  $\alpha$  (Fig. 5) between the charge axis and the lateral rarefaction front (determined by the curvature of the wave at the edge) remains sufficiently large. The angle a is determined by the angle  $\varphi = \alpha + \Theta$  between the wave front and the side of the charge. But  $\varphi$ decreases from 180° at L = 0.5 d to a minimum value of  $90^{\circ}$  +  $\sin^{-1}y^{\dagger}/R_{m}$ However, 0 might be expected to remain approximately constant being determined solely by the hydrodynamics at the wave front near the edge of the charge which should be approximately constant in geometrical expansion. The angle  $\alpha$  is thus at the maximum value (greater than 90°) at L = 0.5 d and decreases steadily as L increases reaching a minimum value at L =  $R_m$ . While  $\alpha$  continues to decrease until L = 3.5 d for  $a_o \ll d$ , for finite values of the ratio  $a_o/d$  the critical value of  $\alpha$ is reached at L =  $R_m$  < 3.5 d. Apparently for values of  $\alpha$  less than sin-ly'/Rm impulse cannot be fed into the annulus from the rear of the wave as rapidly as it is needed to maintain approximately a constant pressure within the detonation head. The angle  $\alpha$  is thus critical at

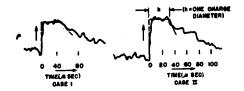


Fig. 10 - Density Distance (or Time) Contours in the Detonation Wave of a Gaseous Explosive (Solid Line Measurements by Kistiakowsky and Kydd, Dotted Line Detonation Head Model)

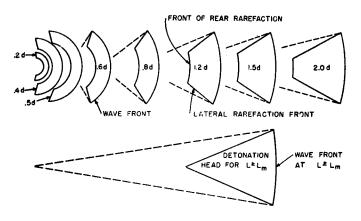


Fig. 11 - Development of Detonation Head in an Ideal Detonation with  $a_0/d << 1.0$  (Dotted lines extend point of initiation for  $L < L_m$  and to apparent initiation point for  $L \ge L_{m^*}$ )

#### Cook

 $L=R_m$ . Since the tendency for the head to remain isobaric is (experimentally) greater than the tendency for wave shape to continue to increase, a steady state wave front is established at this critical value of  $\alpha$ , and  $\alpha$  as well as wave curvature then becomes steady.

A complete description of wave shape would provide a description of factors determining the minimum value of  $\alpha$  (or  $\alpha_m$ ) or the dependence of  $R_m/d$  upon these factors through the functions X and f in equation (4). This problem is a difficult one and has not yet been solved. The experimental evidence appears to be of such a nature, however, to require theoretical concepts of the type employed in the detonation head model as indicated above.

#### ACKNOWLEDGMENT

This work was supported by Office of Naval Research, Contract Number N7-onr-45107, Project Number 357 239, and was carried out by the Explosives Research Group. The excellent work of Dr. G. Smoot Horsley, Dr. William S. Partridge, and Mr. Wayne O. Ursenbach, together with other members of the Explosives Research staff is gratefully acknowledged.

#### BIBLIOGRAPHY

- (1) H. Eyring, R. E. Powell, G. H. Duffey, R. B. Parlin, Chem. Rev. 45, 1 (1949).
- (2) M. A. Cook and E. F. Pound, "'Pin Oscillograph' for Measurement of Detonation Velocity", Technical Report No. XXXIII, May 4, 1954, ERG, Utah University.
- (3) M. A. Cook and W. O. Ursenbach, "Velocity-Diameter and Wave Shape Studies in Low Density 50/50 TNT-SN Mixtures", Technical Report No. XXXVI, July 30, 1954, ERG, Utah University.
- (4) G. I. Taylor, Proc. Roy. Soc. <u>A200</u>, 235 (1940).
- (5) G. B. Kistiakowsky and P. H. Kydd, "The Rarefaction Wave Following a Gaseous Detonation", Report submitted under Contract N5-ori-76, T. O. XIX, NR-053-094, Office of Naval Research.
- (6) M. A. Cook, "Detonation Head Model and Chemical Reaction Rates in Detonation" (submitted for publication).

# DETERMINATION OF REACTION RATE OF SODIUM NITRATE AND THE EQUATION OF STATE OF 50/50 TNT-NaNO<sub>3</sub>

Melvin A. Cook and Wayne O. Ursenbach University of Utah Salt Lake City, Utah

#### ABSTRACT

Reaction rates of sodium nitrate (SN) in low density mechanical and high density cast mixtures of 50/50 TNT-SN were determined by each of the three theories extant (nozzle, curved front, and detonation head) using the experimental velocity (D) vs. diameter (d) curves measured over a broad range of diameters from the critical diameter d<sub>c</sub> up to 25 cm. The total reaction times found for SN may be expressed by the equations

$$T_2 = 6.8 \times 10^{-4} \, \overline{R}_g \cdot f \; ; \; (\overline{\rho}_1 = 1.83)$$

$$T_2 = 2.1 \times 10^{-3} \, \overline{R}_g \cdot f \; ; \; (\overline{\rho}_1 = 1.15)$$

where  $\mathcal{T}_2$  = reaction time of SN in seconds,  $\overline{R}_g$  = grain radius of SN in centimeters, and f = 1.0 for the detonation head model, 0.07 to 0.09 for the nozzle theory, and 0.03 to 0.04 for the curved front theory.

The approximately three times greater total reaction time or slower reaction rate of SN in the explosive at  $\rho_1$  = 1.15 than in that at  $\rho_1$  = 1.83 (irrespective of the theory used to determine it) implies a temperature difference  $T_2$  ( $\rho_1$  = 1.83) -  $T_2$  ( $\rho_1$  = 1.15) of about 600°C in agreement with the  $\alpha(\mathbf{v})$  equation of state which leads also to a value of 600°C for this difference.

#### INTRODUCTION

Cook, Mayfield, and Partridge (1) determined the velocity-diameter D(d) curves for ammonium nitrate (AN) in 50/50 TNT-AN at  $\overline{\rho}_1$  = 1.55 (cast) and  $\overline{\rho}_1$  = 0.9 (loose-packed), 70.7/29.3 composition B-AN (cast  $\overline{\rho}_1$  = 1.59) and pure AN ( $\overline{\rho}_1$  = 1.04). They found that the reaction time ( $\gamma_2$ ) of AN in the detonation of these widely different

explosives followed in all cases (within a factor of 1.5) the equation

$$T_2 = 1.7 \times 10^7 \, \overline{R}_g/k!$$
 (1)

where k', the specific rate constant, is given by

$$k' = 4 \times 10^9 T_2 \exp -38,300/RT_2$$
 (2)

Here  $f_2$  (in seconds) was determined by the detonation head model; (2) equation (2) was determined in this laboratory in isothermal decomposition studies; Rg is the average radius of the AN in centimeters and T2 is the detonation temperature computed by the a(v) equation of state, calculated temperatures for the above four explosives being  $T_2 = 3510$ , 3300, 4150, and  $1720^{\circ}$ K, respectively. The nozzle theory (3) gave reaction times ranging from 0.04 to 0.12 times as long as those given by equations (1) and (2) and the curved front theory (4) gave values of  $ilde{ au_2}$  ranging from 0.025 to 0.085 times those computed by these equations. Hence the correlation between the  $\mathcal{T}_2$ 's themselves as well as with isothermal decomposition studies was much better in these studies with the detonation head model than with the latter two theories. Moreover, the fit of the experimental D(d) curves by the detonation head model was consistently better than by the nozzle theory which in turn was better than by the curved front theory. The constant factor in k' would necessarily be in the range from 8 to 60 times greater than the value found in isothermal decomposition studies to agree with the  $\frac{7}{2}$  results found by the latter two theories. Factors ranging only from 0.7 to 1.5 are required, however, to bring the results for the detonation head model into agreement with equations (1) and (2). Note that the theoretical Eyring equation for k'

$$k' = kT/h e^{\Delta S^{\#}/R} e^{-\Delta H^{\#}/RT}$$
(3)

gives for this constant the value  $2 \times 10^{10} \, \mathrm{e}^{\Delta S^{7}/R}$ . The values of the constant factor obtained in the nozzle and curved front theories for AN were even larger than k/h (k and h are the Boltzmann and Planck constants) by a factor ranging from 4 to 20. This gave  $\Delta S^{7}$  values ranging from 2.8 to 6.0 E.U. The factor 4 x 109 in equation (2) which was the isothermal decomposition value gave  $\Delta S = -3.2$  e.u.

Direct comparison of the reaction rates of AN in 50/50 TNT-AN at  $\rho_1$  = 0.9 and 1.55 showed that the reaction rate was about 3.5 times faster at the high density than at the low one. This requires a temperature about 500°C higher at 1.55 than at 0.9 g/cm. The calculated difference by the  $\alpha(v)$  equation of state was 240°C if the molecules CH<sub>2</sub>OH and CH<sub>2</sub>O<sub>2</sub> are assumed to form making use of the equilibrium constants determined by statistical mechanics. However, by omitting the equilibrium equations for the molecules CH<sub>2</sub>OH and CH<sub>2</sub>O<sub>2</sub> the computed equilibrium constants for which were somewhat doubtful, the computed temperature difference was about 500°C in agreement with that required by the observed reaction rates. The Kistiakowsky-Wilson-Brinkley equation of state leads to about -400°C for this temperature difference and it was

therefore concluded that the  $\alpha(v)$  equation of state is much better than the K-W-B equation of state for 50/50 TNT-AN.

SN lends itself well to a study of the type carried out for AN. The two systems, in fact, are much alike not only in the nature of the mixtures but also in the shapes of the D(d) curves. This article presents the experimental velocity-diameter (D(d)) curves for cast and loose-packed 50/50 TNT-SN mixtures measured over the diameter range from the critical diameter  $d_c$  to diameters up to 25.2 cm.

Measurements of the shape of the front of the detonation wave were also carried out for the TNT-SN mixtures and are described in a separate paper in this symposium. (5) They showed spherical wave fronts throughout (aside from a few scattered non-reproducible traces of slightly tipped or asymmetrical wave fronts). The radius of curvature R of the spherical wave for a given set of conditions was reproducible within  $\pm$  10 percent for both the cast and loose-packed products in this case. The radius of curvature/diameter ratios (R/d) in diameters of 5 and 10 cm and  $\rho_1 \sim 1.15$  g/cc increased at first geometrically (R = L) with length L but changed abruptly to the steady state wave shape of R = R<sub>m</sub> at L = R<sub>m</sub> remaining at this value for L > R<sub>m</sub>. Values of R<sub>m</sub>/d were 1.45 at d = 5 cm and 1.8 at d = 10 cm. The R<sub>m</sub>/d curves increased from unity near the critical diameter to about 2.5 at d = 25.2 cm. The significance of these data are discussed in terms of reaction rates in reference (5).

#### EXPERIMENTAL METHODS AND RESULTS

The SN used in the loose-packed TNT-SN mixtures was screened through 28 on 48 mesh standard Tyler screens. Closer screen cuts were taken for the cast charges. While the effect of particle size was clearly evident and seemed to follow the Eyring surface burning law, it was too small in this case owing to the small range of sizes available for quantitative study of the Eyring surface burning model other than by the D(d) curve itself. The TNT used was the regular fine-grained product. The loose-packed charges were vibrator packed in manila paper tubes and densities determined by total weight/total volume measurements. Cast charges were poured also in manila paper tubes using 6-8" "heads" which were removed and only the bottom portion of length L  $\geq$  6d was used. Velocities were measured primarily by a pin oscillograph (6) although a high speed, rotating mirror camera was used to measure velocity in the smallest diameter charges. Pin oscillograph measurements were made in all cases at L > 3d.

In initial studies (7) with 50/50 TNT-SN, the ideal velocity-density (D\*( $\rho_1$ )) curve was calculated from the  $\alpha(v)$  equation of state and the 'universal'  $\alpha(v)$  curve established primarily with C-H-N-O explosives. The D(d) curve at d = 25.2 cm for the low density product was only 200 m/sec lower than the calculated ideal velocity, and this curve appeared still to be increasing at d = 25.2 cm. The D(d) curve for the cast product was flat for diameters above d = 12.7 cm and the

observed velocity was 250 m/sec higher than the calculated value. To determine D\* at the low end of the D\*( $\rho_1$ ) curve, therefore, two charges of 50/50 TNT-SN at d = 20 cm were prepared using ball-milled SN. These results (with corrections for density) checked very closely the values found at d = 25.2 cm with the -28 + 48 mesh SN indicating that the velocity had reached the hydrodynamic one (D\*) at d = 25.2 cm. Assuming a linear D\*( $\rho_1$ ) curve this result together with the large diameter values for the cast product established the experimental D\*( $\rho_1$ ) curve for 50/50 TNT-SN shown in Fig. 1. The equation for D\* was

$$D* = 4100 + 2580 (\rho_1 - 1.0)$$
 (4)

Using the slope 2580 m/sec/g/cc to correct the velocities of the cast product to  $\overline{\rho}_1$  = 1.83 and those of the loose-packed one to  $\overline{\rho}_1$  = 1.15, the velocity-diameter curves given in Fig. 2 were obtained.

# THERMO-HYDRODYNAMIC PROPERTIES OF 50/50 TNT-SN

Thermo-hydrodynamic properties were computed by the inverse method using the equation of state (8)

$$pv = nRT e^{X}; x = K(v)/v$$
 (5)

and the observed  $D^*(\rho_1)$  data (equation (4)). In these calculations the molecules CH<sub>2</sub>OH and CH<sub>2</sub>O<sub>2</sub> were neglected even though the calculated equilibrium constants indicated that they should be appreciable at high fugacity. The reason for neglecting these molecules as mentioned previously was the uncertainty in the theoretically computed equilibrium constants. The results of these calculations are given in Table I together with a comparison of the calculated  $\alpha(v)$  curve and the 'universal' one (9) equation (5) being identical with the  $\alpha(v)$  equation of state

$$pv = nRT + \alpha(v) p$$

with  $e^{X} = v/(v - \alpha)$ . The maximum difference was 0.02 l/kg in  $\alpha$  and occurred on the low density side. The difference corresponds to a velocity difference of about 200 m/sec, which is just outside the range of experimental error in velocity determinations at low density owing to density and composition fluctuations.

#### REACTION RATE DETERMINATIONS

Using the values D\*(1.83) = 6240 m/sec and D\*(1.15) = 4390 m/sec, the experimental D(d) curves were analysed by the nozzle, curved front and detonation head theories. Although a careful study of the nozzle theory shows that such is not necessarily the case, Taylor (10) states that a plot of  $(D*/D)^2$  against  $1/R^2$  should give a straight line. Also the initial curved front theory indicated that a plot of D vs. 1/d should give a straight line although the more recent formulation of the

curved front theory (11) shows that this too is not the case. Accordingly the data obtained here are plotted both as  $1/D^2$  vs.  $1/d^2$  and as D vs. 1/d in Fig. 3. One will note that the Taylor condition is approximately satisfied for cast sodatol, but for the loose-packed product the curve differs widely from a straight line both at small and large diameters. The curve at low density, however, does not agree in shape with the nozzle theory.

Using the nozzle theory directly and the most recent formulation of the curved front theory the following values of the reaction zone length  $a_0$  were obtained from computations at various values of  $D/D^*$  across the D(d) curves.

Noza	zle	Curved Front						
$\rho_1 = 1.83$	$\rho_1 = 1.15$	ρ <sub>1,</sub> = 1.83	$\rho_{1} = 1.15$					
d(cm) a <sub>o</sub> (cm)	d(cm) a <sub>o</sub> (cm)	d(cm) a <sub>o</sub> (cm)	$d(cm)$ $a_o(cm)$					
3.8 1.25 5.0 1.32 7.5 1.42 10.0 1.50	3.8 1.2 4.45 1.4 6.38 1.7 8.4 1.9	3.2 0.6 4.3 0.6 6.65 0.51 9.15 0.39	3.2 0.67 4.65 0.73 9.1 0.78 15.0 1.20					
$\bar{a}_0 = 1.4$	$ \begin{array}{rrr} 12.5 & 2.4 \\ 15.7 & 2.5 \\ 17.0 & 2.2 \\ \overline{a}_0 = 1.9 \end{array} $	$ \begin{array}{rcl} 10.2 & 0.36 \\ 12.0 & 0.15 \\ \overline{a}_0 = 0.4 \end{array} $	$\overline{a}_0 = 0.8$					

The detonation head model leads generally to a better fit of the D(d) curves than either of the above theories. However, in this case the shape of the curve is such that the reaction time  $\mathcal{T}_2$  for SN in the case of the low-density mixture is very sensitive to the particular value one selects for D\*. For the cast sodatol  $\mathcal{T}_2$  was not as sensitive to the value one chooses for D\* and moreover D\* in this case could be readily established without ambiguity. Using D\* (1.15) = 4700 m/sec (computed from the  $\alpha(v)$  curve), for example,  $\mathcal{T}_2$  was about 180 usec, and the general fit of the D(d) curve was excellent for d > 3 cm. However, using the experimental value D\*(1.15) = 4390 m/sec one obtains  $\mathcal{T}_2$  = 60 usec. Despite this relatively large difference the computed D(d) curve for  $\mathcal{T}_2$  = 60 usec was still within experimental error of the observed data for d > 3.0 cm (Fig. 4).

While the fit by the detonation head model at small diameters was not perfect, the  $\widehat{\gamma}_1$  (for TNT) values obtained were consistent for both sodatol and amatol. In both cases  $\widehat{\gamma}_1$  was 8.5 µsec in the cast products and increased to 20 µsec and 26.5 µsec in the loose-packed amatol and sodatol, respectively. This increase was about the same relative amount as for  $\widehat{\gamma}_2$  (for AN and SN) in going from the cast to the low density mixtures.

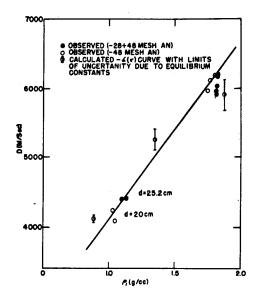


Fig. 1 - Maximum or Hydrodynamic Velocity-Density Curve for 50/50 TNT-SN

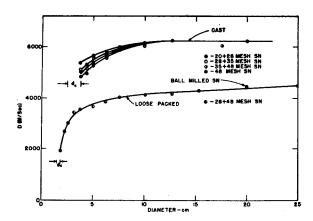


Fig. 2 - Velocity-Diameter Curves for 50/50 TNT-SN. (Each Point is an Average of 2-5 Measurements.)

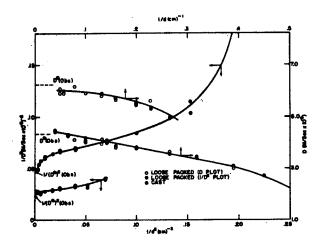


Fig. 3 -  $1/D^2$  vs.  $1/d^2$  for 50/50 TNT-SN

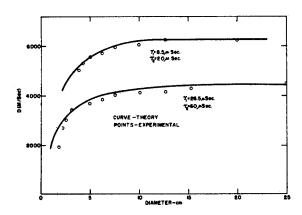


Fig. 4 - Comparison of Theoretical D(d) Curves (Detonation Head Theory) with Experimental Results

The total reaction times may be expressed in terms of the Eyring surface burning equation

$$\widehat{f} = \overline{R}_{g} / \lambda k!$$
 (6)

which may be shown to be consistent with results obtained in this study and has been verified quantitatively in previous studies. The results of these studies may therefore be summarized by the equations

$$\gamma_2 = 2.1 \times 10^{-3} \, \overline{R}_g \cdot f \, (\rho_1 = 1.15)$$
(7)

$$\gamma_2 = 6.8 \times 10^{-4} \,\overline{R}_g \cdot f \, (\rho_1 = 1.83)$$
(8)

where f = 1.0 in both equations for the detonation head model (from the average  $a_0$ ), f = 0.09 and 0.07 in equations (7) and (8), respectively for the nozzle theory, and (from the average  $a_0$ ) f = 0.04 and f = 0.03 for equation (7) and (8), respectively, for the curved front theory.

As in the case of AN in amatol, the reaction time of SN in sodatol increased by a factor of about three in decreasing the density from  $\overline{\rho}_1$  = 1.83 to  $\overline{\rho}_1$  = 1.15. This shows that the detonation temperature increased with density. If one assumes (1) that the activation energy of SN is the same as for decomposition of SN (61 kcal/mol), (2) the temperatures in Table I, and (3) the equation

$$k' = AT e^{-61,000/RT}$$
 (9)

of absolute reaction rate theory, the ratio  $\widehat{\gamma}_2(1.15)/\widehat{\gamma}_2(1.83)$  turns out to be 3.0 in agreement with the value found by the detonation head model and (within the limits of uncertainty) with the values found by either the nozzle or curved front theory. This shows, as in the case of amatol, that the  $\alpha(v)$  equation of state is essentially correct. The Kistiakowsky-Wilson-Brinkley equation of state

$$pv = nRT (1 + x e^{x}); x = KT^{-1/4}/v$$

gives for  $T_2(1.83)$  - T(1.15) a value of about -500°. This would require by equation (9) a ratio  $f_2(1.15)/f_2(1.83)$  of about 0.3 which is too low by a factor of about ten.

The remarkable consistency of the detonation head model may be shown also by noting the absolute values of k' found in this investigation in comparison with those for AN, TNT, and others found in previous studies. Values of k' for SN computed from equation (6) were  $10^{9.93}$  for the low density product and  $10^{10.4}$  for the cast product. Equation (9) with  $\Delta H = 61$  kcal/mole requires  $\Delta S^{\neq} = -2.0$  E.U. to give these values of k'. This value is practically the same as that found for AN. Again values of  $\Delta S^{\neq}$  from + 3 to + 6 E.U. are required to give the values of  $\Delta S^{\neq}$ , one computes through equations (6) and (9). Positive values of  $\Delta S^{\neq}$ , however, seem highly improbably for a process such as this. While autocatalysis leads to positive values of  $\Delta S^{\neq}$ , autocatalysis can hardly come into play in a surface burning reaction of the type involved in detonation.

Thermo-Hydrodynamic Properties of Cast and Loose-Packed 50/50 INT-SN Table I:

P2 (atm)	59,000	158,000									N&20	2.94	2.94
(m/sec)	1155	1395									<b>7</b> СН	0.1	1.2
(g/cc)	979.0	0.424		2.0	0.348	0.391		0.340	0.391	(8)	NH3	9.0	1.4
C <sub>V</sub> (kcal/ kg/deg)	0.287	0.307	Curve	1.8	0.377	0.431	rve)	0.375	0.431	on (mols/k	H <sub>2</sub> 0	3.5	9.0
C <sub>v</sub> (kcal/mol) kg/deg)	850	076	Calculated $\alpha(\mathbf{v})$ Curve	1.6	0.409	0.479	(Universal Curve)	0.420	0.479	Products of Detonation (mols/kg)	8	5.3	1.4
n (mol/kg)	26.0	23.0	Calc	1.4	0.447	0.540	n)	094.0	0.540	Products	8	10.0	12.9
$r_2^{(oK)}$	3750	4350		1.2	0.491	0.620		0.510	0.620		N S	6.2	5.5
D*(obs) (m/sec)	0644	6240		1.0	0.543	0.723		0.565	0.723		H <sub>2</sub>	0.3	_
(g/cc)	1.15	1.83		٩	<sup>1</sup> 당	42		븅	<b>4</b>			p, = 1.15	ρ <sub>1</sub> = 1.83

#### ACKNOWLEDGMENT

This work was supported by Office of Naval Research, Contract Number N7-onr-45107, Project Number 357 239, and was carried out by the Explosives Research Group, Utah University.

#### **BIBLIOGRAPHY**

- (1) M. A. Cook, E. B. Mayfield, and W. S. Partridge, "Reaction Rates of Ammonium Nitrate in Detonation" (submitted for publication).
- (2) M. A. Cook, "Detonation Head Model and Reaction Rates in Detonation" (submitted for publication).
- (3) H. Jones, Proc. Roy. Soc. (London) A189, 415 (1947).
- (4) H. Eyring, R. E. Powell, G. H. Duffey, and R. B. Parlin, Chem. Rev. 45, 1 (1949).
- (5) M. A. Cook, "Detonation Wave Fronts in Ideal and Non-Ideal Detonation", This Symposium.
- (6) M. A. Cook and E. F. Pound, "'Pin Oscillograph' for Measurement of Detonation Velocity", Technical Report No. XXXIII, May 4, 1954, ERG, Utah University.
- (7) M. A. Cook and W. O. Ursenbach, "Velocity-Diameter and Wave Shape Studies for Low Density 50/50 TNT-Sodium Nitrate Mixtures", Technical Report No. XXXVI, July 30, 1954, ERG, Utah University.
- (8) M. A. Cook, R. T. Keyes, G. S. Horsley, and A. S. Filler, "A Study of the Equation of State for EDNA", Accepted for Publication, J. Phys. Chem.
- (9) M. A. Cook, J. Chem. Phys. <u>15</u>, 518 (1947).
- (10) J. Taylor, "Detonation in Condensed Explosives", Oxford Press, (1952).
- (11) R. B. Parlin and D. W. Robinson, "Effect of Charge Radius on Detonation Velocity", Technical Report No. VII, October 3, 1952, ERG, Utah University.

#### THE DECOMPOSITION OF ALPHA-LEAD AZIDE

J. M. Groocock C.S.A.R., Ministry of Supply Great Britain

# General Introduction

Detonation, from a chemical viewpoint, is essentially an extremely rapid exothermal reaction, but there is little certain evidence to show that this reaction for any given initiator is simply the thermal decomposition reaction greatly accelerated by extreme physical conditions. However, it would seem that a clear understanding of the kinetics of the low-rate decomposition of initiators and of the decomposition that, under suitable conditions, can be observed prior to detonation is a necessary precursor of an understanding of the chemistry of detonation. A study of the reaction kinetics of the decomposition of lead azide is therefore being made at the Armament Research Establishment in Great Britain. So far, work has been completed on the photolysis and electron bombardment decomposition under vacuum of pure alpha lead azide and this paper will deal mainly with these. Reference will also be made to a study of the thermal decomposition of lead azide at moderate temperatures, which experimentally has reached a fairly advanced stage and to some preliminary results obtained at higher temperatures, where the decomposition passes into detonation.

#### Decomposition of Azides

The study of solid reactions has made rapid progress in recent years since the importance of lattice defects was pointed out by Frenkel (1) and Wagner and Schottky (2) and further impetus was given by the development of the theory of electrons in solids (3 and 4). The first detailed elucidation of a solid reaction using these ideas was given by Gurney and Mott (5) for the photochemical process taking place in silver bromide. In recent years considerable attention has been given to the metallic azides (6 to 17). There is a series of these of the general formula MN<sub>3</sub> for monovalent, MN<sub>6</sub> for divalent metals and they all decompose stoichiometrically under suitable conditions according to the equation:

#### Groocock

$$2 MN_3 -> 2M + 3N_2$$

The reaction can be studied by measuring the build up of the pressure of nitrogen in a vacuum system. Thermochemical data shows that the decomposition of one azide radical to give a nitrogen molecule plus a nitrogen atom is endothermic, i.e.

$$N_3 -> N_2 + N - 37 \text{ k-cals.}$$

whereas the decomposition of two azide reaicals to give three nitrogen molecules is exothermic,

$$2N_3 -> 3N_2 + 151 \text{ k-cals.}$$

and most methods of decomposition involve the latter. In the crystal there is some stabilisation by resonance but this is low for metals with high ionisation potentials.

The kinetics of the thermal decompositions of lead, sodium and potassium, calcium, strontium and barium azides have been studied (6 to 15) but these will not be discussed here. The photochemical decompositions of barium and potassium azides (11, 14, 15) and the electron bombardment decomposition of sodium and barium azides (16 and 18) have also been studied.

# The Photolysis of Barium and Potassium Azides

The reflection spectra of barium, potassium and sodium azides have been measured by Jacobs and Tompkins (15) and it was found that absorption of wavelengths shorter than 2700 to 2800 A took place. They found no evidence of photoconductance in these salts. The photolysis of barium azide has been investigated by Garner and Maggs (11) and in more detail by Thomas and Tompkins (14). The latter found that on irradiation with light of wavelength 2537%, nitrogen is evolved and the rate becomes linear with time. In fresh unirradiated barium azide there is an initial fast rate of decomposition which gradually decays to a constant value. Between -1060 and 4000 the rate is proportional to the square of the intensity. Between -106° and -52° the activation energy is 200 cals., between -52° and -10° 1700 cals., and between -10° and  $40^{\circ}$  the activation energy is 4500 cals. Similar results have been obtained by Jacobs and Tompkins (15) for potassium azide. An immediate emission of nitrogen occurs at a rate which increases slightly for the first five minutes and then becomes constant, at a rate proportional to I'. Activation energies of 700 cals. below 1°C, and 2,700 cals. above 1°C were obtained and slow decomposition was found to continue after switching off the light source.

According to Thomas and Tompkins, absorption of a quantum of light must excite an electron either into the exciton level or the conduction band. They then consider that it is likely that

#### Groocock

decomposition involves two positive holes or excitons which must be trapped at adjacent sites. Positive holes in the lattice will be held apart by their charges, and reaction with the low activation energy found experimentally will be possible only if the centre as a whole is uncharged; i.e. the trap is a doubly charged vacant cation site. The rate of decomposition is constant and thus the number of these centres must be independent of time and reaction must therefore regenerate a trapping centre. Thomas and Tompkins first consider the rate of decomposition as proportional to the rate at which traps containing two positive holes are formed. The formation of traps containing one positive hole is proportional to the concentration of free positive holes, while they can be destroyed in three ways; by trapping an electron, by thermal liberation of the hole, and by reaction with a neighbouring positive hole giving the measured reaction rate. By means of a detailed analysis of such factors Thomas and Tompkins obtained an expression for the rate of formation of traps containing two positive holes and then showed that if the traps are deep, the rate of decomposition is proportional to I rather than I2 as found experimentally. If the traps are shallow, however, the temperature dependence is incorrect and the mobility of the positive holes should give photoconductivity. Thomas and Tompkins suggest that the mechanism involved two excitons and show by a treatment similar to that outlined above that the experimental facts can be explained in terms of this. The difference is that excitons having no net charge can be trapped at any discontinuity in the lattice. The temperature dependence found is explained in terms of two possible processes for the reaction together of the excitons, one utilising the energy released by the trapping of one of the excitons, and the other requiring thermal energy from the lattice.

#### The Electron Bombardment Decomposition of Barium and Sodium Azides

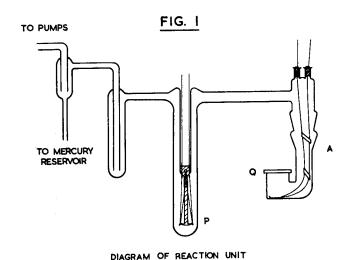
The electron bombardment decomposition of sodium azide has been studied by Muller and Brous (18), and Groocock and Tompkins (16) who also investigated barium azide by this technique. They found that on bombardment of both compounds with electrons of constant velocity and intensity there was an immediate evolution of gas and that the decomposition rate rose quickly to a maximum and then slowly decayed approximately exponentially finally to approach a constant rate after long periods of bombardment. If now bombardment was stopped and the salt was left under high vacuum for some hours, on recommencing bombardment the rate of decomposition was found to have recovered completely and the first curve could be repeated exactly. Detailed investigation showed that the recovery process had first order kinetics. No colour change was produced by the bombardment. variation in the decomposition rate with the intensity of bombardment was complex but all the results could be adequately explained in terms of a theory which postulated that the action of the electron beam was to produce positive holes and conduction band electrons in a relatively thick layer. Decomposition to give nitrogen occurred whenever two positive holes were produced in adjacent positions in

the surface; therefore the reaction was controlled by the number of single surface positive holes present. This in turn was determined by the concentration of azide ions in the deeper layer penetrated by the electron beam but where decomposition aid not take place. The recovery process was seen in terms of the recombination of positive holes and conduction band electrons in this lower layer.

## The Photolysis of $\alpha$ -Lead Azide

# Experimental details

The apparatus consisted of the reaction cell A (Fig.1)



connected to a high vacuum system comprising a Pirani gauge P, a liquid nitrogen trap, a mercury cut-off and a mercury diffusion pump with a rotary oil pump. The azide was contained in a flat tray of pyrex glass 12 mm's. in diameter and the junction of a copper constantan thermo-couple was sealed with Araldite into a groove ground into the face of the tray. Using this the temperature of the azide could be measured and the values

are accurate to ± 0.2°C. The Pirani gauge had a sensitivity such that pressure differencies of 1x10<sup>-5</sup>mms. could be detected easily. The ultra-violet light was obtained using a low pressure mercury vapour lamp having 90 per cent of its total radiation in the 2537 Å line. A calibration of intensity of radiation against current through the lamp was obtained with excellent reproducibility, using a zirconium cathode photocell sensitive in the ultra-violet only.

Measurements of rate of decomposition against time were obtained as follows: The time \$\Delta t1\$, for a small pressure increase in the system closed by the cut-off was measured; this part of the apparatus was then quickly pumped out and the time \$\Delta t2\$ for the same small pressure increase measured again. As \$\Delta t\$ is small \frac{1}{\Delta t}\$ is proportional to the rate of decomposition at time t, and from a series of values of \$\Delta t\$, a plot of rate of decomposition against time can be obtained for any period of decomposition, while the pressure within the cut-off system varies between small limits only. This technique has the further advantages that measurements are independent of the shape of the Pirani gauge calibration curve and that the resulting rate of change of pressure/time curves are more useful theoretically

than the more usual pressure/time curves.

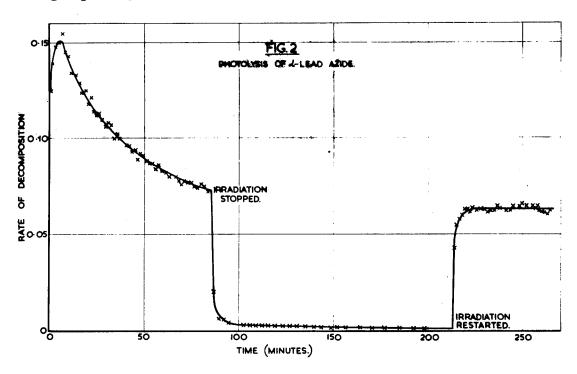
#### Results

## Photolysis at constant intensity

Fig.2 shows the plot of rate of decomposition against time for the photolysis of  $40 \text{ mg} \cdot \text{ of } \alpha\text{-lead azide} \cdot$  The temperature of the azide rose from  $3.6^{\circ}\text{C}$  to  $7.0 \pm 0.2^{\circ}\text{C}$  during the first ten minutes of the photolysis due to the heating effect of the beam, but in view of the low activation energy of the reaction (reported later) this would increase the rate by only 2 per cent and no correction is therefore made. Gas is evolved immediately on commencing the irradiation and the rate reaches a maximum within a few minutes and then falls approaching a constant value after some hours. Mathematical analysis of this and other decomposition curves shows that the final decay in rate is exponential in form:

i.e. 
$$R - R_{\infty} = (Ro - R_{\infty}) \exp(-kt)$$

where R is the rate of decomposition at time t, Ro is the rate extrapolated to zero time and R 2 is the rate approached after prolonged photolysis.



This exponential decay in rate is held fairly closely for the later stages of the photolysis, but in all cases in the region immediately following the maximum the rate was too high to accord with an exponential decay. As the temperature is low at this time

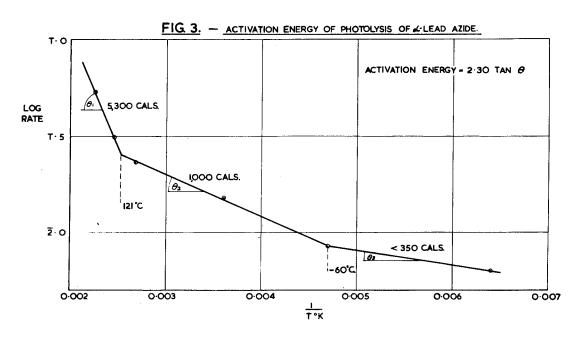
and the effect of the initial rise will still be tending to reduce the rate, this result is unexpected. Within a few minutes of the commencement of the photolysis, the surface of the azide had become noticeably yellow, and the colour rapidly darkened through orange to brown, and finally black.

After 85 minutes the irradiation was stopped but gas continued to be evolved although at a much reduced rate. This "dark rate" decayed rapidly and after about an hour was 1/50 x R... On recommencing irradiation there was again an immediate evolution of gas at a rate which increased rapidly to a constant value, but lower than the rate at which irradiation had been stopped. The dark rate was checked after allowing the azide to stand unirradiated in high vacuum overnight, and then had a very low value probably accounted for by the outgassing of the apparatus.

Re-irradiation again showed a rise to a constant value lower than the rate at which the previous irradiation had been stopped.

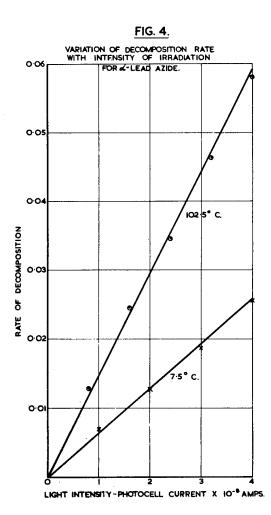
# Variation of photolysis rate with temperature

The rate of decomposition at constant intensity of illumination was measured at several temperatures in the range -  $117^{\circ}C$  to +  $171^{\circ}C$ , and in all cases the general form of the rate/time curve was the same as that outlined above. Values of  $R_{\infty}$  were selected such that plots of  $\log (R - R_{\infty})$  against time gave the best possible straight lines and these values of  $R_{\infty}$  were then plotted in a conventional activation energy curve. (Fig.3). This graph of  $\log R_{\infty}$  against  $1/T^{\circ}K$  has three straight regions of different slopes: above 121°C there is an activation energy of 5,300 cals; between 121°C and some temperature below  $-60^{\circ}C$  it is 1,000 cals, and at very low temperatures the reaction has an activation energy of less than 350 cals.



# Variation of photolysis rate with intensity

The intensity of irradiation was varied by altering the current passing through the mercury vapour lamp to correspond with the photocell calibration curve, as noted above. Two temperatures, 7.5°C and 102.5°C were used for these experiments; at lower temperatures, except at maximum intensity of irradiation, the rates of decomposition were too low to be measured with sufficient accuracy. The procedure adopted was to irradiate a fresh sample of the azide at the maximum intensity until the rate was falling only very slowly. The intensity was then reduced by a known amount and irradiation continued while 12 readings of rate were taken, these in general showing merely a scatter about a constant value. Their mean could therefore be taken as the decomposition rate for this intensity. By successively reducing the current (lamp) through fixed amounts a series of readings of rate against intensity were obtained. Although the bath temperature was kept constant throughout a run, the varying intensities of illumination used affected the actual temperature of the azide; the



temperature of the salt at maximum illumination was up to 5°C higher than that of the unilluminated salt. However, this corresponded to a rate change of only 3 per cent and was not therefore corrected for. The results obtained at the two temperatures are shown graphed in Fig.4. In both cases the plot of rate against intensity is a good straight line passing through the origin. The rate of decomposition is therefore proportional to the intensity.

#### Discussion of results

For the photolysis of  $\alpha$ -lead azide the main experimental facts which must be explained are as follows:-

- (i) At constant intensity of irradiation and constant temperature, the rate of decomposition rises first to a maximum and then decays probably exponentially to a constant value.
- (ii) There is an immediate colour change followed by blackening.
- (iii) On ceasing irradiation there is a slow "dark rate" which decays to zero.
- (iv) Re-irradiation produces a rapid rise to a constant value which is lower than the final value of the previous irradiation.
- (v) The R<sub>∞</sub> value varies as the first power of the intensity.
- (vi) The temperature dependence is complex, but is very similar to that of barium and potassium azides.

Theoretical treatments of the results obtained for the photolysis of barium and potassium azides have been given by Thomas and Tompkins (14) and Jacobs and Tompkins (15) and as noted in the introduction they postulate a mechanism involving the reaction together of two excitons produced by the radiation. Similar assumptions applied to lead azide demand that the rate of decomposition shall be proportional to the square of the intensity of illumination rather than the first power, as found experimentally. A theory based on reaction of positive holes however overcomes this difficulty. Although the direct excitation of an electron into the conduction band by absorption of a quantum of light is thought to be a forbidden transition, if the exciton level is very near to the conduction band most electrons which reach the exciton level will then be thermally excited into the conduction band. For lead azide it is therefore a reasonable assumption that absorption of a quantum of light excites an azide ion giving a conduction band electron and a positive hole. It is now assumed that whenever two positive holes are trapped at adjacent positions in the lattice reaction can then occur to give three molecules of nitrogen. The number of effective traps is taken as constant because an equilibrium rate of decomposition is soom reached and this implies that reaction of a trap releases it for further trapping. Let there be N traps of which n are empty, n<sub>1</sub> contains one positive hole and n<sub>2</sub> two. let the probability of trapping a positive hole be P and of trapping a free electron (destroying a positive hole) be P.

In addition centres containing one and two positive holes may thermally dissociate, but if reaction takes place at cation vacancies which are deep traps this effect should be negligible. Finally kn<sub>2</sub> is the decomposition rate to give gaseous nitrogen. At equilibrium, i.e. when the rate has fallen to R<sub>m</sub>

$$\frac{dn}{dt} = kn_2 + p_n_1 - p_n = 0$$

$$\frac{dn}{dt}^2 = p_1 n_1 - p_2 n_2 - kn_2 = 0$$

and as the number of traps remain constant  $N = n + n_1 + n_2$ . Now p and p are proportional to the intensity of irradiation, i.e. p = C I and p = C I. Solution of these equations gives the following expression for the measured rate:

Rate = 
$$\frac{kC_{+}^{2} \text{ N I}}{\sqrt{C_{+}^{2} + C_{-}^{2} + C_{+}^{2} + C_{-}^{2} / I + k \sqrt{2}C_{+} + C_{-}^{2} / I}$$
If now 
$$\sqrt{C_{+}^{2} + C_{-}^{2} + C_{+}^{2} + C_{-}^{2} / I \ll \sqrt{2}C_{+} + C_{-}^{2} / k}$$

the rate will be proportional to I. C, and C, must be less than unity and are likely to be small as most of the electrons and positive holes will not be trapped before recombining. The lifetime of a cation vacancy containing two positive holes must be short in view of the low activation energy of the overall process so k must be large; therefore unless I is large the rate should be proportional to I. At very high intensities the rate should become independent of the intensity. Although the above mechanism utilises positive holes and conduction hand electrons it does not necessarily demand a high photoconductivity, for the reacting positive holes are immobilised in deep traps and reaction produces many anion vacancies which are deep electron traps. The absorption bands associated with the resulting F centres undoubtedly give rise to the colour changes observed during decomposition. The blackening observed after further decomposition indicates that coalescence of n Pb++ ions with 2n F-centres is taking place, the azide lattice is collapsing and particles of colloidal metallic lead are being produced.

Analysis of the initial stages of the decomposition curves, i.e. before the rate has become constant  $R_{\infty}$ , requires solution of the initial differential equations for non-equilibrium conditions. The following expression then results:

$$\frac{\text{Rate}}{k} = S \left\{ 1 - \exp_{\frac{1}{2}} \left[ -(k + 2p_{+} + 2p_{-}) - \sqrt{f} \right] \right\}$$

$$+ T \left\{ \exp_{\frac{1}{2}} \sqrt{-(k + 2p_{+} + 2p_{-})} + \sqrt{-7} t - 1 \right\}$$
where  $\sqrt{-\sqrt{k^2 - 4p_{+}}(k - p_{-})}$ 
and  $-S + T = -\frac{R_{\infty}}{k}$ 

i.e. an equation of the form.

$$\frac{R}{k} = S \sqrt{1 - \exp \cdot (-\alpha t)} + T \sqrt{\exp \cdot (-\beta t)} - 1 \sqrt{2}$$

This equation is the sum of two exponential terms the first of which is zero at t=0 and rises to a maximum  $R_{\infty}^{-1}$  when  $t\to\infty$ , and the second of which is zero at t=0 and then falls to a minimum  $R_{\infty}^{-11}$  = - T when T ->  $\infty$ . It gives a very good qualitative representation of the experimental curve provided certain conditions, such as that both  $\alpha$  and  $\beta$  are positive, are satisfied. Further examination shows in general that these conditions are fulfilled.

A "dark rate" is logically predicted by the above theory. When the irradiation is stopped production of positive holes and free electrons will cease and a source of energy will be removed, but double positive holes trapped at cation vacancies will continue to decompose unimolecularly. Furthermore free positive holes and those released from shallow traps will continue to be trapped at cation vacancies and there decompose, this being a much slower bimolecular process. Combination with F-centres and conduction band electrons will also destroy positive holes and when all have been destroyed or immobilised singly the rate will become zero. From this it would be expected that on stopping the irradiation the decomposition rate would first fall very rapidly and then finally approach zero at a much slower rate, as found experimentally.

If irradiation is now restarted after a waiting period the initial rate should be low while the number of traps containing double positive holes builds up to its equilibrium value. This build up as found experimentally should however be more rapid than the build up that takes place on first irradiating a sample of the salt, for many of the cation vacancies will already contain a single positive hole. During the waiting period it is possible that in the absence of a large excess of positive holes, some of the cation vacancies might trap two anion vacancies produced during the irradiation, this giving effective destruction of the trap. This would explain the lower equilibrium reaction rate after a waiting period.

The activation energy values are very similar to those found for the photolysis of barium and potassium azides and the explanation is the same; the final reaction to give nitrogen can take place in two ways, either with zero activation energy, all the energy being supplied by the radiation, or with the addition of a thermal activation energy. These two result in the temperature dependence found. (This point is discussed in detail by Thomas and Tompkins).

As noted above the colour changes produced by the irradiation are due to the production of additional adsorption bands, probably F-bands, and the blackening is due to the production of metallic lead. In the thermal decomposition of barium azide the presence of nuclei of barium metal has the effect of greatly catalysing the decomposition and the same is true to a lesser degree in the thermal decomposition of  $\alpha$ -lead azide. There is no experimental indication that this is so, for the photolysis of  $\alpha$ -lead azide and no modification of the theory is thus needed.

## Electron Bombardment Decomposition of a-Lead Azide

# Experimental details

The apparatus was identical with that described above for the photolysis experiments except that the irradiation cell was replaced by a bombardment cell. This reaction cell was fundamentally a simple diode electronic valve in which the cathode and anode were supported in glass cones so that the whole cell could be easily dismantled.

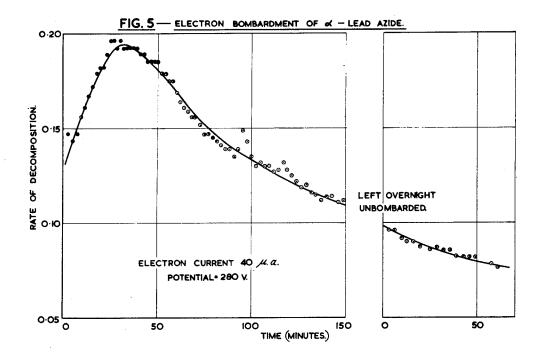
The technique used was to place a weighed sample of the finely powdered azide on the anode and to flatten and smooth this to give complete coverage of the metal. After pumping overnight, a known A.C. potential was applied to the anode. The temperature of the directly heated cathode, which was a short length of electric light filament. was then adjusted to give the desired electron current and the rate of decomposition of the azide measured using the method described above for the photolysis experiments. The number of electrons reaching the anode in unit time was measured using a D.C. micro-ammeter (the reaction cell behaved as a half-wave rectifier) and kept constant by adjusting the cathode temperature. The earlier work of Groccock and Tompkins had shown that serious irregularities of behaviour were found if a D.C. potential was used, because of the build up and discharge of space-charges in the cell. It had also shown that it was experimentally impossible to work at very low potentials and that above 50 volts, variations in potential had little effect on the reaction rate. Therefore, so long as the conditions remained constant, there was little disadvantage in using an A.C. potential. All experiments were carried out at room temperature.

Experimentally it is difficult to get satisfactory results from the electron bombardment method. It is necessary to have an electrode system that allows insertion of the azide on the anode and gives sufficient cathode anode separation to ensure that the azide is not thermally affected by heat from the cathode. High voltages are undesirable because the electrons then have sufficient energy to produce multiple effects in the azide, making interpretation of the results more difficult. Consequently high electron currents giving easily measurable decomposition rates cannot be obtained. Electron space charges form about the relatively non-conducting azide layer covering the anode and produce further difficulties. Neutralisation of the space charges is aided by allowing the gas pressure to rise when positive ions are formed, but these in turn have their own complicating effects. The best compromise found was to use a cathode anode separation of 2.5 cms, a potential difference by 200 volts A.C. and a gas pressure of about 3 x 10<sup>-3</sup>mms. 15 mg. of azide was spread on the anode which was 1 sq.cm. in area.

## Results

# Decomposition at constant electron current

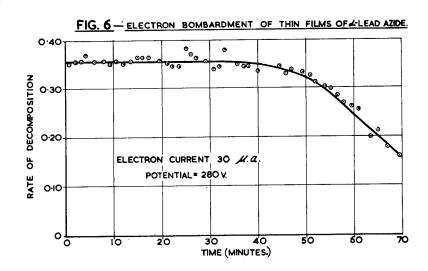
Fig.5 shows a typical decomposition curve at constant electron current and applied voltage. It is very similar to the curves found for sodium and barium azide by Groccock and Tompkins. With lead azide however there was no recovery of rate after standing unbombarded under vacuum. In fact as in the photolysis work the rate



was lower on re-bombarding. Experimentally this meant that the sample of lead azide had to be changed after each run. With sodium and barium azides which "recovered" completely on standing it was possible to adopt the much more satisfactory procedure of doing a whole series of runs on the same sample. Electron bombardment of lead azide produced the same permament colour changes as shown in the photolysis experiments.

# Thin azide layers

Because of the quantitatively irreproducible results a different method of applying the azide to the anode was tried. A particularly fine sample of the azide was sieved into the top of a long glass tube and fell onto the anode at the bottom. Complete coverage was thus obtained with only 1 mg. of azide. The results were now markedly different from those obtained with the thicker layers. The shape of the decomposition curves at constant electron current showed an immediate evolution of gas which stayed constant for an hour or more (Fig.6). There followed a fairly sharp fall in rate and this was associated with a considerable fall in conductivity. At higher electron currents (50 to 80  $\mu$ a) the region of



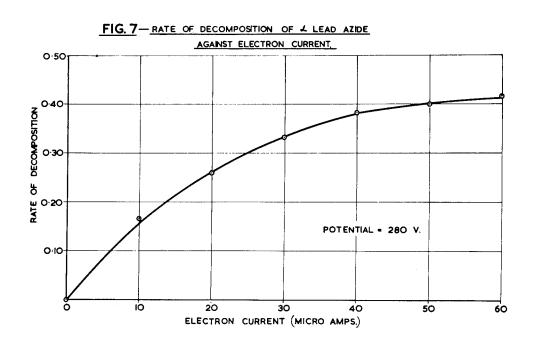
constant decomposition was comparatively short, the fall in rate occuring when relatively little of the azide had decomposed. With lower electron currents (10 to 20  $\mu$ a) a much larger proportion of the azide could be decomposed before the fall in conductivity made the continuation of the run impossible.

With a 1 mg. sample of azide a few minutes bombardment caused darkening of a well defined but irregular shaped patch of the azide, the remainder staying white. As bombardment continued this patch darkened, the remainder of the surface still being unaffected.

with an azide sample of only 0.7 mg the whole of the azide surface rapidly discoloured on bombardment while with 1.5 mg there was no rapid discolouration, the whole of the surface darkening after an hour or more. The conductivity variations noted above were also affected by the layer thickness. The 1.5 mg samples showed the sudden fall in conductivity after 1 to 2 hours bombardment, but the 0.7 mg samples did not show this fall in rate and conductivity till after 10 to 20 hours bombardment, if at all.

# Variation of decomposition rate with electron current

The effect of variations in the electron current on the rate was determined both by varying the electron current during a run and also by varying the current from run to run. Similar results were obtained and these resembled those found for sodium and barium azides. in that the rate was roughly proportional to the current at low electron currents and approached a maximum as the current increased (Fig. 7). At low electron currents for these thin azide samples, the ratio of the number of azide radicals decomposed to the number of incident electrons was about 0.75; the energy of the electrons was probably about 280 ev. For the earlier work using thicker azide samples there was no long period of constant decomposition rate, but even the highest rates reached during the course of the runs corresponded to an electron yield value lower (0.3 to 0.75 ev) than that found for the thinner samples. These electron yields are of the same order as those found for sodium and barium azides.



#### Discussion of results

For the electron bombardment decomposition of  $\alpha$ -lead azide the main experimental facts which must be explained are as follows:-

- (i) At constant bombardment flux the rate of decomposition rises first to a maximum and then decays probably exponentially to a constant value.
- (ii) There is an immediate colour change followed by blackening.
- (iii) There is no "dark-rate" on stopping bombardment.
- (iv) Re-bombardment after a waiting period shows no "recovery process"; the rate rises rapidly to a constant value which is lower than the final value of the previous bombardment.
- (v) The variation of the rate with the electron flux is complex but appears to be the same as that for barium and sodium azides.
- (vi) Finally the special phenomena associated with very thin azide layers need explanation.

Groocock and Tompkins (16) have discussed the electron bombardment decomposition of sodium and barium azides in terms of a theory which has several major differences from that applied by Thomas and Tompkins (14) to the photolysis results. It was thought unlikely that the electrons used, which had an energy roughly 50 times that of light of wavelength 2537A, would produce excitons. Ample energy is available to give decomposition of single azide ions, but the very simple kinetics which would result from a mechanism of this kind do not accord with experiment. A further difference from the photolysis theory is that a mechanism depending upon a thermal activation energy is thought unlikely. Experimentally the absence of a "dark rate" indicates a different mechanism. They therefore postulated that decomposition occurs instantaneously without further activation energy when an azide ion adjacent to a surface hole is excited by an electron of the primary beam. Positive holes formed at a deeper level in the azide do not decompose to give nitrogen. The recovery in decomposition rate on re-bombardment after a waiting period is due to the regeneration in the bulk layer of azide ions from positive holes by the trapping of conduction electrons. A mathematical treatment based on these postulates gave quantitative agreement with the experimentally found curves for the rate of decomposition against time at constant electron current, for the variation of the rate with electron current and for the recovery in rate with time of standing.

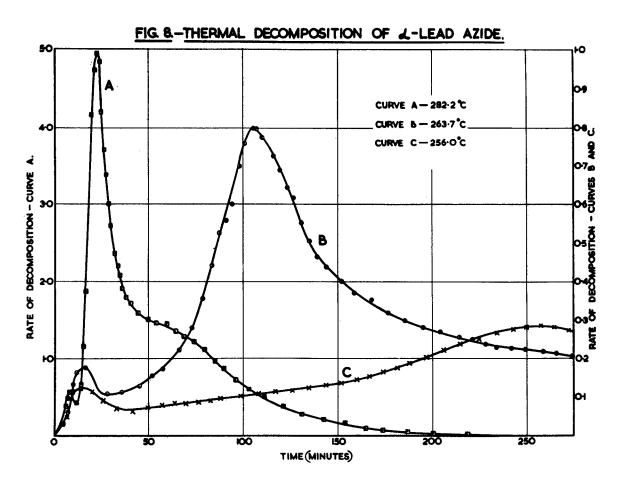
The above arguments which were formulated for barium and sodium azides apply also to lead azide. While the lead azide results are not sufficiently reproducible to give the quantitative correspondence with the theory that the sodium and barium azide results gave, qualitatively the agreement is good. Two points need further explanation: the colour changes produced in lead azide, and the absence of a recovery process. The former, which are also produced by ultra-violet irradiation are readily explained. In all three azides large number of F-centres must be produced during bombardment and the absence of colour in barium and sodium azides, as suggested by Thomas and Tompkins is probably due to their F-bands being in the near ultraviolet rather than the visible part of the spectrum. The blackening of  $\alpha$ -lead azide shows the presence of colloidal metallis lead produced by the reaction: Pb<sup>++</sup> + 2F-centres → Pb + 2 vacant anion sites. followed by collapse of the lattice. Experimentally however there is no indication that the electron bombardment decomposition (or the photolysis) is catalysed by metallic lead, nor do F-centres or metallic nuclei play any important part in the mechanism postulated by Groocock and Tompkins. These special effects in α-lead azide do not therefore call for any important change in the mechanism. That there is no recovery process in a-lead azide implies that the regeneration of azide ions from positive holes does not take place in the absence of the electron beam probably because the conduction electrons are preferentially trapped at some other type of trap e.g. anion vacancies or metallic particles or possibly at a deeper level in the azide beyond the region where positive holes are formed.

The special effects found with very thin layers of a-lead are probably electrical rather than chemical in nature. The bombarding electrons penetrate into the solid and lose energy by collision with the lattice electrons, exciting these into the conduction band and leaving behind positive holes. Finally the electrons and positive holes will tend to be trapped at suitable lattice imperfections or to recombine and it is during these transitions that they may take part in chamical reactions. Under the conditions used for electron bombardment decomposition studies, there will be a potential gradient across the solid and consequently there will be a directional motion superimposed upon the random thermal motion of the conduction electrons and positive holes. As a result the trapping of the positive holes and electrons will tend to take place respectively near and far from the bombarded surface. It can be seen that when the above factors are considered together with the actual chemical reactions taking place in the decomposition the overall picture must be complex, but some explanation of the observed effects can be given in terms of the strong internal space-charges formed in the solid.

#### Thermal Decomposition of a-Lead Azide

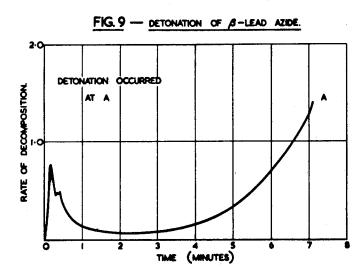
A study is being made of the thermal decomposition of  $\alpha$ -lead azide under vacuum. While this work is not yet complete it has already shown that the kinetics of the decomposition are more

complex than earlier workers believed. Experimentally the azide (c.1 mg.) contained in a platinum bucket is lowered under vacuum by means of a magnetic device into a furnace chamber maintained at the desired temperature (to  $\pm$  0.1°C) by an electric furnace. Decomposition rates are then measured by the method used for the photolysis experiments. The most fruitful work has been done on good crystals of pure  $\alpha$ -lead azide, sieved to give particles of roughly constant size. Fig.8 shows the rate of decomposition of



lead azide sieved between 150 and 200 mesh at temperatures of 256.0°C, 263.7°C and 282.2°C. Features to be noticed are the region in the lowest temperature curve, where the rate increases linearly and the very sharp peak in the highest temperature curve. The very rapid decay after the peak cannot be explained in terms of destruction of material or reduction of the area of the reaction interface. Work with other sieve fractions has shown that the height of this peak is proportional to the surface area of the crystals.

In the experiments being carried out at the higher temperatures above 300°C the azide is tipped under vacuum by a magnetic device onto a copper block heated in a furnace and the reaction rates prior



to detonation are recorded automatically. Using this system with small crystals, isothermal conditions are established very quickly and selfheating is minimised. Fig.9 shows a typical trace obtained from 2 mg. of crystalline β-lead azide (120 5 200 mesh) at 304.5°C. The initial peak is probably outgassing and detonation occurred at A on the curve.

Work on the thermal decomposition of lead azide is being continued and a more comprehensive report will be prepared later.

## Bibliography

- 1. Frenkel: Zeits. f. Physik. (1926) 35,652.
- 2. Wagner and Schottky: Z.Phys. Chem. B. (1930) 11,163.
- 3. Mott and Gurney: "Electronic Processes in Ionic Crystals". 0.U.P. (1948)
- 4. Seitz: "Modern Theory of Solids" MoGraw Hill (1940).
- 5. Gurney and Mott: Proc. Roy. Soc. A. (1938) 164,151.
- 6. Garner and Gomm: J.C.S. (1931) 2123.
- 7. Harvey Trans. Far. Soc. (1933) 29,653.
- 8. Garner and Moon: J.C.S. (1933) 1398.
- 9. Garner and Marke: J.C.S. (1936) 657.
- 10. Maggs: Trans. Far. Soc. (1939) <u>35</u>,433
- 11. Garner and Maggs: Proc. Roy. Soc. A(1939) 172,299
- 12. Wischin: Proc. Roy. Soc. A (1939) 172,314.
- 13. Audubert and Roberts: J. Chem. Phys. (1946) 43,127.
- 14. Thomas and Tompkins: Proc.Roy.Soc. A. (1951) 209,550.  $1951) \overline{210,111}$
- 15. Jacobs and Tompkins: Proc. Roy. Soc. A. (1952) 215, 254, 265.
- 16. Groccock and Tompkins: Proc. Roy. Soc. A. (1954) 223, 267
- 17. Mott: Proc.Roy.Soc. A. (1939) 172,325.
- 18. Muller and Brous: J. Chem. Phys. (1933) 1,482

### Acknowledgments

Acknowledgment is made to the Chief Scientist, British Ministry of Supply, for permission to publish this paper for this symposium.

British Crown Copyright reserved. Reproduced with the permission of the Controller, H.B.M.S.O.

## THE DETONATION OF AZIDES BY LIGHT

J.S. Courtney-Pratt, B.E. Ph.D. and G.T. Rogers, M.A. Research Laboratory for the Physics & Chemistry of Surfaces, Department of Physical Chemistry, Cambridge, England.

## Introduction.

It is well known that crystalline azides decompose slowly when irradiated with ultra violet light of normal intensity (1,2,3). The present work shows that if the intensity is raised sufficiently the detonation of silver azide can be initiated. Besides its intrinsic interest, this result provides a useful approach to a more fundamental study of the processes leading to stable detonation in these compounds.

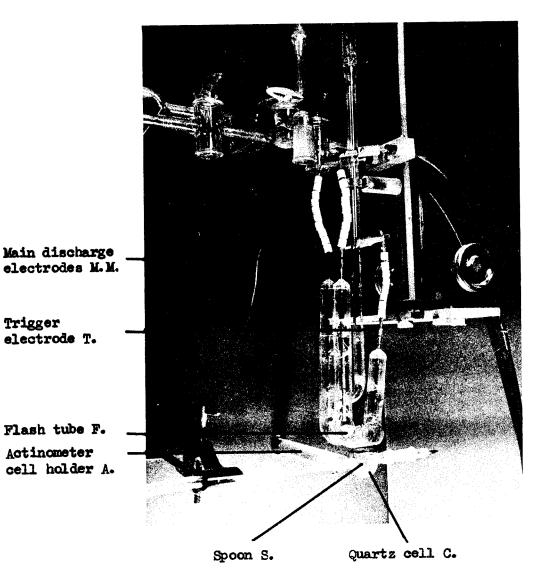
In many experiments on initiation it is very difficult to obtain an estimate of the amount of energy actually received in the explosive since this often depends on a number of unknown factors. With initiation by light absorption this difficulty is largely overcome as the amount and initial distribution of energy within the crystal can be obtained from absorption spectrum and actinometric measurements. Further a light source which will both provide illumination and initiate explosion in what might be expected to be a reproducible manner, will be of considerable

advantage for high speed photographic studies of these reactions. Eggert (4) has investigated the initiation of nitrogen iodide by the light from a flash lamp. More recently Berchtold and Eggert (5) have initiated explosion in a variety of sensitive substances. They interpret their results as indicating a thermal mechanism. Work by Bowden et. al. (6) has shown that the initiation of explosion by friction and impact proceeds through the formation of a small thermally hot region. This work shows that the overall description of initiation by light is beyond reasonable doubt a thermal one. The absorbed light is degraded to heat forming a hot surface layer on the crystal. This layer is responsible for setting up the detonation.

# Experimental

Silver aside has been used for all the experiments described in this paper. Pure and fairly perfect crystals of silver aside were prepared by crystallisation from an aqueous ammonia solution in the dark and irradiated with ultraviolet light of high intensity in the apparatus shown in Figure 1.

A crystal of silver aside is placed in the stainless steel spoon S mounted in the quartz cell C. The cell is evacuated. The crystal is irradiated with a high intensity flash from the krypton filled flash tube F of the shape shown in Figure 1. This design was employed to give the maximum useful efficiency. The flash tube has a quartz envelope and is filled with 18 cms. of pure krypton. A bank of condensers of  $80~\mu$  F which can be charged to any voltages V between 2.0 and 4.0 Ky is connected between the main



Trigger electrode T.

Actinometer

Apparatus for irradiating crystals of silver Figure 1. azide with high intensity ultra violet light. The crystal is placed on the spoon S in vacuum and is irradiated with light from the quartz flash tube F.

electrodes M. M. The lamp is fired by applying a high voltage trigger pulse to the third electrode T.

In all experiments the horizontal positioning of the spoon relative to the basal plane of the flash tube was unchanged. The vertical distance between the spoon and the basal plane of the lamp was adjusted to 1.0  $\pm$  0.1 cm. for each experiment; this represents a variability of  $\pm$  5% in the light received on the spoon.

The perspex rod A holds a small liquid irradiation cell used for calibrating the photometer described in the next section.

Characteristics of the flash and measurement of the integrated absorption Q.

The intensity versus time curves for flashes at various voltages were measured using a photocell and cathode ray tube. A typical curve shown in Figure 2. These curves show that over the range in which the lamp is used the peak intensity increases with the voltage while the time integrated intensity is proportional to the square of the voltage. For flashes at greater than 2.5 Kv the duration of the flash is sensibly constant at 61  $\pm$  2  $\mu$  secs.

Results are expressed in terms of the integrated specific absorption Q defined as the total number of quanta per flash falling on one square millimetre of surface at the position of the crystal in the wavelength step 2000 - 3600 A.

The flash has a low intensity "tail" lasting some 40  $\mu$ sec. As the integrated output of the tail is small the flash duration is taken as the time between the start of the initial rise and the point where the intensity has fallen to 1/10 peak intensity.

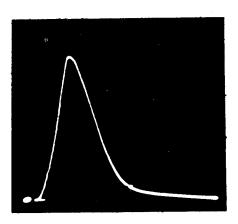


Figure 2. Light output versus time curve for a flash using 80  $\mu$  F capacity at 2.5 Kilovolts.

This quantity was measured for each flash using an integrating photoelectric photometer calibrated against the uranyl oxalate actinometer<sup>(7)</sup> an accuracy of ± 10% is possible for comparing results obtained in the same apparatus. Light losses due to reflection and scattering at the various quartz-air interfaces make less certain the absolute accuracy of Q but it is reliable within a factor of two.

The spectral distribution of the light from flash tubes with similar characteristics to the one used here has been investigated by Christie and Porter. (8)

The visible and ultraviolet absorption spectrum of silver azide was measured using a Unicam ultraviolet spectrophotometer.

Transparent platelike crystals of about 0.06 mm thickness were prepared for these measurements.

# Results.

Values of the absorption coefficient for thin plates of

silver azide are given in Table I.

TABLE I.

wavelength in A	absorption coefficient in k.cm <sup>-1</sup>	
4000	103	
3800	111	
3700	183	
3600	920	
3550	920 10 <sup>5</sup>	

These show that for the thicknesses of crystal used in these experiments all light of wavelength less than 3600 A entering a crystal would be completely absorbed. Below 2000 A quartz absorbs a large part of the radiation. The azide therefore absorbs energy in the same range as the uranyl oxalate. Q is then a measure of the total ultraviolet energy absorbed by the crystal. The crystalline azides absorb in the infra red<sup>(9,10)</sup>. Quartz does not transmit wavelengths > 35,000 A so that any effects produced by infra red absorption must be confined to absorption at wavelengths shorter than this. The only band reported is at 29,000 A. With a water filter, which removes all radiation > 10,000, explosion was still obtained though absorption of the infrared does make a contribution to initiation. Experimentally it has been more convenient not to filter out the infrared in most cases.

When small crystals of silver azide were irradiated with single flashes such that Q progressively increased very little decomposition occurred until a critical value Q<sub>crit</sub> was reached when explosion occurred.

The value of Q<sub>crit</sub> does not depend on the mass of the crystal in the range 0.2 to 1.5 milligrams, the projected area of the crystal facing the lamp in the range 0.3 to 2.0 mm<sup>2</sup>, or the area per unit mass. A sample of silver azide powder particle size ca 10<sup>-3</sup> cms diameter had the same sensitivity as individual crystals.

TABLE II.

The critical integrated specific absorption for silver azide.

Range of Q quanta/mm <sup>2</sup>	Number of experiments	Number of explosions	% explosions
< 4.6 x 10 <sup>15</sup>	12	1	8
4.6 to 4.8 x 10 <sup>15</sup>	9	2	22
4.8 to 5.0 x 10 <sup>15</sup>	8	5	63
5.0 to 5.2 x 10 <sup>15</sup>	6	4	67
> 5.2 x 10 <sup>15</sup>	All explode		100

The results in Table II. show that the value of Q needed to give 50% probability of explosion lies between 4.8 and 5.2 x 10<sup>15</sup> quanta/mm<sup>2</sup> in the wavelength range 2000 - 3600 Å. The range of Qorit is probably much narrower than this since the two values of Q bounding Qorit differ by only 10% which is the same as the error in the measurement of Q. Because the effects of preirradiation on Qorit are not quite clear a fresh crystal was used for every determination. No appreciable amount of decomposition was ever detected when the crystal did not explode. However, if by chance a crystal was flashed at a value of Q very close to but below Qorit, the crystal, which is always heavily darkened, usually broke up into a number of

quite large fragments. This effect is particularly striking if thin flat crystals are used when the pieces are seen to have straight sides generally at right angles to each other, and fit together exactly, on a microscopic scale, to reform the crystal.

Preirradiation with ultra violet light is known to modify
the kinetics of subsequent thermal decomposition of solid azides.

Preliminary experiments on the effects of preirradiation on Q suggest
that if there is any increase in sensitivity it is small < 10%.

A preliminary study of the times involved in the photochemical initiation has been made. A two beam cathode ray oscillascope was used to record the light intensity time curve of the flash on one beam while the moment of explosion was detected on the other by the ion current flowing between the spoon S and a small ring electrode mounted ca 2 mm. above the azide crystal. The results indicate strongly that the moment of explosion is connected with the integrated light intensity rather than with the peak intensity.

Silver azide may be markedly sensitised to photochemically initiated explosion by colouring it with an adsorption indicator. Samples of powder coloured by precipitating 0.1 gms AgN<sub>3</sub> in the presence of 0.010 gms of erythrosin and excess silver ions had a value of Q<sub>crit</sub> 2.1 x 10<sup>15</sup> quanta/mm<sup>2</sup>. Control experiments showed that this increase in sensitivity was due to the presence of the dye and not to adsorbed silver ions or the physical form of the precipitate. It must be remembered that Q refers only to light absorbed in the wavelength range 2000 - 3600 Å. Erythrosin dyed

silver azide also absorbs light in the region 3600 - 5500 Å so that if the coloured and normal azides are compared in terms of total energy absorbed at all wavelengths the sensitivity of the two may be identical. That the absorption of visible light makes a definite contribution is shown by the fact that erythrosin dyed azide may be detonated with the light from a medium sized photographic flash bulb while the largest flash bulbs do not even produce darkening of normal silver azide.

# Discussion.

These results show clearly that the absorption of sufficient ultra violet light can initiate the explosion of silver azide.

Consider a square millimetre of the face of a silver azide crystal uniformily illuminated by a flash so that it explodes. The absorption coefficient is very high ca 10<sup>3</sup> at 3600 Å so that the light is absorbed close to the surface. Although the light initially causes electronic excitation this energy is very rapidly degraded to heat and this will raise a surface layer to a high temperature which may be calculated in the normal way.

The energy equivalent to an integrated specific absorption of Q quanta mm<sup>-2</sup> in the range 2000 - 3600  $\mathring{A}$  is easily shown to be given by

Total energy = 
$$7.0 \times 10^{-12} Q \text{ ergs/mm}^2$$
  
=  $1.6 \times 10^{-19} Q \text{ cals/mm}^2$ 

The absorption coefficient increases very rapidly with decreasing wavelength around 3600 Å Table I. Taking the absorption

coefficient as 10<sup>4</sup> cm<sup>-1</sup> between 3600 Å and 3550 Å 95% of the incident radiation is absorbed in 3 x 10<sup>-4</sup> cms. The density of silver azide is 4.8 gm/cm<sup>3</sup> (11,12) and its specific heat 0.12 cals/grm. (13) The critical value of Q for explosion of pure silver azide is 5 x 10<sup>15</sup> quanta/mm<sup>2</sup>, the energy absorbed from the flash Q<sub>crit</sub> is therefore 8 x 10<sup>-4</sup> cals/mm<sup>2</sup>. If no energy losses from the surface layer occurred in the time of the light pulse or during the time taken for all the energy absorbed to be degraded to heat, whichever is the longer, this surface layer 3 x 10<sup>-4</sup> cms thick would be raised 480° i.e. to about 500°C by that amount of light energy. This is well above the ignition temperature of silver azide, 273°C<sup>(14)</sup> or 380°C<sup>(13)</sup>.

Considering the surface layer as the explosion nucleus its volume and the amount of heat in it are proportional to the projected area. Since the results show that Q<sub>crit</sub> is independent of the projected area it seems likely that the thickness and temperature are the two important parameters determining the onset of explosion.

It has been shown<sup>(6)</sup> that the explosion nucleus must exceed a critical size before for it to result in explosion. This work suggests that the smallest dimension, here the thickness of the explosion nucleus, is a critical factor.

So far heat losses from the surface have been neglected.

The main source of heat loss will probably be by conduction through
the azide. The temperature of the surface layer will not be
uniform throughout its thickness and, if heat losses are appreciable

vary with time depending on the shape of the light intensity versus time curve of the flash tube. One advantage of this method of studying the initiation of explosion is that this variation of temperature with time and distance from the surface can be obtained explicitly from experimental data. At the present time not all the data has been obtained but an estimate of the order of magnitude of the heat losses can be obtained by considering the surface layer as at a uniform steady temperature of 500°C and calculating how much heat is lost through a square millimetre of surface in the duration of the flash which is 60 μsec. This shows that about  $4 \times 10^{-5}$  cals is lost i.e. about 1/20 the energy input  $2 \times 10^{-5}$  cals is lost i.e. about 1/20 the energy input  $2 \times 10^{-5}$  cals area.

The absorption of ultra violet light produces initially electronic excitation; electrons being raised to exciton or conduction levels. Estimates of the life time of these excited states indicate that the time for the degradation of electronic excitation to heat is probably very short compared with the 60 µsec duration of the flash. Hence both photochemical and thermal decomposition will occur in this period at a high temperature. It is not possible to make any quantitative estimate of the amount of heat liberated under these conditions. We may expect it to be somewhat greater than the amount of heat lost but still small compared with the incident energy. The incident energy is then the critical factor.

Providing no appreciable decomposition occurs during the time of the flash the thickness of the surface layer and relative variation of temperature with distance perpendicular to the surface would depend only on the absorption coefficient, and would therefore be constant for a given wavelength range. The temperature at a given distance increases with increasing time integrated intensity unless the thermal conductivity were exceptionally high.

The rates of heat loss and generation will depend on the temperature so that the critical value of Q, table II required to produce explosion may reasonably be associated with a minimum temperature requirement.

Erythrosin alters the absorption spectrum and the nature of the surface of silver azide.

It is not possible to draw any fundamental conclusions from the results for coloured azide but the results are compatible with the proposed thermal mechanism and support Berchtold and Eggert<sup>(5)</sup> who also found that the more highly coloured compounds were the more sensitive.

In conclusion the results so far obtained indicate that the photochemical initiation of the explosion of silver azide involves the creation of a hot surface layer by the degradation of the energy of the absorbed light. For successful initiation a minimum thickness and temperature of the layer are required.

Bowden and Singh<sup>(15,16)</sup> have found a similar temperature thickness relation for thermally initiated explosion. The minimum thicknesses and temperatures found by them are of the same

order of magnitude as those deduced here.

The investigation provides further evidence that the setting up of an explosive reaction which will lead to detonation involves energy considerations on a scale which is very large measured on a molecular scale.

# Acknowledgements.

We wish to express our thanks to Dr. F.P. Bowden for his interest in the work, to the Ramsay Memorial Fellowship for an award to one of us (G.T.R.), the Ministry of Supply (Air) for a grant to the Laboratory, and the Royal Society for a grant for equipment.

## References.

- 1. Garner, W.E. and Maggs, J. Proc. Roy. Soc. A172, 299, (1939).
- 2. Thomas, J.G.N. and Tompkins, F.C. Proc. Roy. Soc. A209, 550, (1951).
- 3. Jacobs, P.W.M. and Tompkins, F.C. Proc. Roy. Soc. <u>A215</u>, 254, (1952).
- 4. Eggert, J. Fundamental Mechanisms of Photographic Sensitivity Butterworth (1951) p.94.
- 5. Berchtold, J. and Eggert, J. Naturwissenschaften 40, 55, (1953).
- 6. Bowden, F.P. and Yoffe, A.D. The initiation and Growth of Explosions in liquids and solids. Cambridge Monographs on Physics (1952).
- 7. Leighton, W.G. and Forbes, G.S. J.A.C.S. <u>52</u>, 3139, (1930).
- 8. Christie, M.I. and Porter, G. Proc. Roy. Soc. A212, 398 (1952).
- 9. Garner, W.E. and Gomm, A.S. J. Chem. Soc. 2123, (1931).
- 10. Delay, A., Duval, C and Leconte, J. Bull. Soc. Chim. 12, 581, (1945).
- 11. Bassiere, M. Compt. Rend. 201, 735, (1935).
- 12. Hughes, E.W. Thesis Cornell University (1935).
- 13. Yuill, A.M. Thesis, Cambridge University (1954).
- 14. Taylor, C.A. and Rinkenback, W.H. J. Franklin Inst. 204, 369, (1927).
- 15. Bowden, F.P. and Singh, K. Nature 172, 378, (1953).
- 16. Bowden, F.P. and Singh, K. Proc. Roy. Soc. (to be published).

# DETONATION IN AZIDES WHEN THE DIMENSIONS ARE COMPARABLE WITH THE LENGTH OF THE REACTION ZONE

F.P. Bowden F.R.S. and A.C. McLaren
Research Laboratory for the Physics and Chemistry of Surfaces,
Department of Physical Chemistry,
Cambridge, England.

#### Introduction.

We now have a good deal of evidence that the initiation of explosives by impact and by friction is generally thermal in origin. The mechanical energy of the blow or of rubbing is degraded into heat and concentrated to form a "hot spot". These hot spots are readily formed in two main ways: 1. By the adiabatic compression of small included gas bubbles. 2. By friction on the confined surfaces, on grit particles or on crystals of the explosive itself. Under very extreme conditions a sufficient temperature rise can be produced by viscous heating of the rapidly flowing explosive. For a general survey of this see Bowden and Yoffe (1).

More recently Dr. A.M. Yuill (2) has been investigating a new type of hot spot formed by the impact of a sharp point on a hard surface. The work done in plastically deforming a pointed metal striker causes its temperature to rise to a value of several hundred degrees. This temperature rise is proportional to the hardness of the striker and inversely proportional to the heat capacity of the metal. These hot spots caused by plastic deformation can initiate explosion. (See Figure 1.).

The actual value of the hot spot temperature necessary to initiate explosion varies but there is evidence that for a wide range of explosives it is in the vicinity of  $400 - 500^{\circ}$ C, when the duration is of the order of about  $10^{-5}$  sec. There is also strong evidence that the hot spots must be much larger than molecular dimensions if they are to lead to explosion. Again the limiting size depends upon the explosive and upon its temperature but experiments show that the size may vary from  $10^{-5}$  to  $10^{-5}$  cms. in diameter.

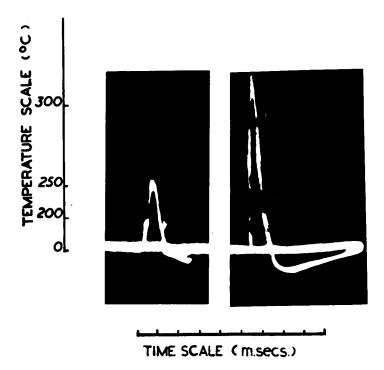


Figure 1: Cathode ray oscilloscope traces of the high temperature pulses obtained with tungsten needle strikers on a steel anvil. The first trace, for a 1,100 g.cm. impact, gives a maximum temperature rise of 250°C and is not sufficient to initiate cyanuric triazide at 95°C. The second trace gives a peak temperature of 315°C, with a 3,300 g.cm. impact, an energy sufficient to cause 100% initiation.

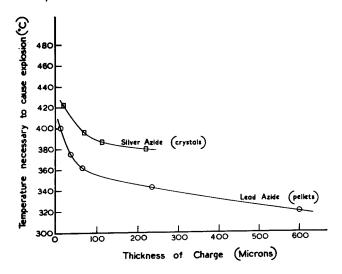


Figure 2: Curves showing the increase in temperature necessary to cause explosion of thin charges of lead azide.

## Bowden and McLaren

The existence of the burning stage means that there may, in initiation by impact, friction or shock, be an appreciable time delay before detonation occurs. This can vary from a few to several hundred microseconds (3). It should be emphasised that the failure of an explosive to detonate is frequently due to a failure in this burning stage rather than to a failure in stage (i).

With simple metallic azides such as those of lead and silver, this burning stage, if it exists at all, is very short. With the more complex azides, such as cyanuric triazide, the burning stage is, however, observed. This is associated with the fact that in a complex molecule the decomposition can occur in more than one way. Experiments show that the products of decomposition during the burning stage are quite different from those obtained during detonation (4).

## Size effects in the initiation and growth of an explosion.

The growth of a thermal explosion from a small nucleus is governed by simple physical considerations. A theoretical treatment of the factors involved in this simple thermal theory for gaseous systems was first given by van't Hoff (5) and has been re-examined by Frank-Kamenetski (6), Rice (7) and also Dainton (8). It has been applied by Rideal and Robertson (9) to condensed high explosives and their calculations indicate that for hot spot temperatures of  $400 - 500^{\circ}$ C the minimum size is in the range mentioned above.

A series of experiments has been performed to study the effect of crystal size on the explosive decomposition of metallic azides. The thermal theory of explosion, outlined above, suggests that if we take crystals of smaller and smaller size and heat them at a fixed temperature we should find a size limit below which explosion does not occur.

The critical size appears to be determined by the smallest dimension of the crystal, its thickness if it has a plate-like structure. Experiments (10) with small crystals of lead and cadmium azide show, as we should expect, that the

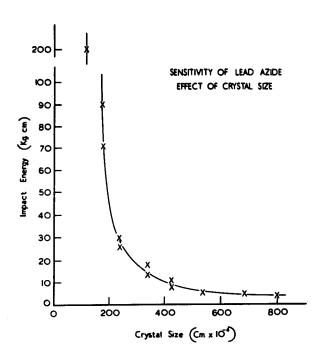


Figure 3: Curves showing the increase in impact energy necessary to cause the explosion of very small crystals of lead azide.

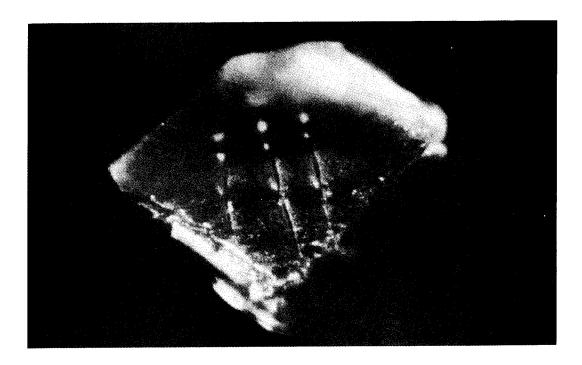


Figure 4.: A crystal of cadmium azide after heating at 317°C, showing the cracking and breaking up along crystallographic planes. X400.

## Bowden and McLaren

critical size depends on the temperature and with cadmium azide, for example, it is about 24 microns at 320°C.

In a further series of experiments, thin compressed sheets of lead azide and single crystals of silver azide of thicknesses varying from 10 to 600 microns were placed on a mica hot plate in a small electrically heated oven, the temperature of which was indicated by a thermocouple. The results are shown in Figure 2, where it will be seen that as the thickness of the pellet is decreased the temperature necessary to cause explosion increases. If we extrapolate these results to a temperature of 500°C the critical thickness is about a micron which is of the same order of magnitude as the critical hot spot size for the same temperature, estimated by the earlier methods. It is interesting to note that this limiting size of a few microns is similar to the thickness of the "hot layer" obtained by Dr. Courtney-Pratt and Dr. Rogers in their recent experiments of the explosion of azides by light. (See paper in this symposium).

From similar considerations we may expect the impact sensitivity of a crystal to be dependent upon its size. Dr. A.M. Yuill (2) has recently investigated the effect of crystal size on the impact sensitivity of lead azide. His results are illustrated in Figure 3. It will be seen that the impact energy necessary to cause explosion increases as the size of the crystal is reduced in a manner similar to that observed when the crystals were heated. It should be noted that under impact, the crystals are crushed and flow plastically to form a pellet the thickness of which is about one-tenth to one-quarter that of the original crystal, suggesting that if the explosion starts at a late stage of the impact, the thickness may be the limiting factor.

Initiation of explosion with high speed particles. effect of irradiating a number of sensitive explosive crystals (such as lead azide, silver azide, cadmium azide and nitrogen iodide and silver acetylide) with high speed particles has been studied by Bowden and Singh (10). They were subjected to irradiation by electrons, by neutrons, by fission products and by X-rays. All these substances were exploded by an intense electron stream but experiment showed that this is a thermal effect and is due to a bulk heating of the crystal. Nitrogen icdide is exploded by fission products but this substance is anomalous. With other substances interesting changes within the crystal are observed and these affect the subsequent thermal decomposition but no explosion results. The experiments show that, in general, the activation of a small group of adjacent molecules is not enough to cause explosion and support the view that the necessary "hot spot" size is large on a molecular scale (ca. 10-6 cms in diameter).



Figure 5: Electron microscope picture (X50,000) of a partially decomposed lead azide crystal. The crystal is apparently breaking up into tiny blocklets about 10<sup>-5</sup>cm. across.

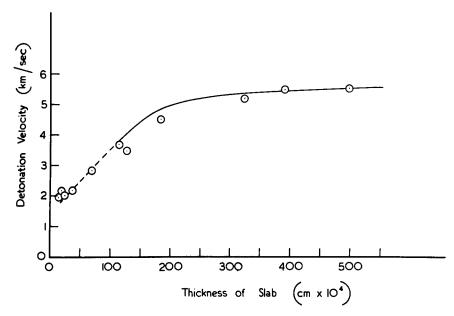


Figure 6: The relation between the thickness of a sheet of lead azide and the detonation velocity. The continuous curve is the relation to be expected from the modified Jones' theory taking the length of the reaction zone as 75 microns.

#### Bowden and McLaren

Changes within the crystal. If the crystals are below the critical size or if larger crystals are heated at a lower temperature so that only thermal decomposition takes place, the crystals split and break up along crystallographic planes (10). This is illustrated in Figure 4, for cadmium azide. This suggests that the rate of decomposition may be a maximum along preferred directions within the crystal. The decomposition involves the formation of metallic nuclei and the evolution of gaseous nitrogen, accompanied by a large amount of heat, and this may easily lead to a splitting of the crystal. This splitting can occur with violence. The spreading of the defects and cracks through the crystal may play a part in the propagation process. It will also influence the rate of thermal decomposition by exposing a large amount of fresh surface. In addition to the development of cracks a darkening of the crystal takes place showing that nuclei are being formed within the crystal.

The electron micrograph (Figure 5) of a small partially decomposed crystal of lead azide is of particular interest. The photograph which is taken at high magnification (50,000) shows that during decomposition the crystal appears to break up into very small blocks about 10<sup>-5</sup>cms. across indicating that preferential decomposition occurs at the surface of these blocks. These may correspond to the elementary mosaic structure of the crystal. Since we would expect decomposition to occur preferentially at the crystal defects these elementary blocks may be more resistant to reaction and require a higher temperature to decompose them. These small crystal fragments can detach themselves from the parent crystal and quite frequently this happens with explosive violence. These flying fragments may play a part in propagating the explosion from crystal to crystal.

## Size effects in the detonation of azides.

We have, up till the present, been considering the influence of size on the initiation or the growth of explosion - that is on stages (i) and (ii). It is of interest to consider the influence of physical dimensions on the last stage of the explosion, that is on the stable detonation - stage (iv) - in azides.

The effect of charge diameter on the detonation velocity of a high explosive has been studied by a number of workers (e.g. Bichel, Mettegang, Dautriche, Kast, Hiscock, E. Jones, Paterson and Ford) and the results have been summarized by J. Taylor (11). The experiments have been almost exclusively concerned with high explosives such as TNT and complex nitroglycerine explosives, and in all cases the diameters were large (of the order of 1-20 cm) compared with the lengths of the reaction-zones. The estimated length of the reaction zone of finely powdered TNT is, for example, about 0.3 cm. and that of

### Bowden and McLaren

liquid nitroglycerine is 0.04 cm. It was observed that the detonation velocity increased with the diameter of the explosive charge, approaching a maximum asymptotically. The results may be explained in terms of the hydrodynamic theory.

Little work seems to have been done with the initiating explosives and recently experiments have been made to analyse the effect of change of thickness on the detonation velocity of lead azide when pressed into thin sheets or slabs. The thickness of these was comparable with the length of the reaction zone and varied from about 20 to 500 microns. The sheets were 1.3 cm. long and 0.5 cm. wide and were made in a device which ensured that the density did not vary by more than a few percent from one sheet to another. The mean density of the sheets was 3.14 gm.cm<sup>-3</sup> compared with the crystal density of about 4.60 gm.cm<sup>-3</sup>. "Pure" lead azide from a single batch was used throughout.

The detenation velocity was determined by means of a simple drum camera. A sheet of known thickness was placed at the end of a trail (about 2 cm long) of powdered lead azide on a glass plate over a slit, and the explosion initiated by means of an electrically heated wire in the powder. The results are plotted in Figure 6. It will be seen that for sheets of thickness of 400 microns and greater the detonation velocity is constant at approximately 5.5 km/sec, and decreases steadily to about 2 km/sec for a thickness of about 20 microns.

An attempt has been made to explain these results in terms of the expanding jet theory of J. Jones (12), itself an extension of the hydrodynamic theory, modified to apply to the present experimental conditions. The theory is based upon the fact that in solid explosives a certain lateral expansion of the decomposing materials will always take place with any practical degree of confinement. If this expansion within the reaction zone takes place before the reaction is complete, part of the explosive decomposes at a lower effective loading density, and hence, a lower detonation velocity than that which would occur if no lateral expansion took place, is to be expected. Jones' calculations were made for cylindrical charges where the constraint is symmetrical about the axis.

In our experiments, with very thin sheets of explosive, this was not the case since the width of the charge is so much greater than the thickness. We have assumed that the expansion is symmetrical in a vertical direction about the axis of the charge and that no lateral expansion takes place horizontally. We should thus expect the detonation velocity to decrease more slowly with decreasing thickness than in the case of a cylindrical charge where expansion in two dimensions will take place. The reaction is initiated at the shock-wave front and develops over a certain distance, X; - the reaction zone.

#### Bowden and McLaren

The theory provides an expression for the detonation velocity V, for any thickness of charge in terms of the maximum stable velocity  $V_0$  and the ratio of the length of the reaction zone (X) to the thickness of the charge. From the thickness for which  $V = V_0$  we can calculate X. We see from Figure 6 that for lead azide the critical thickness lies between 400 and 600 microns. This gives a value for X of approximately 75 microns. The theoretical relationship between the detonation velocity and the thickness of the charge is plotted (continuous curve) in Figure 6, where it may be compared with the experimental results. Fairly good agreement between experiment and theory is obtained over the range of thicknesses for which the theory is valid, i.e. for thicknesses greater than the length of the reaction zone. Below 100 microns the curve (dotted) joining the experimental points is a smooth continuation of the theoretical curve.

We may conclude, therefore, that the variation of detonation velocity with thickness of charge for azides is analogous, though on a very different scale, from that observed for high explosives and can be explained reasonably well in terms of the hydrodynamic theory. The calculated length of the reaction zone for lead azide is from these experiments approximately 75 microns.

# Influence of prior-heating on the detonation velocity.

Some experiments have also been carried out to investigate the effect of heating on the subsequent detonation of lead azide. Compressed sheets of the explosive were heated in an oven to a fixed temperature lying between 200° and 300°C. The heating was carried out for periods of five minutes or longer. The explosive was then allowed to cool and the detonation velocity determined. It was found that a comparatively gentle heating of the explosive could cause a marked diminution in the detonation velocity.

In a parallel series of experiments, the explosive was heated in vacuo under identical conditions and the pressure of gas evolved measured as a function of time; it was found that the decomposition was small. The mechanism of this retardation is not yet clear and further work is in progress.

# Acknowledgements.

We thank the Ministry of Supply (Air) for a grant to the Laboratory, and the Royal Society for a grant for apparatus.

### Bowden and McLaren

# References

- (1) Bowden, F.P. and Yoffe, A.D. (1952); Initiation and Growth of Explosion in Liquids and Solids (Cambridge Univ. Press).
- (2) Yuill, A.M. Ph.D. Thesis, Cambridge. See also (10).
- (3) Bowden, F.P. and Gurton, O.A. (1949) Proc. Roy. Soc. A198, 337.
- (4) Robertson, A.J.B. and Yoffe, A.D. (1948) Nature, 161, 806.
- (5) van't Hoff, J.H. (1884) Etudes de Dynamique Chimique.
- (6) Frank-Kamenetski, D. A. (1939) Acta Phys-Chim U. R. S. S. 10, 565.
- (7) Rice, O.K. (1940) J. Phys. Chem. 8, 727.
- (8) Dainton, F.S. (1942) Trans. Faraday Soc. 38, 227.
- (9) Rideal, E.K. and Robertson, A.J.B. (1948) Proc. Roy. Soc. A195, 135.
- (10) Bowden, F.P. and Singh, K. (1953) Nature, 173, 378.
- (11) Taylor, J. (1952) Detonation in Condensed Explosives (Oxford University Press).
- (12) Jones, H. (1947) Proc. Roy. Soc. A189, 415.

### ORIGIN OF LUMINOSITY IN DETONATION FLAMES

Elwyn Jones
Imperial Chemical Industries Limited,
Nobel Division,
Stevenston, Ayrshire, Scotland

When Mallard and Le Chatelier(1) first used a rotating-drum camera to study detonation in explosive gases, it was at once apparent that the luminosity of the phenomenon varied according to the chemical nature of the medium, being much brighter in some gases Such photographs normally show an initial bright than in others. line or "streak", coinciding with the passage of the "detonation-wave", and a residual glow which may be traversed by similar streaks representing the passage of "shock-waves"(2). The residual glow often shows striations, commonly attributed to mass movement of incandescent matter, and sometimes alternating bright and dark bands, supposed by some to indicate the helical progression of the Thus, the luminous effects accompanying "detonation head"(3). detonation in gases reflect the train of chemical and physical events occurring in the medium following the initiation of the explosive reaction.

The flames of condensed explosives appear to be equally complex and have attracted considerable attention, particularly where photography has been used in the development of "flameless" explosives for use in fiery coal mines. Three different kinds of flame have been noted in condensed explosives and, according to Lemaire(4), these represent three distinct chemical stages in the detonation process, namely, the fast "primary reaction", in which the condensed explosive is suddenly converted into gas at high temperature and pressure, the slower "secondary reactions" which take place among the products of the primary reaction and the "tertiary reaction" in which the hot secondary products combine with atmospheric oxygen. Thus, Lemaire attributes all detonation luminosity to chemical action.

On the other hand, Moraour(5) asserts that most, if not all, of the light accompanying detonation arises from the physical impact of the detonation-wave on the ambient medium, this type of luminosity being strikingly demonstrated in the "argon photographic flash"(6).

According to this view, the light emanates from sources entirely outside both the explosive and its detonation products, and so would appear to be only remotely connected with the chemistry of detonation. Thus, the two current views on this matter appear to be contradictory.

It will be seen from this short review that detonation flames make an interesting study and, if the sources of these transient luminosities can be identified, information may be obtained on the chemical and physical behaviour of matter under the influence of detonation-waves and shock-waves.

# Analysis of Detonation Flames

The flames from condensed explosives may be conveniently illustrated by means of photographs taken in the dark with an ordinary camera with its shutter open. With powerful explosive compounds, in contrast with weak explosive mixtures, a "still" photograph obtained in this way usually shows little more than an illuminated cloud. This is evident in the photographs of Will(7), Hiscock(8) and others, and is illustrated in Fig. 1, which was obtained with a small pellet of tetryl, (NO<sub>2</sub>)<sub>2</sub>C<sub>6</sub>H<sub>2</sub>N(NO<sub>2</sub>)CH<sub>3</sub>. Anything which may have happened in the immediate vicinity of the cartridge is obscured by this highly luminous cloud and the first task is to remove this obstacle.

One way in which this may be done is by reducing both the oxygen deficiency of the explosive and the size of the charge. The photograph reproduced in Fig. 2 shows simultaneously the position, size and shape of each flame relative to the cartridge and to each other for a particular explosive. Like Fig. 1, this is an ordinary still photograph, taken in the dark, of a small cylindrical cartridge, 1 in. long by 0.5 in. diameter, of granular explosive wrapped in cellophane and fired vertically downwards. In this case, however, the explosive used was pentaerythritol tetranitrate,  $C(CH_2NO_3)_L$ .

Reading from the cartridge outwards or, in other words, taking the flames in chronological order, we have first the "primary flame" which seems to fill the cartridge but keeps rigidly inside it, then the "secondary flame" characterised by luminous streamers issuing from the explosive and, finally, the "tertiary flame" which, in this instance, is somewhat attenuated and has risen just enough to let the primary and secondary flames be seen. The buoyancy of the detonation products and the appreciable delay before the cloud burst into flame are interesting to note.

Our identification of the three flames of detonation in condensed explosives is confirmed in Fig. 3 and 4, where the tertiary and secondary flames of nitroglycerine,  $[C_2H_5(NO_2)_2]$  have been extinguished in that order by adding increasing proportions of inert matter, this being the traditional method of producing "flameless" explosives for use in coal mines(9). Here, the cartridges were much larger and the photographs illustrate the effect of cartridge size and shape on these flames. In conjunction with Fig. 1 and 2, these photographs show certain characteritics of high explosive flames which are very suggestive, namely:-

The primary flame takes its size, shape and even its texture from the unexploded material; it illuminates the stationary matter and goes out again before movement begins or, at least, before it becomes noticeable.

The secondary flame consists of luminous streamers which travel mainly in straight lines and diminish in width with increasing distance from the cartridge; the incandescent material behaves more like projected matter than an expanding gas.

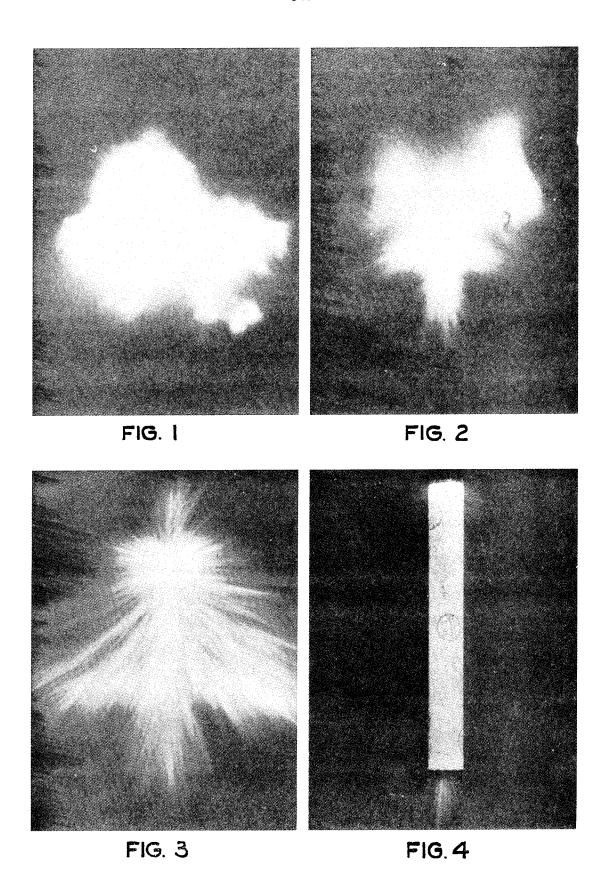
The tertiary flame increases in size and intensity with increasing oxygen deficiency of the explosive, c.f. Fig. 1 and 2. It appears, therefore, that this flame represents the deflagration of a cloud of combustible residues and, further, that ignition occurs sponteneously after an appreciable delay in an upward-moving cloud which, until then, is invisible.

These inferences tend to support a chemical interpretation of the origin of detonation luminosity and, so far, give little evidence of shock-wave luminosity. Nevertheless, there are certain features of the primary and secondary flames which suggest that the explanation offered by Lemaire is not wholly acceptable. Moreover, the apparent absence of shock-wave luminosity is rather surprising in view of Muraour's experiments and it seems desirable to take a closer look at the primary and secondary flames.

# Primary Flame

To study the primary flame, it is convenient to use a "streak" camera which provides a time scale whereby the speed and duration of the flame may be estimated. The photographs which we shall reproduce were obtained with a rotating-mirror camera capable of writing speeds up to 400 m. per sec., the optical system comprising two lenses with the conventional "slit" located between them. This arrangement is not recommended.

As illustrated in Fig. 5, the photograph of the primary flame takes the form of an inclined streak which plots its progress along the cartridge against a vertical time scale. The explosive cartridges



were usually around  $1\frac{1}{4}$  inch in diameter and up to a foot in length. In the present context, numerical details are unimportant because our analysis is qualitative rather than quantitative.

Fig. 5 was obtained with a cartridge of granular pentaerythrital tetranitrate, and it should be remarked that the lens aperture was adjusted to avoid recording the less luminous secondary flame. would be incorrect, therefore, to assume that the absence of secondary and tertiary flames in detonation photographs signifies that none On the contrary, Fig. 2 shows that even small charges of this explosive produce both secondary and tertiary flames. this point is often overlooked, this situation is inevitable because, even with a constant aperture, the apparent intensity of the light would still depend on other factors such as, for example, the speed of Comparison of luminous intensities should therefore be the flame. made with some caution, especially when one photograph is compared with On the other hand, since Fig. 2 and 5 both agree on this point, it seems reasonable to conclude that the primary flame in gramular pentaerythritol tetranitrate is much more vivid than either the secondary or tertiary flames.

The most remarkable feature of this photograph, a feature common to all primary flame photographs, is the extremely short duration of the primary luminosity. Measurements of such photographs suggest that the emitters are active for probably less than one microsecond. They seem to appear abruptly and to disappear with the same abruptness. which suggests that they may be atoms or free radicals, their brief period of activity being a measure of their limited life.

The photograph reproduced in Fig. 6 was obtained with the same explosive as before, but on this occasion half of the cartridge was infused with argon and the other half with butane. Where the intergranular spaces were filled with the monatomic gas argon, the primary flame is much more luminous than where the interstics were filled with the complex gas butane. This leads to two interesting inferences, namely, that the emitters are probably atoms and that they derive, at least partly, from the interstitial gas.

The latter inference is borne out by the remarkable fact that pure explosive compounds in the form of cast or highly compressed pellets give surprisingly little primary luminosity, the same being true of liquid and gelatinous explosives. A striking demonstration of this fact is given by Taylor(10) who reproduces a streak photograph of a composite charge made up of alternate layers of a high density explosive and an inert salt. In these circumstances, the primary luminosity is very intense in the granular salt, but is hardly visible in the explosive. Moreover, in mixtures of nitroglycerine and common salt, the intensity of the primary flame seems to increase with decreasing proportion of nitroglycerine. In other words, the presence of chemically inert matter tends to intensify the primary flame.

These apparently irrational facts admit of a very simple explanation, namely, that the initial products of detonation possess kinetic energy rather than heat. It may be recalled that Berthelot's(1) theory of detonation implies that the energy released in an explosive reaction appears first as kinetic energy of the newly-created molecules and that the fundamental difference between deflagration and detonation resides in the fact that the motion of the molecules is random in the former case, but unidirectional in the latter. It follows from this that collisions occur immediately in deflagration and similar slow reactions, giving the spontaneous effect of heat, but, because the molecules are travelling in the same direction in detonation, collisions are fewer and less energetic with the result that there is little heat as ordinarily understood. To produce collisions, the molecules must encounter resistance.

This inference suggests that confinement should increase the luminosity of the primary flame and Fig. 7 demonstrates the effect of removing the cellophane wrapper from part of an explosive cartridge, the brighter portion corresponding to the wrapped explosive. Bowden(12) and his collaborators have shown, thin films of explosive caught between impacting surfaces give out a surprising amount of Again, if a high density explosive is fired in a vacuum and light. an obstacle is placed in the way of the expanding products, the sudden conversion of their kinetic energy into "heat" produces a brilliance far transcending the light from the primary flame. As a vacuum can neither support a shock-wave nor emit light, this incandescence must occur in the products of detonation. Ratner(13) seeks to explain this effect, which is also apparent in air, by assuming that the outer skin of explosive escapes decomposition in the primary flame but is overtaken at an obstacle. Even this explanation associates the light with the explosive rather than the ambient medium.

Thus the evidence suggests that the energy released in the primary reaction is contained in the products largely in the form of kinetic energy in the direction of propagation and that any resistance they meet causes kinetic energy to be converted into the equivalent of heat and so leads to incandescence. If the resistance is offered by a gas, incandescence may be induced in the gas, provided not too much energy is absorbed in its chemical dissociation.

# Shock-wave Luminosity

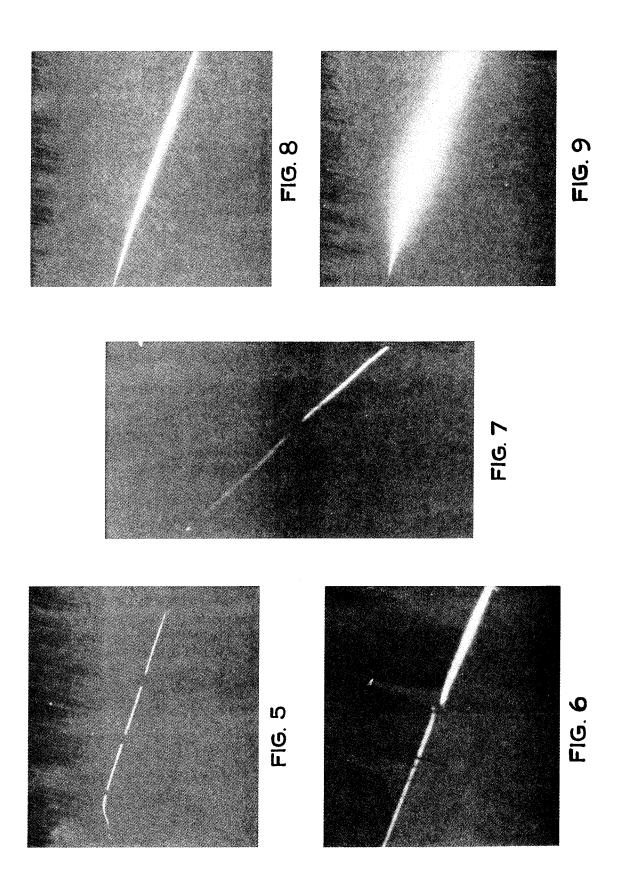
The reality of shock-wave luminosity is demonstrated in a very convincing manner by Muraour(14) who produced incandescence at the meeting point of two non-luminous shock-waves. It may be deduced from this experiment that before a shock-wave can become self-luminous, it would have to travel at a speed approximating to the relative velocity of Muraour's shock-waves, which would suggest a figure of the order of 5 km. per sec.

It has been demonstrated (15), however, that when an explosive is fired in or into the air, the shock-wave does not separate from the expanding products until the speed of the combined disturbance has fallen to about 2 km. per sec., at which speed the shock-wave is quite definitely non-luminous. It appears, therefore, that shock-wave luminosity is likely to appear only with high velocity explosives and, when it does appear, it will be difficult to distinguish it from product luminosity or, in other words, Lemaire's secondary flame.

It has been said already that the primary flame is rather feeble in a homogeneous explosive so that this type of explosive might be very suitable for studying shock-wave luminosity. directing the disturbance from the end of such a cartridge into a close-fitting tube, lateral expansion is prevented and the high velocity is maintained over greater distances. Moreover, lateral losses being small, the "wave" may be expected to assume a plane front, so that, by viewing it from the side, some idea of the depth This technique was used by of the luminous zone may be obtained. Laffitte(16) but, being handicapped by the low resolving power of his camera, he was unable to disclose the fine structure of the We therefore reproduce in Fig. 8 a high-speed camera photograph of the luminous effects produced in an air-filled tube on firing a charge of compressed pentaerythritol tetranitrate at one end. Fig. 9 shows the same shot fired into argon but with a considerably Except for the fact that the disturbance is reduced aperture. very much more luminous in argon than in air, the two photographs are almost identical. It may be added that, on replacing the air by butane, the luminosity is markedly decreased.

These results agree with those of other observers and confirm that the luminosity of the disturbance varies according to the nature of the surrounding gas, but whether the ambient medium contributes to the emission or interferes with it is open to question. It is well-known that the secondary flame can be suppressed by firing the explosive in an atmosphere of butane or some other complex organic vapour and it seems likely in this case that the kinetic energy is absorbed in dissociating the vapour. In other words, if the chemical energy of the explosive can be given out as kinetic energy of the products, it is equally possible for the kinetic energy of the products to be absorbed in the chemical dissociation of the medium. Moreover, if the emitters are atoms, the difficulty of producing luminosity in complex organic vapours is explained.

On this view, the heavy monatomic gas, argon, is a major contributor to this type of luminosity but, since action and reaction are equal but opposite, the product molecules involved in these collisions are also liable to be dissociated and contribute to the luminosity, as they do on striking a rigid obstacle. Thus, the difficulty in separating shock-wave luminosity from product luminosity still persists.



On examining the detailed structure of the two photographs, it will be seen that the evidence is consistent with this mechanism of light emission. The products of detonation are relatively non-luminous to begin with and their first encounter with the ambient medium is at a surface. This surface approximates to a plane which is viewed from the side and so appears, at first, very thin. As the products advance into the gas, the collision zone increases in depth according to the time and space required for the alien particles to accommodate themselves to the movement of the medium they have entered. Once they fall into step, order is restored and the luminosity ceases.

# Secondary Flame

It appears from the foregoing that the distinction is difficult to draw between shock-wave luminosity and product luminosity due to collision, both of which may be regarded as This representing the type of luminosity which Muraour describes. part of the secondary flame arises from physical causes, but, if emission is due to atoms, their presence is indicative of chemical The chemical changes which may be initiated depend on the nature of the explosive and here it is necessary to distinguish between explosive compounds and explosive mixtures. Most military high explosives are substantially pure chemicals but commercial explosives are often heterogeneous mixtures of different explosives, In this way, the characteristics with or without inert diluents. of an explosive are adapted to the purpose for which it is intended. Coal mining explosives, in particular, contain flame-suppressing ingredients so that it would be wrong to judge all explosives by the amount of flame produced by these explosives. By the same token, photographic techniques, like flashlight and Schlieren photography, which are effective only with substantially flameless explosives, are On the other hand, military high open to the same criticism. explosives, which by virtue of their high rates of detonation exaggerate the importance of shock-wave luminosity, present an equally one-sided picture of high explosive flame. To obtain a comprehensive view, due regard should be given to both types of explosive, but they should be considered spearately.

Fig. 3 is typical of the kind of photograph obtained with some of the British coal mining explosives in present use, and it is worth noting that the shock-wave velocity in this case is too low to produce luminosity due to collision. Nevertheless, the secondary flame is still in evidence and the origin of this luminosity must be sought in the explosive itself. Besides nitroglycerine, these explosives contain such combinations as ammonium nitrate and woodmeal which react much slower than nitroglycerine. It is understandable, therefore, that anyone working with this class of explosive should attribute the secondary luminosity to chemical reactions initiated by the primary detonation reaction.

It will be apparent that the picture of the detonation process presented here differs from that normally assumed for theoretical purposes, but it is felt that any theory which ignores the activation energy of the reaction, and so fails to take cognisance of the sensitivity factor, can not be complete. The emphasis here is on the energy absorbed in the dissociation of the explosive molecule and, indeed, of any unstable complex molecule which may become entrained in a high velocity shock-wave.

The author is indebted to Messrs. T.A. Brown and I.G. Cumming for supplying the photographs from which the accompanying illustrations were selected.

### REFERENCES

- 1. Mallard, E. and Le Chatelier, H.L. Ann. Mines, Ser. 8, 4, 296, 1883
- 2. Dixon, H.B. Phil. Trans., A, 184, 97, 1893
- 3. Campbell, C. and Finch, A.C. J. Chem. Soc., 8, 2094, 1928
- 4. Lemaire, E. Ann. Mines. de Belg., 19, 37, 1914
- 5. Muraour, H. and Michel-Levy, A. Mem. des Poudres, 26, 171, 1934-5
- 6. Grimshaw, H.C. and Hardy, V.O. Safety in Mines Res. Est. Rept. No. 32, 1951
- 7. Will, W. Schiess-und Spreng., 323, 343, 1909
- 8. Hiscock, W.G. Iron and Coal Trades Rev., 1, 18, 1924
- 9. Marshall, A. "Explosives", London, 1915
- 10. Taylor, J. "Detonation in Condensed Explosives", Oxford, 1952
- 11. Berthelot, M. Compt. rend. 94, 149, 1882; 96, 672, 1883
- 12. Bowden, F.P., and Yoffe, A.D. "Initiation and Growth of Explosion in Liquids and Solids", Cambridge 1952
- 13. Ratner, S.B. J. Tech. Phys. USSR, 20, 1422, 1951
- 14. Muraour, H. Compt. rend. 198, 1499, 1934
- 15. Laffitte, P. and Patry, M. Compt. rend., 191, 1335, 1930 Payman, W. and Woodhead, D.W. Proc. Roy. Soc., A. 163, 575 1937
- 16. Laffitte, P. Ann. de Phys. 4, 587, 1925

# THE ROLE OF GAS POCKETS IN THE PROPAGATION OF LOW VELOCITY DETONATION

Owen A.J. Gurton
I.C.I. (Nobel Division)
Stevenston
Ayrshire, Scotland.

For many years it has been known that nitroglycerine and explosives based on nitroglycerine detonate at either of two If the explosive receives a heavy shock from a priming velocities. charge it will detonate at a rate approaching the maximum or hydrodynamic velocity, but if it receives a weaker shock (such as the blow from a detonator) it may detonate at a much slower rate. nitroglycerine may detonate at about 8,000 m. per sec., or at about High velocity detonation of liquid 1.000 to 2.000 m. per sec. nitroglycerine is very constant in character. The detonation front seems to advance at a steady rate through the explosive and the detonation velocity does not vary from experiment to experiment. This is not true of low velocity detonation which does not propagate with a very steady front, in the pure liquid(1).

However, nitroglycerine is not usually used commercially in a pure condition, but is mixed with other materials which remove its obvious fluid properties. The simplest admixture, and the one which leads to the least change in thermochemical properties, is the addition of small quantities of nitrocellulose. H.C. Clapham 1930 showed that this addition had a profound effect on the ease with which He showed that if nitrolow velocity detonation would propagate. cotton was allowed to gel in nitroglycerine without stirring, the resultant mixture would detonate at high velocity if adequately primed, but either failed to detonate or gave rise to a very low velocity propagation if an attempt was made to set up normal low velocity When one of these gels was aerated by stirring, the detonation. propagation of low velocity detonation in liquid nitroglycerine again In fact, low velocity detonation in liquid nitrobecame possible. glycerine is much less steady than low velocity detonation in an aerated gel(1). Thus, the aeration of an explosive gelatine was in some way related to the ease with which low velocity detonation would propagate in it.

The phenomenon of dual velocity of detonation has been

observed not only in other liquid explosives(2), but also in granular solid explosives including T.N.T. and tetryl(3). To achieve a steady low velocity detonation in solid explosives two requirements had to be met. Firstly, the grain size of the explosive had to be moderately coarse, and secondly, the cartridge density had to be fairly low, (about 1 g. per c.c.). In other words, the explosive had to contain gas pockets.

Bowden, Mulcahy, Vines and Yoffe(4), showed that the inclusion of small bubbles of air in nitroglycerine and in other liquid explosives increased their sensitivities to initiation by impact. The reason for the high sensitivity of the aerated liquid was traced to the high temperatures which were attained in the gas pockets when they were suddenly compressed. Yoffe(5) replaced the air by other gases and vapours and also by gases at higher pressure. He showed that as the ratio of the specific heats of the gases increased, the sensitivity of the explosive appeared to increase, but that as the pressure of gas increased the sensitivity decreased. This second effect was observed in solid explosives as well as liquids.

Ratner(6), calculated the temperature to which the shock wave accompanying detonation would raise liquids like nitroglycerine, etc., and concluded that if high velocity detonation occurred, the temperatures would be about 3,000°C. However, in low velocity detonation, the temperature rise of a liquid or solid due to compression in the shock front would be insignificant. Bowden and Gurton(7), pointed out that if gas bubbles were present the temperatures produced in the bubbles would be very high, and the hot spots at the bubbles would become new explosion centres. Consequently, low velocity detonation in an aerated explosive was probably maintained by these hotspots.

Evidence in support of this has been obtained with small scale experiments by Bowden & Williams (8).

In this paper direct experimental evidence will be brought forward to indicate that these views are substantially correct for large charges, at least in the low velocity detonation of solids, but that some other mechanism is probably operative in the low velocity detonation of nitroglycerine.

The methods employed were similar in principal to those used on a smaller scale by Yoffe(5), and Bowden and Williams(8), but since larger quantities of explosives were being detonated, the apparatus used was of a different form.

#### I. EXPLOSIVES CONTAINING VARIOUS GASES

In the adiabatic compression of an ideal gas

$$T_2 = T_1(\frac{p_2}{p_1}) \frac{\gamma - 1}{\gamma}$$
 (1)

where  $T_1$  and  $T_2$  are the initial and final temperatures,  $p_1$  and  $p_2$  the initial and final pressures, and  $\gamma$  the ratio of the specific heats of the gas at constant pressure, and constant volume. If one were to replace the gas by one of lower  $\gamma$  value, provided the initial temperature and the compression ratio were constant, the final temperature would be decreased. The effect of this change on the initiation of explosives has been fully discussed by Bowden & Yoffe(9).

Experiments were carried out with three solid explosives, namely, granulated tetryl, flake T.N.T., and nitroguanidine. The nitroguanidine was obtained in the form of fine crystals, and had a very low natural bulk density. The tetryl and the T.N.T. were packed loosely in thin paper or celluloid wrappers to form cylinders \( \frac{3}{4}\)" in diameter and 5" long. The packing density aimed at was 0.9 g. per c.c. for tetryl and 0.8 g. per c.c. for T.N.T. Nitroguanidine was packed in increments into cylindrical paper or celluloid wrappers 7/16" in diameter, and was compressed to a bulk density of 0.5 g. per c.c.

The paper or celluloid wrappers were thoroughly perforated and the cartridges inserted in wide bore glass tubes. The assemblies were primed with detonators and evacuated. Since the wrappers were perforated, the gas between the grains of explosive was removed. Ether vapour or pentane were then introduced until the saturation vapour pressure was reached. The velocities of detonation were then measured photographically (See E. Jones (10)), and compared with the detonation velocities measured in air. In some cases the detonation velocities of the explosives were measured by the Dautriche method using the system which will be described in the next section. results which have been arranged in Table 1 gave little indication that replacing air by ether or pentane vapour has any effect on the detonation velocities. In the course of this work several failures were obtained when pentane vapour had been introduced into T. N. T. cartridges, but in those cartridges which did detonate the velocity of detonation was never much less than the velocity of detonation in a similar cartridge of T.N.T. interspersed with air.

Velocity of detonation of granular explosives set off by a No. 6 A.S.A.T. copper detonator

The land	:Diameter	r:Densi	y:Gas con- :l	Method of: Vel	ocity of :
Explosive	: inches	:g./c.	::tained in:	neasure- : de	tonation :
•	:	:	:explosive:		per sec.
: Nitroguani-	: <sup>3</sup>	: 0.5	: Air :I	Dautriche:2,5	<b>-</b> .
: dine	:	:	: Ether :	" :2,5	
: 1st batch	:	:	: Pentane :	" :2,2	
Nitroguani-		:	: Air :	High :2,6	
: dine	: 7/16	: 0.5	: Ether :	speed :2,6	20 :
: 2nd batch	:	:	: Pentane :	camera :2,6	
:	:	:		Dautriche:1,7	_
:	: 3/4	: 0.9	: Ether :	" :1,7	
Towns 1	:	:	: Pentane :	" :1,8	المستقبل الم
Tetryl	:	:	: Air :	High :1,4	
•	: 7/16	: 0.9	: Pentane :	speed :1,4	,60 :
:	•	:		camera :	
:	: _	:		Dautriche:1,7	-
T.N.T.	: 3/4	: 0.8	: Ether :	":1,7	
:	:	:	: Pentane :	":1,7	<u>25 1,818 :</u>

# II. EXPLOSIVES CONTAINING GAS UNDER HIGH PRESSURE

Since a change of gas from air to a vapour of low  $\gamma$  value (like ether and pentane) at a low pressure did not effect any marked change in the properties of the detonating explosives, experiments were carried out with methane ( $\gamma = 1.31$ ) at high pressure. According to equation 1 an increase in the initial gas pressure would reduce the compression ratio and, therefore, reduce the maximum temperature to which the gas would be raised, provided that the maximum pressure was not increased. In fact, the final pressure in detonation is increased by an increase in the initial pressure, but it was found that for the initial pressure range used in these experiments, the change in the detonation pressure was insignificant.

#### Experimental Method

The experiments were carried out in a gas tight vessel of 15 litres capacity. The vessel had very thick walls and was built to stand pressure up to several thousands of atmospheres. Cylindrical cartridges of explosives were prepared in waxed paper wrappers which were thoroughly perforated. Figure 1 shows how the cartridge was set up so that its velocity of detonation could be measured by the Dautriche method. In order to avoid damage to the vessel the length of detonating fuse employed was cut to a minimum which was usually 25 cm. Plastic covered Cordtex fuse with a core of PETN was used.

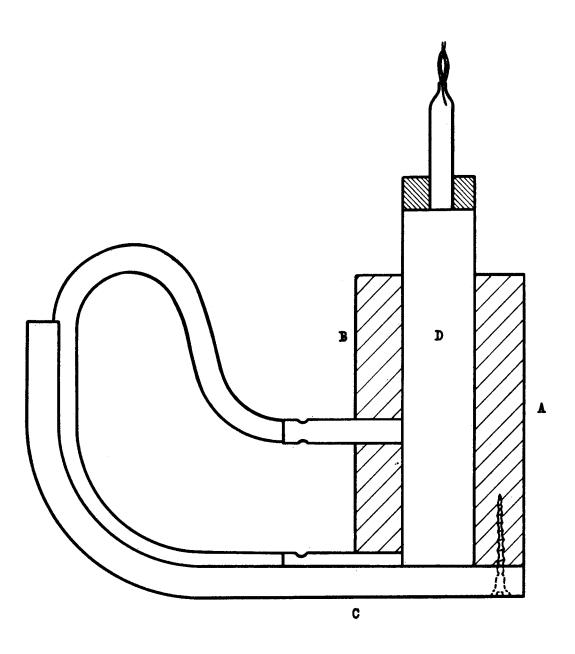


FIG. 1.

Arrangement of explosive and detonating fuse for the measurement of detonation velocity by the Dautriche method.

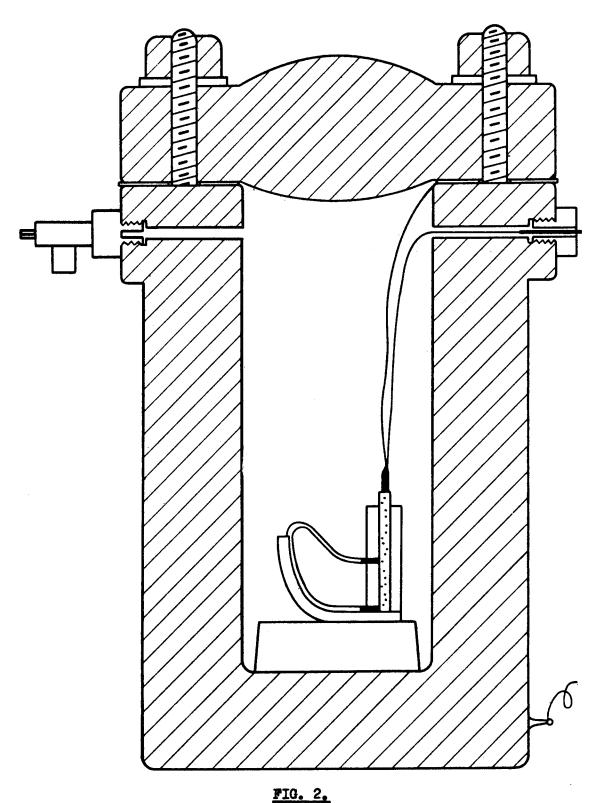
This had a detonation velocity of 6,600 m. per sec. The fuse was capped with No.6 fulminate detonators. A small strip of wood, A, was screwed to a curved lead plate, C. The cartridge of explosive, D, was strapped to this strip of wood. Another piece of wood, B, had a 1" diameter hole drilled in it 3 cm. from its edge, where a 1" diameter groove of semicircular cross section had been cut parallel This piece of wood was strapped to the cartridge and to the hole. The detonators capping the fuse were inserted in the its support. two holes, one in the wooden block, B, and the other in the hole formed by the adjacent grooves in the wooden block, B, and the lead The lead plate was bent so that the fuse rested in the plate, C. The plate was marked at the position where the mid-point groove. A detonator was inserted in the of the fuse rested against it. cartridge, and the whole assembly was lowered into the gas tight The complete assembly is shown in Figure 2. This vessel Gas was then injected until the required was closed and evacuated. pressure was reached, and the detonator fired electrically. these experiments the gas used was methane so that the combined effect of low value and high initial pressure would be exerted. Since the cartridge wrappers were thoroughly perforated, the injected gas was able to enter the spaces between the grains of explosive in the cartridge without compressing the whole charge. The loading density of the explosive was, therefore, unaltered, except for the insignificant increase in the mass of the gas pockets. detonator was fired, detonation was set up in the cartridge and a wave of explosion travelled down to the first detonator capping the A new detonation wave was then initiated in the detonating fuse. first arm of the fuse, while the original wave continued to the second detonator where another detonation wave was initiated in the By this time the wave in the first arm had second arm of the fuse. travelled a distance  $2\ell = dt$  where d is the detonation velocity of the fuse and t the time taken for the detonation wave in the cartridge to travel 3 cm. (the distance between the detonators). This interval is, of course, 3/D where D is the detonation velocity The two waves in the fuse would meet at the midof the cartridge. point of the fuse if both arms had been set off instantaneously, but since the first arm had a lead 20 over the second arm they met at a distance & from the mid-point and made a mark on the lead plate.

But 
$$D = \frac{3d}{2\ell}$$

A measurement of  $\ell$  therefore gave a measure of the unknown detonation velocity D.

# Experiment with Grained Tetryl

Grained tetryl was loosely packed into cartridge wrappers 7/16", 3", and 15/16" diameter at a loading density of 0.9 g./c.c. and each cartridge set up as shown in Figures 1 and 2. The vessel was evacuated and then filled with gas. The pressure was measured by a Bourdon gauge, and then the cartridge was set off by a No.6 A.S.A.T. copper detonator.



Arrangement for firing an explosive charge under pressure.

It was found that as the gas pressure increased, the detonation velocity became progressively slower, and above a threshold pressure the explosion did not propagate. Some typical results are given in Table 2. Some results obtained by the high speed camera method described in part 1 are included to show that the Dautriche method was not highly inaccurate.

Effect of pressure on the velocity of detonation of grained tetryl density 0.9 g./c.c. set off by a No.6 A.S.A.T. copper detonator

Diamete	r:	Pressure	:	Gas filling	;:	Velocity of
inches	:a	tmospheres	:	voids	:	detonation
	:	-	:		:	m./sec.
7/16	:	0.03	:	Air	:	1460*
Ħ	:	1.0	:	Air	:1	,480, 1,300, 1,330
	:		:		:1	,430 <b>*</b> , 1,540 <b>*</b>
17	:	14.3	:	Methane	:	910
11	:	27.7	:	11	:	Failed
<u>3</u> 4	:	1.0	:	Air	:	1,700
Н	:	14.3	:	Methane	:	1,890
11	<del></del>	21	:	11	:	450
11	:	27.7	:	19	:	1,330
**	:	47.7	:	11	:	Failed
15/16	:	1.0	:	Air	:	2,860
H	:	14.3	:	Methane	:	2,330
Ħ	:	17.6	:	11	:	2,085
11	:	21.0	:	17	:	1,695
11	:	41.0	:	17	:	Failed

\* Determined by high speed camera method.

In all these experiments the distance from the initiating detonator to the first pick-up detonator, the "run-up", was kept constant at 6 cm. and it might be argued that the average velocity between the pick-ups appeared to fall as the pressure increased because the acceleration to maximum velocity was being slowed. A few experiments were, therefore, carried out in which the "run-up" was varied. For these experiments some \(\frac{3}{4}\)" diameter cartridges were used. In Table 3 results obtained at one atmosphere in air are compared with those obtained at 14.3 atmospheres in methane.

Velocity of detonation of grained tetryl density 0.9 g./c.c.

:Lei	ngth of r	un up: (	as pressure	:Ve	locity of deton	ation:
:	cm.	: 8	tmospheres	:	m./sec.	<u> </u>
:	1	:1 8	atm. of air	:	1,670	:
:	4	:		:	1 <b>,</b> 930	:
:	7	:		:	2,440	:
:	<u>1</u> 0	:			2,380	:
:	1	:14.	3 atm. of metl	nane:	1,615	:
:	4	:		:	1,515	:
:	7	:		:	1,515	
:	10	:		:	1,500	:

These results showed a definite tendency for acceleration of the detonation wave to a steady velocity of about 2,400 m./sec. at 1 atmosphere pressure of air, but an apparent deceleration of the velocity to about 1,500 m./sec. if the intergranular spaces were filled with methane at 14.3 atmospheres. This suggests that high pressure reduced the final steady velocity of detonation.

In all these experiments only velocities between 900 and 2,500 m./sec. were recorded, but if the explosive was sufficiently primed it would detonate at a much higher velocity. Sufficient priming was obtained when 2 g. of fine PETN was put on top of the cartridge of tetryl, and was set off by a No.6 A.S.A.T. copper detonator. When 7/16" diameter cartridges were set off by this means the following velocity records were obtained:-

1. At one atmosphere pressure in air, run up 6 cm. 4,550 m./sec.

2. At 67.7 " " in methane, run up 6 cm. 4,550 m./sec.

3. At 64.3 " " " " 25 cm. 4,550 "

Obviously the high velocity detonation of this explosive was unaffected by a change in the pressure of the gas in the intergranular spaces up to 67.7 atmospheres.

#### Experiments with Flake T.N.T.

The low velocity regime of a batch of flake T.N.T. was studied in experiments essentially similar to those carried out with grained tetryl. Only two cartridge diameters were investigated,  $\frac{3}{4}$ " and 15/16" and the results have been set out in Table 4.

Velocity of detonation of T.N.T. flake density 0.8 g./c.c. fired by a No.6 A.S.A.T. copper cased detonator

:Diameter	:	Pressure	:		:Velocit	y of	-:
: inches	:	atmospheres	:Gas	s present	: deto	nation	:
:	:		:			/sec.	_:
:	:	0.03	:	Air	:2020*	2020*	:
:	:	0.12	:	Ħ	:1754	1818	:
: 3	:	1.0	:	11	:1750	2040	:
3 4	:	21	:	Methane	: 20	80	:
:	:	24.3	:	11	:No read	ing obtained	i:
:	:	27.7	:	**	:Some T.	N.T. left	:
:	:	41	:	#		completely	_:
:	:	1.0	:	Air	: 2,	380	:
:	:	9.3	:	Methane	: 2,	,330	:
: 45/46	:	11.0	:	17	: 1,	020	:
15/16	:	14.3	:	tt	: 2,	000	:
:	:	26	:	Ħ	: 1,	,820	:
:	:	41	:	Ħ	: Failed	completely	_:

The velocities recorded in these experiments were not as regular as those recorded in the experiments with grained tetryl, but the continual propagation of low velocity detonation was prevented if the gas pressure between the grains of explosive was above a critical value.

It was found that high velocity detonation could be initiated in  $\frac{3}{4}$ " diameter cartridges of this flake T.N.T. if a primer of 5 g. of powdered PETN was placed on top of the charge. The primer was then set off by a No.6 A.S.A.T. electric detonator. High velocity detonation was observed when pressures of one atmosphere of air or 67.7 atmospheres of methane were applied in the gas spaces, and no drop in detonation velocity occurred.

### Experiments with Nitroguanidine

Very fine nitroguanidine was stemmed in increments into paper shells to form cartridges of bulk density 0.5 g. per c.c. wrappers were perforated and the cartridges set up in the arrangement shown in Figures 1 and 2. The explosive was quite porous in spite of the stemming, and gases at low pressure could be swept through the cartridges with ease. The experimental procedure followed was essentially similar to that employed in the experiments The vessel was evacuated with tetryl and T.N.T. described above. The charge was fired, and the gas injected to the required pressure. The detonation velocity was then and the lead plate recovered. calculated from a measurement of the distance between the zero mark on the plate and the mark due to the collision of the two approaching waves in the fuse. Typical results have been set out in Table 5.

Detonation velocity of nitroguanidine density 0.5 g./c.c. set off by a No.6 A.S.A.T. copper cased detonator

:Diameter of cartridge	: Pressure : atmospheres	: Gas : injected	: Velocity of : detonation
: inches	•	:	: m./sec.
: 7/16	: 0.03	: Air	: 2650*
:	: 1.0	: "	<b>:</b> 2750
:	: 6.0	: Methane	: 2500
:	: 7.0	: #	: 1490
:	: 11.0	: "	: 2170
:	: 17.7	: "	: Failed
: <del>3</del>	: 1.0	: Air	: 3130
:	: 6.7	: Methane	: 3220
:	: 11.0	: "	: 3030
<b>:</b>	: 14.3	: "	: Failed

<sup>\*</sup> Determined by high speed camera methods.

Once again there was a tendency for the detonation velocity to fall as the pressure increased, and if the pressure exceeded about 11 to 15 atmospheres the propagation did not continue.

In the experiments with coarse tetryl and T.N.T. heavier priming caused a marked increase in the velocity of detonation. two distinct velocities at which detonation could propagate. However, fine nitroguanidine detonated at its maximum velocity when set off by a weak detonator, and no amount of priming could establish a steady propagation at a higher rate. It might be argued that the effect of pressure on the results obtained with tetryl and T.N.T. was merely to reduce the effectiveness of the detonator, for, if heavier priming was employed (and high velocity established) pressures of methane up to 67.7 atmospheres had no effect. Experiments were, therefore, carried out with cartridges of nitroguanidine 7/16" diameter primed with 2 g. of fine PETN powder. Table 6 shows the They showed that there was a marked effect due to results. increasing the gas pressure, and the continued propagation of detonation was eventually stopped.

Table 6

Velocity of detonation of nitroguanidine density 0.5 g./c.c. diameter 7/16", primed with 2 g. of PETN and set off by a

No.6 "Briska" type detonator

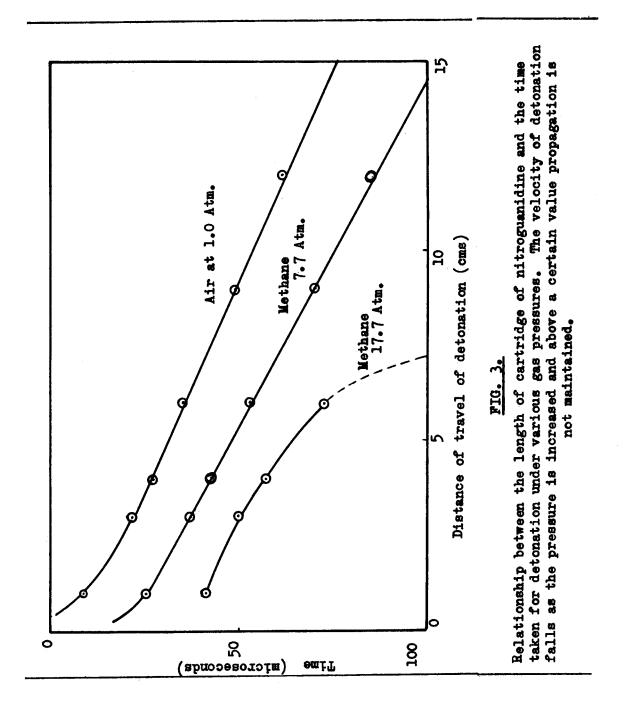
	Pressure	: Gas	:Velocity of detonation	
: <u>a</u>	tmospheres	:injected	: m./sec.	
:	1.0	: Air	: 2,000	
:	14.0	: Methane	: 1,750	
:	14.3	: "	: 2,130	
:	16.7	: "	: 2,330	
:	17.7	: "	Failed	
:	19.3	: "	: 11	
:	27.7	: "	: "	
:	41.0	: "	1 #	

Further proof that the propagation of explosion rather than the initiation process was being modified by the increase in pressure was provided by some experiments in which the length of "run-up" between the initiating detonator and the first pick-up was changed. 7/16" diameter cartridges of various lengths were set up in the system shown in Figures 1 and 2. A series of velocity determinations over the last three centimetres of cartridges of increasing length provided a picture of the way in which the velocity of detonation increased along the length of a single cartridge. Experiments were performed with the gas spaces filled with air at one atmosphere, methane at 7.7 atmospheres, and methane at 17.7 atmospheres, and the results are set out in Table 7. The cartridges fired at 17.7 atmospheres pressure were primed with 2 g. of PETN and a No.6 Briska detonator.

Velocity of detonation of nitroguanidine density 0.5 g./

Initiator		Run cm.		Pressur		Gas	:	Velocity of detonat	tion
No C A C A C		Citta		atmosphe	res:1		ea:	m./sec.	
No. 6 A. S. A. T.	:	1	:	1.0	:	Air	:	1670	
	:	3	:	1.0	:	11	:	2330	
	:	6	:	1.0	:	11	•	2130	
	:	9	•	1.0	•	18	:		
11 11	÷	4	<del></del>	7 7		- 11		2380	
	•		•	<u>/•/</u>	IN	ethan	<b>e</b> :	1725	
	:	3	:	7•7	:	11	:	1820	
	:	6	:	7•7	:	Ħ	:	1700	
	:	9	:	7.7	•	Ħ		2040	
2 g. PETN + a	:	1	<del></del>	17.7	<del></del>	11	÷		
No.6 Briska			•	47.7	•		i	1930	
No. 6 Briska	•	ڔ	:	17•7	:	11	:	1330	
	:	6	:	17.7	:	17	:	Failed	
	:	9	:	17.7	•	tt	•	Failed	

These results may be translated into the distance time curves shown in Figure 3.



It can be seen that the detonation velocity as measured by the slope of these lines rapidly settled to a steady value when the cartridges were fired in air at one atmosphere. If the cartridges were fired in 7.7 atmospheres of methane the same thing happened, but the steady value reached was somewhat lower. When the cartridges were fired with a pressure of 17.7 atmospheres of methane in the intergranular spaces, the velocity fell rapidly and with cartridges over 6 cm. in length complete consumption of the explosive did not occur.

# Experiments with Liquid Nitroglycerine

The experiments with tetryl, T.N.T., and nitroguanidine showed that low velocity detonation could be prevented by increasing the included gas pressure. High velocity detonation of tetryl and T.N.T. was unaffected by a pressure of 67.7 atmospheres. Since liquid nitroglycerine was known to detonate at two discrete velocities it was of interest to study the effect of pressure on the propagation of explosion in this substance.

Nitroglycerine was poured into thin walled shells made of cellophane. It was found that low velocity detonation would not propagate in charges of ½" diameter or less, and so for all experiments the lowest practicable diameter 7/16" was used. The cartridges were set up in the same way as those of T.N.T. tetryl and nitroguanidine (as shown in Figures 1 and 2) but the cartridge wrapper was not, of course, perforated.

It has already been mentioned that low velocity detonation in liquid nitroglycerine is an irregular propagation differing markedly from the steady low velocity detonations observed in aerated gelatines or coarse powders. It is not surprising, therefore, that the low velocities recorded at atmospheric pressure varied from 1410 to 950 m. per sec. Velocities below about 900 m. per sec. were often not recorded by the Dautriche method because the fulminate detonators capping the fuse were not sensitive enough to be set off by such weak explosion waves.

In the first series of experiments the initiator used was a No.1 fulminate detonator, the weakest detonator available. the pressure was increased to 11.3 atmospheres no velocity readings were obtained, although the fuse detonated, and the lead was dented by the explosion when it reached the end of the cartridge. probable that only one of the detonators capping the fuse was set off by the explosion, consequently there was no mark due to the At higher pressures the complete fuse with meeting of two waves. detonators was often recovered, but even when the pressure was 71 atmospheres the explosion of the liquid was complete, for its "brisance" caused a dent to be punched in the lead plate. The did not appear to grow smaller as the pressure increased. experiments were repeated with a heavier initiator, a No.4 fulminate Occasionally this initiated high velocity propagation. detonator.

However, as the pressure increased, the incidence of high velocity detonation became less frequent and there was a definite tendency for the low velocity records to be reduced in value, although no complete failure was observed. The results have been set out in Table 8.

Table 8

Velocity of detonation of liquid nitroglycerine
7/16" diameter

· T 2 + 2 - 4	:	Pressure	: Gas		:Vel	ocity o	of	:		-:
Initiator	:a	tmospheres	: used		: de	tonatio	on	: Re	marks	1
:	:		:			per se		:		_;
: NO. 1	:	1.0	: Air		:141	0, 1160	950	:		1
:detonator	:	11.3	:Metha	ne	:	No rea	ading	:Fuse	detonated	:
:	:	30.3	: "		:	11	Ħ	:Fuse	recovered	:
:	:	71.0	: "		:	11	Ħ	: "	pt	_;
: NO.4	:	1.0	: Air		:	1250		:		:
:detonator	:	1.0	: "		:	7690		:		:
:	:	14.3	:Metha	ne	:	6670		:		:
•	:	17.7	: 11		:	1205		:		:
•	:	20.5	. 11		:	1040		:		:
:	:	32.7	. 11		:	1010		:		:
•	:	44.3	: 11		:	807		:		8
:	<u>:</u>	67.7	. 11		:	909		:		_:

If the propagation depended on the presence of small bubbles one A number of attempts were made to remove might expect this result. all gas bubbles from the liquid before firing by leaving the cartridges several hours before firing them, and by storing the cartridges under vacuum, but low velocity propagation was still Finally, small quantities of nitroglycerine were outgassed under a vacuum of 10<sup>-2</sup> mm. of mercury, and then poured into the The cartridges were returned to the vacuum cartridge shells. chamber which was opened just before the cartridge was inserted in the A cartridge so assembled was set off by assembly shown in Figure 1. a No.1 detonator at one atmosphere air pressure and detonated at high velocity. It gave a reading of 6670 m. per sec. Two other cartridges were removed in turn from vacuum chambers, and rapidly arranged in the Dautriche assembly (Figure 1) inserted in the pressure vessel (Figure 2) and rapidly raised to a high pressure. It was very unlikely that any air bubble could remain in the liquid after outgassing, but if any invisible one was left it was compressed by the applied pressure to an insignificant volume. Pressures of 47.7 atmospheres and 64.3 atmospheres were used and the initiator was a No.1 detonator. In both cases complete low velocity propagation occurred. explosive was left, a distinct dent was made in the lead plate, and Although no velocity records were obtained, it the fuse detonated. was clear that low velocity detonation had propagated in liquid nitroglycerine when gas bubbles were completely excluded.

#### Discussion

These experimental results reveal a striking similarity between the initiation of explosion by the impact of a hard body, and the propagation of explosion by the impact of a low velocity detonation wave. In order to initiate explosion by impact it is apparently necessary to have within the explosive something which will provide a local high temperature or hot spot. The most effective hot spot source is a small bubble of gas. During impact this bubble is rapidly compressed, and reaches a high temperature. The explosion is then initiated at the hot spot. If no bubbles are present it is very difficult to start an explosion.

# Low Velocity Detonation in Solid Explosives

In order to maintain low velocity detonation in solid explosives like T.N.T. or tetryl, or in gelatinous mixtures containing nitroglycerine it is again of great advantage, if not essential, that gas pockets should be present. In the experiments with tetryl, T.N.T., and nitroguanidine subjected to increasing gas pressure, it was clear that as the gas pressure increased, the ease of propagation of low order detonation was reduced, and above a threshold pressure, which varied with the explosive and with the cartridge diameter, ceased to maintain a steady rate.

This effect cannot be explained by hydrodynamic considerations of the explosive as a homogeneous body, for the pressures used in these experiments were insignificant in comparison with the detonation We must, therefore, look at the mechanism of detonation pressures. Detonation waves which all travel at supersonic for an explanation. velocities are really shock waves maintained by chemical reactions. The front of the shock wave on meeting a new layer of explosive compresses it very rapidly and thereafter the chemical reaction begins Bridgeman(11), has shown that static pressures of the same order as detonation pressures do not initiate explosion in solid explosives, and it seems reasonable to attribute initiation to the suddenness of the pressure rise. Such compressions bring about a rapid increase in temperature and since the shock wave also brings about a change in the kinetic energy of the material, the temperature attained is even higher than the temperature in adiabatic compression During the high velocity detonation over the same pressure range. of nitroglycerine the compression of the liquid phase may bring about temperature rises of 3,000°C.(6), but in low velocity detonations the pressure changes cannot be great enough to raise the temperature of a liquid or solid phase more than a few tens of degrees. more compressible gas pockets would, however, be raised to very high Hot spots would be formed at the gas bubbles and temperatures. these would initiate explosion in their vicinity immediately a shock Thus a low velocity detonation in a granular wave encountered them. solid would appear to be a shock wave supported by a chemical reaction which is initiated at the gas bubbles encountered by the shock wave.

Support for this view has been obtained in the study of the light emitted in explosions.

A considerable amount of study has been given to the origin of the luminosity near detonating explosives and Muraour(12) has shown that the majority of the light comes from the surrounding gas which is raised to a very high temperature by the compression it suffers in the passage of a shock wave (Michael Levy and Muraour(13)) showed that if grains of lead azide were separated by 3 mm. gaps, an explosion would propagate from grain to grain in air, but if the air was replaced by carbon dioxide at 22 atmospheres pressure, the luminosity was reduced, and propagation of the explosion was Paterson(14) has obtained evidence that luminosity incomplete. may be produced within a granular material by the passage of a shock wave, and since this may be brighter than the luminosity of an explosion supported by a shock wave of greater intensity, it is reasonable to suppose that the luminosity comes from the compressional This may be regarded as evidence heating of the small gas pockets. that the gas pockets within a granular explosive do become very hot when a detonation wave passes over them, and we would expect that these hot spots would act as centres of explosion. initial pressure of the gas in the pockets were increased, the compression ratio in the detonation wave would be reduced, and so the Eventually, maximum temperature in the gas pockets would be reduced. if the compression ratio were sufficiently reduced the hot spot temperatures would not be high enough to initiate local explosions. On this view of the Thereafter the detonation would not propagate. mechanism of initiation of explosion in the wave front we would expect that there would be a threshold pressure in the gas pockets above which low velocity detonation would no longer be possible. experiments with tetryl, T.N.T. and nitroguanidine confirm that there is such a threshold pressure.

If air was replaced by other gases of lower γ value at low pressures there was no substantial drop in the velocity of detonation At first sight a drop in velocity, or of the granular solids. complete failure in the propagation might have been expected, but Firstly, the gases of lower several factors have to be remembered. Y value cannot be considered to behave as ideal gases during such large compressions, and the temperatures produced by adiabatic compression would be higher than those predicted by the ideal Secondly, since it is a shock wave compression rather equation(1). than an adiabatic compression, the effect of  $\gamma$  variations would be considerably less than the effect in adiabatic compression. more likely however that the change in the specific heat of the gas pockets brought about by the replacement of air by pentane or ether vapour was not sufficient for it to have a distinctly measurable Some cartridges of effect on the properties of the explosive. T.N.T. failed to detonate when they contained pentane vapour, whilst similar cartridges containing air detonated completely, but this occurred only when the diameter was near the minimum diameter for

propagation, and it would be unwise to base any conclusions on these results alone.

# Low Velocity Detonation in Liquid Nitroglycerine

In the introduction to this paper it was pointed out that the low velocity detonation of nitroglycerine is more irregular than the low velocity detonation of granular solids or aerated gelatines. This suggests that low velocity detonation of liquid nitroglycerine may differ in mechanism from low velocity detonation in granular The experiments described above have shown that the complete absence of gas bubbles in the liquid does not prevent the propagation of low velocity detonation. An increase in the external pressure does seem to reduce the velocity of detonation, but pressures up to 71 atmospheres failed to prevent propagation of the explosion. The only reasonable explanation would appear to be the one previously offered for the detonation of thin films of nitroglycerine (Bowden and Gurton(7)) that the mechanical effects of the detonation wave rapidly broke up the explosive to provide a large burning surface which was ignited by conduction of heat from the reacting material. There is no obvious explanation for the apparent drop in velocity with pressure, but since the variation in records obtained at atmospheric pressure covered almost the whole range observed under pressure, this drop in velocity may not have any significance.

In general it may, therefore, be concluded that in most explosives the chemical reaction responsible for the propagation of low velocity detonation of solids is continuously initiated in the shock front of the detonation wave by the hot spots formed in the compression of gas pockets. There is no evidence that the presence of gas pockets is essential for the maintenance of high velocity detonation in solids, or low velocity detonation in liquid nitroglycerine.

This work followed logically from the study of detonation in thin films which the author carried out in conjunction with Dr. F.P. Bowden, F.R.S., and I thank him for suggesting the investigation. The author also wishes to thank Dr. J. Taylor, M.B.E. for his constant encouragement, and Messrs. G. Boyd and I.G. Cumming who helped to carry out the experimental work.

# REFERENCES

(1) Taylor, J., 1952	Detonation in condensed explosives. Oxford University Press
(2) Ratner, S., 1944	C.R. Acad. Sci. U.R.S.S., 42, 265
(3) Jones, E. and Mitchell, D., 1948	Nature <u>161</u> , 98
(4) Bowden, F.P., Mulcahy, M.F.R., Vines, R.G. and Yoffe, A., 1947	Proc.Roy.Soc. (A) 188, 241, 311
(5) Yoffe, A., 1949	Proc. Roy. Soc. (A) 198, 373
(6) Ratner, S., 1947	Acta Physicochemica U.R.S.S., 22, 357
(7) Bowden, F.P. and Gurton, O.A., 1949	Proc.Roy.Soc. (A) 198, 350
(8) Bowden, F.P. and William, H.T., 1951	Research <u>4</u> , 1951
(9) Bowden, F.P. and Yoffe A., 1952	Initiation and growth of explosion in liquids and solids. The University Press, Cambridge
(10) Jones, E., 1928	Proc. Roy. Soc. (A), 120, 603
(11) Bridgeman, P., 1947	J.Chem. Phys. <u>15</u> , 311
(12) Muraour, H., 1942	Chemie et Industrie, 47, 3
(13) Michael-Levy, A. and Muraour, H., 1936	Comptes Rendues, 202, 755
(14) Paterson, S., 1951	Nature <u>167</u> , 479

#### SENSITIVENESS TO DETONATION

Elwyn Jones and Ian G. Cumming I.C.I. (Nobel Division) Stevenston, Ayrshire, Scotland.

A sensitive explosive is one which needs little encouragement to induce it to explode or, at least, to undergo chemical changes leading to explosion. The necessary stimulus may come from any one of a number of sources, such as friction, impact, flame, electric sparks and so on, and since explosives vary in their reactions to different stimuli, it is desirable in discussing sensitiveness to specify the kind of initiating agency in mind. Thus, one explosive may be very sensitive to ignition by an electric spark whereas another may be more susceptible to impact or friction. In fact, the same explosive can be made sensitive to electrical discharges or to friction merely by introducing a little graphite in the one case and a few particles of grit in the other.

In some explosives the explosive reaction, however initiated, inevitably builds up to detonation, sometimes with astonishing rapidity. Other high explosives require a "detonator", or even a "booster" or "primer", to initiate reaction; in these cases, if the initiating device does its work, detonation sets in immediately. It is necessary, therefore, to distinguish between the direct initiation of detonation and its initiation through an intermediary. In other words, the sensitiveness of an explosive to detonation is not to be confused with its sensitiveness to ignition.

As its name implies, sensitiveness to detonation is an exclusive property of the so-called high explosives. There are circumstances, however, where a high explosive may lose its ability to detonate as, for example, when spread in a thin layer on an anvil. It appears, therefore, that sensitiveness to detonation is a property, not of the explosive substance, but of the explosive system. In other words, the geometry of the explosive charge and its environment are factors which must be

# Jones and Cumming

taken into account both in defining sensitiveness to detonation and in developing methods for its measurement.

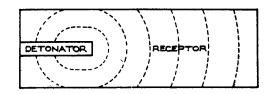
# Sensitiveness Tests

It has been indicated that direct initiation of detonation, particularly in condensed explosives, normally requires a detonator or primer. Hence, sensitiveness to detonation may be measured by the weakest detonator or primer capable of initiating detonation in the explosive charge in question(1). For reasons of symmetry, the explosive charge is usually prepared in the form of a cylindrical cartridge and, for convenience, the cartridge is fired in the open. Thus the conditions of test are arbitrarily chosen, but experience has shown that initiators which function satisfactorily under these conditions perform equally well, if not better, under field conditions as, for example, in borehole charges or high explosive bombs.

The almost universal use of detonators for initiation in practice makes a minimum detonator test very attractive from the practical point of view, but the geometry of this system is unnecessarily complicated for initial study, see Fig. 1 (a). A primer, on the other hand, can be made to match the shape of the receptor and its strength varied without necessarily affecting the geometrical requirements of the test. Primer and receptor cartridges placed in line would appear to offer the simplest and most convenient arrangement for experimental purposes. It may be worth noting here that the geometrical basis of this model is a straight line, namely, the axis of symmetry.

To measure the sensitiveness to detonation of the receptor cartridge, it is necessary to be able not only to vary the strength, or "initiating power", of the primer but also to express this property in terms of some numerical quantity. This is usually done by separating the primer and receptor cartridges and increasing the intervening gap in successive experiments until the point is reached at which, on firing the primer, the receptor just fails to detonate, the critical distance being taken as an arbitrary measure of the sensitiveness of the receptor. The space between the cartridges may be filled with any homogeneous medium but it is convenient in practice to use air. The arrangement of the gap test is illustrated in Fig. 1(b).

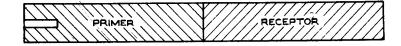
The presence of a gap in the explosive column is a complication which, as will be seen shortly, is not altogether desirable and the alternative may be suggested of varying the initiating power of the primer by diluting it with inert material and, this time, taking the critical amount of diluent required to cause failure as a measure of sensitiveness. This is essentially the same test only that in this version the receptor cartridge is initiated by a true "detonation-wave" in an explosive rather than by the "shock-



(a) MINIMUM DETONATOR TEST
(ILLUSTRATING CHANGING SHAPE OF DETONATION FRONT)



(化) GAP TEST



(c) CONTACT TEST

FIG. I SENSITIVENESS TO DETONATION TESTS

#### Jones and Cumming

wave" set up in the medium separating the two cartridges, see Fig. 1(c). Whether or not there is any real difference between a detonation-wave and a shock-wave as regards initiating power is a matter which need not concern the present discussion because the work to be described was done with explosives in intimate contact.

The gap test, however, will serve to illustrate a point of some significance which may be conveniently considered at this stage. If the test is carried out with a constant primer, the critical gap at which detonation is just transmitted to each of a series of different receptors will, as already seen, arrange these receptors in order of their sensitiveness to detonation. Conversely, if a standard receptor is used with a range of primers, the critical gap now arranges the primers in order of initiating power. Actually, the converse is not strictly true because it depends on the doubtful hypothesis that the decay of initiating power with distance is the same for all explosives; this is why a contact test presents fewer complications than a gap test.

If, as is more usual in carrying out the gap test, the same explosive is used as primer and receptor, explosives are again arranged in a definite order of sensitiveness to detonation but this arrangement is not necessarily the same as that obtained with a standard primer. It appears, therefore, that there are two kinds of sensitiveness to detonation and, since one is measured by the maximum gap over which transmission occurs in a given explosive, this is called "sensitiveness to propagation" and the other "sensitiveness to initiation". There are, therefore, three primary factors concerned in the double cartridge test, namely, initiating power, sensitiveness to initiation and sensitiveness to propagation.

An elementary relation between these quantities may now be noted. To measure the sensitiveness to initiation of a receptor, the initiating power of the primer must be reduced until it just fails to initiate the receptor. In other words, the sensitiveness to initiation equals the minimum effective initiating power.

Again, the sensitiveness to propagation is the margin by which the actual initiating power exceeds the minimum effective value, or sensitiveness to initiation. At the limit for propagation the initiating power of an explosive cartridge coincides with its sensitiveness to initiation and the sensitiveness to propagation vanishes. These statements reduce to the following equality:-

Initiating power - sensitiveness to initiation

= sensitiveness to propagation.

This relationship derives from our definitions of these quantities and must now await experimental verification. Nevertheless, it is interesting to note that, if this relation holds, these three quantities have the same dimensions in the mathematical

sense and so can be measured in the same units, an encouraging prospect.

#### Experimental

As already indicated, the experimental procedure for carrying out the preferred form of the double-cartridge test is to join the primer and receptor cartridges end to end in the same straight line and to vary one or other in a systematic way until the point is reached when, on firing the primer, the receptor just fails to detonate. If the cartridges are carefully made and are long enough to ensure steady detonation, the end-point is usually remarkably sharp. By varying the primer and receptor in turn, results will be obtained showing how the sensitiveness to initiation on the one hand, and the initiating power on the other, vary with certain physical and chemical properties of the explosives.

For example, a series of receptor cartridges might be prepared to cover a certain range of sensitiveness to initiation; these could be a series of trinitrotoluene/ammonium nitrate mixtures cartridged at a constant density or, alternatively, a particular trinitrotoluene/ammonium nitrate mixture cartridged at different In these cases the sensitiveness to initiation might be expected to increase with increasing proportion of trinitrotoluene in the mixture and to decrease with increasing density. The primer for either or both series of constant receptors could be nitroglycerine absorbed in kieselguhr, the proportion of nitroglycerine to kieselguhr being varied for each test until the point The proportion of nitroglycerine in of failure is established. the critical mixture is taken to represent the sensitiveness to initiation of the particular receptor concerned and, when this has been done for all the receptors, the combined results show how the sensitiveness to initiation varies with the composition of the trinitrotoluene/ammonium nitrate mixture in the one case and with The complementary process, of cartridging density in the other. course, provides similar information about the initiating power.

Such experiments can be made with almost any explosive or explosive/inert combination but it is not the intention here to compare explosives but rather to illustrate certain general principles. It is proposed, therefore, to describe an experiment involving a receptor cartridge having two stable rates of detonation and so combining two explosives in one. Such a cartridge may be expected to show two levels of initiating power, sensitiveness to initiation and sensitiveness to propagation. The particular explosive chosen for this experiment was flaked trinitrotoluene, size 20 x 30 B.S.S. cartridged at a density of 1.0 g./c.c. A 3 cm. diameter cartridge of this explosive, for example, detonates at 1900 or 4100 m./sec. depending on the strength of

#### Jones and Cumming

the initiator. The problem is, as before, to determine the minimum primer required to initiate each of these detonation regimes.

Even with two rates of detonation, one cartridge can only give two results and, since this is not enough to solve a problem involving three variables, it becomes necessary to vary the detonating properties of the cartridge in a way which will not alter the explosive or disturb the basic model. This may be done quite simply by varying the diameter of the cartridge, which is obviously an arbitrary factor. Thus it becomes possible, at least in theory, to produce two infinite series of results from one explosive of one grain size at one density. By varying the size and density, the results may, if necessary, be multiplied without end.

It remains now to find a common unit for measuring the explosive properties of the cartridge. If, as seems likely, the initiating power is a function of the velocity of detonation, a weak primer may be expected to initiate detonation in the receptor at a lower rate than a strong one and we can therefore measure the strength of a primer by the magnitude of the initial velocity induced in the receptor. On this view, the minimum initiating power needed to ensure complete detonation of a receptor, i.e. the sensitiveness to initiation of the receptor, is measured by the minimum initial rate of detonation which ensures Similarly, the sensitiveness to propagation complete propagation. is represented by the margin between the stable value of the detonation velocity and this critical initial value. photographing the double-cartridge test on a moving film and measuring the initial and final rates of detonation in the receptor, it should be possible to obtain quantitative measurements of the initiating power, sensitiveness to initiation and sensitive-This assumes, of course, that all three ness to propagation. quantities are functions of the rate of detonation and that the process of attaining stable detonation is sufficiently gradual to be observable.

As will be seen from the specimen photographs reproduced in Fig. 3, the explosive chosen for the experiment does in fact lend itself to this technique and it was found possible, by examining the photographs with a comparator and measuring the tangents to the trace at various points, to plot the rate of detonation against distance along the receptor cartridge. By extrapolating to the point where primer and receptor meet, the starting rate in the receptor was obtained. The method is not very accurate but by using different sets of primers, several values for the same result were obtained and an average taken.

The primers used were in two groups, (a) picrite, nitrated cotton wool and a commercial explosive (Glasgow Dynamite), all cartridged at varying densities and (b) nitroglycerine/kieselguhr, pentaerythritol tetranitrate/common salt and trinitrotoluene/common salt mixtures of varying proportions. The primer cartridges were usually 6 in. long, which is normally sufficient to establish stable detonation. By varying the density in group (a) and the composition in group (b), the critical conditions for initiation were established for the trinitrotoluene receptor cartridge in different diameters.

#### Results

In  $\frac{7}{8}$  in. diameter cartridges, flaked trinitrotoluene, size 20 x 30 B.S.S., cartridged at a density of 1.0 g./c.c. did not propagate detonation, however well primed.

In 1 in. diameter cartridges, this explosive, if initiated at any speed between about 1,600 and 3,200 m./sec., accelerated or decelerated until the rate of detonation reached a figure of approximately 1,700 m./sec., after which it remained steady. If initiated at anything below 1,600 m./sec., detonation died out and, if initiated at anything above 3,200 m./sec., the rate of detonation became steady at approximately 3,400 m./sec.

In 1 3/16 in. diameter cartridges, the same explosive, if initiated at speeds between about 1,400 and 2,400 m./sec., settled down to a stable regime at approximately 1,900 m./sec., whereas if initiated at speeds exceeding 2,400 m./sec., its final velocity of detonation was approximately 4,100 m./sec.

In  $1\frac{1}{2}$  in. diameter cartridges, this explosive had only one stable velocity of detonation which was approximately 4,400 m./sec. This required a minimum initiating speed of about 1,200 m./sec.

Difficulty was experienced in producing primers which were too weak to initiate this explosive so that the minimum initiating velocities for the low velocity regime are a little uncertain.

The results are reproduced graphically in Fig. 2 and it will be seen that they form two pairs of intersecting lines, the upper line of each pair representing the stable velocity of detonation, or initiating power, of the regime concerned and the lower representing the minimum effective initiating rate, or sensitiveness to initiation. Thus, AB represents the initiating power of the high velocity regime, BC the sensitiveness to high velocity initiation, CD the initiating power of the low velocity regime and DE the sensitiveness to low velocity initiation.

M/SEC. **5000** INITIATING POWER (H.V.) 4000 OF RATE 3000 SENSITIVENESS TO INITIATION (H.V) INITIATING POWER 2000 Ε 1000 SENSITIVENESS TO INITIATION (L.V.)

SENSITIVENESS TO INITIATION (TWO - VELOCITY EXPLOSIVE)

FIG. 2 RELATION BETWEEN INITIATING POWER AND

#### Jones and Cumming

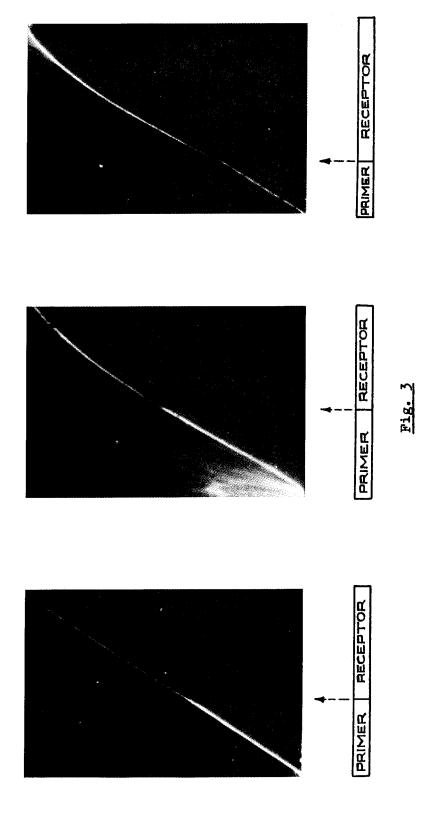
At the points of intersection B and D, the initiating power equals the sensitiveness to initiation and, by definition, this distinguishes the limiting diameter for propagation. The fact that cartridges of slightly lower diameter could not be made to detonate completely, even with the heaviest priming, thus confirms expectations. Moreover, as the cartridge diameter increases above the limiting value, the lines are seen to diverge, showing that the sensitiveness to propagation increases with cartridge diameter. This is also a well-established experimental fact.

At C the initiating power of the stabilised low velocity regime equals the sensitiveness to initiation of the high velocity regime, with the result that the one leads to the other. seems likely, the build-up of detonation occurs at different rates under the two regimes, the velocity curve should suffer an abrupt change of slope at this point. For example, if a cartridge of the critical diameter were to be initiated at the minimum effective rate, which according to Fig. 2 is approximately 1,400 m./sec., detonation accelerates at the characteristic "low velocity" rate up to about 2,000 m./sec., at which point the change-over occurs and, thereafter, acceleration proceeds at the "high velocity" rate. It may be further anticipated that the line BC continues beyond C and that, above the critical diameter, the low velocity regime gradually disappears. Photographs taken in this region bear out these inferences, at least in a qualitative way. In fact, this phenomenon has been observed and commented on before(2) but no adequate explanation of the mechanism of the change-over has previously been offered.

Another interesting feature of the results is the indication that the sensitiveness to initiation of a given explosive varies with cartridge diameter, the smaller diameter cartridges being more difficult to initiate. This confirms the earlier inference, based on other evidence, that sensitiveness to detonation is a property of the explosive cartridge or charge rather than that of the explosive substance.

The fact that the minimum diameter for propagation of detonation is the same for both high and low velocities of detonation may be fortuitous because there is evidence that this is not the case with other two-velocity explosives. Thus Blasting Gelatine detonates at the high velocity in diameters too small to propagate low velocity detonation whereas the opposite is true for Polar Saxonite No. 3.

It may be said in conclusion that the results of the experiments described above confirm predictions relating to the behaviour of detonation in a two-velocity explosive which were based on the assumptions that initiating power, sensitiveness to initiation and sensitiveness to propagation are inter-related and can be defined in terms of the rate of detonation.



Transmission of Detonation - High Speed Camera Photographs

# Jones and Cumming

# References

(1) A. Marshall "Explosives" Vol. 2, p. 429.
London, 1917.

(2) E. Jones Nature, <u>161</u>, 1948, 98. D. Mitchell

#### INITIATION OF MILITARY EXPLOSIVES BY PROJECTILE IMPACT

# J. M. Dewey Ballistic Research Laboratories Aberdeen Proving Ground, Md.

#### INTRODUCTION

An experimental study of the factors controlling initiation of detonation in impact of high speed fragments has been undertaken. The first phase has been aimed at an understanding of the many discrepancies in the literature. (1) Tetryl was used because of the convenience of its relatively high sensitivity, with Composition B (60/40 cyclonite TNT) for comparison.

#### RESULTS AND DISCUSSION

It was found that detonation was initiated, if at all, either at the surface of impact or where explosive was trapped between a projectile and a backing plate. Neither a backing plate nor the thickness of the explosive (above the critical diameter) affected the first process. No burning starting at the initial impact of the projectile has been observed. Ignition frequently results from flash of the projectile against a backstop, following break-up of the charge by the projectile, as seen in Figure 1. In one case a 2-1/2" x 1" Composition B disc struck by a Caliber .50 flat-ended steel slug spalled, apparently in powdered form, and the spall was ignited or detonated at impact on the metal backstop, giving a bright flash. Tetryl pellets (density 1.48 - 0.04 g/cc) 1/2" thick burned, under the conditions of these experiments, when struck by Caliber .30 carbine ball (which has an approximately hemispherical nose) at velocities above 700 m/s, while a velocity of 900 m/s was required with 1" thick pellets. At velocities up to 1000 m/s neither Caliber .30 nor Caliber .50 standard ball, which have streamlined contours, caused burning or detonation of an unbacked charge. The charge, whether of cast or pressed explosive, simply broke up under impact. As Kouba(2) reported in 1947, shape, size, and velocity, not mass and velocity, of the projectile determine the result. Charges backed by metal detonated within the hole in the back plate, as could be seen by observation of the plate.



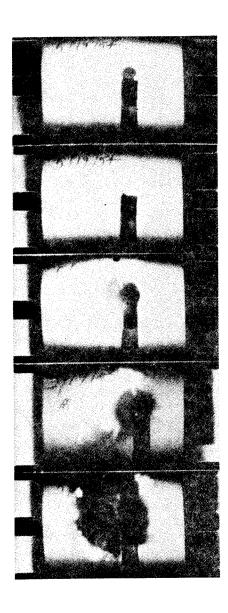


Figure 1 - Ignition of Comp. B Discs by Flash at Backstop, about 5000 Frames/Sec.

Flat-ended brass cylinders of various lengths were fired against Tetryl and cast Composition B. As far as possible in rapid setting up of charges, impact was normal. The results on the effect of the shape of the impacting surface of the projectile lead to the conclusion that small variations from normal would have little effect, since a small area of contact is ineffective at the velocities used. No effect of mass was observed with differing lengths. The lowest velocity at which a projectile caused detonation was sensitive to the diameter of the projectile but not to its length. Caliber .30 cylinders do not detonate Comp B at velocities up to 1000 m/sec. Figure 2 gives results with Caliber .50 cylinders. Figure 3 gives results with Caliber .30 cylinders fired against Tetryl, plotted against velocity and against kinetic energy. It is seen that the slight correlation with kinetic energy results only from the small range of masses used. "Partial detonation" means that detonation was followed by burning. This is shown by the jagged irregularities in the luminosity seen in frames of the high-speed motion pictures following the single frame overexposed by the luminous airshock resulting from detonation, as well as by very assymetric shock fronts in one-half microsecond single frame photographs. Figure 4 gives examples, while Figure 5 shows detonations believed to be complete. The term "low order detonation" has been avoided because it appears to have as many meanings as there are authors in the literature of initiation. Incomplete detonation can also be detected by the apparent duration of the luminosity. With the 22g to 45g Tetryl pellets used, film blackening followed detonation for 3 to 12 milliseconds. When burning but no detonation occurred. the apparent luminosity persisted for 30 to 80 milliseconds. particular values are, of course, without significance, since they depend on the photographic method and on the size of the charge, but the absence of overlap suggests that a practical field test for complete detonation could be developed from observations of times of luminosity with particular charges and cameras. Probably the longer times of luminosity observed following detonations result from burning following incomplete detonation. The data reported here are not suited to a statistical test of the reliability of this method of identifying complete high order detonations, as most of them were obtained in the course of experimentation with the instrumentation.

#### INTERPRETATION IN PHYSICAL TERMS

All of the results are consistent with the idea that impact is effective in initiating detonation when it produces a high gradient of compression and therefore of temperature. In backed explosives, this may occur in a layer trapped between projectile and backing. With a bare free charge struck by a blunt-ended projectile a strong compression shock is propogated, while with a streamlined projectile the pressure is relieved by the motion of the explosive sidewise. Hot spots, which Bowden and co-workers (1) have found so important in thin films, may be essential also in initiating detonation in bulk

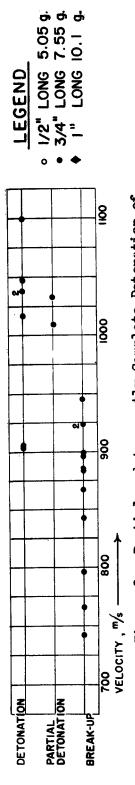
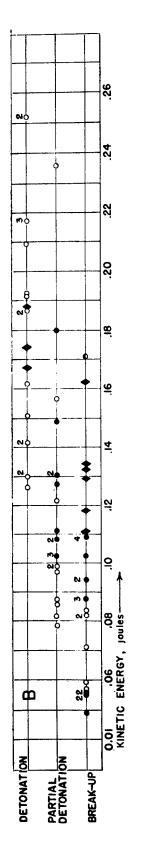
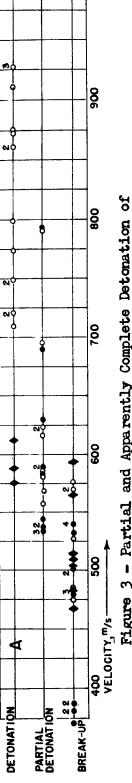


Figure 2 - Partial and Apparently Complete Detonation of Composition 'B' by Impact of .50 Caliber 21g. Cylinders (3/4") long) vs Velocity of Cylinders





8

Figure 3 - Partial and Apparently Complete Detonation of Tetryl by Normally Impacting Flat-ended .30 Caliber Cylinders: A, vs Velocity of Cylinders; B, Kinetic Energy of Cylinders

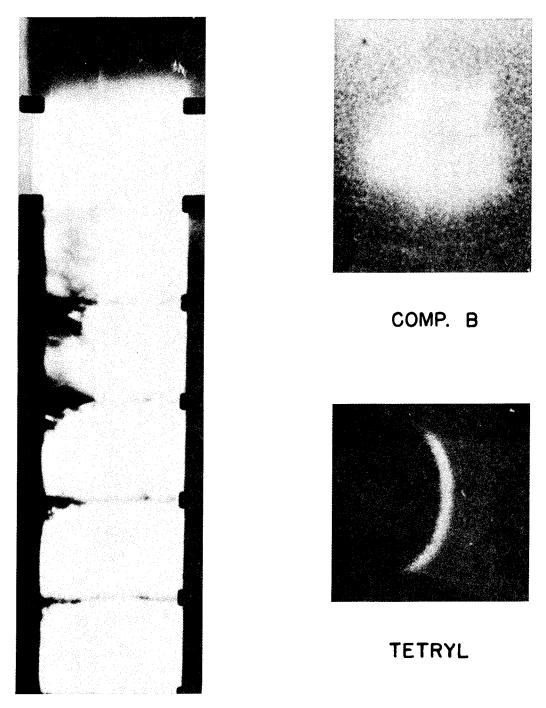
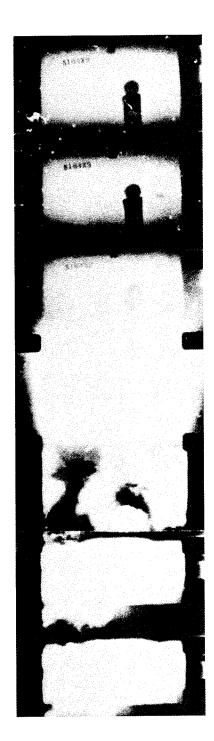


Figure 4 - Partial Detonations. Single Repatronic Frame at Upper Right of Same Detonation as Fastax Frames



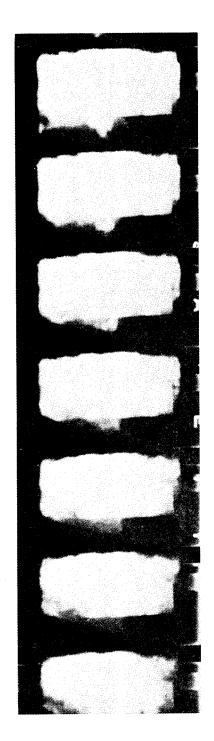


Figure 5 - Apparently Complete Detonation

explosives. They will always be provided by the granular nature of military explosives, even in the absence of the foreign material usually present. A gradual rise in temperature is ineffective because the explosive decomposes thermally or burns before the temperature required for detonation is reached, while a shock or entrapment of a thin layer raises the temperature too rapidly for the slow reaction to occur before the more rapid one. If a shock mechanism is the effective one, no effect of the mass per unit area of projectiles impacting on a bare charge should be observable, since the detonation occurs within a few microseconds after impact. An extremely short projectile would be required to show a mass effect in this short time. Nor should the material of the projectile be of importance. Only a material softer than the explosive would be sufficiently easily deformed to reduce the shock strength appreciably.

The effectiveness of backing a thin layer of explosive may under some circumstances result from the increase in shock strength occurring at reflection. In thicker layers decay would prevent initiation at the surface of reflection by shocks too weak to be effective at the surface of impact.

It is planned to check these points and to greatly extend the range of projectile masses used in order to distinguish more positively between area and mass effects.

#### INSTRUMEN TATION

Projectiles are fired from a modified machine gun or a Mann barrel, varying the velocity by changing the powder load. The velocity of each round is measured by foil screens triggering 1.6 megacycle Potter counters through a simple pulse shaping and lock-out circuit. Three screens are used in a distance of 1 meter.

Observations are made with Kodak or Fastax high-speed cameras and with Model No. 2208-1 (one-half microsecond exposure) Rapatronic cameras. (2) The photoelectric trigger circuit of the latter camera furnished with the Faraday shutter is not satisfactory for initiation work as the delay varies with light intensity, usually exceeding 20 microseconds from the time of impact. Thus, the air shock following complete detonation is all that is seen. As it would be excessively inconvenient to use any other type of triggering, a circuit with a smaller delay was substituted. Triggering on the initial flash is still not obtained and further work is required to give a reliable interpretation of all the results. It is hoped to improve this part of the instrumentation and use two Faraday cameras with a known interval between exposures to observe separately the first stage of initiation and the airshock formed when detonation is complete. photoelectric trigger does not operate unless some detonation occurs. Each round which triggers the Faraday camera gives a single overexposed frame on the Fastax followed by a short period of luminosity. In spite of the close agreement of results of the two types of cameras

on the occurrence of detonation, the use of two types of camera should lead to a better understanding of the partial detonations by giving an extended view and one rapid enough to show the form of the airshock. A Polaroid-Land back on the Rapatronic camera makes immediate observation of the result of each round possible, a great convenience in field firings.

Little reliance can be placed on direct observation. With bare charges the sound correlates with the occurrence of detonation but gives no indication of its extent. With backed charges even this cannot be said. Some effort was made in the first firings to improve the estimates made without instrumentation by the use of witness plates, viewing in a mirror, etc. The reliability of such estimates remained so low that they were abandoned.

As hits near the edge of a charge are relatively ineffective, the high-speed camera record was used to determine the point of impact. Rounds on which neither the projectile nor the point of impact could be seen were discarded. The cast charges were X-rayed for uniformity but only those with gross defects, such as cavities, were discarded. They were prepared by cutting from a carefully cast cylinder and are considerably more uniform than service rounds. Nine Tetryl pellets had densities ranging from 1.45 to 1.55, suggesting a lower degree of uniformity. As sensitivity is known to vary with density, this variability may account for much of the variation in results seen in Figure 4A.

Future work will be directed toward a better understanding of results of practical weapons tests, so that reliable predictions can be made of the results of new conditions.

#### REFERENCES

- 1. Most of the literature is confidential. Important exceptions include:
  - E. K. Rideal and J. B. Robertson, Proc Roy Soc A195, 135, (1948).
  - G. B. Kistiakowsi, Third Symposium on Combustion and Flame, The Williams and Williams Co., Baltimore (1949) p. 560.
  - F. P. Bowden and A. D. Yoffe, The Initiation and Growth of Explosions in Liquids and Solids, Cambridge Monographs on Physics, Cambridge University Press (1952). The Fourth Symposium on Combustion, The Williams and Wilkins Company (1953) p. 161.
  - 2. NOrd Contract with Hercules Powder Company.
- 3. M. Sultanoff and R. A. Bailey, The Application of the Faraday Magneto-Optic Effect, etc., BRL 791, (1951).

# FACTORS AFFECTING THE TRANSMISSION OF DETONATION BETWEEN SMALL EXPLOSIVE CHARGES

L.D. Hampton, J. Savitt, L.E. Starr, R.H. Stresau U.S. Naval Ordnance Laboratory Silver Spring, Maryland

#### Introduction

Almost all intentionally established explosive reactions, whether for laboratory experiments, commercial applications, or in ordnance items, are initiated by means of relatively weak impulses. These weak impulses, whether mechanical, electrical, or thermal, generally ignite deflagration of the explosive material which, under favorable circumstances, accelerates rapidly, generating shock waves which may be intense enough to establish detonation. By the nature of this process, the incipient detonation thus established is the mildest reaction which can propagate as a detonation and must grow to its stable rate. The various phases of this process have been discussed by Kistiakowski(1), Bowden and Yoffe(2), Eyring et al(3) Andreev(4), Gamow and Finklestein(5), and many others.

The use of a large charge of an explosive in which this entire process will readily take place is so hazardous that it is almost never done. The usual practice is that of subdividing the explosive charge into two or more components in which there is a general inverse relationship between size and sensitivity and of isolating the smaller, more sensitive, components from the larger ones until as shortly as possible before the charge is to be detonated.

Mechanical design considerations and the fact that the most effective material for one phase of this process is not necessarily the most effective for another phase results in further subdivision of explosive charges. Practically every detonation of intentional origin, in the course of its growth, has encountered one or more discontinuities. The reliability with which detonation can be transmitted across these discontinuities is affected by a wide variety of factors including the properties of the explosive materials involved, the densities at which they are loaded, the materials in which they are confined, their absolute and relative

sizes, their relative positions, and the nature and position of any intervening materials. It is obvious that so many permutations of these factors are possible that there will never be time to investigate all of their interactions.

Most of the work which has been done by the authors in this field has involved determinations of the conditions under which one charge, which we have called the "donor", will initiate another known as the "acceptor". In some cases, the donors and acceptors were standard or proposed explosive train components such as detonators, leads, boosters, or simulated main charges. More often, special, idealized components have been used.

Experimentally, detonation is usually considered to have been transmitted between two charges if the acceptor detonates with nearly its maximum intensity. Under some circumstances the criterion used to differentiate between "fires" and "misfires" introduces questions of orders of detonation, but in most experiments the output of the acceptor is either practically negligible or so near the maximum that the differences are difficult to detect. It does not follow that all charges classified as "fires" are initiated at their stable detonation rates. The usual situation is quite the opposite since, in experiments aimed at determining the threshold conditions for initiation, most trials will be made under conditions very near the threshold. It does follow that most explosive charges, if they detonate at all, build up to stable detonation quite quickly. The transmission of detonation involves the completion by the donor of the establishment of conditions which insure the growth of detonation. Whether the dominant initiation mechanism is homogeneous compressive heating of the solid explosive, interstitial heating related to inhomogeneity, or ignition by air shock and reaction products, conditions necessary for the growth of detonation are those of high temperature and pressure.

In each of the transmission mechanisms mentioned, the growth of detonation depends upon the rise of temperature and pressure due to the excess of heat and gas evolved over that lost to the system. Due to the short times involved in these processes, heat losses due to conduction are probably second order effects so that the principal cooling mechanism is the expansion of the gases and other materials present. The most important factors which affect the transmission of detonation are those which affect the vigor of the reaction which is established in the acceptor and those which retard the expansion of the products of the reaction. In most experimental situations, the various factors involved are so interwoven that it is difficult to separate their effects, but most of the experimental results illustrate these generalities so obviously that this fact hardly needs to be pointed out.

# Experimental Procedure

#### General

The data discussed herein were obtained by a variety of experimental procedures. Quite a few of these experiments were determinations of the critical conditions for the initiation of detonation in one explosive element by means of another. The critical condition is defined as the least favorable of the series of related conditions for which the donor will initiate detonation of the acceptor. Such information unfortunately cannot be obtained for any one combination of a donor and an acceptor. All that can be learned from one shot is that the acceptor was or was not initiated. The first experiment which suggests itself is that of "working up" to the critical point from each side with a series of straddling shots using identical donors and acceptors. However, it is impractical, if not impossible, to make components which are nearly enough identical for this type of experiment, thus each set of donor and acceptor has a unique critical point. The experiment must be directed toward determining the average critical point which, upon a little reflection, can be seen to be the point at which 50% of the acceptors fire. During the past war a method for determining such statistics was devised by the Explosives Research Laboratory, Bruceton, Pa. It was analyzed and refined by the Statistical Research group of the Applied Mathematics Panel at Princeton. method. which will be referred to herein as the Bruceton method, involves a series of trials the conditions for each of which are determined by the result of the previous trial, and is described in more detail in a report of the Statistical Research group of the Applied Mathematics Panel (6).

#### Criteria of Detonation

The Bruceton method is applicable only where the result of a single trial can be placed definitely in one of two categories; in the case of propagation tests, detonation or failure of the acceptor.

Detonation in a marginally initiated charge, quite obviously, is initiated at something less than its stable rate. Stable detonation is achieved only after a certain amount of the acceptor explosive has been consumed. As the vigor of initiation is increased, the quantity of explosive consumed in the growth process should be expected to decrease with a corresponding increase in the output of the acceptor as indicated by the damage to its case or by other criteria which might be used. Thus, in an experiment to determine the conditions under which detonation is transmitted from one charge to another, the result may depend upon the criterion of detonation used to classify a given trial as a "fire" or "misfire". The seriousness of this effect depends upon the relationship between the rate of build-up and the variation of characteristics from one individual donor or acceptor to another. It will be shown in a later section

of this paper that this effect can be quite serious under some conditions but that it has negligible influence in the range of conditions under which most of the data reported herein were obtained. In the Bruceton up and down experiments which were used to obtain a large part of these data, individual trials in which the classification would have been changed by a reasonable change in the criterion of detonation were rare.

#### Physical Arrangement

Although data obtained by means of a variety of experiments are discussed herein, experiments of the kind schematically illustrated in Figures 1 and 2 are the sources of most of the data.

SOLID EXPLOSIVE

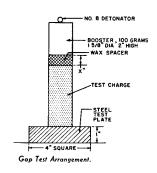


Figure 1
Booster Sensitivity Test(7)

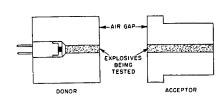


Figure 2
Small Scale Gap Test(7)

The experimental arrangement shown in Figure 1 was used by Eyster, Smith, and Walton (8) to investigate the effect of a variety of factors upon the transmission of detonation. That shown in Figure 2 has been used extensively by the authors of this paper. The energy transfer between donor and acceptor in the booster sensitivity test is accomplished by the transmission of shock waves through and between solid materials, a relatively simple process. Transmission across an air gap as in Figure 2 is somewhat more complicated since the air in a shock zone is extremely hot, of the order of 10,000°C(9), and is followed by a mass of product gases whose particle velocity is close to the shock velocity and whose

density is quite appreciable. Both the high temperature of the air and the high kinetic energy of the product gases may be more important factors in the transmission of detonation than the air shock as such. The confinement, which is necessary because of the small scale, adds further complexity. The differences between these two types of experiments are such that any points on which they agree must be of reasonably general applicability.

#### Observations and Discussion

# Factors Related to Dimensions of Explosive Charges

It is self evident that the effectiveness of the transmission of detonation should increase with the size of the donor charge. With very small donors, the diameter effect can cause significant decrease in the stable detonation velocity and the detonation may not grow to its maximum stable rate. After stable detonation at a rate closely approximating the plane wave detonation rate has been achieved, the effectiveness of a donor continues to increase with size because the larger mass of explosive products takes longer to expand and thus maintains conditions conducive to growth of detonation in the acceptor for a longer time. In a gap or barrier test, this combines with the general scaling law which applies generally to explosion phenomena. As the diameter of the donor is increased the critical gap or barrier thickness increases more rapidly. In Table I some data of Eyster, Smith, and Walton (8) show this relationship.

		Critic	cal Thicknes	ss, Wax	Barrier
Booster Diam.	Weight				
(inches)	(gm)	Pentolite	Comp A-3	Comp E	Picrate

(inches)	(gm)	Pentolite	Comp A-3	Comp B	Picratol 52/48
1.00	40.8	1.13	0.99	0.79	0.41
1.57	100.	2.08	1.70	1.32	1.00
2.50	254.	3.50	3.91	2.29	1.77

Table I
Booster Sensitivity Test - Scaling Experiments
(Tetryl Booster - Two Inches Long)

The relationship is also apparent in Figure 3 from data of some of the present authors. The deviation from geometrical scaling can be ascribed to the time factors involved. The times associated with the hydrodynamic shock phenomena are essentially transit times and hence vary proportionally with linear dimensions while the reaction time of the acceptor explosive is dependent upon local conditions in the reaction zone.

The principal effect of acceptor diameter is that upon the resistance of the system to the expansion of the material of the

reaction zone. When an explosive charge is unconfined, its resistance to expansion increases, of course, with its diameter so that larger charges are more easily initiated. This effect has been demonstrated by Eyster, Smith, and Walton(8). When the acceptor is heavily confined in a metal such as copper, the effect of its diameter upon its apparent sensitivity is somewhat more complex. The explosive material affords less resistance to expansion than the confining medium so that a small reaction nucleus is supported by the proximity of the walls. Thus the apparent relative sensitivity of the acceptor depends upon the donor diameter. Figure 3 shows this quite forcibly. Note that, under the conditions of these experiments, the optimum acceptor diameter is slightly less than the donor diameter.

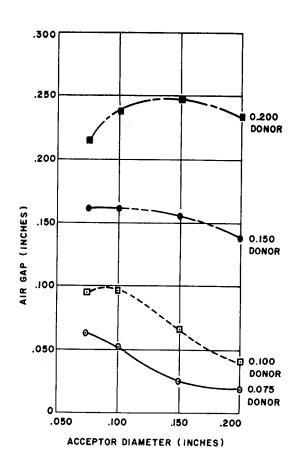


Figure 3
Air Gap in the Small Scale Gap Test as Related to Acceptor and Donor Diameter

Where the growth of detonation is incomplete, the effectiveness of a donor may be expected to increase sharply with length. This principle is of great practical importance when the donor and acceptor are the intermediate and base charge of a detonator. It is

discussed in some detail by the present authors in a recent paper (10). Where the transition from burning to detonation takes place in lead azide it is so rapid that the effect of column length observed in most experiments is that associated with the growth of the "head" of reaction products rather than that of the detonation. As the length of a donor column is increased the length of the head of gases behind the detonation front is increased up to the point where radial losses become prepoderant. Beyond this point, further increases in length result in no increase in effectiveness. This point depends upon the manner in which the donor is confined. The length of the head affects gap test results through its effect on the attenuation of the transmitted shock and accompanying phenomena and in resisting the rearward expansion of the acceptor reaction products. As might be expected, a given increase in charge weight is less effective in increasing the effectiveness of a donor when it is added by increasing the length than when the diameter is increased, Figure 4.

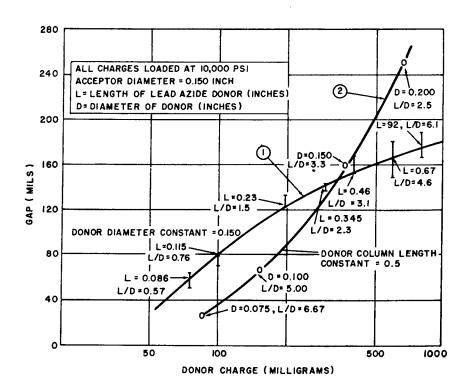
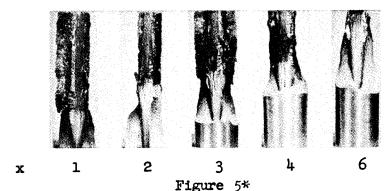


Figure 4
Critical Axial Air Gaps Across Which Detonation is
Transmitted Between Lead Azide and Tetryl

The effect of acceptor length upon the transmission of detonation is usually quite small. Where a short denor is backed

by a metal plate, the shock reflected from the backing plate might be expected to reinforce the incident shock and increase the apparent sensitivity. One of the present authors has shown(11) that for one such system, the length of the donor had to be reduced to 0.025 inches, a very small fraction of any other dimension involved, before this effect could be detected. A second effect of acceptor length upon sensitivity which may be real or apparent depending upon interpretative point of view is that related to growth of detonation in the acceptor. Under circumstances where the growth of detonation may require a column length of the same order of magnitude as the acceptor, a longer acceptor might build up to a point where it would be classified as a "fire" while a similarly initiated acceptor of lesser length would be classified as a "misfire". In Figure 5 it is demonstrated that circumstances are possible under which appreciable column lengths are required for the growth of detonation.



Explosive Container Fragments Showing the Effect of the Vigor of Initiation Upon the Growth of Detonation in Tetryl

\*The distance (x) between a donor of PETN loaded at a pressure of 10,000 psi and the three inch long acceptor of tetryl, with a diameter of 0.300 inches, loaded at a pressure of 4,000 psi, was varied as indicated. Note that the growth to high order detonation in the acceptor as reflected by the distortion of the acceptor container can be quite gradual for large values of x and that the distance required in the tetryl for the reaction to grow to high order detonation increases with increasing x, that is with decreasing vigor of initiation.

# Factors Related to Composition of Explosive

In general, explosives which are more "brizant" as indicated by high detonation velocity, large plate dent results, etc., are more effective as donors, and those which are more sensitive by other standards, such as impact sensitivity obtained using drop tests, are more sensitive acceptors. In experiments to determine the minimum booster required to initiate cast TNT it was found that 6.1 grams of RDX/wax, 97/3 is equivalent to 8.3 grams of tetryl. Figure 6 shows the correlation between impact sensitivity and critical air gap.

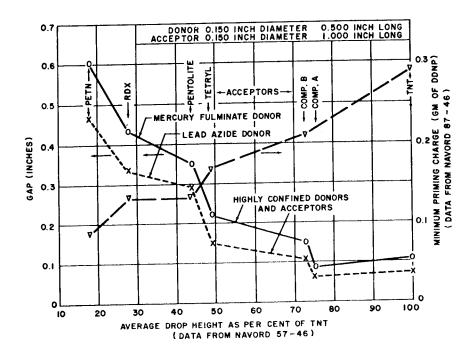


Figure 6
Minimum Priming Charge and Gap for Critical Propagation
as Related to Impact Sensitivity

Where the donor is very small, as for example in "minimum priming charge" experiments, the rapidity with which the explosive effects the transition from burning to detonation is the predominant factor in its effectiveness. Good correlation has been obtained between minimum priming charge experiments and other measurements of the rate of this transition (10).

The effect of additives upon sensitivity to initiation is not necessarily proportional to that upon impact sensitivity. The sensitivity of RDX to initiation by other explosives, for example, is much more sharply reduced by the addition of wax or similar materials than is its impact sensitivity. Note, in Figure 6, the inversion between Comp A and TNT.

The correlation between impact and initiation sensitivity apparently does not apply to explosives which are mechanical mixtures of fuels and oxidizers. This may be related to the necessity for more intimate mixing during the reaction time. In some such mixtures considerable difficulty has been experienced in producing a material with acceptable impact sensitivity which can be initiated with a booster of reasonable size.

# Factors Related to States of Aggregation

Charges of solid explosives are made either by casting them or by pressing from granular material. In either case large variations in grain or particle size are possible. In addition, the density of pressed granular explosives may be varied over a wide range. The effects of the voids in pressed granular explosives may be enumerated as follows:

- 1. A large increase in effective surface area which makes the material more ignitable and increases the mass reaction rate for a given surface burning rate.
- 2. An increase in the overall compressibility and the proportion of the energy of a shock converted to interstitial heat. The result is that much weaker shocks can cause reactions of sufficient vigor to propagate as detonations.
- 3. An increase in the effective free volume with the result that a given reaction rate results in a slower pressure rise and thus tends toward less rapid acceleration of the reaction.
- 4. A decrease in the velocity and pressure of stable detonation with increasing percentage voids.
- 5. A reduction in the "acoustic impedance" both because of the reduced density and the increased compressibility. This results in an improvement of shock transmission between the explosive and low impedance media such as air and deterioration of shock communication with high impedance media such as steel.

It is quite plain that these effects may reinforce or counteract one another in their influence upon the transmission of detonation depending upon circumstances.

Most primary explosives depend upon a combination of the first two of these effects to promote the transition from burning to detonation. When pressed to a density above a limit characteristic of the explosive they refuse to effect this transition. This phenomenon is known as "dead pressing". It has been stated frequently that mercury fulminate is dead pressed at loading pressures in excess of 25,000 psi. Some of the present authors have shown that this figure may vary from 5,000 to 80,000 psi depending upon

conditions of confinement. Lead azide shows less tendency than other explosives to "dead press" probably because its extreme hardness results in quite high percentages of voids at practical loading pressures. However, "dead pressing" effects have been observed with lead azide and may cause trouble where confinement is poor, particularly if the lead azide has been loaded in a high humidity atmosphere. Where "dead pressing" is not a factor, the third and fourth effects mentioned above result in a general increase in the effectiveness of donors with increasing density.

The manner in which these effects combine to determine the sensitivity of an acceptor is quite obvious when considered qualitatively. Quantitative consideration of the effect of density on the transmission of detonation has not been undertaken. The combined effects can be observed experimentally but it is difficult to separate them. In air gap experiments, the apparent sensitivity decreases with increasing density within the usual range of densities used in ordnance. Where barriers of other materials are involved, this relationship may change. In Figure 7 the effect of density on critical gap is compared with that on critical aluminum barrier. Note that the air gap varies much more sharply with density than does the barrier. Dodd(12) found that, with combined air gaps and steel barriers, the optimum density of tetryl as an acceptor was in the neighborhood of 1.5.

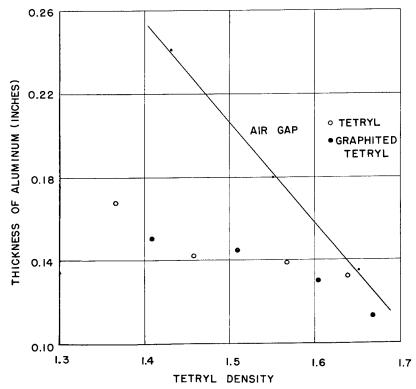


Figure 7
Propagation of Detonation Lead Azide to Tetryl

In explosives loaded to densities lower than is the usual ordnance practice, the growth of detonation is slower and the line between "fires" and "misfires" becomes more nebulous. The choice of criterion of fire can have a substantial effect upon the estimate of the critical gap, Figure 8.

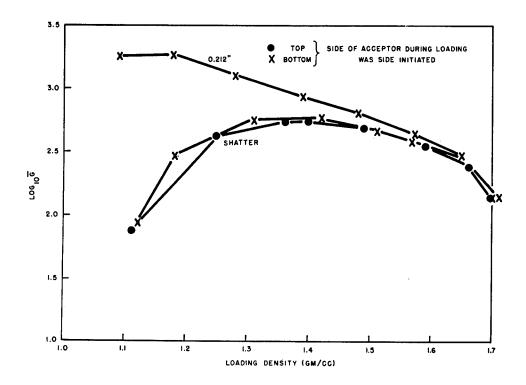


Figure 8\*
Dependence of Air Gap Sensitivity of Tetryl Upon Loading Density and Criterion of Fire

<sup>\*</sup>Regular Bruceton type air gap sensitivity tests were performed with donors of PETN loaded at pressures of 10,000 psi and acceptors of tetryl loaded at pressures varying from 500 to 80,000 psi. Note that for the lower densities there is a complete reversal in the order of sensitivity with density when the criterion of the Bruceton test is varied from one requiring that the acceptor container be shattered to one requiring that the end of the explosive cavity farthest from the donor be expanded from 0.200 inches to 0.212 inches diameter.

Similarly particle size effects on the transmission of detonation may be taken as evidence of the role of surface burning in incipient and growing detonation. In an investigation of such effects coarse sieve cuts were invariably less sensitive to initiation than fine cuts of eight different lots of tetryl(13). Typically, the critical gap for the initiation of tetryl which was held on a number 35 sieve was 0.128 inches while that for tetryl of the same lot which passed through a number 45 screen was 0.150 inches.

Cast charges are less sensitive than pressed charges of the same explosive. The difference is more than can be explained in terms of loading density. Eyster, Smith, and Walton(8) report 0.82 inches for the critical thickness of wax barrier for the initiation of cast TNT (density 1.60) and 1.68 inches for pressed TNT (density 1.55). The grain size of cast explosives affects their sensitivity, in a manner similar to that of the particle size of pressed explosives. In minimum booster tests carried out by present authors(14) a booster of 9.3 grams of tetryl was required to initiate TNT cast at 100°C under conditions where "creamed" TNT, cast at its melting point, was initiated by 8.3 grams of tetryl. The crystals of TNT in the case of the hot charges were of the order of an inch in length, while those in the creamed material were microscopic.

#### Factors Related to Confinement

Rather few explosive experiments are carried on in vacua. Explosive charges are generally bounded by inert (non-explosive) media. Whenever a detonation reaches a boundary the shock is transmitted to the adjacent medium, with a resultant displacement of the interface between the explosive and the inert medium. Similarly, the more gradually rising pressure associated with growing deflagration can cause motion of the interface. When a wave such as a shock is transmitted from one medium to another the concept of impedance coupling is useful. The characteristic acoustic impedance of a medium is defined as the product of its density and the velocity at which sound propagates in it. Similarly, the characteristic shock impedance of a medium might be defined as the product of the density and the velocity at which a shock propagates in the medium. The variation of shock with amplitude is reflected in a variation of the shock impedance. A rigorous treatment taking this variation into account would be severely limited by the lack of equation of state data in the pressure range associated with detonation phenomena. For some materials, information is available regarding the velocities of shocks of this strength. For these a useful approximation is the assumption that the velocity is constant for that part of the shock wave which is important in the propagation of detonation.

In another paper of this conference (15) it is shown that the length of the head of reaction products behind the detonation front of a confined column of explosive is directly related to the shock

impedance of the confining medium. As mentioned above, the length of the detonation head of the donor can have an effect on the transmission of detonation. In one experiment(13), lead azide donors 0.10 inches in diameter, confined in steel and brass, initiated tetryl acceptors across mean gaps of 0.057 inches and 0.058 inches respectively, while those confined in aluminum would initiate the same acceptors across a mean gap of only 0.030 inches. The shock impedances of steel, brass, and aluminum are 4.2, 3.9, and 1.7 megarayls\* respectively.

As pointed out in the introduction, the growth of detonation in the acceptor depends upon an increase in pressure resulting from the excess of gaseous products and heat produced by the reaction over losses, which are associated with expansion. In an air gap test the rearward expansion of the reaction products of a recently initiated acceptor is retarded by the presence of the donor product gases to an extent related to their mass and density. The resistance of the confining medium to radial expansion is related to its shock impedance. Table II gives critical air gaps obtained with a series of systems which were made as similar as possible except for the confining medium of the acceptor. Also given are shock impedances of the acceptor materials as obtained by Slie (15).

Confining Medium of Acceptor	Shock Impedance of Acceptor Confinement(1 (megarayls)	Critical Air Gap (16) (15) (lead azide to tetryl) (0.150 inch diam.columns)
Lucite	0.7	0.063 inches
Magnesium	1.4	0.088 "
Zinc (die cast)	2.6	0.101 "
Babbitt	3.2	0.148 "
Bronze	4.2	0.105 "
Brass	3.9	0.153 "
Steel (SAE 1020)	4.2	0.260 "

Table II

Critical Air Gaps Related to Acoustic Impedance of
Acceptor Confining Medium

The effect of confinement upon acceptor sensitivity varies with the explosive material. Table III, from some measurements of  $\operatorname{Dimmock}(17)$ , gives critical gaps obtained for a number of acceptor explosives using two systems which differed mainly in the confinement of the acceptor. Note the inversions between tetryl and RDX and between TNT and Comp A.

<sup>\*</sup>One rayl or acoustic ohm is equal to one gram per square centimeter per second.

cceptor Explosive	Acceptor Confinement			
Material	Brass	Aluminum		
Comp A	0.046 inches 0.049 "	0.017 inches < 0.010 "		
Comp B Tetryl	0.062 " 0.082 "	0.039		
RDX	0.101 "	0.050 "		

Table III Critical Gaps for Various Explosives for Two Confinements

The above discussion has concerned itself with the effects of confinement of explosives by containers so thick that they may be considered to be infinite. No systematic data are at hand regarding the effect of confinement in thinner walled vessels upon the transmission of detonation. The scattered data which are at hand suggest to the authors that, as in most confinement effects, the sensitivity or effectiveness rises sharply with thickness at first and approaches a maximum at a point where the wall thickness is of the order of the diameter of the explosive column.

Confinement of an air gap between two explosive charges can have a very large effect upon the critical length of such a gap. Notice the order of magnitude difference between the confined gaps used in the experiments illustrated in Figure 5, and the unconfined gaps associated elsewhere in this paper with explosive charges of the same size. Here again systematic data are lacking. Dodd(12) showed that, for one system, a gap smaller in diameter than the donor resulted in more effective transmission of detonation than one much larger. Using another system, one of the present authors showed that a gap equal to or slightly larger than the donor resulted in more reliable transmission than a gap somewhat smaller in diameter than the donor. With still another system, others of the present authors could detect no difference between a gap confined in a tube slightly larger than the donor and one three times the diameter of the donor. In all three of these experiments, the donors were detonators with metal cups and additional barriers were involved.

# Factors Involving the Nature of the Separation Between the Charges

Most of the experiments discussed above are determinations of critical air gaps between coaxial cylinders of explosive. Although this type of experiment is a convenient tool for the investigation of the effects of many of the factors involved in the transmission of detonation, most practical transmission problems involve more complex systems. The permutations of the interactions involved in such systems are overwhelming in number. The data available are too diverse and "spotty" to give a clear, connected picture. Some of

them, however, are quite revealing.

The transmission of detonation between two separated charges involves the transmission of a shock wave from the donor explosive to the intervening medium, through the medium, and to the acceptor explosive. Unless the shock impedance of the intervening medium is an exact match to that of the explosive, the shock must be partially reflected, either as a shock or as a rarefaction, at the interface. Either type of reflection will cause the energy of the transmitted wave to be less than that of the incident wave.

The application of the concept of impedance coupling to detonation transmission and the limitations of this application may be illustrated using some data of Eyster, Smith, and Walton(8). Determinations were made of the critical barrier through which detonation could be transmitted from tetryl boosters to various explosives. Measurements were also made of the dents made in steel by tetryl boosters from which they were separated by various thicknesses of the same barrier materials. By interpolation, these data may be used to obtain the depth of dent produced by a combination of booster and barrier which will initiate a given explosive 50% of the time. This depth varies with the barrier material. If it is assumed that the shock energy which must be transmitted to the explosive in order to initiate it is independent of the transmission medium and that the depth of dent produced is a direct measure of the energy transmitted to the steel block, impedance coupling principles may be used to compute the relative depth of dent which should be associated with 50% functioning. Table IV gives the critical barrier thicknesses for the initiation of Comp B together with the corresponding depth of dent as interpolated from experimental data and as computed using impedance coupling considerations.

Comp B Acceptor  Barrier Material Barrier Thickness (50% Point) Corresponding De				
Dallier Processor	2011201 1112011010 () 0 10 10 10 10	Int.*	Comp**	
Air	1.21	0.039	0.006	
Wax Aluminum	1.46 1.51	0.013 0.0195	0.007	
Copper	1.17	0.032	0.031	
Polystyrene Wood (oak)	1.43 1.04	0.0115	0.0115 0.0093	

Table IV

Critical Barriers of Various Materials with Corresponding Dents Produced in Steel Plates

<sup>\*</sup>Interpolated from experimental data. \*\*Computed using impedance coupling principles. \*\*\*The dent produced by the 50% combination of booster and aluminum barrier was used in the computation of the computed barrier thickness of other materials.

It will be noted that the experimental and computed values give very good agreement between aluminum, copper, and polystyrene and somewhat worse for wax, while the experimental values for air and wood are completely out of line. The poor agreement for the wax barrier may reflect the lack of equation of state data for this material. As pointed out earlier in this paper, the phenomena associated with the transmission of detonation across air gaps is too complex to be characterized in terms of simple impedance coupling. Apparently this observation also applies to wood.

In some cases air gaps and barriers are combined. A special case of combined barriers and gaps is that in which a relatively thin solid barrier is in direct contact with the donor explosive and is followed by a gap. Under these circumstances, the barrier material which is hurled across the gap plays an important role in the initiation of the acceptor. Since it takes some distance of travel for the solid material to reach its maximum velocity, the most favorable conditions for transmission of detonation involve an optimum gap. Dodd(12) found that the optimum gap for one such system was about 1/16 of an inch. Graumannand Robertson(18) in another system, involving transmission between a detonator and a lead, found that the optimum was in the neighborhood of 1/8 of an inch, while some of the present authors, in a system involving the initiation of HBX by a booster, found that the optimum was in excess of a quarter of an inch. The data in Table V were obtained in some experiments directed toward determination of the critical length of booster for the initiation of cast TNT. In these tests, the booster was well confined both radially and from the rear. The booster cups of aluminum and of steel had bottoms about 0.070 inches thick. All boosters were a mixture of RDX and wax (97/3). In each test the thickness of booster for 50% initiation was determined by a variant of the Bruceton method.

Standoff Distance	Booster :	Length for	50% Initiation of TNT
	Steel	Cup	Aluminum Cup
0.000 0.050 0.100	0.347 : 0.325 0.215	inches	0.238 inches 0.181 "

Table V
Minimum Booster Length for Initiation of TNT at
Various Standoff Distances

An interesting feature of the results obtained with the steel booster cup is the substantial change in booster requirement as the gap was increased from 0.050 to 0.100 inches although the booster length needed with zero gap was not very different from that with 0.050 gap. An explanation which has been proposed for this effect is that the velocity of the bottom of the cup increases in steps as

it reverberates. Note that smaller boosters are required when aluminum cups are used. In another experiment(14) where determinations were made of the critical thickness of a second barrier of steel which was in direct contact with an HBX acceptor, this thickness was found to be 0.236 inches when aluminum cups were used and 0.400 inches when brass cups were used. Where a gap is interposed between a donor and an acceptor a barrier in contact with the donor can help bridge it and where a barrier is interposed a gap beyond it is conducive to improved transmission of detonation. Perhaps more surprisingly, it was observed that a tetryl booster which failed to initiate a charge of TNT when in direct contact with it in three consecutive trials caused high order detonation in eight of nine trials when an air gap was interposed.

When the donor is displaced from its alignment with the acceptor as shown in Figure 9 the transmission of detonation from donor to acceptor becomes more difficult. In Figure 10 the critical transverse displacements for the transmission of detonation between donors of lead azide and mercury fulminate and acceptors of various high explosives are graphically compared with critical axial air gaps for the same combinations of explosives. The "S" shape of these curves is apparently related to the point at which the expanded hole in which the donor charge had been loaded is tangent to the unexploded acceptor explosive. The initiation of some explosives, including tetryl, is apparently quite probable when the holes overlap, but quite improbable when they do not. This fact suggests that the initiation is related to contact with the acceptor explosive of the hot gases produced by the reaction of the donor explosive. For the more sensitive high explosives such as RDX and PETN the metal borne shock is apparently an important initiation mechanism. The deformation of the containers of these explosives sometimes showed evidence that initiation occurred at a point other than the end.

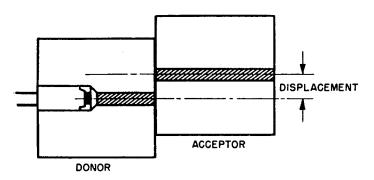


Figure 9
Arrangement of Donor and Acceptor in the Transverse
Displacement Tests

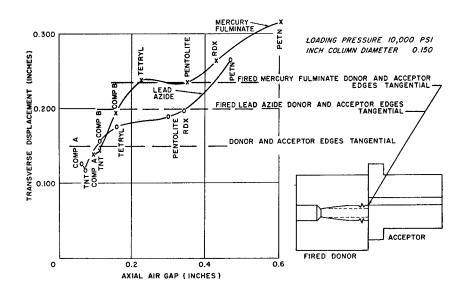


Figure 10
Initiation Properties of the Explosive Across Transverse
Displacement and Axial Air Gaps

In some cases explosive charges are initiated by means of smaller charges which are inserted in holes in the acceptor charges. This type of system may be quite effective. Army Engineer Corps special blasting caps of an old lot which were incapable of initiating Comp B charges reliably from any external position initiated the same charges quite reliably when inserted only 0.2 inches in holes over an inch deep. These results were obtained with holes ranging in diameter from 5/16 inch, which is a sloppy clearance fit, to 1/2 inch. Other evidence is also at hand which indicated that this type of initiation can be quite effective.

#### Factors Involving Special Geometry

One way in which detonation is transferred from one element to the next is by the use of the shaped charge principle in the so called "spit back" fuze. In the shaped charge a special shape is used on the end of the detonator which has the form of a cone with the apex pointing into the detonator. The detonation, upon reaching this cone causes it to collapse and forms a jet which concentrates the energy and makes it effective at considerable distances. This is used in certain applications in which it is desired to have a detonator in the nose of a shell initiate a booster in the rear. It should be pointed out that, since the shaped charge action is one of concentrating the energy put out by the detonator, the problem of aiming the jet becomes critical. If this jet does not strike the

booster properly it will, of course, not initiate it. It should also be pointed out that, under some circumstances the concentration of the energy in two dimensions by a shaped charge can result in greatly increased dispersion in the third. Where initiation is marginal because of the small diameter of the donor, the use of a shaped charge can result in complete failure (19). Such failures are characterized by extremely deep narrow holes in the acceptor.

Use has also been made of the shape of the boundary between two explosives loaded into the same element to control the form of the detonation wave as it reaches the exit end of the element. If a detonator, for instance, contains two explosive materials, the first having a detonation velocity less than that of the second, a curved interface, Figure 11, between the two explosives can be used to reduce the curvature of the detonation wave as it diverges from the point of initiation. If properly designed this could give a plane or converging wave at the exit end of the element.

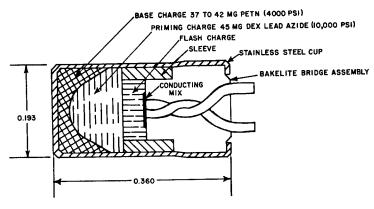


Figure 11
Eastman Form Charge Detonator

#### Conclusions

A number of reasonable mechanisms have been proposed for the transmission and growth of detonation, and for the losses which oppose these processes. The temptation exists to propose a mechanism, preferably one which can be reduced to manageable mathematics, and to try to explain all observable phenomena in terms thereof. The most emphatic conclusion which can be drawn from the observations discussed above is that yielding to any such temptation can lead only to confusion.

The transmission and growth of detonation involves a series of chemical and physical processes, each quite simple in itself, which

# Hampton, Savitt, Starr, Stresau

interact differently under different circumstances. These conclusions are generalities. More specific conclusions may be found above.

# Hampton, Savitt, Starr, Stresau

# References

- (1) Third International Symposium on Combustion and Flame and Explosion Phenomena, Williams and Wilkins, Baltimore, 1949, Initiation of Detonation of Explosives, pg. 560, G.B. Kistiakowski
- (2) Cambridge University Press, 1952, The Initiation and Growth of Explosions in Liquids and Solids, F.P. Bowden and A.D. Yoffe
- (3) Chemical Reviews, Vol. 45, pp. 69-181, The Stability of Detonation, H. Eyring, R.E. Powell, G.H. Duffey, and R.B. Parlin
- (4) Comptes Rendus de l'Academie des Sciences de l'URSS, 1946, Vol. 51, No. 1, pp. 29-32, On the Dependence of the Burning Velocity of Secondary and Initiating Explosives Upon the Pressure, K.K. Andreev
- (5) NAVORD Report 90-46, Theory of the Detonation Process, R.J. Finkelstein and G. Gamow, 20 April 1947
- (6) AMP Report No. 101.1R, OSRD Report 4040, Statistical Analysis for a New Procedure in Sensitivity Experiments, Statistical Research Group, Princeton University, July 1944
- (7) NOIR 1111, Ordnance Explosive Train Designers Handbook, April 1952
- (8) NOLM 10336, The Sensitivity of High Explosives to Pure Shocks, E.H. Eyster, L.C. Smith and S.R. Walton, 14 July 1949
- (9) NAVORD Report 2285, Shock Velocities in the Immediate Neighborhood of Detonating Explosives, R.H. Stresau and J. Savitt, 27 December 1951
- (10) Electric Detonator Symposium, Franklin Institute, September, 1954, Factors Affecting the Output of Electric Detonators, R.H. Stresau, L.D. Hampton, J. Savitt and W.M. Slie
- (11) NAVORD Report 2844, The Propagation of Detonation in Some Special Explosive Systems, J. Savitt, 13 April 1953
- (12) Ordnance Board Proceedings No. 30878 with enclosure dated 15 April 1945
- (13) NAVORD Report 2385, Investigation of the Propagation of Detonation Between Small Confined Explosive Charges, Progress Report, W.E. Dimmock, L.D. Hampton and L.E. Starr, 1 April 1952

# Hampton, Savitt, Starr, Stresau

- (14) Unpublished Results of the Present Authors.
- (15) Second ONR Detonation Conference, February 1955, Conditions Behind the Reaction Zone of Confined Columns of Explosives, Notions Derived from Plate Dent Experiments, R.H. Stresau and W.M. Slie
- (16) NAVORD Report 2938, Effect of Acceptor Explosive Confinement Upon Acceptor Sensitivity, J. Savitt, 13 November 1953
- (17) NAVORD Report 2494, A Small Scale Gap Sensitivity Test, W.E. Dimmock, 2 July 1952
- (18) NOIM 9707, The Effect of Air Gaps on the Initiation of a Lead by a Detonator, R.L. Graumann and A.E. Robertson, 25 June 1948
- (19) NAVORD Report 2134, Studies of the Propagation of Detonation Through Barriers Separated by Air Gaps, W.E. Dimmock, L.D. Hampton and R.H. Stresau, 29 June 1951

# THE CORRELATION OF THE SENSITIVENESS OF EXPLOSIVES WITH COMBUSTION DATA

E. G. Whitbread & L. A. Wiseman Explosives Research & Development Establishment Ministry of Supply, England

# SUMMARY.

During the last few years at E.R.D.E. the sensitiveness of a large number of liquid explosives, and of a few solid explosives, has been determined by the gap test, in which the explosive is subjected to a shock wave. It is shown that the sensitiveness of liquid explosives, measured in this way, can be correlated with the product, in x Q, where in is the mass rate of combustion at an arbitrary pressure of 50 atms, and Q is a calculated heat of explosion. It appears also that, for a given value of in x Q, sensitiveness increases with increasing value of Q, where P is the density of the explosive.

These results have been interpreted in terms of the following model. It is assumed that the shock wave initiates a combustion reaction in some region of the liquid explosive; the mechanism and location of the initiation is not yet known. In order to produce a positive effect, i.e. an explosive increase in pressure or a reactive shock wave, it is necessary for the pressure in this combustion region to increase rapidly and it is shown that the rate of increase of pressure depends directly on  $m \times Q$ , pQ, and the pressure, and inversely on the linear dimensions of the combustion region.

The product, m x Q, gives a broad correlation with sensitiveness over the range of explosives from those as inert as ethyl nitrate and T.N.T. to those as sensitive as the initiator class. It fails, in this simple form, with plastic propellants but it is shown that this apparent lack of correlation may arise from the particular type of dependence of rate of burning on pressure. T.N.T. and Picric Acid have been examined in greater detail. The sensitiveness of liquid T.N.T. at 90°C and of pressed charges of granular T.N.T. of different grain sizes over a range of densities have been measured. It is shown that the sensitiveness of pressed charges of T.N.T. (and of Picric Acid) can be interpreted in terms of cavity initiation, i.e. "hot spots" created by the adiabatic compression of gases in a

cavity. In the pressed charges so far examined, initiation of the combustion reaction is the controlling process whereas, for liquid explosives, initiation appears to be easy, and growth (the rate of increase of pressure in the combustion domain) is the controlling process. Liquid and solid T.N.T. at the same density, are about equally sensitive on both the gap test scales used in this work. This agreement is shown to be fortuitous and this deduction was later confirmed by measurements of the sensitiveness of liquid and solid Picric Acid.

The correlation of the rifle bullet sensitiveness of liquid explosives with the gap test sensitiveness suggests that the rifle bullet initiates a combustion reaction. This idea is supported by the different behaviour of plastic propellants when subjected to the rifle bullet test and to the gap test.

The initiation process in liquid explosives, when assessed by the gap test, is discussed in the light of this experimental work and the negative conclusions reached that the initiation is not due to the presence of small air bubbles or to density fluctuations in the liquid. The mechanism, whereby a low-order detonation is propagated in a liquid explosive, remains a mystery.

The relationship between sensitiveness as measured by the gap test and by other tests, such as the impact test, is discussed. In order to be able to do this, some measurements of the conditions in the gap test have been made. The shock pressures necessary to produce an explosion or reactive shock in the explosive have been measured, and it is deduced from the results on granular explosive charges, that the "effective" duration of the pressure pulse increases with increasing pressure and that this factor must be taken into account when assessing the results of the gap test.

The object of this work was to obtain a detailed knowledge of the initiation and growth processes in explosion phenomena, so that the possibilities of more efficient desensitisation of explosives could be assessed. For homogeneous solid and liquid explosives, the "intrinsic" sensitiveness can be assessed from the mass rate of burning, which is a measureable property. It appears to be difficult if not impossible, to lower the rate of burning, except by reducing the energy, which is clearly undesirable. We must, therefore, concentrate on studying the effect of the physical state of the explosive on its sensitiveness. For liquid explosives we propose to study the effect of increasing viscosity on sensitiveness. In the case of solids, energy can be concentrated locally by friction, by stress concentration and by adiabatic compression of trapped air. Some of these factors may be controllable by altering crystal habits and crystal sizes. The role of desensitisers, such as wax, is discussed and it is suggested that smaller quantities, i.e. less than the customary 10 - 15 per cent, might be effective if the surfaces of the individual crystals of the explosive can be

completely covered with the wax.

It is known that, for a given value of Q, the rates of burning of explosive compounds decrease in the sequence: nitramines, nitroxy-compounds and nitro-compounds. It would, therefore, appear to be worthwhile exploring the field of nitro-compounds, particularly of the aliphatic series, more thoroughly.

## 1. INTRODUCTION.

Any discussion of the sensitiveness of explosives must consider two main factors:

- (a) the mechanism by which mechanical energy (in the case of initiation by impact, shock wave or friction) or electrical energy (in the case of spark initiation) is converted into thermal energy, or initiates some reaction which releases thermal energy, and
- (b) the conditions under which a "hot spot", i.e. a localised region at a higher temperature than the bulk explosive, will be formed and grow until an explosive reaction ensues.

This paper is concerned primarily with the second of these features.

The conception of hot spots is by no means new (c.f. Bowden and Yoffe, ref 15) and one of the earliest attempts to put it on a quantitative basis was made by Rideal and Robertson (1) who studied the minimum size and temperature of a region in an explosive material in which the rate of production of heat would be greater than the rate of loss of heat by conduction to the rest of the explosive. In this, values of the rate of decomposition of the explosive are required under conditions which admit only of gross extrapolation of low temperature kinetic data.

Another approach to this problem was made by Adams and Wiseman (2) in their consideration of initiation of explosive reaction by adiabatic compression of a cavity within an explosive. It is clear that an exothermic reaction, under conditions such that the rate of production of heat is greater than the rate of loss of heat, will eventually become a combustion reaction. These authors, therefore,

considered the conditions necessary to initiate a combustion reaction over the surface of the cavity and showed that the important properties of the explosive were the heat of explosion, Q(cal/g) and the mass rate of burning,  $m(g/cm.^2 sec)$ . It was shown that the sensitiveness of the explosive to this type of initiation increased with increasing values of the quotient, m/Q.

In order to put sensitiveness studies on a more quantitative basis, it was decided at E.R.D.E. some years ago, to study the sensitiveness of explosives to shock waves by the Gap Test (3). In an analysis of these results (4) it was shown that the sensitiveness of liquid explosives measured by this test, could be correlated with the product m x Q, where m was measured at an arbitrary pressure of 50atms.

This report is an attempt to clarify the present position of the application of these concepts, involving rates of burning, to sensitiveness and it falls into the following sections:-

- (a) an analysis of the range of validity of the product,fix Q, as a measure of sensitiveness,
- (b) an examination of the significance of the gap test,
- (c) an experimental approach to the correlation of the sensitiveness of liquid and solid explosives with each other, and
- (d) some tentative suggestions on the mechanism of initiation and growth of explosive reactions.

# 2. VALIDITY OF CORRELATION FACTOR, & x Q.

The important factor in this correlation is the rate of burning, since Q for weak and strong explosives does not vary by more than a factor of about 5, whereas in can vary by a factor of at least 30 in liquid explosives (the difference between methyl nitrate and propyl nitrate) and by a factor of about 1000 between an initiator, such as mercury fulminate, and a weak explosive such as ethyl nitrate. The uncertainty in the value of Q is, therefore, relatively unimportant. Q, in this paper is calculated for the hypothetical reaction (at constant pressure).

$$C_x O_y H_z N_w = x CO + (y - x) H_2 O(g) + (\frac{1}{2}z + x - y) H_2 + \frac{1}{2}w N_2$$

If there is more than sufficient oxygen to oxidise all the carbon and hydrogen, it is used to oxidise the CO to CO<sub>2</sub>. Theoretically, the heat of explosion should be calculated as for a constant volume explosion but, since the products in transient reactions are not as simple as those indicated above, there would be no gain in accuracy in so doing and we have, therefore, used Q calculated by the simple process given above. The heats of formation used are given in Appendix 1.

At what pressure to compare the rates of burning is not known (this is discussed later). We have used 50 atms., where data is available, but in the case of initiators, it has been necessary to use a reference pressure of 1 atm.

# 2.1 Liquid Explosives.

Many of these have been assessed for sensitiveness at E.R.D.E. under two arbitrarily chosen conditions of confinement:— Scale I and Scale III. (Scale II has been used for only a few cases, which are referred to later). The details of these scales are given in Ref 3, but for this discussion it is sufficient to know that Scale III represents the "heavier" confinement, and that a larger initiating charge is used which delivers a greater impulse to the test assembly. The results for Scale III are shown in Table I and Fig. 1.

The other simple forms of correlation are with Q, with m and with m/Q. Correlation with Q is good for the organic nitrates but does not extend to those mixtures containing nitro compounds or to the Dithekites (stoichiometric mixtures of nitrobenzene and nitric acid, with added water). Correlation with m/Q is bad, while that with m is fair but not as good as that with m x Q.

Provisionally, therefore, we shall accept that the product, in x Q, is the best correlation factor. In reference 4, it was suggested that, on the available combustion data, the dinitrate of butane 2:3 diol should be less sensitive than ethyl nitrate. This was found not to be true. A possible reason for this will be discussed later.

The results for Scale I are shown in Table II and Fig II.

On Scale I results with C (the card value) greater than 50 cards are not reproducible and the effect with C less than 5 cards is not a pure shock initiation since hot particles from the donor are known, by photographic observation, to penetrate the gap under these conditions. The main anomaly is the apparently large difference between the sensitiveness of butane 2:3 diol dinitrate and the 75/25 (w/w) mixture of ethylene glycol dinitrate and triacetin. These two explosives have about the same density, heat of explosion and rate of burning. A possible explanation of this is that Scale I only gives a significant result when the rate of growth of the explosion centre from the point of initiation is sufficiently fast. If two explosives can be initiated with equal ease but in one the growth, i.e. rate of increase in pressure, is faster than in the other then, since the criterion is the damage done to the container, the one in which the rate of growth is faster will appear to be more sensitive by this test. From Fig 2 it will be seen that, for a given value of m x Q, the explosive having the higher value of Q is the more sensitive. fact, with C greater than 20, the sensitiveness correlates better with Q than m x Q. However, correlation with Q cannot accommodate

TABLE I.

SENSITIVENESS OF LIQUID EXPLOSIVES ON SCALE III.

(m at a combustion pressure of 50 atms.).

,	T	losive.	8	Q	R <sub>b</sub>	m	c*	фхQ
	Component A.		g/cm <sup>3</sup>	cal/g	cm/sec	$g/cm^2$		cal/cm <sup>2</sup>
						sec		sec
	Ethyl Nitrate.			751	0.77	.41	43	309
1.	100	o	1.11	754 662	0.37 0.31	• 4± • 34	45 35	225
2.	96	4	1.09			.28	29	160
3.	92.1	7.9	1.08	572	0.26	.255	28	136
4.	90.4	9.6	1.07	534	0.24		22	
5.	84.1	15.9	1.05	388	0.18	.19		74
6.	80.1	19.9	1.03	297	0.14	• 145	19	43
		Propyl Nitrate.		"		70	77	007
7.	80	20	1.10	662	0.29	.32	37	201
8.	70	<b>3</b> 0	1.10	603	0.26	. 285	31	172
9•	60	40	1.09	570	0.23	. 25	27	
10.	0	100	1.05	294	0.14	.145	16	43
	Ethyl Nitrate.	Nitromethane.						
11.	60	40	1.12	840	0.19	.21	31	
12.	40	60	1.13			.17	29	
13.	0	100	1.14	969	0.10	.115	24	111
	Ethyl Nitrate.	Nitromixture.*						
14.	80	20	1.11	757		. 265	35	
15.	70	<b>3</b> 0	1.12	<b>75</b> 9		.215	29	163
16.	60	40	1.12	761	0.16	.18	27	137
	Butylene 2:3	Ethyl Alcohol.						
	glycol dinitra							
17.	96	4	1.27	729	0.15	.191	40	139
18.	92.1	<b>7.</b> 9	1.24	637	0.121	.150	31	96
19.	90.4	9.6	1.23	596	0.109	.134	29	80
20.	84.1	15.9	1.18	450	0.078	-	22	41
21.	80.1	19.9	1.16	353	0.063		18	26
C.A.	Nitroglycerine							
22.	67.5	32.5	1.41	656	0.175	. 247	29	162
23.	65	35	1.40	592	0.150		24	124
24.	<b>6</b> 0	40	1.37	464	0.104		16	66
25.	55	45	1.36	336	0.074	-	11	34
26 <b>.</b>	Dithekite D13		_,,,			-		- •
20.	DIGHT OF DIA	w/w H <sub>2</sub> O)	1.37	1265	_	_	30	
27.	Dithekite D20						-	
41.	DICHEKIRE DEC	w/w H <sub>2</sub> 0)	1.36	1146	-	-	19	

A C is a measure of the thickness of the gap. The gap consists of cards and C is the number of cards in the gap.

Nitromixture = 83% nitromethane + 17% 2-nitropropane (w/w).

TABLE II.

SENSITIVENESS OF LIQUID EXPLOSIVES ON SCALE I.

(m at a combustion pressure of 50 atms).

	Explorement A.	osive. Component B.	<b>&amp;</b> g/cm <sup>3</sup>	Q cal/g	R <sub>b</sub>	m g/cm <sup>2</sup> sec	С	mxQ cal/cm <sup>2</sup> sec
	Nitroglycerine.	Triacetin.						
1.	90	10	1.54	1286	1.02	(1.51)	65	1941
2.	85	15	1.50	1124	. 69	(0.96)	47	1080
3.	82.5	17.5	1.49	1049	•54	(0.78)	31	816
4.	80	20	1.47	970		.65	26	630
5.	<b>7</b> 5	25	1.45		.29	.42	22	341
5. 6.	70	<b>3</b> 0	1.42	694	.21	. 285	5	185
	Ethylene Glycol	Triacetin.						
	Dinitrate.							
7.	89	11	1.45	1267	.56	.81	52	
8.	84	16	1.43	1108	•43	.61	29	683
9.	80	20	1.41		.305		27	429
10.	<b>7</b> 5	25	1.39				21	254
	Ethyl N		1.11			0.41	2	309
	Nitrome		1.14	969	.10	.115	_	111
	Dithekite D20.		(1.36)		-	-	4.	(60)*
	Dithekite D13.		1.37	1265	-	-	16	(160)*
		2:3 dio1		_		_	_	
	din	itra <b>te.</b>	1.303	815	.22	. 285		-
	D.E.G.N	•	1.39	989	.61	. 85	27	841

<sup>\*</sup> m x Q value from Fig. 1

Dithekite D20 or D13.

# 2.2 Rates of Burning of Liquid Explosives.

The values of m quoted in Table I and Table II are for a combustion pressure of 50 atms. The sources of this information are in references 5, 6, 7 and 8. Values in brackets were obtained by extrapolation of the plot of log m against Q. Values for the series based on the dinitrate of butane 2:3 diol were obtained from the results on the other glycol dinitrates (ref 7) since the log m value gives a linear relationship with Q.

The values of m have been deduced from the linear rate of regression of the liquid meniscus when the liquid burns in a capillary tube. There is, therefore, some uncertainty in the value of m since it is not known whether the flame zone is parallel to the meniscus or flat and perpendicular to axis of the tube in which the

liquid is burnt. Furthermore, the shape of the meniscus varies somewhat with pressure and nature of the explosive: there is, therefore, both an absolute and a relative uncertainty in the values of m. This aspect has been considered by Stocks (6) but we propose to ignore it in the treatment of this report since the uncertainty in the rate of burning is of about the same order as the uncertainty in Q.

It is shown later that the shock pressures in gap test initiation are of the order of 10<sup>4</sup> atms. If the rates of burning depend linearly on the pressure, any reference pressure, e.g. 50 atms, can be used to compare the magnitude of the product, m x Q, for different explosives. For most of the explosives examined, the rate of burning is a linear function of the pressure. The rate of burning, at a given pressure, increases smoothly with increasing Q, but it has been found that the explosives examined fall into a number of classes. The evidence is as follows (7, 8): at 50 atms if log m is plotted against Q we find that:-

- (a) propyl, ethyl and methyl nitrates, mixtures of ethyl and propyl nitrates and ethyl and methyl nitrates diluted with hydrocarbons or alcohols lie on a straight line,
- (b) glycol (ethylene, propylene, butylene) dinitrates also lie on a straight line but for a given value of Q, the m values are about half those in (a),
- (c) mixtures of nitroglycerine with triacetin lie on an intermediate line.
- (d) an ether link in the molecule leads to an increased rate of burning, e.g. D.E.G.N. compared with glycol dinitrates and CH<sub>3</sub>.O.CH<sub>2</sub>.ONO<sub>2</sub> compared with the alkyl nitrates.

It is difficult to see why the rates of burning of methyl nitrate, nitroglycerine and ethylene glycol dinitrate should differ so much since the heats of explosion are approximately the same and it is probable that, at high pressures, the rate controlling reaction is the reduction of NO. At high combustion temperatures this reaction probably proceeds by the homogeneous mechanism.

$$NO + NO \rightarrow N_2 + O_2$$

The homogeneous bimolecular decomposition of NO has a large energy of activation (70 to 80 k. cals/mole) and, therefore, there may be other routes for the reduction of NO at lower combustion temperatures.

From these facts and discussion it appears possible that the rates of burning of the hotter organic nitrates at high pressures depend only on the value of  $\mathbb{Q}$ . This would explain the rather better correlation of C with  $\mathbb{Q}$ , on Scale I, than with  $\mathbb{R} \times \mathbb{Q}$ . Secondly,

above 50 atms, the rate of burning of ethyl nitrate depends approximately on  $\sqrt{P}$ , and therefore the rate of burning of ethyl nitrate systems may not, at sufficiently high pressures, be appreciably different from those of compositions based on the dinitrate of butane 2:3 diol and, hence, the correlation of C with  $m \times Q$  on Scale III might be better than that shown in Fig 1 if the rates of burning at high pressures were known.

# 2.3 Solid Explosives.

The sensitiveness of a pressed solid explosive depends markedly on the grain size and packing density and, of a cast explosive, on the crystal size. It is, therefore, not immediately obvious under what conditions comparisons of sensitiveness should be made. Qualitatively, however, the factor m x Q does appear to give good correlation. Available results are shown in Table III.

TABLE III.

RATES OF BURNING OF SOLID EXPLOSIVES.

Compounds. R	ate of ] cm/sec.	Burning, g/sec.	Dens Pres g/cm <sup>3</sup> .	sure.	Q s. calsy	mxQ I g.cal/cm <sup>2</sup> sec.	Ref.
1. Mercury Fulminate. 2. Trinitrotriazidobenzene. 3. Potassium Picrate. 4. Diazodinitrophenol. 5. Lead Styphnate. 6. 40% " "+ 60" talcum. 7. R.D.X. 8. P.E.T.N. 9. Tetryl. 10. T.N.T. (cast). 11. Nitroglycerine. 12. Methyl Nitrate. 13. Ethyl Nitrate.	1.50 2.15 exp: 14.5 36 22 8-9 13-14 0.2	1.05 2.75 3.1 lodes - 58 37 13-14 22 0.3 0.12	1.45 3.07 1.60 1.70 1.57 1.60 1.59 1.20	1 1 1 1000 1000 1000 1000	1280 469 - 880 - 1250 1390 920 653 1466 1450	1350 - - >12000 - 73 51 12-13 14.5 440	9999991010222

# Notes to Table III.

- (1) m x Q estimated at P = 1 atms. (linear extrapolation being used to obtain m where necessary).
- (2) Q estimated as described previously; any metal assumed to be present in normal state.
- (3) Only approximate figures of the densities of R.D.X., P.E.T.N.

and tetryl are quoted since the densities used are not given in Ref 10.

# (4) Rates of Burning.

- (a) Below 1 atm pressure, rates of burning of trinitrotriazidobenzene and mercury fulminate depend linearly on the pressure (12); above 1 atm pressure there are no data.
- (b) The data on the solid high explosives may not be reliable since they were obtained from p/t records of the combustion of granular material. Further we find it difficult to accept that T.N.T. burns faster than tetryl since tetryl is "hotter" than T.N.T. and is a nitramine, and in general nitramines burn faster than nitrohydrocarbons (refs 4 and 7). The only other data, known to the authors, is that of Andreew (ref 13) quoted below.

DATA OF ANDREEW.

COMPOUND.	m g/cm²/sec.	CONDITIONS.	
P.E.T.N. R.D.X. (s) Tetryl. (l) T.N.T. (s) T.N.T. (l)	0.055 0.057 0.15 0.017 0.033	130°C 100°C 133°C room temp. 250°C	

(c) The rate of burning of nitroglycerine is also obtained from data of Andreew. Other data on nitroglycerine diluted with triacetin, obtained at E.R.D.E. suggest that the rate of burning of pure nitroglycerine is much nearer to that of methyl nitrate than the value given in Table III.

The sequence of the values of M x Q in Table III is:- initiators, nitroglycerine, methyl nitrate, (R.D.X., P.E.T.N.), (Tetryl, T.N.T.), and ethyl nitrate, which is in good agreement with the accepted sequence of sensitiveness and also with gap test results, e.g. T.N.T. less sensitive than Tetryl (19) and T.N.T. Tetryl R.D.X. P.E.T.N. (20). The small anomalies e.g. inversion of R.D.X. with P.E.T.N. and T.N.T. with tetryl may be due either to errors in measured rates of burning or non-linear dependence of rate of burning on pressure. The quantitative value of the scale is suspect in any case, because of the neglect of the mechanism whereby energy is transmitted to the explosive and converted into thermal energy and it seems unlikely that this is the same for liquids and crystalline solids.

In the absence of strictly quantitative data, we can conclude only that m is an important factor in the sensitiveness of solid explosives, and not that m x Q has a quantitative significance.

Before concluding this section, it should be pointed out that there is an upper limit to the rate of combustion. Compounds, whose "ideal" rate of burning is greater than this, will therefore, show no combustion regime on initiation (c.f. Bowden, Ref 15) but will give immediate detonation. Certain of the azides may show this behaviour. Further consideration of the matter is given in Appendix II.

# 2.4 Plastic Materials.

The plastic materials considered are Plastic Propellants, which consist of a crystalline oxidant, e.g. ammonium perchlorate, cemented with a binder such as polyisobutylene and a wetting agent, e.g. lecithin. Some gap test results, on Scale III, are given in Table IV.

The C values in Table IV are much smaller than would be expected from the value of m x Q. Further, the presence of materials, e.g.  $Cr_2O_3$ , which catalyse the low pressure combustion process appears to have a slightly negative effect on the sensitiveness. This may be because the catalyst has no kinetic effect under the pressure conditions of the gap test and, therefore, reduces the rate of burning by lowering the value of Q. The effect of occluded air on the sensitiveness of plastic propellants is similar to that produced by air bubbles in liquids.

Two possible reasons why the C values should be unexpectedly low can be suggested. Firstly the pressure exponent of the rates of burning is about 0.7, i.e. less than unity and, therefore, the value of m x Q under the pressure conditions of the shock wave would be very much less than if the pressure exponent were unity as it appears to be for many one phase systems. Secondly, the transmitted shock pressures in the explosive material depend on the physical properties of the latter and may be greater or smaller than the pressure of the incident shock. Relative to liquids, this would have the effect of displacing the card values for a given range of m x Q either to larger or smaller values.

#### 3. SIGNIFICANCE OF GAP TEST.

3.1 In an adiabatic system having perfect mechanical confinement any compound which decomposes exothermically will eventually explode. The times required for this to happen are, however, very long at ordinary temperatures. If, in such a system, a sufficiently large "hot spot" is formed then the resultant explosion will centre about this point. In practical systems the critical energy required to start an explosive event depends very much on the mechanical and thermal confinement. Let us now consider the gap test with these ideas in mind. In the gap test a strong shock or sequence of shocks

TABLE IV.

GAP SENSITIVENESS (SCALE III) OF PLASTIC PROPELLANTS.

CODE NO. OF			burning	Q	mxQ	, C	
COMPOSITION.	Density		00 p.s.ji.	cal/g	cal/cm	/ "Fre <b>e"</b>	Contair
(See Appendix III)		om/sec	g/cm²/sec		sec	from	ing air
E202.	1.70	1.80	3.06	958	2931	16	-
E260.	1.67	1.50	2.51	865	2167	13	-
E261.	1.65	1,15	1.90	773	1391	10	-
E911 = (E202 + 3% Cr <sub>2</sub> 0 <sub>3</sub> ) E912 =	1.73	2.25	3.89	9 <b>31</b>	3624	15	22
(260 + 3% Cr <sub>2</sub> 0 <sub>3</sub> ) E913 =	1.71	2.0	3.42	840	2873	12	20
(E261 + 3% Cr <sub>2</sub> 0 <sub>3</sub> ) E937 =	1.69	1.70	2.87	751	2158	10	16
$(E202 + 3\% K_2 Cr_2 O_7)$ E938 =	1.71	1.45	2.48	950	2356	12	-
$(E260 + 3\% K_2 Cr_2 O_7)$ E939 =	1.68	1.19	2.00	860	1 <b>71</b> 9	<b>≯</b> 10	-
(E261 + 3% K <sub>2</sub> Cr <sub>2</sub> O <sub>7</sub> ) RD 2200 RD 2043 RD 2331 RD 2332	1.66 1.78 1.73 1.60 1.58	0.94 1.88 0.69 0.30 0.25	1.56 3.35 1.19 0.48 0.40	770 1140 45 <b>3</b> 499 404	1202 3815 541 240 160	→ 10 → 10 → 10 → 10	10

(see Fig. 3) is transmitted to the explosive under examination, the explosive being contained in a standard vessel, a metal tube. The criterion of a positive effect, i.e. addition of energy from the explosive to the shock wave, on Scale I is the fragmentation of the container and, on Scale III, the tearing of a metal end-plate. The initiating shock is not sufficiently strong to cause such damage. This implies that to get a positive effect either a reactive shock, not necessarily a stable one, must be propagated through the explosive or there must be a rapid increase in pressure above that of the shock pressure transmitted to the explosive from the donor across the gap.

It is necessary at this stage to anticipate our conclusion in order to clarify discussion. In some way, the initiating shock starts an exothermic reaction at some point or points in the explosive. We shall regard this exothermic reaction as a combustion reaction and define this whole process as initiation. Under favourable conditions, i.e. a sufficiently high initiating pressure and adequate confinement, the pressure at the point or points of initiation will increase. This process we call growth. If the dimensions and confinement of the explosive are large enough, this

growth process will lead to the formation of a shock wave of sufficient strength to initiate more explosive, i.e. a reactive shock will be formed, and eventually a stable detonation wave may be produced. We imagine, therefore, the sequence of events to be as follows:—initiation— growth— reactive shock—detonation wave.

The growth process may be sufficiently vigorous to give a positive effect in the tests. In Scale I, the photographic evidence shows that in diethylene glycol dinitrate a low velocity detonation wave is propagated. The "positive effect" in Scale I is sufficiently large, i.e. fragmentation of the container, to support the photographic evidence that a detonation wave is produced. The "positive effect" is much weaker in Scale III and it is impossible, at present to state whether an explosive reaction or an unstable reactive shock is produced.

A priori there is no reason to assume that ease of initiation will run parallel with ease of growth as we pass from one explosive to another. The two cases of particular interest are:-

- (a) initiation easy, growth difficult,
- (b) initiation difficult, growth easy.

In case (a), the explosive will have to be over-initiated in order to get a positive effect in the test. In case (b), a shock pressure sufficient to initiate the explosive, will produce a reactive shock of sufficient strength to give a positive result. It does not follow therefore, that the gap test necessarily measures the same property for all explosives.

On an empirical basis it can be argued that the gap test measures ease of propagation. Some sort of assessment of ease of propagation can be made by examining the propagation of detonation of explosives in tubes of differing dimensions. In a few cases direct comparison with gap test results is possible. Such results are given in Table V (details of the propagation test are given in Appendix IV); the figures in the "Results" column give the minimum tube diameter in which the explosive propagates detonation under the conditions of test.

Explosive A propagates more readily than explosive B despite the fact that it is less sensitive than B. In each pair the explosive which propagates better has the higher value of Q. This limited evidence suggests, that Scale III measures either ease of initiation or "build-up" of an explosion wave (growth) rather than ease of propagation.

In Scale I the initiating shock is weaker, the charge diameter is smaller and the wall thickness of the metal container less than in Scale III. It is also possible that the accepted indication of

TABLE V.

COMPARISON OF PROPAGATION AND GAP TEST RESULTS.

A N <sub>2</sub>	H <sub>J.</sub> 54•2%• )			
N <sub>2</sub>	H <sub>1</sub> 54.2%. ) H <sub>2</sub> NO <sub>3</sub> 36.5%. ) O 9.3%. )	10	570	5/8"
B Pr	opyl Nitrate.	16	294	greater than 2".
	thekite Dl3.	<b>3</b> 0	1265	less than 1/16".
	hyl Nitrate.	43	754	1/4".
L	tromethane.	24	969	less than 1/4".
B Et	hyl Nitrate.	43	754	1/4".
	tromethane.	24	969	less than 1/4".
B 60,	40 Etono/Prono	2• 27	570	5/8".

a positive result, namely fragmentation of the containing tube, is more rigorous than that required in Scale III. In reference to Fig. 2 it was pointed out that for a given value of m x Q, the explosive with the higher value of Q was apparently the more sensitive. It was shown in Section 2.2, however, that this effect may also be due to uncertainty in the value assigned to the rate of burning, that observed differences in rates of burning at low combustion pressures may disappear at pressures of 10° or 10° atms. Another aspect of the matter is shown in Fig. 4 where the explosives assessed on Scale I are plotted on a grid of m x Q and  $\rho_{\rm C}Q$ ,  $\rho_{\rm C}$  being the density of the explosive. The explosives fall arbitrarily into two classes:-

(a) 
$$C > 16$$
. and (b)  $C \le 6$ .

and the field can be divided in such a way that the two classes are separated. It appears, therefore, that a C value less than some value between 6 and 16 on Scale I has no quantitative significance. For a given value of m x Q,  $\rho_{\rm C}$ Q must be above a certain value before Scale I gives significant results. We shall assume therefore (see argument in Section 6.2) that only explosives in which the growth of the explosion centre is rapid can be assessed on Scale I; in other words ease of initiation or of growth of the explosion centre is measured if Q is large enough. The factor  $\rho_{\rm C}$ Q is larger for ethylene glycol dinitrate/triacetin (65/35) than for butane 2:3 diol dinitrate and thus may be the cause of the large apparent difference in sensitiveness on Scale I.

3.2 The gap test technique was originally selected for this work at E.R.D.E. because it was thought that, in principle, the strength of the initiation shock could be measured. The properties of the shock wave, which appear to be important, are its peak pressure,

velocity and thickness from which can be deduced the time for which any element of explosive is subjected to pressure. We have not yet obtained adequate photographs of the shock waves in liquids subjected to gap tests but the photographs so far obtained (Fig 3) show that there is a succession of shock waves. However, measurements of shock pressures have been made. The main difficulty in measurement is one of principle. If a shock wave passes from one medium to another, the shock pressure in the second medium may be higher or lower than the shock pressures in the first. For weak shocks the criterion is the acoustic impedance, i.e. product of velocity of sound (c) and the density (p). If the shock is travelling from a medium of low impedance (small pc) into one of high impedance, the shock pressure in the second medium will be higher than in the first. It follows from this that measurement of the shock pressure by the methods described below may not give the pressure in all explosives since they differ so much amongst themselves in physical properties.

Pape (11) has measured the pressure in two ways:-

- (a) by transmitting the shock to a Hopkinson bar, and
- (b) by transmitting the shock to water and calculating the shock pressure from the measured velocity.

Both methods of measurement give about the same values for the pressure (see Fig. 5) although the form of the curve is rather unexpected in the case of water. The main point, however, is that the pressures are about the same despite the large difference in acoustic impedance between water and steel. It should be noted, however, that the Hopkinson bar result is a time averaged result (for the figures quoted below, the time interval is 5 \musecs), whereas that from the velocity in water is an instantaneous one for the leading shock wave (see Fig 3). However, the Hopkinson bar results are simple and are as follows:-

Scale I 
$$log_{10}P = -0.0339 C + 4.63.$$
  
Scale III  $log_{10}P = -0.0250 C + 4.76.$ 

where P is measured in atms and C is the number of cards in the attenuating stack.

Measurements with fewer than 30 cards were not significant because permanent damage was done to the Hopkinson bar and above 50 cards the results were not reproducible. Extrapolation below 30 cards is probably permissible but not above 50 cards (gap test results are irreproducible at card values above 50).

The estimated minimum pressure required to obtain a positive result with Dithekite D13 on Scale III is about 1.0 x  $10^4$  atms and about 1.2 x  $10^4$  atms on Scale I. The only other cases for which a direct comparison is possible fall on that part of Scale I where the

results do not appear to have quantitative significance. If m is a linear function of P and the pressures measured by the Hopkinson bar are reliable, the value of m x Q at the initiation pressures for explosives can be estimated. On Scale I (C > 16) the value of m x Q is about 5 x 10<sup>4</sup> cal/cm<sup>2</sup> sec and on Scale III about 3 x 10<sup>4</sup> cal/cm<sup>2</sup> sec. The scatter is quite large, as the results in Table VI show, but nevertheless the rates of energy release required for initiation on Scale I do appear to be significantly higher than those required on Scale III. This is to be expected in view of the lighter conditions of confinement in Scale I.

It has been mentioned previously that Plastic Propellants (Table IV) are less sensitive than expected from the value of m x Q. It was suggested that a reason for this might be that the pressure exponent of the rate of burning is less than unity. Assuming that the critical rate of energy release on Scale III is 3 x 104 cal/cm2 sec (Table VI) then,  $(\dot{m} \times Q)_1/(\dot{m} \times Q)_2 = (P_1/P_2)^n$ , where n is the pressure exponent, subscript 1 refers to reference conditions (e.g. 50 atms for liquids, 1000 p.s.i. for plastic propellant) and subscript 2 to the conditions in the initiating shock i.e. (m x Q)2 is 3 x 104 cal/cm2 sec and P2 can be calculated from the value of C. The above equation for Plastic Propellant can be written: (m x Q)1/  $3 \times 10^4 = (68/P_2)^n$ . Values of n have been calculated for the compositions RD 2200, E 202, E 260, and E 261 (Table IV), i.e. for compositions containing no combustion catalysts. The values are 0.41, 0.40, 0.44, and 0.50 respectively. Although less than n determined at low pressures (1000 p.s.i.) such values are not unreasonable and, therefore, the low sensitiveness of Plastic Propellants may be ascribed to their combustion properties and not to their physical properties.

3.3 It can be concluded from this discussion that the gap test does not measure ease of propagation of detonation but ease of initiation and/or the growth factor. It appears that at least a low-order detonation is produced under the conditions of Scale I but it has not been proved whether a positive result on gap test Scale III involves a low-order detonation, i.e. the rate of growth under the conditions of Scale III may not be sufficient to set up a reactive shock.

# 4. RIFLE BULLET SENSITIVENESS.

# 4.1 Liquid Explosives.

It was shown in Ref 4 that the sensitiveness of liquid explosives to rifle bullet attack, under the conditions specified in Ref 14, could be correlated with the sensitiveness on gap test (Scale III). An explosion, or partial or complete detonation, was accepted as a criterion. It is possible, however, than an explosion cannot always be regarded as an incipient detonation since it might be argued that the bullet created a large surface in the liquid, e.g. by cavitation, which ignited and gave rise to explosive combustion. This could

# TABLEVI. ESTIMATED RATES OF ENERGY RELEASE FOR INITIATION OF EXPLOSION.

ecai Explosive.	RATE OF	SE EXPLOSIVE.	III. RATE OF C ENERTY RELEASE cal/cm <sup>2</sup> sec
* N.G. T.A. 85 15 80 20 75 25 E.G.N. T.A. 84 16 80 20 75 25 Dithekite D13 D.E.G.N.	47 2.4 x 10 <sup>4</sup> 26 7.1 x 10 <sup>4</sup> 22 5.4 x 10 <sup>4</sup> 29 6.1 x 10 <sup>4</sup> 27 4.6 x 10 <sup>4</sup> 21 4.2 x 10 <sup>4</sup> 21 4.2 x 10 <sup>4</sup> 27 8.9 x 10 <sup>4</sup>	(90.4/9.6) ETONO <sub>2</sub> /PRONO <sub>2</sub> (60/40) Propyl Nitrate. Nitromethane. Butane 2:3 dinitrate + 4% ETOH.	43 3.0 x $10^4$ 28 2.9 x $10^4$ 27 3.3 x $10^4$ 16 2.0 x $10^4$ 24 3.1 x $10^4$ 40 1.6 x $10^4$ 16 2.9 x $10^4$

NOTE: \* T.A. - Triacetin, N.G. - Nitroglycerine, E.G.N. - Ethylene Glycol Dinitrate.

produce a sufficiently rapid rise in pressure to cause severe damage to the container without the onset of detonation. We have, therefore, re-examined the results from Ref 14 although the data are statistically inadequate. Significant results are shown in Table VII.

Apart from anomalies, being within the scatter expected of such a small number of trials, we see that there is a broad correlation with gap test sensitiveness whichever criterion is regarded as a positive event.

# 4.2 Solid Explosives.

We have as yet very few data on solids suitable for comparison with the liquid explosives and gap sensitiveness measurements. The available results are given in Table VIII.

The definition of explosion, used in this work, is:- "Impact accompanied by a flash or slight report. Box split along seams and sometimes thrown as much as 15 yards." (Ref 14). Such an event could easily be produced by vigorous burning inside the box and it is hardly surprising that materials, such as Plastic Propellants, should

TABLE VII.

SENSITIVENESS OF LIQUID EXPLOSIVES
TO RIFLE BUILET ATTACK.

explosive.	no. Of Trials	DETON-	ntage Detona- Tions & Explosio	III
EtONO2/PrONO2, 80/20. EtONO2/Nitromixture, 80/20. EtONO2/Nitromixture, 75/25. EtONO2/PrONO2, 70/30. EtONO2/PrONO2, 50/50. Dithekite D 13. EtONO2/Nitromethane, 40/50. EtONO2/Nitromethane, 40/50. EtONO2/Nitromethane, 70/30. EtONO2/Nitromethane, 60/40. EtONO2/PrONO2, 60/40. Nitromethane. Dithekite D 20. PrONO2.	29 15 25 12 30 29 30 60 17 30 74 30 60 30	55 13 24 50 10 10 7 8 6 0 0		43 37 35 33 31 30 30 29 27 27 24 19 16

TABLE VIII.

SENSITIVENESS OF SOLID EXPLOSIVES TO RIFLE BULLET ATTACK (REF.14).

EXPLOSIVE.	DENSITY g/cm <sup>3</sup>	SCALE I	SCALE III	NO. OF TRIALS		entage. Explo- Sions
Amatol. (80/20).  RDX/BWX. (90/10).  Pressed.  RDX (Pressed).  TNT (Pressed).  RD 2200 )  RD 2201 ) Plastic  E 202 ) Propellants.  RD 2043 )	1.3 ? ? ? 1.78 1.70 1.73	25 23 24 - -	- - - 30 - 16 10	30 29 27 30 30 30 30 30	7 0 81 0 0 0	20 10 19 40 90 27 67 23

give explosions (so defined) under rifle bullet attack since they have much higher rates of burning than liquid explosives at low pressures (compare Table I and Table IV). These results, and the known rates of burning of liquid explosives and Plastic Propellants, suggest that the rifle bullet starts a combustion reaction at a relatively low pressure.

When we consider the few results with pressed solid granular explosives, there is no correlation with liquid explosives. Liquid explosives having C values greater than 20 on Scale I would certainly give rise to a large percentage of detonations in the rifle bullet test. A liquid explosive with a C value of 23 on Scale I would have m x Q (at 50 atms. pressure) equal to about 500 cal/cm2sec. We estimate that the rate of burning of an homogeneous mixture of RDX and Beeswax (90/10) would be about 1.5 g/cm2sec at 50 atms. since its heat of explosion is about 800 cal/g (c.f. Fig 7 of Ref 7), which leads to a value of 1200 cal/cm2sec. for m x Q. The explanation of the discrepancy may stem from the fact that the explosive is inhomogeneous. The same conclusion might be drawn from the relative sensitivenesses of RDX/TNT and T.N.T., i.e. RDX/TNT behaves more nearly like T.N.T. than R.D.X. The effect of inhomogeneity on sensitiveness is discussed later. Other factors not considered are grain size, crystal size and loading density, all of which have an effect on sensitiveness.

#### 5. SENSITIVENESS OF PRESSED CHARGES OF T.N.T.

One of the difficulties in sensitiveness work is to obtain a logical link between the sensitiveness of liquid and solid explosives. Certain explosives, however, are stable in the liquid and solid state. The easiest one to handle is T.N.T.; another is Picric Acid. In these systems it is possible to compare the sensitiveness of a liquid and a solid, for which the chemical nature of the decomposition process is the same, the only difference being the final temperatures of the decomposition process which depends on the magnitude of the latent heat of fusion.

It was decided to determine the sensitiveness of T.N.T. under the following conditions:— (a) as a liquid at 90°C, (b) as a cast solid at ambient temperature, and (c) as a pressed charge in which the loading density, the grain size and the crystal size were varied. Some results obtained at this establishment are shown in Figs. 6a and 6b. These were obtained on gap Scale II which is almost the same as Scale I, except for a difference in the mechanical properties of the steel of the containing tube.

The main conclusions are:-

(a) the sensitiveness is a function of density, increasing with density, passing through a maximum and then decreasing.

- (b) at specified density, pressed charges of large grain size are more sensitive than ones with small grain size,
- (c) a pressed charge of grains made from large crystals is less sensitive than one of grains made from small crystals.

The results with cast T.N.T. and liquid T.N.T. are shown in Table IX.

# TABLE IX. SENSITIVENESS OF T. N. T.

FORM OF T.N.T.	SCALE I. SCALE II. SCALE III			
Normal brown. (cast).	9	12	30	
Liquid at 90.		15	30	

The agreement between the sensitiveness of liquid and cast T.N.T. is thought to be fortuitous because it is well-known that the sensitiveness of cast T.N.T. can be altered appreciably by variation of the crystal size. This matter is discussed in Section 6.

# 6. ANALYSIS OF RESULTS.

- 6.1 Before attempting to analyse the main results, we may summarise them briefly:
  - (a) the product h x Q (at P = 50 atms.) gives a good correlation of the sensitiveness of liquid explosives on gap test Scale III and by the rifle bullet test.
  - (b) generally speaking the product m x Q gives a good correlation qualitatively with sensitiveness over the whole field of explosives.
  - (c) on gap test Scale I the product m x Q is not a sufficient criterion, the magnitude of Q or QQ also appears to be important.
  - (d) there are some anomalies amongst the solid explosives, e.g. R.D.X. which despite a higher value of m x Q, is less sensitive than P.E.T.N. (20) and RDX/BWX is less sensitive on Scale I than would be guessed from its estimated rate of burning (if it were homogeneous).
  - (e) the rifle bullet sensitiveness of amatol, pressed T.N.T. and pressed RDX/TNT is less than that for liquids of similar

gap test sensitiveness.

# 6.2 Growth of an Explosion Centre.

We assume that mechanical action produces a localised high temperature in the explosive. This high temperature can be produced by friction, by shock waves or by local stress concentration or release. We assume, furthermore, that a combustion reaction starts at the hot spots. This process we define as "initiation", and from Bowden's work (15) it would appear generally true. In certain cases, (e.g. certain initiators), it may not be true and the probable reason for this is discussed in Appendix 2. In order to get a measurable explosive effect it is necessary for the combustion reaction to lead to an increasing pressure. Since this also requires an increasing size of the "hot spot", we define this second stage as growth. The rate of increase of pressure in an "explosion centre" of radius \* is given by equation 10 of Appendix V:-

If R<sub>b</sub> is a linear function of pressure, the factor

Repe Q' = Repe Q'

is approximately independent of pressure (p, will increase slowly with pressure). Neglecting changes in M and a with pressure, we can write pressure). Neglecting changes in M and c with pressure, we can write equation 1 in the form

At a given pressure P, a large value of dP/dt is favoured by large values of  $R_{bo}$  and  $\rho_c Q^{\dagger}$  i.e. by large values of  $R_{bo}\rho_c Q^{\dagger}$  which is approximately proportional to  $m \times Q$  (at any reference pressure), and  $\rho_c Q^{\dagger}$ .

If we put 
$$S = R_{bo} \rho_c Q^t$$
 equation 1b can be written 
$$\frac{dP}{dE} = \frac{3P}{F} \left[ \frac{KS - \frac{PS}{P_cQ^t} - YA}{P_cQ^t} \right]$$
 1c i.e. for a given value of S,  $dP/dt$  increases with increasing values

of pcQ'.

If, therefore, initiation is relatively easy and we are using a sensitiveness test in which growth must occur to give a measurable effect, as in gap tests, we should expect sensitiveness to increase with increasing values of S, approximately proportional to m x Q, and of  $\rho_{c}Q^{\bullet}$ . This is, in fact, what we have found with explosives on Scales I and III (see Figs 1, 2 and 4).

If  $R_b = R_{bo} P^n$ , where n < 1, we should expect the material to be less sensitive than would correspond to the value of m x Q at the reference pressure of 50 atms. This appears to be the case with plastic propellants (section 2.4) and hydrazine and hydrogen peroxide (discussed in Ref 4), all of which materials have values of n less

than unity.

# 6.3 Initiation by Cavity Initiation.

A pressed granular explosive must contain gas-filled cavities. It is possible that initiation of detonation of such explosives is produced by the adiabatic compression of the gas in the cavity. The pressure required to initiate a combustion reaction in an explosive material containing cavities is (equation5, Appendix VI):-

log d + 1/3. log { \( \frac{\d - \d \}{d} \) = log D - Blog P3

where d is the grain size, & is the density and Po is the initiating pressure. Accordingly, the pressure required for initiation decreases as the grain size is increased (at constant density). With a fixed grain size, the initiating pressure decreases as density is reduced.

Thus, if initiation is the controlling factor and not growth, (defined in Section 6.2), the sensitiveness of pressed charges of explosive will increase with increasing grain sizes and decreas density. Clearly the sensitiveness cannot increase indefinitely with decreasing density because:-

- (a) at some limiting low density the particles of explosive will only just be in contact, and
- (b) ease of initiation increases with increasing value of d (equation 2) but rate of growth decreases with increasing value of d, i.e. at some density, which will be lower the smaller the value of d, the pressure required for a sufficiently rapid growth will be larger than that required for initiation and hence will become the controlling factor.

If compression of a pressed porous solid is primarily the "compression" of the cavities, the in equation 1 is the radius of the cavity when compressed. The initial radius of the cavities is

where d<sub>c</sub> is the diameter of the cavities. Now for adiabatic compression of the cavity

ln (Pi/Po) = - 38ln(+i/to) = -38ln (2+i/dc)

where i refers to initial conditions (before compression) and o to initiating conditions. Hence

to = dc. {?;} 1/38 = d. { 66-6} 1/3. {?;} 1/38

In Appendix V it was shown that A in equation 1, which is a measure of the confinement conditions can be written (at the beginning of growth)

H= = - = = .d. fo. ( 6-6) }35. ( 7:) -2|38

Combining equations 3 and 4 with equation 1 we obtain for the initial rate of growth

when  $P_1 = 1$  atm. We can see from equation 5 that (dP/dt), decreases with decreasing pressure and decreasing density. This effect of changes in bulk density on the two terms on the R.H.S. is different, but not enormously so, as shown in Table X.

# $\mathbf{f_0} = 1.55 \text{ (as in cast T.N.T.)}$

6	E0/(60-6)	[6/(60-6)]43	Ratio of Factors.
1.4	10.3	2.15	4.7
1.2	4.4	1.5	2.9
1.0	2.7	1.2	2.3
0.8	2.1	1.02	2.1
0.6	1.6	0.86	1.9

Thus at densities of 1.0 g/cm<sup>3</sup> or less the ratio of [((6-6)]]<sup>13</sup> and 6-(6-6) does not depend much on 6 i.e. the relative importance of the confinement factor does not depend markedly on 6. We have, therefore, the following picture. At values of 66 near to unity (not too close to unity, since the confinement term containing A approaches infinity faster than the first term) initiation may be difficult and growth relatively easy. As 6 decreases, initiation becomes easier and growth more difficult. At some 6, the minimum pressure required for initiation may be too low to produce a fast enough rate of growth, i.e. a higher initiating shock pressure will be necessary to get growth fast enough to produce explosive combustion or a reactive shock. The density at which the change over occurs will be lower the smaller the value of d.

# 6.4 Pressed Charges of Explosive.

The behaviour of charges of pressed T.N.T. (Section 5 and Fig 6) approximates to the description in Section 6.3. It is worthwhile inserting numerical values into equation 2 in order to determine whether the theoretical initiating pressure is of the same order as our estimate from other experimental work. In equation 2 we have (Appendix VI).

(Appendix VI).

D. 69R. R. 13V = 6RQ. A. F. (R. 1etm.)

Q. This is somewhat less than the heat of explosion (Ref 2). The

measured value of the heat of explosion is about 1000 cal/gm (Ref 16) and the minimum estimate is 653 cals/gm (Table III). We shall assume a value of 700 cal/gm.

M. Since p/m is approximately independent of pressure (if m depends linearly on pressure) we can use the value of p/m at one atmosphere

According to Andreew (Ref 13),  $\dot{m}$  (1 atm.) = 0.017 gm/cm<sup>2</sup> sec. By linear extrapolation from the value at 1000 atms, we obtain  $\dot{m}$  (1 atm.) = 0.022 g/cm<sup>2</sup>cm. Although this agreement is satisfactory, we find difficulty in accepting this value because

pressure.

- (a) it is higher than that for an alkyl nitrate of the same heat of explosion (Fig 7 of Ref 7), and,
- (b) the value of m x Q (at 50 atms), deduced from the sensitiveness on Scale III corresponds to a value of m (1 atm.) of about 0.005 g/cm² sec. which appears more reasonable on our experience of the rates of burning of different classes of chemical compounds (Ref 7).

For the other physical properties we shall assume:  $\vec{\rho} = 0.002 \text{ g/cm}^3$ ,  $\vec{A} = 10^{-3} \text{ g/cm}$  sec.,  $\vec{M} = 25$ , and  $\vec{R} = 82 \text{ cm}^3$  atm/deg.6. With these values we obtain  $\vec{D} = 3.4$  ( $\vec{m} = 0.02 \text{ g/cm}^2 \text{sec}$ ) and  $\vec{D} = 16.8$  ( $\vec{m} = 0.005 \text{ g/cm}^2 \text{sec}$ ). Equation 2 then becomes  $(\vec{a} + \vec{b} + \vec{$ 

B =  $(3\times-1)$  3%. If Y = 1, B = 0.67; if X is large, B approaches unity. We shall choose therefore X = 1.4 and B = 0.75. Further since the charges were made from cast T.N.T. we shall assume X = 1.55 instead of 1.65, the crystal density.

Evaluating  $P_0$ , with  $6 = 1.0 \text{ g/cm}^3$  and d = 0.01 cm, we obtain a value of  $\log P_0$  between 3.5 and 4.5 i.e. P is between 3 x  $10^3$  and 3 x  $10^4$  atms. Now on Scale II the values of C lie approximately between  $20 \pm 5$ . Scale II is very similar to Scale I, the pressures probably being somewhat higher on Scale II for a given card value. From the formulae in Section 3.2 we find that  $\log P$  varies from about 3.80 to 4.10, which is within the limits of the calculated pressure.

For a given grain size, the sensitiveness increases by an amount corresponding to 5 cards or less as the density changes from 1.3 g/cm<sup>2</sup> to 0.8 g/cm<sup>2</sup>. Equation 2 should give a value which is not less than this since there must be a change over from the control by initiation to control by growth of explosion centres. We have, therefore,

with the above values of  $G_1$ , and  $G_2$  and  $G_0 = 1.55$  we obtain  $\log P_1/P_1 = 0.30$  which corresponds to a difference in C (i.e.  $C_1 - C_2$ ) of about 10 cards. This is reasonable agreement in view of the complications due to the growth of the explosion centres.

We have shown that changes in & and & affect the initiation and growth factors in opposite senses. It follows from this that equation 2 will always overestimate the effect of changes in 🛦 and 🌢 on the initiation pressure Po. On Scale II a pressed charge (6 = 1.05 gm/cm<sup>3</sup>) with grain size between 20 and 36 B.S.S. has a C value of 25. A pressed charge at the same density with grains passing 200 B.S.S. has a C value of 21. A grain size of 20 to 36 B.S.S. size has a mean diameter of about 600 microns; grains passing 200 B.S.S. have a diameter less than 76 microns. Thus a change in d by a factor of 10 changes the C value by 4 cards, corresponding to a change in log P of about 0.14. Now according to equation 6 a change of d by a factor 10 will change log P by 1.33 (corresponding to change in C of about 40 cards). The discrepancy is enormous. Let us, however, consider the effect of change of grain size on the rate of growth of an explosion centre. Neglecting all terms except the first in equation 5 we have, assuming  $P_i = 1$  atm,

we have, assuming  $P_i = 1$  atm, (sy+1)/3y KS Assume that a pressure,  $P_0$ , is required to initiate a charge with grain size d. The pressure required to initiate a pressed charge with grains of 10d is (from equation 6) about Po/20, The initial value of dP/dt for a grain size of 10d, is thus 0.1 x (1/20)12 0.0025 of the value for d. Thus the rate of growth of explosion centres is 400 times slower and if this rate is less than some critical value, a higher value of the pressure will be necessary, i.e. the decrease in initiating pressure will not be as great as that calculated from equation 6.

While this effect may well occur, the effect of changes in d is, according to equations 5 and 6, independent of 6. Now from Fig 6 we can see that a change of d by a factor 10 never has the marked effect calculated from equations 5 and 6. Therefore we conclude that

- (a) our model is incorrect, or,
- (b) our estimate of the size of the cavities is incorrect, or,
- (c) a significant factor has been omitted from our model.

We do not believe that our model is basically incorrect because it leads to ease of initiation increasing with increase in particle size whereas one based on growth as the controlling mechanism would give the opposite result. While the method of estimating the size of the cavity from d and b is crude, we do not believe that a change of d by a factor of 10 can have as little effect as suggested by the experimental results unless some factor has been omitted.

One factor, has certainly been omitted. In Ref 2 it was shown that initiation occurred at a time T after the arrival of the pressure wave, where T is given by T~10/v2P. Here v is the equivalent vapour phase rate of burning of the condensed phase, i.e. the vapour phase

rate of burning of the vapour at such an initial temperature that the final combustion temperature is the same as that for the combustion of the condensed phase. If the mass rate of burning depends linearly on P, v is independent of pressure. We have already estimated that m (1 atm.) for T.N.T. probably lies between 0. 02 and 0.005 g/cm<sup>2</sup>sec. v therefore, lies between 2 and 0.5 cm/sec. i.e. T lies between 2.5/P and 40/P. The pressures which we are considering are about 10<sup>4</sup> atms. Therefore the pressure pulse must have a duration between 2.5 x 10<sup>-4</sup> and 4 x 10<sup>-3</sup> secs.

In the gap test the pressure pulse is produced by attenuating the shock issuing from a tetryl charge. However, we know experimentally that a series of shock waves, rather than a single shock, is transmitted through the explosive. The reason for this has been suggested to us by Professor D. Pack. (Royal Technical College, Glasgow). After the tetryl pellet has detonated, the system consists of the detonation products, the attenuating card stack and the receptor explosive charge. A shock wave is transmitted through the card stack, part of which is transmitted as a shock wave into the explosive - part reflected. The reflected part is again reflected by the hot gases through the card stack towards the explosive. The explosive is thus subjected to a series of shocks; the shock pressures will clearly be larger and the pulse frequency shorter, the thinner the attenuating card stack. We deduce from this that the "effective" pressure may well be of shorter duration when the card stack is thick, i.e. the shock pressure is low. For cavity initiation this is the converse of the requirements for initiation.

Thus, as the grain size is increased, the pressure required for initiation decreases but the time during which this must act increases. We have shown, however, that the "effective" duration of the pressure pulse probably decreases with decreasing pressures in the gap test. If this is so, we can suggest an explanation of the discrepancy between the effect of changing d on the gap sensitiveness and that calculated by equation 2. As d increases, the pressure required decreases but the time during which this must act increases. In order to comply with this time requirement the initiation pressure must, therefore, at some value of d stop falling and start to increase. This is what is observed experimentally and explains why equation 2 must, at least with some explosives, grossly overestimate the effective of changing d on the initiating pressure.

# 6.5 Cast Charges.

Cast T.N.T. has a density of 1.55 g/cm<sup>3</sup> whereas the crystal density is about 1.64 at normal room temperature. The solid thus contains a large proportion of free space. If the cast solid crystal consisted of one large crystal, the gas (air) would be in a solution and uniformly distributed throughout the solid. If the crystal has localised imperfections and/or the charge consists of many crystals, the gas will diffuse and collect between crystal faces and at

crystal imperfections if sufficiently large. It is impossible to make an estimate of the size of pockets of gas, except that in cast charges they should be small since the only gas present is the air originally in solution and that produced by thermal decomposition. We can, however, be certain that the number of such cavities per unit volume whether between crystal faces or at crystal imperfections, will be larger the smaller the crystals. The crystal size is controlled by the rate of cooling. The more rapid the cooling, the smaller the crystals, the greater the number of imperfections and the smaller the amount of dissolved gas that diffuses away. If the attraction of the dissolved gas molecules for each other is greater than the attraction between them and the explosive, there will be a tendency for the dissolved gas to form microscopic imperfections (bubbles).

Let us, therefore, consider the cast solid of density with n

The confinement factor, A, in equation 1, depends on n and i.

The comment factor, k, in equation 1, depends on a manual of is the value of 
$$\frac{1}{1}$$
 at pressure  $P_0$ , then

A =  $\frac{E}{4W} \cdot \frac{1}{2W} = \frac{E}{3} \cdot \frac{1}{2}  

and 7a) is

$$\frac{dP}{dt} = 3P_0 \left\{ \frac{\sqrt{N}m}{3} \right\}^{\frac{1}{8}} \cdot \left\{ \frac{c_0}{c_0 - c} \right\}^{\frac{1}{3}} P_0^{\frac{1}{3}} \left[ KS - \frac{P_0S}{P_0Q} \right] - \frac{\sqrt{E}}{c_0 - c} \cdot P_0^{\frac{1}{3}} \left[ KS - \frac{P_0S}{P_0Q} \right] - \frac{\sqrt{E}}{c_0 - c} \cdot P_0^{\frac{1}{3}} \left[ KS - \frac{P_0S}{P_0Q} \right] - \frac{\sqrt{E}}{c_0 - c} \cdot P_0^{\frac{1}{3}} \left[ KS - \frac{P_0S}{P_0Q} \right] - \frac{\sqrt{E}}{c_0 - c} \cdot P_0^{\frac{1}{3}} \left[ KS - \frac{P_0S}{P_0Q} \right] - \frac{\sqrt{E}}{c_0 - c} \cdot P_0^{\frac{1}{3}} \left[ KS - \frac{P_0S}{P_0Q} \right] - \frac{\sqrt{E}}{c_0 - c} \cdot P_0^{\frac{1}{3}} \left[ KS - \frac{P_0S}{P_0Q} \right] - \frac{\sqrt{E}}{c_0 - c} \cdot P_0^{\frac{1}{3}} \left[ KS - \frac{P_0S}{P_0Q} \right] - \frac{\sqrt{E}}{c_0 - c} \cdot P_0^{\frac{1}{3}} \left[ KS - \frac{P_0S}{P_0Q} \right] - \frac{\sqrt{E}}{c_0 - c} \cdot P_0^{\frac{1}{3}} \left[ KS - \frac{P_0S}{P_0Q} \right] - \frac{\sqrt{E}}{c_0 - c} \cdot P_0^{\frac{1}{3}} \left[ KS - \frac{P_0S}{P_0Q} \right] - \frac{\sqrt{E}}{c_0 - c} \cdot P_0^{\frac{1}{3}} \left[ KS - \frac{P_0S}{P_0Q} \right] - \frac{\sqrt{E}}{c_0 - c} \cdot P_0^{\frac{1}{3}} \left[ KS - \frac{P_0S}{P_0Q} \right] - \frac{\sqrt{E}}{c_0 - c} \cdot P_0^{\frac{1}{3}} \left[ KS - \frac{P_0S}{P_0Q} \right] - \frac{\sqrt{E}}{c_0 - c} \cdot P_0^{\frac{1}{3}} \left[ KS - \frac{P_0S}{P_0Q} \right] - \frac{\sqrt{E}}{c_0 - c} \cdot P_0^{\frac{1}{3}} \left[ \frac{P_0S}{P_0Q} \right] - \frac{\sqrt{E}}{c_0 - c} \cdot P_0^{\frac{1}{3}} \left[ \frac{P_0S}{P_0Q} \right] - \frac{\sqrt{E}}{c_0 - c} \cdot P_0^{\frac{1}{3}} \left[ \frac{P_0S}{P_0Q} \right] - \frac{\sqrt{E}}{c_0 - c} \cdot P_0^{\frac{1}{3}} \left[ \frac{P_0S}{P_0Q} \right] - \frac{\sqrt{E}}{c_0 - c} \cdot P_0^{\frac{1}{3}} \left[ \frac{P_0S}{P_0Q} \right] - \frac{\sqrt{E}}{c_0 - c} \cdot P_0^{\frac{1}{3}} \left[ \frac{P_0S}{P_0Q} \right] - \frac{\sqrt{E}}{c_0 - c} \cdot P_0^{\frac{1}{3}} \left[ \frac{P_0S}{P_0Q} \right] - \frac{\sqrt{E}}{c_0 - c} \cdot P_0^{\frac{1}{3}} \left[ \frac{P_0S}{P_0Q} \right] - \frac{\sqrt{E}}{c_0 - c} \cdot P_0^{\frac{1}{3}} \left[ \frac{P_0S}{P_0Q} \right] - \frac{\sqrt{E}}{c_0 - c} \cdot P_0^{\frac{1}{3}} \left[ \frac{P_0S}{P_0Q} \right] - \frac{\sqrt{E}}{c_0 - c} \cdot P_0^{\frac{1}{3}} \left[ \frac{P_0S}{P_0Q} \right] - \frac{\sqrt{E}}{c_0 - c} \cdot P_0^{\frac{1}{3}} \left[ \frac{P_0S}{P_0Q} \right] - \frac{\sqrt{E}}{c_0 - c} \cdot P_0^{\frac{1}{3}} \left[ \frac{P_0S}{P_0Q} \right] - \frac{\sqrt{E}}{c_0 - c} \cdot P_0^{\frac{1}{3}} \left[ \frac{P_0S}{P_0Q} \right] - \frac{\sqrt{E}}{c_0 - c} \cdot P_0^{\frac{1}{3}} \left[ \frac{P_0S}{P_0Q} \right] - \frac{\sqrt{E}}{c_0 - c} \cdot P_0^{\frac{1}{3}} \left[ \frac{P_0S}{P_0Q} \right] - \frac{\sqrt{E}}{c_0 - c} \cdot P_0^{\frac{1}{3}} \left[ \frac{P_0S}{P_0Q} \right] - \frac{\sqrt{E}}{c_0 - c} \cdot P_0^{\frac{1}{3}} \left[ \frac{P_0S}{P_0Q} \right] - \frac{\sqrt{E}}{c_0 - c} \cdot P_0^{\frac{1}{3}} \left[ \frac{P_0S}{P_0Q} \right] - \frac{\sqrt{E}}{c_0 - c} \cdot P_0^{\frac{1$$

The initiation equation, from equation 2 of Appendix VI and equation 7 above is

As we pass from a microcrystalline casting to a single large crystal the density will approach nearer to  $\bullet_0$ , which in this case is the crystal density and n must approach zero but  $\lceil \log n - \log \rceil$ (60-6)/6] from equation 9, approaches infinity. Thus, on this model, a pure crystal should be insensitive. If we consider a cast explosive consisting of only a few crystals, we cannot define a mean density and therefore & will have no meaning but the number of cavities will be few. If they are small initiation may be difficult but it will be easier than in the pure crystal; growth will be favoured by the smallness of the cavity. The net result will be an increase in sensitiveness but a reproducible sensitiveness will be obtained only with large charges if the crystals are large. As the crystal size decreases, n becomes the main factor since changes in only have a large effect when 6.5 approaches zero. Thus initiation becomes more difficult but growth easier, not only because n increases but because Po, the pressure required to produce initiation also increases. We should, therefore, expect initiation to be the controlling factor at some value of 5 which will be closer to 5, the

smaller the crystal size. Microcrystalline charges should therefore behave like pressed charges.

When a pressed charge of T.N.T. is made from grains obtained from a microcrystalline cast charge it is more sensitive than one made from grains from a cast charge with large crystals. (Figs. 6a and 6b). Now our model assumes that initiation occurs in the cavities between the grains. Any cavities inside the grains must be smaller than the cavities between the grains except possibly when the grains. If initiation occurs, the pressure must momentarily increase and the increase may be sufficient to set off "cavities" in the grains. This explanation is not entirely acceptable because it suggests that growth and not initiation is the controlling process, whereas the dependence on d suggests the converse. The effect is, however, a small one and it may be that we are attempting to make too fine distinctions on a crude theory.

It is impossible to decide whether the controlling process in the sensitiveness of cast T.N.T. (normal brown) is initiation or growth. According to equations 8 and 9, if n decreases, initiation becomes easier and growth more difficult. Comparing a cast material with a pressed material made from particles of the cast material, we should expect n to be smaller for the cast material, i.e. initiation should be easier at a given density and growth more difficult. By extrapolation of the results in Fig 6 we see that the sensitiveness of cast T.N.T. appears to be about the same as that of a pressed composition of the same density. It is possible, therefore, but by no means certain, that growth is the controlling factor in cast (normal brown) T.N.T.

# 6.7 Liquid T.N.T.

Liquid T.N.T. (at  $90^{\circ}$ C) has a C value of 30 on Scale III, i.e. the corresponding value of  $m \times Q$  at 50 atms. is about 150 cal/cm<sup>2</sup>sec. We have already pointed out that there are two possible values of m at 1 atm. viz 0.017 and 0.022 g/cm<sup>2</sup>sec. Taking a mean value of 0.02 g/cm<sup>2</sup>sec at 1 atm. pressure, we obtain 1.0 gm/cm<sup>2</sup>sec. at 50 atms. The value of Q is uncertain. Assuming that all the oxygen is present as CO in the combustion products, Q = 653 cal/gm. However, the experimental value for Q is about 1000 cal/g. The value of  $m \times Q$  (at 50 atms.) thus lies between 653 and 1000 cal/cm<sup>2</sup>sec. This does not correspond

FOOTNOTE: We should point out that the equation  $C_7H_5N_3O_6 \rightarrow 6CO + 2.5H_2 + 1.5N_2 + C$ 

which gives Q = 653 cal/gm is a most unlikely reaction. This value of Q is much lower than the experimental figure. Such a large uncertainty is not found with other explosives examined, except propyl nitrate. In combustion reactions, Q for propyl nitrate is undoubtedly larger than 296 cal/gm but even if it were as high as 400 cal/gm, (since mxQ (at 50 atms.) would increase only from 34 to 46 cals/gm) it would not affect the correlation shown in Fig 1.

with the sensitiveness on either Scale II or Scale III and we find it difficult to accept such a high rate of burning from our knowledge of the combustion of explosives (ref 7). If we accept a value of  $m \times Q$  (at 50 atms.) of 150 cal/cm<sup>2</sup>sec, then m is 0.15 or 0.23 g/cm<sup>2</sup> sec depending on the value of Q. From Table IX we can estimate that liquid T.N.T. would have a value of about 12 on Scale I. Now  $P_CQ^C$  must lie between about 950 or 1500 cal/cm (since  $P_C = 1.46 \text{ g/cm}^2$ ). If we accept that  $m \times Q = 150 \text{ cal/cm}^2$ sec, then Q must be not less than about 850 cal/g for the Scale I result to be comparable with Fig 4.

By analogy with other liquid explosives we assume that growth is the controlling factor in the gap test sensitiveness. We have seen that it is impossible to determine whether the controlling factor in the case of cast T.N.T. is initiation or growth. The pressure corresponding to C = 30 on Scale III is about  $1 \times 10^4$  atms; that corresponding to C = 9 on Scale I is about twice as large. This is consistent with growth rather than initiation being the controlling factor, since the confinement on Scale I is less than that on Scale III.

In the growth process the number of cavities, n, the radius of the cavities r and the value of m x Q are the important parameters. We can be certain that m x Q will be larger for liquid T.N.T. than for cast T.N.T. since both m and Q are larger. However, we should not expect in to be larger than by a factor of two (see Andreew's values in Section 2.3). It is difficult to see what the nature of the cavities in the liquid could be (assuming they exist) but it is certain that they must be smaller in size and in number than those in a cast solid. It is, therefore, impossible to say whether a liquid should be more sensitive than a cast solid since although larger m x Q and smaller r favour growth, the smaller value of n does not. Anticipating the conclusions from our discussion, that the mechanism of initiation in the gap test applied to liquid explosives is different from that for solid explosives, we must conclude that, even if growth is the controlling factor for both cast and liquid T.N.T., the fact that these have the same sensitiveness is a coincidence and not an instance of a general phenomenon.

This conclusion is confirmed by results with Picric Acid (Fig 7). Liquid Picric Acid at 120°C has a C value on Scale II of 34 compared with C values for pressed charges of Picric Acid which are not greater than 27.

These data are not quite conclusive since the gap test sensitiveness might have a temperature coefficient. The limited evidence
available indicates that any such temperature coefficient is small.
Thus the gap sensitiveness of liquid propyl nitrate is not more than
one card different at -15°C from the value at about +15°C. Similarly
the sensitiveness of nitroguanidine changes by one card when the
temperature is increased from 15°C to 95°C. (22).

# 6.8 R.D.X/B.W.X.

In Section 4.2 we have suggested that the sensitiveness of pressed RDX/BWX is less than would correspond to the growth factor in x Q if it were homogenous. In general, whether initiation or growth were the controlling factor we should expect R.D.X. systems to be more sensitive than other solid explosives considered here with the same value of Q because R.D.X. has the highest rate of burning. However, we must remember that R.D.X/B.W.X. is at least a two phase system. When R.D.X. crystals are covered with Beeswax the cavities may be between these coated crystals. The sensitiveness would be much lower because beeswax does not burn (in the absence of air). Such a system should, therefore, be less sensitive than expected from the heat of explosion. It is possible that initiation occurs inside the crystals (c.f. pressed T.N.T. made with grains from cast T.N.T. of large and of small crystals) rather than in the wax between the coated crystals.

# 6.9 R.D.X. and P.E.T.N.

The quoted rate of burning of R.D.X. is definitely greater than that of P.E.T.N. (Table III) and these values agree approximately with the rates of burning of other nitramines and organic nitrates (ref 7). However, Bowden's work on cavity initiation of P.E.T.N. and R.D.X. (21) suggests that P.E.T.N. burns faster under his conditions than R.D.X. Nevertheless P.E.T.N. is, from all experience, (cavity initiation, impact sensitiveness and gap sensitiveness) more sensitive than R.D.X. R.D.X. crystals are harder than those of P.E.T.N. and, therefore, we cannot associate the difference with hot spots produced by intercrystalline friction although it is well-known that grit will sensitize R.D.X. and P.E.T.N. in impact tests. If R.D.X. does burn faster than P.E.T.N., then we must assume that some important factor has been omitted from our model.

#### 7. DISCUSSION.

- 7.1 The results of our analysis can be summarized as follows:-
  - (a) the shock sensitiveness of liquids is determined by the value of the products n x Q and ρ<sub>c</sub>Q, the second factor becoming increasingly important as the confinement is reduced. This behaviour suggests that growth rather than initiation is the controlling factor in sensitiveness,
  - (b) the rate of burning is a major factor in the sensitiveness of all explosives.
  - (c) the sensitiveness of pressed T.N.T. charges can be reasonably explained by a combination of cavity initiation and growth.

- (d) liquid T.N.T. apparently fits in with other liquid explosives but the value of the rate of burning is in doubt. The fact that liquid and cast T.N.T. have the same sensitiveness is probably a coincidence,
- (e) the difference in sensitiveness between R.D.X. and P.E.T.N. may originate in physical, not chemical factors.
- (f) in binary systems, the physical state of the binary system may be of major importance, e.g. RDX/BWX,
- (g) in rifle bullet tests there is a correlation with gap sensitiveness in the case of liquid explosives. If there is a correlation in the case of solid explosives, it is a different one from that valid for liquid explosives.

# 7.2 The Gap Test.

We have obtained some knowledge of the shock pressures transmitted to the explosive in the E.R.D.E. gap tests. It has also been shown (Fig. 3) that a series of shocks is transmitted to the explosive so that the explosive charge is subjected to an "effective" pressure for a time,  $\mathcal{L}$ , which depends on the gap thickness. The consequence of this are analysed in Section 6.4. We can write  $\mathcal{L} = f(P)$ , where P is the "effective" pressure. Clearly f(P) will depend on the type of gap test, i.e. on the material of the gap and on the size of the donor charge.

For the purposes of analysis we have distinguished between initiation, by which we mean the starting of a combustion reaction at some point or points in the explosive, and growth at these points, i.e. a positive value of dP/dt at these points. Initiation may be by adiabatic compression of gas-filled holes in the explosive, i.e. cavities, but it is probable that this is not the mechanism in liquid explosives (see Section 7.4). If the charge is encased in metal, the shock from the gap will be transmitted to the containers as well as to the explosive. The particle velocities in the container and explosive will, in general, be different and viscous heating of the explosive at the boundaries may be the cause of initiation. It has been shown that confinement is an important factor in the growth process. It can be seen, therefore, that the type of container used for the explosive charge may be important.

The two preceding paragraphs can be summed by the statement that the sensitiveness measured by a gap test depends on the experimental technique as well as on the explosive. To illustrate these points we quote the following results:-

(a) we find that cast (normal brown) T.N.T. and liquid T.N.T. at 90°C have about the same sensitiveness on Scales II and

III. American workers (23) using a different experimental arrangements, found liquid T.N.T. to be appreciably less sensitive than cast T.N.T.,

- (b) Dithekite D 13 is less sensitive than ethyl nitrate on Scale III but more sensitive on Scale I.
- (c) J. Savitt (24) mentions that the relative sensitiveness of R.D.X. and Tetryl and of Composition A and T.N.T. is reversed when the container material is changed from brass to aluminium.

Originally this work on the gap test was started at E.R.D.E. on the assumption that the test was physically a simple one, i.e. the propagation of a single shock wave into the explosive. This is not true but the efforts made to obtain a better picture of the events in the gap test have helped to obtain a better understanding of the mechanism of sensitiveness. Thus points (a) and (b) above may be explicable in terms of the confinement factor. Point (c), if confirmed, probably cannot be explained in this way because m x Q and  $\rho_cQ$  for R.D.X. are larger than for tetryl and, therefore, under certain conditions there may be some mechanism of initiation other than cavity initiation, e.g. viscous heating, in which case the low temperature rate of decomposition of the explosive becomes an important factor.

# 7.3 Relation of gap test sensitiveness to results by other methods.

We shall restrict our discussion to impact sensitiveness. Measurements of impact sensitiveness are normally carried out with powdered explosives which have been lightly tamped. In such measurements the particles of the explosive can move relative to each other, i.e. frictional heating is possible, air pockets are enclosed in the explosive, i.e. cavity initiation is possible, and with certain types of striker plastic deformation of the striker can occur and thus a hot spot can be formed on the striker. With P.E.T.N., in the absence of grit the initiation appears to be cavity initiation (21), whereas, with some of the primary explosives, hot spots are formed by frictional heating or localised plastic flow in the crystals (21). According to Eyster et alia (23) the addition of grit to an explosive does not alter its gap test sensitiveness (called "booster" sensitiveness in the U.S.). For assessment of handling hazards, impact tests are more significant than gap tests, despite the fact that the results are generally qualitative.

Another important aspect of an assessment test is the criterion for a "positive" effect in a test. In gap tests we have used either the fragmentation of the container or the amount of damage to a thin metal cover plate. In impact tests, the volume of gas evolved by the explosive (Rotter Impact Machine) or the sound from an explosion is used as a criterion. Now the impact and gap pressures

required to produce these results may be different. With two

explosives A and B, we may have the following state of affairs:- $\begin{array}{c} R_b \text{ (A)} < R_b \text{ (B)} \text{ when P} < P_p \\ R_b \text{ (A)} > R_b \text{ (B)} \text{ when P} > P_p \end{array}$ i.e. A will appear les: sensitive than B under one set of conditions and more sensitive under another set. Thus, at P = 1000 p.s.i., R (TNT) ~ 1.0 cm/sec (extrapolated from Table III) but may well be lower (see Section 6.4) and  $R_b$  (NH<sub>L</sub>CLO<sub>L</sub>) = 0.8 cm/sec but the rate of burning of T.N.T. appears to increase linearly with the pressure whereas that of NH<sub>2</sub>ClO<sub>1</sub> increases as P<sup>2</sup> (unpublished data of Mr. G.K.Adams, E.R.D.E.). At low initiating pressures, i.e. loose powders in impact test, NH, CLO, may be as sensitive or even more sensitive than T.N.T. but at initiating high pressures, i.e. compressed powders in gap test, should be less sensitive. Another case in point is cordite. Impact tests on cordites are always carried out with the finely divided material and under such conditions the cordites are quite sensitive. Gap tests measurements on cordite charges show that they are very insensitive. A good cordite charge has no pockets of gas and, therefore, cavity initiation is impossible. In manufacture, cordite is prepared either by a solventless or solvent process, i.e. the cordite is never in the form of a fine powder. Under manufacturing conditions the impact sensitiveness of finely divided cordite is irrelevant. If, however, it is necessary to machine or saw the cordite charges, the high impact sensitiveness of the finely divided powder is significant.

Nevertheless, there is a broad correlation between the gap and impact sensitivenesses of many explosives and we must ascribe this to the important role played by the rate of burning. Since, from the point of view of handling, explosive burning is a serious hazard, the low pressure rate of burning, which determines the sensitiveness of loose powders of solid explosives or a liquid explosive containing air bubbles, is probably a more important sensitiveness parameter than the high pressure rate of burning.

The case of composite explosives is considered in Section 7.5.

# 7.4 Liquid Explosives.

In the gap test measurement of the sensitiveness of liquid explosives we have shown that the results can be correlated on the assumption that the growth of the explosion centre, and not initiation, is the controlling process. We do not yet know what the mechanism of initiation is but two possibilities must be considered:-

- (a) very small air-bubbles in the liquid, and,
- (b) local fluctuations in density in the liquid.

We can obtain an estimate of the minimum size of air bubble

from equation 2 of Appendix VI (the exact equation would give a higher value of the size). With  $P_1 = 1$  atm. we have,  $\frac{30 R}{M.c} \cdot P^{(1-3Y)/3Y} = \frac{3}{16} \cdot Q \cdot \frac{1}{2} \cdot \frac{R}{Mc} \cdot P^{(1-3Y)/3Y}$ 

The uncertainties in the values of  $\lambda$ ,  $\epsilon$  and  $\lambda$  are not important. If the gas in the bubble is air, we assume  $\lambda = 1.4$ , i.e.  $(1-34)(3\chi-0.75)$ ,  $\lambda \sim 10^{-3}$  g/cm. sec. and  $\kappa \sim 10$  cal/mole.  $\bar{\rho}$  is the density in the precombustion zone. The temperature in the cavity after adiabatic compression is high (about 3000 K) and a value of  $\bar{\rho} = 0.0001$  P g/cm<sup>3</sup> should not be in error by more than a factor of two even with  $P = 10^{4}$  atms. For many liquid explosives  $\hat{\kappa} = \hat{\kappa}_0 \times P$ . With these values the equation above becomes:-  $(2.5 \times 10^{6} \times Q)/(\hat{m}_0 \times P^{0.75})$ 

Some estimates of F from this equation are given in Table XI.

# TABLE XI.

# MINIMUM BUBBLE SIZE FOR CAVITY INITIATION IN GAP TEST.

explosive.	mog/om² sec	Q cal/ gm	Patms x 10 <sup>-3</sup> pressure in gap test.	ro em.
Ethyl Nitrate.	.008	754	4.7 (Scale III)	4 x 10 <sup>-4</sup>
Nitromethane.	.0023	969	14.3 (Scale III)	8 x 10 <sup>-4</sup>
Propyl Nitrate.	.0028	294	22.2 (Scale III)	1 x 10 <sup>-4</sup>
D.E.G.N.	.017	<b>98</b> 9	5.25 (Scale I)	2 x 10 <sup>-4</sup>

Since this is the minimum of gas bubble for initiation under the pressure conditions in the gap test which give a positive effect, and since we have shown that the results can be correlated with  $\dot{m} \times Q$  (growth) and not with  $\dot{m}/Q$  (cavity initiation), any bubbles really responsible for initiation must be larger than this, i.e. at least  $10^{-9}$ cms. It is difficult to believe that degassed liquid explosives do contain bubbles of this size, except an occasional one.

It has been shown that addition of single bubbles (diameter 0.1 cm) to D.E.G.N. increases the sensitiveness very slightly (17). This must facilitate initiation but, since we have found growth to be the controlling mechanism, it would not be expected to have much effect on the gap sensitiveness.

It is known that there are density fluctuations in a liquid. When a liquid is compressed there must be local increases of temperature at the microscopic regions where the density, before compression, was below the mean density. For simplicity in calculation we shall assume that the liquid contains "holes". These "holes" will be distributed at random in the liquid but at any moment there is a finite possibility that any microscopic region contains more than the average number of holes. Such regions will be ones of low density.

We can estimate the minimum size of the regions in the following way. It was shown in ref 2 that the minimum size, r, of cavity in which combustion could be propagated was

With the values in Table XI we find that  $r_c \sim 5 \times 10^{-5}$ cm. The energy necessary to start the combustion reaction is (2)

which for ethyl nitrate is about 3 x 10-9 cals (values for the other explosives in Table XI range between 10-8 and 10-9 cals). This energy however, will not all be produced by adiabatic compression if the local rise in temperature is sufficient to decompose most of the explosive molecules in a time of the order of a few microseconds.

The number of calories released in a domain of radius ra (initially) assuming that complete decomposition takes place, is

which is smaller than the required energy by a factor of 10 (allowance should be made for the fact that the reaction is a constant volume rather than a constant pressure reaction and the adiabatic heat of compression should be added but these corrections will not materially affect the result). This indicates that the complete decomposition of all the ethyl nitrate in such a cavity would not be sufficient to start the combustion reaction, i.e. the minimum cavity size would be about 10 times larger.

If the compression raises the temperature in the small domain from  $T_0 = 300^{\circ}$ K to  $T^{\circ}$ K, a thermal explosion will be produced in a time t. Treating this thermal explosion as an adiabatic first-order process (which gives a minimum value of T), it can be shown that

 $\tau \simeq \frac{\exp(E|RT)}{B} \cdot \frac{RT^2}{QE}$ For ethyl nitrate, E = 39.9 k.cals/mole, Q ~ 70 k.cals/mole, log B = 15.8 and e (for ethyl nitrate vapour) ~ 30 cals/mole. With these values  $\tau = 5 \times 10^{-4}$  secs,  $T = 600^{\circ}$ K;  $\tau = 5 \times 10^{-6}$  secs,  $T = 700^{\circ}$ K;  $\tau = 2 \times 10^{-7}$  secs,  $T = 800^{\circ}$ K. The delay before ignition on cavity initiation (2) is  $\sim 10/\sqrt{P}$  which for ethyl nitrate (P =  $10^4$  atms,  $\nabla = 3$ cm/sec) is ~10-4 secs. Experimentally the delay for D.E.G.N. containing a bubble when initiated by the gap test, Scale I, is about 40 micro sec. (17). Assuming that the hot spot must be formed in a time

certainly not greater than 100 ksec, T must lie between 600 and 700 K.

The bulk rise in temperature when water is adiabatically compressed to 10 tatms. is about 35°C. We shall assume that this rise in temperature is bought about when some of the "holes" in the liquid are filled by compression, i.e. forcing molecules into them. If explosive liquids behave similarly (rough calculations on methyl nitrate (18) give a smaller rise in temperature) 10 times more holes are needed than exist on the average per unit volume of liquid in the domain of radius 10 r<sub>C</sub> = 5 x 10<sup>-4</sup> cm. in order to get a rise in temperature of 300 to 400°C. Since liquids at the melting point are 3% to 5% less dense than solids at the same temperature, we can say crudely that a liquid contains 3% to 5% "holes", i.e. places where molecules were in the solid state. This means that the liquid would have to have regions (with dimensions of 10-4 cm) of less than half the mean density. This is most unlikely.

The two possibilities discussed above are not mechanisms, therefore, for the initiation of liquid explosives in the gap test. Other possible mechanisms are viscous heating between the container and the explosive and concentration of shock waves by reflection from the container walls. Without further experimental data it is futile to speculate. However, even if the mechanism of initiation in the gap test is found, it may still give no explanation of how low velocity detonations propagate in nitroglycerine, methyl nitrate and diethylene-glycol dinitrate where the velocities of propagation are ~2000 m/s and the shock pressures are ~10<sup>4</sup> atms.

# 7.5 Solid Explosives.

On the model discussed in this report, we have shown that the sensitiveness of pressed charges of solid explosive can increase or decrease with density depending on whether the controlling factor is growth or initiation. Similar results have been found by American workers (20, 23). At densities near the absolute density intiation may be by another mechanism, i.e. by the temperature rise produced by compression of the bulk explosive. Our model thus accounts for the phenomenon of "dead pressing".

When we consider composite explosives, the picture becomes much more complicated. Compositions consisting of an explosive plus an inert component, e.g. RDX/BWX are considered in the first place. If the inert component completely covers each crystal of the explosive component, and if the crystals contain no gas-filled cavities, the composition should behave as inert material to pressures less than required for the initiation of "dead pressed" material. We can make an estimate of the thickness of inert layers in the following way, using RDX/Wax as our model. Let us consider crystals of diameter d cm. and cavities of diameter 2d (inspection of equation 4 of Appendix VI shows that this corresponds to a bulk density of about 1/9th of the absolute density). The thermal energy released in the cavity by adiabatic compression from a pressure of 1 atm. to

one of P atms is easily shown to be (assuming air in the cavity with a molecular weight 1)

where  $P = (T/T_0)^{\frac{1}{N}}$  Y = 1.4 and  $C = Specific heat per mole. If <math>P = 1 \times 10^{4}$  atms,  $T \sim 3000^{\circ}$ K and we can therefore neglect  $T_0$  and obtain

望,此.

This heat is to be absorbed by the fusion of the inert material. If the thickness of the inert material is tom., its effective latent heat of fusion, i.e. the energy required to raise the inert material from  $T_0$  to its melting point and to fuse it, L, and its density  $\rho_1$ , then

pi.T. (ad)2.にし=等.はで or = cT/(3取でpiL)

Assuming T = 3000 K, c = 10 cal/mole,  $T_0 = 300$ ,  $\rho_i \sim 0.8$  g/cm<sup>3</sup>, L = 50 cal/g.  $t/d \sim 10^{-2}$ . If  $\rho_e$  is the density of the explosive, the percentage of inert material is 600 . t/d . Fig. For RDX,  $\rho_e = 10.00$ 1.8 g/cm<sup>3</sup> and, for a wax,  $\rho_1 = 0.8$  g/cm<sup>3</sup>, hence about 3% of wax should be sufficient to desensitise R.D.X. Usually about 10% is used but Pennie and Sterling (25) report that 5% Beeswax or Acrawax is sufficient to desensitise fine R.D.X. It should be noted that the density of the wax does not enter into this calculation. The requirements of the wax are that it should have a large heat of fusion, L, be easy to spread over the explosive and adhere strongly to the surface of the explosive so that it is not removed during handling. Since for most purposes, a pourable explosive is required it follows from this discussion that the minimum amount of wax is determined by pourability rather than sensitiveness. A high density wax is clearly undesirable if a pourable composition is required.

The T.N.T. in RDX/TNT compositions can be regarded as the desensitiser and this is supported by the fact that these compositions approximate to T.N.T., rather than R.D.X., in their sensitiveness behaviour.

Composite explosives, such as NH<sub>4</sub>CLO<sub>4</sub>/TNT/AL, present a much more difficult case for analysis. Such compositions, based on NHLClo./Al, are sensitive to impact tests but relatively much less sensitive on gap tests. In impact tests, there is plenty of air in the lightly tamped composition so that oxidation of the aluminium may provide the necessary hot spots, and friction and plastic deformation may play a significant role. In pressed charges of this material there is much less air and, therefore, the necessary oxygen to burn the AL must be obtained from the NHLCLO, which is thermally a very stable material. It is not at all clear that the rate of burning of the composite charge is relevant in this case. It has been shown that pressed charges of NHLCLOL/INT/AL are more sensitive, at the same density, than cast charges of the same composition (26). We suggest that, in the cast charges, the T.N.T. covers the aluminium so that

oxidation of the aluminium by the decomposition products of the NH<sub>L</sub>CLO<sub>L</sub> is prevented. On this basis we can understand qualitatively why loose powders of the three components are as sensitive as R.D.X. om impact tests but relatively much less sensitive in gap tests and even more insensitive as cast compositions.

It was also found (26) that the gap sensitiveness decreased with decreasing density. As the density decreases the mean distance between fuel and oxidant components must increase. In order to get an exothermic reaction between the Al and the NH<sub>1</sub>ClO<sub>1</sub>, a diffusion flame must be set up between them and this will be more difficult the greater the separation.

Sufficient has been said to indicate the complications in interpreting the behaviour of composite systems. It is proposed to investigate the sensitiveness of binary mixtures of NH<sub>2</sub>ClO<sub>1</sub> and certain fuels as E.R.D.E. has a wealth of combustion data on this type of system.

# 7.6 Rifle Bullet Sensitiveness.

It has been shown that there is a reasonable correlation between the sensitiveness of liquid explosives on the gap test and to rifle bullets. Since the gap test measurements can be correlated by the assumption that growth, and not initiation of explosion centres is the controlling mechanism, it is logical to apply the same conclusion to positive effects produced by rifle bullets. We say "positive effects" because the results produced by rifle bullets vary from mild explosions to complete detonations. Further, plastic propellants give a high percentage of explosions although their gap sensitiveness is low. As a possible explanation we have suggested that the "positive effect" in the rifle bullet test starts as a low pressure. i.e. ~107 atm, combustion process. Whether the rifle bullet causes this as a result of frictional heating of the explosive during its passage through the explosive, by forming a hot spot at the back or front of the container from the work done in piercing the container or by the production of shock waves is not known. Whatever the mechanism, however, we cannot espect the correlation between rifle bullet and gap test to be necessarily the same for liquids as that for solids because the initiation process in the gap test is different for the two classes of materials and we suggest that the initial pressure conditions in the two types of test are also different.

Two types of research will be necessary to clarify this crude picture. Firstly a detailed study of the time between impact and a positive effect with different masses and energies of fragment (bullet) under different confinement conditions. Secondly, a comparison of the rifle bullet sensitiveness and gap test sensitiveness of systems for which the R<sub>b</sub>/P curves cross at some pressure. The following systems are quoted as examples:-

(a) ethyl nitrate and 2:3 butane diol dinitrate. It is known

that ethyl nitrate has the higher rate of burning at  $P^{\sim}$  100 atms. whereas it is less sensitive on the gap test Scale III.

- (b) a plastic propellant with and without a combustion catalyst for which the catalysed composition will have the higher rate of burning at low pressure,
- (c) T.N.T. and  $NH_{\downarrow}ClO_{\downarrow}$  since  $R_b$  (TNT) increases linearly with pressure whereas that for  $NH_{\downarrow}ClO_{\downarrow}$  increases as  $P^2$ , and,
- (d) ethyl nitrate alone and catalysed with an amine (5).

# 8. CONCLUSIONS.

Our thesis is that the mass rate of burning combined with the heat of explosion, is a good criterion of the sensitiveness of a compound. In gap test measurements the high pressure (above 1000 atms) rate of burning appears to be relevant whereas in impact, and possibly in rifle bullet tests, the rate of burning at lower pressures appears to be important. However, with a given composition, the sensitiveness can be varied over a certain range by alterations in the density, grain size and crystal size or form ( and \$\beta\$ H.M.X.). Completely satisfactory desensitisation implies that the energy per unit mass and the density of the explosive is not reduced. The method of application of the explosive also adds additional restrictions. Thus, if a pourable composition is required, e.g. RDX/TNT, RDX/PWX, the minimum amount of liquid phase required is probably above the minimum amount necessary for satisfactory desensitisation.

Desensitisation can be achieved basically in two ways. The first requires that the rate of burning should be reduced, with as little reduction in the energy as possible. Reduction in the rate of burning, without reduction in energy, has not been achieved except by mixing systems such as ethyl nitrate with nitromethane (Table I). The second way is to prevent mechanical action from producing hot spots in the explosive. For liquids, this means avoiding the presence of all gas bubbles in the liquid which is difficult. There is some indication, however, from Bowden's work (15) that, in impact tests, the viscosity may be of some importance. In the case of solids, we must reduce frictional heating, localised plastic deformation in the crystals and cavity initiation. In theory it is possible that some control of the first two factors can be achieved by modifications to the crystal form. All three factors can be controlled to some extent, by coating the high energy components with soft materials such as waxes. We have suggested that ~ 3% wax should be sufficient to desensitise a compound, such as R.D.X., against cavity initiation but we do not know whether such small quantities would be effective in impact tests with grit present. We can see that, with such small quantities of desensitiser, the physical properties of the desensitiser, apart from the relevant thermal ones and the ability to adhere strongly to the explosive, are of minor importance. The

greater the quantity of desensitiser, the more important become properties such as density and energy content. Of these, the density is probably most important since detonation pressure is approximately proportional to the energy per unit mass, but to the second power of the density. A high density desensitiser increases the difficulty of application because its volume is smaller.

It is shown in ref 7 that the rate of burning at pressures of 50 atms. is a monotonic function of Q but that explosives can be divided into three broad classes: nitramines, nitroxy compounds and nitro-compounds, the rate of burning at a given Q decreasing in this order. American workers have realised that the aliphatic nitrocompounds offer a fruitful field of research and have specifically looked for a substitute for T.N.T. in this field. R.D.X. and H.M.X. are good explosives because of their stability, fairly high energy content and high density. The efficient utilisation of these explosives requires either,

- (a) desensitisation with small quantities of high density desensitisers, or,
- (b) combination with an aliphatic nitrocompound with the minimum reduction in energy and density.

Class (a) will give compositions which cannot be poured, but must be press-filled. Class (b) can give pourable compositions. The application of these ideas to explosive systems will be discussed in another report at a later date.

#### REFERENCES

E. K. Rideal and
 A.J.B.Robertson.
 G.K.Adams & L.A.Wiseman.
 R.Pape & E.G.Whitbread.
 L.A.Wiseman.
 G.K.Adams & G.W.Stocks.
 G.W.Stocks.
 G.K.Adams & L.J.Drummond.
 G.K.Adams & G.O.Iloyd.

9. A.F.Belayev & A.E.Belayeva.

E.R.D.E. Tech. Memo. No. 2/M/52.
E.R.D.E. Tech. Memo. No. 2/M/52.
E.R.D.E. Tech. Memo. No. 21/M/52.
E.R.D.E. Report No. 42/R/51.
E.R.D.E. Report No. 1/R/51.
E.R.D.E. Report No. 10/R/50.
E.R.D.E. Report No. 4/R/53.
E.R.D.E. Report No. 10/R/53.
Comptes Rendus (Doklady) 1946,
52, 803.

10. S.J.Jacobs & W.B.Buck.	0.S.R.D. Report No. 6329.
11. R. Pape.	E.R.D.E. Tech. Memo. 8/M/54.
12. A.F.Belayev & A.E.Belayeva.	Comptes Rendus (Doklady) 1947, <u>56</u> , 491.
32 V V Andrews	
13. K.K.Andreew.	Comptes Rendus (Doklady) 1946,
	54, 39.
14. L.F.Jones.	E.R.D.E. Report No. 29/R/51.
15. F.P.Bowden & A.D.Yoffe.	The Initiation & Growth of
	Explosion in Liquids and Solids.
	Cambridge University Press 1952.
16.	A.R.E. Memo. No. 1/51.
17. R. Pape & E. G. Whitbread.	E.R.D.E. Report No. 17/R/52.
- 10	
18. S. Ratner.	Acta Physicochimica URSS 1947, 22,
18. S. Ratner.	Acta Physicochimica URSS 1947, 22,
	357•
19. G.K. Hartman.	357. N.O.L. Memo. 10,068.
19. G.K.Hartman. 20. R.H.Stresau & L.E.Starr.	357. N.O.L. Memo. 10,068. N.O.L. Memo. 10,577.
19. G.K.Hartman. 20. R.H.Stresau & L.E.Starr. 21. F.P.Bowden & O.A.Gurton.	357. N.O.L. Memo. 10,068.
19. G.K.Hartman. 20. R.H.Stresau & L.E.Starr. 21. F.P.Bowden & O.A.Gurton. 22. K.A.Cooper, E.Speller &	357. N.O.L. Memo. 10,068. N.O.L. Memo. 10,577. Proc. Roy. Soc. 198A (1949) p.350.
<ol> <li>G.K.Hartman.</li> <li>R.H.Stresau &amp; L.E.Starr.</li> <li>F.P.Bowden &amp; O.A.Gurton.</li> <li>K.A.Cooper, E.Speller &amp; E.G.Whitbread.</li> </ol>	357. N.O.L. Memo. 10,068. N.O.L. Memo. 10,577.
19. G.K.Hartman. 20. R.H.Stresau & L.E.Starr. 21. F.P.Bowden & O.A.Gurton. 22. K.A.Cooper, E.Speller &	357. N.O.L. Memo. 10,068. N.O.L. Memo. 10,577. Proc. Roy. Soc. 198A (1949) p.350. E.R.D.E. Tech. Memo. No. 11/M/51.
<ol> <li>G.K.Hartman.</li> <li>R.H.Stresau &amp; L.E.Starr.</li> <li>F.P.Bowden &amp; O.A.Gurton.</li> <li>K.A.Cooper, E.Speller &amp; E.G.Whitbread.</li> </ol>	357. N.O.L. Memo. 10,068. N.O.L. Memo. 10,577. Proc. Roy. Soc. 198A (1949) p.350.
19. G.K.Hartman. 20. R.H.Stresau & L.E.Starr. 21. F.P.Bowden & O.A.Gurton. 22. K.A.Cooper, E.Speller & E.G.Whitbread. 23. E.H.Eyster, L.C.Smith & S.R.Walton.	357. N.O.L. Memo. 10,068. N.O.L. Memo. 10,577. Proc. Roy. Soc. 198A (1949) p.350. E.R.D.E. Tech. Memo. No. 11/M/51.
19. G.K. Hartman. 20. R.H. Stresau & L.E. Starr. 21. F.P. Bowden & O.A. Gurton. 22. K.A. Cooper, E. Speller & E.G. Whitbread. 23. E.H. Eyster, L.C. Smith & S.R. Walton. 24. J. Savitt.	357.  N.O.L. Memo. 10,068.  N.O.L. Memo. 10,577.  Proc. Roy. Soc. 198A (1949) p.350.  E.R.D.E. Tech. Memo. No. 11/M/51.  N.O.L. Memo. 10,336.  Navord Report 2997.
19. G.K.Hartman. 20. R.H.Stresau & L.E.Starr. 21. F.P.Bowden & O.A.Gurton. 22. K.A.Cooper, E.Speller & E.G.Whitbread. 23. E.H.Eyster, L.C.Smith & S.R.Walton.	357.  N.O.L. Memo. 10,068.  N.O.L. Memo. 10,577.  Proc. Roy. Soc. 198A (1949) p.350.  E.R.D.E. Tech. Memo. No. 11/M/51.  N.O.L. Memo. 10,336.

# APPENDIX I.

# HEATS OF FORMATION.

COMPOUND.	HEAT	OF	FORMATION	(-AHf).
Ethyl Nitrate:			42.0	
Propyl Nitrate.			48.0	
Nitromethane.			25.1	
2 - Nitropropane.			<b>3</b> 8.9	
2:3 Butane diol dinitrate.			72.9	
Diethylene Glycol Dinitrate.			107.0	
Nitroglycerine.			85.4	

# HEATS OF FORMATION - (CONTINUED).

COMPOUND.	HEAT	Œ	FORMATION	(-AH <sub>f</sub> ).
Nitric Acid. Nitrobenzene. Ethyl Alcohol. Methyl Nitrate. Ethylene Glycol Dinitrate. Triacetin. CO2. CO. H2O (gas). H2O (liquid). Hydrazine (liquid). Hydrazine Nitrate. Mercury Fulminate. Trinitrotriazidobenzene. Potassium Picrate. Lead Styphnate. R.D.X.			41.4 5.5 66.1 35.4 61.0 306.2 94.05 26.41 57.80 68.30 12.05 60 65.4 272 110.1 107 - 14.4	
P.E.T.N. Tetryl. T.N.T.			126.7 - 8.0 10.2	

These values are not, in all cases, the best ones. Thus, Gray & Smith (J.C.S. 1954, 769) quote a value of  $\Delta H_f = -45.8$  k.cals/mol for Ethyl Nitrate and a recent redetermination of  $\Delta H_f$  (CH<sub>3</sub>NO<sub>2</sub>) has brought it back to the old value of -27 k.cals/mole. The main sources used were:-

- (a) Springall and Roberts. A.R.D. Report No. 614/44.
- (b) H.H.M.Pike. A.R.E. Report No. 25/49.
- (c) Robinson. Thermodynamics of Firearms. Hill
  1943.

# APPENDIX II.

# MAXIMUM RATE OF BURNING.

All explosives can burn to detonation. The mechanism, in most cases, is that the combustion gases penetrate into the mass of the explosive. This leads to a mass rate of burning per unit area which is much greater than the true mass rate of burning. Under such conditions pressure gradients will be formed and eventually shock waves. Since the gas flow into a shock front is always supersonic, the shock wave will move into the explosive and detonation may result because rates of burning normally increase with pressure. There is another possibility, however, if the true mass rate of burning is high enough a shock wave will be formed as soon as combustion commences,

i.e. true combustion is not possible since detonation intervenes.

Since the gas flow into a shock front must be supersonic intuitively one feels that an approximately necessary condition for this type of phenomenon is that the gas flow from the burning surface should be sonic. The sonic velocity, a, is defined by a  $=\sqrt{RT/M}$  where:- $=\sqrt{T}$  = specific heat ratio,  $=\sqrt{T}$  = temperature of combustion gases, and  $=\sqrt{T}$  = molecular weight of combustion gases. The gas flow velocity from a burning surface is  $=\sqrt{T}$  = m/= m RT/PM, where = density of combustion gases, and = pressure of combustion gases, i.e. initially of surrounding atmosphere. On our argument detonation and not combustion will occur if  $=\sqrt{T}$  a. We can then determine a critical value of m, m<sub>e</sub>, defined by

···中[祭]12

Since  $T \sim Q/c$  where Q = heat of explosion and c = specific heat per unit mass, we can write  $\sim P \left[ \sqrt{RQ} \right]^{1/2}$ 

With Q = 500 cal/gm,  $\overline{M}$  about 30,  $\overline{V}$  = 1.2 and c = 0.4 cal/gm, deg. C, the value of  $m_c$  at P = 1 atm., is about 20 gm/cm<sup>2</sup>sec.

A more rigorous analysis (Navord Report 90 - 46) leads to the expression.

If c is a specific heat at constant volume, the exact expression is smaller than the "intuitive expression" by a factor,  $(2(\chi+1)/\chi)^2 \simeq 2$  If c is a specific heat at constant pressure, the factor is  $(2(\chi+1))^{\frac{1}{2}} \simeq 2$ . Thus, the maximum rate of combustion, when gases do not penetrate into the explosive is, at P=1 atm., about  $10 \text{ g/cm}^2$  sec., which is far greater than the rate of combustion of any materials outside the initiator class (see Table III of text). It is possible that in the azides, particularly lead, thallous and silver azides, the true rate of burning is greater than  $m_c$  and therefore a hot spot goes over to detonation without an intermediate combustion regime. Bowden and Williams (Proc. Roy. Soc. 1951, 208A, 176) have shown that, with thin films (about 0.1 mm. thick) of the azides mentioned above, there

is no build up to detonation but detonation occurs immediately on

initiation.

APPENDIX III.

COMPOSITION OF PLASTIC PROPELLANTS IN TABLE IV.

Code No. of Omposition	NH <sub>1</sub> , C <b>£</b> O <sub>4</sub>	Picrate.	Polyiso- butylene. ts by weig	styrene.	NaNO3	Lecithin
E 202.	86.5	-	12.5	-	-	1
E 260.	76.5	10	12.5		_	1
E 261.	66.5	<b>2</b> 0	12.5	10	•	7
RD 2200.	89	-	-	10		+
RD 2043.	-	55	-	10	34	1
RD 2331.	36.5	50	12.5	-	-	1
RD 2332.	26.5	60	12.5	•		1

# APPENDIX IV.

# PROPAGATION TEST.

Most tests of "detonability" are, in reality, tests of propagation. In the usual form of this test the material to be examined is filled into a number of charge cases of about equal lengths but different diameters, and attempts are made to initiate these charges with primers, the size of which increases with charge diameter. In general the ability to support a detonation wave is greater at the larger diameters and with the more massive confining tubes. Tube strength is of secondary importance since the pressures involved in a detonation (about 10 atms.) are greater than the yield point of any material.

In practice a standard set of charge cases is used, each case with its own size of primer, and the result is quoted as the smallest size of tubing in which the material will propagate detonation. Such a set of tubes is given below.

Inside Diameter.	Wall Thickness.	Primer.
2	8 gauge. 8 gauge. 16 gauge. 16 gauge. 16 gauge. 16 gauge.	60 grams Tetryl. 40 grams Tetryl. 20 grams Tetryl. 10 grams Tetryl. 5 grams Tetryl. Detonator only.

Diameters greater than 2 inches are seldom used because of the quantity of explosive involved. With diameters smaller than  $\frac{1}{4}$ , the charge case is joined on to a section of larger diameter to accommodate the detonator.

# APPENDIX V.

#### COMBUSTION IN A CAVITY.

#### 1. Basic Equation.

Let V be the volume of the cavity in an explosive in which combustion is occurring. The mass, m(t) of gas (combustion products) in the cavity at time t is:-  $m(t) = V(t) \cdot \rho_g(t)$ . where  $\rho_{g(t)}$  = density of gases in cavity. If we assume that the gases behave as ideal gases (consideration of imperfect gases is given later),  $\rho_g = PM/RT$ , whence:- $\rho_g = \frac{M}{R} \left[ \frac{1}{4} \cdot \delta P - \frac{P}{L^2} \delta T \right]$ 

2.

where P = pressure, T = temperature, M = mean molecular weightof gases (assumed independent of P and T), R = gas constant.

At time  $t + \delta t$ ,  $m(t + \delta t) = m(t) + 4\pi r^2 R_b \beta \delta t$ , where r = radius of cavity,  $R_b = linear$  rate of burning of explosive (cms/sec),  $\rho_c = density$  of explosive (the compressibility of the explosive is neglected).

ρ<sub>8</sub> (++6+) = ρ<sub>8</sub>(t) + 3ρ δτ = m (++6+) = V(Hρ<sub>8</sub>(t) + μπ+2 R<sub>4</sub>ρ<sub>8</sub>δτ V(t+6t) = V(t) + μπ+2 δ+ 3.

where or = increase in radius in time

Substituting equation 2 in equation 3 and noting that V(t) =

(4/3).  $r^3$  we obtain  $\rho_{\delta}(t) + \frac{m}{R} \left[ \frac{1}{7} \frac{dP}{dt} - \frac{P}{17} \frac{dT}{dt} \right] \delta t = \frac{\rho_{\delta}(t) + \frac{3}{4} \cdot R_{\delta} \rho_{\delta} \delta t}{1 + \frac{3}{4} \cdot \frac{dT}{dt} \cdot \delta t}$ which neglecting teams in  $(\delta t)^2$ , leads to

#### 2. Value of dT/dt.

In time &t, the radius of the cavity increases by fr and the mass in the cavity by 4Mr Rb ct = m. We shall now divide this process into two stages:-

- (a) addition of hot gases of mass, m, the radius changing from r to r + Rbt, no work is done at this stage,
  - (b) expansion of cavity from r + Rhot to r + or without addition

of hot gases.

(a) If To is the initial temperature of the explosive then m(t).c.  $(T' - T_0) + Q. \Psi r^2 R_b \rho_c \delta t = (m(t) + \Psi r^2 R_b \rho_c \delta t).c. (T' - T_0), where$ T' = temperature after addition of mass m of hot gases, Q = heat of explosion at constant volume at To, c = mean specific heat at constant volume (Toto T).

By rearranging the above equation we obtain: -

(b) For adiabatic expansion - P = const. V (where & is different from the low temperature, low pressure value). Whence dP/P =

Further P = const.  $T^{*}(V-1)$  whence  $dP/P = \frac{X}{X-1} \cdot \frac{dT}{T}$  Therefore  $dT/T = \frac{X}{T} \cdot \frac{dT}{T}$  Therefore  $dT/T = \frac{X}{T} \cdot \frac{dT}{T}$ 

where T' = temperature after expansion of cavity from r + Rb(t) to r + r. The value of r is (Rb + A) t, where A is the linear rate of expansion under the balance of expansion of cavity from r + Rb(t) rate of expansion under the hydrodynamic forces, i.e. or in equation 7 is Act.

From equations 6 and 7

$$T''-T = \frac{3}{7} \cdot \frac{R}{R} \cdot \frac{R_b p_c T (Q'-cT') \delta t}{cP} - 3(Y-1) \frac{A \delta t}{T}$$

which can be written

which can be writ

since T' 🕿 T

Rate of Increase of Pressure in Cavity. 3.

Equation 8 can be substituted into equation 5 to give

Now 
$$dr/dt = R_b + A$$
, where A, a complex function of P and the conditions

of confinement, is the rate of growth of the cavity under the pressure in the cavity. Equation 9 can, therefore, be written

Imperfect Gases. 4.

Instead of assuming that PV = nRT, we can take the next approximation of P(V - nb) = nRT, where b = a constant, n = the number of moles of gas in volume V. It follows from this that  $\rho_0$  =  $P\bar{n}$  (RT+ $b\bar{r}$ )
If the above analysis is repeated with this value for  $\rho_g$ , we obtain:-

where  $\leq$  = bP/RT, which is similar to equation 9.

#### 5. Effect of Number and Size of Cavities on Confinement Factor A in Equation 10.

Let us imagine that the charge, during the build-up process, is expanding at a rate of E (cm /sec) per unit volume of explosive and that the increase in volume is obtained entirely by expansion of the cavities under the hydrodynamic forces, i.e. the compressibility of the condensed phase is neglected. Let there be n cavities. which have a radius r at pressure P, per unit volume of explosive. We then have: -

or

where dre/dt is defined by  $dr/dt = R_b + dr_e/dt = R_b + A$  as in Section 3 of this appendix.

# APPENDIX VI.

#### INITIATION IN A CONDENSED PHASE CONTAINING CAVITIES.

It was shown in ref 2 that the pressure required to produce initiation by the adiabatic compression of gas in a cavity of initial

radius re was given by the equation

3q R (R/R) 3/34

Me Pi [ [ R P: X8-144 + R M . Q - I']

 $q = \mathbf{\tilde{p}}^2 \cdot \mathbf{Q} \cdot \mathbf{k}/\mathbf{\hat{n}},$ 

F = mean gas density at moment of initiation,

Q = heat of explosion,

k = thermal diffusivity of gas,

m = mass rate of burning at pressure P,

 $P_i$  = initial pressure,

 $P_{O}$  = initiating pressure,

R = gas constant,

M = mean molecular weight of gases in cavity.

 $\bar{M}' = molecular$  weight of explosive vapour,

c = specific heat,

p = vapour pressure of explosive in cavity, Y = specific heat ratio,

T' = mean temperature in cavity at moment of initiation, and,

To = initial temperature.

Now if m is a linear function of pressure, q is approximately independent of pressure since  $k \vec{p} = \hbar/c$  is also approximately independent of pressure. For most explosives p is very small and the term containing

this can be neglected. In ref 2, it was estimated that  $T'/T_0$  was about 3 and therefore if  $P_0 \approx 10^3$  atms. we can also neglect this term. Equation 1 can therefore be written

tc = [34 R . P' | 3V] . [Po | -|3Y | 3Y]
= log D' - B log Po. Where D' = (3qR/Mc) P' | 3Y

whence  $\log r_c = \log D' - B \log P_o$ . Where  $D' = (3qR/Mc)P_c$  and B = (3y-1)/3y

2. Equation 2 will now be applied to a pressed charge. Let the charge be made up of particles of explosive of grain size d. If the density of the explosive is do and that of the pressed charge is do the number of explosive particles per unit volume of pressed charge is

n. T. d. 6. = 6 or n = \(\frac{1}{2}\).

The fraction of free space is (6-6)/6 and if we regard this as distributed over n cavities per unit volume of diameter d<sub>c</sub>, we obtain w. \( \begin{align\*} \lambda \left( \frac{1}{2} \right) \right) \left( \frac{1}{2} \right) \right( \frac{1}{2} \right)

 $\log d + \frac{1}{3} \log \left[6 - 6/6\right] = \log D - B \log P$ 

where  $D = 2D^{\bullet}$ .

Whitbread & Wiseman

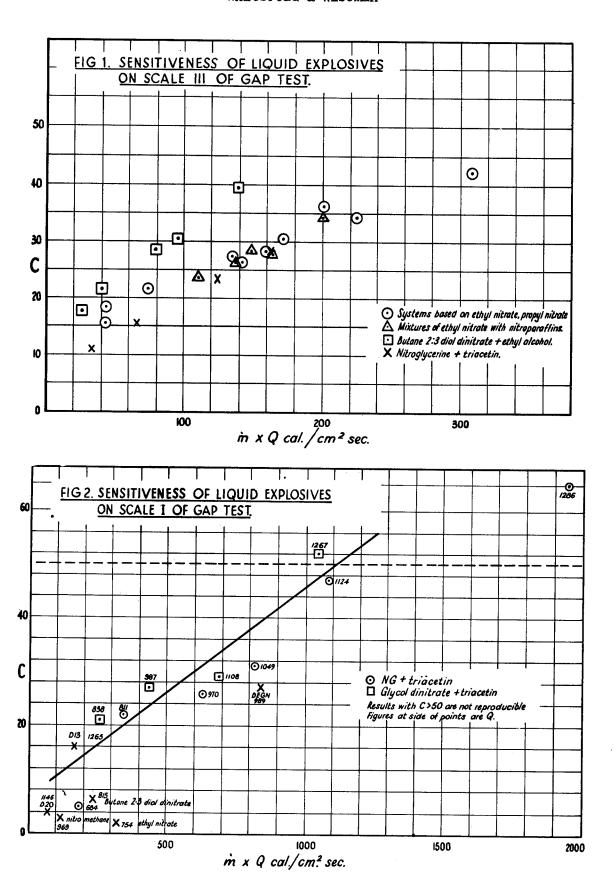
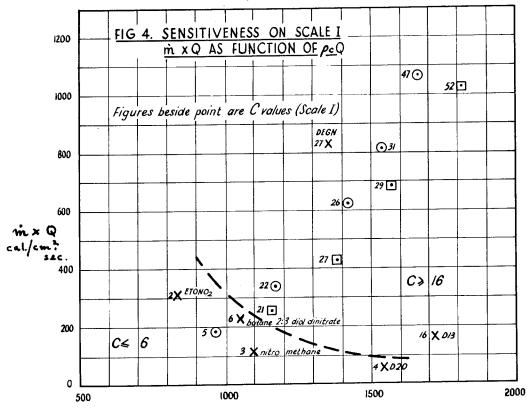


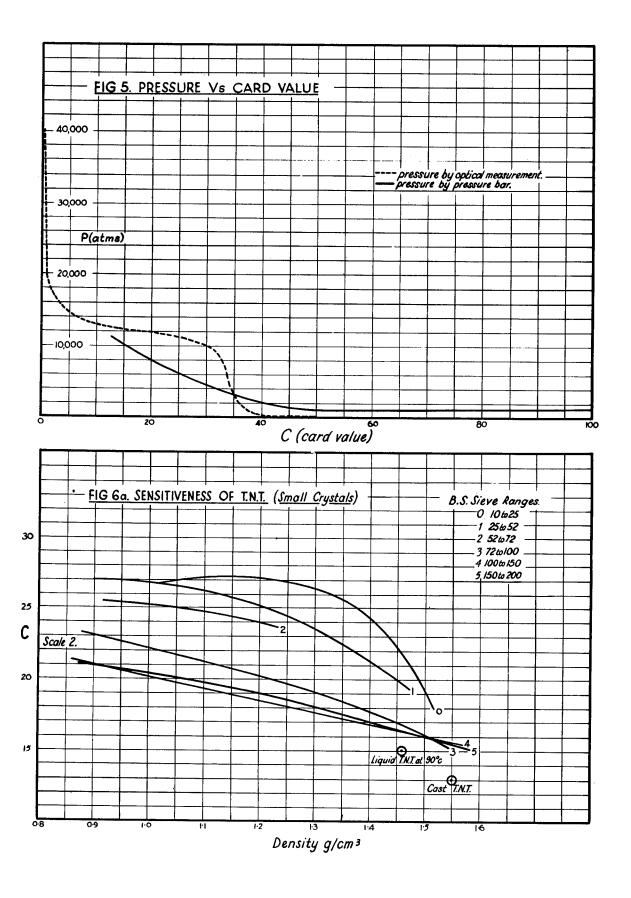
FIG. 3

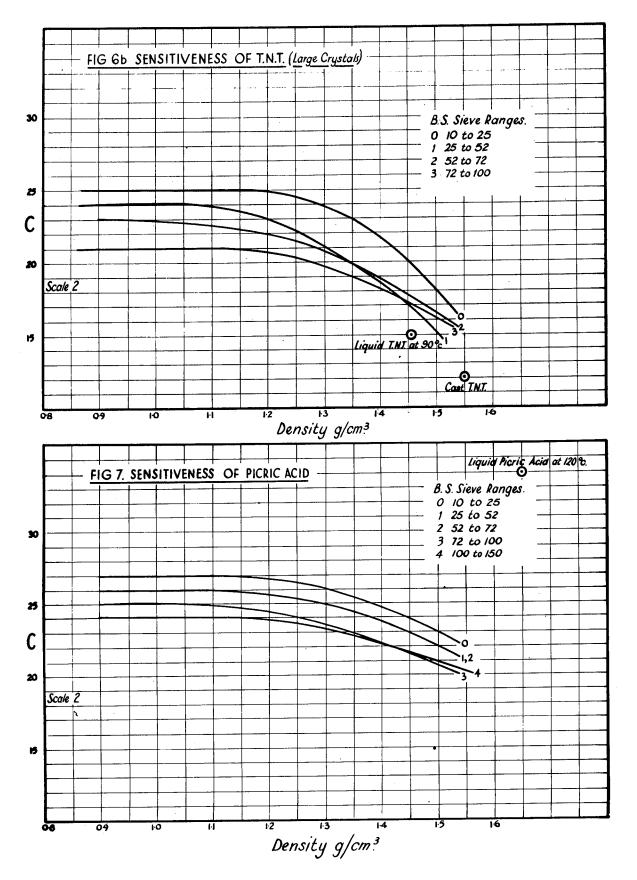
Edge of opaques cloud from donor & gap.

Mirror Camera photograph showing multiple shocks and reflections in Scole III type test (Water in perspex tube)

Flash from donor charge.







### PROBLEMS OF INITIATION IN TESTS OF SENSITIVENESS

E.G. Whitbread
E.R.D.E., Ministry of Supply
Great Britain

# SUMMARY

The prime purpose of tests of sensitiveness is to assess the probability of accidental explosion occurring in explosive charges of practical size. Information is accumulating at E.R.D.E. that in the case of some tests of sensitiveness it is the chance of growth, not of initiation, that is assessed. In this category are the 'Gap' test and tests of sensitiveness to attack by small arms ammunition and by high-velocity fragments, possibly excepting when they are applied to materials of a high order of sensitiveness such as R.D.X.

Perhaps the most important part of this information is the proved correlation between sensitiveness and an arbitrarily defined 'rate of energy release' deduced from combustion data. The correlation, however, tends to break down for materials of high sensitiveness, and also fails for plastic propellants and colloidal propellants (cordite).

Recent work at E.R.D.E. on the mechanism of tests by projectile attack has revealed induction periods of up to 500 microseconds between impact and explosion, thus confirming the importance of the growth phase. There is evidence of two mechanisms operating in the explosion process though it is probable that their overall pattern is the same, the features contributing to the pattern varying in degree. The particular mode prevailing is a function of the level of sensitiveness of the explosive tested, and this may result in tests of the 'Gap' type being much less reliable criteria for very sensitive explosives than for, say, liquid monopropellants.

If, with a particular explosive, it is clear which of the three phases of the explosive reaction is the most significant, initiation, growth or propagation, and if this is also the controlling phase under the conditions prevailing in the 'Gap' test, then the results

will be of value even if relating to a different parameter and shewing wider scatter than with the liquid propellants.

# INTRODUCTION

Sensitiveness tests are usually performed in order that the chame of an explosion in a charge of practical size may be estimated. In such a practical charge initiation is usually important only when accompanied by the subsequent growth of the explosion process.

There is a growing body of information at E.R.D.E. that in a number of tests of sensitiveness the mechanism of the test is related to combustion processes, and that what is being measured is not the probability of initiation but the rate of growth of the process once initiated. If this is so, then the properties measured by these tests will not be the same as those measured by other tests which do, in fact, measure initiation (e.g., some impact machines). If the data are to be intelligently used it will be necessary to decide both what is required and what is provided by the tests used.

# TYPES OF TEST CONSIDERED

# 1. Gap Test.

It has been observed by several authors - notably Eyring (1) - that some tests, particularly those using a high-intensity shock to initiate the explosive, give results which are very reproducible. In order to put sensitiveness studies on a quantitative basis it was therefore decided at E.R.D.E. some years ago to use the 'gap' test. The precise forms used at Waltham Abbey have been described elsewhere (2) and it is sufficient for the purposes of this paper to state that there are two patterns of immediate interest, described as Scales I and III, the major differences being (a) that in Scale I the case used to contain the charge under test is lighter than that used in Scale III, and (b) that whereas in Scale I the criterion of a 'fire' is the fragmentation of the charge case, in Scale III it is the rupture of the test plate placed on the top of the charge under test. In both cases the result obtained is a number, known as the 'card value', which increases with increasing sensitiveness.

# 2. Projectile Tests

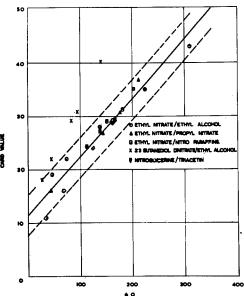
Since in the past it has been believed to be of 'practical' (as opposed to 'academic') importance, and because the results have some significance in relation to the 'gap' test, a considerable volume of work has been done on the 'rifle bullet attack' test and on the 'high-velocity fragment attack' test. In these tests the explosive is subjected to projectile attack while confined in a container, the subsequent condition of which, in conjunction with blast effects, is used to determine whether or not a charge has exploded.

# EVIDENCE AVAILABLE

In an analysis of the results obtained by the foregoing tests (3) it was shown:-

(a) That sensitiveness, as measured by Scale III (which deals with less sensitive explosives than does Scale I), correlates linearly with the product mQ, where m is a mass rate of burning under monopropellant conditions at an arbitrary pressure, 50 atmospheres, (the units of m are ML-2T-1) and Q is the heat of explosion (water gaseous) at constant pressure. The data are summarised in Table 1 and graphically represented in Fig. 1.

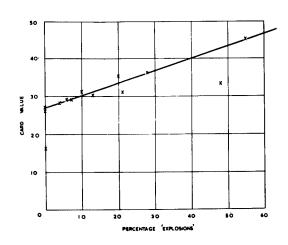
For any two-component system (e.g., ethyl nitrate/ethyl alcohol) the correlation between sensitiveness and the combustion data is excellent, deviations from the linear relation amounting usually to one unit (card) of sensitiveness.



CORRELATION BETWEEN SENSITIVENESS (CARD VALUE, SCALE III) AND RATE OF ENERGY RELEASE. FIG. I.

As can be seen from Figure 1, the overall correlation is very good; if the case of 2:3 butanediol dinitrate is excepted the regression coefficient is 0.96, which is significant at the 0.001 level for the number of materials tested. It is of interest that even the 2:3-butanediol dinitrate system shows the correlation between sensitiveness and make when considered by itself.

(b) That a linear relation exists between the percentage explosions obtained in the 'rifle bullet' test and the sensitiveness as measured by the 'gap' test, Scale III (and therefore, the 'rifle bullet' results correlate with mQ) (Fig. 2.).



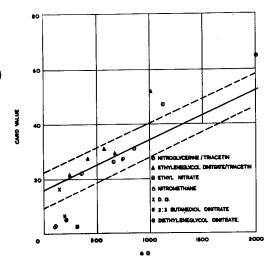
Percentage explosions in the Rifle Bullet Test Vs. Card Value (Gap Test Scale III). Fig. 2.

(c) That no simple correlation could be found between mQ and the card value for the materials tested on Scale I (i.e., for the more sensitive class of materials) (Table 2) Fig.3.)

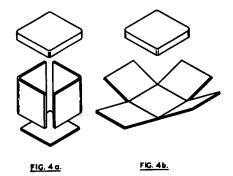
While the bulk of the work described deals with liquids, extension to solids is under way. The most outstanding result so far is that the plastic propellants and cordites, when fired in the form of a single cord, are very insensitive, as judged on the basis of the mQ relation. (Table 3).

While it is important that, eventually, the mechanisms for all tests of sensitiveness are understood, work directly aimed at the evaluation of mechanism has, at E.R.D.E., been restricted to the fragment' and 'rifle bullet' tests. In view of the links both have with fiQ, it is probable that similar mechanisms will be found for both the projectile and the Scale III 'gap' test. The details of the results of this investigation are as follows (4):-

(a) The tests are very sensitive to the construction of the container, for example, a change in the proportion of welded to folded edges has been found to



CORRELATION BETWEEN SENSITIVENESS (CARD VALUE SCALE I) AND RATE OF ENERGY RELEASE. FIG. 3.



have a marked influence on the results. Ethyl nitrate, fired in a box constructed as shown in Figure 4(a), gave 60% of explosions, but if the box was made as in Fig.4(b) the percentage of explosions fell to 40, a significant decrease in the 50-shot samples used.

(b) The tests are relatively insensitive to the energy of the projectile, provided that this exceeds some minimum value. Thus if in a steel box of uniform thickness a 'window' of varying thickness is fitted at the point of entry of the bullet, the results shown in Table 4 are obtained. The slight increase in lethality with thickness of entry windows from 1/16 to \frac{1}{4} inch is not statistically significant in the sample size (50 shots) used. The sharp decrease at 5/16 inch is significant and would seem to indicate that the projectile must have a certain minimum energy for initiation; but if it has this minimum energy, the probability of explosion is determined mainly by the explosive container. If the thickness of the whole

Table 1. Sensitiveness of liquid explosives in Scale III.

	Explos	i ve	е_	Rb	Q	í	iq	6 <b>d</b>	
No	Component, A.	Component, B.	g/cæ <sup>3</sup>	Cm/80C	cal/g	g/cm <sup>2</sup> / Sec.	cal/cm <sup>2</sup> /	cal/cm3	C#
	Ethyl Nitrate	Ethyl Alcohel							
1	100	0	1.11	0.37	754	0.41	309	837	43
2	96	ŭ	1.09	0.31	662	0.338	224	722	35
3	92.1	7.9	1.08	0.26	572	0,281	161	618	29
4	90.4	9.6	1.07	0.24	533	0.257	137	570	28
5	84-1	15.9	1.05	0.18	388	0.189	73	407	22
6	80.1	19.9	1.03	0.14	297	0.144	42	306	19
	Ethyl Nitrate	Propyl Nitrate					ľ		
7	80	20	1.10	0.29	662	0.319		728	37
ė	70	30	1.10	0.26	616	0.286		678	31
9	60	40	1.09	0.23	570	0,251	143	621	27
10	0	100	1.05	0.14	294	0.147	43	309	16
	Ethyl Nitrate	Hi trome than e	1						
11	60	40	1.12		839	0.213		940	31
12	40	60	1.13	0.15	883	0.170		998	29 2h
13	0	100	1.14	0.10	969	0.114	110	1105	24
	Ethyl Nitrate	"Nitro mizture"#	]	1					
14	80	20	1.11		757	0.266		840	35
15	70	30	1.12	0.19	759	0,213		850	29 27
16	60	40	1.12	0.16	761	0.179	136	852	2/
	2:3 B.D.D.N.	Ethyl Alcohol					4.50	2006	40
17	96	4	1.27			0.191		926 790	31
18	92.1	7.9	1.24			0.150			
19	90.4	9.6	1.23			0.134		744 531	29 22
20	84-1	15.9	1.18			0.094		409	18
21	80.1	19.9	1.16	0.063	353	0.073		405	10
	Nitroglycerin	Triacetin			656	0.017	162	925	29
22	67.5	<b>32.</b> 5	1.41			0.247		829	24
23	65	<b>35</b>	1.40			0.142		636	16
24	60	40	1.37	0.10		0.142		457	11
25	55	45	1.36		1265	1 0.101	75	401	30
25	D•13 ≠		1.37	ł	1146	ł			19
27	D.20 §		1.36	Į	1140	ł		ł	'7
	1	<u> </u>	<u> </u>	ļ	<u> </u>	<u> </u>	<u> </u>	<u> </u>	I

<sup>#</sup> C is a measure of the thickness of the gap. The gap consists of cards and C is the number of cards in the critical size of gap.

<sup># &</sup>quot;Nitromixture" = 83% Nitromethane + 17% 2-Nitropropane

<sup>#</sup> D.13 = 24.6% Mitrobenzene : 62.4% Mitric Acid : 13% Water D.20 = 22.6% Mitrobenzene : 57.4% Mitric Acid : 20.0% Water

<sup>• 2:3-</sup>Butene diol Dinitrate

TABLE 2
Sensitiveness of liquid explosives in Scale 1

T	Explosive		9.	Rb	a	1	iq	eq		
No.		Component B	€/cm³	Cm/800	cal/g	g/cm²/ sec.	cal/cm?	cal/	C ¥	Group
1 23 4	Nitroglycerin 90 85 82.5 80	Triacetin 10 15 17.5 20	1.54 1.50 1.49 1.47	0.98 0.64 0.52 0.44	1330 1170 1090 1009	1.51 0.96 0.78 0.65	2008 1123 850 656	2048 1755 1624 1483	65 47 31 26	C C B B
406	75 <b>70</b>	25 30	1.45	0.29	849 720	0.42 0.285	357 205	1231 1022	<b>22</b> 5	B
	Ethyleneglycol dinitrate	Triacetin								
789	89 84	11 16	1.45 1.43	0.559		0.81 0.61	1012 665	1811 1560	52 <b>29</b>	B
10 11	82 <b>.</b> 5 80 75	17.5 20 25	1.42 1.41 1.39	0.378 0.304 0.214	965	0.54 0.43 0.30	564 415 247	1482 1361 1144	31 27 21	B B B
12 13	Ethyl Nit Nitrometh	rate	1.11	0.37 0.10	754 969	0.41 0.114	309 110	8 <i>3</i> 7 1105	2 3	A
14 15 16	D.13. D.20. Butane 2:3 diol	dinitrota	1.37 1.36 1.303	0-18	1265 1146 824	0.117	1486	1733 1559 1074	16 4 6	В
17	Diethyleneglyco		1.39	0.61	877	0.848	744	1219	27	B

<sup>\*</sup>C is a measure of the thickness of the gap. The gap consists of cards and C is the number of cards in the critical size of gap.

 $<sup>\</sup>emptyset$   $\mathring{m}Q$  (and hence  $\mathring{m}$ ) obtained from Figure 1.

Table 34

Gap test Scale III Sensitiveness of Plastic Propellants

Code Number of Composition	Density gm/ml.		f Burning O p.s.i.	Q cal/gm	m x Q cal/cm <sup>2</sup> sec	C (Free from	C con-
or composition	<b>5</b>		gm/cm <sup>2</sup> /sec			air)	taining air)
E202	1.70	1.80	3.06	948	2931	16	
E260	1.67	1.50	2,505	865	2167	13 10	
E261 E911 )	1.65	1.15	1.898	773	1391		
(E202 + 3% Cr <sub>2</sub> 0 <sub>3</sub> )	1.73	2,25	3 <b>.8</b> 93	931	3624	15	22
E912 (E260 + 3% Cr <sub>2</sub> 0 <sub>3</sub> )	1.71	2,00	3 <b>,42</b> 0	840	2873	12	20
E913 (E261 + 3% Cr <sub>2</sub> 0 <sub>3</sub> )	1.69	1.70	2,873	751	2158	10	16
E937 (E202 + 3% K2Cr207 }	1.71	1.45	2 <b>.</b> 480	950	2356	12	
E938 (E260 + 3% K2Cr2O7 )	1.68	1.19	1.999	860	1719	10	
E939 (E261 + 3% K <sub>2</sub> Cr <sub>2</sub> O <sub>7</sub> )	1,66	0.94	1.560	770	1202	10	·
RD.2200	1.78	1,88	3,346	1140	3815	30	
RD,2043	1.73	0.69	1.194	453	541	10	
RD.2331	1.60	0.30	0.480	499	240	10	
RD.2332	1,58	0,25	0.395	404	160	10	10

- Notes:- (1) These propellants are putty-like materials made by coating a salt oxidant with a high polymer binder.
  - (2) The air content of the 'Free from air' material is about ½.
  - (3) The rates of burning are for 1000 p.s.i., data in other tables in this report are for 50 Atm. The correction factor, which is not known exactly, should not be less than 0.75.

Table B

Compositions of Plastic Propellants

	Parts by Weight								
Composition	Ammonium Perchlorate	Ammonium Picrate	Polyiso- butylene	Polystyrene Binder	Sodium Nitrate	Lecithin			
E202 E260	86.5 76.5	10	12 <b>.</b> 5 12 <b>.</b> 5	-	•	1			
E261	76 <sub>•</sub> 5 66 <sub>•</sub> 5	20	12.5	•	•	i			
RD.2200 RD.2043	89 -	<b>-</b> 55	-	10 10	34	1			
RD.2331 RD.2332	36 <sub>•</sub> 5 26 <sub>•</sub> 5	50 60	12 <b>.</b> 5 12 <b>.</b> 5	•	•	1			

Table 3C

Gap Test Scale III Sensitiveness of Cordite

Cordite	Density gm/ml.		burning 50 Atm.	cals/gm.		Card Value
***************************************		Rb	Å	Q	<u> </u>	C
SC Chopped **	1.5 <del>69</del> 1.0	0 •73	1•15	810	931	10 (a) 31 (b) 34
RS	1.578	0.81	1.28	890	890	10
F.488/649	1.550	0 -84	1.30	670	670	10

<sup>\*\* &#</sup>x27;SC chopped' consists of pressed charges, made from chopped SC cord, (a) of diameter and length = 0.205 inch each, and (b) of diameter and length = 0.048 inch each.

### Whithread

Yariation in Lethality with Thickness of Point of Entry

Rifle Bullet Attack = 3 inch cubical steel boxes of 4/8-inch well thickness filled with Ethyl Nitrate

Thickness of 'Window' (inch)	Percentage Explosions	Total Humber of Trials
1/16	42	50
1/8	40	50
3/16	46	50
1/4	50	50
5/16	0	10

<u>Table 5</u>

<u>Yariation in Lethelity with Thickness of Wall</u>

Rifle Bullet Attack - 3-inch cubical steel Boxes, filled with Ethyl Nitrate.

Thickness of Wall (inch)	Percentage Explesions	Total Number of trials
1/16	0	20
1/8	40	50
3/16	90	20

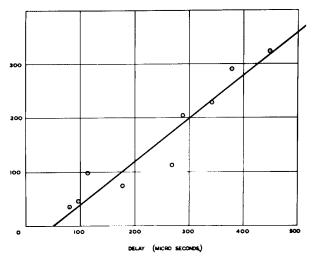
box is varied, and not just the point of entry, then there is a profound effect on the lethality, as is shown in Table 5.

The way in which the energy of the projectile is made up (i.e., the relative importance of mass and velocity) has a considerable effect on the lethality. Boxes made by welding 1/16 inch sheet steel end plates to 3-inch long sections of 3\frac{1}{4} inches 0.D. x 8 gauge pipe were attacked by high-velocity fragments and rifle bullets, the projectile passing axially through the box. The results with ethyl nitrate are given in Table 6, and it can be seen that, compared with the 1.7 gm. fragment, the 7.5 gm. fragment is not more lethal, in spite of its increased energy, and that the rifle bullet is (in this context) quite harmless!

When using boxes with perspex windows, high-speed photography of the entry cavities produced showed that, whereas the rifle bullet made a clean tunnel through the liquid, the bomb fragment made a large hemispherical cavity. It was thought that the blast pressure from the bomb used to drive the fragment was inflating the cavity through the entry hole, thus artificially increasing the surface and internal pressure, an effect absent in the case of the bullet. A number of shots were fired in which bombs without fragments were used to attack filled boxes with a previously made hole. In no case did initiation occur, nor was any cavity formed. It would seem, therefore, that the greater lethality of the smaller fragment, as compared with the bullet, is a real phenomenon and not produced by the experimental conditions.

- (c) It is possible to observe a delay between the impact of the projectile and the explosion. Three methods have been used in this work:-
- (i) varying the construction, and thereby the bursting time, of the box,
- (ii) high speed cinematography, and
- (iii) observation of the light evolved from the box, by means of a photomultiplier coupled to a cathode ray oscillograph.

The third method gives results more suited to exact analysis than the other two, and by the use of a number of mixtures of differing mQ the variation of the delay with this parameter has been observed. (Tab



VARIATION OF DELAY WITH M.Q. FIG. 5.

parameter has been observed. (Table 7 Fig. 5), and the delay found to be

Table 6.

Variation in Lethality with Projectile.

'Pipe' - type boxes filled with Ethyl Nitrate.

Projectile and Weight	Energy (Joules)	Percentage Explosions	Total Number of Trials
Fregment 1 gm.	2.50 x 10 <sup>3</sup>	22	23
Freguent 1.7 gm.	3.64 x 10 <sup>3</sup>	5 <del>f</del>	50
Fragment 7.5 gm.	6.70 x 10 <sup>3</sup>	10	20
Bullet 11.3 gm.	3.18 x 10 <sup>3</sup>	0	20

Table 7

Delay in Appearance of Flash in the Rifle Bullet Test as a function of mQ

Explosive		₽Q.	1	Delay
Component A	Component B	(cals./sec./cm²)		(Microseconds)
Ethyl Nitrate	Nitroglycerine			
100	0	309	0.00324	448
95	5	343	0.00291	<i>3</i> 78
85	15	437	0.00228	341
80	20	<i>1</i> <b>0</b> 0	0.00204	288
48	52	1010	0.00099	113
23	77	2128	0.00047	97
0	100	2784	0.00036	81
Nitromethane	Nitroglycerine			
l <b>şi</b> ş	56	904	0.00111	270
34.5	65.5	1376	0.00073	178

inversely proportional to mQ.

# DISCUSSION

In view of the correlation with mQ for both 'Gap' and Projectile tests, it would appear reasonable to suppose that we are dealing not with initiation itself but with the growth of the process subsequent to initiation, and that this process is similar to combustion.

Examining the relation between the delay and mQ in the rifle bullet test shown in Table 7 (Fig. 5), it can be seen that it is of the form:-

$$D - A = \frac{k}{mQ}$$

where D = measured delay A and K are constants.

Since mQ is a rate of energy release per unit area it follows that k/mQ is the time for some given quantity of energy to be produced. It is not surprising, therefore, that this will correlate with the observed delay from impact to some defined phenomenon such as the appearance of light. What is surprising is the length of the delays (up to nearly 500 microseconds) which can only re-emphasise that the rate of energy production in the early stages must be low, as, by consequence, must be the pressure.

The actual observation in a series of rifle bullet tests is the probability of explosion, as determined by the proportion of boxes actually exploding under set conditions. Initiation by any one or more of what might be termed the primary processes (i.e., shock produced by impact, viscous heating of the liquid flowing round the projectile, heating by the projectile which has itself heen heated by its passage through the front plate, and 'nipping' of the explosive between the projectile and the back plate) occurs in the first 120 -150 microseconds, and where the delay is longer than this there is strong presumptive evidence that the chance of explosion is not the chance that one of these processes will occur, but is rather the probability that a subsequent process is allowed to continue without Such a conclusion is supported by the relative interruption. insensitivity of the tests to the energy of the projectile and by their sensitiveness to the nature of the construction of the box. The high lethality of a small fast fragment appears anomalous but is explained later.

The most likely sequence of events is that one, or more, of the 'primary' processes starts a combustion-like reaction which either builds up to an explosion or is stopped by the dispersal of the system, and it is the variations in the middle stage that produce the variation in the results when different explosives are tested.

The way in which the rifle bullet test depends for its

discrimination on the differing rates of energy release is now reasonably obvious. Consider Figure 6 in which energy release, E, is plotted against time, T. A given energy release history is plotted on this diagram as a curve through the origin. Three such curves corresponding to rates R4 Ro and Rz are shown. (It is not assumed that the shapes shown are correct). In most forms of the test (5) 'Partials' are recognised as well as 'Detonations', (so called); these correspond to levels of energy release E4 (Partial) and E2 (Detonation). If we take a box of definite design, then the bursting time under the conditions of the test will vary in a statistical manner between limits Now, for an explosive T<sub>1</sub> and T<sub>2</sub>. corresponding to R<sub>4</sub> 100 per cent.

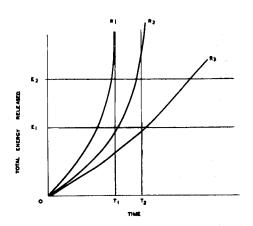


Fig. 6

of detonations will be observed since the R, energy release line reaches E<sub>2</sub> before T<sub>1</sub>; for R<sub>2</sub> there will be a statistical distribution of 'Partials' and 'Detonations', and for R<sub>3</sub> the prior advent of time T<sub>2</sub> will always ensure a failure.

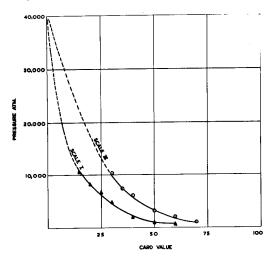
The two constants in the expression D - A =  $\frac{K}{MO}$  have a physical

meaning. If mQ is infinite, energy is released at an infinite rate and the intrinsic delay must be zero. We are, however, considering the delay from impact to the observation of light when using a steel box; to be observed, the light must get out of the box, so that either the projectile must go right in or, alternatively a split must appear in the box itself. 'A' represents this delay and will be roughly constant for all explosives. It was checked by the substitution of an all-perspex box for the usual steel one, using a filling of pure nitroglycerine; the observed delay was reduced, but the dispersion of D about the regression line for delay on 1/mQ is too great for A to be accurately measured by this experiment.

K is much more interesting than A. If D - A is a time and mQ a rate of energy release per unit area, K must have the dimensions of energy per unit area and represent the ratio of the total energy required to satisfy the criterion of a fir (in this case the light flash) to the area of reacting surface available. Now the surface available will be due largely to the material shattering under stress, and this is a very complex phenomenon depending (in the case of a liquid) on viscosity and tensile strength. It is interesting to note that all the liquids used to compile Table 7 have similar viscosities (their tensile strengths are unknown) and it is probable that if a major charge in viscosity had been made the correlation

would break down. It is possible that the increased lethality and the large cavity produced by the small fast fragment as opposed to the bullet is due to the lack of aerodynamic form and to the tumbling motion of the former, producing a larger zone of 'shattered' liquid. An attempt was made to check this by using 'dum-dum' bullets (i.e., with the ogive truncated); the cavity was altered in shape and the delay reduced, but not significantly so in a statistical sense.

In the case of the 'Gap' Test, the most important evidence for the existence of a slow combustion stage is the correlation between the card values and combustion data measured at a pressure which is very low (50 Atm.) compared with the pressures measured by the Hopkinson Pressure Bar on the 'gap' surface. (6) (Figure 7.) It is unlikely that the pressure exponents will be so consistent that the relative rates of burning for different explosives will be the same at the  $10^3$  to  $10^4$  atm.,



Hopkinson Pressure Bar Measurements on Gap Test Card Stacks. (Fig. 7).

shown in Figure 7, as they are at 50 atm.. The reaction will be stopped in the gap test not so much by dispersal - as in the projectile test - since the tube is often recovered, but by the onset of rarefaction waves from the top of the tube, and, ultimately, through the 'gap' itself. The time available for the induction period probably increases with increasing 'gaps' (because the gap is thicker the rarefactions take longer to enter the explosive), but this is more than offset by the decreasing pressure behind the shock front.

Solids may be divided into more or less porous solids and homogenous types such as cordite. In the former, the area of reacting surface is largely determined by the internal structure (i.e., by grist, crystal size, etc.); in the latter, we have materials which may be considered as liquids of enormous viscosity and considerable tensile strength. These will yield very small reacting areas (i.e., high values of K) and their intrinsic delays will be long, i.e., the probability of explosion is low.

There is no a priori reason why all 'gap' and 'projectile' tests should not conform to this scheme, and some explanation is necessary for the 'Scale I' results. If these data are examined (Table 2) they will be seen to fall into three groups (marked A, B and C in the table). Of these, group B correlates with fig in the same

manner as do the materials tested by 'Scale III', i.e., there is a relation of the form:

$$C = a + b \quad (\hbar Q)$$

The values of the constants a and b are, however, different for the two scales. It is thought that group A has failed to correlate because it consists of materials which, in the size of tubing used as a charge case, will fail to propagate a detonation. criterion of a 'fire' is that the tube is shattered, the test is not applicable to such materials which are certain to give anomalous By reference to Table 2 it will be seen that they all have relatively low values for e Q, the energy density, and this indicates lack of ability to propagate detonation, particularly in small diameters where the energy losses due to the lateral expansion of the confining tube in the region of the reaction zone are high. reason for the failure in the correlation in materials of high mo (i.e., those in group C) is more subtle, and in some respects more important. It is known that for 'gaps' in excess of 50 cards on 'Scale I' the pressure in the shock front is below 1000 atm. (6) (Fig. 7). and that under these conditions the attenuation is no longer exponential or reproducible (a peculiarity of the cardboard system). This, however, is not the whole story since, if the correlation has been obeyed, then with at least two of the materials card values of less than 50 should have been obtained. A probable reason for the failure is that for material of high mo the build-up of the reaction from initiation is so rapid that it is not possible to extinguish it by mechanical dispersal. The limit for control in this way, must vary with the system, and for 'Scale I' appears to have been reached at mQ = 850 cals./sec.cm<sup>2</sup>.

### CONCLUSIONS

It is concluded that there is a common mechanism for all explosions in the tests described, viz:- (i) initiation of a combustion, (ii) increase in rate of burning and extent of combustion surface, (iii) a change to detonation if the burning surface has a velocity exceeding the local speed of sound, thus generating a shock wave. It is with the probability of the third step, detonation or, if this does not occur, the virtual completion of the second by the consumption of all the available material, that we are concerned in sensitiveness testing.

Within this general pattern occur two modes of operation. If the second stage is slow - because of a low rate of burning, low energy or too little surface available for combustion - then it will become important because, being slow, it will provide a delay in which it is possible to "put out the fire." If, however, the second step is fast then every initiation becomes a detonation and we must measure the chance of initiation.

### Whi thread

It has been seen that our tests commonly measure the rate of growth, i.e., step (ii), but that in some cases (e.g., explosives of high mQ) they might measure chance of initiation because in the The question then arises: does the test the second step is fast. test provide the information required for all explosives for which mechanical considerations (such as the failure of large cardboard gaps) do not preclude its use? To answer this question, we must know the operating mechanism in the explosion of the practical The investigation of this charges which are our primary concern. while not more difficult, is much more expensive than the corresponding work with small charges, and may be prohibitively so. We have, however, some information: it is certain that if delays are not important in a small charge, they are even less so in a No-one doubts that if nitroglycerine (an extreme case) is initiated there is no way of stopping it; the difficulty is that even with less sensitive explosives, if they are in the form of a large charge, every initiation may become a detonation simply because the transit time of the shock wave and the returning rarefaction is so great that, without the aid of confinement, there is ample time for the 'growth' stage.

We have little information to enable us to decide at what size a particular explosive will pass into this class, but if the importance of such tests as the 'gap' test is to be assessed it will have to be obtained.

# BIBLIOGRAPHY

- 1. H. Eyring, Chem.Rev., 45 1 69-181, 1949.
- 2. R. Pape and E.G. Whitbread, E.R.D.E. Tech. Memo. 21/M/52.
- 3. L.A. Wiseman E.R.D.E. Report 42/R/51.
- 4. P.C. Hobbins and E.G. Whitbread E.R.D.E. Report in preparation.
- 5. L.F. Jones E.R.D.E. Report 29/R/51.
- 6. R. Pape E.R.D.E. Tech. Memo. 8/M/54.

# LEAD AZIDE PRECIPITATED WITH POLYVINYL ALCOHOL

T. Gaynor Blake Olin Mathieson Chemical Corporation East Alton, Illinois

> Donald E. Seeger Picatinny Arsenal Dover, New Jersey

Richard H. Stresau Naval Ordnance Laboratory White Oak, Maryland

# Introduction

Although the virtues of lead azide as an initiating explosive have long been known, its use has been somewhat limited by the hazards involved in uncontrolled crystallization. Accidental explosions which occurred in early manufacture were variously explained in terms of large crystals, twin crystals and formation of the beta polymorph. Many materials have been used for the purpose of directing the formation of the stable alpha form during the precipitation. The best known crystal controlling material, which is also the most used in the United States is dextrin (1). Typical dextrinated lead azide contains between 92 and 95% lead azide.

The British have used a material termed "Service" lead azide (2), characterized by a minimum lead azide content of approximately 97%. The crystal control of this material is achieved without the use of an organic protective colloid. Due to its higher purity, "Service" lead azide will usually out-perform dextrinated lead azide, but its handling and storage characteristics are less desirable.

During World War II, in the loading of detonators containing Service Lead Azide, some United States installations experienced prohibitively high rates of

inadvertent explosions during the pressing operations. This led to attempts in the chemical laboratories to modify the lead azide in order to reduce the handling hazards, while maintaining the desirable characteristics of Service Lead Azide.

One of the resulting lead azides which seemed to have improved sensitivity characteristics was a sample precipitated in the presence of polyvinyl alcohol (3), hereinafter referred to as PVA lead azide, and having a lead azide content somewhat reduced from that of Service Lead Azide. This material, however, was not approved for production prior to the end of World War II. In 1949, the Naval Ordnance Laboratory began an investigation of the properties of this lead azide, which led to the discovery of some interesting characteristics. These characteristics include low hygroscopicity, an ability to accelerate to maximum rate of detonation in a shorter period of time (and column height), and a slight increase in the terminal rate for the same loading pressures.



Dextrinated Lead Azide (75X)



Polyvinyl Alcohol Lead Azide (75X)

#### FIGURE I

## Experimental

During the development of the T196E4 (M505) Fuze for use in 20 mm. ammunition, it became evident that a detonator smaller than the standard M29 detonator (which was the smallest available at that time) would be needed in order that the safety requirements could be realized. The

space available for the detonator, later to be designated the T32, was approximately .145" in diameter and .290" long. It was required that this detonator be capable of initiating high order detonation in an RDX booster charge across a minimum air gap of .050".

At the outset of the development of the T32 detonator, the PA-100 and Standard Primer Mixtures, dextrinated lead azide, tetryl, PETN and RDX were the only explosives standard for use in detonators. It soon became evident that, using these materials, the optimum explosive train was one made up of PA-100 Primer Mixture, dextrinated lead azide and RDX. A shellac coated gilding metal cup, hand loaded with these explosives produced a detonator that met the requirements set forth and functioned satisfactorily in fuzes. However, since the critical weight tolerances required on the charges of explosive of this detonator could not be held in mass production, the detonator failed to satisfy the need. In order that such a small detonator could be mass produced, it was necessary to look for more efficient explosive materials.

Information on the availability of new explosives and explosive mixtures suggested two paths of solution to the problem. One involved the use of a more efficient primer mixture; the other the use of a more efficient lead This problem was finally resolved after exhaustive azide. investigation and subsequent adoption of the NOL No. 130 Primer Mixture. It was found that as little as 5 mg. of this primer (compared with 25 mg. of PA-100 Primer Mixture) is required to initiate dextrinated lead azide reliably. The quantity of primer mixture used in this detonator was therefore cut to approximately one-half the amount originally used. The space made available was used by increasing both the dextrinated lead azide charge and the RDX charge. This detonator, designated originally as the T32El Detonator and finally standardized as the M47 Detonator has been mass produced with little difficulty.

During the investigation of the second possible solution to this problem, several new types of lead azide were investigated. Among these was the Polyvinyl Alcohol (PVA) lead azide. Modified T32 Detonators loaded with this lead azide in place of the standard dextrinated lead azide proved to be far superior from a functioning point of view. Figures II, III and IV show results of T32 Detonator shellac coated gilding metal cups loaded with 30 mg. of PA-100 mixture and the intermediate and base charges as noted. Each charge was consolidated at 10,000 p.s.i. As noted, the space available from the decrease in the lead azide charge was filled with base charge.

Blake, Seeger and Stresau

Quanti	ty (n	ıg.)				Hole :	Size (Ir	nch)
PbN <sub>6</sub>	RDX	PETN	#Tested	НО	LO	Ave.*	Max.	Min.*
100 95 90 85 80 70 65 55		30 34 38 42 44 46 45 54	50000000000000000000000000000000000000	50 49 37 25 33 30 33 11 0	0 13 25 17 20 17 39 50	.227 .223 .220 .228 .228 .230 .232 .227	.248 .250 .237 .247 .250 .261 .248	.209 .164 .203 .207 .180 .204 .200 .200
100 95 90 85 80 70 65 55	236 344 446 480 552		50 50 50 50 50 50 50 50 50 50 50 50 50 5	50 50 50 50 50 50 50 50 50 50 50 50 50 5	0 0 0 0 0 2 5 0 0 5 0 0 5 0 0 5 0 0 0 0	.229 .233 .233 .227 .218	.248 .250 .251 .252 .242	.212 .214 .213 .187 .172

Figure II

PbN6	RDX	#Tested	НО	LO	Ave.	Max.	Min.
80 75 70 65 65 55 45	45 48 54 57 60 61 62	50 50 50 50 50 50 50	500009999 5555444	0 0 0 0 0 1 1	.258 .258 .260 .263 .266 .267 .266	.289 .278 .281 .284 .294 .306 .293	.233 .231 .237 .237 .231 .225 .212

Figure III

Similar tests were conducted in a modified T32El Detonator. In this case the shellac coated gilding metal cups were loaded with 13 mg. of NOL No. 130 Primer Mixture, lead azide and RDX as noted. Each charge was consolidated at 15,000 p.s.i.

Blake, Seeger and Stresau

Quanti Dex.	<u>ty</u>				Lea Hol	d Disc Le Size*	<del>,</del>
PbN <sub>6</sub>	RDX	<u>#Tested</u>	<u>#HO</u>	<u>#LO**</u>	Ave.	Max.	Min.
110 100 90 85 80 75 70 65	36 45 45 55 55 58	45 45 45 45 45 45 45 45	45 45 44 20 0	0 0 0 1 17 43 45 45	.212 .218 .194 .219 .149 .163	.232 .244 .228 .251 .214 .245	.177 .170 .081 .159 .075 .081
Py PbN <sub>6</sub>	RDX						
70 60 55 50 45 40 35 30	60 62 64 67 70 72 74 76	45 45 45 45 45 45 45	44444 4444 4444	0 0 0 0 0 0	.260 .267 .264 .263 .252 .269 .224	.308 .291 .298 .303 .290 .302 .275	.230 .230 .206 .206 .192 .231 .186

<sup>\*</sup> Low order detonation not included in hole size.

#### Figure IV

As can be seen from the data presented in Figures II, III and IV, PVA lead azide is twice as efficient as an intermediate charge for use in small detonators as the standard dextrinated lead azide.

Under Project "Jackstraw" one of the approaches to the problem called for the design of a very small stab type primer-detonator having great sensitivity. This detonator was to occupy a space having a diameter of .145" and an overall height of 1.40". Moreover, there was a section at the base of the cylinder which had a diameter necked in to .090". This detonator was required to initiate high order detonation of an RDX-Hystrene (98-2) lead across a .035" air gap. Because earlier fuze design work on this task had been carried out with the M26 primer which appeared to have almost the desired sensitivity, the first efforts were toward increasing the initiating ability of the M26. It was very quickly found that neither the sensitivity nor the required initiating ability could be achieved.

<sup>\*\*</sup>Low order - no hole in lead disc.

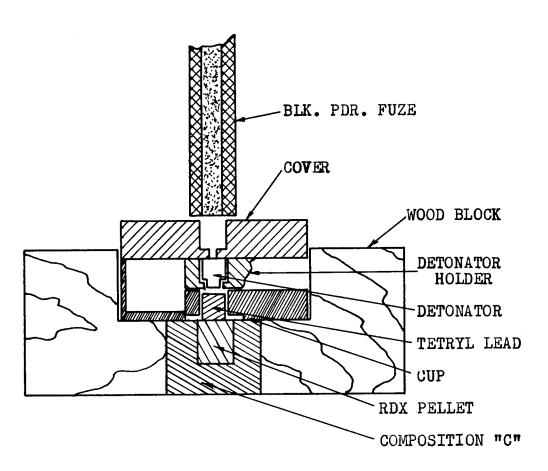
The successful approach was made as follows:
Using the cup described above and holding the initiator constant at a value considered to be well above minimum, the base charge was progressively reduced to determine the minimum quantity which would give the initiating power required.

In order to eliminate the variables associated with sensitivity and firing pin shape, the lead azide charge was subjected to the spit of a section of safety burning fuse. Because with the small quantities of explosive the degree of confinement provided by the test fixture was considered to be extremely critical, it was decided that measurements such as plate indentation should be avoided and the test shots would be in fuze rotors which in turn would fire the normal lead and the ability of this lead to propagate to a booster would be determined by having the lead shoot a small sample of Composition-C contained in a wood block. Figure V, Drawing A-2 shows this This proved to be a very noisy test and the test fixture. wood blocks were, of course, completely demolished when a high order detonation was achieved. On the other hand, it eliminated any possibility of misinterpretation of results because the Composition-C, in those cases where the detonator was sub-marginal was merely scattered around and the wood block was not destroyed. At this time three base charge materials were under consideration, tetryl, PETN and RDX, in the belief that small differences in their sensitivity to initiation and output might be significant in achieving a workable system.

Having determined the minimum quantity of base charge, this was held constant and the minimum initiating charges, both of dextrinated and PVA lead azide were determined. In this case it was found that less than 30 mg. of PVA lead azide would initiate the base charge high order whereas 55+ mg. of dextrinated azide were required. These data were plotted as % fires vs. base charge.

Next the minimum quantity of priming necessary to initiate the lead azide satisfactorily was determined holding the azide and base charge constant, at a value above the minimum previously determined. It was found that as little as 5 mg. of NOL No. 130 would give reliable initiation of the system. This determination was made using the assembly shown in Figure VI, Drawing A-3 which re-introduced the problem of input energy now that initiator and base charge had been removed from the area of suspicion.

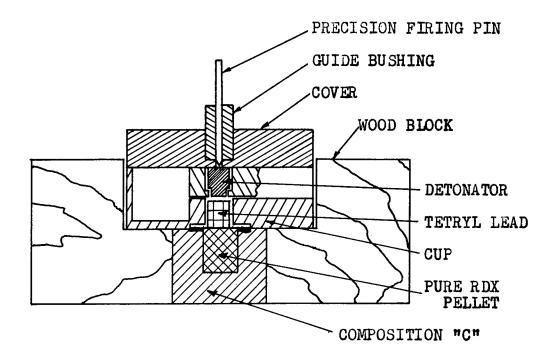
The 100% firing values for charge weight were then calculated in terms of inches of column height in the detonator, and were plotted in terms of base charge vs.



Test Assembly (Without Priming)

Figure V

Drawing A-2



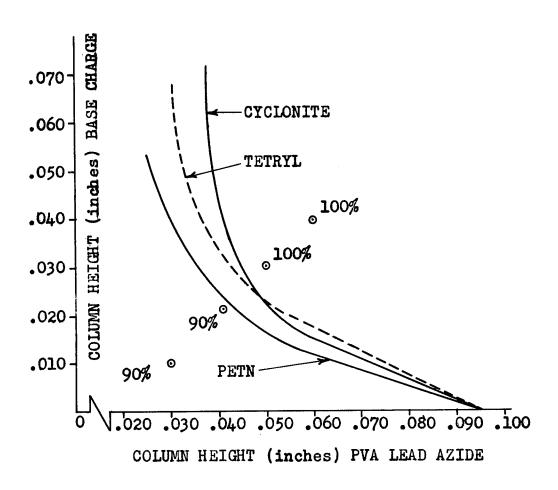
Test Assembly (For complete primer - detonator)

Figure VI

Drawing A-3

100% FUNCTIONING CURVES

Base Charge Column Height vs. PVA Azide Column Height



VARIATION OF INITIATOR VS. BASE CHARGES FOR 100% FUNCTIONING WHEN TESTED AS IN SKETCH A-2

THE FOUR POINTS WERE ESTABLISHED IN TEST ASSEMBLY A-3 WITH COMPLETE DETONATORS

Figure VII

Drawing A-1

initiator in inches. This gave the curves shown in Figure VII, Drawing A-1.

All of the potentially useful values for column height of initiator and base charge fall above the curves. The area below the curves gives unreliable functioning. A study of the tolerances experienced in production loading then permitted the selection of a point above the curves and yet within the total length of the detonator which would permit the normal variables in production (i.e., charging of lead azide and the base charge) without getting outside that useful area.

The final loading recommended for production was: Base Charge, Tetryl .010 grams, PVA Lead Azide .040 grams, and NOL No. 130 Priming .015 grams, permitting considerable safety margin, percentage-wise, on each charge, whereas the volume available did not permit an acceptable design using dextrinated lead azide.

Although not discussed above, it is interesting to note that a condition of dead pressing of tetryl was experienced in several of the experimental detonators in which the lead azide charge was marginal, such that a decrease in loading pressure from 25,000 p.s.i. to 15,000 p.s.i. caused an otherwise identical design to change from 100% failures to 100% high order detonations.

A number of fuze designs have been built around an electric detonator of about the size and input characteristics of the Mk 124 Primer. As its name implies, this item was not originally designed as a detonator. However, it has been found to function satisfactorily as a detonator under certain circumstances. These circumstances are not prevalent in all of the proposed designs, so that the problem arose of producing a detonator of the same dimensions but with greater effective output. One expedient which was suggested by S. Kolodny of the Diamond Ordnance Fuze Laboratories was that of inserting a steel washer at the beginning of the explosive column to increase the confinement and promote the growth of detonation. Another was the substitution of PVA for dextrinated lead azide.

Special detonators were fabricated from Mk 124 Primer parts. The detonators were divided into two groups, a confined group and an unconfined group. Each group had two series, one with dextrinated lead azide and the other with polyvinyl alcohol lead azide, as intermediate and flash charges, Figures VIII and IX. All four series had base charges of PETN. Members of each series were loaded with various amounts of lead azide and PETN and the output of each item was obtained using the dent test. (4)

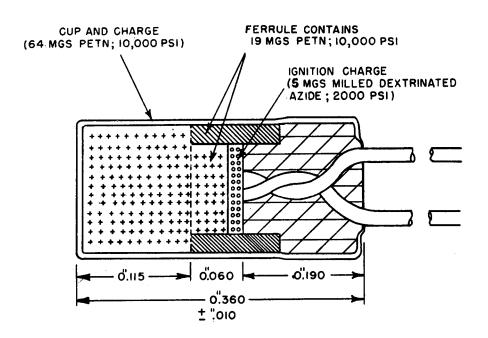


Figure VIII

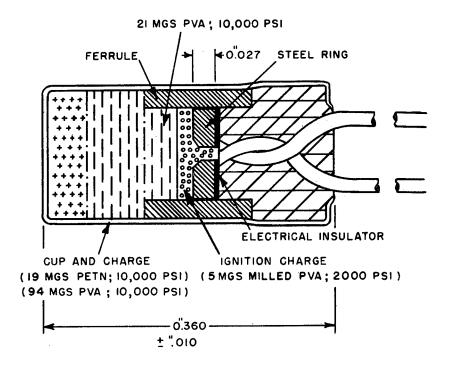


Figure IX

The results are plotted in Figure X, next page. It will be noted that the dextrinated lead azide, unconfined, gave no measureable output when only five milligrams were used and that the maximum for this series was that with forty milligrams of lead azide. The effect of the confining disc upon the shorter columns of dextrinated lead azide is quite dramatic. In contrast, the PVA lead azide detonators without the confinement were more effective than those with it. In this case apparently, the principal effect of the steel washer was that of displacing some explosive.

## Other Properties

The two outstanding features of PVA lead azide are (a) the ability of small charges to initiate RDX very efficiently and (b) its pressure density relationship is such that a quantity (by weight) of PVA lead azide can be pressed into a smaller volume than the same quantity of dextrinated lead azide consolidated at the same pressure. In very small detonators, this latter feature is almost as important as the former. The following table shows the pressure density relationship of dextrinated and PVA lead azide.

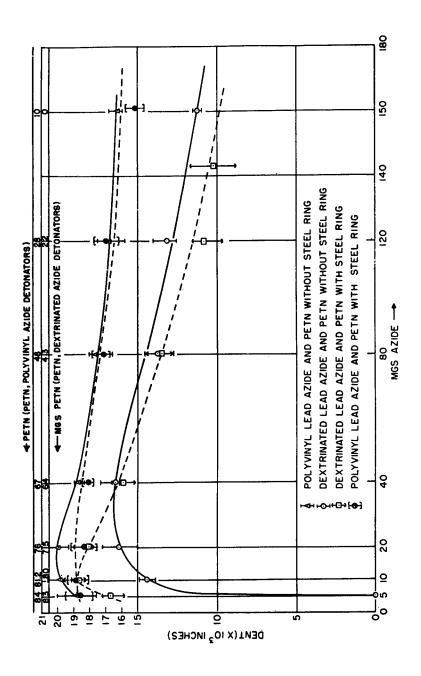
## Pressure-Density Relationship of Dextrinated and PVA Lead Azides

Pressure of Consolidation (p.s.i.)	<u>Density</u> Dextrinated Lead Azide	gm./cc PVA Lead Azide
3,000 6,000 9,000 12,000 15,000 20,000 25,000 30,000	2.62 2.88 3.27 3.08 3.14 3.27 3.30 3.34	3.51 3.55 3.55 3.81 3.84 3.94

Figure XI

The increased ability of PVA lead azide as an initiating explosive does not show up in the quantity of sand crushed in the so-called "brisance test". Six hundred milligrams of both types of lead azide crushed an average of approximately 25 grams of sand.

A third interesting feature of PVA lead azide is that it is practically non-hygroscopic. The moisture



THE RESULT OF DEAT TEST FOR AZIDE/PETM DETONATORS CONFINED AND UNCONFINED

Figure X

picked up by a typical lot of dextrinated lead azide is as follows:

## Hygroscopicity of Dextrinated Lead Azide

Exposure Period (Hours)	% Increase in Weight of Dextrinated Lead Azide Exposed to 90% R. H. at 30° C.
1 2 3 4 5 6 7 24 28 48 120	0.55 0.64 0.64 0.68 0.71 0.71 1.00 1.05 1.16 1.17

### Figure XII

By comparison PVA lead azide when exposed to 90% R. H. and 21°C. picked up only 0.03% moisture before coming to constant weight. It was found that moisture content of the lead azide used in the T32 Detonator was critical. When dextrinated lead azide containing more than 0.7% moisture was used, a large number of (low order) failures of the detonator was experienced.

Results of stability tests indicate that PVA lead azide is a stable explosive. Laboratory tests involving the determination of weight lost and quantity of gas evolved during prolonged heating show:

Loss in wt. on heating at  $100^{\circ} + 1^{\circ}C$ . #1 #2 Ave. for 8 hours. (in duplicates),%. 0.14 0.10 0.12

Quantity of gas evolved from at 100°C.

I gram of sample during 40 hrs.

(Vacuum stability test),ML

In addition, results of firing tests on modified T32 Detonators containing PVA lead azide, as the initiating charge, during storage at 71°C. over a period of 12 months indicated that this explosive is stable and compatible with the other ingredients which make up the detonator.

At the present time the Ordnance Corps will permit the use of PVA lead azide in explosive trains only

where it is not feasible to use dextrinated lead azide. The restricted use of PVA lead azide is attributed to the presence of log or lath shaped crystals having dimensions as great as .4 mm. Pertaining to the sensitivity of lead azide as a function of the crystal size, Tenny L. Davis states that "The sensitivity of lead azide to shock and friction increases rapidly as the size of the particle in-Crystals 1 mm. in length are liable to explode spontaneously because of internal stresses within them. "(5) The Ordnance Corps to the present time has specified that the lead azide to be used will contain no needle-like Considerable amount crystals exceeding .1 mm. in length. of work has been conducted to determine if the larger crystals found in the PVA lead azide render this material unduly hazardous. To date no significant difference between impact sensitivity of the standard lead azide and PVA lead azide has been found, except where abrasive is present.

Several references, one in a recent issue of Nature (6), however, state that the idea that large crystals of lead azide are always excessively sensitive to shock or friction has been widely received, but seems to have little foundation.

Regarding the possible presence of the unstable beta form crystals in PVA lead azide, X-ray diffraction patterns of both the dextrinated and PVA lead azide were obtained. Examination of these patterns indicated that they were identical.

Figure XIII following presents data showing typical impact, stab and hot wire sensitivities for PVA lead azide and dextrinated lead azide.

#### Discussion

The growth of detonation in most explosives involves a period of burning, followed by a low velocity detonation phase, and finally stable detonation. The outstanding "priming efficiency" of lead azide among common primary explosives is undoubtedly related to the extreme rapidity with which it undergoes this process. The burning phase which is quite visible in streak camera photographs of incipient detonation of most explosives is not generally observed in lead azide. (9)

This behavior has inspired the idea that the mechanism of initiation of lead azide and explosives which behave similarly is different from that of other explosives. Garner (10) has proposed a mechanism involving a chain reaction and has concluded that the decomposition of two

adjacent molecules in a period of ten to the minus 13 seconds is sufficient to start a spherical wave of reaction which may develop into an explosion. He also concludes that the probability of this event in normal initiating conditions is sufficiently high to account for the

Figure XIII - Sensitivity							
	NOL	PVA Lead Azide Lab Sample X-105	PVA 1 Azio Plant X-1:	de Sample	Azide	d na Le e Az	ctri- ated ead zide
Impact	No.				X-73	3 Lot	<del>5 64</del>
Type 3 tools (2.5 kg wt.) (7)		36 cm.	55	cm.	33 (	em.	
Type 12 tools * (500 gm. wt.) (8)			9	cm.	28 (	cm.(8)	20 cm.
Type 12 tools * (1 kg. wt.) Type 12 tools *			3	cm.	14 (	cm.(8)	8 cm.
(2.5  kg. wt.)	)		2	cm.	10 0	cm.(8)	4 cm.
Type 3 tools (2.5 kg. wt.) As a component of primer mix	(7)		5	em.	21 0	em.	
Stab							
As a component a priming mix : Mk 102 primers		1.61 in.	2.2	25 in.	2.12	in.	
As a component priming mix in detonators	of Mk	a 28 4.50 in.			4.63	3 in.	
As a component priming mix in detonators	of Mk	a 44 2.3 in.			3.42	? in.	
Hot wire 0.0002	27"	dia. wire 1412 erg	ន		1288	ergs	
Hot wire 0.000	l" d	ia. wire 222 erg	s		257	ergs	

<sup>\*</sup>In type 12 tools the explosive is placed on sandpaper

initiation of lead azide. Bowden and Yoffe, (11) have expressed the opinion that lead azide may be initiated by tribochemical excitation. The hot spot mechanism of initiation, the broad applicability of which has been established by Bowden and various co-workers, (9), (11) and (12) may also apply to lead azide. The rapid acceleration of the action of this material may be the result of its high melting point and mechanical strength, both of which are conducive to the formation of hot spots.

The transition from a less vigorous reaction to detonation depends upon the acceleration of weaker reactions and the consequent development of strong shock waves. In all of these incipient reaction processes which have been proposed as peculiar to lead azide and similar explosives as well as the more common incipient burning, the condition of the surfaces of the grains and crystals is important. A coating of a foreign material can serve as a barrier to retard the propagation of burning or chain reactions or as a cushion and lubricant to reduce crystalline stresses and inter-crystalline friction. The effect of an impurity upon the propagation rates and acceleration of such reactions may be much greater than would be predicted on the basis of dilution, and may be expected to depend strongly upon the nature of its distribution as well as its properties and concentration.

Each individual grain of dextrinated lead azide is an agglomerate of perhaps a million crystallites, Figure I, while each particle of PVA lead azide is an individual crystal, usually several times as long as it is wide, Figure I. It is inconceivable that PVA lead azide could be consolidated by pressure without breaking many crystals The conand exposing a large number of clean surfaces. solidation of dextrinated lead azide by redistribution of the crystallites within a dextrin matrix would appear The existence of clean surfaces of explosive possible. could be very conducive to the operation of some of the propagation processes mentioned above, and might help to explain some of the differences in performance between dextrinated and PVA lead azide reported above. Detonation may be defined as a self propagating explosive reaction in which the controlling mechanism whereby energy is transmitted from the reacted to the unreacted explosive is that of a hydrodynamic shock. The parameters of stable detonation, including its propagation velocity, are determined by equilibrium conditions at the end of the reaction zone, in which the losses of material exactly balance the influx due to the propagation of the wave into virgin explosive and the losses of energy exactly balance the sum of the thermal and available chemical energy of the unreacted material overtaken. These conditions are affected by the

reaction rate only to the extent that it affects the geometry of the reaction zone and the consequent deviation from one dimensional flow in this region. The design of most explosive components is such that this deviation is quite small. The acceleration of detonation from a lower rate to the stable rate requires an increase in pressure in the reaction zone, and depends upon the rate of this increase. In turn, increase in pressure depends upon the excess of either the material influx, the energy liberated by the reaction, or both over the losses from the reaction zone. The growth of detonation may be expected to be closely dependent upon the reaction rate.

The surface burning model has been shown to explain observable phenomena associated with the detonation of solid explosives. (13) Detonation of various explosives, including lead azide (14), has been observed wherein the propagation rate is so low that the temperature necessary for rapid reaction is attainable only by concentrating the heat of compression at "hot spots". Whether the hot spots result from intercrystalline friction or compressive heating of interstitial gases, the presence of voids is important in the formation of hot spots. As the percentage of voids is decreased either by filling them with another material or loading the explosive at a higher density, its structure becomes more rigid and the shock pressure necessary to disrupt it becomes greater. Failure of the structure, of course, is necessary for either intercrystalline friction or appreciable compression of the gases. the propagation and acceleration of weak detonation is directly related to the proportion of voids in the material through which it is propagating. (13)

The rapid acceleration of detonation in lead azide may be attributable to the fact that under normal loading conditions, loading pressures between ten and twenty thousand pounds per square inch, a charge usually contains more than twenty percent voids. In considering the effect of organic impurities upon lead azide, the large density difference must be kept in mind. The eight percent by weight of impurities which is typical of dextrinated lead azide furnished under United States military specifications (1) would amount to over twenty-seven percent by volume, if it were all dextrin, and would reduce the voidless density to 3.7 grams per cubic centimeter as compared with 4.8 for pure lead azide. What might seem a small weight percentage of organic impurities may be expected to have a considerable effect upon the rate at which stable detonation is approached in lead azide.

The term "void" is used here in the sense of the absence of liquid or solid material. The presence of gases is, of course, necessary for one of the mechanisms proposed.

Whether the initiation and growth of stable detonation in lead azide is a process similar to but faster than that in other explosives or a unique process, the time and material expended in the process can be expected to be influenced by impurities, particularly if the impurities coat the particles of lead azide.

Measurements of the Detonation Properties of - PVA and Dextrinated Lead Azide

The velocities of both PVA lead azide and dextrinated lead azide were measured for columns 0.2 inches in diameter heavily confined in brass. Each velocity was measured over the second inch of a two inch long column. The results are given in Figure XIV.

## Pressure-Density-Velocity Relationship of Dextrinated and PVA Lead Azide\*

Loading Presure p.s.i.	PVA Lead Azide		Dextri Lead <i>l</i>	
• 12.	Density gm./cc.	Det. Vel. m/sec.	Density gm./cc.	Det. Vel. m/sec.
4,000 16,000 32,000 64,000	2.99 3.45 3.77 3.85	4060 4620 4930 5410	2.60 2.96 3.35 3.57	3800 4130 4400 4880

#### Figure XIV

Note that for equivalent loading pressures the detonation velocity of PVA lead azide is substantially higher than that of dextrinated lead azide, but that, for equivalent densities the dextrinated material detonates at a slightly higher velocity. An increased detonation velocity for given density with the addition of a diluent to an explosive may be expected where the decomposition products of the diluent have lower average molecular weights than those of the explosive. Some investigators (15) have observed slightly higher detonation velocities in Composition A than in RDX for equal densities. In the manufacture of detonators, the density is limited by the loading pressure which can be used, so that the velocity attainable with a given loading pressure is of more significance. Since the shock pressure associated with a detonation is nearly proportional to the product of the density and the square of the detonation velocity, the detonation pressure of PVA lead azide which has been pressed at 16,000 p.s.i. is about half again as large as that of dextrinated lead

<sup>\*</sup>Differences in values in Fig. XI and XIV are in line with variations in unpressed density and loading components.

azide loaded at the same pressure. This difference is substantial, but not sufficient to account for all of the difference in performance which has been observed between lead azide manufactured by the two processes.

The possible influence of impurities upon the rate of growth of detonation in lead azide has been discussed. An experiment which may be considered to be evidence of a difference between the two types of lead azide involves the measurement of functioning times of electric detonators. Two groups of detonators were made which were similar except that the flash charge, that charge in direct contact with the bridge wire, was dextrinated lead azide in one case and PVA lead azide in the other. These detonators were fired by the discharge of a 0.2 mfd. condensor charged to various voltages. The functioning times were measured by means of the vacuum thermocouple timer. (16) The results are given in Figure XV.

## Functioning Times of Detonators

	Flash Char	ge Material
	Dextrinated	PVA
Firing Voltage	Lead Azide	Lead Azide
(Volts)	(Microseconds)	(Microseconds)
40	4.0 - 8.0*	1.95 - 2.4*
140	3.8 - 3.12	1.45 - 1.9
350	2.5 - 3.05	1.45 - 1.75
700	2.15 - 2.68	1.25 - 1.75
1400	1.50 - 2.55	1.28 - 1.45
2800	1.56 - 2.02	1.38 - 1.50

\* Spread of four to eight measurements.

## Figure XV

It will be noted that the detonators with PVA lead azide functioned more rapidly at each voltage and that the dextrinated lead azide showed a progressive decrease in functioning time with increasing voltage while the PVA lead azide changed hardly at all except at the lowest voltage used. Taken by itself, this data might be taken to indicate that the detonators loaded with PVA lead azide were much more sensitive. Measurements of the minimum firing energy, however, fail to bear this out. The energy required for fifty percent firing of the detonators with the dextrinated lead azide flash charges was found to be about 1300 ergs and that for the PVA lead azide 1400 ergs. This difference in energy requirement is not statistically significant. Note that the energy used in the time experiments ranged from 1600 ergs up. The difference in the

times must be attributed to the difference in the rate of growth of detonation in the two materials. The measured functioning times for the PVA lead azide are quite close to the time which a detonation might be expected to require to traverse the distance between the bridge wire and the probe used to detect functioning of the detonators. The difference in functioning time between the PVA and dextrinated lead azides is obviously much more than can be accounted for on the basis of the difference in their stable detonation rates.

If this time data are considered in conjunction with the output data of Figure X, it becomes quite apparent that an important difference between PVA lead azide and dextrinated lead azide is in the rapidity with which they grow to detonation. The lack of any improvement in the PVA lead azide results can be considered evidence that this material builds up to stable detonation so rapidly that little is to be gained by confinement of this kind.

### Conclusions

From the foregoing, it may be concluded that: Dextrinated lead azide grows to detonation more slowly than PVA lead azide.

A significant quantity of explosive is expended in this growth process. The explosive consumed in the growth of detonation is less effective in initiating the subsequent charge than that which detonates at the stable rate. For these reasons, and because it can be consolidated at higher densities, PVA lead azide is appreciably more effective as an initiator, particularly where space is at a premium.

#### References:

- (1) Military Specification for Lead Azide, MIL-L-3055, 30 September 1949, Amendment 1, 24 March 1952
- (2) British Service Azide Specification IG237,  $\frac{A}{163}$  E
- (3) U. S. Patent 2,421,778
- (4) NAVORD Report 2815 Direct Initiation of Boosters, by R. H. Stresau, W. M. Slie and L. D. Hampton
- (5) The Chemistry of Powder and Explosives, by Tenny L. Davis
- (6) Nature, 172 (Aug. 29) p. 379, 1953, Size Effects in the Initiation and Growth of Explosions by F. P. Bowden and K. Singh
- (7) NAVORD Report 1589, N. D. Mason, Impact Sensitivity Determinations of Explosive Compounds Tested During the Period from 1 January 1950 to 1 November 1950
- (8) NAVORD Report 2111, George Svadeba, Impact Sensitivity of Primary Explosives, 1 June 1951
- (9) F. P. Bowden and A. D. Yoffe, The Initiation and Growth of Explosions in Liquids and Solids, Cambridge University Press, 1952.
- (10) W. E. Garner, Transactions of the Faraday Society, 34, 985, 1008, 1938.
- (11) F. P. Bowden and A. D. Yoffe, Research 1, 581, 1948
- (12) F. P. Bowden and O. A. Gurton, Proc. Roy. Soc. A, 1938, 337, 350, 1949
- (13) H. Eyring, R. E. Powell, G. H. Duffey, and R. B. Parlin, Chem. Rev. 45, 69, 1949
- (14) R. H. Stresau, NAVORD Report 2460, 28 May 1952
- (15) L. D. Hampton, NAVORD Report 3731, September, 1954
- (16) R. H. Stresau and C. Goode, NAVORD Report 2137, 29 June 1951

# THERMO-HYDRODYNAMICS AND REACTION KINETIES IN SOME METALIZED EXPLOSIVES

Melvin A. Cook, Aaron S. Filler, Robert T. Keyes
William S. Partridge, and Wayne O. Ursenbach
University of Utah
Salt Lake City, Utah

#### ABSTRACT

Experimental velocity-diameter curves are presented for 80/20 TNT-AN, 45/30/25 HBX-TNT-Al, 75/25 HBX, various mixtures of AN-Al ranging from pure ammonium nitrate to 60 percent AN, RDX, and 95/5 RDX-boron. Velocity-density relations are presented for all except the last two explosives. Wave shape vs. diameter measurements for the aluminized explosives are also summarized.

Results show that the Al reacts too rapidly for rate to be a real limiting factor in TNT and RDX-Al mixtures, but relatively slowly in the AN-Al mixtures. The familiar properties of the high temperature Al explosives are attributed to the thermodynamics of Al reactions in which the  $Al_2O(g)/Al_2O_3(c)$  ratio is appreciable in the detonation wave and negligible as far as the maximum available work integral  $A = \int p dv$  is concerned. The change of this ratio from a high value in the detonation wave to a low one later on gives aluminized explosives low "brisance" but high blast potential. Preliminary results suggest a similar effect for boron.

The AN-Al mixtures were shown to be non-ideal over the entire range of conditions studied. Reaction rates in these mixtures depend on the particle size of both the AN and the Al. They seem to be controlled by mass transfer which leads to anomalous  $D(\rho_1)$  curves showing a maximum at a relatively low density around 1.0 to 1.2 g/cc.

#### INTRODUCTION

The studies summarized in this article represent investigations described in three technical reports (1,2,3) on this project in addition to work not previously reported on the variation of velocity with density in AN-Al and AN-DNT and preliminary velocity vs. diameter results for 95/5 RDX-boron. The studies of aluminized explosives

include rather complete investigations with 80/20 TNT-A1, 45/30/25 RDX-TNT-A1, and 75/25 HBX together with various mixtures of ammonium nitrate (AN) and aluminum ranging from zero to 40 percent Al.

Aluminized explosives are characterized in general by relatively low "brisance" but high (underwater, open air and underground) blast potential. The low relative "brisance" of aluminized explosives has been attributed in the past to incomplete reaction of Al at the C-J plane and the high blast potential to after burning of aluminum. Early shaped charge studies with torpex and other aluminized explosives interpreted in light of the observed linear variation of hole volumes produced in uniform targets with detonation pressure in charges of constant geometry and constant cones using C-H-N-O explosives where detonation pressures could be computed unambiguously, (4) indicated that aluminum acted effectively as a diluent as far as shaped charges are concerned. More careful studies of this nature carried out in this laboratory showed, however, that the effective (or 'measured') detonation pressures in some aluminized explosives were even considerably lower than one can account for by mere dilution with an inert additive. Moreover, extensive velocity-diameter studies showed that aluminum reacts very rapidly in tritonal and HBX, diameter effects disappearing in relatively small diameters. These results described below brought out that an explanation of the behavior of aluminum in tritonal and HBX was to be found not in the kinetics of reaction of aluminum but in the thermodynamics of aluminum reactions.

A careful study of the thermodynamics of various aluminum products was therefore carried out and results showed that the possible detonation products of aluminum in C-H-N-O explosives were Al<sub>2</sub>O(g), AlO(g) and Al<sub>2</sub>O<sub>3</sub>(c), (g = gas, c = condensed). Approximate constants were computed from statistical mechanics from which the distribution of aluminum in these three products could be computed approximately by including these equilibrium constants along with others applicable in C-H-N-O explosives in the computation of the thermo-hydrodynamics of aluminized explosives. Alo03 apparently does not exist in the vapor phase. (Later computations showed that AlO is also unimportant at least at low oxygen balance.) The results of the thermo-hydrodynamic calculations incorporating these equilibrium constants for tritonal and HBX were very enlightening; they showed that the ratio Al<sub>2</sub>O(g)/ Al<sub>2</sub>O<sub>3</sub>(c) was large at low densities and did not reach zero even at the maximum possible densities. Moreover, by reference to the empirical (universal) a(v) curve, it became evident that the velocity-density curves of TNT-Al and RDX-TNT-Al mixtures should not be linear as in normal C-H-N-O explosives but should show considerable curvature. This prediction was later verified by velocity D vs. density  $\rho_{\text{l}}$  measurements in these explosives. The results of these studies therefore appeared to give a satisfactory explanation of the characteristic behavior of the aluminized explosives, HBX and tritonal, presented later in the discussion.

It was expected that the situation would be somewhat different in explosives of higher oxygen balance. To study the aluminum

reactions in detonation at high oxygen balances therefore various AN-Al mixtures were studied. Thermo-hydrodynamic calculations in this case showed that the ratio Al<sub>2</sub>O(g)/Al<sub>2</sub>O<sub>3</sub>(c) should be negligible up to 15 percent Al, owing to the relatively low temperature of these mixtures. While it was expected that AlO would become important, contrary to expectation the calculated ratio AlO(g)/Al<sub>2</sub>O(g) proved negligible even at the highest oxygen balances studied. However, this result remains uncertain since the calculated equilibrium constants may not be sufficiently reliable to insure the accuracy of this conclusion. While the rate of reaction of Al in tritonal and HBX was relatively high, it was relatively slow in the AN-Al mixtures. Indeed, the properties of these mixtures were found to depend critically on the rates of reaction of both AN and Al. Sample thermo-hydrodynamic calculations for the above three series of explosives are given in Table I.

While Al has great practical importance, other metals are also of considerable interest in explosives. Studies of metallized explosives being carried out at the present time thus have as their objective the elucidation of the behavior of these metals also. To date only preliminary studies of boron in RDX have been carried out and are summarized here.

The experimental results obtained in the above studies are summarized in this article together with a discussion of the behavior of aluminum and boron in the explosives studied. In addition to the velocity-diameter (D(d)) and velocity-density (D( $\rho_1$ )) studies carried out in connection with determinations of the reaction rates and thermohydrodynamics of the aluminized explosives, extensive measurements of wave shape were also carried out. These results are also summarized in this article.

#### **EXPERIMENTAL**

### D(d) Curves for Tritonal and HBX

Velocity-diameter studies of cast and loose-packed 80/20 TNT-Al, cast 75/25 HBX, and loose-packed 45/30/25 RDX-TNT-Al are presented in Fig. 1. Velocities were measured in these and other cases described here by pin oscillograph (5) and rotating mirror camera methods. (6) The charges all had a length/diameter (L/d) ratio of six or more. They were contained in thin-walled (larger diameters) or plastic tubes (smallest diameters). Densities were measured in samples of the cast charges by sectioning them. They were found to show some axial and radial density fluctuations limited in all cases, however, to two percent or less. The loose-packed charges were vibrated for density uniformity, care being taken to avoid segregation by excessive vibration. Densities were determined in all cases by total weight/total volume measurements. Velocities were corrected to an average density in each case by appropriate  $D(\rho_1)$  relations.

No systematic aluminum particle size or diameter effects were found in either the 80/20 TNT-Al or 45/30/25 RDX-TNT-Al except for the former at diameters less than 5 cm. In fact in the HBX series no definite diameter or particle sizes effects were observed even in the lowest diameters studied. These results show clearly that the reaction rate of aluminum is not a limiting factor in the behavior of tritonal and HBX.

Of particular interest are the following comparisons:

Explosive	$ ho_{\mathtt{l}}$	D(m/sec)
TNT	1.59	6910
80/20 TNT-Salt	1.75	6900
80/20 TNT-A1	1.75	6800
TNT	0.85	4525
80/20 TNT-Salt	1.00	4400
80/20 TNT-Al	1.00	3840
60/40 RDX_TNT	1.70	7800
45/30/25 RDX-TNT-Salt	1.77	(7430)*
45/30/25 RDX-TNT-A1	1.77	7200
60/40 RDX-TNT	1.00	(5650)*
45/30/25 RDX-TNT-Salt	1.15	(5400)*
45/30/25 RDX-TNT-A1	1.15	4600

\*By linear interpolation of results for TNT-salt and RDX-salt mixtures.

These results show that aluminum lowers the velocity of TNT, 60/40 RDX-TNT and composition B more than salt which acts (if not as a pure diluent) as a slightly heat absorbing solid. Clearly, therefore, aluminum must have a strongly endothermic effect at the C-J plane. This would be the result if  $Al_2O(g)$  were to form in appreciable amounts. But if  $Al_2O_3(c)$  were to become the sole aluminum product, the large diameter velocity of the TNT-Al and RDX-TNT-Al mixtures would have been appreciably higher (even at the same density) than the velocity in the corresponding explosives without aluminum.

The effectively endothermic reaction of Al in the detonation wave may be seen also in the following results of detonation pressure measurements by the shaped charge method.(8)

Explosive	ρ <sub>1</sub>	p <sub>2</sub> (atm x 10 <sup>-3</sup> )*
TNT	1.59	150
80/20 TNT-Al	1.68	140
TNT	0.81	46
80/20 TNT-Al	0.94	45
Composition B	1.71	230
80/20 HBX	1.81	170
73.2/26.8 HBX	1.83	155

\*Average deviation from mean 5-10 percent.

Thus the actual detonation pressures of tritonal and HBX were less.

than in TNT and composition B even though the densities of the former explosives were 6 to 8 percent higher  $(p_2 = \rho_1 \text{ DW} \approx \rho_1 \text{D}^2/4)$ . The density increase was not enough except in the low density TNT-Al, however, to make up for the endothermic reaction.

## $\mathtt{D}( ho_1)$ Curves for Tritonal and HBX

Thermo-hydrodynamic calculations for tritonal and HBX using a linear  $D(\rho_1)$  curve and the new Al-distribution equilibrium constants in the inverse solution method (9) gave inconsistent results. values of  $p_2$  were too large and the computed a(v) curve deviated considerably from the 'universal' one. (10)) These results suggested, therefore, that the  $D(\rho_1)$  curve should not be linear. Measurements of the  $D(\rho_1)$  curves for pressed 80/20 TNT-Al in 8.5 cm (L/d = 6) charges 45/30/25 RDX-TNT-Al at d = 5.2 cm and L/d  $\geq$  6 were therefore carried out. These diameters were chosen to insure ideal detonation. The results are shown in Fig. 2. The a(v) curves calculated using the observed  $D(\rho_1)$  curves were in much better agreement with the 'universal' curve and the calculated pressures were also in much better agreement with the observed ones. There remained a discrepancy in the  $\alpha(v)$ curve for tritonal, although the calculated pressures were in good agreement with the observed ones in this case. For HBX the computed c(v) curve was in excellent agreement with the 'universal' curve, but the calculated pressure at high density was still about 25 percent too high. However, this discrepancy was of the order of magnitude associated with the limits of uncertainty in the equilibrium constants determining the  $Al_2O(g)/Al_2O_3(c)$  ratio.

## D(d) Curves for AN-Al Mixtures

Experimental D(d) and D vs. percent Al (constant d) data for AN-Al mixtures varying in composition from 100/0 to 70/30 are shown in Fig. 3 and 4. The influence of Al particle size is also indicated by some of the results shown in Fig. 5 for 8 to 20 percent Al. Additional data showing Al particle size effects are given in Tables II and III. The AN-Al mixtures were all non-ideal at velocities far below the ideal velocities in all cases irrespective of the particle size of either the AN or Al. No attempt was made to correct velocities for small density fluctuations owing to the anomalous  $D(\rho_1)$  relations noted in Fig. 3. For example, the velocity was in general considerably lower on the high density side than on the low density side. Previous unpublished studies have shown that this is a characteristic of fuel or combustible sensitized AN explosives at  $D/D^*$  considerably less than unity.

In order to show the anomalous density effect unambiguously,  $D(\rho_1)$  measurements were carried out with the 90/10 AN-Al mixture using a single uniform unscreened Al sample throughout. These results are shown in Table IV. In the first series using a fine AN product (sample 1, Table IV), the  $D(\rho_1)$  curve was found to go through a maximum somewhere between a density of 1.09 and 1.28. These measurements were repeated about three weeks later using the same lot of AN. However, clearly this sample had changed during the three week interval, as

noted, for example, by the fact that it packed to a lower density. this series the maximum velocity (3485 m/sec) was observed at about  $\rho_1$  = 1.12 and the velocity was 950 m/sec lower at  $\rho_1$  = 1.25 than at  $\rho_1^-$  = 1.12. Pressing crushes the AN somewhat, hence the anomalous D( $\rho_1$ ) effect should be even more pronounced than indicated by these two series (AN samples 1 and 2, Table IV). To show the real  $D(\rho_1)$  effect, one s should use constant particle size. To accomplish this, several shots were made in which the pressed charges were compared with loose-packed ones made by first pressing the AN to the density of the corresponding pressed charge, crumbling the mixture and loose packing it in charges of the same diameter and length. Three comparisons of this sort are shown in Table IV (AN samples 3, 4, and 5). Note that the low density product showed a higher velocity than the higher density one, and the difference increased with the density difference. These results show that the  $D(\rho_1)$  curve for 90/10 AN-Al with fine AN and fine Al exhibits a maximum at some value of density below  $\rho_1$  = 1.25. Another more easily reproducible example of the anomalous  $D(\rho_1)$  effect in AN explosives is shown in Table IV for a 90/10 AN-DNT mixture using liquid DNT and fine AN. Again the  $D(\rho_1)$  curve is shown to go through a maximum in this case near  $\rho_1 = 1.18$  g/cc.

The AN-Al mixtures are complicated non-ideal explosives; besides the anomalous  $D(\rho_1)$  relations, particle size effects may be observed not only in Al but also in AN. The AN particle size was not allowed to vary more than the amount caused by crystal growth in the AN and the ability to reproduce particle size in AN from one lot to another. As a result, no definite particle size effects of AN were noted. To show that the AN particle size also influences velocity in these mixtures, therefore, two shots were made in 10 cm diameter charges using a much coarser AN product and the same grade of aluminum as in the comparative examples. The results (AN sample 6 in Table IV) showed an average velocity about 1000 m/sec lower than for the finer grade AN charges of the same density and Al particle size.

## D(d) Curves for RDX and 95/5 RDX-Boron

A preliminary (partial) D(d) curve for loose-packed 95/5 RDX-boron is compared with the D(d) curve for RDX in Fig. 5. The RDX used in both cases was 65 to 100 mesh. The boron was a sample of quality still to be determined. These results are as yet too meager to allow reliable conclusions to be made, but they indicate that the reaction at the C-J plane for boron as for aluminum may also be an endothermic one relative to the products of detonation of RDX. Note, for example, that the reaction rate of RDX seems to be considerably retarded in the mixture indicating a considerable drop in detonation temperature. For diameters above 1 cm, RDX appears to detonate with ideal velocity (D/D\* = 1.0). However, the results for the 95/5 RDX-B mixture showed D still to be increasing even at d = 7.5 cm. At d = 1.3 cm the velocity of the mixture was about 10 percent lower than for pure RDX, and at d = 7.5 cm it was about 5 percent lower. If B were a pure diluent, the ratio of the D\*'s for the two explosives would be about 0.975.

## Wave Shape Measurements in Aluminized Explosives

After considerable effort to obtain quantitative wave shape results in cast tritonal and HBX, studies were discontinued owing to the very erratic results obtained. The cause of these irreproducible results was not only the difficulties inherent in casting such mixtures, but also a tendency toward segregation of the aluminum causing it to concentrate along the charge axis enough to attenuate the wave at this position more than toward the sides. Apparently relatively slight segregation of this sort is sufficient to flatten and even invert the wave from its normal value for an homogeneous charge. The effect of Al segregation is much more pronounced than density fluctuations along the charge axis which also tends to flatten or distort the wave.

In the loose-packed and pressed charges of 80/20 TNT-Al and 45/30/25 RDX-TNT-Al, the wave shapes showed normal reproducibility and normal curvature. The waves were spherical in shape and showed a constant or steady state value  $R_m$  at large L/d. Values of  $R_m/d$  obtained for the loose-packed mixtures of TNT-Al and RDX-TNT-Al with two grades of Al (-325 mesh and 65 to 100 mesh) are plotted against diameter in Fig. 6.  $R_m/d$  vs.  $\rho_1$  curves for pressed 80/20 TNT-Al and 45/30/25 RDX-TNT-Al obtained at d = 8.5 cm and d = 5.2 cm, respectively, are shown in Fig. 6.  $R_m/d$  increased for TNT-Al from 1.45 at  $\rho_1$  = 1.0 to 2.5 at  $\rho_1$  = 1.56 at which density the  $R_m/d$  vs.  $\rho_1$  curve still had a fairly steep slope. In the RDX-TNT-Al mixture, however,  $R_m/d$  increased from 1.95 at  $\rho_1$  = 1.18 to the limiting value of about 4.0 at  $\rho_1$  = 1.48. This mixture showed no further increase in  $R_m/d$  with density as the wave increase from  $\rho_1$  = 1.48 to 1.57, the average limiting value of  $R_m/d$  being 3.85.

Wave shape data obtained for the AN-Al mixtures are given in Table V. They show  $R_{\rm m}/d$  to be confined to the relatively narrow range between 0.9 and 1.7 in the diameters studied.

### DISCUSSION OF RESULTS

Temperatures and pressures at the C-J plane for low density TNT-Al and RDX-TNT-Al mixtures are such that the chief product of aluminum is  $Al_2O(g)$ . This forms endothermically with respect to the products of detonation of these explosives and as a result the intensity of the detonation wave is reduced by aluminum. Owing to the much more rapid increase of pressure than temperature with density, however, the ratio  $Al_2O(g)/Al_2O_3(c)$  decreases with density but remains appreciable even at the maximum density. As a result the influence of the highly exothermic product  $Al_2O_3(c)$  never is sufficient in tritonal and HBX to overcome the endothermic effect of  $Al_2O(g)$  at the C-J plane. The detonation velocities and detonation pressures (and "brisance") of these high temperature aluminized explosives are thus always lower than those of the corresponding explosives without aluminum even at the maximum densities, despite a 6 to 8 percent higher density for the aluminized explosive.

The ratio Al<sub>2</sub>O(g)/Al<sub>2</sub>O<sub>3</sub> falls to zero at temperatures below about 3500°K at the "explosion pressures" p<sub>3</sub> of the high density aluminized explosives or below about 3000°K at very low pressures. This effect will, therefore, cause the temperature to be buffered at a value between 3000 and 3500°K during adiabatic expansion. The maximum available energy or total blast potential is determined by the integral

$$A = \int_{\mathbf{v}_{4}}^{\mathbf{v}_{4}} p d\mathbf{v} = Q - q$$
 (1)

where A is the maximum available work in expansion of the products of detonation from specific volume  $v_3$  to  $v_4$ . Q is the heat of explosion and q is the heat retained by the products of detonation at  $v_4$ . In general detonations are very efficient in utilizing Q in work processes as long as the resistance of the burden is adequate. In open air blasts the resistance is low such that A/Q  $\sim$  0.15 to 0.2, but in underground and underwater A/Q  $\sim$  0.8 to 1.0 depending on the explosive. In either case, however, the buffering action of the ratio Al20(g)/Al203 (c) on temperature will tend to increase Q and A in aluminized explosives approaching as far as maximum available energy is concerned, the high value corresponding to zero in this ratio. Only where v4 is effectively only slightly greater than v3, as in applications requiring high brisance (e.g., shaped charge phenomena including impulsive loading of targets, cavity effect, etc.) will the high Al<sub>2</sub>O(g)/Al<sub>2</sub>O<sub>3</sub>(c) ratios applicable in the wave front of detonation be important in lowering intensity. In cases where  $\mathbf{v}_{l_i}$  is effectively much greater than  $\mathbf{v}_{3}$ , this ratio should be effectively zero. The thermodynamics of the Al20(g)/Al203(c) ratio thus appears to give a complete qualitative explanation of the behavior of the important high temperature, aluminized explosives. Quantitative computation should be possible for any particular set of conditions.

The situation is somewhat different in AN-Al mixtures. In the first place these mixtures have low enough detonation pressures and sufficient oxygen at Al < 15 percent that the Al<sub>2</sub>O(g)/Al<sub>2</sub>O<sub>3</sub>(c) ratio is practically zero in this range. At 20 percent Al, where the explosive is approximately oxygen balanced, this ratio is still quite low and Q for detonation conditions is a maximum (at 1355 kcal/kg) since the ratio Al<sub>2</sub>O(g)/Al<sub>2</sub>O<sub>3</sub>(c) increases rapidly as Al is further increased owing to the rapidly increasing temperature. However, A (in work processes where v<sub>4</sub> is effectively much greater than v<sub>3</sub>) should continue to increase with percent aluminum in the AN-Al mixtures, perhaps to as high as 35 to 40 percent Al. The AN-Al explosives in this composition range should thus be very powerful ones for underwater, airblast, and underground use. However, while they should develop sustained pressures their peak pressures under all circumstances should be very low, particularly in small sizes where the D/D\* ratio is low.

Finally, let us consider briefly the kinetics of the reactions of AN-Al and AN-DNT mixtures in detonation. In previous studies of non-ideal explosives, including both pure explosives and mixtures, the surface burning (two-thirds order) rate law described by Eyring,

et al.(12) was found to apply. The explosive mixtures studied, however, were of a type in which the temperature generated by the reaction of at least one of the ingredients alone without mixing would raise the temperature in the products to near or even above the final equilibrium temperature after thermodynamic equilibrium of the products. In AN-Al mixtures, however, the temperature attained by reaction of AN alone cannot exceed about 1700°K, whereas that for the complete mixture rises much higher. Hence mass transfer and possibly heat transfer are much more important factors in these mixtures than in a mixture such as TNT-Al. The latter temperature in the gaseous phase will always be in the neighborhood of the final temperature, but this is by no means true in the mixture. Two other possible limiting factors besides heat transfer in the condensed phases thus arise. The limiting factor determining rate in the AN-Al mixtures might be either (1) mass transfer in the gas phase or (2) heat transfer in the gas phase.

In the previous examples studied these processes are apparently unimportant and the rate of reaction is limited by the upper limit of temperature and reaction rate in the solid (the Eyring process). However, in AN-Al mixtures apparently the gaseous phase is effectively not in equilibrium, and factor (1),(2) or both thus limit the rate of reaction. The fact that the rate decreases rapidly with density indicates that the limiting factor is mass transfer. (Diffusion falls rapidly with increasing density or pressure in the vapor phase, but thermal conductivity does not.) This situation corresponds approximately to that occurring in granular "low" explosives such as black powder in which the burning rate decreases with increasing density.

Single and double-base propellants in which the solid phase is homogeneous have apparently thermal conductivity as the rate determining factor. That is, apparently the rate in these explosives is determined by the temperature at the solid-vapor interface, but the initial process of decomposition is endothermic or much less exothermic than the overall reaction. Most of the heat is thus generated a short distance away from solid-vapor interface and must be transferred back to support the reaction. The temperature gradient away from the surface (temperature being smallest at the solid surface) therefore increases with pressure, and the effective surface temperature also increases with pressure. The result is that the burning rate increases with pressure.

The anomalous  $D(\rho_1)$  curves observed at d=10 cm in 90/10 AN-DNT are believed characteristic of AN-combustible mixtures in small diameters.

Quantitative studies of the D/D\* vs.  $\rho_1$  curves of such mixtures by means of the detonation head model should thus provide the necessary reaction rate data for the study of their reaction kinetics. It is possible that such studies would lead to valuable information on mass transfer in gases at high densities and pressures in addition to important practical and theoretical information on the reaction kinetics of AN-combustible mixtures.

#### ACKNOWLEDGMENT

This work was supported by Office of Naval Research, Contract Number N7-onr-45107, Project Number 357 239, and was carried out by the Explosives Research Group, Utah University.

#### BIBLIOGRAPHY

- (1) "Reaction Kinetics and Thermo-Hydrodynamics of 80/20 Tritonal", Technical Report No. XXIX, March 10, 1954, ERG, Utah University (Confidential).
- (2) "Reaction of Aluminum in 75/25 HBX", Technical Report No. XXXIV, May 7, 1954, ERG, Utah University (Confidential).
- (3) "Velocity and Wave Shape Studies of AN-Al Mixtures", Technical Report No. XXXV, June 7, 1954, ERG, Utah University (Confidential).
- (4) This correlation was first presented by M. A. Cook and L. B. Seely, DuPont shaped charge studies during World War II.
- (5) "'Pin Oscillograph' for Measurement of Detonation Velocity", Technical Report No. XXXIII, May 4, 1954, ERG, Utah University.
- (6) "Construction of Rotating Mirror 'Streak' Cameras and Synchronizers", Technical Report No. XII, April 30, 1953, FRG, Utah University (Confidential).
- (7) "Detonation Velocities of Ideal Explosives with Inert Additives", Technical Report No. XVIII, August 15, 1953, ERG, Utah University (Confidential).
- (8) "Recent Developments in Theory of Detonation", Technical Report No. XXV, November 23, 1954, ERG, Utah University (Confidential).
- (9) "Calculation of Products of Detonation Using IBM Machines", Technical Report No. XXI, October 16, 1953, FRG, Utah University.
- (10) M. A. Cook, J. Chem. Phys. <u>15</u>, 518 (1947).
- (11) M. A. Cook, "Detonation Wave Fronts in Ideal and Non-Ideal Explosives", This Symposium.
- (12) H. Eyring, R. E. Powell, G. H. Duffey, R. B. Parlin, Chem. Rev. 45, 1 (1949).

Cook, Filler, Keyes Partridge, Ursenbach

3.248 0.582 2.312 0.727 28.8 1.05 1165 7360 5380 8 0.582 0.875 AN-Al Mixtures (log F = 3) 0.727 1.05 1355 2835 0097 5760 ଷ 얺 0.582 0.023 0.727 33.2 0077 5810 1.05 1305 2757 15 82 Thermo-Hydrodynamic Properties of Aluminized Explosives 0.582 1.855 0.727 1.06 36.6 3580 5550 9 Я 2,7 0.582 0.727 42.7 2180 7,400 1.07 0.37 0.0 780 53 ~ %A1=0 0.582 0.727 43.7 1.07 1780 4380 355 \$ 0.396 3.082 0.432 1.553 45/30/25 RDX-TNT-A1 14.9 1.82 1630 5700 7635 6.0 222 0.518 0.442 3.361 1.274 1065 19.5 00<del>11</del> 5735 1.51 0.4 107 0.560 0.712 194.4 0.174 0.99 3900 4410 23.1 3.0 885 26 0.405 1.785 0.435 12.8 1750 5410 0.28 3.45 7025 196 0.528 9,446 1.416 1100 4100 4930 2.29 1.41 3.5 Table I: 85 179.0 0.497 1.105 3630 2.79 4054 0.91 2.5 880 52  $\text{Al}_2^{0_3} \text{ (mol/kg)}$ Al<sub>2</sub>0 (mol/kg) n (moles/kg) Q (kcal/kg) D\* (m/sec)  $ho_{
m l}$  (g/cc) v2 (cc/g) α (cc/g)

Table II: Influence of Al Particle Size in AN-Al Mixtures in 9.94 (d) x 61 (L) cm Charges

Al Particle Size*	- ρ <sub>1</sub> (g/cc)	$\overline{D}(obs) \ (m/sec)$	Al Particle Size*	- <del>ρ</del> η (g/cc)	$\overline{\mathbb{D}}(\text{obs})$ $(\text{m/sec})$	
6 Percent Al			10	10 Percent Al		
-100 + 150 -150 + 200 -200 + 325 -325	1.13 1.13 1.14 1.20	Failed Low 2495 3050	- 65 + 100 -100 + 200 -200 + 325 -325	1.15 1.12 1.15 1.20	Failed 3085 3090 3225	
12 Percent Al			AN F	article S	<u>ize</u>	
- 65 + 100 -100 + 150 -150 + 200 -200 + 325 -325	1.15 1.14 1.16 1.18 1.20	Failed 3170 2865 2880 2900	+ 48 - 48 + 65 - 65 + 100 -100 + 150	13.3 60.2 22.5 4.0	Percent Percent Percent Percent	

\*Standard Tyler Mesh

Table III: Critical Diameter Data for AN-Al Mixtures

Percent Al	Particle Size* Al	Critical Diameter d <sub>c</sub> (cm)
0	<b>-</b> 325	$12.7 < d_{c} < 16.0$
2	<b>-</b> 325	5.0
4	<del>-</del> 325	2.5
4 6	-325	2.5
8	<b>-</b> 325	<2.5
10	<b>-</b> 325	2.5
15	<b>-</b> 325	2.5
20	<b>-</b> 325	2.5 < d < 5.0
30	<b>-</b> 325	5.0
40	<b>-</b> 325	>7.5
10	- 48 + 325	5.0
12	- 48 + 325	$5 < d_c < 7.5$
	<b>-</b> 48 + 325	5.0
15 6	-150 + 200	10.0
10	-100 + 200	10.0
15	- 65 + 100	10.0
-		

\*AN approximately the same throughout-see Table II

Table IV: Variations of Velocity with Density in AN-Al and AN-DNT Mixtures

<u>90/</u>	LO AN-Al	(10 x 60	cm)	90/10 AN-DNT (1) (10 x 60 cm)					
AN Sample	ρ <sub>1</sub> (g/cc)	Charge	D (m/sec)	AN Sample	$\overline{\overline{\rho}}_{1}$ (g/cc)	Charge	D (m/sec)		
1*	1.06	LP**	3260	1	0.88	LP	3310		
ī	1.09	p	3390	1	1.00	LP	3480		
1	1.19	p	3550	1	1.08	р	3560		
1	1.28	P	3350	1	1.17	p	3330		
2	0.96	ĹP	3365	1	1.27	р	3120		
2	1.12	p	3485	7	1.08	р	3315		
2	1.17	P	3290	7	1.04	pc	3340		
2	1.25	p	2530	7	1.17	p	3210		
3 3	1.07	p	3520	7	1.03	pc	3735		
3	0.96	pc	3490	7	1.27	p	2905		
4	1.18	p	3405	7	1.07	pc	3700		
4	1.00	pc	3715						
5	1.28	P	Failed						
5	0.95	pc	3675						
6	1.12	LP	2595						
6	1.11	LP	2525						

\*Screen Analysis of samples 1, 6, 7 were as follows:

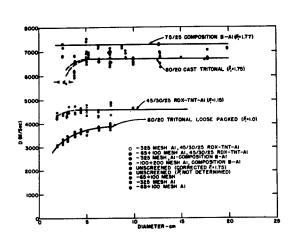
## AN Particle Size Data

Mesh	(1)	(6)	(7)
- 10 + 20		5.1	
- 20 + 35		70.9	
- 35 + 48		20.2	6.0
- 48 + 65	48.5	2.9	48.4
- 65 + 100	28.5	0.9	36.9
-100 + 150	10.1		4.3
-150 + 200	4.8		2.0
-200	8.1		2.4

Samples 2, 3, 4, and 5 were the same as sample 1 but had aged to 27 days. Aging of AN causes definite changes, the most significant of which is the packing quality.

\*\*LP = loose packed, p = pressed, pc = pressed and crushed to a loose powder which was then loose-packed. This gave a loose-packed product of the same particle size as in the corresponding pressed charges.

<b>m</b>	76.0		1.03											
Observed Variations of $R_{ m m}/{ m d}$ with Composition and d in AN-Al Explosives	0.04		0.78					ard**)					le Size	14.9 percent 13.1 percent 20.9 percent 12.7 percent 38.4 percent
n AN-Al	25.0		96.0		1.35			m stand	1.67	1.45			l Partic	
n and di	0.0		1.09		1,2			erial fro	1.37	1.42			**Standard Al Particle	65 mesh 100 mesh 200 mesh 325 mesh
nposition	17.5	ne AN*	1.16		1.31			325 Mesh Al (by removing -325 mesh material from standard**)	1.50	1.52	h Al		*****	+ 6 - 65 + 10 -100 + 20 -200 + 32 -325 mesh
with Com	15.0	Al, Fine AN*			1.21			ng -325 r	Ċ	1.63	200 Mesh			
of R <sub>m</sub> /d	12.5	-325 Mesh	Failed	1.31	1.43	1.6.27		y removi	1.50	1.33	150 to			percent percent percent percent
iations	10.0	Α.	ò	1.27	1.3	1.47		sh Al (b	1.48	1.48	ပ	0.99	Size	- 31 - 40 - 40 - 25 Ligib
erved Var	7.5			1.31	11.3%	2.1	1.53	+ 325 Me	1,61	1.30			*AN Particle S	
	5.0		ר ני	1.33	1.37		1.39 Failed	Fine AN,	Failed	ralled Failed			*AN Pa	+ 48 mesh + 65 mesh + 100 mesh + 150 mesh mesh
Table V:	d=2.5			Failed 0.92	1.35	1.07	Failed	B.						- 48 + - 65 + -100 + -150 me
	Percent Al		0 (	ソセク	, <b>ω</b> ζ	1; E	ጼጹ		95	i;		6 10 15		



TOOO - 326 MESH LOSE PACKED 48/30/ES RDX-TNT-AL (424.48cm)
- 48-100 MESH LOSE PACKED 48/30/ES RDX-TNT-AL (424.48cm)
- 326 MESH PASSED 48/30/ES RDX-TNT-AL (424.48cm)
- 326 MESH PASSED 48/30/ES RDX-TNT-AL (424.48cm)
- 326 MESH PASSED 48/30/ES RDX-TNT-AL (424.48cm)
- 326 MESH ALI (424.48cm)
- 326 MESH ALI (424.48cm)
- 326 MESH ALI (424.48cm)
- 326 MESH ALI (424.48cm)
- 326 MESH ALI (424.48cm)
- 326 MESH ALI (424.48cm)
- 326 MESH ALI (424.48cm)
- 326 MESH ALI (424.48cm)
- 326 MESH ALI (424.48cm)
- 326 MESH ALI (424.48cm)
- 326 MESH ALI (424.48cm)
- 326 MESH ALI (424.48cm)
- 326 MESH ALI (424.48cm)
- 326 MESH ALI (424.48cm)
- 326 MESH ALI (424.48cm)
- 326 MESH ALI (424.48cm)
- 326 MESH ALI (424.48cm)
- 326 MESH ALI (424.48cm)
- 326 MESH ALI (424.48cm)
- 326 MESH ALI (424.48cm)
- 326 MESH ALI (424.48cm)
- 326 MESH ALI (424.48cm)
- 326 MESH ALI (424.48cm)
- 326 MESH ALI (424.48cm)
- 326 MESH ALI (424.48cm)
- 326 MESH ALI (424.48cm)
- 326 MESH ALI (424.48cm)
- 326 MESH ALI (424.48cm)
- 326 MESH ALI (424.48cm)
- 326 MESH ALI (424.48cm)
- 326 MESH ALI (424.48cm)
- 326 MESH ALI (424.48cm)
- 326 MESH ALI (424.48cm)
- 326 MESH ALI (424.48cm)
- 326 MESH ALI (424.48cm)
- 326 MESH ALI (424.48cm)
- 326 MESH ALI (424.48cm)
- 326 MESH ALI (424.48cm)
- 326 MESH ALI (424.48cm)
- 326 MESH ALI (424.48cm)
- 326 MESH ALI (424.48cm)
- 326 MESH ALI (424.48cm)
- 326 MESH ALI (424.48cm)
- 326 MESH ALI (424.48cm)
- 326 MESH ALI (424.48cm)
- 326 MESH ALI (424.48cm)
- 326 MESH ALI (424.48cm)
- 326 MESH ALI (424.48cm)
- 326 MESH ALI (424.48cm)
- 326 MESH ALI (424.48cm)
- 326 MESH ALI (424.48cm)
- 326 MESH ALI (424.48cm)
- 326 MESH ALI (424.48cm)
- 326 MESH ALI (424.48cm)
- 326 MESH ALI (424.48cm)
- 326 MESH ALI (424.48cm)
- 326 MESH ALI (424.48cm)
- 326 MESH ALI (424.48cm)
- 326 MESH ALI (424.48cm)
- 326 MESH ALI (424.48cm)
- 326 MESH ALI (424.48cm)
- 326 MESH ALI (424.48cm)
- 326 MESH ALI (424.48cm)
- 326 MESH ALI (424.48cm)
- 326 MESH ALI (424.48cm)
- 326 MESH ALI (424.48cm)
- 326 MESH ALI (424.48cm)
- 326 MESH ALI (424.48cm)
- 326 MESH ALI

Fig. 1- Velocity-Diameter Curves for 80/20 Tritonal and 45/30/25 RDX-TNT-Al.

Fig. 2 - Ideal Velocity-Density Curves for 80/20 TNT-Al and 45/30/25 RDX-TNT-Al.

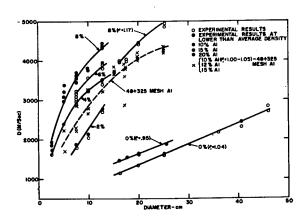


Fig. 3 - Velocity-Diameter Curves for AN-Al Mixtures (-35 + 150 mesh AN, Al was -325 mesh except as indicated,  $\bar{\rho}_1$  = 1.0-1.05).

# Cook, Filler, Keyes Partridge, Ursenbach

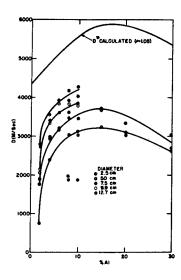


Fig. 4 - Velocity vs. Percent (-325 mesh)Aluminum  $(\overline{\rho}_1 = 1.0-1.05)$ 

Fig. 5 - Velocity vs. Diameter Measurements in RDX and 95/5 RDX-Boron Mixtures (Corrected to  $\overline{\rho}_1$  = 1.1)

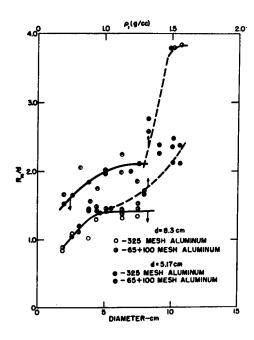


Fig. 6 -  $R_{\rm m}/d$  vs. Diameter Curves for Aluminized Explosives

# CONDITIONS BEHIND THE REACTION ZONE OF CONFINED COLUMNS OF EXPLOSIVE — NOTIONS DERIVED FROM PLATE DENT EXPERIMENTS

W. M. Slie, R. H. Stresau U.S. Naval Ordnance Laboratory Silver Spring, Maryland

# Introduction

It is convenient to consider detonation in one dimensional terms. Much of our insight regarding the processes involved is derived from such considerations. In physical terms, one dimensional consideration of detonation is equivalent to the assumption of an infinite plane wave, or perfect confinement of a finite column. Of course, neither of these conditions is realizable in that rarefaction waves close in radially as well as from the rear. In columns larger than an inch or so in diameter, for most explosives, the effect of the rarefaction waves upon the reaction zone, and hence upon the stability and velocity of detonation, are negligible. Even quite small columns of most high performance explosive compounds, when highly confined in metals, show relatively little diameter effect(1). In any size charge, however, the dimensions and conditions of the head of rapidly moving, high pressure gases which follows the detonation are directly determined by the nature of these rarefactions. The detonation head is a manifestation of flow conditions behind the detonation front. The pressure, density, and temperature drop are determined by these flow conditions, which are in turn determined by the geometry of the case in which the charge is confined. The geometry of the case, of course, is continuously modified by the forces of the detonation.

A rigorous treatment of flow conditions in and behind the reaction zone is beyond the scope of available methods, and would require information which is not available. Treatments based upon reasonable assumptions, sometimes quite obvious approximations, have provided bases for qualitative understanding and sometimes lead to semi-empirical equations which check well with experiment.

Important contributions to the understanding of the effect of radial losses upon the stability of detonation were made by Jones (2) and by Eyring and his co-workers (1). For these purposes, the flow

need be considered only to the extent that it affects conditions within the reaction zone. The curved front theory of Eyring and his co-workers(1) is quite useful for this purpose. The relation between the curvature of the front and conditions several charge diameters back would be difficult to establish and more difficult to work with. The flow behind the reaction zone has been analyzed for several sets of special conditions including those for the edge of a semi-infinite charge(3) and a thin cased cylinder(4).

It has been noted that a very small charge of explosive heavily confined in metal, behaves quite similarly, in some respects, to a much larger bare charge. This fact has led to the development of a small scale technique for the measurement of detonation velocity(5). Associated with the proven usefulness of larger scale plate dent tests(6) it inspired the hope that a useful means of evaluating explosives of which only small quantities are available might lie in a dent test in which the dents are produced by small, highly confined, charges.

The results obtained in the first small scale dent experiments were systematically related to properties of the explosives used, but do not correlate well with the larger scale results of Smith and Eyster(7). The obvious reason for this difference in results was the large difference in the confinement used in the two types of test. Since explosives were included which exhibited little diameter effect, it was reasoned that the effect of confinement upon dent test results must be a manifestation of its effect upon the conditions behind the reaction zone. The explosive columns used in most of the small scale experiments were confined in metal cylinders so thick that further increase had negligible effect upon the results. The thin cased charge analyses quite clearly do not apply to these experiments but the outer boundaries of the case need not be considered.

A useable expression has been derived which relates the depth of dent to the properties of the explosive and confining medium. An important assumption in this derivation is that the length of the "head" of high pressure product gases following the detonation is determined by the relation between the equations of state of the explosive and the confining medium. The present paper includes a discussion of the application and limitations of the use of this expression together with illustrative data.

#### Experimental Technique and Arrangement

As stated above, the dent produced by small, highly confined, columns of explosives was first considered as an economical means of evaluating experimental explosives. The small amount of equipment needed was a very attractive feature. To explore the possibilities of such a test a series of trials was made with the general arrangement shown in Figure 1.

The explosives were loaded into heavy walled brass tubes made by drilling and reaming bar stock. The tubes were counterbored at one end for the insertion of an electric initiator. Most of the tubes were two inches long with about a half inch deep counterbore, leaving about one and a half inches for the explosive column. Several sizes of tubes were used including 0"10, 0"15, 0"20 and 0"25 inside diameters. The ratio of the outside diameter of the tubes to the inside diameter was never less than 6.67. It is believed that this ratio was large enough for adequate confinement in each case, and that any further increase would have had a negligible effect. The blocks in which the dents were made were two inch long pieces cut from one by two inch cold finished, SAE 1020, steel bars. The dent was made in one of the broad faces which was cold finished.

The explosive was loaded by increments at 2,000 psi, 8,000 psi, or 32,000 psi. Increments were limited in length to not more than the diameter of the hole in order to reduce the variations in density due to wall friction which occur when longer increments are used. Densities were determined from the loading pressures using the relations given by Hampton(8). In some cases, these values were verified by measurements of the volume and mass of explosive columns. Electric initiators with bridge wires attached by the spray-metal process(19) loaded with flash charges of fifty milligrams of milled lead azide at 4,000 psi were used.

The depths of dents were measured to the deepest part of the dent from the flat surface of the block at a distance far enough from the dent to have been undisturbed by the explosion. An Ames dial indicator pedestal height gage was used. The deepest point can easily be located by moving the block with respect to the feeler of the gage until a maximum deflection is observed. The depth was measured with respect to at least two opposite points on the surface to check the flatness. If the two readings agreed within one thousandth of an inch they were averaged. Greater disagreement indicated dirt under the block, since the flatness had been checked before the test.

The results of the exploratory tests indicated that the effect of confinement upon dent test results might be much greater than upon detonation velocity measurements. For this reason, a number of trials were made using a variety of confining media and tubes of varying thickness.

The detonation velocities of the explosives used in the first group of experiments were estimated from the densities, which in turn were estimated from the pressures at which they were loaded. In the more recent experiments both the density and the detonation velocity were measured for each trial. The densities were computed from measurements of the dimensions of the hole into which the explosive was loaded and weights of explosives determined by weighing the containers before and after loading. The detonation

velocities were determined by measuring the time required for the detonation to traverse the last inch of the column. The velocity measurement was essentially that described by Hampton (5). The timer used was the vacuum thermocouple timer described by Stresau and Goode (9). In order to measure the detonation velocity, the container, as well as the explosive column, was made in sections to facilitate the insertion of an ionization probe one inch from the end. An inch long column, as nearly identical to the final inch as possible, both as to loading and confinement, preceded the section over which the velocity was measured. This latter section was for the purpose of insuring that the detonation had stabilized before the velocity was measured.

#### Results and Discussion

The dents obtained, Figure 2, were more or less cylindrical with nearly flat bottoms. The charges used were small enough so that the only measurable deformation of the plate other than the dent was a slight swelling, about 0.002, which was radially symmetrical to the dent. In Figure 3 the depths of dents obtained with four high explosives and four column diameters are plotted versus the detonation velocities of the explosives loaded at the same densities. The velocities used in this plot were determined from the loading densities using detonation velocity-density data from M.D. Hurwitz(10). Note the linear relationship of depth of dent to detonation velocity. The convergence of the lines at a point is probably not significant. The charge was detonated with a few increments of lead azide between the initiator and the main charge, Figure 1. This detonator charge could cause considerable difficulty if it had to be considered in the interpretation of results. However, if the assumption can be made that the dent is caused entirely by the charge material, a fairly simple relationship between the depth of dent and the properties of the explosive may be derived. It was therefore necessary to determine the variation of depth of dent with length of explosive column.

A study of the effect of charge dimensions on the depth of dent was undertaken. Charges of lead azide and tetryl in which the fractional column lengths of the two materials were varied were detonated on the surface of metal plates and a measure of the depth of dent was made. The explosives were loaded in columns of total length 0.5, 1.0, and 1.5 at 8,000 psi in heavy walled containers.

The results of these experiments are plotted in Figure 4. Note that both the total column length (Y) and the length of the tetryl column (y) affect the depth of dent when these quantities are small, but when the total column length exceeds about an inch and the length of the tetryl column is over approximately five diameters, the depth of dent becomes independent of both of these dimensions. A similar experiment was performed in which the depth of dent was determined as a function of total column length for lead azide,

Figure 5. In this experiment a standard length of tube was used so that the air gap between the initiator and the column decreased as the column length increased. The shape of the curve seems to indicate that the effect of this change in gap between the initiator and explosive column is negligible. The depth of dent becomes independent of the length of the column when the column length exceeds about a half inch. The larger relative dispersions with lead azide may be attributed at least in part to the residue of lead which had to be removed from the dent before making measurements.

A rather interesting feature of the results of these experiments is the nearly linear relationship between the depth of dent and the detonation velocity, Figure 3. These results may be contrasted with those obtained in larger scale experiments, Figure 6, in which it was found that the depth of dent varied linearly with  $\rho_0 D^2$ , where D is the detonation velocity and  $\rho_0 D^2$  is the density at which the explosive was loaded. This apparent contradiction may be explained by the fact that the larger charges were bare while the smaller charges discussed herein were highly confined in metal. It is believed that the following qualitative discussion may aid in understanding what was experimentally observed. Consideration of dents in metals has usually been in connection with measuring their hardness. A generality which may be inferred from hardness theory and data is that the work done in producing a dent is proportional to the volume of the dent.

The size and condition of the "head" of rapidly moving, high pressure gases which follows a detonation is directly determined by the nature of the rarefaction waves which follow from the rear and close in radially. In columns whose lengths are large enough compared with their diameters, the head reaches a stable condition which is determined by the boundary conditions at the cylindrical surface of the column. Both the size of the head and the length of the column required for it to stabilize itself depend upon what is considered to be part of the head. Gamow and Finkelstein(11), define the head as all of the forward moving gases, but for the purpose of the present discussion, it will be arbitrarily defined as the material which contributes measurably to the deformation of the steel block. By definition metal can be permanently deformed only by stresses in excess of its elastic limit. The pressure which a moving fluid can exert upon a surface, is the sum of the static pressure (P) and the kinetic pressure  $\frac{\rho u^2}{2}$ , where  $\rho$  is the density and u is the particle velocity normal to the surface. This sum

1) 
$$\rho \frac{u^2}{2} + P = H$$

will be known herein as the "total pressure". It will be assumed that the head includes that gas for which the total pressure exceeds the elastic limit of the metal.

In considering the effect of diameter and confinement upon the detonation velocity of explosives, Jones (12) develops his argument on the basis that the expansion of the case allows expansion of the explosives during the reaction time, an approach characterized by Eyring (1) as the "nozzle theory". In considering conditions behind the reaction zone, the nozzle concept becomes even more useful. At the end of the reaction zone, according to the Chapman-Jouguet theory, the sum of the sound velocity and the particle velocity is equal to the detonation velocity. In terms of ordinates moving at the detonation velocity this means that the particle velocity is equal to the sound velocity which is the throat condition of an ideal de laval nozzle.

Courant and Friedrichs describe a "hydraulic" treatment, similar to that of Reynolds, whereby very good approximations of flow conditions in a de Laval nozzle may be obtained. Introducing a set of surfaces of revolution, perpendicular to the wall, it is assumed flow is orthogonal to them and that all relevant quantities are constant on them. Further assuming that the adiabatic expansion of the gas follows the law that PV is constant, that the flow is irrotational, and Bernoulli's law, a set of equations is derived relating the particle velocity, the cross section area, the sound velocity, the density, and the pressure by various functions of gamma.

The shape of the nozzle formed by the expanding case is determined by the interaction of the explosive forces and the resistance of the metal to deformation. The assumption of a simple conical nozzle, while satisfactory for consideration of reaction zone phenomena becomes increasingly unrealistic as the length under consideration increases because it implies an unlimited source of energy. An assumption which is not unreasonable is that at all points on the surface of the nozzle the pressure is equal to the product of the shock velocity, the particle velocity, and the density of the metal. This follows from a not too critical application of the law of conservation of momentum. If this relationship is combined with the nozzle equations, a completely unmanageable set of expressions can be derived. If, however, simple integers, such as two or three, are substituted for gamma, it is possible to obtain numerical solutions for the various flow quantities by a process of iteration. The system scales in terms of the dimensionless quantity  $L \rho_e D_e / r \rho_c D_c$ , where L is the distance behind the front,  $\rho_e$  is the density of the explosive,  $\textbf{D}_{\textbf{e}}$  is the detonation velocity, r is the radius of the explosive charge,  $ho_{
m C}$  is the density of the confining medium, and Dc is the velocity of a shock in the confining medium.

If it is assumed: that the detonation "head" scales in terms of the dimensionless quantity mentioned above; that the volume of a dent in steel is proportional to the energy expended in producing it; that the energy delivered to the plate is proportional to that in the "head"; and that, for a constant diameter explosive charge, the volume of the dent produced is proportional to its depth, the following

expression may be derived by some rather simple but space consuming algebra (20):

$$d/r = k P_c D_c (D_e - S/P_e D_e)$$

where S is a constant related to the strength of the steel. S and k can be determined using two experimental points obtained with explosives for which the relationship between density and detonation velocity is known. In Figure 7, the agreement between the experimental data and the curves plotted from the equation is quite remarkable.

It will be noted that equation 2) predicts that the depth of dent should be proportional to the shock impedance, the product of the density and the shock velocity, of the case. A series of experiments was undertaken to test this prediction. These experiments differed from the previous ones mainly in that the confining medium was varied. The results of these experiments are shown in Tables I and II. The compositions of the confining media are given in Table III. It is seen from Table I, which shows the effect of case confinement for small charges of PETN, that the detonation velocity of the PETN does not change as a function of the confining media. However, the output of the charge, as measured by a dent test, does change with the confining case and is directly related to the characteristic shock impedance of the confining case. Note the agreement between the shock velocities measured using entirely different methods. This is an indication that the time for the reaction of the PETN to be completed is so short that the conditions in the reaction zone are not changed by confinement, but, since the measured output of the PETN charge is changed, the flow conditions in the detonation head must have changed.

The process which takes place in TNT when confined in various media is not so simple, as shown by an inspection of Table II, and in a more specific case, that is, for TNT confined in steel, as shown in Figure 8. For this explosive there is both a velocity change and an output change due to confinement. This is seen by comparing the measured velocity and the large scale velocity for the same density. The detonation velocity called large scale velocity in this report is that obtained from experimental rate-loading density data, and for TNT the difference between the measured velocity and this value decreases as the loading density is increased. This indicates that the reaction zone length of the explosive is an inverse function of density.

A comparison of the reaction zone lengths for PETN and TNT may be obtained using relationships derived by Eyring et al(14).

tan 
$$= \sqrt{\frac{D}{n}} - 1$$

$$\frac{D}{D_i} = 1 - .88 \text{ a sin }$$
assuming  $\cos \phi \approx 1$ 

$$\frac{D}{D_i} = 1 - .88 \text{ a } \sqrt{\frac{D^2}{D_i^2} - 1}$$

where D = detonation velocity (measured)

D; = ideal detonation velocity (large scale)

a = reaction zone length

R = radius of the charge

f = density of explosive charge

c = density of case

D = shock velocity

substituting values from Table I for PETN confined in steel (P = 1.35) a = .12 mm

substituting values from Table II for TNT ( $\ell$  = 1.36) a = 2.4 mm substituting values from Table II for TNT ( $\ell$  = 1.58) a = .106 mm

The values obtained for the length of the reaction zone agree in a quantitative way with the upper limit values given by Herzberg(21), if we assume that the reaction zone length of PETN is shorter than that of TNT from the effect of confinement on each explosive, and from the comparative sensitivity of each explosive. Thus one sees that the reaction zone lengths for the two explosives, TNT and PETN differ appreciably for similar conditions of confinement and loading.

The results obtained with aluminum and magnesium are an odd combination of a vindication of these equations and an illustration of their limitations. It is clear from a glance at equation 3) that the predicted effectiveness of a confining medium increases so sharply as its shock velocity approaches the detonation velocity of the explosive that its density assumes a secondary importance. It will be noted that the detonation velocities of TNT columns loaded in aluminum and magnesium, which have high shock velocities but low densities, are higher than those confined in babbitt. As predicted by equation 3), which applies to the reaction zone, aluminum is a better confining medium than babbitt so far as detonation velocity is concerned, but as predicted by equation 2) which was derived considering the whole detonation head, babbitt is a better confining

medium than aluminum as indicated by the dent test. The difficulty arises when an attempt is made to use equation 3) quantitatively. The meaning of the imaginary quantity resulting from the substitution of a shock velocity higher than the detonation velocity is somewhat difficult to grasp.

All of the confining tubes used in the experiments described above were so thick that it was assumed that further increase in thickness would have negligible effect. A series of experiments was run with tubes of varying thicknesses. The results of these experiments are given in Tables IV and V. The one inch outside diameter tubes used in the previously mentioned experiments are obviously large enough to justify this assumption. Results obtained with PETN are given in Table IV. Neither the material nor the thickness of the confining tube has an effect on the detonation velocity of PETN which is large enough to be detected with the instrumentation used. The dent produced, however, varies systematically with the outside diameter for each confining medium.

Since the results of the experiments with the denser confining media were more nearly as expected, these experiments will be considered first. In terms of the interpretation of dent test data on which this paper has been based, the effect of the outside diameter of the tube upon the dent should be felt when this diameter is small enough that the rarefaction wave which is the reflection of the shock wave from the surface reaches the bore of the tube within the length of the detonation head. If it is assumed that shock and rarefaction waves of all amplitudes have a constant velocity, the distance, "L", from the detonation front to the point where the rarefaction wave intersects the bore can be obtained from the simple trigonometric relationships:

4) 
$$\sin B = D_c/D_e^{(5)} L = 2t\cot B$$

where B is the angle between the axis and the shock front in the metal and "t" is the thickness of the tube. If we apply these equations to the data for PETN confined in steel, the length of head determined is in the neighborhood of three millimeters. The larger variation of shock velocity with amplitude in the other materials makes the wave front geometry too complicated to express in these simple terms, but an order of magnitude correlation might be expected. Brass, whose shock velocity and density are close to those of steel, is quite similar in its behavior as a confining medium both with thick and thin walls. The outside diameter at which the effect of the surface rarefaction is noticeable should be smaller for babbitt both because as a poorer confining medium it would support a shorter detonation head and because of its lower shock velocity, the ratio of "L" to "t" in equations 4) and 5) is larger. This expectation is realized, Table IV.

Equations 4) and 5) cannot be applied to aluminum and magnesium because their shock velocities exceed the detonation velocity of the explosive. An interesting feature of the magnesium and aluminum data is the sharp increase in depth of dent with decreasing diameter at about 0.45 inch outside diameter. Observation of the shapes of the dents produced left no doubt that this increase was associated with a substantial contribution by the case to the denting. Apparently these materials, due to their good impedance match to the explosive, acquire enough forward momentum to contribute appreciably. The rather sharp break at 0.45 inch diameter may be associated with the distribution of this momentum over so large an area that the pressure exerted on the steel was reduced below the rather definite yield point of this material.

The results obtained with TNT in tubes of varying diameter, Table V, are quite similar to those obtained with PETN, except that both the material and thickness of confinement affect the detonation velocity. The decrease of detonation velocity with the outside diameter of the steel tubes is about what might have been anticipated. The apparent increase of detonation velocity with decreasing outside diameter of the babbitt tubes was quite unexpected and has not yet been explained. The possibility of measurement aberrations is being investigated.

The "hydraulic" treatment of the de Laval nozzle is based on the assumption that radial pressure gradients are negligible. For nozzles with small expansion angles this assumption is quite realistic. As expansion angles increase, however, so do radial pressure gradients. The expansion angles of the nozzles formed by the interaction of detonating explosives with the confining media increase as the shock impedance of the media decrease. The resulting increase in radial pressure gradients is quite apparent in the shapes of dents produced by the impingement of the detonation on steel plates. As the shock impedance of the confining medium is decreased, the shape of the dent changes from the nearly flat bottomed configuration of Figure 2 to the nearly conical dents produced by unconfined charges.

A nozzle promotes the conversion of thermodynamic energy to kinetic energy by presenting a surface to the expanding gases at such an angle that a component of the force is in the direction of acceleration. The magnitude of this component is proportional to the product of the pressure and the sine of half the expansion angle. For small angles, the pressure change is small and the acceleration increases with the angle. For larger angles where the radial pressure gradients are appreciable, the pressure at the surface decreases until, at some angle depending upon the thermodynamic characteristics of the gas, it reaches zero. The axial component of force, in such a system, must go through a maximum. In the nozzles formed from confining tubes by detonations, the nozzle angles, varying in accordance with the principles discussed above, also may

be expected to go through optimums for acceleration of the gases as they change with the shock impedance of the tubes. It should be kept in mind that this acceleration is in the opposite direction to the detonation velocity so that the optimum acceleration would correspond with a minimum forward momentum and a minimum dent. In Table VI some data obtained by Savitt(18) seem to support this expectation.

The agreement between equation 2) and experimental data shown in Figure 3 was partly the result of the similarity of the equations of state of the reaction products of the explosives used in these experiments. The general usefulness of detonation velocity as a criterion of explosive performance also stems from this similarity. For some purposes and with certain explosives the lack of correlation between detonation velocity performance is probably related to variations in equation of state. An example of this was a mixture of RDX with about twenty-three percent of wax and plastic resins. Fragmentation results with this explosive gave much poorer results than would be anticipated from the detonation velocity. This explosive also made smaller dents than were predicted by equation 2). Further investigation may lead to more accurate predictions of explosive performance by the use of the small scale dent test combined with the small scale detonation velocity measurements.

# Conclusions

Some conclusions which may be drawn from the foregoing are that:

- 1. The depth of the dent which is produced by the impingement of a detonation upon a steel plate is a function of the length of the detonation head as well as the peak detonation pressure.
- 2. That the use of the concept of a de laval nozzle, formed by the action of the explosive on the confining medium, which travels with the detonation makes possible the derivation of an expression relating the depth of dent to the properties of the explosive and of the confining medium which correlates well with experimental data for charges confined in thick metal tubes.
  - 3. That the nozzle concept may be applied to thinner tubes.
- 4. That the nozzle concept also may be applied to long cylindrical charges of any confinement if a more generalized treatment of nozzle flow than the "hydraulic" treatment is used.
- 5. That the dent test, combined with detonation velocity measurements, can make more reliable predictions of explosive performance possible where equation of state variations affect the reliability of prediction based on detonation velocity alone.

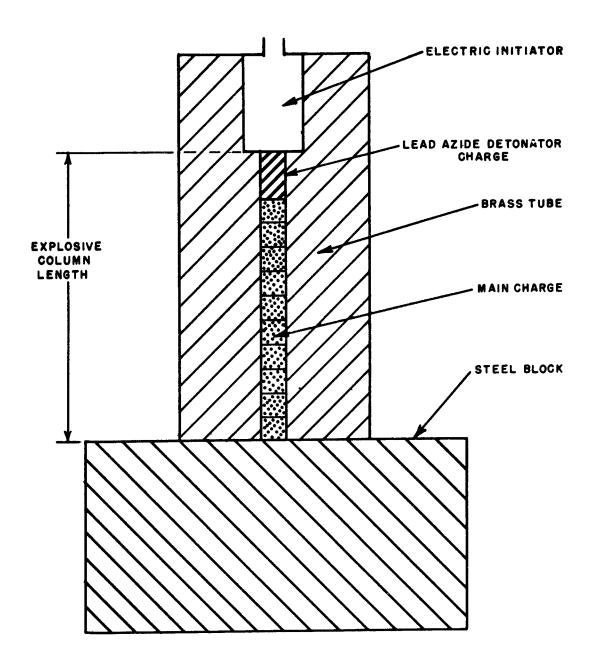


FIG. I SMALL SCALE DENT TEST (EXPERIMENTAL ARRANGEMENT)

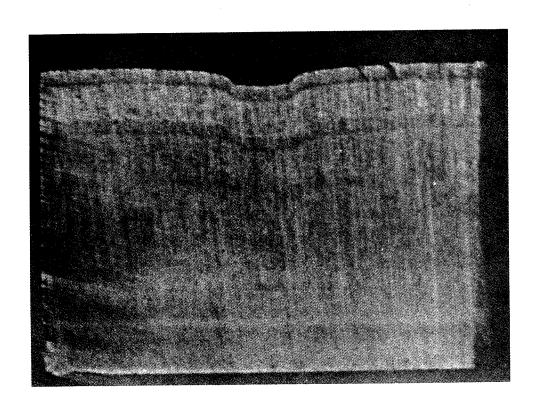
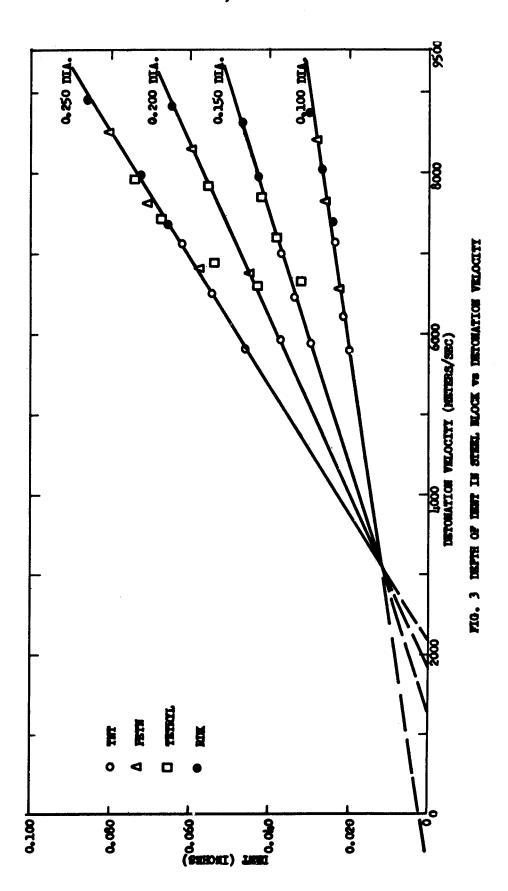
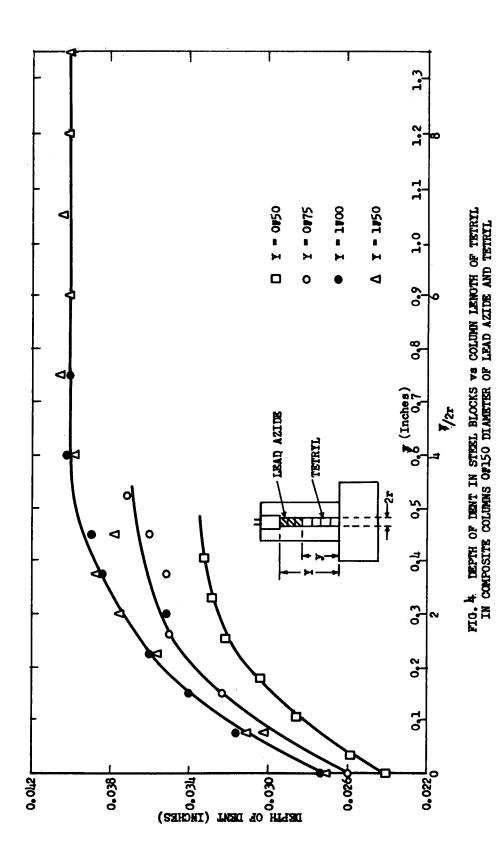
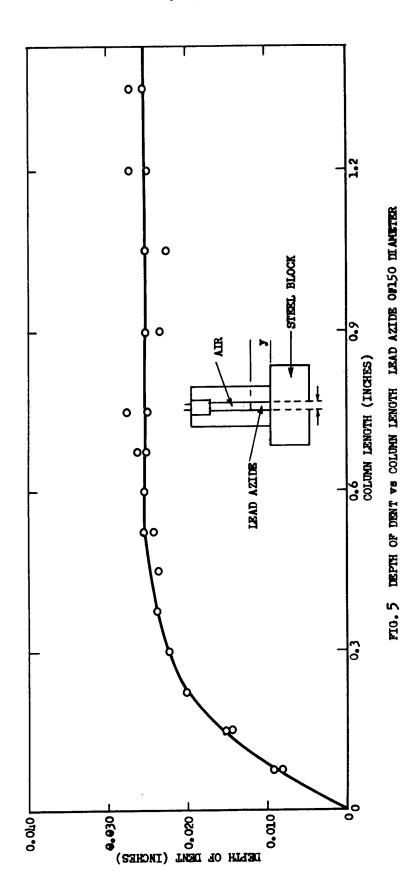


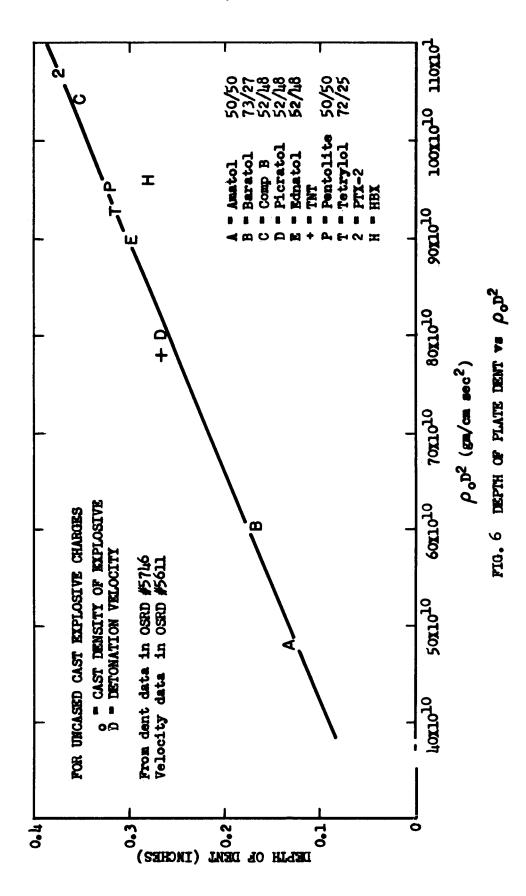
FIG. 2

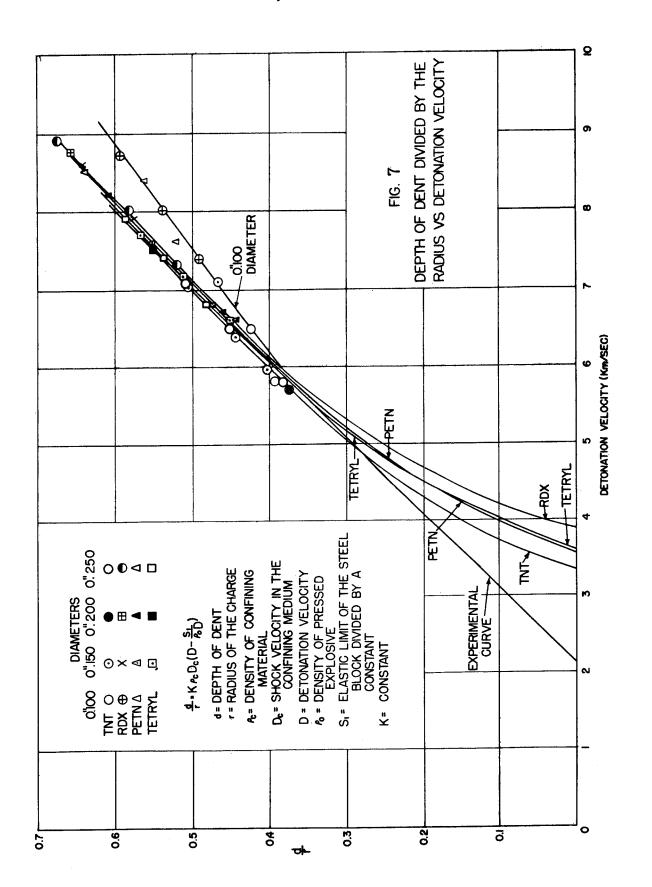
CROSS SECTIONAL CUT OF METAL BLOCK SHOWING DENT











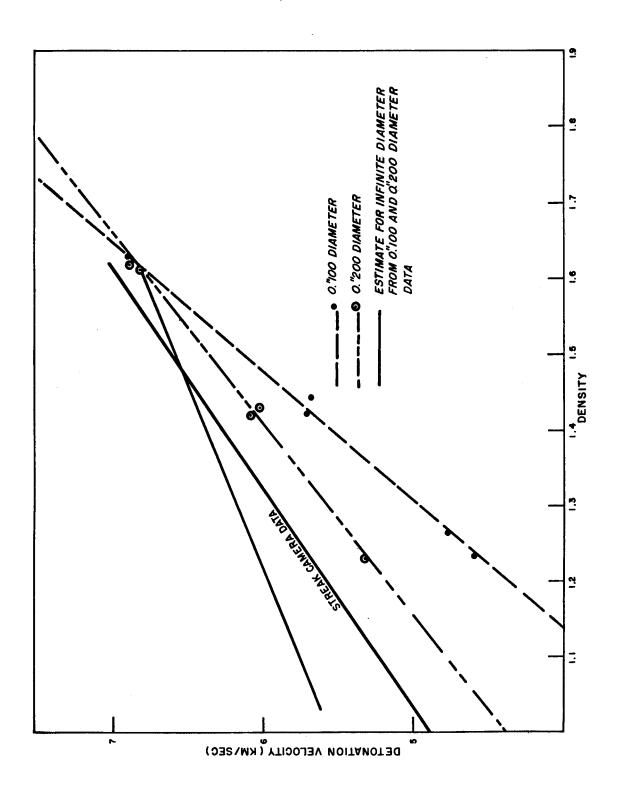


Figure 8
Detonation Velocities of Small Diameter Columns of
TNT Confined in Heavy Steel Tubes

Table I

Effects of Radial Case Confinement for Small
Cylindrical Charges of PETN

Confining Medium	đ	đ/ <sub>T</sub>	D <sub>e</sub>	Di	Pe	<b>P</b> c	D <sub>c</sub>	D.
Zinc Alloy Die Cast	24 22	0.32 0.30	6750 6850	6850 6850	1.362 1.368	6.60	4050 3850	
Magnesium Die Cast	12 12	0.17	6750 6700	6950 6950	1.380 1.380	1.81	7834 7834	
Brass	35	0.47	6850	6850	1.365	8.50	4519	4350 <sup>(13)</sup>
Regular Brass	36	0.48	6650	6950	1.370	8.50	4615	4291(14)
Bronze	31 30	0.42	6700 6600	6950 6850	1.376 1.357	8.80	<b>45</b> 19 <b>51</b> 35	*4730 <sup>(15)</sup>
Ketos Steel	31 35	0.41 0.47	6050 6250	6400 6350	1.242 1.224	7.84	4850 5450	
Regular Steel (1020 Steel)	36 37	0.48 0.50	6500 6400	6500 6800	1.250 1.351	7.85	5240 5610	5882 (14) 5240 (16)
Babbitt	27 27	0.37 0.37	6550 6650	6700 6750	1.312	9•73	3274* 3217	**3020(16)
Magnesium	13	0.17	6800	6950	1.383	1.76	7834	
Aluminum	17 18	0.23 0.24	6900 6800	6950 6950	1.382 1.385	2.71	6886 7150	7103(17)

d-depth of dent (thousandth of an inch); r-radius of explosive column (thousandths of an inch);  $D_e$ -detonation velocity (meters/sec) as measured;  $D_i$ -detonation velocity (meters/sec) from large scale measurements for density ( $P_e$ );  $P_e$ -density at which each specimen was loaded;  $P_c$ -density of confining medium;  $D_c$ -shock velocity in confining medium (meters/sec) calculated from data for each trial using equation 2);  $D_c^i$ -shock velocity in confining medium measured by others, using various techniques, for shocks produced by explosives

<sup>\*</sup>Copper

<sup>\*\*</sup>Iead

Table II

Effects of Radial Case Confinement for Small
Cylindrical Charges of TNT

Confining Medium	đ	<b>₫/</b> r	D <sub>e</sub>	Di	<i>P</i> <sub>e</sub>	<b>P</b> c	D <sub>c</sub>	D.
Zinc Alloy Die Cast	15 15 19 21	0.20 0.20 0.26 0.28	5000 4900 6530 6650	6100 6100 6800	1.37 1.37 1.58 1.58	6.60	3500 3536 3450 3645	
Magnesium Die Cast	10 13 12	0.14 0.17 0.16	6450 6850 6800	6050 6900 6950		1.81	7100 7620	
Brass	29 28 40 41	0.35 0.35 0.38 0.39	5582 5582 6775 6775	6050 6050 6850 6850	1.36	8.50	4200 3700	4291 (13) 4350 (14)
Steel 4140	28 27 32 32	0.38 0.36 0.43 0.43	5850 5725 6700 6650	6100 6100 6800 6800	1.37 1.36 1.58 1.58	7.84	4475 4070	
Steel 1020	30 30 32	0.40 0.40 0.43	5532 5507 6675 6650	6100 6100 6850 6850	1.36 1.36 1.59 1.58	7.85	4950 4580	5882 <sup>(14)</sup> 5240 <sup>(16)</sup>
Babbitt	24 26	0.32 0.35	5465 6700	6300 7000	1.45 1.63	9•95	3343 3000	
Aluminum Magnesium	15 11	0.20	5910 5474 6725	6150 6200 7100	1.43 1.65	2.71	7135 7400	7103(17)
	11	0.15	6625	7100	1.65		7515	

d-depth of dent (thousandth of an inch);r-radius of explosive column (thousandths of an inch); $D_e$ -detonation velocity (meters/sec)as measured; $D_i$ -detonation velocity (meters/sec) from large scale measurements for density ( $P_e$ ); $P_e$ -density at which each specimen was loaded;  $P_c$ -density of confining medium; $D_c$ -shock velocity in confining medium (meters/sec) calculated from data for each trial using equation 2);  $D_c^i$ -shock velocity in confining medium measured by others, using various techniques, for shocks produced by explosives

# Table III

# Composition of Metals Used for Confinement

Zinc Alloy Die Cast	Aluminum 4.1%; Magnesium 0.04% Zinc remainder
Magnesium Alloy Die Cast	Aluminum 9.0%; Manganese 0.13% Zinc 0.70%; Magnesium remainder
Brass	Copper 62.00%; Zinc 35.00%; Lead 3.00%
Bronze	Copper 80.0%; Tin 10.00%; Lead 10.00%
Commercial Brass (Regular)	Copper 61.5%; Zinc 35.5%; Lead 3%
Ketos Steel	Carbon 0.90%; Manganese 1.25%; Tungsten 0.50%; Chromium 0.50%
Steel (1020)	(a) (a) (b) (b) (c) (c) (c) (c) (c) (c) (c) (c) (c) (c
Babbitt	Lead 77.50%; Tin 10.00%; Antimony 12.00%; Copper 0.50%
Magnesium	Aluminum 2.5-3.5%; Manganese 0.20 min; Zinc 0.7-1.3%; Si .3 max; Cu05% max. Ni. 005% max; Fe .005% max. other elements .3 max - Remainder % Mg
Steel (4140)	Carbon 0.38%; Manganese 0.92%; Phos. 0.017%; Sul 0.021%; Ni 0.19%; Cr 0.99%; Mg 0.20%

Table IV

Dents and Measured Detonation Velocities for Small PETM Charges Confined in Various Materials, and for Various Wall Inicknesses

ŀ	<b>(</b> 3	
	<pre>P = 1.34 gm/cc D = 6650 (m/sec) Babbitt Case</pre>	Dert x 10 <sup>3</sup> (in.) 28 29 30 30 28 29 28 29 28 29 26
ALK DOCO	<pre>P = 1.42 gm/cc D = 7020 (m/sec) Aluminum Case</pre>	Dent x103(in.) 18 20 20 29 29 29 29 29 29 29 20 20 20 20 20 20 20 20 20 20 20 20 20
TOT 10T TOM NOT THE THEODES	<pre>p = 1.35 gm/cc D = 6760 (m/sec) Steel Case</pre>	Dent x103(in.) 36 36 35 35 35 33 30 29 22 22
	<pre>P = 1.35 gm/cc D = 6720 (m/sec) Brass Case</pre>	Dent x 103(in.) 36 36 37 37 38 31 31 27 27 28
	(gm/cc) (m/sec) m Case	x <sup>103</sup> (th. 33(th.) 33 44 25(th.) 35 44 25(th.)
	*/e 1.37 (gm/cc D = 6740 (m/sec Magnesium Case	0.D.(in.) 1.00 0.90 0.80 0.70 0.50 0.45 0.375 0.375 0.325 0.225 0.225 0.100

\* $\rho$ is the average density of the PEIN charges. D is the average detonation velocity.

Table V

Dent and Detonation Velocity Measurements for Small Confined TNT Charges for Various Confining Materials, and Various Wall Thicknesses

· 'ਚ	₹	₹	52	ನ	な	છ	g	£	ช	52	સ	છ	ನೆ	22	77	8	1	1	1	;
H H	5945	1 <sub>7</sub> 80	14870	4930	1810	1985	09 <u>8</u> 4	00g <sub>1</sub>	<b>1</b> 950	4920	088 1	0464	5085	218	5204	5285	!	:	;	;
B B I	1.45	1.36	1.39	1.40	1.38	1.39	٦	1.39	٦	٦	ij	H	H	Ä	Ä	Ä	ŀ	;	1	!
B A 0.D.	1.0	oʻ	7.	۲.	<u>.</u> ,	9.	ů.	.450	904.	.375	.350	.325	<u>8</u>	-275	.250	82.	*	₽ ₽£	1	1
ರ	4	⋨	73	73	4.5	57,	91	17	:	19	1	8	8	ဓ္ဘ	ജ	17	15	!		
M C D	5670	±295	9295	5665	5657	5626	5615	5714	!	, 1808	!	5682	5726	25	5757	5590	5535	failed	i i	failed
UMIN	1.40																1.42			1.43
A L O.D.	2.00	1.75	1.50	1.25	1.00	8	800	0.70	0.50	0.50	0,40	0.350	0.325	0.300	0.250	0.225	0.200	0.175	0.165	0.160
ෆ්			31													1				
De	5732	5707	5750	5682	5650	5708	5613	5474	5474	5501	5501	5523	2,00	1	į	!				
ਜ਼ ਜ਼ <b>੍ਰ</b> ੰ	1.36	1.36	1.38	1.37	1.36	1.37	1.37	1.36	1,38	1.37	36.	1.37	1.26	failed	i	failed				
s T 0.0.	1.0	6.0	, φ	0.7	9.0	0.5	7.0	0.35	0.325	0.3	0.25	0.225	. 2.0	0.175	0.165	0,160				
್	62	20,0	\&	S	8	30,	9	8	30,	27	25	`ನ	22	16	1	i				
D e	ıc	VП	5585	VИ.	ישי	$\sim$	5524	5552	5619	5505	5637	5522	5552	なん	failed	failed				
Α Ω Ω	1.36	1.37	36	•	1.36	1.37	1.37		1,35		1.36	1.36	36.1	1.36	1.37	98.1				
B R O.D.	0.1	0.0	0	0.7	9.0	0.5	0,10	0.35	0.325	) () ()	200	0.225	0.0	0.175	0.165	091.0				

0.D. - Outside diameter of case in inches - e loading density of explosives in gm/cc -  $D_e$  detonation velocity of explosive meters/sec - d depth of dent in thousandths of an inch \*The column diameter was .150 inches.\*\*Unable to load smaller diameter pieces.

Table VI The Depths of the Dents Produced in Steel by Various Diameter Tetryl Charges Showing the Effect of Confinement

Diameter of Column	Wall Thickness (inches)	Dents Prod Brass	luced by Tetryl Bakelite	Confined in Air
0.2	0.4	50	19	23
0.3	0.35	73	30	41
0.4	0.3	93	40	52
0.5	0.25	114	53	71
0.6	0.2	138	70	85

Density - 1.6 gm/cc Column length - 0.75 inches

Dents are measured in thousandths of inches

# References

- (1) The Stability of Detonation, H. Eyring, R.E. Powell, G.H. Duffey and R.H. Parlin, Chemical Reviews, Vol. 45 pp 69-181
- (2) The Detonation Velocity of Solid Explosives Contained in Long Cylindrical Tubes of Varying Weight, AC 1168, 6 September 1941, H. Jones
- (3) Note on the Lateral Expansion Behind a Detonation Wave, AC 2093, 16 May 1942, G.I. Taylor, M. Jones
- (4) Analysis of the Explosion of a Long Cylindrical Bomb Detonated at One End, RC 193, G.I. Taylor
- (5) NAVORD Report 2282, Small Scale Technique for Measurement of Detonation Velocities, 27 December 1951, L. Hampton, R. Stresau
- (6) NOIM 10381, Miscellaneous Physical Testing of Explosives, L.C. Smith, S.R. Walton, 1949
- (7) OSRD 5746, Physical Testing of Explosives, L.C. Smith, E.H. Eyster, 1945
- (8) NOIM 10765, Density of a Pressed Explosive as a Function of Loading Pressure, L. Hampton
- (9) NAVORD Report 2137, Recent Developments in the Vacuum Thermocouple Timer, R. Stresau, C. Goode
- (10) OSRD 5611, The Rate of Detonation of Various Explosive Compounds and Mixtures, Part II, M.D. Hurwitz
- (11) NAVORD Report 90-46, Theory of the Detonation Process p 90, R.J. Finkelstein, G. Gemow
- (12) AC 1168, RC 247 Phys. Ex. 150, H. Jones
- (13) J. Appl. Phys. 2444 (1953) R.C. Shreffler, W.E. Deal
- (14) Phy. Rev. 75 (1522) 1949, D.S. Hughes, W.L. Pondrom, R.I. Mimes
- (15) J. Appl. Phys., Vol. 25 (1954) No. 10, J. Savitt, R. Stresau, L.E. Starr
- (16) Proceedings of the Physical Society, Vol. 60, 1 January 1948, D.C. Pack, W.M. Evans, H.J. James

- (17) NAVORD Report 2864, The Propagation of Shock Waves in Aluminum, 28 April 1953, H. Dean Mallory
- (18) NAVORD Report 3753, Some Observations of the Growth of Detonation, J. Savitt
- (19) NOLM 8696, A Method for the Fabrication of Low Energy Electric Initiators, R.H. Stresau
- (20) NAVORD Report 2422, Small Scale Plate Dent Test for Confined Charges, W.M. Slie, R.H. Stresau, 23 April 1952
- (21) NAVORD Report 84-46, Detonation Time and Length of Reaction Zone, G. Herzberg, G.B. Walker

# INDEX TO AUTHORS

```
Kantrowitz, A. — 79
Keyes, R. T. — 733
Kirkwood, J. G. — 71, 107, 312, 424
Kistiakowsky, G. B. — 45, 105, 187, 198
Kydd, P. H. — 187
Lewis, B. — 43
Malin, M. E. — 136, 454, 478
Mallory, H. D. — 358
Mason, C. M. — 12, 157, 281
Mautz, C. W. - 478
McLaren, A. C. — 561
Morrison, R. B. - 266
Nicholls, J. A. — 266
Parlin, R. B. — 93, 404
Partridge, W. S. — 733
Peek, H. M. — 231
Price, D. — 22
Reed, S. G., Jr. — 295
Rinehart, J. S. — 31
Rogers, G. T. — 547
Roth, J. — 57
Savitt, J. - 620
Scott, F. — 157
Seeger, D. E. — 711
Seely, L. B., Jr. — 439
Slie, W. M. — 749
Starr, L. E. - 620
Stresau, R. H. — 620, 711, 749
Summers, C. R. — 157
Thrap, R. G. - 231
Ursenbach, W. O. — 519, 733
Walker, G. R. — 39
Wedaa, H. W. - 251
Whitbread, E. G. — 643, 695
Wiseman, L. A. — 643
Wood, W. W. — 312, 424
Zinman, W. G. - 198
```